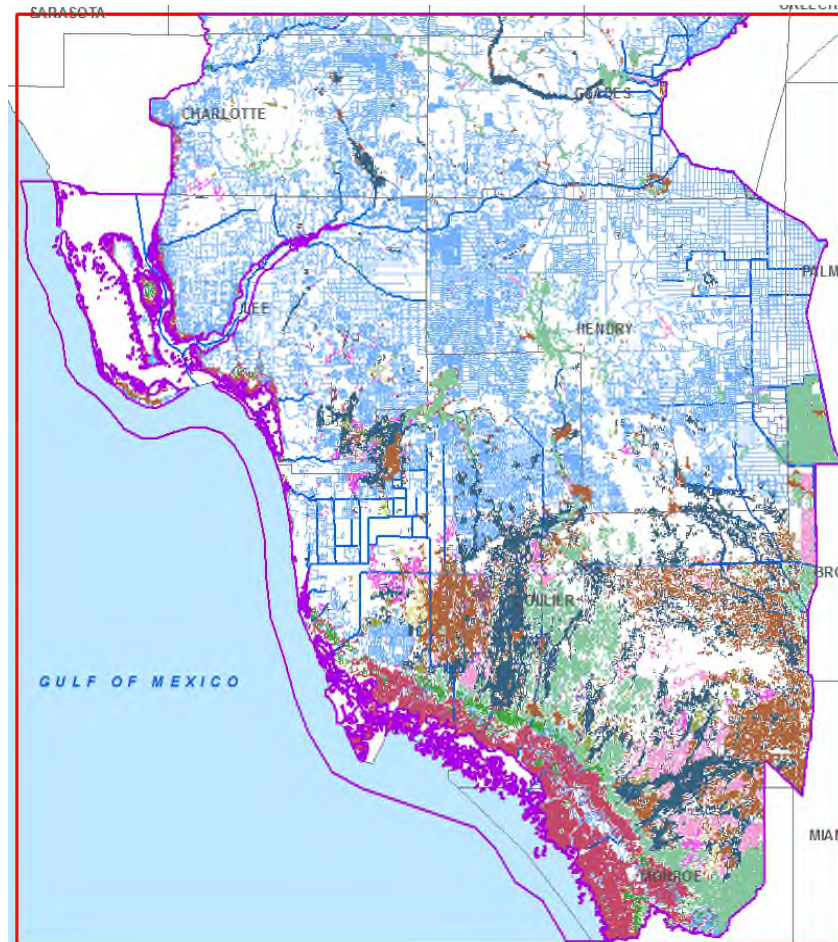


Model Documentation Report for the Lower West Coast Surficial and Intermediate Aquifer Systems Model (LWCSIM)

November 2020



Prepared by:

Uditha Bandara, Rob Earle, David Butler, Yirgalem Assegid, and D. Michael Parrish



South Florida Water Management District | 3301 Gun Club Road | West Palm Beach, FL 33406

ACKNOWLEDGMENTS

The modeling team wishes to recognize the invaluable commitment of the South Florida Water Management District (SFWMD) staff and others who have contributed to the success of the Lower West Coast Surficial and Intermediate Aquifer Systems Model development and calibration. From the SFWMD, this includes Jeff Giddings, Anushi Obeysekera, Pete Kwiatkowski, David Welter, and Emily Richardson as well as former staff Angela Montoya, Laura Kuebler, and Jorge Kappa. Also from the SFWMD, Kevin Rodberg and Alexandra Hoffart provided post-processing and GIS support, Manuel Zamorano provided database support, and Natalie Kraft provided technical editing of this report.

EXECUTIVE SUMMARY

The Lower West Coast (LWC) Planning Area of the South Florida Water Management District (SFWMD) faces numerous water management challenges. Growing freshwater demands, dwindling traditional water sources, increased levels of environmental protection, and sea level rise need to be addressed and managed to protect the area's water resources and provide adequate water supply. Regional water supply plans are the SFWMD's primary tools to address these issues.

To evaluate potential impacts to water supply and provide a tool to support water supply planning, a three-dimensional groundwater flow model of the surficial and intermediate aquifer systems underlying the LWC Planning Area was developed. The Lower West Coast Surficial and Intermediate Aquifer Systems Model (LWCSIM) was designed to simulate the response of the aquifers and natural systems (e.g., wetlands) to stresses such as proposed wellfield pumping. Results of the model applications can provide guidance in developing water management strategies, support periodic updates to the regional water supply plans, and be used in regulatory applications.

The LWCSIM was developed using the United States Geological Survey's MODFLOW model code. The geographic extent of the model covers extends from Charlotte County down the Gulf Coast to Everglades National Park in Monroe County, and from Lake Okeechobee in Glades County to the northwestern corner of Miami-Dade County. This area was divided into a uniform rectangular grid, oriented north to south, with grid cell spacing of 1,000 feet. The model comprises nine primary layers, including five productive aquifers: Water Table aquifer, Lower Tamiami aquifer, Sandstone aquifer-carbonate zone, Sandstone aquifer-clastic zone, and Mid-Hawthorn aquifer, and four semi-confining zones between the aquifers.

The model was calibrated to steady-state and transient conditions. The steady-state model was calibrated to average 1999 water levels, which ensured the water budget was reasonable. The steady-state model represents the approximate conditions of 1999, which was a period of minimal change in storage in the study area, and a period of increased monitoring that provided the initial conditions for the transient model. The transient model was calibrated to the period from January 1999 through December 2012, a total of 192 monthly stress periods, with a validation period from January 2013 through December 2014. Approximately 500 measured groundwater levels were used as head calibration targets. Four measured structure flows and estimated baseflows were used as flux calibration targets. Manual and automatic calibration (Parameter Estimation software [PEST]) methods were used iteratively during the model calibration process. The primary purpose of the transient model is to provide a tool to conduct long-term (20 to 50 years) planning and evaluate water supply issues. The LWCSIM is designed to evaluate regional conditions from stresses on the surficial and intermediate aquifer systems in the LWC Planning Area.

TABLE OF CONTENTS

| | | |
|----------|---|-----------|
| 1 | Introduction..... | 1 |
| 1.1 | Water Supply Geography and Issues | 2 |
| 1.2 | Objectives | 2 |
| 1.3 | History of Modeling in the LWC Planning Area..... | 4 |
| 1.4 | Peer Review | 4 |
| 2 | Description of the Study Area..... | 5 |
| 2.1 | Rainfall..... | 5 |
| 2.1.1 | Adjustment of NEXRAD Rainfall Data..... | 7 |
| 2.2 | Evapotranspiration | 11 |
| 2.3 | Recharge | 15 |
| 2.4 | Soil Infiltration Groups | 18 |
| 2.5 | Land Use..... | 20 |
| 3 | Physical Setting | 25 |
| 3.1 | Surface Water Flow System..... | 25 |
| 3.2 | Hydrostratigraphy | 25 |
| 3.2.1 | Geological Framework..... | 25 |
| 3.2.2 | Hydrostratigraphic Framework..... | 27 |
| 3.2.3 | Conceptualized Groundwater Flow | 28 |
| 3.2.4 | Data Collection and Analysis..... | 28 |
| 3.2.5 | Hydrostratigraphic Data..... | 28 |
| 3.2.6 | Hydraulic Data | 29 |
| 3.2.7 | Hydraulic Conductivities/Storage Coefficients..... | 29 |
| 3.3 | Water Use..... | 39 |
| 3.3.1 | Water Use Summary | 39 |
| 3.3.2 | Public Supply | 42 |
| 3.3.3 | Agriculture and Landscape/Recreational | 44 |
| 3.3.4 | Commercial/Industrial/Institutional | 48 |
| 3.3.5 | Domestic Self-Supply | 50 |
| 3.3.6 | Southwest Florida Water Management District Pumpage | 53 |
| 4 | Model Conceptualization and Design..... | 54 |
| 4.1 | Software Selection | 54 |
| 4.2 | Model Boundaries..... | 54 |
| 4.3 | Spatial Discretization | 56 |
| 4.4 | Temporal Discretization..... | 56 |
| 4.5 | Calibration Period..... | 56 |

| | | |
|----------|--|------------|
| 5 | Model Implementation | 59 |
| 5.1 | Boundary Conditions | 59 |
| 5.1.1 | General Head Boundaries | 61 |
| 5.2 | Initial Conditions | 64 |
| 5.2.1 | Initial Heads | 64 |
| 5.3 | Rivers | 74 |
| 5.4 | Drains | 76 |
| 5.5 | Wetlands | 78 |
| 5.6 | Landscape Irrigation Return Flow | 80 |
| 5.7 | ET-Recharge-Runoff Methodology | 83 |
| 5.7.1 | Input Requirements | 83 |
| 5.7.2 | Evapotranspiration | 84 |
| 5.7.3 | Runoff Calculations | 85 |
| 5.7.4 | Recharge to the Saturated Zone | 86 |
| 5.7.5 | Land Use Impact on Evapotranspiration and Recharge | 103 |
| 5.7.6 | Extinction Depths Variation with Land Use Types | 105 |
| 5.8 | Pumping Wells..... | 106 |
| 6 | Calibration..... | 107 |
| 6.1 | Methodology | 108 |
| 6.1.1 | Calibration Targets..... | 108 |
| 6.1.2 | Automated Calibration..... | 113 |
| 6.2 | Calibration Parameters | 113 |
| 6.2.1 | Hydraulic Conductivity..... | 113 |
| 6.2.2 | Leakance Values | 114 |
| 6.2.3 | Storage Parameters..... | 114 |
| 6.2.4 | Crop Coefficients | 114 |
| 6.2.5 | Extinction Depths..... | 114 |
| 6.2.6 | Curve Numbers | 115 |
| 6.2.7 | River and Drain Conductance | 115 |
| 6.2.8 | Pumping Rates | 115 |
| 6.3 | Steady-State Calibration | 115 |
| 6.4 | Transient Calibration | 116 |
| 6.4.1 | Transient Calibration Setup | 117 |
| 6.4.2 | Transient Calibration Procedure | 117 |
| 6.4.3 | Transient Calibration Criteria | 119 |
| 6.4.4 | Model Fit/Statistics | 122 |

| | | |
|----------|--|------------|
| 6.5 | Model Verification..... | 140 |
| 6.6 | Simulated Heads | 141 |
| 6.7 | Water Budget | 151 |
| 6.7.1 | Surface Water Budget..... | 151 |
| 6.7.2 | Groundwater Water Budget | 152 |
| 7 | Sensitivity Analysis | 160 |
| 7.1 | Parameters and Methodology..... | 160 |
| 7.2 | Sensitivity Results..... | 161 |
| 7.3 | Monitor Well Water Level Sensitivity..... | 162 |
| 7.4 | Results by Layer Parameter | 164 |
| 7.4.1 | Stresses and Related Variables | 169 |
| 7.4.2 | Conclusion of the Sensitivity Analysis | 169 |
| 8 | Model Limitations..... | 169 |
| 9 | Recommendations for Future Data Collection..... | 170 |
| 9.1 | Water Use Data | 170 |
| 9.2 | Water Level (Head) Data | 170 |
| 9.3 | Hydraulic Conductivity Data | 170 |
| | Literature Cited | 171 |
| | Appendices..... | 175 |
| | Appendix A: NEXRAD Correction | 1 |
| | Appendix B: Layer Tops/Bottoms and Thicknesses..... | 1 |
| | Appendix C: Domestic Self-Supply Coverage Procedure | 1 |
| | Appendix D: River Stage Missing Data Gap Filling | 1 |
| | Appendix E: Drain Coverage Procedure..... | 1 |
| | Appendix F: Wetland Coverage Procedure | 1 |
| | Appendix G: Landscape Irrigation Data Development Procedure | 1 |
| | Appendix H: Final Adjusted Model Properties..... | 1 |
| | Appendix I: Hydrographs | 1 |
| | Appendix J: R-squared versus TNSE for LWCSIM Calibration Targets | 1 |
| | Appendix K: Sensitivity Run Plots | 1 |

LIST OF TABLES

| | | |
|-------------|---|-----|
| Table 1-1. | Model layering nomenclature across multiple models..... | 4 |
| Table 2-1. | Land use summary for 2000, 2004, 2010, and 2014 in the Lower West Coast Planning Area..... | 20 |
| Table 3-1. | Water use, in million gallons per day, by county and use type, of the surficial and intermediate aquifer systems, for the Lower West Coast Planning Area in 1999..... | 39 |
| Table 3-2. | Water use demands by use type from 1999 to 2014, in million gallons per day, of the surficial and intermediate aquifer systems, for the Lower West Coast Planning Area..... | 41 |
| Table 3-3. | Agriculture water use demand by county, in million gallons per day, of the surficial and intermediate aquifer systems within the Lower West Coast Planning Area. | 46 |
| Table 3-4. | Agriculture acreage by county within the Lower West Coast Planning Area and model domain..... | 46 |
| Table 3-5. | Landscape/Recreational water use demand by county, in million gallons per day, of the surficial and intermediate aquifer systems within the Lower West Coast Planning Area..... | 46 |
| Table 3-6. | Landscape/Recreational acreage by county within the Lower West Coast Planning Area..... | 47 |
| Table 3-7. | Acreage by crop/use type within the Lower West Coast Planning Area. | 47 |
| Table 4-1. | Model layers and corresponding hydrogeologic units. | 56 |
| Table 5-1. | Density differences of water samples relative to total dissolved solids concentration..... | 61 |
| Table 5-2. | Florida Land Use Cover Classification System (FLUCCS) descriptions. | 103 |
| Table 6-1. | Residual statistics after parameter estimation (PEST) calibration of steady-state model..... | 116 |
| Table 6-2. | Transient model calibration statistics of the target monitoring wells in the model..... | 122 |
| Table 6-3. | Transient structure flow calibration statistics for major watersheds in LWCSIM..... | 136 |
| Table 6-4. | Transient wetland water level calibration statistics in the model..... | 136 |
| Table 6-5. | Transient model verification statistics of the target monitor wells. | 140 |
| Table 6-6. | Simulated water budget summary..... | 153 |
| Table 7-1. | Parameters varied by model layer. | 160 |
| Table 7-2. | Parameters and multipliers of sensitivity analysis for the model..... | 161 |
| Table 7-3. | Range of relative mean absolute error, by aquifer, for the scenario Kh (layer 6) = 0.2×. | 162 |
| Table 7-4. | Parameters with significant sensitivity..... | 162 |
| Table 7-5. | Summary of sensitive parameters by aquifer. | 164 |
| Table 7-6. | Significant sensitivity of the Water Table aquifer. | 164 |
| Table 7-7. | Significant sensitivity of the Lower Tamiami aquifer. | 165 |
| Table 7-8. | Significant sensitivity of the Sandstone aquifer – clastic zone. | 166 |
| Table 7-9. | Significant sensitivity of the Sandstone aquifer – carbonate zone..... | 167 |
| Table 7-10. | Significant sensitivity of the Mid-Hawthorn aquifer. | 168 |
| Table 7-11. | Significant sensitivity to stresses. | 169 |

LIST OF FIGURES

| | | |
|--------------|---|----|
| Figure 1-1. | Model location and boundary..... | 1 |
| Figure 1-2. | South Florida Water Management District planning areas. | 3 |
| Figure 2-1. | Annual average rainfall distribution in the Lower West Coast Planning Area from 1965 to 2013. | 6 |
| Figure 2-2. | Monthly rainfall distribution for 1999 and the average monthly rainfall from 1999 to 2014. | 6 |
| Figure 2-3. | Rainfall distribution across the model domain in 2005 (wet year). | 9 |
| Figure 2-4. | Rainfall distribution across the model domain in 2007 (dry year)..... | 10 |
| Figure 2-5. | Annual average reference evapotranspiration from 1965 to 2013. | 12 |
| Figure 2-6. | Monthly reference evapotranspiration distribution for 1999 and average monthly reference evapotranspiration distribution from 1999 to 2014..... | 12 |
| Figure 2-7. | Spatial distribution of reference evapotranspiration in 2005 (wet year). | 13 |
| Figure 2-8. | Spatial distribution of reference evapotranspiration in 2007 (dry year)..... | 14 |
| Figure 2-9. | Spatial distribution of gross groundwater recharge rates in 2005 (wet year)..... | 16 |
| Figure 2-10. | Spatial distribution of gross groundwater recharge rates in 2007 (dry year). | 17 |
| Figure 2-11. | Spatial distribution of hydrologic soil groups across the model domain, as classified by the Natural Resource Conservation Service..... | 19 |
| Figure 2-12. | 2000 land use/land cover map..... | 21 |
| Figure 2-13. | 2004 land use/land cover map..... | 22 |
| Figure 2-14. | 2010 land use/land cover map..... | 23 |
| Figure 2-15. | 2014 land use/land cover map..... | 24 |
| Figure 3-1. | Generalized geologic and hydrogeologic units of the Lower West Coast Planning Area (From: Geddes et al. 2015)..... | 26 |
| Figure 3-2. | Horizontal hydraulic conductivity of the Water Table aquifer. | 30 |
| Figure 3-3. | Horizontal hydraulic conductivity of the Tamiami confining unit..... | 31 |
| Figure 3-4. | Horizontal hydraulic conductivity of the Lower Tamiami aquifer. | 32 |
| Figure 3-5. | Horizontal hydraulic conductivity of the Upper Hawthorn confining unit. | 33 |
| Figure 3-6. | Horizontal hydraulic conductivity of the Sandstone aquifer – clastic zone. | 34 |
| Figure 3-7. | Horizontal hydraulic conductivity of the Sandstone aquifer confining unit. | 35 |
| Figure 3-8. | Horizontal hydraulic conductivity of the Sandstone aquifer – carbonate zone..... | 36 |
| Figure 3-9. | Horizontal hydraulic conductivity of the Mid-Hawthorn confining unit. | 37 |
| Figure 3-10. | Horizontal hydraulic conductivity of the Mid-Hawthorn aquifer. | 38 |
| Figure 3-11. | Water use distribution by use category, in million gallons per day, of the surficial and intermediate aquifer systems, for the Lower West Coast Planning Area in 1999..... | 40 |
| Figure 3-12. | Water use distribution by county, in million gallons per day, of the surficial and intermediate aquifer systems, for the Lower West Coast Planning Area in 1999..... | 40 |
| Figure 3-13. | Water use distribution by aquifer layer, in million gallons per day, of the surficial and intermediate aquifer systems, for the Lower West Coast Planning Area in 1999..... | 41 |
| Figure 3-14. | Water use summary for the Lower West Coast Planning Area, 1999 to 2014..... | 42 |
| Figure 3-15. | Public Supply pumping facilities using the surficial and intermediate aquifer systems within the Lower West Coast Planning Area. | 43 |
| Figure 3-16. | Agriculture and Landscape/Recreational pumping facilities using the surficial and intermediate aquifer systems in the Lower West Coast Planning Area. | 45 |
| Figure 3-17. | Location of Commercial/Industrial/Institutional pumping facilities using the surficial and intermediate aquifer systems in the Lower West Coast Planning Area. | 49 |
| Figure 3-18. | Domestic Self-Supply well locations using the surficial and intermediate aquifer systems in the model domain..... | 52 |

| | | |
|--------------|---|-----|
| Figure 4-1. | Location of water withdrawal facilities by aquifer in the Lower West Coast Planning Area..... | 55 |
| Figure 4-2. | Rainfall probability exceedance curve for the Lower West Coast Planning Area, 1965 to 2014. | 57 |
| Figure 4-3. | Annual distribution of groundwater monitor wells in the Lower West Coast Planning Area..... | 58 |
| Figure 4-4. | Annual average rainfall for the transient simulation period in the Lower West Coast Planning Area..... | 58 |
| Figure 5-1. | Location of the general head boundary, layers 1 through 9. | 59 |
| Figure 5-2. | Surface water stations used to develop the general head boundary in the Water Table aquifer. | 60 |
| Figure 5-3. | National Oceanic and Atmospheric Administration tidal stations. | 62 |
| Figure 5-4. | Average monthly stages (in feet mean sea level) at the Fort Myers and Naples tidal stations. | 63 |
| Figure 5-5. | Starting heads of the Water Table aquifer..... | 65 |
| Figure 5-6. | Starting heads of the Tamiami confining unit..... | 66 |
| Figure 5-7. | Starting heads of the Lower Tamiami aquifer..... | 67 |
| Figure 5-8. | Starting heads of the Upper Hawthorn confining unit. | 68 |
| Figure 5-9. | Starting heads of the Sandstone aquifer, clastic zone. | 69 |
| Figure 5-10. | Starting heads of the Sandstone aquifer confining unit..... | 70 |
| Figure 5-11. | Starting heads of the Sandstone aquifer, carbonate zone. | 71 |
| Figure 5-12. | Starting heads of the Mid-Hawthorn confining unit. | 72 |
| Figure 5-13. | Starting heads of the Mid-Hawthorn aquifer..... | 73 |
| Figure 5-14. | Location of rivers simulated in the model..... | 75 |
| Figure 5-15. | Location of drains used in the model. | 77 |
| Figure 5-16. | Wetlands coverage in the model. | 78 |
| Figure 5-17. | Convention for numbering cell faces in the MODFLOW Wetlands package. | 79 |
| Figure 5-18. | Example of a levee acting as a barrier to flow in the MODFLOW Wetlands package. | 80 |
| Figure 5-19. | Potable water used for landscape irrigation in the model. | 81 |
| Figure 5-20. | Reclaimed water used for landscape irrigation in the model. | 81 |
| Figure 5-21. | Landscape irrigation application rates used to calculate infiltration by curve number method for 1999..... | 82 |
| Figure 5-22. | Inputs and outputs for the ET-Recharge-Runoff program. | 83 |
| Figure 5-23. | Flow chart describing the ET-Recharge-Runoff program..... | 88 |
| Figure 5-24. | Spatial distribution of simulated runoff in 2005 (wet year). | 90 |
| Figure 5-25. | Spatial distribution of simulated runoff in 2007 (dry year). | 91 |
| Figure 5-26. | Spatial distribution of unsaturated zone evapotranspiration in 2005 (wet year). | 92 |
| Figure 5-27. | Spatial distribution of unsaturated zone evapotranspiration in 2007 (dry year). | 93 |
| Figure 5-28. | Maximum evapotranspiration in 2005 (wet year). | 94 |
| Figure 5-29. | Maximum evapotranspiration in 2007 (dry year). | 95 |
| Figure 5-30. | Gross recharge in 2005 (wet year). | 96 |
| Figure 5-31. | Gross recharge in 2007 (dry year)..... | 97 |
| Figure 5-32. | MODFLOW-simulated evapotranspiration in 2005 (wet year). | 98 |
| Figure 5-33. | MODFLOW-simulated evapotranspiration in 2007 (dry year)..... | 99 |
| Figure 5-34. | Extinction depths in 2005..... | 100 |
| Figure 5-35. | Simulated net recharge in 2005 (wet year)..... | 101 |
| Figure 5-36. | Simulated net recharge in 2007 (dry year). | 102 |
| Figure 5-37. | Gross recharge, runoff, unsaturated zone evapotranspiration, groundwater evapotranspiration, total evapotranspiration, and net recharge variation with land use. (Refer to Table 5-2 for the FLUCCS codes.)..... | 104 |

| | | |
|--------------|---|-----|
| Figure 5-38. | Average simulated extinction depths for different land use types. (Refer to Table 5-2 for the FLUCCS codes.)..... | 106 |
| Figure 6-1. | Flow calibration targets..... | 109 |
| Figure 6-2. | Surface water calibration targets..... | 110 |
| Figure 6-3. | Evapotranspiration calibration targets..... | 111 |
| Figure 6-4. | Groundwater level calibration targets..... | 112 |
| Figure 6-5. | Observed versus simulated steady-state heads in all model layers..... | 116 |
| Figure 6-6. | Spatial distribution of groundwater target wells and the average errors of simulated heads in the Water Table aquifer (layer 1)..... | 123 |
| Figure 6-7. | Spatial distribution of groundwater target wells and the average errors of simulated heads in the Lower Tamiami aquifer (layer 3)..... | 124 |
| Figure 6-8. | Spatial distribution of groundwater target wells and the average errors of simulated heads in the Sandstone aquifer – clastic zone (layer 5)..... | 125 |
| Figure 6-9. | Spatial distribution of groundwater target wells and the average errors of simulated heads in the Sandstone aquifer – carbonate zone (layer 7)..... | 126 |
| Figure 6-10. | Spatial distribution of groundwater target wells and the average errors of simulated heads in the Mid-Hawthorn aquifer (layer 9)..... | 127 |
| Figure 6-11. | Comparison of observed water levels in cluster wells open to Mid-Hawthorn aquifer (BICY-MZ1) and Upper Floridan aquifer (BICY-MZ2)..... | 128 |
| Figure 6-12. | Mean simulated versus observed water levels in the Water Table aquifer..... | 129 |
| Figure 6-13. | Mean simulated versus observed water levels in the Lower Tamiami aquifer..... | 129 |
| Figure 6-14. | Mean simulated versus observed water levels in the Sandstone aquifer – clastic zone..... | 130 |
| Figure 6-15. | Mean simulated versus observed water levels in the Sandstone aquifer – carbonate zone..... | 130 |
| Figure 6-16. | Mean simulated versus observed water levels in the Mid-Hawthorn aquifer..... | 131 |
| Figure 6-17. | Histogram of simulated versus observed water level differences in the Water Table aquifer..... | 131 |
| Figure 6-18. | Histogram of simulated versus observed water level differences in the Lower Tamiami aquifer..... | 132 |
| Figure 6-19. | Histogram of simulated versus observed water level differences in the Sandstone aquifer – clastic zone..... | 132 |
| Figure 6-20. | Histogram of simulated versus observed water level differences in the Sandstone aquifer – carbonate zone..... | 133 |
| Figure 6-21. | Histogram of simulated versus observed water level differences in the Mid-Hawthorn aquifer..... | 133 |
| Figure 6-22. | Observed versus simulated structure flow in the West Caloosahatchee watershed..... | 134 |
| Figure 6-23. | Observed versus simulated structure flow in the East Caloosahatchee watershed..... | 135 |
| Figure 6-24. | Spatial distribution of wetland surface water gauges and the average errors of simulated water levels..... | 137 |
| Figure 6-25. | Measured versus simulated total evapotranspiration at the Ave Maria agricultural site..... | 138 |
| Figure 6-26. | Measured versus simulated total evapotranspiration at the marsh site..... | 138 |
| Figure 6-27. | Measured versus simulated total evapotranspiration at the Cypress swamp site..... | 139 |
| Figure 6-28. | Measured versus simulated evapotranspiration at the SGGEX agricultural site..... | 139 |
| Figure 6-29. | Simulated water levels for the Water Table aquifer..... | 142 |
| Figure 6-30. | Simulated water levels for the Lower Tamiami aquifer..... | 143 |
| Figure 6-31. | Simulated water levels for the Sandstone aquifer – clastic zone..... | 144 |
| Figure 6-32. | Simulated water levels for the Sandstone aquifer – carbonate zone..... | 145 |
| Figure 6-33. | Simulated water levels for the Mid-Hawthorn aquifer..... | 146 |

| | | |
|--------------|---|-----|
| Figure 6-34. | Simulated potentiometric surface differences between the Water Table aquifer and the Lower Tamiami aquifer..... | 147 |
| Figure 6-35. | Simulated potentiometric surface differences between the Lower Tamiami aquifer and the Sandstone aquifer – clastic zone..... | 148 |
| Figure 6-36. | Simulated potentiometric surface differences between the Sandstone aquifer – clastic zone and carbonate zone..... | 149 |
| Figure 6-37. | Simulated potentiometric surface differences between the Sandstone aquifer – carbonate zone and the Mid-Hawthorn aquifer..... | 150 |
| Figure 6-38. | Average water budgets, by county, as simulated in the ET-Recharge-Runoff program..... | 152 |
| Figure 6-39. | Average net general head boundary flow in the Water Table aquifer..... | 155 |
| Figure 6-40. | Average net general head boundary flow in the Lower Tamiami aquifer..... | 156 |
| Figure 6-41. | Average net general head boundary flow in the Sandstone aquifer – clastic zone. | 157 |
| Figure 6-42. | Average net general head boundary flow in the Sandstone aquifer – carbonate zone. | 158 |
| Figure 6-43. | Average net general head boundary flow in the Mid-Hawthorn aquifer. | 159 |

ACRONYMS AND ABBREVIATIONS

| | |
|----------|---|
| AFSIRS | Agricultural Field-Scale Irrigation Requirements Simulation |
| AG | Agriculture |
| APT | aquifer performance test |
| BCB | Big Cypress Basin |
| CII | Commercial/Industrial/Institutional |
| cfs | cubic feet per second |
| CN | Curve Number |
| District | South Florida Water Management District |
| DSS | Domestic Self-Supply |
| DWRM | Districtwide Regulation Model |
| ET | evapotranspiration |
| FLUCCS | Florida Land Use Cover Classification System |
| ft | foot |
| GHB | general head boundary |
| GIS | geographic information system |
| gpd | gallons per day |
| gpd/p | gallons per day per person |
| IAS | intermediate aquifer system |
| K_c | crop water use coefficient |
| K | hydraulic conductivity |
| K_h | horizontal hydraulic conductivity |
| K_v | vertical hydraulic conductivity |
| L/R | Landscape/Recreational |
| LECsR | Lower East Coast Subregional (Model) |
| LFA | Lower Floridan aquifer |
| LSI | landscape irrigation |
| LTA | Lower Tamiami aquifer |
| LWC | Lower West Coast |
| LWCSIM | Lower West Coast Surficial and Intermediate Aquifer Systems Model |
| MAE | mean absolute error |
| mgd | million gallons per day |
| MHA | Mid-Hawthorn aquifer |
| MODFLOW | Modular Groundwater Flow Model |

| | |
|----------------|---|
| NEXRAD | Next Generation Weather Radar |
| NGVD29 | National Geodetic Vertical Datum of 1929 |
| NRCS | Natural Resources Conservation Services |
| PCUR | per capita use rate |
| PS | Public Supply |
| PZ | Permeable Zone |
| R ² | Pearson coefficient of correlation |
| SAS | surficial aquifer system |
| SFWMD | South Florida Water Management District |
| SSA | Sandstone aquifer |
| SWFWMD | Southwest Florida Water Management District |
| TCU | Tamiami confining unit |
| TNSE | transformed Nash-Sutcliffe efficiency (coefficient) |
| UFA | Upper Floridan aquifer |
| USACE | United States Army Corps of Engineers |
| USGS | United States Geological Survey |
| WHAT | Web-based Hydrologic Analytical Tool |
| WTA | Water Table aquifer |

1 INTRODUCTION

This document presents the Lower West Coast Surficial and Intermediate Aquifer Systems Model (LWCSIM), including its purpose and development. The LWCSIM boundary (**Figure 1-1**) encompasses the Lower West Coast (LWC) Planning Area, one of five water supply planning regions in the South Florida Water Management District (SFWMD or District). The LWCSIM was created to assist with long-term (20 to 50 years) planning and evaluation of water supply issues in the LWC Planning Area. The model may also be used for regulatory applications, which could require modifications to the model to meet regulatory criteria. The LWCSIM was developed following standard industry protocols (Franke et al. 1987, Anderson and Woessner 1992, Reilly 2001, Reilly and Harbaugh 2004).

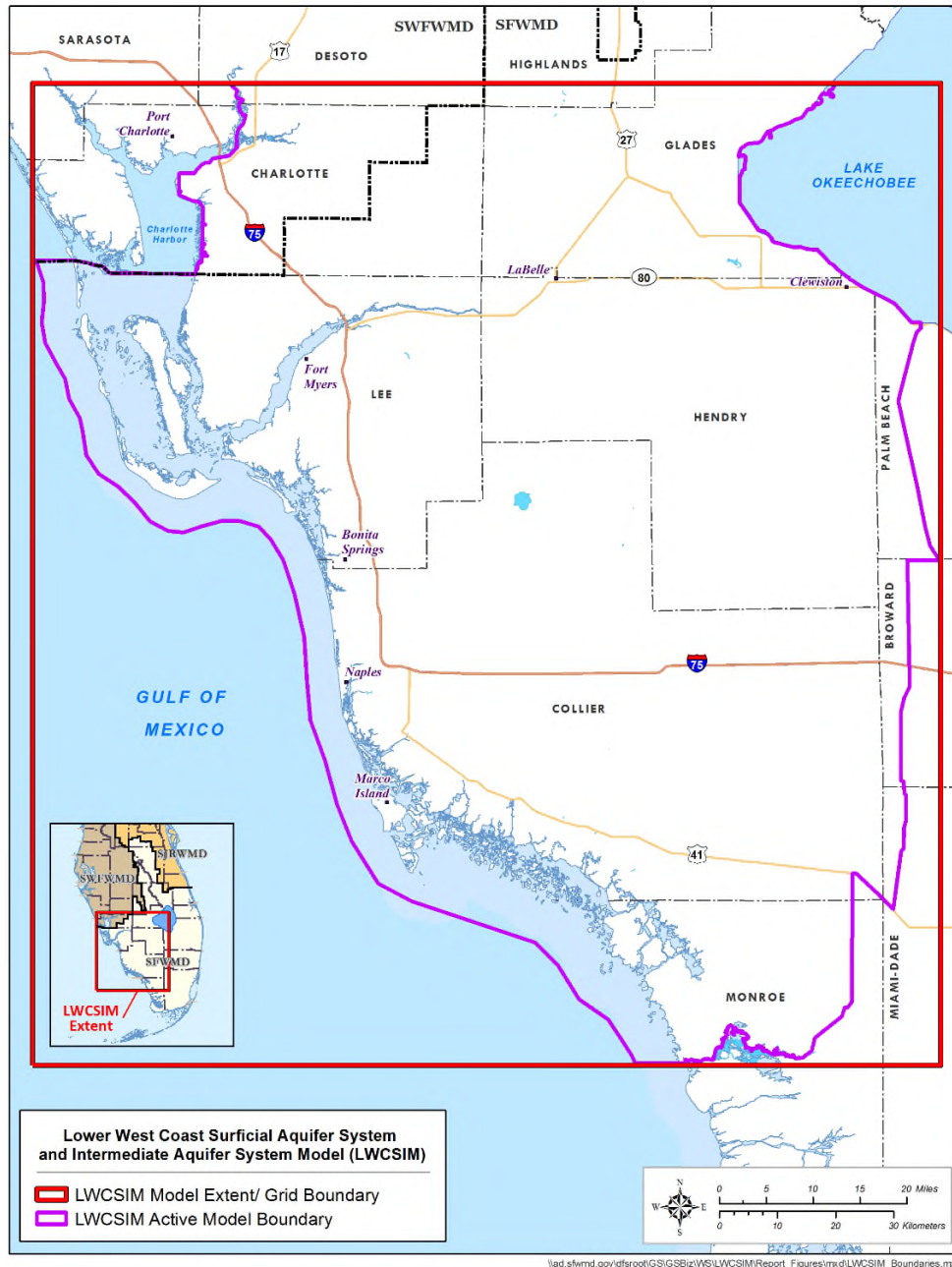


Figure 1-1. Model location and boundary.

1.1 Water Supply Geography and Issues

The LWC Planning Area includes all of Lee County, most of Collier County, and portions of Hendry, Glades, Charlotte, and mainland Monroe counties (**Figure 1-2**). The region generally reflects the drainage patterns of the Caloosahatchee, Imperial, Estero, and Cocohatchee river basins. The LWC Planning Area includes many coastal and inland natural systems, including Big Cypress Swamp and a large part of Everglades National Park.

The LWC Planning Area faces numerous challenges to maintaining adequate water supply for growing urban and agricultural demands while simultaneously meeting the needs of the environment. Detailed information on estimated and projected demands for the LWC Planning Area can be found in the most recent update to the water supply plan (SFWMD 2017).

Historically, water demands in the LWC Planning Area were met using surface water and groundwater. Surface water has been the primary source of water supply for the agricultural industry in the Caloosahatchee River (C-43 Canal) watershed. However, surface water from the existing canal and storage networks alone is insufficient to meet agricultural water use demands and environmental needs during 1-in-10-year drought conditions. Past analyses concluded that additional storage was necessary to provide adequate resources to meet existing legal user and natural system needs in the LWC Planning Area.

Throughout the LWC Planning Area, the surficial aquifer system (SAS) historically served as the major source of fresh groundwater for Public Supply (PS), Landscape/Recreational (L/R), and Agriculture (AG). However, analyses of the SAS indicate it is a limited water source in many areas.

Saltwater intrusion is an ongoing concern, resulting from continued use of shallow groundwater sources near the coast, potential sea level rise, movement of connate water in the SAS, and upconing of poor-quality water from deeper aquifers.

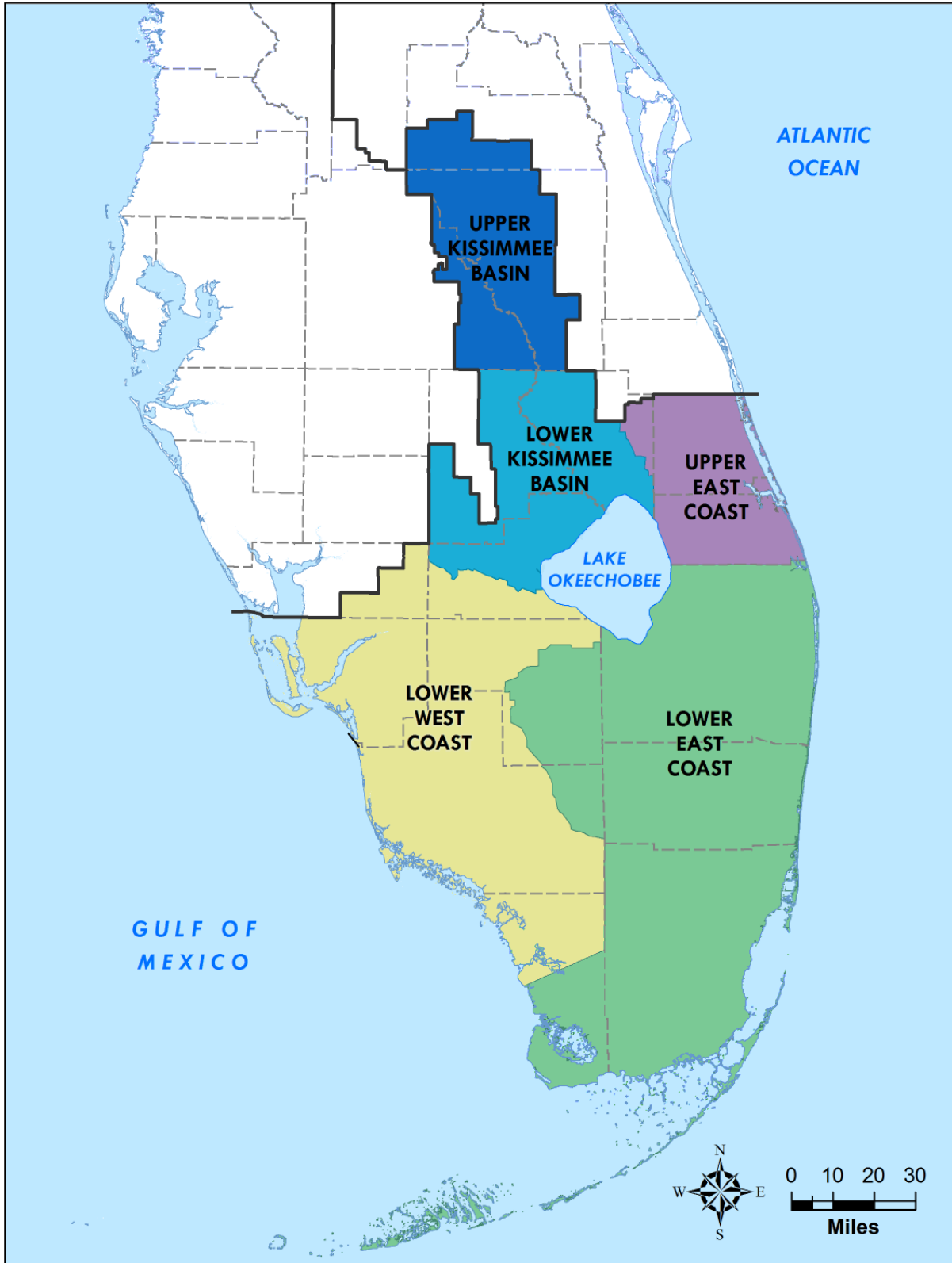
Historically, the Sandstone aquifer (SSA) and Mid-Hawthorn aquifer (MHA) within the intermediate aquifer system (IAS) have been important sources of fresh water for portions of Lee and Hendry counties. However, the freshness and productivity of these local aquifers are not consistent throughout the LWC Planning Area. Analyses indicate these localized aquifers are limited water sources in portions of the planning area due to the cumulative effects of withdrawals by all water users, which decrease water levels in the IAS and could harm the resource (e.g., through saltwater intrusion).

To reduce the potential impacts to traditional freshwater sources, future increased demands are projected to gradually shift to alternative water sources, including increased use of the underlying Floridan aquifer system and reclaimed water. The Floridan aquifer system is a regional resource, underlying portions of Georgia, South Carolina, and Alabama as well as the entire Florida peninsula.

1.2 Objectives

The objective of this work was to develop a calibrated groundwater flow model that incorporates the SAS and IAS in the LWC Planning Area to support the regional water supply plan updates. The intended purposes of the model include the following:

- 1) Facilitate the SFWMD's evaluation of the current and future availability of groundwater in the SAS and IAS;
- 2) Assess future water supply and management strategies; and
- 3) Evaluate potential impacts of groundwater withdrawals on wetlands and natural areas in the LWC Planning Area.



\\ad.sfwmd.gov\dfsroot\GIS\GSBiz\WSIWSP_Areas\mxd\WSPAreas_20180320.mxd

Figure 1-2. South Florida Water Management District planning areas.

1.3 History of Modeling in the LWC Planning Area

The SFWMD retained Marco Water Engineering, Inc. (2006) in April 2005 to develop a MODFLOW-based groundwater flow model of the SAS in the LWC Planning Area. The Marco Water Engineering, Inc. (2006) model, covering 5,129 square miles, simulated the Water Table aquifer (WTA), Lower Tamiami aquifer (LTA), and SSA. The model grid consisted of 765 rows and 622 columns, and the cells were 704 feet (ft) by 704 ft. A transient model calibration was conducted for a 15-year period (January 1986 through December 2000). **Table 1-1** illustrates how the LWCSIM layers relate to the Marco Water Engineering, Inc. (2006) model as well as nearby models (Lower East Coast Subregional Model [LECsR; Giddings et al. 2006] and Districtwide Regulation Model [DWRM; Environmental Simulations, Inc. 2014]).

Table 1-1. Model layering nomenclature across multiple models.

| Aquifer System | LWCSIM Model Layer # | LWCSIM Model Layer Name | Districtwide Regulation Model | Marco Water Engineering, Inc. Model Layer Number | Lower East Coast Subregional Model Layering |
|-----------------------------|----------------------|-------------------------------|-------------------------------|--|---|
| Surficial Aquifer System | 1 | Water Table aquifer | Water Table | 1 | Layers 1 and 2: Holocene + Q5 + Q4 + Q3 + Q2 + Q1 |
| | 2 | Tamiami confining unit | | | |
| | 3 | Lower Tamiami aquifer | | 2 | Layer 3: T2 + T1 |
| Intermediate Aquifer System | 4 | Upper Hawthorn confining unit | Peace River Aquifer (PZ1) | 3 | |
| | 5 | SSA clastic zone | | | |
| | 6 | SSA confining layer | | | |
| | 7 | SSA carbonate zone | | | |
| | 8 | Mid-Hawthorn confining unit | | | |
| | 9 | Mid-Hawthorn aquifer | Upper Arcadia Aquifer (PZ2) | | |

LWCSIM = Lower West Coast Surficial and Intermediate Aquifer Systems Model; SSA = Sandstone aquifer.

The LWCSIM was developed to incorporate a) the IAS in addition to the SAS, b) 15 years of additional water use and water level data, and c) updated hydrogeologic data and hydrostratigraphic interpretation of the data. It is important to periodically update models with current data. The improved model will facilitate evaluation of the current and future availability of groundwater in the SAS and IAS.

1.4 Peer Review

An independent, scientific peer-review panel evaluated each major phase of LWCSIM development and calibration. The following groundwater modeling experts with experience in Florida composed the peer-review panel:

- David F. MacIntyre, P.E. (Chair), AquaSciTech Consulting, PLLC
- James O. Rumbaugh, P.G., President, Environmental Simulations, Inc.
- Mark A. Ross, Ph.D., P.E., President, Hydrosystems, Inc.

The peer-review panel was engaged from the conceptual model development phase through calibration and model documentation. The first panel meeting occurred in October 2016. Throughout the peer-review process, publicly noticed teleconferences were conducted periodically to update the panel on the LWCSIM progress and solicit input via a series of tasks outlined in the Scope of Work. All communication with the panel was conducted through an SFWMD web board, which also was available to the public. Publicly noticed meeting dates were posted prior to the meetings. Correspondence between SFWMD staff and the peer-review panel was conducted through the web board, and all documents, meeting summaries, and task deliverables were posted on the web board. Major discussion topics included the model input data sets, conceptual model, calibration strategy, model calibration results, and final model documentation.

2 DESCRIPTION OF THE STUDY AREA

2.1 Rainfall

Rainfall is an important part of the hydrologic cycle. The spatial and temporal distribution of rainfall influences other variables in the LWCSIM. Long-term (1965 to 2013) historical annual rainfall averages 54 inches in the LWC Planning Area, and the distribution is shown in **Figure 2-1**. The driest year recorded is 2000, with 41 inches of rainfall, while the wettest year recorded is 1995, with 71 inches of rainfall.

Rainfall data for the transient simulation period (1999 to 2014) were derived from a combination of Next Generation Weather Radar (NEXRAD) and DBHYDRO (the SFWMD's corporate database) gauge data coupled with a simple spatial interpolation technique (Brown 2014). NEXRAD data were used from the beginning of May 2002, while gauged data were used from January 1999 through April 2002. NEXRAD data provide complete spatial coverage of rainfall amounts using a predetermined grid resolution (2 kilometers by 2 kilometers). Four NEXRAD sites operated by the National Weather Service cover the LWCSIM domain: KBYX in Key West, KAMX in Miami, KMLB in Melbourne, and KBTW in Tampa. Although these sites are not within the LWCSIM boundary, their coverages encompass the model domain. The monthly distribution of rainfall across the LWCSIM domain for 1999 and an average of 1999 to 2014 is shown in **Figure 2-24**.

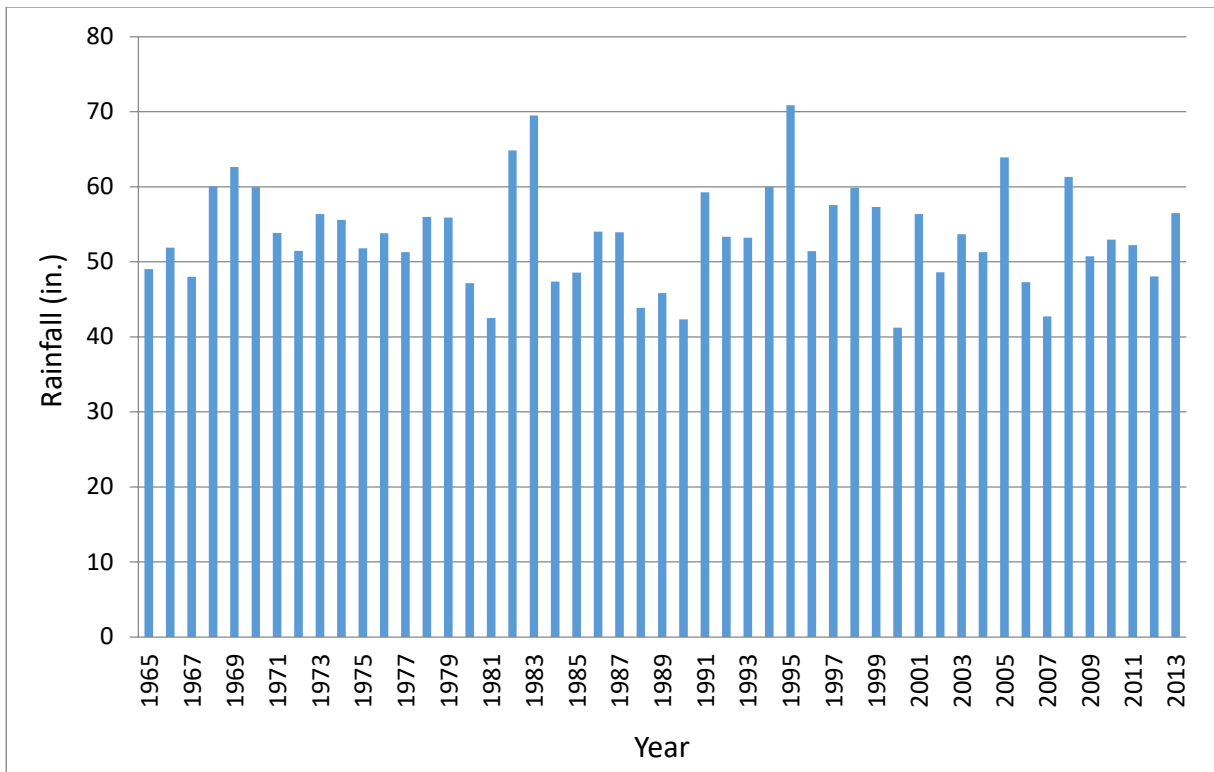


Figure 2-1. Annual average rainfall distribution in the Lower West Coast Planning Area from 1965 to 2013.

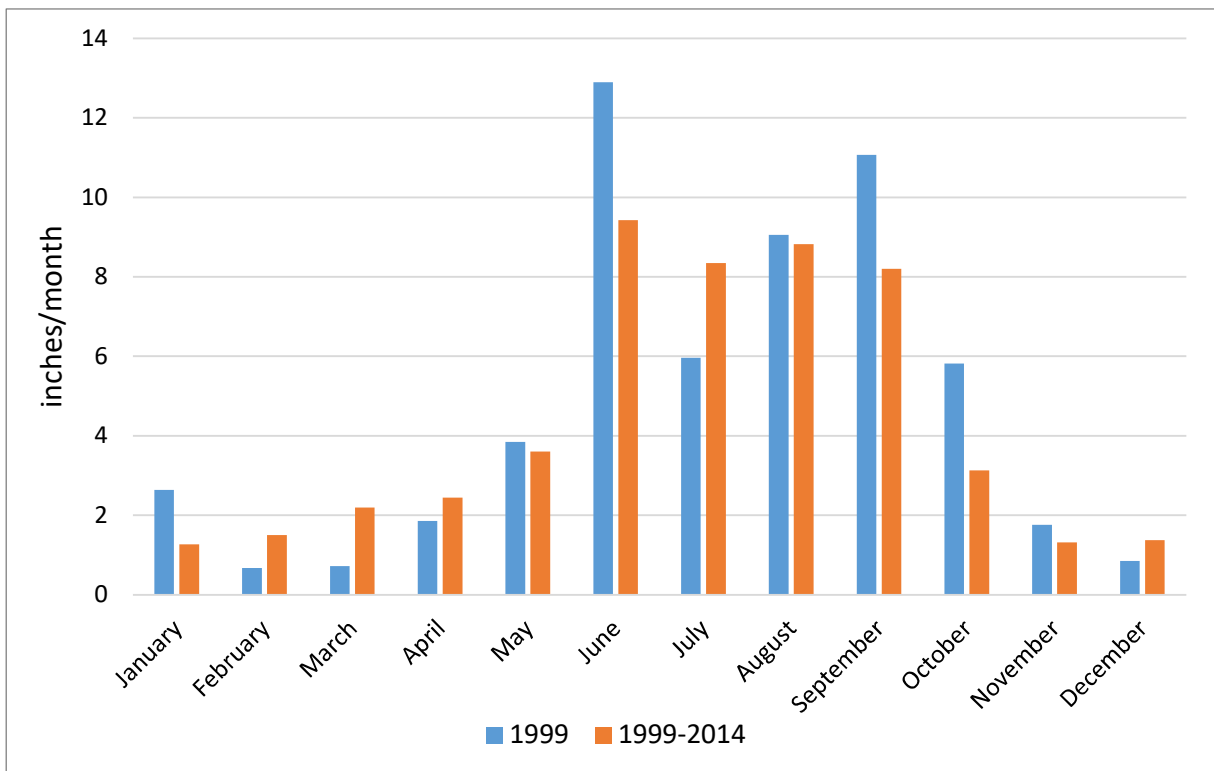


Figure 2-2. Monthly rainfall distribution for 1999 and the average monthly rainfall from 1999 to 2014.

2.1.1 Adjustment of NEXRAD Rainfall Data

A statistical analysis comparing the daily rain gauge timeseries values with nearby NEXRAD rainfall data revealed a seasonal bias in the NEXRAD daily data. The relative bias between the monthly and yearly recorded rain gauge and estimated NEXRAD rainfall totals was calculated as follows:

$$Relative\ bias = \frac{\sum NRD_i - \sum RG_i}{\sum RG_i} \times 100 \quad (1)$$

Where NRD_i and RG_i represent the mean rainfall estimated by NEXRAD and recorded by the rain gauge, respectively. The mean rainfall difference (RD) can be calculated as follows:

$$RD = \overline{NRD_i} - \overline{RG_i} \quad (2)$$

The bias was determined to represent overestimation of small rainfall accumulations (≤ 0.1 inches/day) and an underestimation of more extreme events (> 20 inches/day). A method was developed and used to adjust the NEXRAD data to reduce this bias. The correction involves identifying a multiplier to apply to each daily NEXRAD data value in a manner that a) does not significantly increase or decrease the overall volume of water for each year, and b) maintains the same general daily spatial distribution or rainfall patterns. The correction does not significantly increase or decrease the annual total NEXRAD data because the NEXRAD and rain gauge annual totals have a very good correlation and are very similar.

To eliminate the bias for other models, the NEXRAD data have been adjusted using a single non-linear equation or performing separate adjustments for wet season and dry season with different equations. However, the spatial extents of those models were much smaller than this LWCSIM effort required, and developing a suitable equation was unnecessary.

Linear regression of yearly, monthly, and daily rain gauge and NEXRAD rainfall totals was performed to evaluate the overall relationship between the variables. Furthermore, the Kolmogorov-Smirnov statistical test for normality showed a positive skew of the daily values, indicating a considerable number of small values near or equal to zero, which is not surprising because rainfall does not occur every day. Therefore, the relationship between NEXRAD data and individual rain gauges was evaluated using the Kendall's tau (τ) rank-based correlation method (Helsel and Hirsch 1992). Monthly correlation for each rain gauge and NEXRAD pixel pair was calculated using daily values ($n \geq 14$), and correlation coefficients were used to discern which rain gauges displayed a good relationship ($\tau \geq 0.75$) with the NEXRAD pixels. Rain gauges showing a poor relationship with the NEXRAD pixels were excluded from further analysis. Yearly and monthly rain gauge and NEXRAD totals were calculated. The bias between the rain gauge and NEXRAD data was determined by the ratio between the two (Steiner et al. 1999, Goudenhoofd and Delobbe 2009, Smith and Rodriguez 2017). The resulting value was used as the NEXRAD adjustment factor, calculated as follows:

$$AdjF(bias) = \sum \frac{RG_i}{n_1} / \sum \frac{NRD_i}{n_1} \quad (3)$$

Where AdjF is the multiplicative factor used to adjust the daily NEXRAD value, and RG_i and NRD_i are the monthly rainfall recorded by the rain gauge and estimated by NEXRAD, respectively, during an equally match-paired number of days ($n \geq 14$).

The statistical analysis performed did not consistently show a strong correlation when comparing daily rain gauge data with NEXRAD data at nearby pixels. However, there was a strong correlation, for most rain gauges, when comparing the same data for annual totals and a very good correlation with monthly totals.

The method developed to reduce bias uses monthly adjustment factors at each rain gauge with a suitable correlation and number of observations within the selected month. The adjustment factor is calculated as the ratio of the monthly sum of rain gauge values divided by the sum of the nearest monthly NEXRAD rain pixel values. Rain gauge stations with adjustment factors were filtered prior to creating NEXRAD bias corrections. Included stations must have adjustment factors between 0 and 10, Kendall τ correlation values less than 0.6, and 15 or more daily values per month.

To prevent overcorrection of NEXRAD daily values and to include most adjustment factors, the adjustment factor was arbitrarily constrained to between 0.7 and 1.3. Adjustments less than 0.7 were assigned the minimum adjustment factor of 0.7 and adjustments greater than 1.3 were assigned 1.3. Rain gauges with monthly adjustment factors equal to 0 were set to 1 providing no adjustment. Visual examination of the resulting bias showed several rain gauges located less than 2 kilometers from each other, which can produce inconsistencies in the bias arising from high and low values in spatially close stations. Therefore, the resulting monthly bias value at each rain gauge station was normalized using a complete hierarchical cluster analysis (Müllner 2013, Maechler et al. 2018), in which bias points are the result of the averaged bias of each rain gauge within 2 kilometers. The resulting monthly bias was used as the multiplicative adjustment factor to correct the daily NEXRAD pixel value using geostatistical processes.

Adjustment factors were interpolated across the entire NEXRAD grid using the automated autoKriging method described by Hiemstra et al. (2009). The autoKriging function tests different interpolation models (linear, spherical, exponential, Gaussian, and Matern [M. Stein's parameterization]) by estimating semi-variograms and selecting the best fit kriging model (Hiemstra et al. 2009). This process produced a monthly bias grid with adjustment factors at each NEXRAD pixel. The adjustment factors were applied to the uncorrected NEXRAD values to produce corrected NEXRAD values. Point values for the bias and the uncorrected and corrected NEXRAD were converted into a raster for visual evaluation. During this process, a few inconsistencies associated with the NEXRAD and rain gauge pairing were observed. The inconsistencies resulted from mismatched NEXRAD and rain gauge daily values, and the data were examined and removed from daily values. Subsequently, the entire process was repeated and a new set of raster plots was created. The difference or change in rainfall was calculated by subtracting the corrected from the uncorrected NEXRAD, and the results were displayed in a separate raster. The model cell locations were used to extract values from the corrected NEXRAD raster and exported as data for each model mesh cell. All statistical and spatial data analyses were performed using R programming language (version 3.5.1; R Development Core Team 2018).

The results obtained by applying adjustment factors for each temporal aggregation to make bias adjustments and recalculating monthly and annual sums near observed locations were reviewed to ensure the correction did not create or eliminate significant amounts of rainfall. Monthly totals provided significantly better correction than wet season/dry season totals. There was not a significant benefit to using bi-weekly or weekly corrections because the observed and NEXRAD values did not correlate well at those levels of discretization. More detailed description of the adjustment of the NEXRAD rainfall data is provided in **Appendix A**.

The steady-state model used rainfall data from 1999. The maximum monthly rainfall in 1999 (12.9 inches) occurred in June, and the minimum amount of rainfall (0.7 inches) occurred in February. Average annual rainfall across the model domain in 1999 was 57.3 inches. Spatial distribution of adjusted NEXRAD rainfall data for 2005 (wet year) and 2007 (dry year) within the model domain are shown in **Figures 2-3** and **2-4**, respectively. Average rainfall across the model domain was 63.8 and 42.7 inches in 2005 and 2007, respectively.

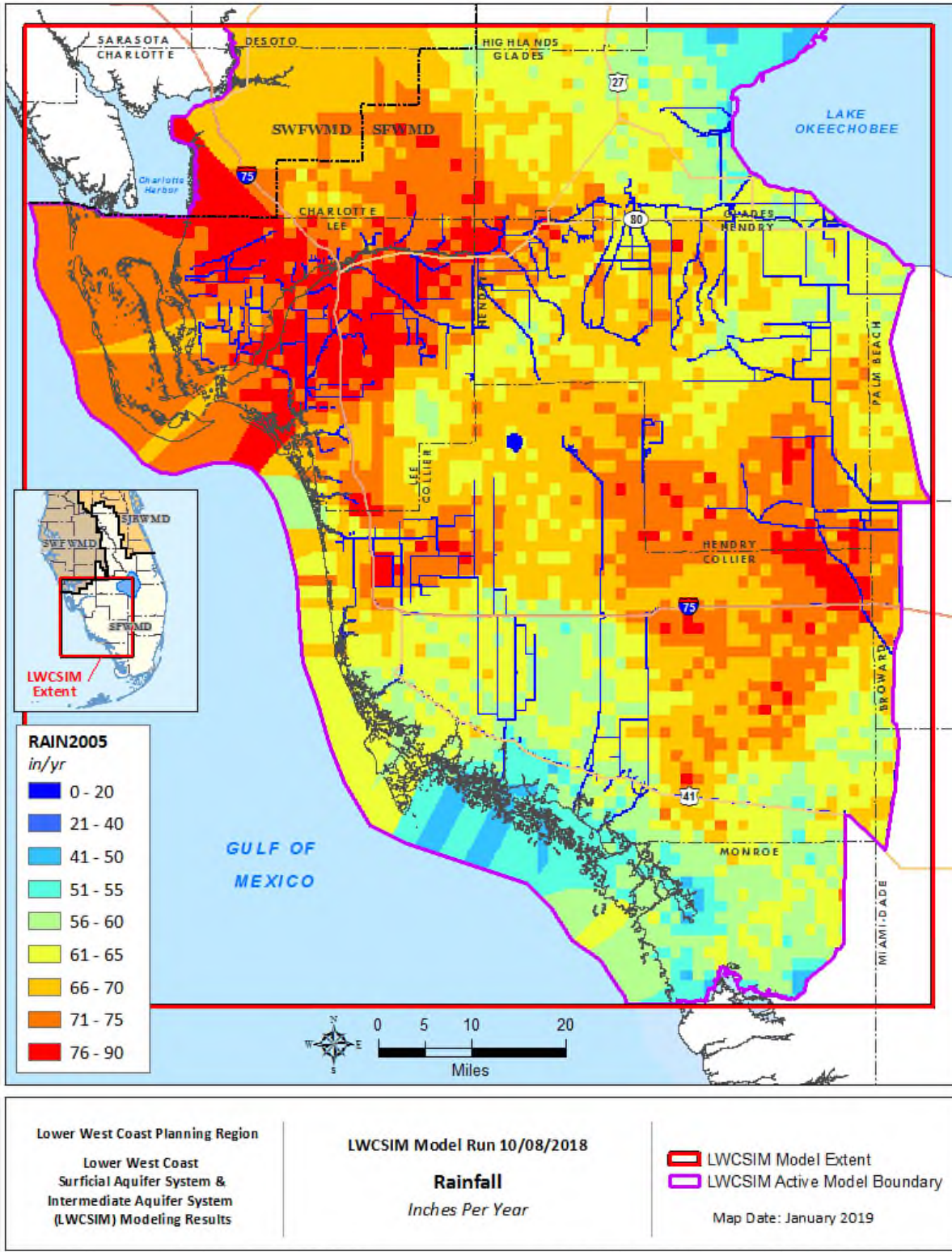


Figure 2-3. Rainfall distribution across the model domain in 2005 (wet year).

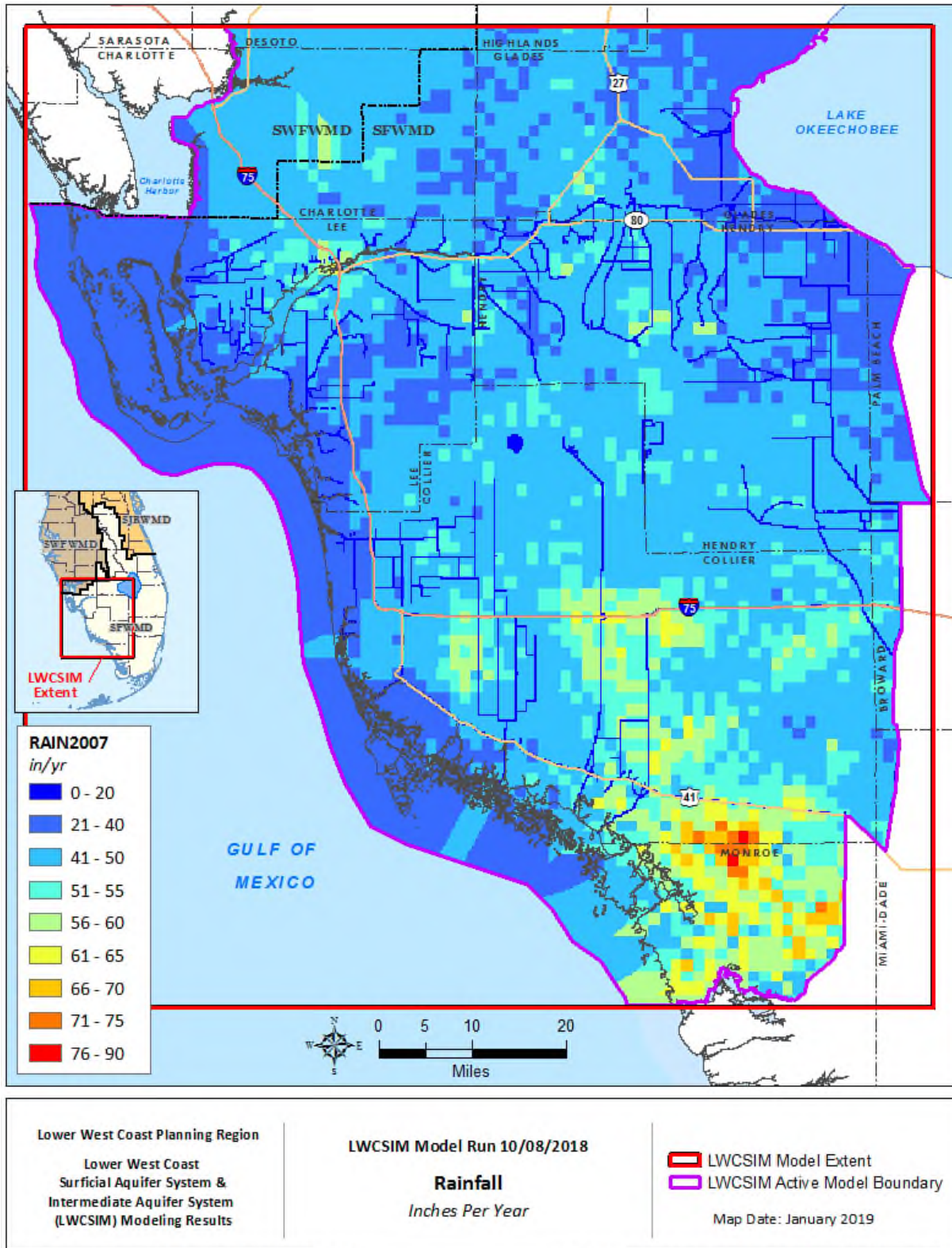


Figure 2-4. Rainfall distribution across the model domain in 2007 (dry year).

2.2 Evapotranspiration

Evapotranspiration (ET) is the sum of the evaporation from water bodies and transpiration losses from plant systems to the atmosphere. ET plays a major role in the hydrologic cycle in the LWC Planning Area because the water table is near land surface throughout the year. In fact, ET causes the largest loss of water from the system.

Reference ET is the rate of ET from a hypothetical reference crop with an assumed crop height of 0.12 meters, a fixed surface resistance of 70 seconds per meter, and an albedo of 0.23, closely resembling the ET from an extensive surface of green grass of uniform height, actively growing, well-watered, and completely shading the ground (Jensen et al. 1990, Doherty et al. 2010). Potential ET is the amount of water used by a crop and can be estimated by multiplying the reference ET by a crop water use coefficient (K_c). The K_c is specific to a particular crop or vegetation and can vary from month to month.

Reference ET data were obtained from the SFWMD's updated data set (Brown 2013). The updated data have a domain consistent with the jurisdictional boundary for the SFWMD and were created from two data sets. The first data set was the 51-year hydrological re-analysis (HYDRO51) and the second data set was generated by the North American Land Data Assimilation System (NLDAS). The long-term data set was created incrementally, and the completed set is believed to be the best available because the data from 1979 to present used the NLDAS-based satellite data (Brown 2013).

Historical reference ET distribution from 1965 to 2014 is shown in **Figure 2-5**. The average value over this period is 57 inches/year. The monthly distribution of reference ET across the LWCSIM domain is shown in **Figure 2-6**. The maximum reference ET rate (6.24 inches) occurred in April, and the lowest reference ET rate (3.01 inches) occurred in December (Smajstrla 1990). **Figure 2-6** also includes the average reference ET rates for the LWCSIM transient calibration period (1999 to 2014). **Figures 2-7** and **2-8** show the spatial distribution of reference ET across the LWCSIM domain for 2005 (wet year) and 2007 (dry year).

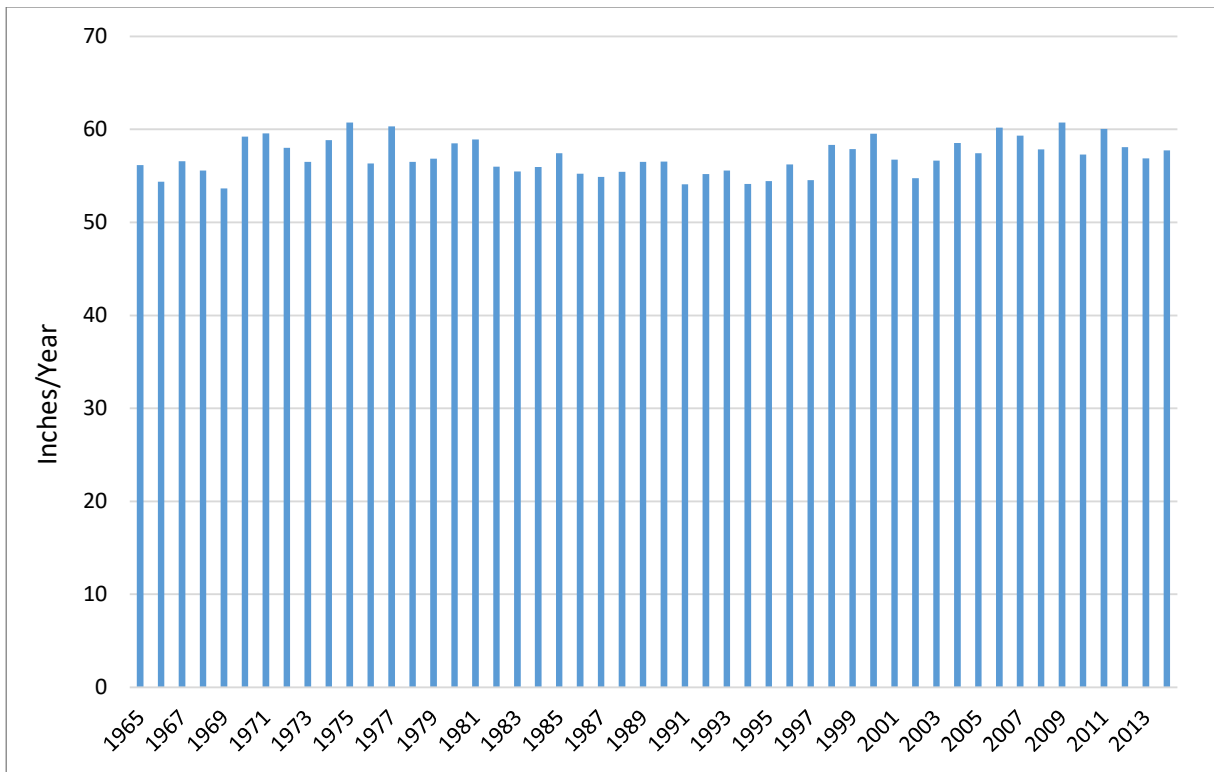


Figure 2-5. Annual average reference evapotranspiration from 1965 to 2013.

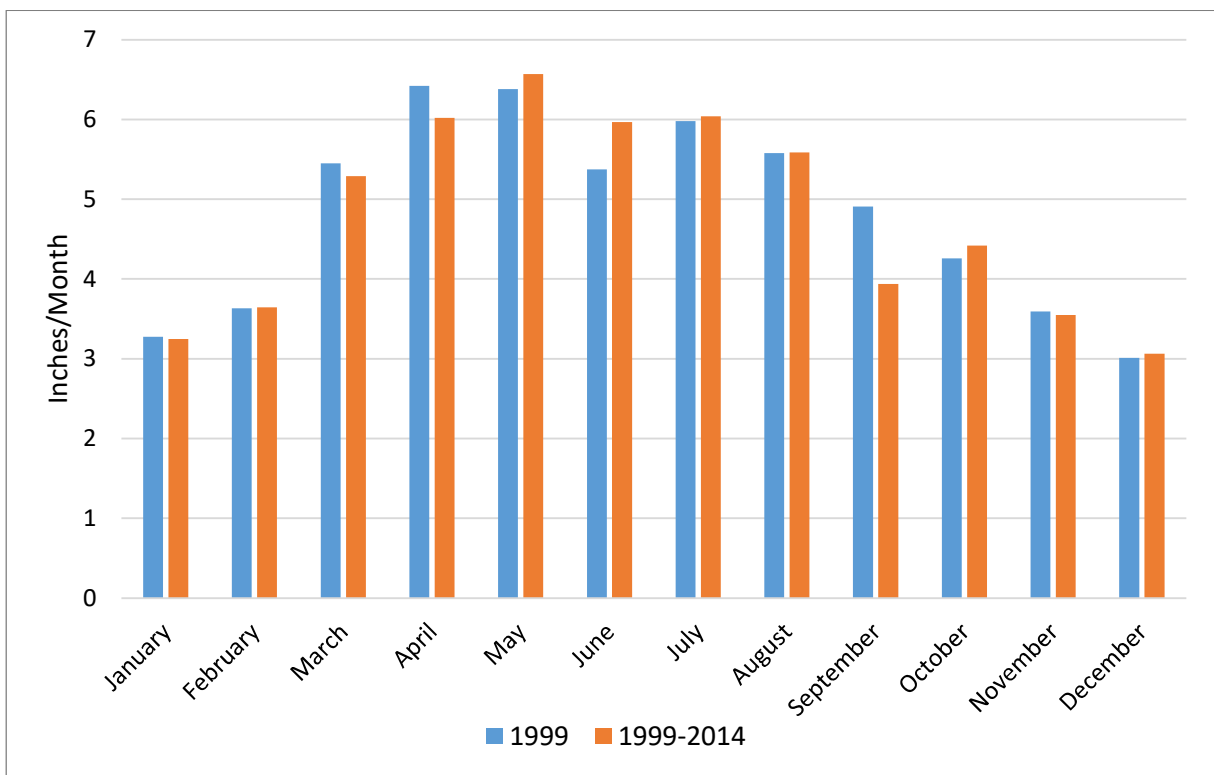


Figure 2-6. Monthly reference evapotranspiration distribution for 1999 and average monthly reference evapotranspiration distribution from 1999 to 2014.

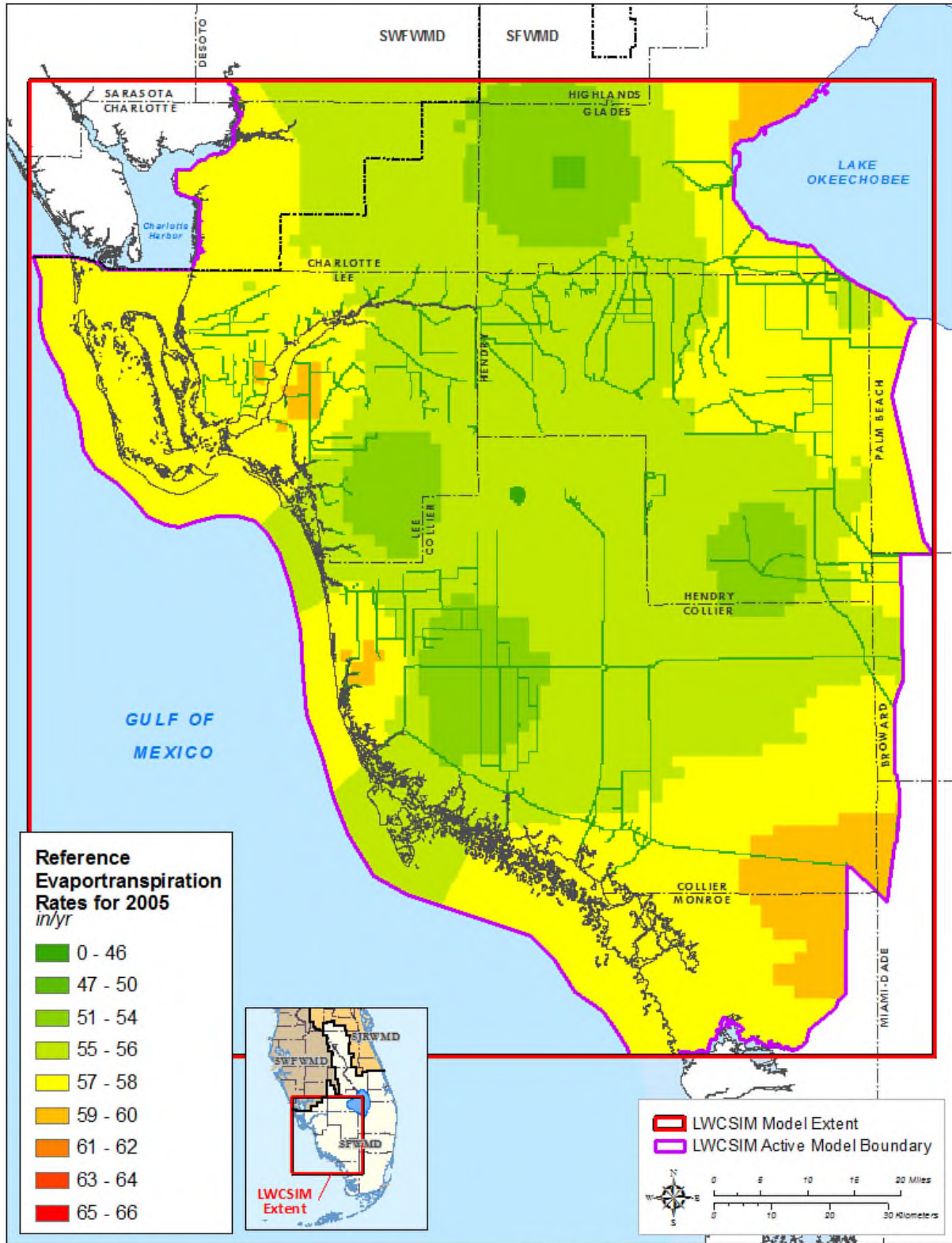


Figure 2-7. Spatial distribution of reference evapotranspiration in 2005 (wet year).

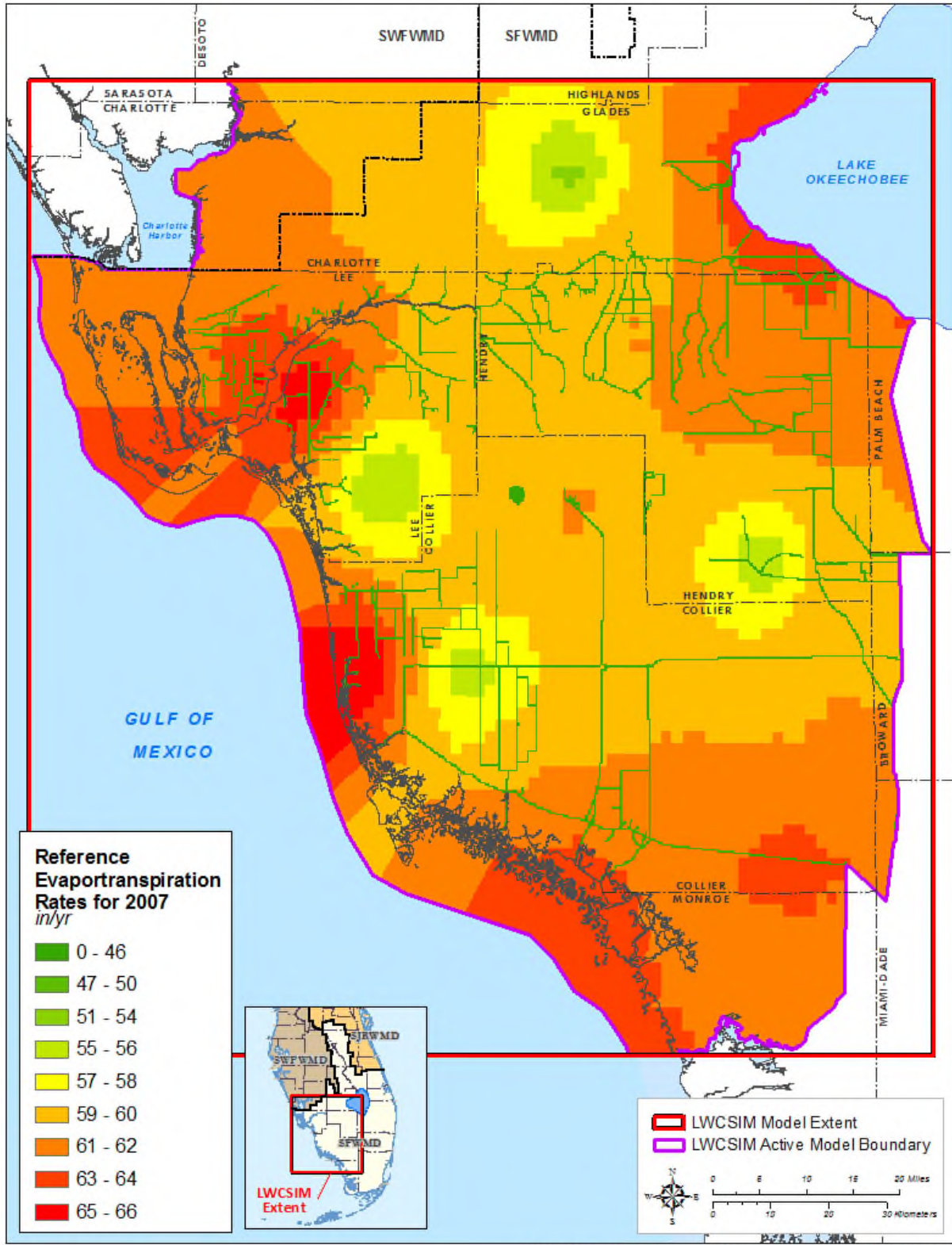


Figure 2-8. Spatial distribution of reference evapotranspiration in 2007 (dry year).

2.3 Recharge

Within the LWC Planning Area, groundwater recharge primarily occurs through rainfall and, to a lesser extent, through irrigation return flows. Groundwater flow occurs from high to low elevation areas, the amounts of which can vary dramatically throughout the year.

Although the average annual rainfall and temperatures are relatively similar across the planning region, large variations in spatial and temporal distributions occur daily. These differences are obtained daily from rain gauges, NEXRAD, and climatic stations. This site-specific information is used when calculating the supplemental irrigation demands using the Agricultural Field-Scale Irrigation Requirement Simulation (AFSIRS) program (Smajstrla 1990) for specific properties.

The amount of rainfall available for recharge to the SAS is reduced by runoff and ET. In this area, ET generally accounts for 60% to 70% of rainfall, and the remaining 30% to 40% runs off the land into drainage networks/streams/rivers or percolates into the ground as recharge.

The amount of water available from the SAS as recharge to the IAS depends on several variables. Areas where the soil is well drained are potentially good areas of moderate to high recharge capacity, while in areas with poorly drained soil, the recharge potential could be near zero because of higher runoff and ET in these areas. A second variable is the thickness and characteristics of the confining units. Areas in which a) the confining units are thin, b) the aquifers have a higher hydraulic conductivity (K), or c) local aquifers make up a dominant percentage of the overall unit thickness are prime areas for recharge because flow through these units is less restrictive. The third primary variable is the downward hydraulic gradient between the SAS and IAS. For recharge to occur, water levels in the SAS need to be higher than water levels in the underlying IAS.

Figures 2-9 and **2-10** show the spatial distribution of annual average gross recharge provided to MODFLOW in 2005 (wet year) and 2007 (dry year), respectively. Gross recharge is defined as follows:

$$\text{Gross Recharge} = \text{Rain} + \text{Irrigation} - \text{Initial Abstraction} - \text{Runoff} - \text{Unsaturated/Vadose Zone ET} \quad (4)$$

Gross recharge was estimated using a pre-processor, which is described in **Section 5.7** and should not be confused with net recharge, which is the combined effect of applied recharge and ET. The ET-Recharge-Runoff pre-processor separates runoff from rainfall using the United States Department of Agriculture (1986) National Resources Conservation Service (NRCS) Curve Number (CN) approach and estimates the vadose/unsaturated zone ET. Gross recharge is provided as input to MODFLOW. Net recharge is defined as follows:

$$\text{Net Recharge} = \text{Gross Recharge} - \text{Saturated Zone/Groundwater ET (from MODFLOW)} \quad (5)$$

Net recharge is the SAS recharge that remains after MODFLOW rejects some of it as groundwater ET using the ET package. Thus, net recharge is calculated after the MODFLOW simulation is complete. The highest gross recharge occurs in the southern portion of the model domain, which is primarily wetland areas such as Everglades National Park and Big Cypress National Preserve (**Figures 2-9** and **2-10**). This is because, in wetland areas, runoff is routed through the Wetlands package and is not included in the gross recharge equation (4). Also, the unsaturated zone is not present in wetland areas during most of the year (shallow water table condition); thus, very small unsaturated zone ET is removed from the system. The lowest gross recharge is applied to the northeastern portion of the model domain (Hendry and Glades counties), where the unsaturated zone is present (deeper water table condition); thus, a significant amount of unsaturated zone ET is removed from the system.

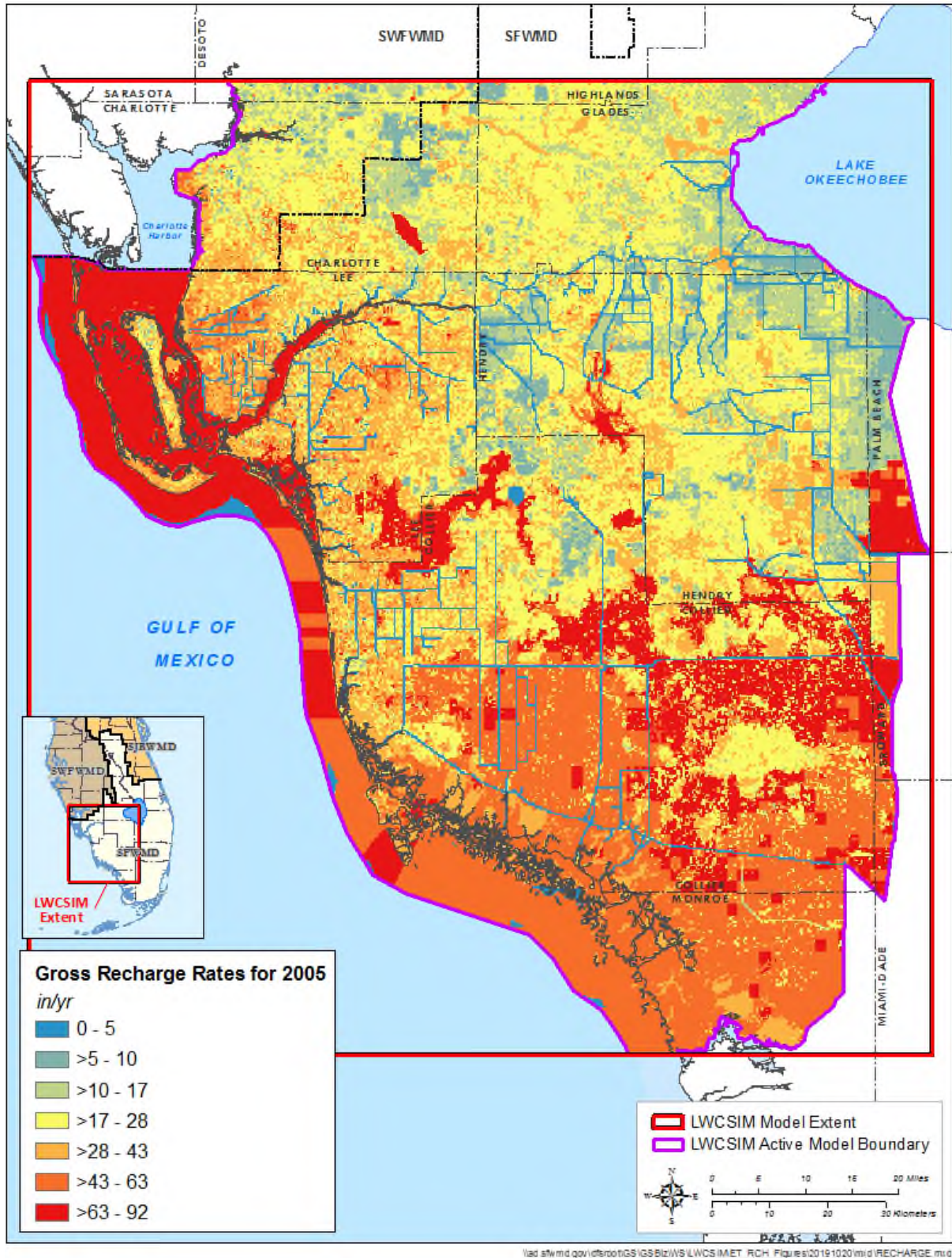


Figure 2-9. Spatial distribution of gross groundwater recharge rates in 2005 (wet year).

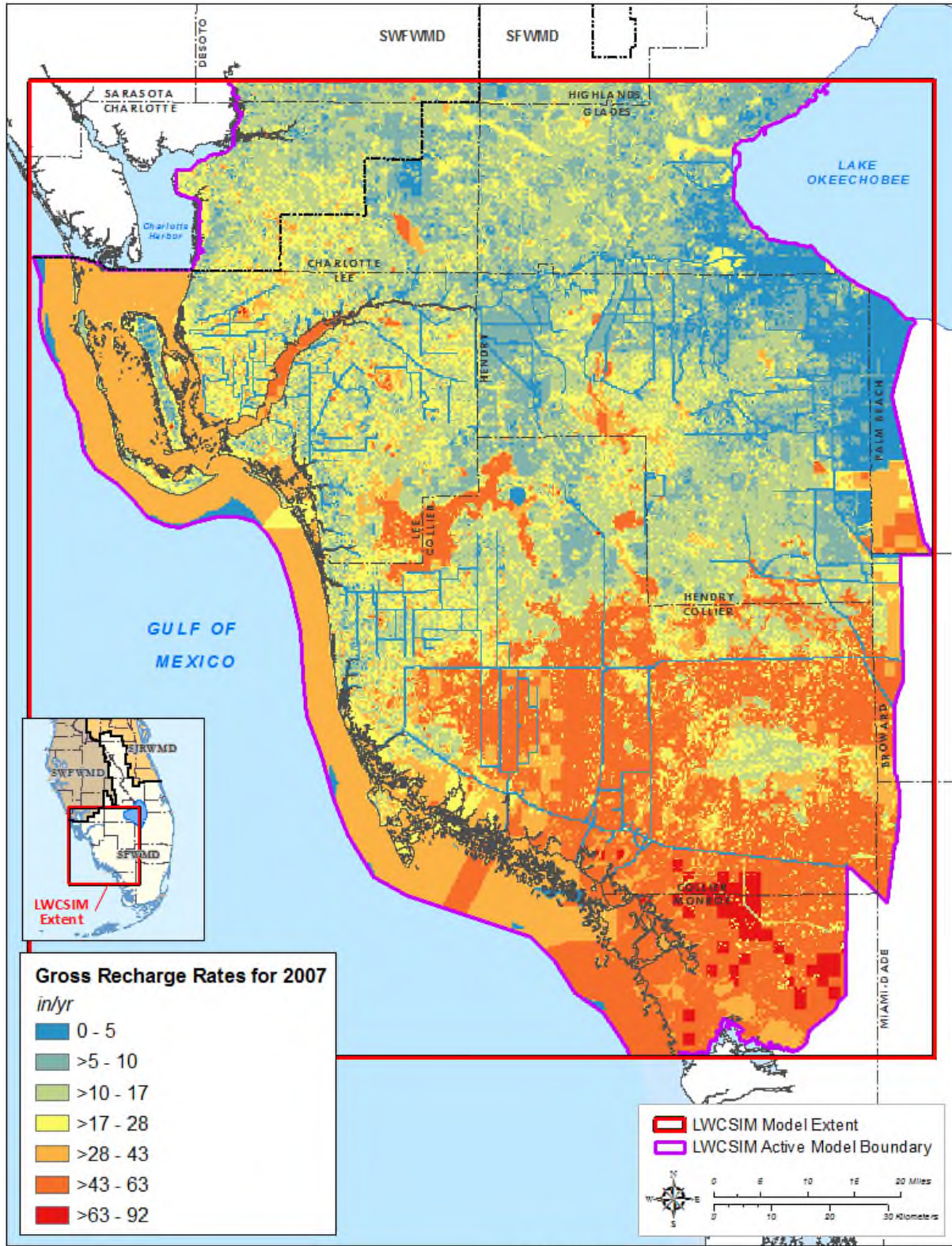


Figure 2-10. Spatial distribution of gross groundwater recharge rates in 2007 (dry year).

2.4 Soil Infiltration Groups

Infiltration rates of soils in the LWCSIM domain vary widely, from high infiltration capacity (low runoff potential) to low infiltration capacity (high runoff potential). The runoff-rainfall potential depends on the hydrologic soil group, as classified by the NRCS. Soils are classified into four hydrologic soil groups with specific letter designations: A, B, C, and D designations indicate high, moderate, low, and poor infiltration capacities, respectively. Dual designations, such as A/D, B/D, or C/D are assigned where a high water table may limit infiltration. In these cases, the first letter applies to the drained condition, while the second applies to the undrained condition. The ET-Recharge-Runoff pre-processor that generates recharge to the LWCSIM uses the hydrologic soil group information during the rainfall-runoff separation process of the NRCS CN approach.

With 59% of areas classified as A/D, soils in the LWCSIM domain predominantly have high infiltration rates that may be limited by a shallow water table condition (**Figure 2-11**). Most A/D soils in southern Collier County behave as D soils due to the undrained condition (shallow water table). The next most prevalent soil group is C/D (16%); these are poorly drained, low-infiltration soils commonly observed in the central and northwestern areas of the LWCSIM domain. The third most common soil group is B/D (11%), which consists of moderately drained, somewhat low-infiltration capacity soils found throughout the model domain.

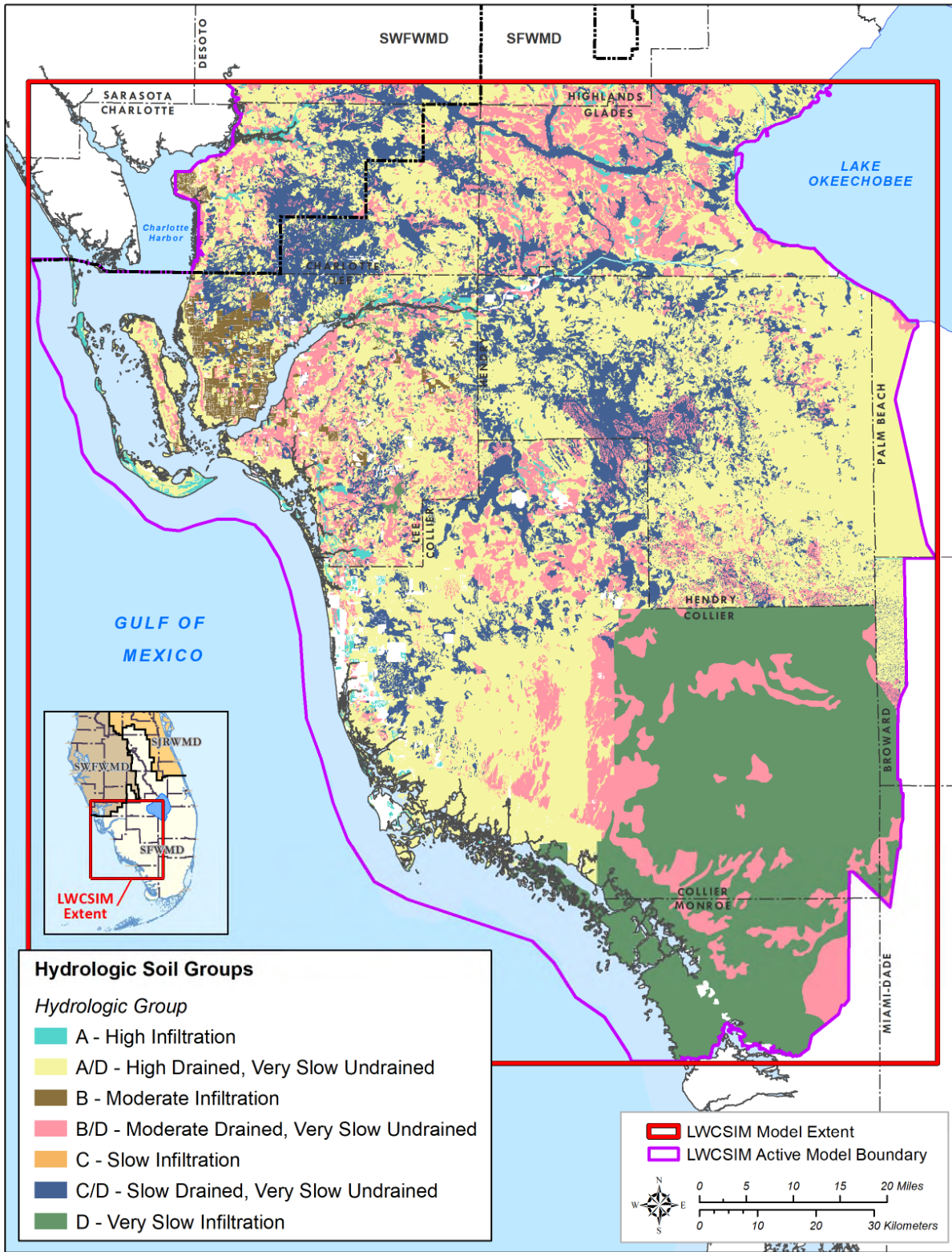


Figure 2-11. Spatial distribution of hydrologic soil groups across the model domain, as classified by the Natural Resource Conservation Service.

2.5 Land Use

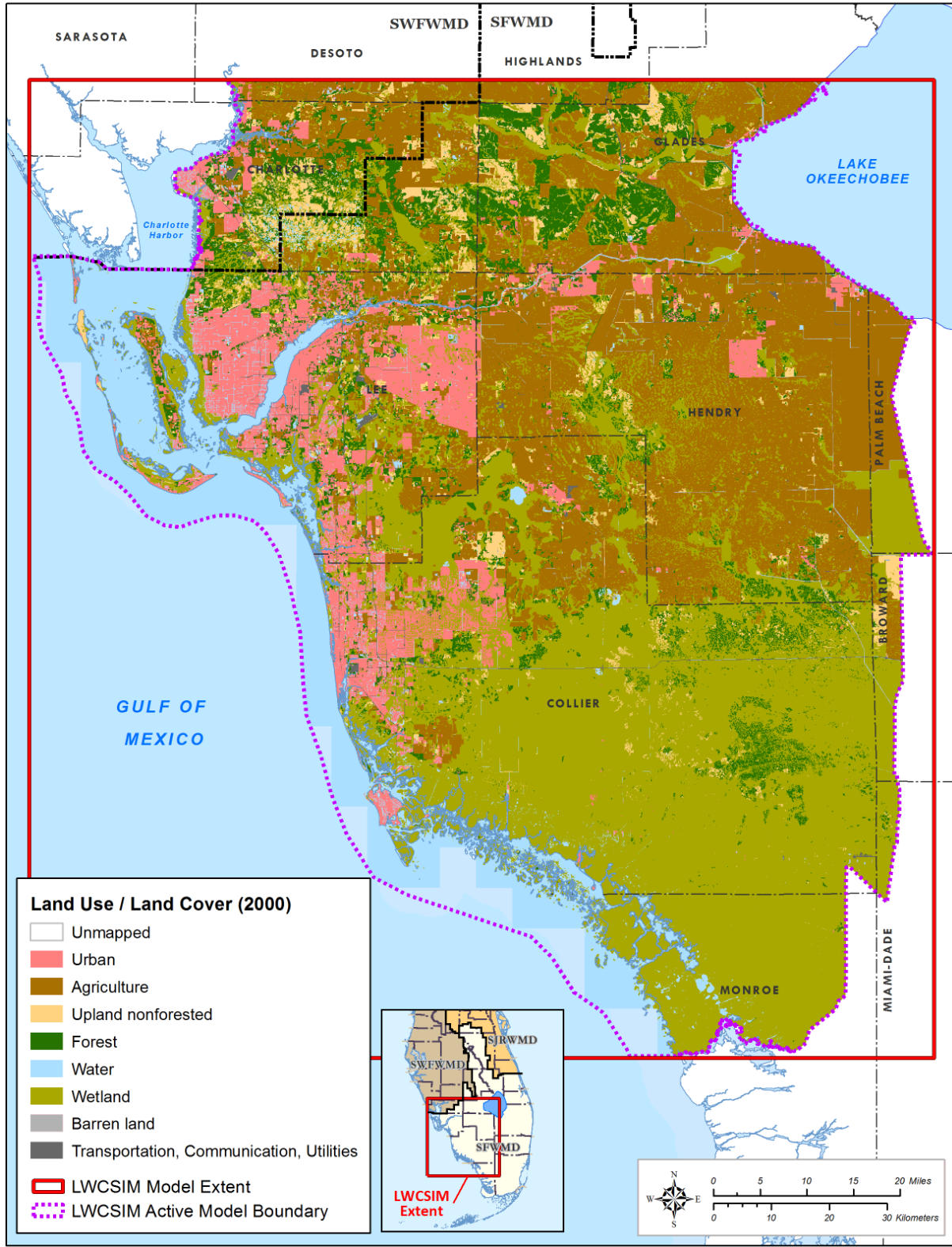
Land use represents a spatial distribution of pervious and impervious surfaces used to separate runoff and infiltration from total rainfall and irrigation. The steady-state model used the SFWMD's 2000 land use map, which was produced using data obtained between 1998 and 2000. The transient version of the model used four land use maps: 1) 2000, representing 1999 to 2001; 2) 2004, representing 2002 to 2006; 3) 2010, representing 2007 to 2011; and 4) 2014, representing 2012 to 2014. These maps used the Florida Land Use and Cover Classification System (FLUCCS) (SFWMD 2009), which updates land use every 5 years based on the SFWMD's enterprise data collection.

Land cover and land use areas primarily were used in the model to estimate maximum ET and recharge rates, AG and L/R irrigation water demands, and irrigation return flow rates. The NRCS CN method (United States Department of Agriculture 1986) was used in an external pre-processing routine to separate runoff from the combination of rainfall and irrigation as a function of land cover and properties of the surface soil. Land use-based crop type and permeability were developed for the FLUCCS codes.

Table 2-1 provides the various land use classifications and acres within the LWCSIM domain. **Figures 2-12** through **2-15** depict the land use/land cover maps for 2000, 2004, 2010, and 2014, respectively.

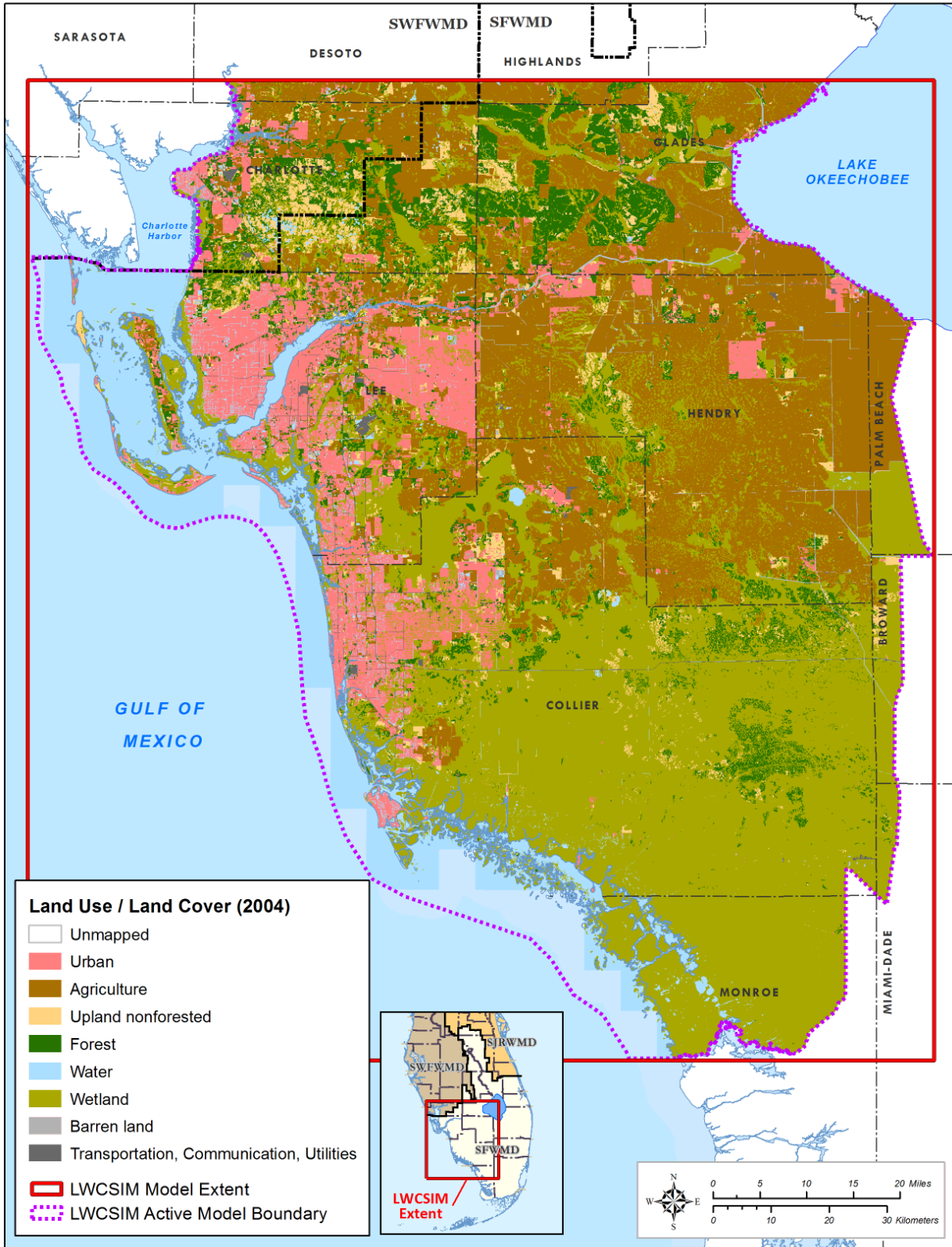
Table 2-1. Land use summary for 2000, 2004, 2010, and 2014 in the Lower West Coast Planning Area.

| Land Use | 2000 (acres) | 2004 (acres) | 2010 (acres) | 2014 (acres) |
|------------------------|--------------|--------------|--------------|--------------|
| Barren Land | 24,919 | 26,676 | 29,336 | 42,327 |
| Citrus | 230,519 | 223,901 | 197,053 | 173,996 |
| Forest | 298,340 | 284,009 | 309,884 | 297,247 |
| Golf | 17,511 | 23,097 | 24,533 | 25,347 |
| Improved Pasture | 391,506 | 370,311 | 397,770 | 389,238 |
| Non-Urban Natural Land | 311,619 | 266,190 | 227,613 | 261,059 |
| Nursery | 4,010 | 4,312 | 8,787 | 8,395 |
| Pasture | 123,174 | 109,669 | 94,552 | 101,046 |
| Row Crops | 102,465 | 103,384 | 107,549 | 79,508 |
| Sod | 1,262 | 684 | 1,179 | 2,326 |
| Sugar | 183,730 | 190,867 | 187,823 | 203,918 |
| Urban | 232,584 | 308,853 | 374,024 | 372,426 |
| Water | 501,508 | 458,332 | 485,624 | 447,284 |
| Wetlands | 1,721,845 | 1,724,757 | 1,694,417 | 1,697,201 |



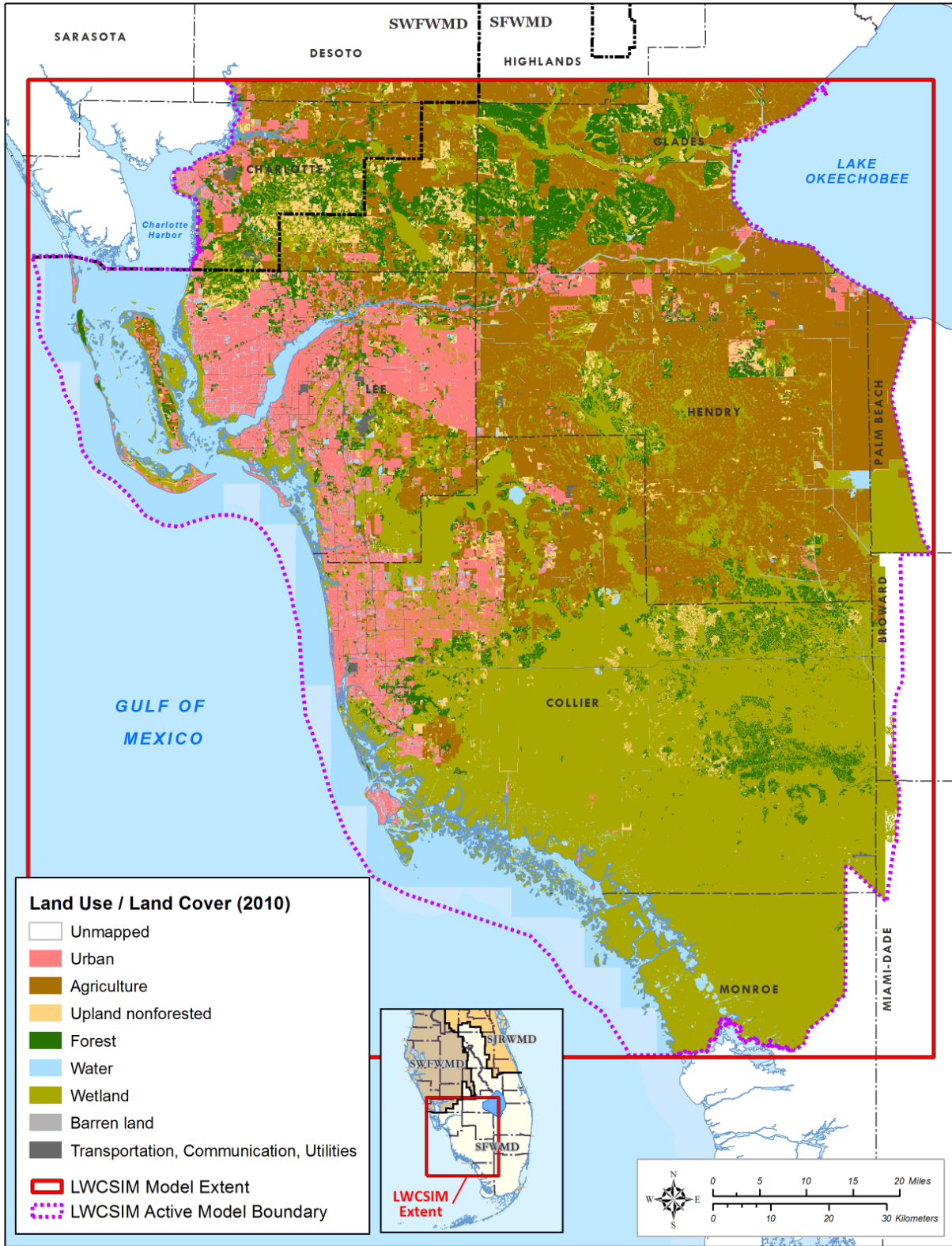
\\ad.sfwmd.gov\dfsroot\GIS\GSBiz\WS\LWCSIM\Report_Figures\mxd\LCLU_2000.mxd

Figure 2-12. 2000 land use/land cover map.



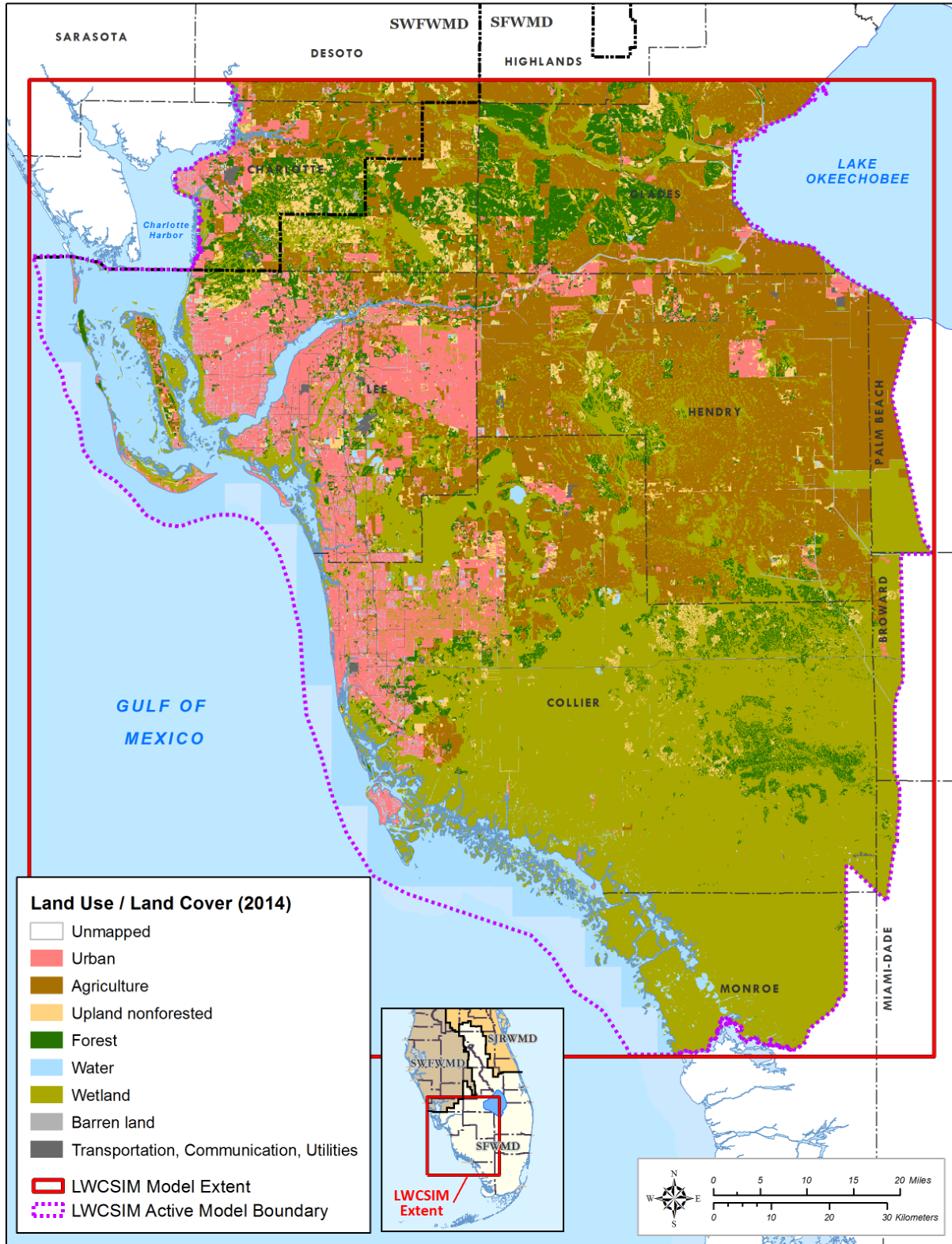
\\ad.sfwmd.gov\dfsroot\GIS\GSBiz\WS\LWCSIM\Report_Figures\mxd\LCLU_2004.mxd

Figure 2-13. 2004 land use/land cover map.



\\ad.sfwmd.gov\dfsroot\GIS\GSBiz\WS\LWCSIM\Report_Figures\mxd\LCLU_2010.mxd

Figure 2-14. 2010 land use/land cover map.



\\ad.sfwmd.gov\dfsroot\GIS\GSBiz\WS\LWCSIM\Report_Figures\mxd\LCLU_2014.mxd

Figure 2-15. 2014 land use/land cover map.

3 PHYSICAL SETTING

3.1 Surface Water Flow System

Primary surface water sources in the LWCSIM domain include the Caloosahatchee River (C-43 Canal) and connected water bodies, such as the Townsend Canal, Roberts Canal, and City Ditch. Cape Coral and Big Cypress Basin (BCB) canal systems also provide surface water supply, and to a lesser extent, local storm water ponds provide water for landscape irrigation. AG is the primary consumer of surface water in the LWC Planning Area.

The BCB canal system in Collier County was constructed as a surface water drainage system. Since 2000, improvements to structures, operations, management, and monitoring have resulted in an estimated 850 acre-feet of additional surface water storage in BCB canals (SFWMD 2012). The BCB capital improvement program includes projects for the Golden Gate canal system, Henderson Creek, FAKA Union, and Barron River. These projects and others provide water resource benefits through reduction of over-drainage and restoration of groundwater and surface water levels to more natural conditions. In addition to providing environmental benefits, these improvements enhance water supply opportunities by increasing groundwater storage and improving the timing and duration of surface water discharges. As a result, the canal system holds more water for longer periods of time than previously capable, capturing water that used to be lost to tide.

The City of Naples Utility Department is developing surface water sources from the BCB canal system to supplement its reclaimed water supply. Cape Coral Utilities also uses a freshwater canal system to augment the City of Cape Coral's reclaimed water supply for residential and commercial landscape irrigation. The City of Marco Island (Marco Island Utilities) uses surface water from Henderson Creek/Marco Lakes, and Lee County Utilities uses some surface water from the Caloosahatchee River.

3.2 Hydrostratigraphy

3.2.1 Geological Framework

South Florida, including the LWC Planning Area, is underlain by a thick sequence of carbonate and clastic sedimentary rocks ranging in age from Paleocene to Recent. Because this study is limited to the SAS and IAS, only the deposits ranging in age from late Oligocene through the Holocene are discussed. The stratigraphic units of interest to this study include the Peace River and Arcadia Formations of the Hawthorn Group, the Tamiami Formation, and the undifferentiated sediments of Holocene/Pleistocene age. **Figure 3-1** shows the general geology and hydrostratigraphy within the LWCSIM domain.

| System | Hydrogeologic Unit | | Lithostratigraphic Unit | | Subject of this Study |
|-------------------------------|-------------------------------|--------------------------|-------------------------|---|-----------------------|
| Surficial Aquifer System | WATER TABLE AQUIFER | | Tamiami Formation | Undifferentiated Holocene/Pleistocene | |
| | TAMIAMI CONFINING UNIT | | | Pinecrest Sand Member | |
| | LOWER TAMIAMI AQUIFER | | | Bonita Springs Marl Member / Caloosahatchee Clay Member | |
| | | Ochopee Limestone Member | | | |
| Intermediate Aquifer System | UPPER HAWTHORN CONFINING UNIT | | Hawthorn Group | Peace River Formation | |
| | SANDSTONE AQUIFER (SA) | CLASTIC ZONE | | | |
| | | CARBONATE ZONE | | | |
| | MID-HAWTHORN CONFINING UNIT | | | | |
| | MID-HAWTHORN AQUIFER | | | | |
| LOWER HAWTHORN CONFINING UNIT | | Arcadia Formation | | | |
| Floridan Aquifer System | UPPER FLORIDAN AQUIFER | | Suwannee Limestone | Avon Park Formation | |
| | | | | | Ocala Limestone |
| | MIDDLE CONFINING UNIT | | | | |
| | LOWER FLORIDAN AQUIFER | | | | |
| | SUB-FLORIDAN CONFINING UNIT | | | | |
| | LOWER HAWTHORN PRODUCING ZONE | | | | |
| | AVON PARK PERMEABLE ZONE | | | | |

Figure 3-1. Generalized geologic and hydrogeologic units of the Lower West Coast Planning Area (From: Geddes et al. 2015).

The lithology of the undifferentiated surficial Holocene/Pleistocene sediments is highly variable. Medium- to fine-grained quartz sand, fossils, clays, and some freshwater limestone and marl are present within this unit. These extend to the top of the Tamiami Formation.

In a few areas, the Tamiami Formation is entirely absent, and the surficial sediments rest directly on top of the Peace River Formation. The undifferentiated surficial sediments grade into the Anastasia Formation to the east and into the Miami Limestone to the south (Bryan et al. 2013). The Tamiami Formation is composed of two units and nine members, none of which are present throughout the entire project area. The upper portion of the Tamiami Formation is predominantly marl, and the lower portion is the Ochopee Limestone. Lithology of this unit varies from fine- to coarse-grained sand and fossiliferous limestone (Scott 2001). The presence of these two units varies spatially, and the Ochopee Limestone is absent in much of southwestern Hendry and northeastern Monroe counties.

The Peace River Formation of the Hawthorn Group is Miocene in age and consists of clays and carbonates interbedded with quartz sands. Phosphate may be gravel to sand sized. Approximately two-thirds of the formation is siliciclastic, and one-third (typically the lower portion) is carbonate. The Peace River Formation underlies the entire project area.

The underlying Arcadia Formation of the Hawthorn Group is predominantly carbonate and spans the entire project area. The contact between the two formations may be distinct or gradational. The Arcadia Formation is primarily dolostone and limestone with beds of clay, quartz sand, and phosphate grains (Scott 1988). The base of the Arcadia Formation is confining in nature and primarily clay and mud.

3.2.2 Hydrostratigraphic Framework

Due to the presence of a thick clay layer underneath the SAS/IAS systems in the LWC Planning Area, the Floridan aquifer system typically is hydraulically disconnected from the overlying SAS/IAS system; therefore, the Floridan aquifer system is not included in the LWCSIM and will not be discussed further.

The hydrogeology of southwestern Florida is complex. Lateral facies changes and variable thicknesses lead to large local variations in hydrogeologic units. The heterogeneous nature of the units and the sparse availability of data in some places pose difficulties for regional mapping. The hydrogeologic units of interest for the LWCSIM effort include the WTA, Tamiami confining unit (TCU), LTA, SSA (clastic and carbonate zones), Mid-Hawthorn confining zone, and the MHA. Geddes et al. (2015) provides further details on these hydrogeologic units.

The WTA is composed primarily of quartz sand and shell, with minor amounts of organic material. A dense limestone cap rock is present in some areas. The WTA is absent or insignificant in places within the LWCSIM domain (e.g., south-central Collier County), and the basal confinement is geographically variable. Where present, the Bonita Springs Marl and low-permeability portions of the Pinecrest Sand facilitate confinement at the base of the WTA. Confinement between the WTA and the underlying LTA, however, is not consistent. Where the TCU is absent or insignificant, the LTA, by definition, could be considered part of the WTA.

The LTA is predominantly a sandy, biogenic limestone and calcareous sandstone. It encompasses all the water-producing limestone and, in some areas, portions of the underlying permeable sand. The upper confinement (TCU) is absent or insignificant in several areas throughout the LWCSIM domain. In northern portions of the modeled area (i.e., Charlotte County into the Southwest Florida Water Management District), well reports typically do not distinguish sub-units of the SAS. Throughout most of the LWCSIM domain, the less permeable clay and fine-grained sands of the Peace River Formation provide basal confinement (Upper Hawthorn confining unit) to the LTA. However, in some areas, this confinement is absent or insignificant. In some locations, the LTA or undifferentiated SAS lay directly on top of the SSA.

The SSA, except where absent or insignificant, is contained entirely within the Peace River Formation of the Hawthorn Group and is part of the IAS. It typically occurs as two distinct permeable units: an upper clastic zone and a lower carbonate zone. The SSA is composed of sandstones, sandy limestones, dolostones, and calcareous sands. These may be contiguous or separated by varying amounts of low-permeability silt and clay. Where a confining unit is present, the SSA is separated from the LTA by lower-permeability clays and dolosilts of the Peace River Formation (Upper Hawthorn confining unit). The SSA is separated from the underlying MHA by low-permeability clays and marls of the basal Peace River Formation (Mid-Hawthorn confining unit), which are present throughout the LWCSIM domain. The SSA is absent or insignificant throughout the eastern portions of the model domain and some smaller areas along the Gulf coast.

The MHA, except where absent or insignificant, is composed of biomicritic limestone, phosphate, shell, and lime mud. It lies entirely within the Arcadia Formation of the Hawthorn Group. The MHA is separated from the overlying SSA by the low-permeability clays and marls of the basal Peace River Formation (Mid-Hawthorn confining unit). Where the SSA is absent or insignificant, the entire thickness of the Peace River Formation isolates the MHA from the overlying SAS. The confinement from the underlying Lower Hawthorn producing zone (not simulated in this model) consists of carbonate muds and terrigenous clays of the Upper Arcadia Formation (Lower Hawthorn confining unit) and is present throughout the study area. For the most part, use of the MHA for water supply purposes occurs in the western part of the LWCSIM domain. Some investigators have defined the MHA as two distinct zones: a shallow zone occurring primarily in the Fort Myers-Cape Coral area, and a deeper zone occurring primarily in the Estero-Bonita

Springs-Fort Myers Beach region. Lacking the data to support a more detailed breakdown of the aquifer throughout the LWCSIM domain, the MHA is considered a single unit for this modeling effort.

3.2.3 Conceptualized Groundwater Flow

Regional groundwater flow is consistent across the WTA, LTA, and SSA. Loosely following land surface elevations, regional flow patterns in the LWCSIM domain can be subdivided into two components. In the northern portion of the modeled area, flow is in a general northeast-to-southwest direction from a regional high along the southern portions of the Highlands Ridge in Polk and Highlands counties towards the Gulf coast and the Caloosahatchee River. In the central portion of the modeled area, flow in all three aquifers generally radiates out in all directions from a regional high located close to the Hendry-Collier county border north of the Town of Immokalee.

Regional flow patterns in the MHA show a general northeast-to-southwest flow pattern throughout the LWCSIM domain. Due to its greater degree of confinement and lower levels of productivity, the MHA is more likely to show impacts from well pumping than the shallower, more productive aquifers. An area of regional decline in the potentiometric surface of the MHA is centered around Cape Coral, which corresponds to an area of historically high pumpage from PS wells and small domestic and irrigation wells.

3.2.4 Data Collection and Analysis

Data collection and assembly of the corresponding computer-model input data sets are among the most time-consuming elements of model development, particularly for a model with as large a geographic extent and complex hydrostratigraphy as the LWCSIM. The following sections describe the data used to construct the steady-state model and how the data were obtained.

3.2.5 Hydrostratigraphic Data

The conceptual groundwater model was divided into hydrostratigraphic units following the primary water-producing units and confining units identified by Geddes et al. (2015). Data from their work and the District's DBHYDRO database provided most of the information used to construct the conceptual model. The groundwater flow model was constructed based on hydrostratigraphic units and may not necessarily follow geological formation contacts.

Once all data were assimilated and checked for quality assurances, they were combined into a single data set to develop the model layers. To solve the flow equations in MODFLOW 2005, the continuous presence of aquifers is required. In other words, aquifer or layer thickness must be greater than zero everywhere in the model domain regardless of whether or not the aquifer is present. To satisfy this condition and to ensure numerical stability during model execution, a minimum thickness of 30 ft was assigned to all layers. Where aquifers are absent, the hydraulic properties of the aquifer(s) below were used. The hydrostratigraphic layers were created by kriging the surfaces of each major hydrostratigraphic unit. **Appendix B**, Figures B-1 to B-10 depict the surface elevations for each of the nine model layers, beginning with the top of layer 1 (the topographic surface), then progressing downward through each layer's bottom surface. The bottom of a layer represents the top of the subjacent layer.

Some of the hydrostratigraphic control points indicate a unit may be extremely thin or absent (defined as 5 ft or less). **Appendix B**, Figures B-11 to B-19 are isopach maps of the aquifers and confining zones. Simulated layer top elevations are show in **Appendix B**, Figures B-20 to B-28. **Appendix B**, Figures B-29 to B-37 provide the simulated layer thicknesses.

3.2.6 Hydraulic Data

Multiple types of hydraulic data are required to develop a multi-layered groundwater flow model. For this section of the model development discussion, the data are divided into the following four categories:

- Hydraulic conductivities and storage coefficients
- Pumpage rates
- Boundary conditions
- Initial conditions

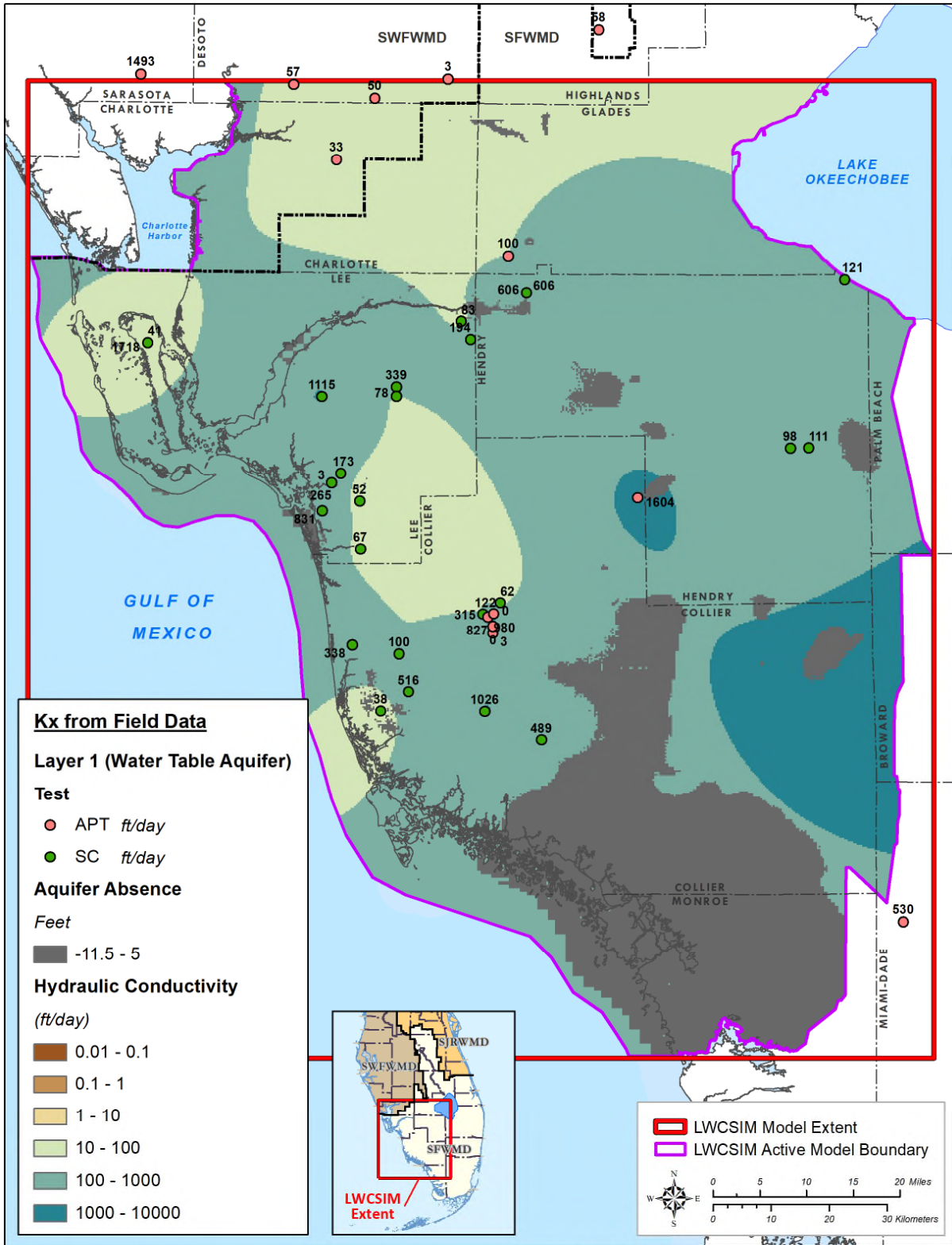
The first two categories are directly related to aquifer properties and hydraulic data, while the remaining two represent aquifer stresses and observed conditions.

Data collection procedures generally require that data be collected both from within and outside the model domain to define conditions along the model boundaries as accurately as possible. The discussion that follows focuses on the data collected within the model boundaries unless specifically stated otherwise.

3.2.7 Hydraulic Conductivities/Storage Coefficients

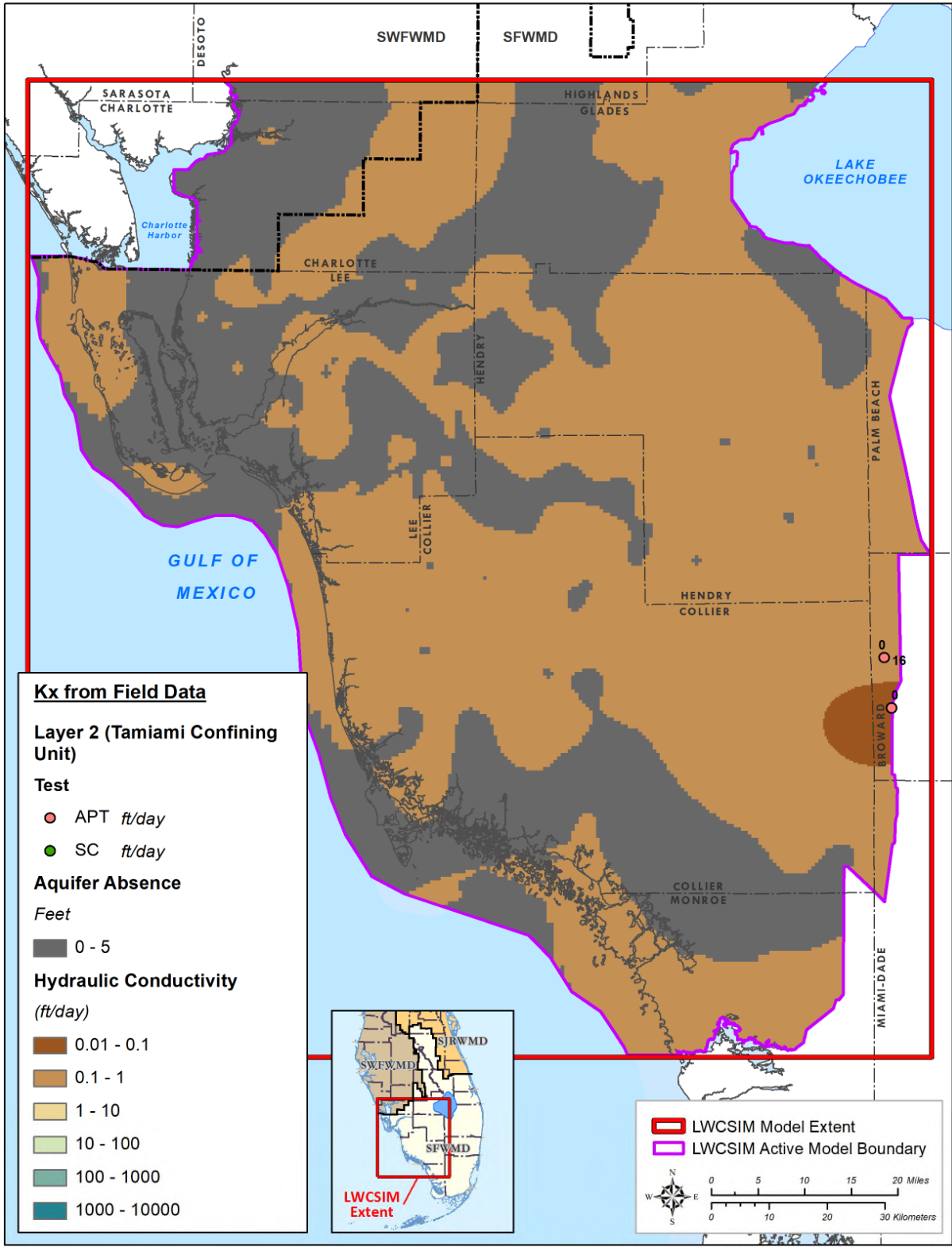
Hydraulic conductivity (K) is an important parameter in development of a groundwater flow model. It represents the aquifer's ability to transmit water under hydraulic gradients and hydraulic stresses such as pumping wells. When multiplied by the aquifer thickness, the resulting term is called transmissivity, which can be readily obtained from aquifer performance tests (APTs). For the LWCSIM, aquifer and confining unit top and bottom elevations are considered static input parameters. The thickness of the aquifer, and consequently the transmissivity of the aquifer, was calculated internally by the model code. Therefore, vertical and horizontal hydraulic conductivities were used in place of transmissivity values. **Figures 3-2 to 3-10** present the interpolated horizontal hydraulic conductivity (Kh) surfaces for each model layer used to define this value in each model cell. The figures were created by interpolating the actual field data values collected from APTs, specific capacity, and slug tests and then using kriging and spline with barriers. When multiple test data points were available in close proximity, priority was given to APT values due to their inherent higher quality. The surfaces were used as the starting point for the steady-state model calibration. The K distribution in all nine layers was adjusted as a result of steady-state and transient calibration. The adjusted K distributions are presented and discussed in the *Calibration* section. A discussion of how layer pinch-outs (absences) were represented within the K distribution of each layer also is presented in **Section 6**.

Another important parameter needed for the transient simulations is the storage coefficient of the aquifers. Storage coefficients can be readily obtained from APTs. Like the relationship between K and transmissivity, the model code requires a specific storage value, which is the quotient of the aquifer storativity divided by aquifer thickness. Storage coefficient (storativity) values were entered directly into each model layer as a property based on APT data.



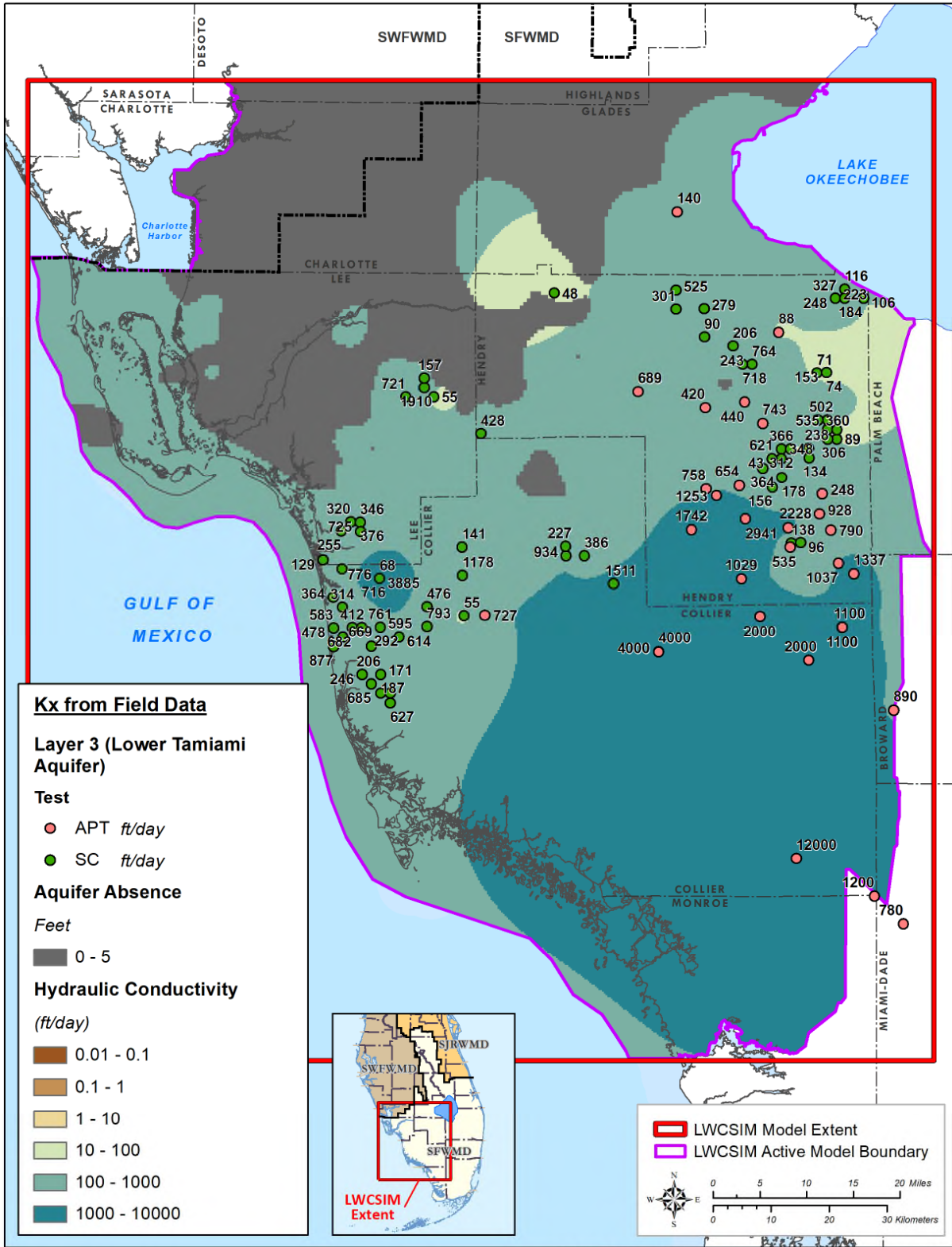
\\ad.sfwmd.gov\dfsroot\GIS\GSBiz\WS\LWCSIM\Report_Figures\mxd\KxfromFieldData.mxd

Figure 3-2. Horizontal hydraulic conductivity of the Water Table aquifer.



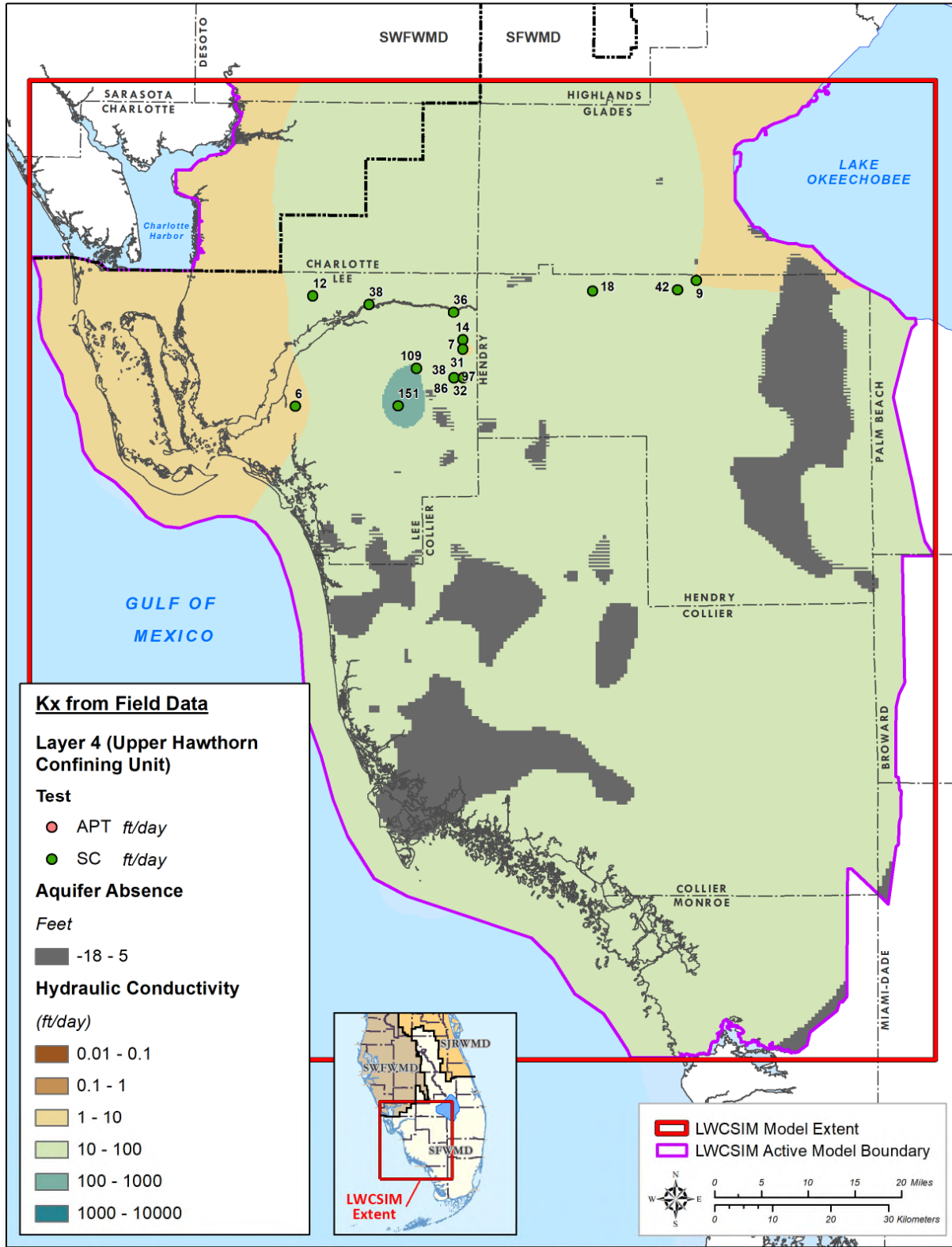
\\ad.sfwmd.gov\dfsroot\GIS\GSBiz\WS\LWCSIM\Report_Figures\mxd\KxfromFieldData_1.mxd

Figure 3-3. Horizontal hydraulic conductivity of the Tamiami confining unit.



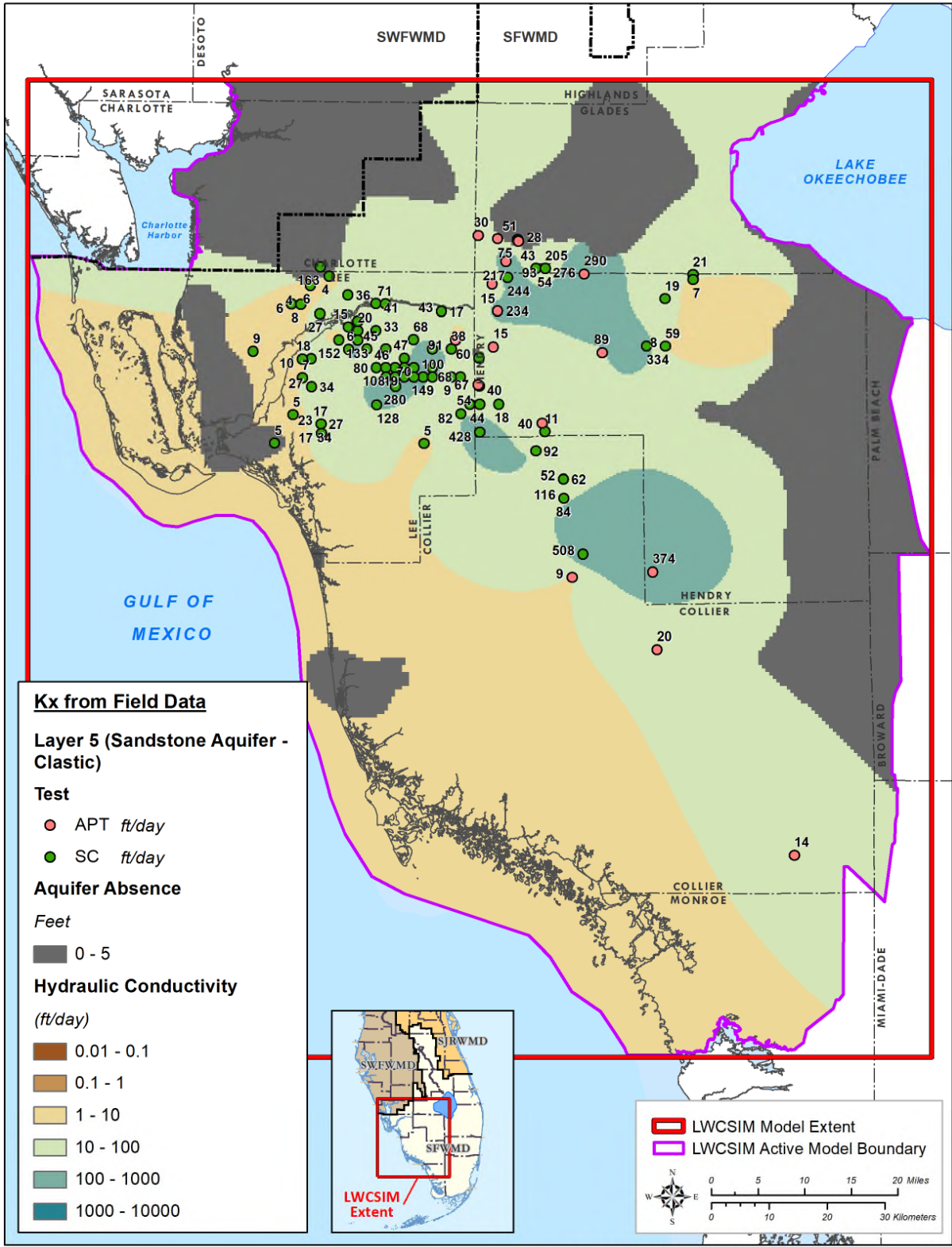
\\ad.sfwmd.gov\dfsroot\GIS\GSB\z\WS\LWCSIM\Report_Figures\mxd\KxfromFieldData.mxd

Figure 3-4. Horizontal hydraulic conductivity of the Lower Tamiami aquifer.



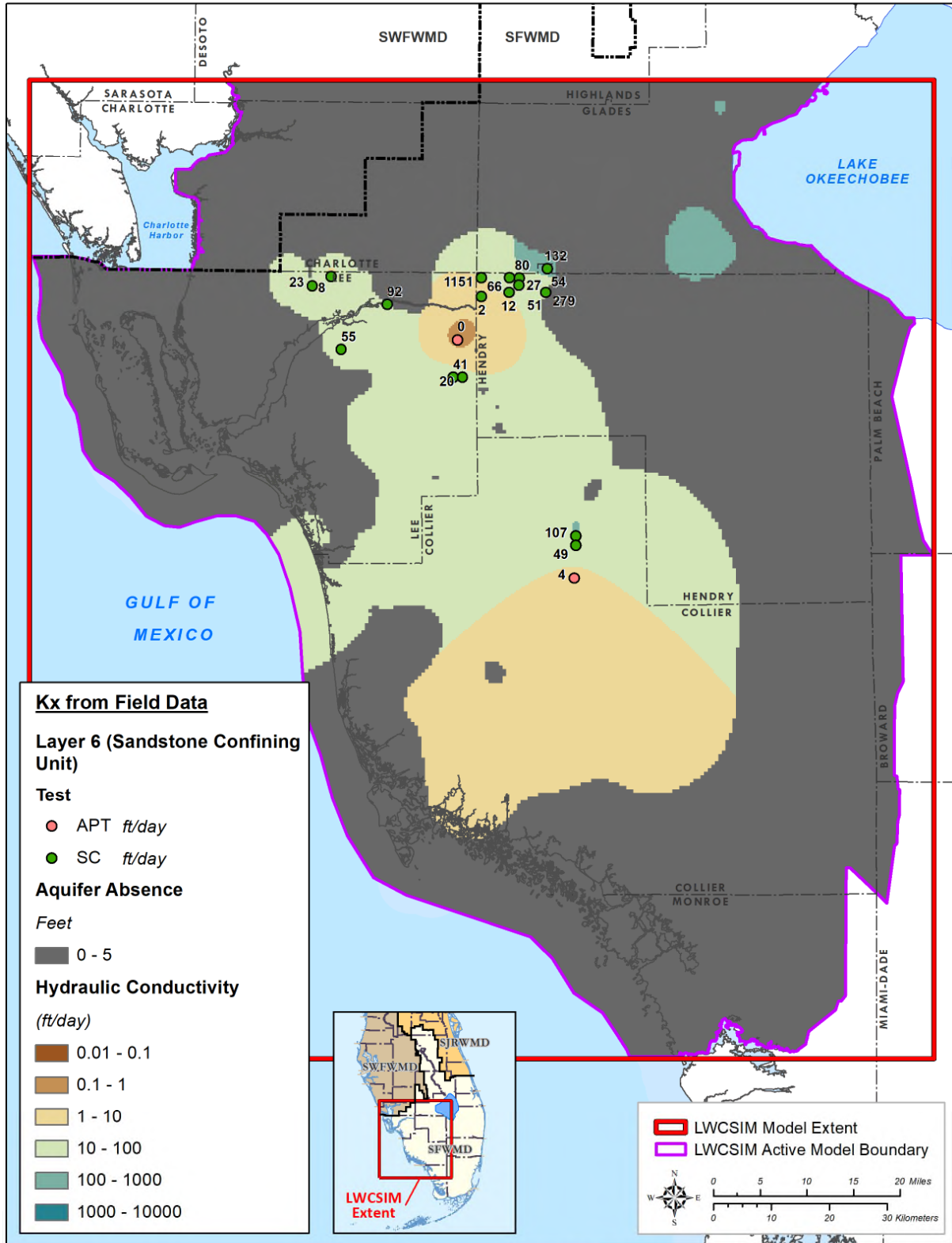
\\ad.sfwmd.gov\dfsroot\GIS\GSBiz\WS\LWCSIM\Report_Figures\mxd\KxfromFieldData.mxd

Figure 3-5. Horizontal hydraulic conductivity of the Upper Hawthorn confining unit.



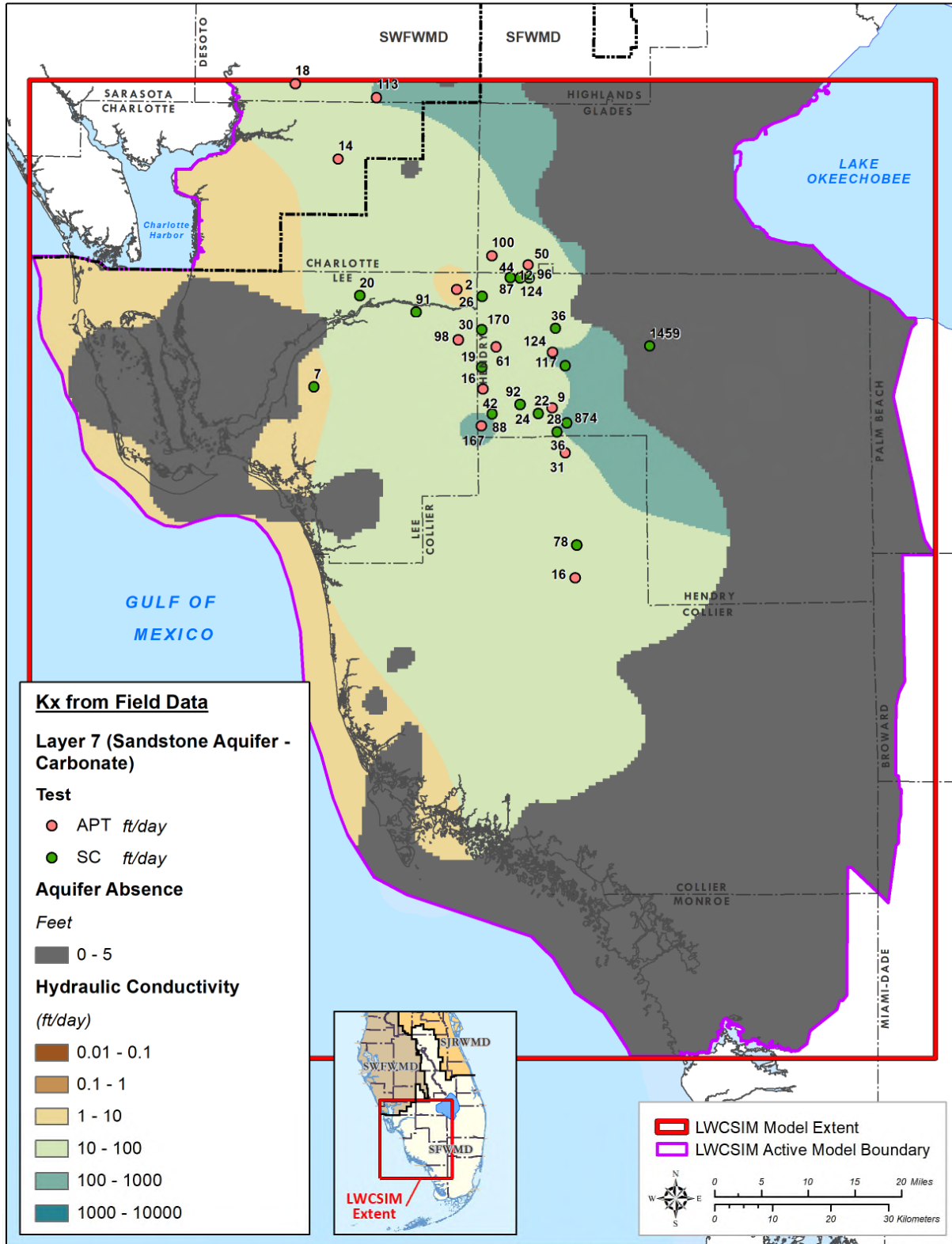
\\ad.sfwmd.gov\dfsroot\GIS\GSBiz\WS\LWCSIM\Report_Figures\mxd\KxfromFieldData.mxd

Figure 3-6. Horizontal hydraulic conductivity of the Sandstone aquifer – clastic zone.



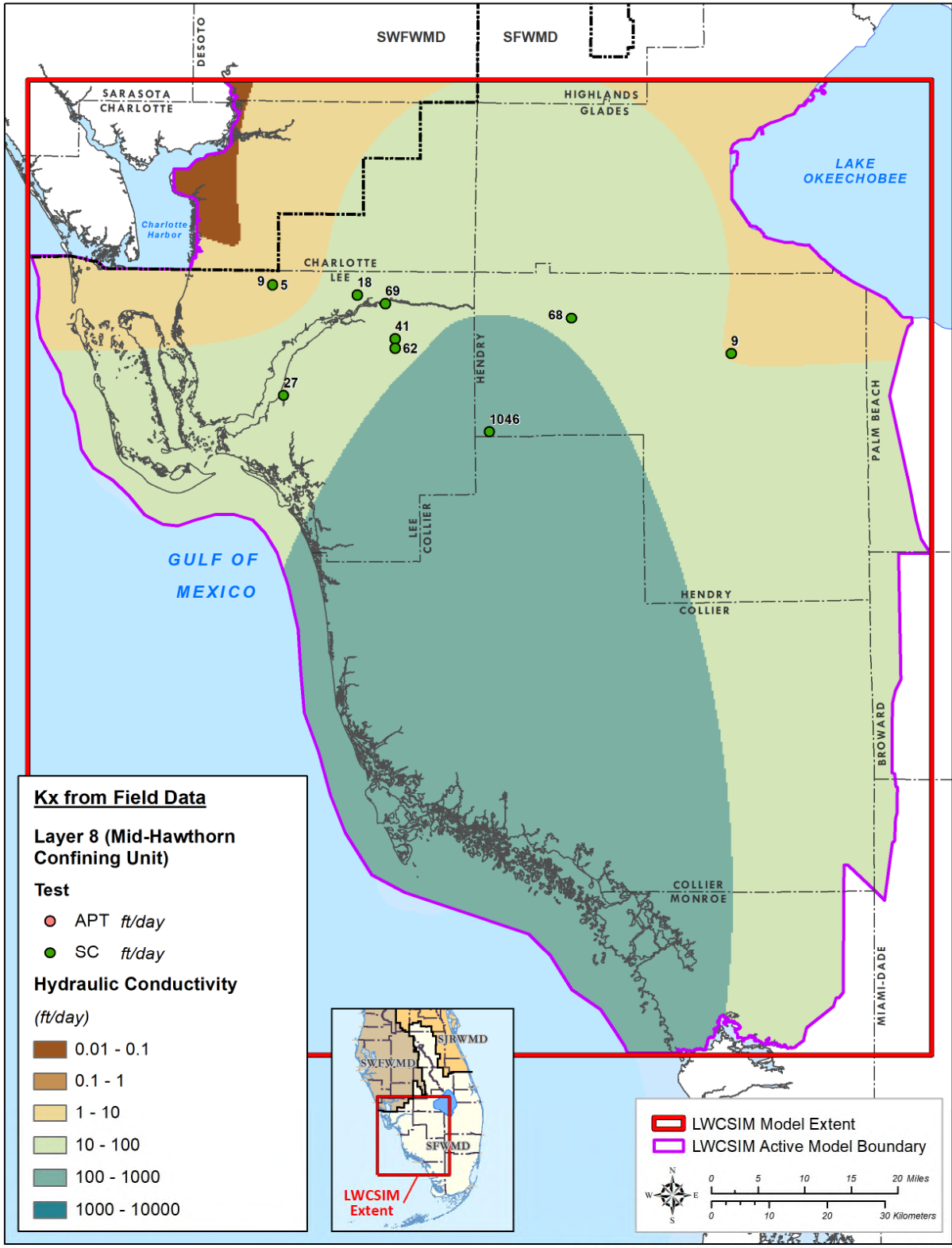
\\ad.sfwmd.gov\dfsroot\GIS\GSBiz\WS\LWCSIM\Report_Figures\mxd\KxfromFieldData.mxd

Figure 3-7. Horizontal hydraulic conductivity of the Sandstone aquifer confining unit.



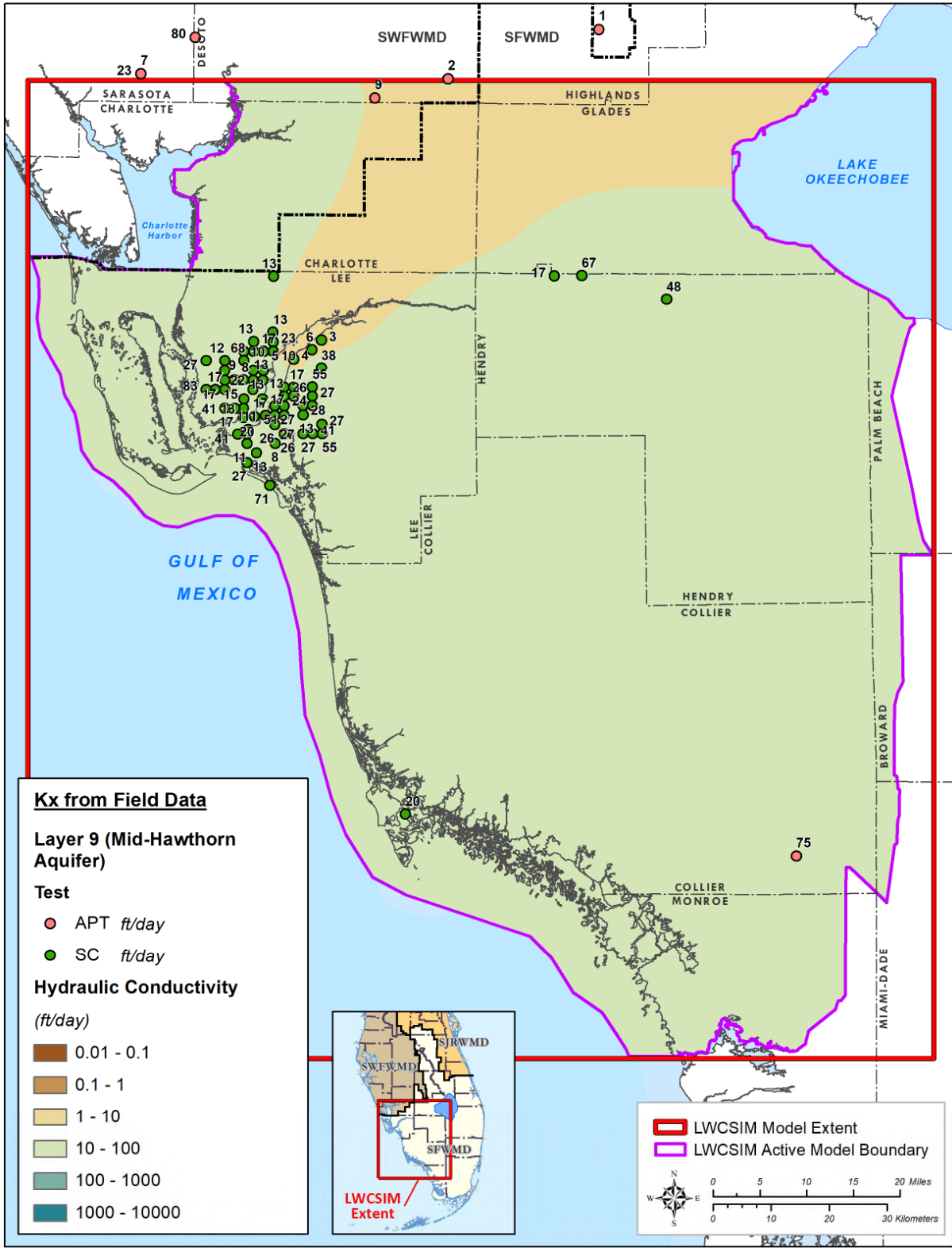
\\ad.sfwmd.gov\dfsroot\GIS\GSBiz\WS\LWCSIM\Report_Figures\mxd\KxfromFieldData.mxd

Figure 3-8. Horizontal hydraulic conductivity of the Sandstone aquifer – carbonate zone.



\\ad.sfwmd.gov\dfsroot\GIS\GSBiz\WWS\LWCSIM\Report_Figures\mxd\KxfromFieldData.mxd

Figure 3-9. Horizontal hydraulic conductivity of the Mid-Hawthorn confining unit.



\\ad.sfwmd.gov\dfsroot\GIS\GSBiz\WS\LWCSIM\Report_Figures\mxd\KxfromFieldData.mxd

Figure 3-10. Horizontal hydraulic conductivity of the Mid-Hawthorn aquifer.

3.3 Water Use

Creation of the MODFLOW WEL package for the LWCSIM required extensive data related to historical water use. The overall goal was to use the best available information related to historical use as well as the best available methods for estimating historical use when no withdrawals were reported. Therefore, the data used for the WEL package were extracted from individual water use permits, actual water use reported to the SFWMD, and demand estimates.

3.3.1 Water Use Summary

There are six water use categories used in water supply planning in South Florida: Public Supply (PS), Agriculture (AG), Landscape/Recreational (L/R), Commercial/Industrial/Institutional (CII), Domestic Self-Supply (DSS), and Power Generation (PG). There are no Power Generation permits within the SAS/IAS, so the category is not discussed in this report.

1999 Steady-State Water Use Summary

Table 3-1 shows the total SAS/IAS water use demands in 1999 for each county and water use category within the LWC Planning Area. **Figure 3-11** shows the total amount and corresponding percentage for each water use classification. AG is the largest water use category within the model domain, making up 71% of total water use. **Figure 3-12** shows the total amount and corresponding percentage for each county within the model domain. Collier County is using the largest volume of water. **Figure 3-13** shows the distribution of water withdrawals from each layer of the model. The LTA is the most used aquifer in the LWCSIM domain, with approximately 228 mgd withdrawn.

Table 3-1. Water use, in million gallons per day, by county and use type, of the surficial and intermediate aquifer systems, for the Lower West Coast Planning Area in 1999.

| County | AG | CII | DSS | L/R | PS |
|-----------|--------|------|-------|-------|-------|
| Charlotte | 9.12 | 0.00 | 0.03 | 0.00 | 0.05 |
| Collier | 126.95 | 1.13 | 2.26 | 28.71 | 63.85 |
| Glades | 9.46 | 0.00 | 0.00 | 0.10 | 0.01 |
| Hendry | 177.30 | 0.71 | 0.00 | 0.51 | 0.00 |
| Lee | 63.93 | 0.25 | 15.13 | 36.09 | 11.09 |

AG = Agriculture; CII = Commercial/Industrial/Institutional; DSS = Domestic Self-Supply; L/R = Landscape/Recreational; PS = Public Supply.

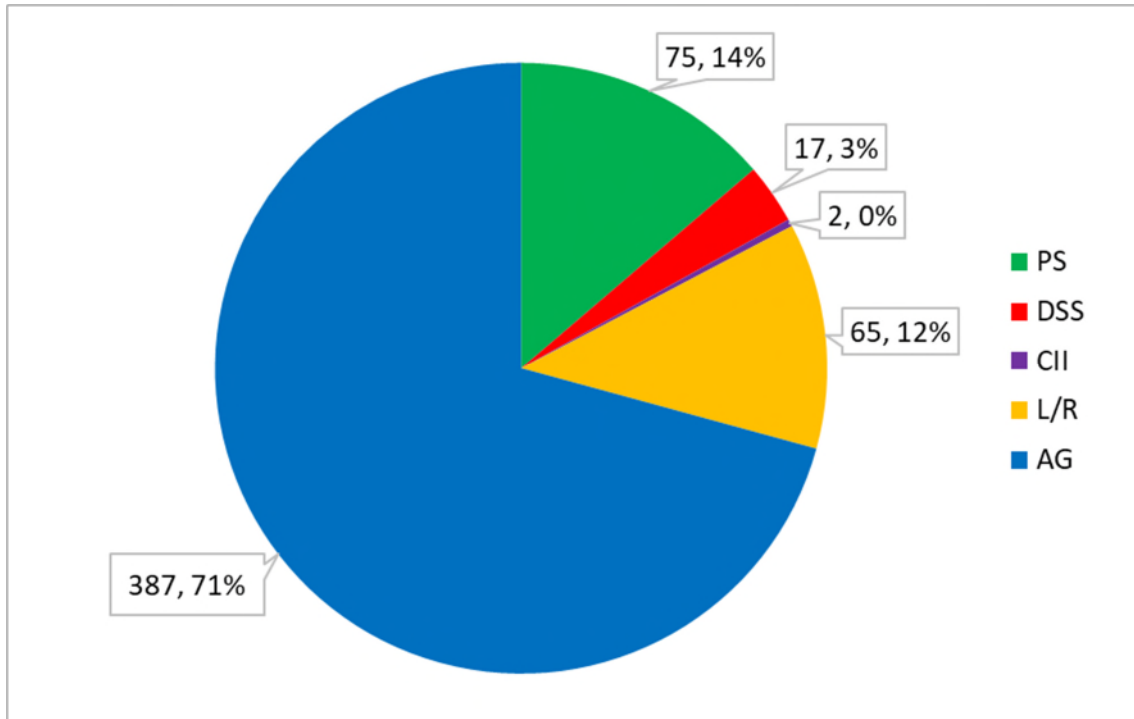


Figure 3-11. Water use distribution by use category, in million gallons per day, of the surficial and intermediate aquifer systems, for the Lower West Coast Planning Area in 1999.

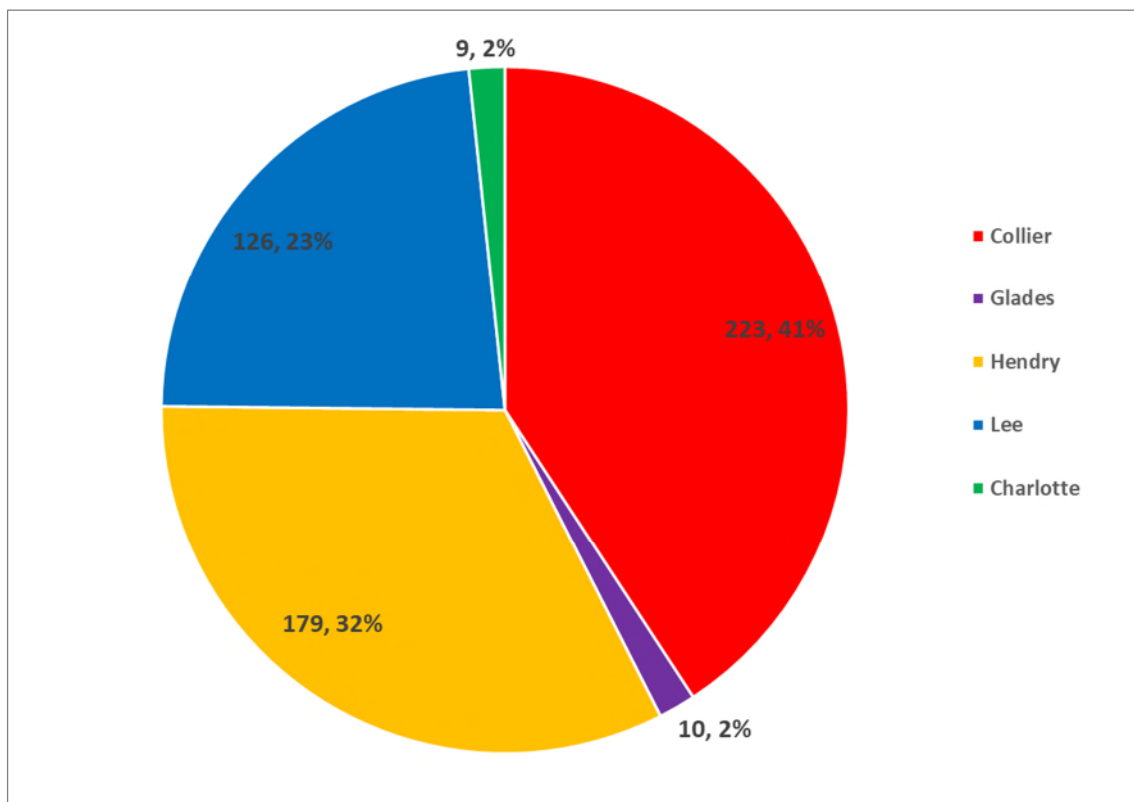


Figure 3-12. Water use distribution by county, in million gallons per day, of the surficial and intermediate aquifer systems, for the Lower West Coast Planning Area in 1999.

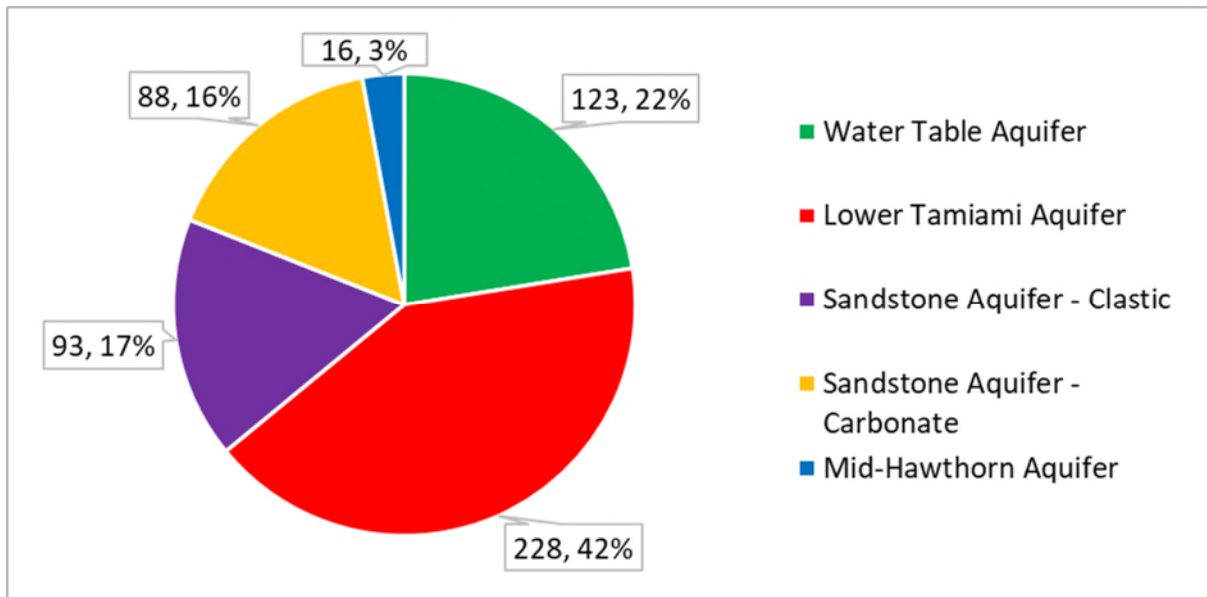


Figure 3-13. Water use distribution by aquifer layer, in million gallons per day, of the surficial and intermediate aquifer systems, for the Lower West Coast Planning Area in 1999.

Transient Period (1999 to 2014) Water Use Summary

Table 3-2 shows the water use demands, by use type, for the transient calibration and verification periods (1999 to 2014). **Figure 3-14** shows the trends in water use demands from 1999 to 2014. AG demands were consistently higher than the other water use categories throughout the calibration and verification periods. The graph also shows that L/R demands increased in 2007. DSS demand increased gradually up through approximately 2007.

Table 3-2. Water use demands by use type from 1999 to 2014, in million gallons per day, of the surficial and intermediate aquifer systems, for the Lower West Coast Planning Area.

| Year | AG | CII | DSS | L/R | PS |
|------|--------|------|-------|--------|-------|
| 1999 | 387.49 | 2.08 | 17.42 | 68.17 | 11.15 |
| 2000 | 447.99 | 1.97 | 19.88 | 70.81 | 11.43 |
| 2001 | 389.13 | 1.66 | 23.29 | 67.33 | 34.64 |
| 2002 | 392.03 | 2.19 | 25.77 | 63.79 | 38.54 |
| 2003 | 318.63 | 1.18 | 30.41 | 92.56 | 36.17 |
| 2004 | 378.47 | 1.15 | 36.91 | 104.47 | 43.40 |
| 2005 | 332.45 | 1.24 | 43.40 | 93.72 | 64.73 |
| 2006 | 426.60 | 1.05 | 51.86 | 112.27 | 71.30 |
| 2007 | 428.08 | 0.96 | 55.33 | 112.09 | 75.74 |
| 2008 | 488.67 | 2.22 | 54.79 | 130.99 | 69.84 |
| 2009 | 538.18 | 3.42 | 55.11 | 136.12 | 69.80 |
| 2010 | 433.89 | 4.28 | 56.78 | 120.87 | 64.73 |
| 2011 | 514.23 | 4.88 | 51.51 | 130.89 | 64.49 |
| 2012 | 512.72 | 4.75 | 51.72 | 126.38 | 63.43 |
| 2013 | 447.07 | 4.06 | 51.88 | 125.78 | 61.22 |
| 2014 | 425.25 | 3.53 | 52.26 | 118.06 | 62.04 |

AG = Agriculture; CII = Commercial/Industrial/Institutional; DSS = Domestic Self-Supply; L/R = Landscape/Recreational; PS = Public Supply.

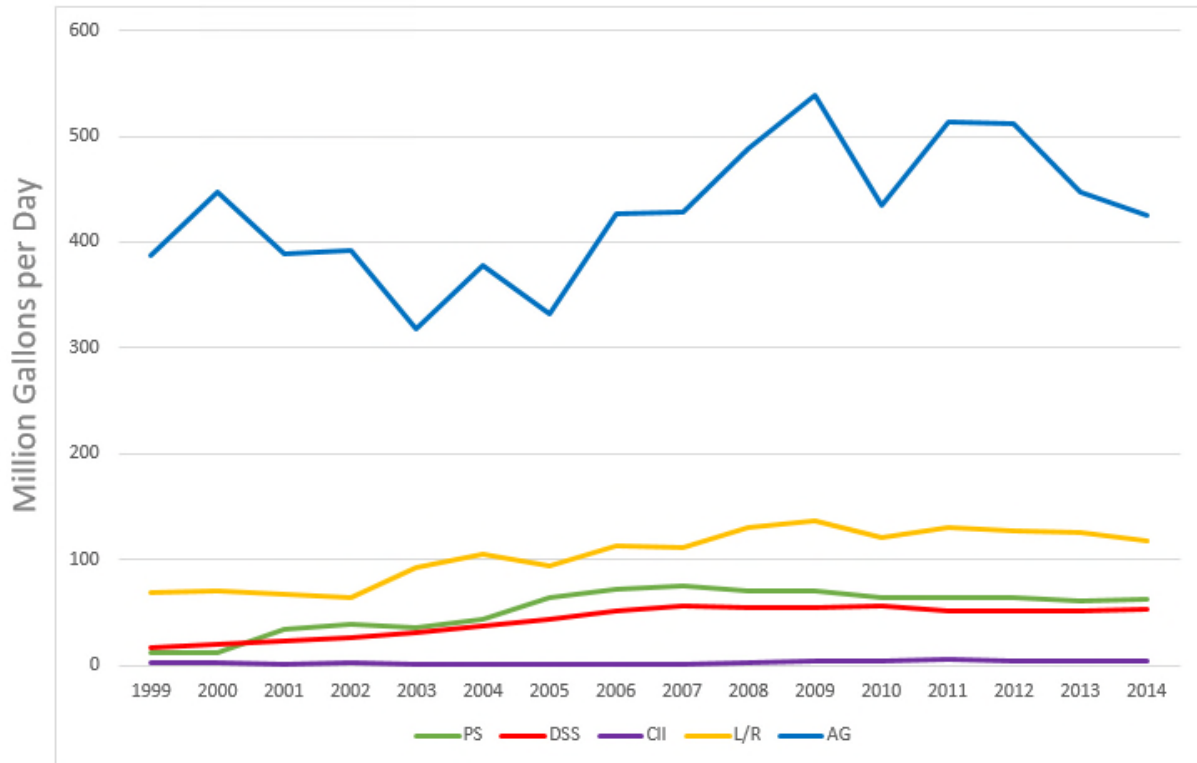


Figure 3-14. Water use summary for the Lower West Coast Planning Area, 1999 to 2014.

The following sections describe how the various water use information was compiled and incorporated into the model.

3.3.2 Public Supply

PS is the second largest water use category within the LWCSIM domain, with 32 individual water use permits and 509 facilities. These permits and facilities are spread throughout Charlotte, Glades, Lee, Collier, and Hendry counties, with most facilities located in Lee and Collier counties. **Figure 3-15** shows the location of PS pumping facilities within the LWCSIM domain.

Historical withdrawal records for PS are available throughout the LWCSIM domain and the calibration period via reported values submitted by permittees to the SFWMD’s Water Use Bureau. Raw water volumes pumped during a given month and year are reported by the corresponding utility. Throughout the calibration period, individual well pumping records were reviewed and used when available. Historical individual well pumping records were used to create facility distribution ratios. Facility distribution ratios were developed based on per-well historical usage and applied to the period of time when per-well pumpage records were not available. At the beginning of the simulation period, historical pumping sometimes was only reported by permit (a summation of all wells providing water for the utility) or by aquifer (a summation of all wells withdrawing water from a specific aquifer). In these cases, it was assumed that facility distribution ratios from later years were applicable in preceding years.

Production wells with open-hole sections penetrating multiple layers were identified and examined. For these wells, the withdrawal at the affected well location was divided among the productive layers (excluding confining units) proportional to the transmissivities of the contributing open intervals.

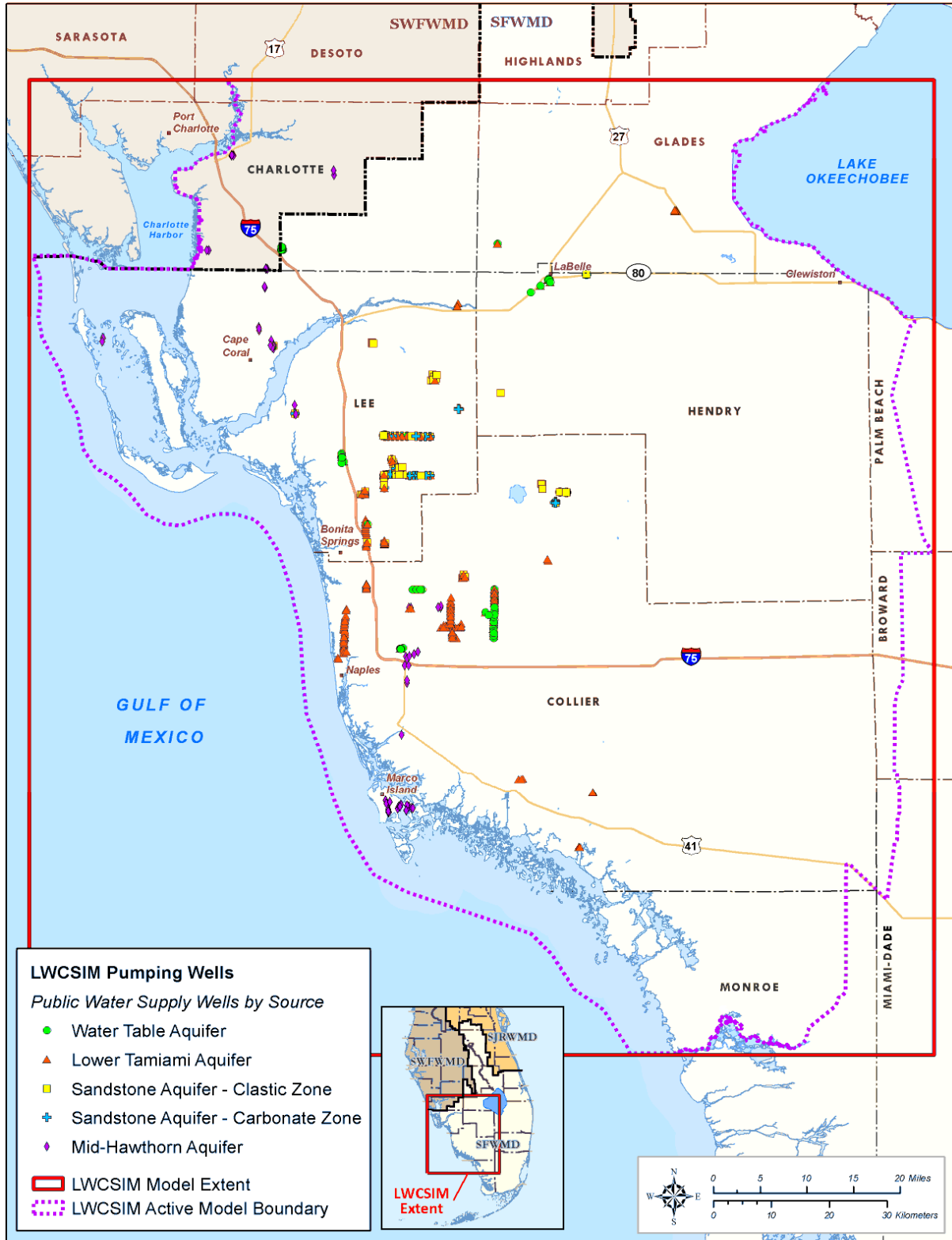


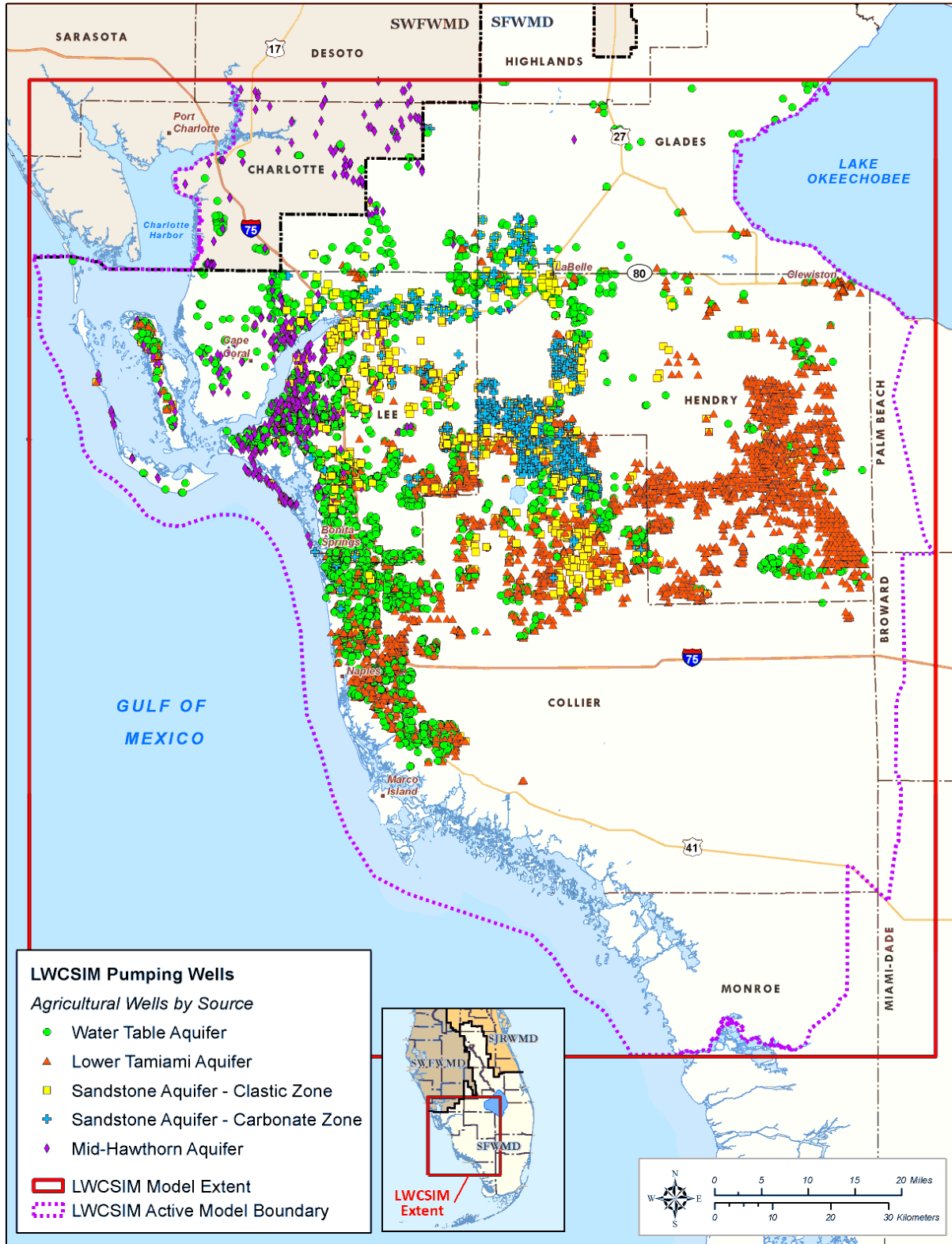
Figure 3-15. Public Supply pumping facilities using the surficial and intermediate aquifer systems within the Lower West Coast Planning Area.

3.3.3 Agriculture and Landscape/Recreational

AG and L/R combined are the largest water use in the LWC Planning Area. These water uses are primarily in north-central Collier County, eastern Lee County, Hendry County, and Glades County. The major agricultural crops are citrus, sugar cane, turf, improved pasture, and various vegetable crops (e.g., beans, tomatoes, melons, other row crops). AG can be subdivided into agriculture, diversion and impoundment, aquaculture, livestock, and nursery, while L/R can be subdivided into golf and landscape. The crop type for L/R is turf.

Within the LWCSIM domain, there are 4,504 water use permits and 11,563 facilities in the AG and L/R categories. These permits and facilities are spread throughout Lee, Collier, Hendry, Glades, and Charlotte counties, with most permittees and facilities located in Lee, Collier, and Hendry counties. **Figure 3-16** shows the locations of AG and L/R pumping facilities within the LWCSIM domain.

Throughout the calibration period, pumping records by permit and by individual well were reviewed. Unfortunately, withdrawal records for the calibration period for AG and L/R users was very limited in availability. Therefore, irrigation demands were determined using the AFSIRS program (Smajstrla 1990). AFSIRS provides an estimate of daily irrigation requirements based on observed rainfall and ET rates, crop types, and land use. A detailed description of how AFSIRS is used to estimate AG demand is described at the end of this section. The SFWMD's water use permit database was queried to determine the predominant crop type and irrigation efficiency for each permit. This information was input into AFSIRS, and irrigation requirements were calculated for each day of the simulation period for each individual water use permittee. Demands were summarized to produce a yearly demand in million gallons per year. Results from AFSIRS for AG and L/R permittees are summarized in **Tables 3-3** and **3-5**, respectively. **Tables 3-4** and **3-6** provide the acreages by county for AG and L/R uses, respectively. **Table 3-7** shows the acreage by crop type for each of the land use/land cover maps. During the years with significant increases in acreage, there also are corresponding increases in demand. The biggest AG users in the LWCSIM domain are Babcock Ranch, located in Charlotte County, and Southern Division Ranch Unit 1, located in Hendry County.



\\ad.sfwmd.gov\dfsroot\GSGS\Bz\WLS\LWCSIM\Report_Figures\trxd\20190307_PumpingWellsAGR.mxd

Figure 3-16. Agriculture and Landscape/Recreational pumping facilities using the surficial and intermediate aquifer systems in the Lower West Coast Planning Area.

Table 3-3. Agriculture water use demand by county, in million gallons per day, of the surficial and intermediate aquifer systems within the Lower West Coast Planning Area.

| Year | Charlotte | Glades | Lee | Hendry | Collier |
|------|-----------|--------|-------|--------|---------|
| 1999 | 23.52 | 4.09 | 29.32 | 135.30 | 115.86 |
| 2000 | 34.18 | 7.97 | 37.57 | 194.14 | 142.98 |
| 2001 | 30.76 | 6.44 | 38.72 | 188.89 | 124.85 |
| 2002 | 26.50 | 6.76 | 28.37 | 140.71 | 111.34 |
| 2003 | 30.54 | 6.37 | 26.94 | 140.62 | 105.51 |
| 2004 | 35.45 | 7.89 | 31.43 | 163.38 | 129.86 |
| 2005 | 33.17 | 7.02 | 30.01 | 146.83 | 121.06 |
| 2006 | 37.90 | 9.18 | 35.91 | 192.45 | 143.54 |
| 2007 | 29.19 | 10.38 | 31.44 | 171.63 | 136.63 |
| 2008 | 23.76 | 7.56 | 24.61 | 150.75 | 114.63 |
| 2009 | 30.79 | 11.18 | 33.94 | 202.72 | 153.81 |
| 2010 | 26.96 | 8.58 | 24.72 | 151.28 | 105.11 |
| 2011 | 31.05 | 9.86 | 27.90 | 184.44 | 139.14 |
| 2012 | 27.29 | 8.63 | 26.77 | 142.77 | 134.02 |
| 2013 | 24.22 | 7.90 | 24.66 | 144.27 | 122.37 |
| 2014 | 22.98 | 6.70 | 21.14 | 126.85 | 108.59 |

Table 3-4. Agriculture acreage by county within the Lower West Coast Planning Area and model domain.

| Year | Charlotte | Glades | Lee | Hendry | Collier |
|------|-----------|--------|--------|---------|---------|
| 2000 | 15,755 | 42,799 | 25,841 | 240,669 | 68,020 |
| 2004 | 15,493 | 43,184 | 23,931 | 229,687 | 68,683 |
| 2010 | 11,081 | 47,347 | 20,418 | 237,883 | 65,475 |
| 2014 | 11,346 | 45,464 | 17,068 | 216,104 | 63,725 |

Table 3-5. Landscape/Recreational water use demand by county, in million gallons per day, of the surficial and intermediate aquifer systems within the Lower West Coast Planning Area.

| Year | Charlotte | Glades | Lee | Hendry | Collier |
|------|-----------|--------|-------|--------|---------|
| 1999 | 0.00 | 0.01 | 19.43 | 0.25 | 17.36 |
| 2000 | 0.00 | 0.01 | 21.77 | 0.29 | 18.17 |
| 2001 | 0.00 | 0.01 | 20.60 | 0.26 | 15.87 |
| 2002 | 0.00 | 0.01 | 28.28 | 0.14 | 20.90 |
| 2003 | 0.00 | 0.01 | 27.21 | 0.14 | 19.13 |
| 2004 | 0.00 | 0.01 | 28.34 | 0.17 | 21.87 |
| 2005 | 0.00 | 0.01 | 21.94 | 0.14 | 18.20 |
| 2006 | 0.00 | 0.01 | 31.06 | 0.20 | 26.81 |
| 2007 | 0.00 | 0.13 | 45.88 | 0.99 | 35.13 |
| 2008 | 0.00 | 0.09 | 39.68 | 0.79 | 29.61 |
| 2009 | 0.00 | 0.13 | 46.06 | 1.05 | 33.80 |
| 2010 | 0.00 | 0.10 | 37.10 | 0.87 | 24.92 |
| 2011 | 0.00 | 0.12 | 43.49 | 1.01 | 31.37 |
| 2012 | 0.00 | 0.12 | 48.42 | 1.05 | 32.16 |
| 2013 | 0.00 | 0.12 | 45.20 | 1.00 | 33.64 |
| 2014 | 0.00 | 0.10 | 40.49 | 0.89 | 29.88 |

Table 3-6. Landscape/Recreational acreage by county within the Lower West Coast Planning Area.

| Year | Charlotte | Glades | Lee | Hendry | Collier |
|------|-----------|--------|--------|--------|---------|
| 2000 | 21 | 477 | 13,059 | 1,413 | 13,041 |
| 2004 | 21 | 422 | 19,750 | 908 | 17,593 |
| 2010 | 25 | 552 | 25,432 | 2,007 | 21,259 |
| 2014 | 76 | 357 | 28,775 | 2,035 | 22,524 |

Table 3-7. Acreage by crop/use type within the Lower West Coast Planning Area.

| Year | Citrus | Crops | Nursery | Pasture | Sod | Sugar | Golf | Landscape |
|------|---------|--------|---------|---------|-----|---------|--------|-----------|
| 2000 | 168,790 | 74,414 | 2,263 | 20,256 | 811 | 126,550 | 13,297 | 14,714 |
| 2004 | 157,863 | 70,558 | 2,380 | 18,472 | 360 | 131,345 | 16,902 | 21,792 |
| 2010 | 142,645 | 74,185 | 5,517 | 23,190 | 527 | 136,140 | 19,655 | 29,620 |
| 2014 | 125,798 | 73,267 | 5,116 | 22,556 | 681 | 126,289 | 20,924 | 32,843 |

AG and L/R permittees often use several sources of water. Within the LWC Planning Area, permittees can withdraw from surface water and groundwater sources, including the Lower Hawthorn and Upper Floridan aquifers. Therefore, it was essential to create facility ratios that allowed for irrigation demands to be applied to the correct aquifers. Facility ratios were created by querying the SFWMD’s regulation database for historical water use data from 1999 to 2014, which were sporadic for AG and L/R permittees and had several outliers. A thorough quality assurance process examined each pumpage record and attempted to adjust any incorrect values. Following the quality assurance process, a facility ratio was created by taking the summation of each individual facility’s withdrawal and dividing by the total permit withdrawal. This allowed for each facility, regardless of the source of water, to have a ratio.

Once the ratios were created, the SFWMD’s regulation database was queried for facility information, including x and y coordinates, pump capacity, and year in addition to well-specific information such as cased depth, total depth, and well diameter. Facilities were filtered to exclude wells using the Lower Hawthorn and Upper Floridan aquifers, which are not part of the LWCSIM. Also excluded were facilities pumping water from external sources (e.g., canals, lakes, reservoirs) or on-site surface water sources hydraulically connected to external sources. Finally, facilities were filtered to include only primary wells and pumps. This filter aligned with the assumption that permittees use only facilities that already had a pump installed. Facilities were placed in the model based on the x and y coordinates in the SFWMD’s water use database. If the x and y coordinates were missing or incorrect, the facility was placed in a reasonable location within the permit boundary. When historical pumping reports were not available, the facility ratio was assumed to be equally distributed among the primary facilities, as indicated in the SFWMD’s water use database.

AFSIRS Model for Estimating AG and L/R Water Use

AFSIRS was developed for Florida’s water management districts by the University of Florida Institute of Food and Agricultural Sciences as a method to determine agricultural water use allocations for consumptive use permitting programs (Smajstrla 1990). The model estimates irrigation requirements for Florida crops, soils, irrigation systems, and climate conditions. The irrigation requirement for crop production is the amount of water, excluding precipitation, that should be applied to meet a crop’s supplemental demand requirements without a significant reduction in yield.

The AFSIRS model is based on a water budget of the crop root zone and the concept that crop ET can be estimated from potential ET and K_c . The water budget includes inputs to the crop root zone from rain and irrigation, and losses from the root zone by drainage and ET. The water storage capacity in the crop root zone is the product of the soil's water-holding capacity and the depth of the effective root zone for the crop being grown. Irrigation is scheduled based on an allowable level of soil water depletion from the crop root zone. This level of simulation model development produced a functional model capable of addressing the wide variety of crops, soils, and irrigation systems in Florida and including variations in daily rainfall and ET rates.

Reference Crop and Crop Coefficients

Reference crops were used to develop the water demands for various crops grown in Florida. Daily ET for each crop was calculated as the product of reference ET and the crop K_c for that day. The K_c values varied with crop growth stage. Crop K_c values were obtained from the literature and revised by the Institute of Food and Agricultural Sciences for bahia grass, citrus, and sod. Three separate sets of K_c values were examined and included in the AFSIRS updates for this modeling effort.

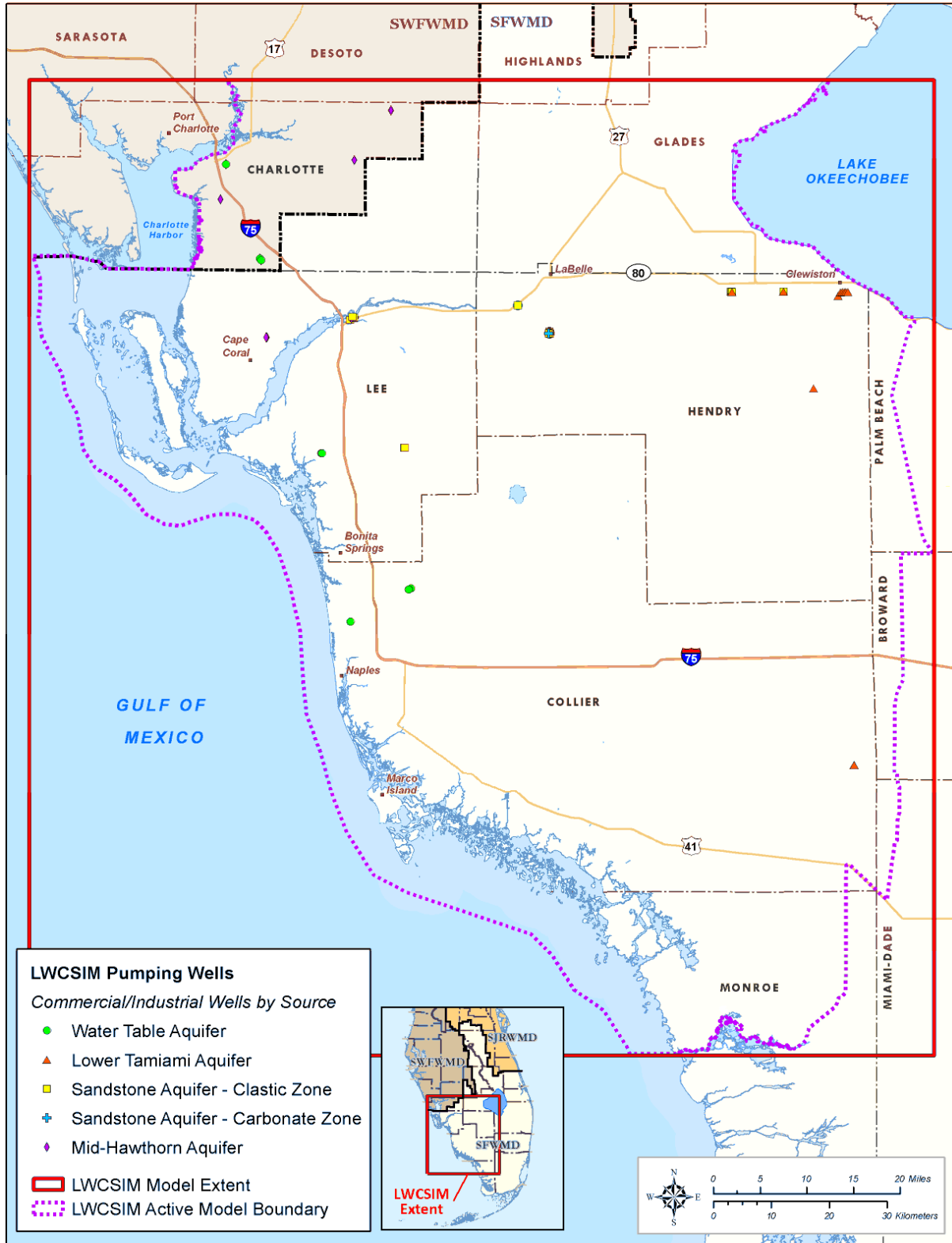
All individual and general irrigation permits issued within the LWCSIM domain were reviewed. Information obtained from the permits included crop type, irrigation method, irrigation source, and irrigation withdrawal facilities. The permitted average annual allocations also were collected and reviewed to ensure the AFSIRS-generated demand was less than the permitted annual allocation. Individual demands were calculated on a crop-by-crop basis and aggregated up to a monthly irrigation demand for each permit.

For the transient model, estimated demands were applied to permitted groundwater withdrawal facilities. Surface water withdrawals were not included in the model unless the permittee used an isolated lake. In this case, the demand was applied to the SAS (layer 1 – Water Table aquifer). Irrigation demands were calculated from AFSIRS and varied based on climatic conditions. The SFWMD's water use database was reviewed to determine when a newly issued permit became operational within the simulation period. For these users, pumpage values before permit issuance were assigned a value of zero.

3.3.4 Commercial/Industrial/Institutional

CII water use is the smallest use category of the SAS/IAS within the LWCSIM domain, making up less than 10% of total water use. CII includes permitted commercial, industrial, and institutional users who are self-supplied and do not receive water from a PS utility. Examples of CII use types include concrete processing, mining, and food processing. Uses that return water back to the withdrawal source (e.g., rock washing, heating and cooling, equipment washing) are not included. Within the LWCSIM domain, there are 15 CII permits and 71 facilities (**Figure 3-17**). The largest CII users are the Ortona and Palmdale sand mines in Glades County.

Within the LWCSIM domain, CII water use for the transient model was obtained on a well-by-well basis from reported pumping values submitted by permittees to the SFWMD or from estimates based on reported values. When only total permit pumping values were available, pumping was assumed to be equally distributed among all facilities associated with the permit. This allowed for creation of a master well file that provides individual pumping rates for each well.



\\ad.sfwmd.gov\dfsroot\GIS\GISB\z\WLS\LWCSIM\Report_Figures\mxd\20190307_PumpingWellsCI.mxd

Figure 3-17. Location of Commercial/Industrial/Institutional pumping facilities using the surficial and intermediate aquifer systems in the Lower West Coast Planning Area.

3.3.5 Domestic Self-Supply

DSS wells in Lee, Collier, Glades, and Hendry counties and associated DSS well data were compiled from several sources. The SFWMD contacted county officials to request information on DSS wells, including location, casing depth, and total depth. Information was provided as a geographic information system (GIS) shapefile or an Excel spreadsheet that could be converted to a GIS shapefile, so all DSS wells could be located in the LWCSIM domain. Information from Lee and Collier counties was the most extensive and complete. DSS wells in Charlotte and DeSoto Counties (within the LWCSIM model domain) were obtained from SFWMD, as discussed in the next section.

All DSS well data were combined into a comprehensive, consistent Excel table containing county, state plane coordinates, well casing depth, well total depth, and per capita use rate (PCUR). GIS was used to intersect these points with the LWCSIM grid to assign a row and column to each well.

The PCUR was calculated from information in the 2012 LWC Water Supply Plan Update (SFWMD 2012). The planning document contains projections of DSS user populations and water demand for each county. Specifically, in Appendix A of the 2012 LWC Water Supply Plan Update, Tables A-1 through A-8 contain the data used to calculate a PCUR for all DSS wells in each county. According to the 2012 LWC Water Supply Plan Update (page 6 of Appendix A), the PCUR is the total annual water use divided by the number of permanent residents.

For example, to calculate the net average PCUR for DSS wells in Lee County in 2005:

1. DSS-using population = 68,566 permanent residents (SFWMD 2012, Table A-2)
2. Net average DSS water demand = 8.37 million gallons per day (mgd) (SFWMD 2012, Table A-7)
= 8,370,000 gallons per day (gpd)
3. $PCUR = 8,370,000 \text{ gpd} \div 68,566 \text{ permanent residents} = 122 \text{ gpd per person (gpd/p)}$

The PCUR also was calculated for the net 1-in-10-year drought (129 gpd/p), the gross average (147 gpd/p) and the gross 1-in-10-year drought (156 gpd/p). The average of all the above is 139 gpd/p.

Each county's overall average PCUR based on the 2012 LWC Water Supply Plan Update (SFWMD 2012) was as follows:

- Collier County: 219 gpd/p
- Glades County: 139 gpd/p
- Hendry County: 131 gpd/p
- Lee County: 139 gpd/p

Discussions with SFWMD planning staff indicated a better estimate of the PCUR might be obtained using the SFWMD's Water Supply Utility Project (WaSUP) database of finished residential water demand as reported for each PS utility in the LWC Planning Area. Based on information in the WaSUP database, each county's average PCUR was adjusted to the following:

- Collier County: 123.67 gpd/p
- Glades County: 114.58 gpd/p
- Hendry County: 67.43 gpd/p
- Lee County: 71.05 gpd/p

The derived PCURs were used as starting points for assigning extraction rates to model cells representing DSS wells. The rates per model layer per model cell were determined and assigned using a method developed by the SFWMD, which uses well casing depth and total depth to determine which model layer(s) are being tapped. The method accounted for model cells that contain more than one DSS well. It was decided that the PCUR represents water used per person and that each household well provides water for an average of three persons. Therefore, a factor of 3 was included when arriving at the final per-model-cell pumping rate. In other words, each DSS well represents three persons. Application to all four counties resulted in the following:

- Collier County: $123.67 \text{ gpd/p} \times 3 = 371.01 \text{ gpd/well}$
- Glades County: $114.58 \text{ gpd/p} \times 3 = 343.74 \text{ gpd/well}$
- Hendry County: $67.43 \text{ gpd/p} \times 3 = 202.29 \text{ gpd/well}$
- Lee County: $71.05 \text{ gpd/p} \times 3 = 213.15 \text{ gpd/well}$

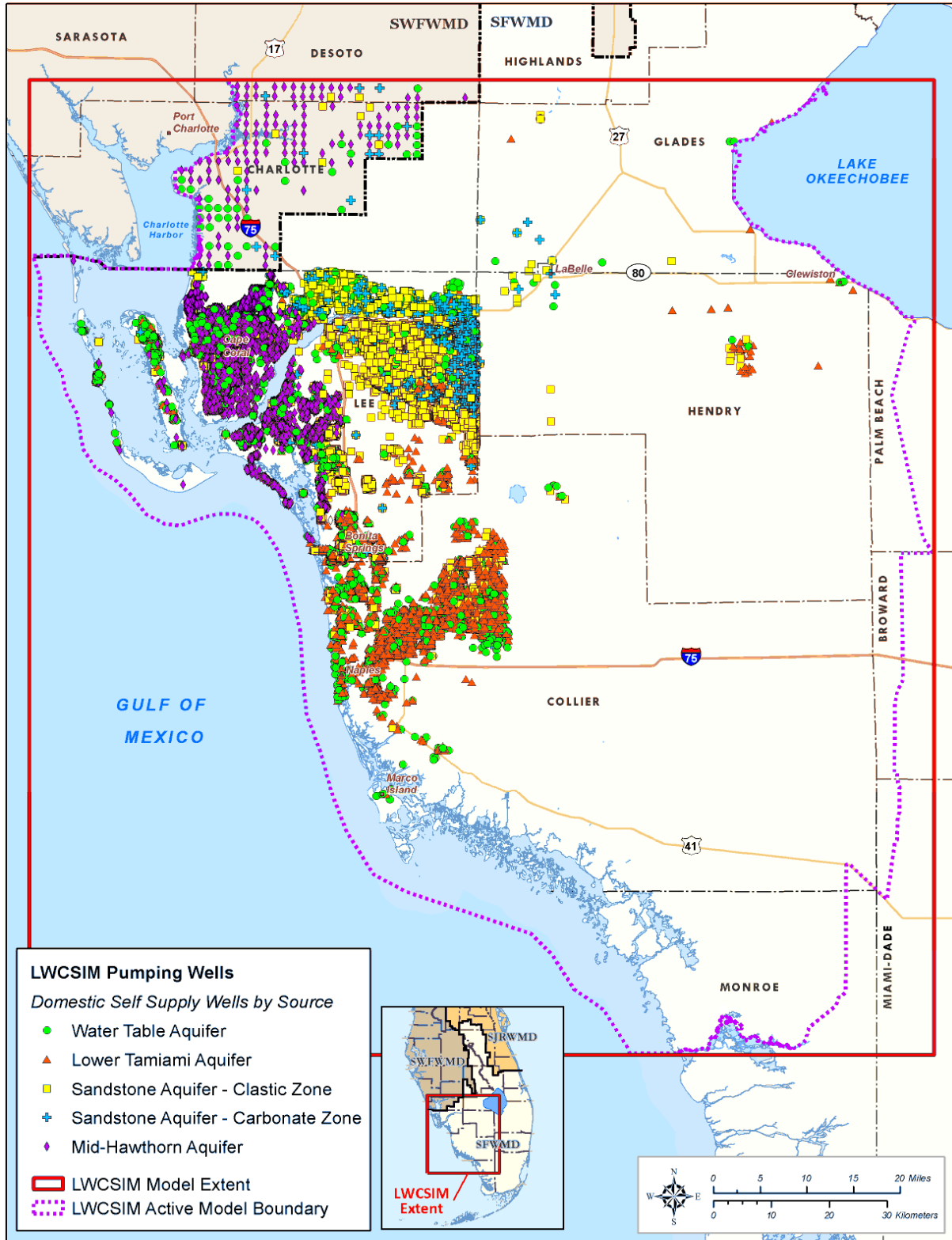
Based on information received from Lee County and discussions with SFWMD planning staff, two additional pieces of information were used to refine the DSS pumping rates. First, the DSS well average PCUR for each county was increased by a factor of one to account for private landscape irrigation, which resulted in the following:

- Collier County: $371.01 \text{ gpd/well} + 123.67 \text{ gpd/well} = 494.68 \text{ gpd/well}$
- Glades County: $343.74 \text{ gpd/well} + 114.58 \text{ gpd/well} = 458.32 \text{ gpd/well}$
- Hendry County: $202.29 \text{ gpd/well} + 67.43 \text{ gpd/well} = 269.72 \text{ gpd/well}$
- Lee County: $213.15 \text{ gpd/well} + 71.05 \text{ gpd/well} = 284.20 \text{ gpd/well}$

Second, the pumping rates for all DSS wells were adjusted over time according to seasonal variations measured at DSS wells in a portion of Lee County. This information was obtained from a Lehigh Acres groundwater flow model developed by Copp (2015). Mr. Copp provided the SFWMD with calibrated DSS well pumping rates, partly based on private landscape irrigation use, and information on how these rates vary monthly over a 2-year period (January 2013 through December 2014). The monthly variation in DSS well pumping rates was used to derive a multiplier (ranging from 0.86 to 1.14) that was applied to the PCUR for each DSS well for each month of the LWCSIM calibration/verification period (January 1999 through December 2014).

As a check on the above water extraction rate-per-well, the four-county average PCUR of 373 gpd/well divided by 3 persons/well = 124 gpd/p. This number is almost identical to the 2015 WaSUP finished residential water demand value for Collier County (123.67 gpd/p).

The final PCUR per well per county was assigned to DSS wells in the LWCSIM cells, with adjustment for seasonal variations applied monthly from January 1999 through December 2014. In the LWCSIM domain, there are 59,340 DSS wells in Collier, Glades, Hendry, and Lee counties, represented by a total of 22,139 model cells (**Figure 3-18**). **Appendix C** contains a detailed presentation of how the DSS coverage was developed.



\\ad.sfwmd.gov\dfsroot\GIS\GISBiz\WLS\LWCSIM\Report_Figures\mxd\20190307_PumpingWellsDSS.mxd

Figure 3-18. Domestic Self-Supply well locations using the surficial and intermediate aquifer systems in the model domain.

3.3.6 Southwest Florida Water Management District Pumpage

Different methodologies were used to prepare the Southwest Florida Water Management District (SWFWMD) pumpage data that are beyond the LWC Planning Area but still inside the LWCSIM domain. Therefore, these processes are discussed separately.

Non-DSS Wells

The SWFWMD maintains a pumpage database for the DWRM (Environmental Simulations, Inc. 2014). SWFWMD staff received non-DSS (e.g., PS, AG, CII) pumpage data from the SWFWMD (R. Peterson, SWFWMD, personal communication, January 2019). The data were plotted in ArcGIS, and wells within the LWCSIM domain were selected (**Figures 3-15 to 3-17**). Because the data were monthly, reported in cubic feet per day, and formatted for MODFLOW, no additional work was needed regarding the flows. However, the layering needed to be adjusted to be compatible with the LWCSIM. For DWRM, layers were assigned based on open interval and geographic location (Environmental Simulations, Inc. 2014). Nine geographic zones were used because several wells had poor well construction information:

- Zone 1: Upper Floridan aquifer (UFA) and Lower Floridan aquifer (LFA)
- Zone 2: UFA and LFA
- Zone 3: SAS, UFA, and LFA
- Zone 4: SAS, UFA, and LFA
- Zone 5: Permeable Zone 3 (PZ3) and UFA
- Zone 6: UFA and LFA
- Zone 7: UFA and LFA
- Zone 8: PZ2, PZ3, and UFA
- Zone 9: SAS, UFA, and LFA

According to Figure 3-12 from Environmental Simulations, Inc. (2014), the SWFWMD portion of the model area falls into Zone 3. In addition, Figures 3-13 to 3-15 were used to evaluate the model layering. SWFWMD staff attempted to follow the layering methodology as much as possible. However, issues that complicated this process included the following:

- There is little geologic control in the area.
- Some model layers thin or pinch out in the SWFWMD.
- Some wells are completed in confining units, while the LWCSIM team agreed to assign withdrawals to aquifers only.

The following strategy was used for layering:

- a) Wells open to a single aquifer layer were assigned to that layer. Most of these were in layers 1 or 9, but a few were in layer 7.
- b) Wells open to layer 4 were reassigned to layer 1. Layers 2 and 3 are thin or absent in these areas. Thus, layer 1 is the most likely source. This is consistent with the DWRM.
- c) Wells open to multiple zones in the SAS were assigned to layer 1. This is consistent with the DWRM.
- d) Wells open to layers 5 through 7 were assigned to layer 7. This corresponds to layer PZ1 in the DWRM.
- e) Wells open to layers 7 through 9 were assigned to layer 9. This corresponds to layer PZ2 in the DWRM.
- f) Wells withdrawing below layer 9 were considered to be withdrawing from PZ3 and/or the UFA. These withdrawal zones are below the LWCSIM base.

DSS Wells

The SWFWMD hired Janicki Environmental to prepare the DSS data. The following is an extraction from a memo from Janicki Environmental (2018) to SWFWMD staff, describing the process (using SAS program) for preparing DSS data for the DWRM:

- “1. Extract data from WMIS and subset based on established selection criteria
2. Fix STR’s (section, township, and range) where necessary in historic database
3. Calculate proportion of total county wells in each county STR
4. Read in county usage and apportion STR usage based on number of wells in each STR
5. Merge in STR centroid information
6. Export as a txt file to read into GIS (Invariant DSS annual for GIS.txt) to final deliverables folder
7. Apply seasonality coefficients to create monthly timeseries for each STR
8. Export to a txt file (Invariant DSS monthly.txt) to final deliverables folder”

A similar procedure was applied to the DSS wells to prepare them for the LWCSIM. An additional step was needed because the DSS data were given in million gallons. The data had to be converted to cubic feet per day.

4 MODEL CONCEPTUALIZATION AND DESIGN

4.1 Software Selection

The MODFLOW code (Harbaugh 2005), which is an industry standard computer program for finite-difference, three-dimensional groundwater flow modeling, was used for this modeling effort. Specifically, MODFLOW 2005 containing the SFWMD wetland module, was used. MODFLOW was selected for the following reasons:

1. It has been widely accepted in the groundwater modeling profession for more than 30 years.
2. The code is well documented and within the public domain.
3. The code is readily adaptable to a variety of groundwater flow systems.
4. The code is modular and easily facilitates any modifications required to enable its application to the types of unique groundwater flow problems encountered in South Florida.
5. It has been used extensively in existing groundwater flow models built for SFWMD water supply planning areas.
6. The SFWMD version of MODFLOW 2005 has been customized to include the Wetlands package.

4.2 Model Boundaries

Boundary conditions can determine model flow patterns and the model’s water budget. Therefore, defining the model boundaries is an important aspect of model design. In order to minimize potential errors during the simulation, physical or hydrologic features are selected as the model boundary conditions when available. When unavailable, specified head boundaries are selected a great distance away from areas of concern in the model domain. The primary imposed stresses in the LWCSIM domain are pumping wells (e.g., for AG or PS), and the model will be used to evaluate the impacts of current and future pumping from these locations. **Figure 4-1** shows the locations of current pumping wells (excluding DSS wells) in the SAS and IAS.

The western boundary coincides with the Gulf of Mexico and Peace River and includes Pine Island and Sanibel Island. The eastern boundary coincides with Lake Okeechobee and the SFWMD’s primary water

management canals (from north to south, L-24, L-25, L-4, and L-28) out to Everglades National Park. The southern boundary coincides with the Lostmans River and Big Lostmans Bay tidal boundaries. The northern boundary is a specified head boundary located a reasonable distance from areas of concern in the model (about 20 miles away from the northernmost pumping well).

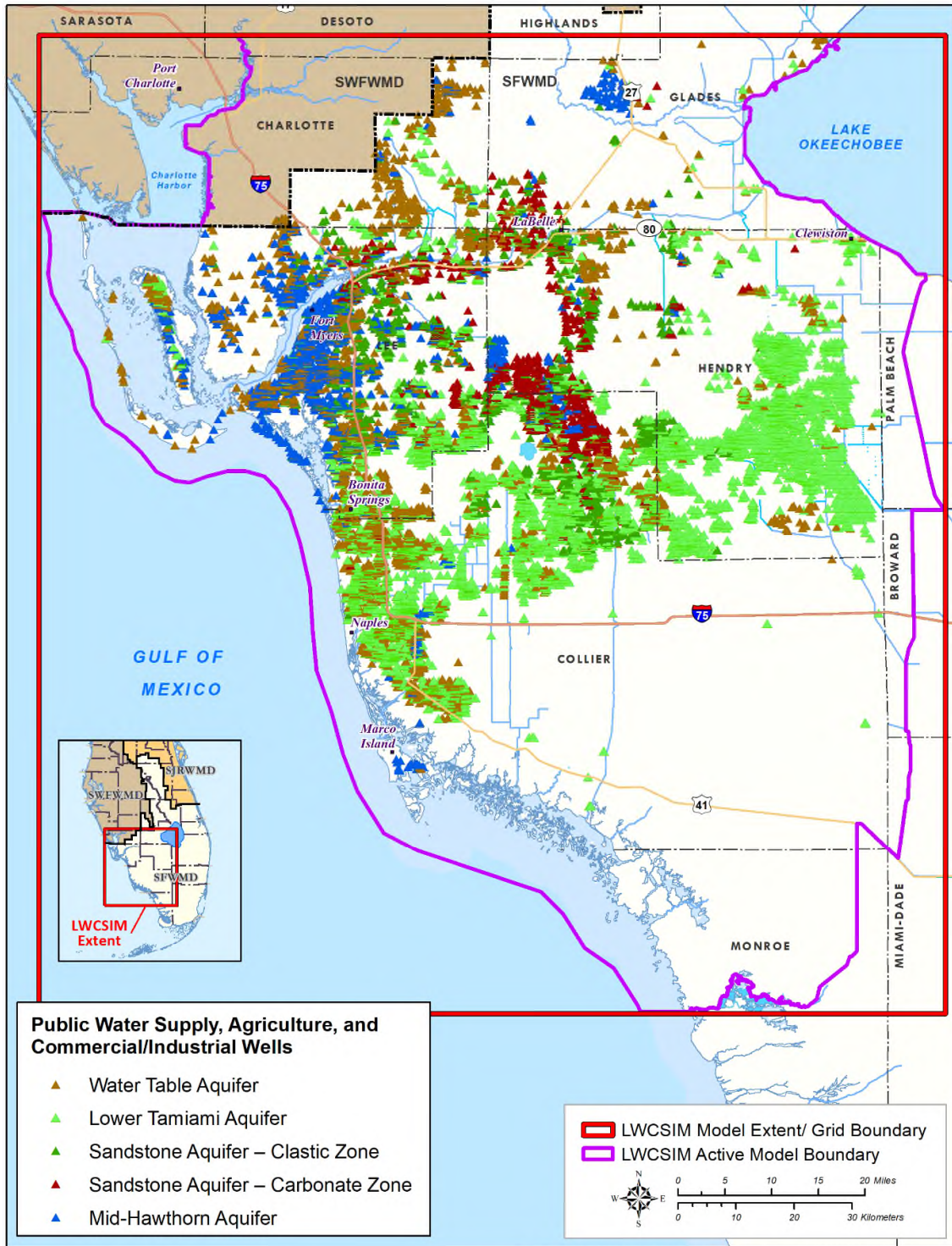


Figure 4-1. Location of water withdrawal facilities by aquifer in the Lower West Coast Planning Area.

4.3 Spatial Discretization

The LWCSIM domain covers an area from the southern edge of Highlands County at the north to Key McLaughlin in Monroe County at the south, and from Charlotte Harbor and the Gulf of Mexico on the west to approximately the western borders of Palm Beach and Broward Counties to the east. The model grid is aligned in a north-south orientation. The model grid is composed of 553 rows and 512 columns, with uniform grid spacing of 1,000 ft. Vertically, the model is composed of nine layers. There are 2,548,224 cells in the model. Of these, 1,670,609 cells are active and 877,615 cells are inactive or no-flow. Grid size selection was based on the planned use of the LWCSIM, data availability, and computational considerations. Based on the North American Datum 1983 State Plane Florida East coordinates (FIPS 0901 feet), the model origin at the southwest corner of the model is: X-direction: 218,436; Y-direction: 441,788.

Model layer definitions and the corresponding hydrogeologic units are provided in **Table 4-1**. The aquifers and confining units are treated as separate layers in the model. Future revisions to the model, or the development of sub-regional models, may require additional sub-layers to obtain local spatial resolution or computational stability.

Table 4-1. Model layers and corresponding hydrogeologic units.

| Model Layer | Hydrogeologic Unit | Abbreviation |
|-------------|----------------------------------|---------------|
| 1 | Water Table aquifer | WTA |
| 2 | Tamiami confining unit | TCU |
| 3 | Lower Tamiami aquifer | LTA |
| 4 | Upper Hawthorn confining unit | H1 |
| 5 | Sandstone aquifer clastic zone | SSA-clastic |
| 6 | Sandstone aquifer confining unit | SC |
| 7 | Sandstone aquifer carbonate zone | SSA-carbonate |
| 8 | Mid-Hawthorn confining unit | H2 |
| 9 | Mid-Hawthorn aquifer | MHA |

4.4 Temporal Discretization

The major stresses to the LWCSIM are boundary conditions related to recharge from rainfall, ET, recharge in the northern portion of the model, wellfield withdrawals, and seasonal tidal patterns. The primary purpose of the LWCSIM is to address long-term (20 to 50 years) planning issues, where a longer stress period could be used. A secondary application may include development of a companion tool for water use permitting purposes, which would require shorter stress periods. Considering the scale and resolution of the LWCSIM, the model’s intended use, and temporal data availability, especially withdrawal data, monthly stress periods were selected.

4.5 Calibration Period

Because the LWCSIM will be used to predict the availability of water resources for the next 20 years or more, the transient model had to be calibrated to extreme conditions (e.g., floods, droughts) to have greater confidence in the model’s predictive capability. Based on historical rainfall data in the LWC Planning Area from 1965 to 2014 (described in **Section 2.1**), average annual rainfall is 53.6 inches. The probability exceedance curve developed for this period shows average annual rainfall during 1-in-10 year drought conditions is 44.8 inches, while the average annual rainfall during 1-in-100 year drought conditions is approximately 41 inches (**Figure 4-2**). Representing 1-in-10 year drought conditions, 42.7 inches of rainfall were recorded in the LWC Planning Area in 2007, while there was 41 inches of rainfall in 2000, which represented 1-in-100-year drought conditions.

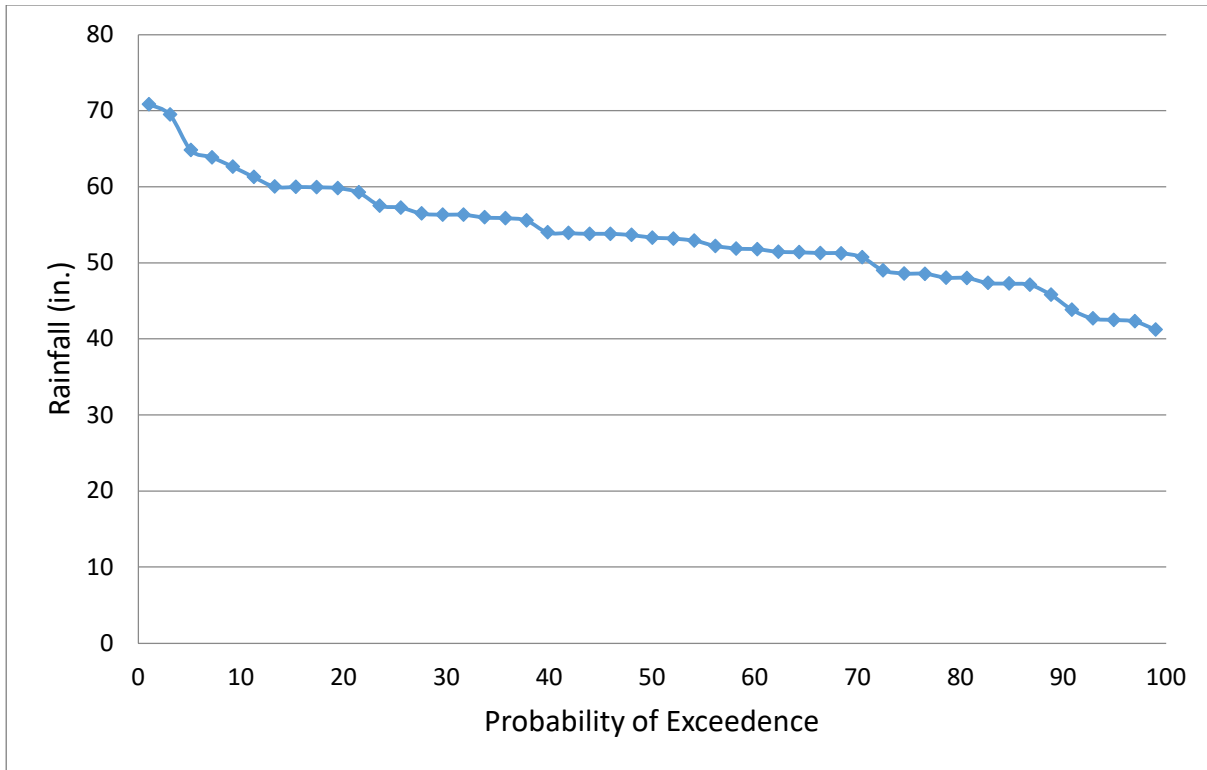


Figure 4-2. Rainfall probability exceedance curve for the Lower West Coast Planning Area, 1965 to 2014.

In the LWC Planning Area, available monitor wells for calibration purposes increased from 30 wells in 1998 to 106 wells in 1999. Considering extreme dry conditions (droughts in 2000, 2001, and 2007), extreme wet conditions (hurricanes in 2005), and data availability (**Figure 4-3**), the 16-year period from January 1999 through December 2014 was selected as the transient model period of record. As a result, this approach provided insight to the potential changes in hydrologic conditions to meet projected needs during extreme conditions. Due to time and computational constraints, a shorter transient calibration period (2008 to 2012) was chosen for use in the Parameter Estimation software (PEST; Doherty 2010) transient calibration. For the transient calibration, 2008 was a wet year and 2012 was a dry year. For manual calibration, 1999 through 2012 were used (**Figure 4-4**). Years 2013 and 2014 were used for model verification.

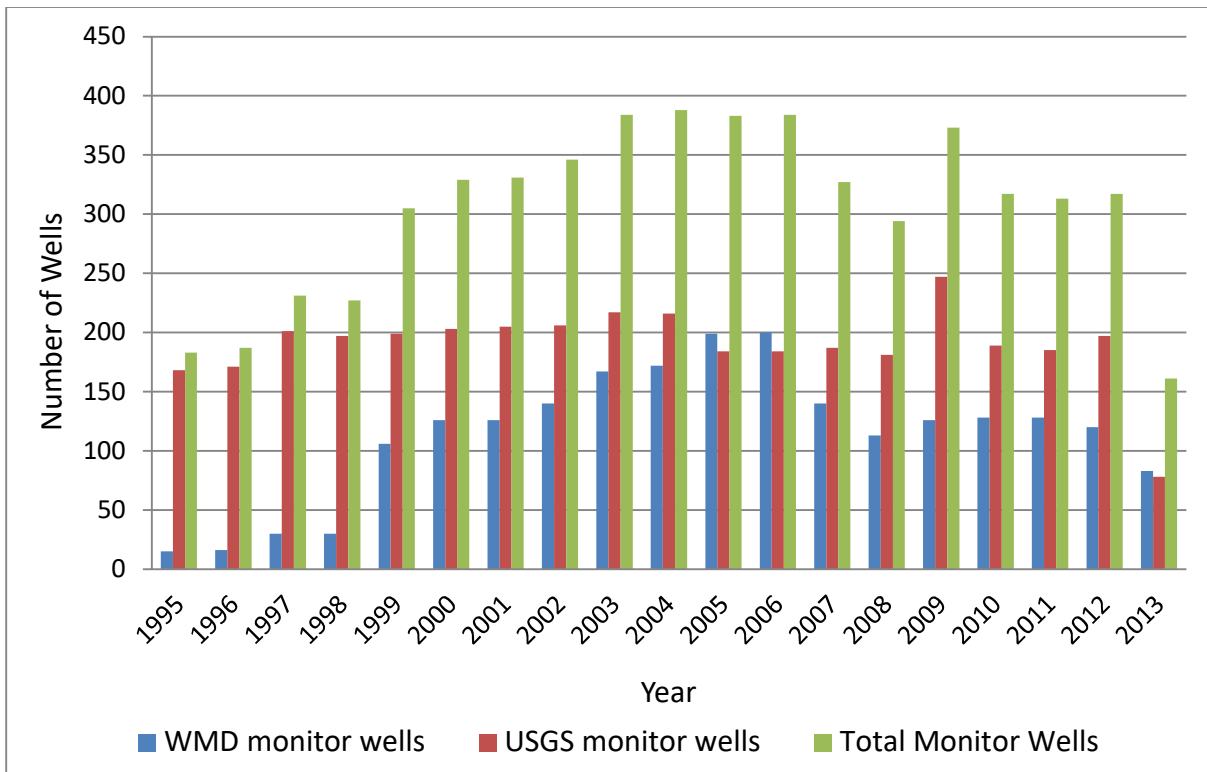


Figure 4-3. Annual distribution of groundwater monitor wells in the Lower West Coast Planning Area.

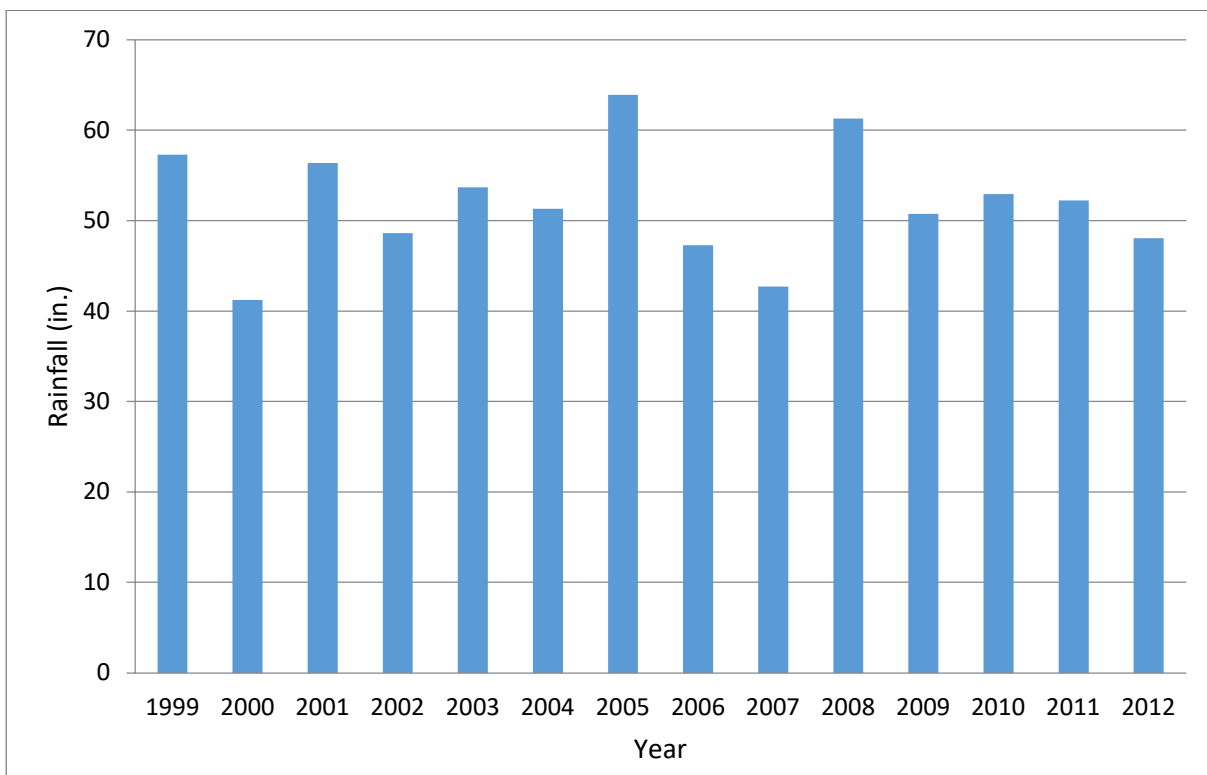


Figure 4-4. Annual average rainfall for the transient simulation period in the Lower West Coast Planning Area.

5 MODEL IMPLEMENTATION

5.1 Boundary Conditions

Figure 5-1 depicts the general head boundary (GHB) around the perimeter of the active model domain, and the no-flow boundary (inactive cells) that lie outside the active model domain. Whenever possible, hydrologic features were used as boundary conditions. **Figure 5-2** shows the surface water stations associated with the GHB cells in the WTA and TCU. The station names in **Figure 5-2** coincide with the station names in DBHYDRO.

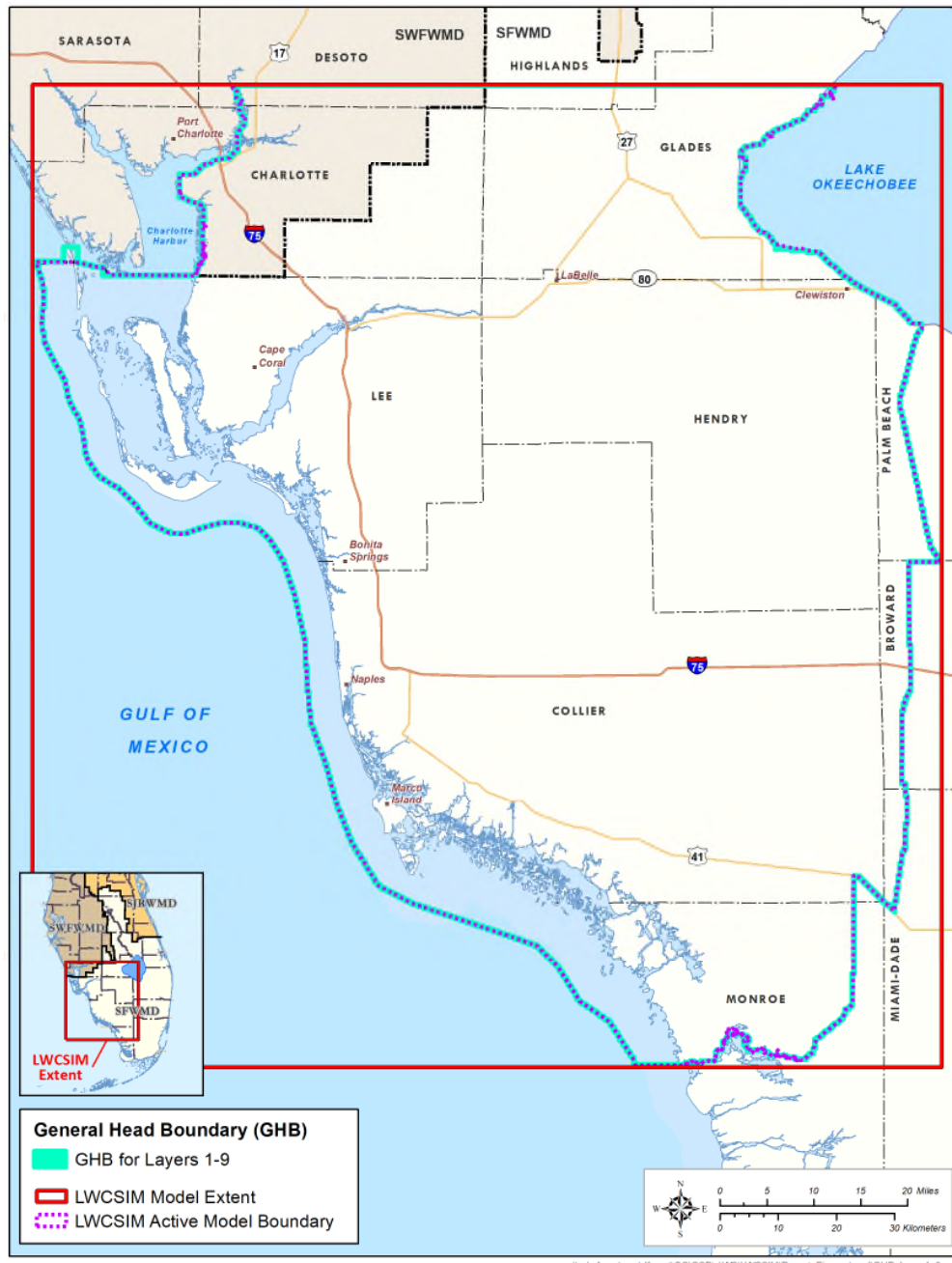
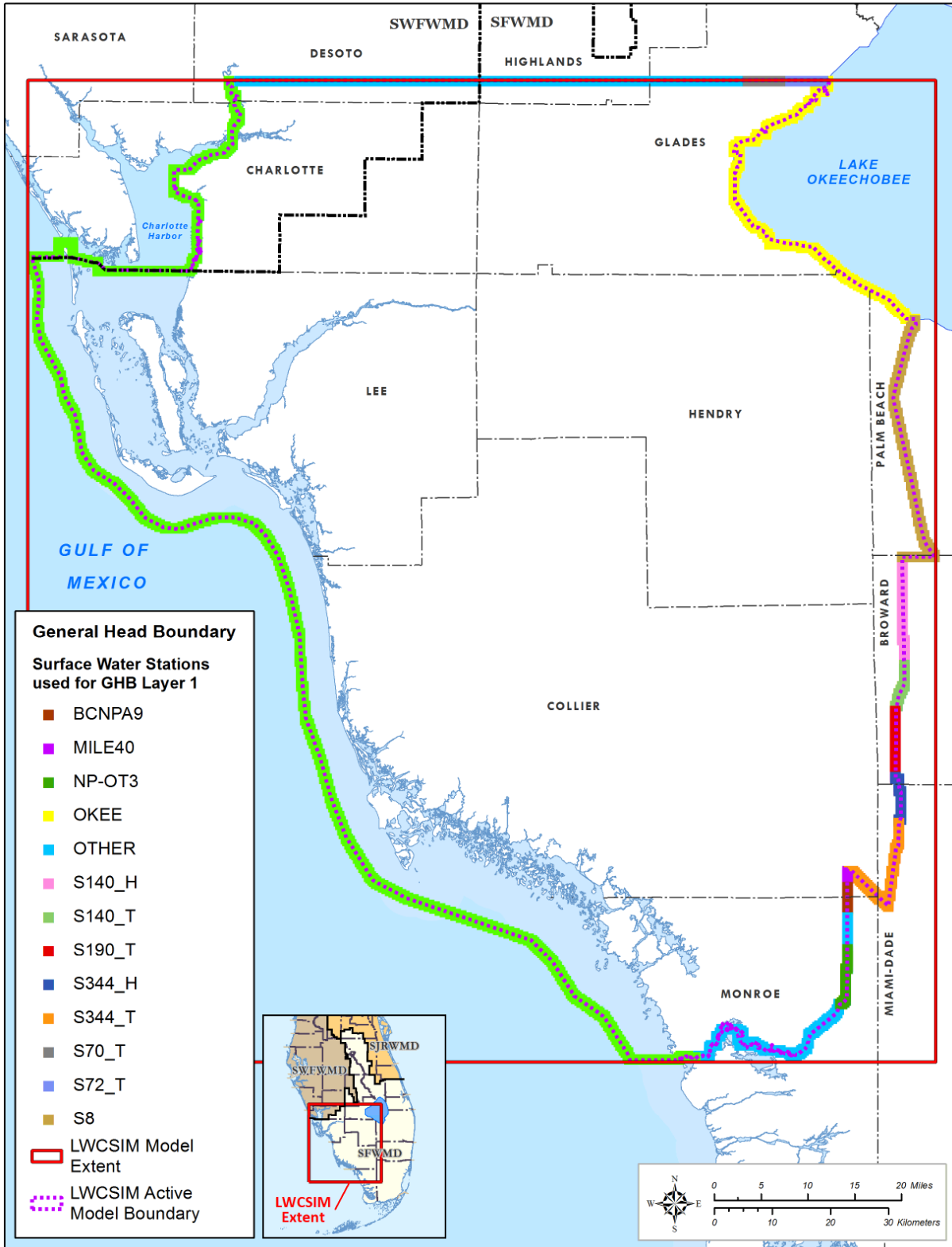


Figure 5-1. Location of the general head boundary, layers 1 through 9.



\\ad.sfwmd.gov\dfsroot\GIS\GSBiz\WLS\LWCSIM\Report_Figures\lrx\d\GHB_Surface_Water_Stations.mxd

Figure 5-2. Surface water stations used to develop the general head boundary in the Water Table aquifer.

5.1.1 General Head Boundaries

According to McDonald and Harbaugh (1988), a GHB consists of a water source outside the modeled area that supplies or removes water to a model cell at a rate proportional to the head difference in the active cell and the head assigned to the external source by the user. The rate at which water is supplied to a cell is given by equation (6):

$$Q = C \times (H_S - H_C) \quad (6)$$

Where:

Q is the flow rate (ft³/day) to or from the boundary cell

C is the constant of proportionality for the boundary (conductance)

H_S is the average head at the source boundary

H_C is the average head in the cell

Along the eastern border for the WTA (layer 1), initial conductance values were obtained from the LECsR Model (Giddings et al. 2006). For the northern, southern, and western boundaries, the conductance values were calculated using equation (7):

$$C = K \times B \quad (7)$$

Where:

C is the conductance value (ft²/day)

K is the hydraulic conductivity of the cell (ft/day)

B is the thickness of the layer (ft)

Hydraulic conductivities were interpolated from field measured data. Initial conductance values for the remaining layers also were determined by equation (7).

Conductance values were adjusted by PEST during the calibration process. The stages for the boundary heads vary horizontally and vertically. For the WTA and TCU, the boundary heads were based on monthly stages at the surface water stations, if available. If there were no adjacent surface water bodies, the boundary heads were based on topographic elevations and physiographic regions (White 1970). For the remaining layers, the boundary heads were based on the monthly estimated stage for the GHB cells. For the LWCSIM, the Gulf of Mexico was considered a physiographic region and divided into five parts to facilitate the PEST calibration.

MODFLOW is not a density-dependent model; therefore, water levels along the coast were adjusted based on total dissolved solids concentrations. There is a significant difference in density between fresh water and salt water when the total dissolved solids concentrations increase (**Table 5-1**).

Table 5-1. Density differences of water samples relative to total dissolved solids concentration.

| Temperature (°C) | Concentration (mg/L) | Density (kg/m ³) |
|------------------|----------------------|------------------------------|
| 23 | 50 | 997.606 |
| 23 | 500 | 997.948 |
| 23 | 5000 | 1001.345 |

°C = degrees Celsius; kg/m³ = kilograms per cubic meter; mg/L = milligrams per liter.

Note: Calculations based on <http://www.csgnetwork.com/h2odenscalc.html>.

According to **Figure 5-1**, there are active cells within the Gulf of Mexico and other saltwater bodies. These areas are tidally controlled. Data from the National Oceanic and Atmospheric Administration (2015) were used to obtain tidal stages. According to the National Oceanic and Atmospheric Administration (2015) there are two active tidal stations within the LWCSIM domain: Fort Myers and Naples (**Figure 5-3**).

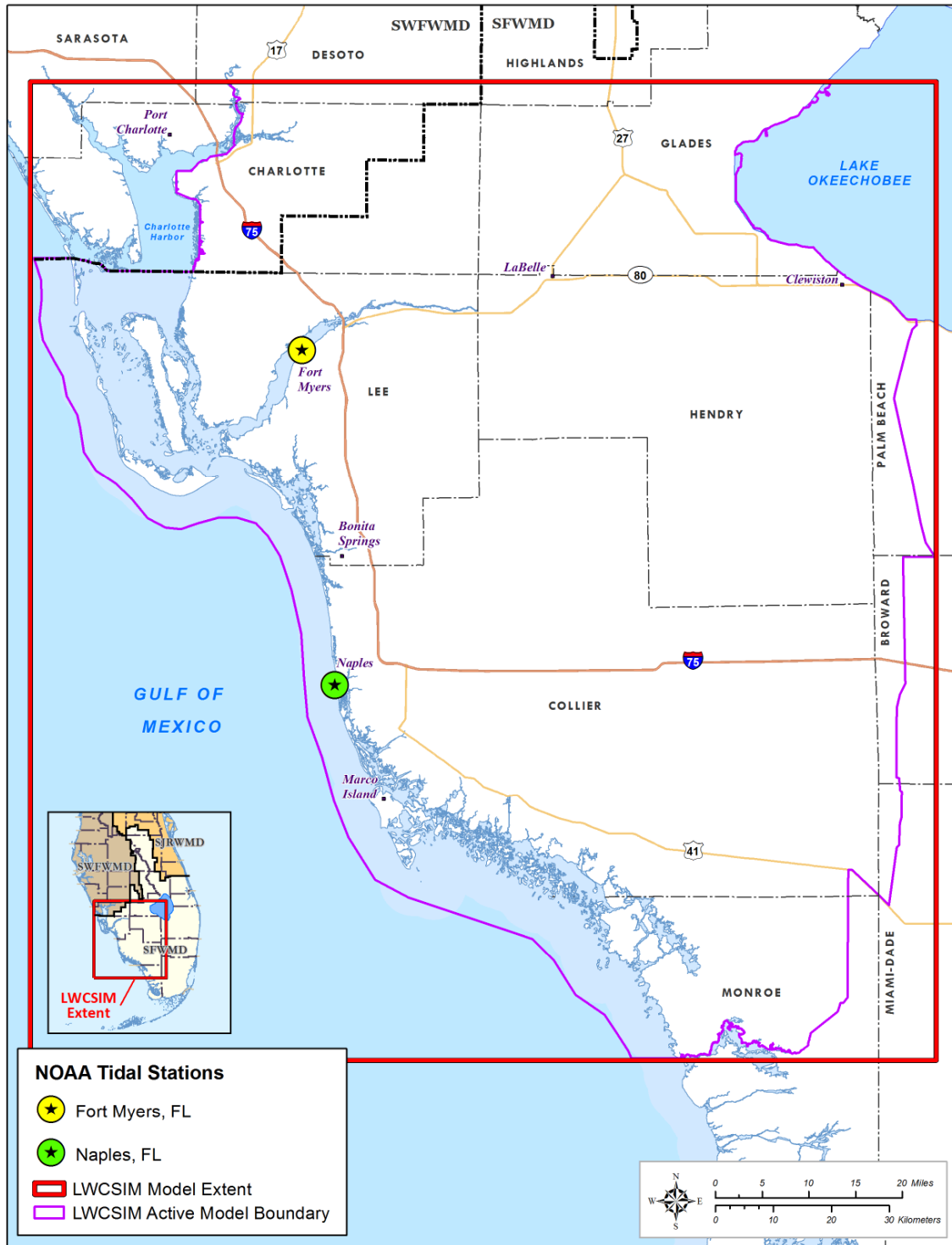


Figure 5-3. National Oceanic and Atmospheric Administration tidal stations.

Figure 5-4 is a hydrograph of the monthly stages at the Fort Myers and Naples tidal stations. Analyses of the data indicate the two stations have similar stages. Therefore, Fort Myers was chosen to represent stages in the tidal areas.

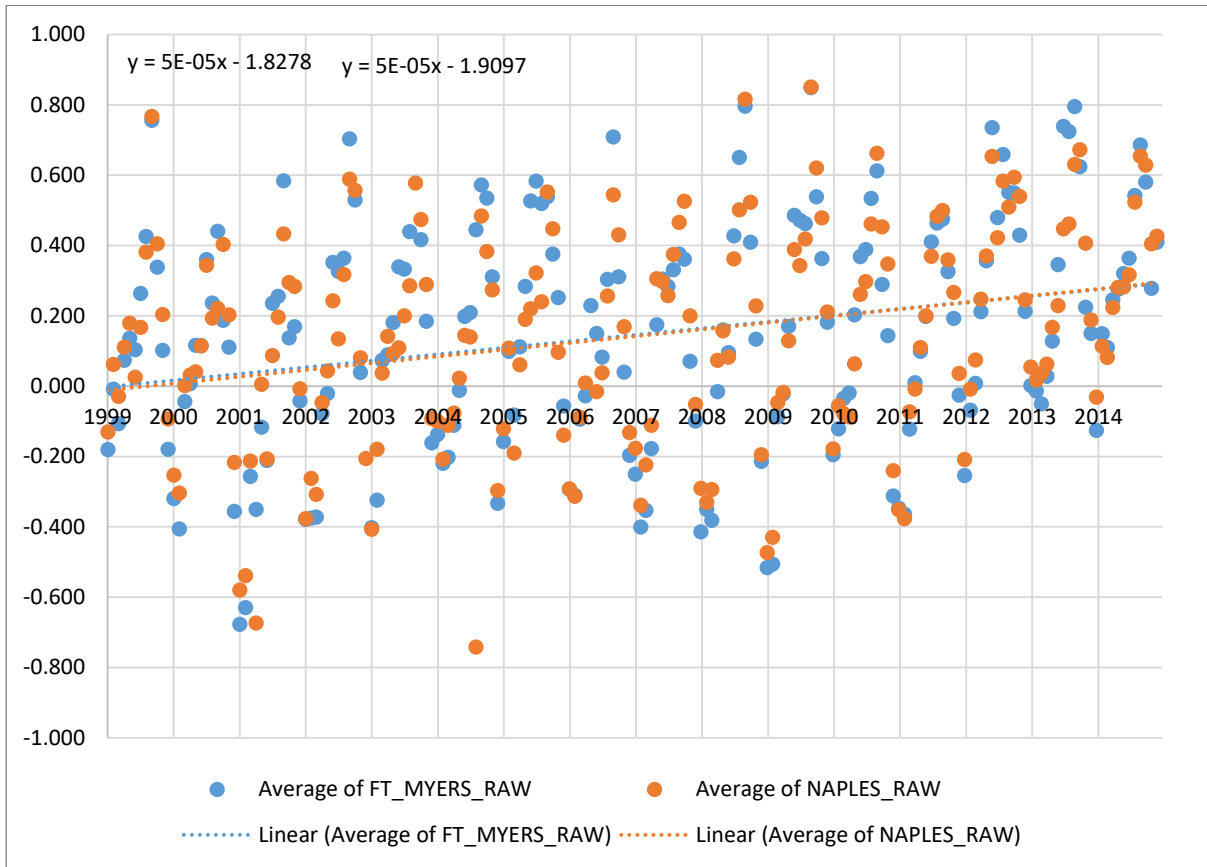


Figure 5-4. Average monthly stages (in feet mean sea level) at the Fort Myers and Naples tidal stations.

Because MODFLOW is not a density-dependent model, water levels along the coast needed to be converted to an equivalent freshwater head. The following procedure was used to estimate the equivalent freshwater heads. Beach and Hood (2003) used equations (8) through (11) from Lusczynski (1961) to calculate the equivalent freshwater head. In addition, water level data from observation wells with total dissolved solids concentrations greater than 5,000 milligrams per liter (mg/L) were corrected with the same procedure.

$$htf = hpf + Zi \quad (8)$$

$$hpf = sg(Zwl - (Zlc - Dcsg)) \quad (9)$$

$$Zi = Zls - Dcsg \quad (10)$$

Therefore:

$$htf = \left(sg(Zw - (Zls - Dcsg)) \right) + (Zls - Dcsg) \quad (11)$$

Where:

htf is the total freshwater head in the well
 hp is the pressure head in the well
 hpf is the freshwater pressure head in the well
 Z_i is the elevation at base of casing
 Z_{ls} is the land surface elevation
 Z_{msl} is sea level, elevation = 0
 Z_{wl} is the measured water level elevation
 D_{csg} is the casing depth, below land surface
 sg is the specific gravity of water in the well

5.2 Initial Conditions

5.2.1 Initial Heads

Starting heads were prepared for the steady-state model layers using the following methodology. January 1999 was used as the starting date.

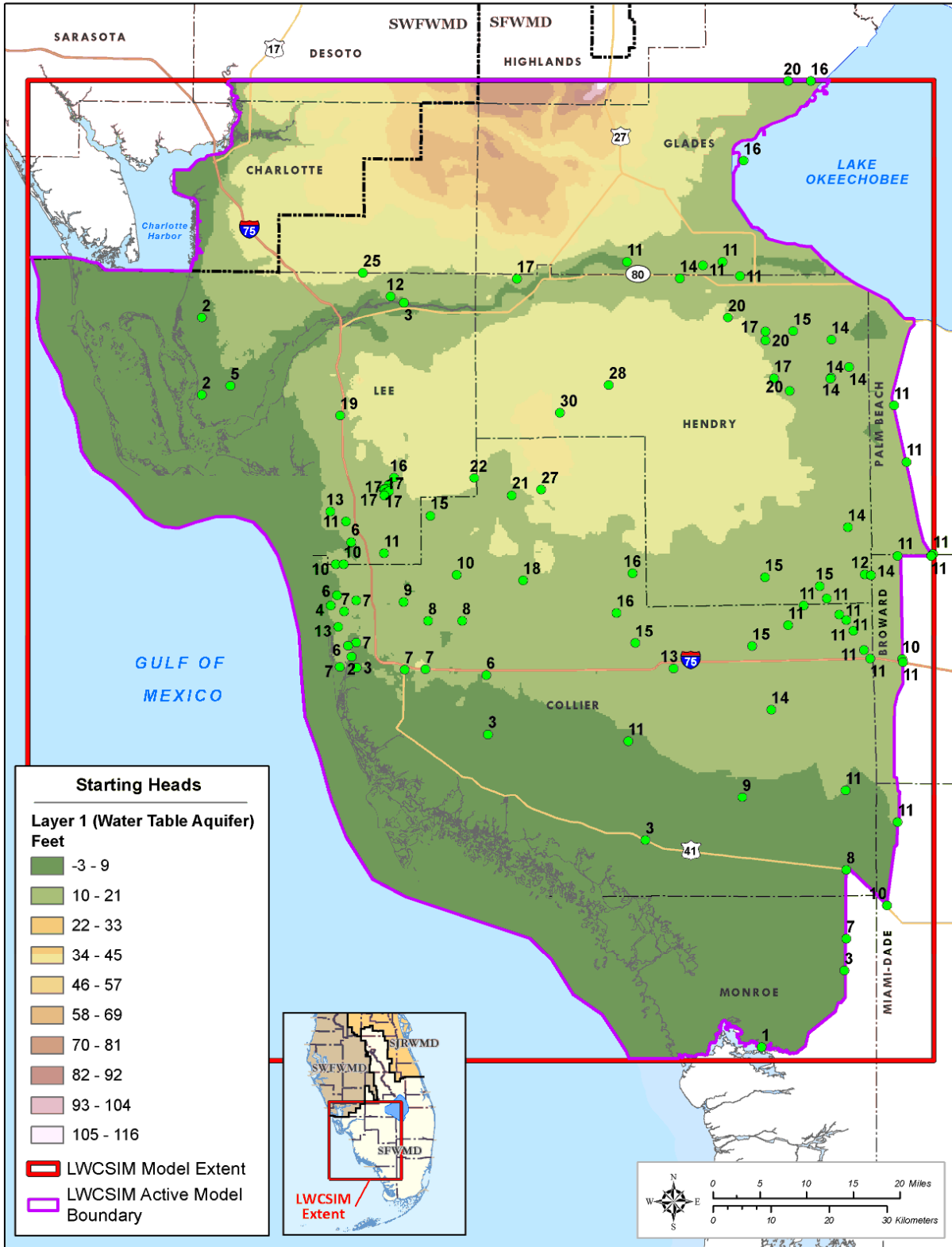
1. Groundwater levels and surface water stages were collected and compiled from databases maintained by the SFWMD (DBHYDRO), United States Geological Survey (USGS), and SWFWMD. Groundwater levels were assigned to the appropriate aquifer layer based on well construction and hydrostratigraphic layer definitions. Surface water levels were applied to layer 1 to augment the groundwater data.
2. Topographic data and a water level contour map from the nearby DWRM (Environmental Simulations, Inc. 2014) were used to supplement layer 1.
3. The Geostatistical Analyst (a commercially available geostatistical tool) was used to determine the best interpolation method and compare the results with the actual data.
4. Once reasonable results were obtained, the starting heads for the confining units were calculated by averaging the two adjacent aquifers. For example, the starting heads for the TCU were calculated using equation (12):

$$H_{TCU} = (H_{WTA} + H_{LTA}) \div 2 \quad (12)$$

Where:

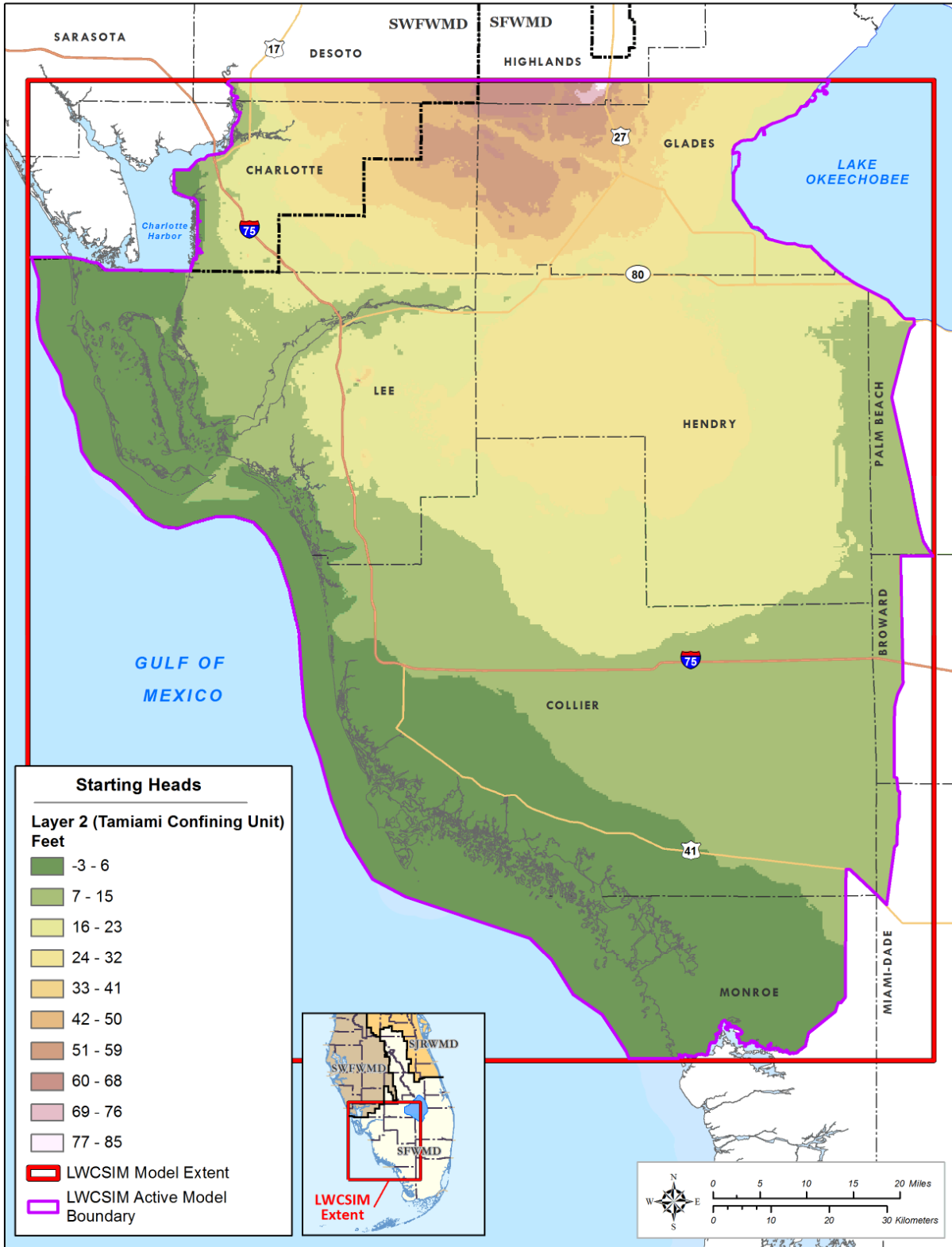
H_{TCU} is the water level in the TCU
 H_{WTA} is the water level in the WTA
 H_{LTA} is the water level in the LTA

Figures 5-5 through 5-13 provide the starting heads in January 1999 for each model layer. These data were used for the steady-state model. Once the steady-state model was calibrated, the resulting heads were used for the transient version of the LWCSIM.



\\ad.sfwmd.gov\dfsroot\GIS\GISB\z\WLS\LWCSIM\Report_Figures\mxd\StartingHeads_WTA_Lyr1.mxd

Figure 5-5. Starting heads of the Water Table aquifer.



\\lad.sfwmd.gov\dfsroot\GIS\GSB\z\WS\LWCSIM\Report_Figures\mxd\StartingHeads_TCU_Lyr2.mxd

Figure 5-6. Starting heads of the Tamiami confining unit.

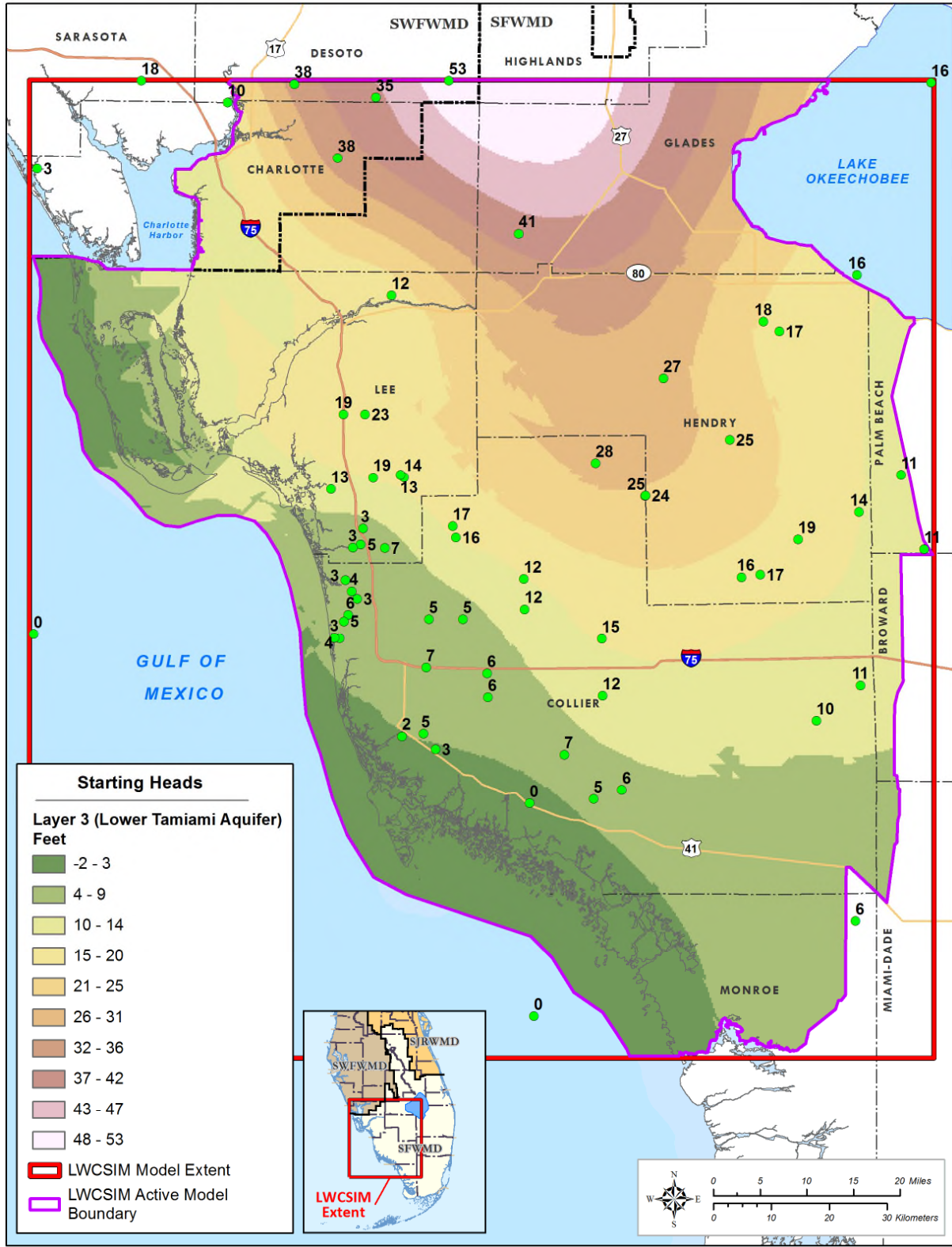
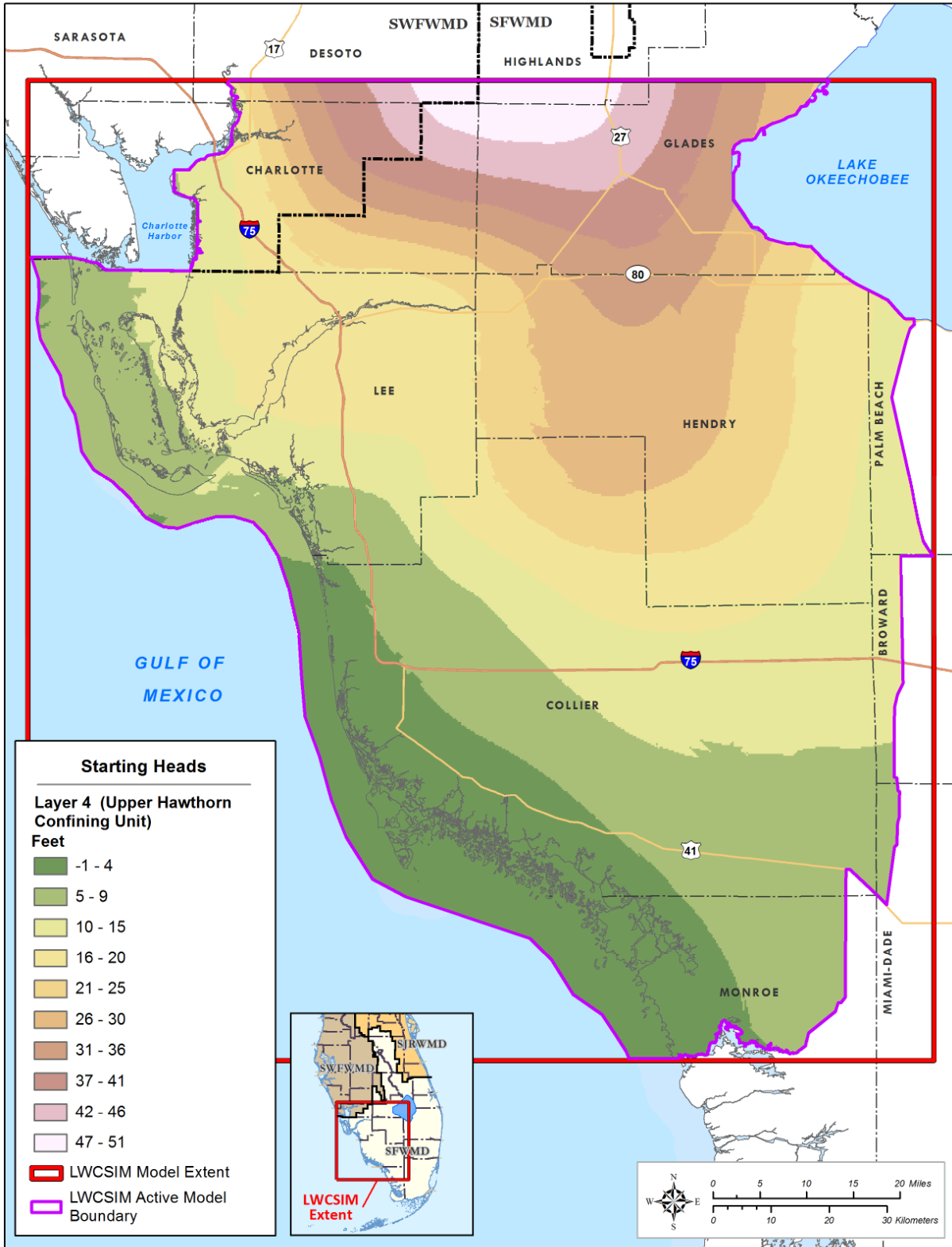
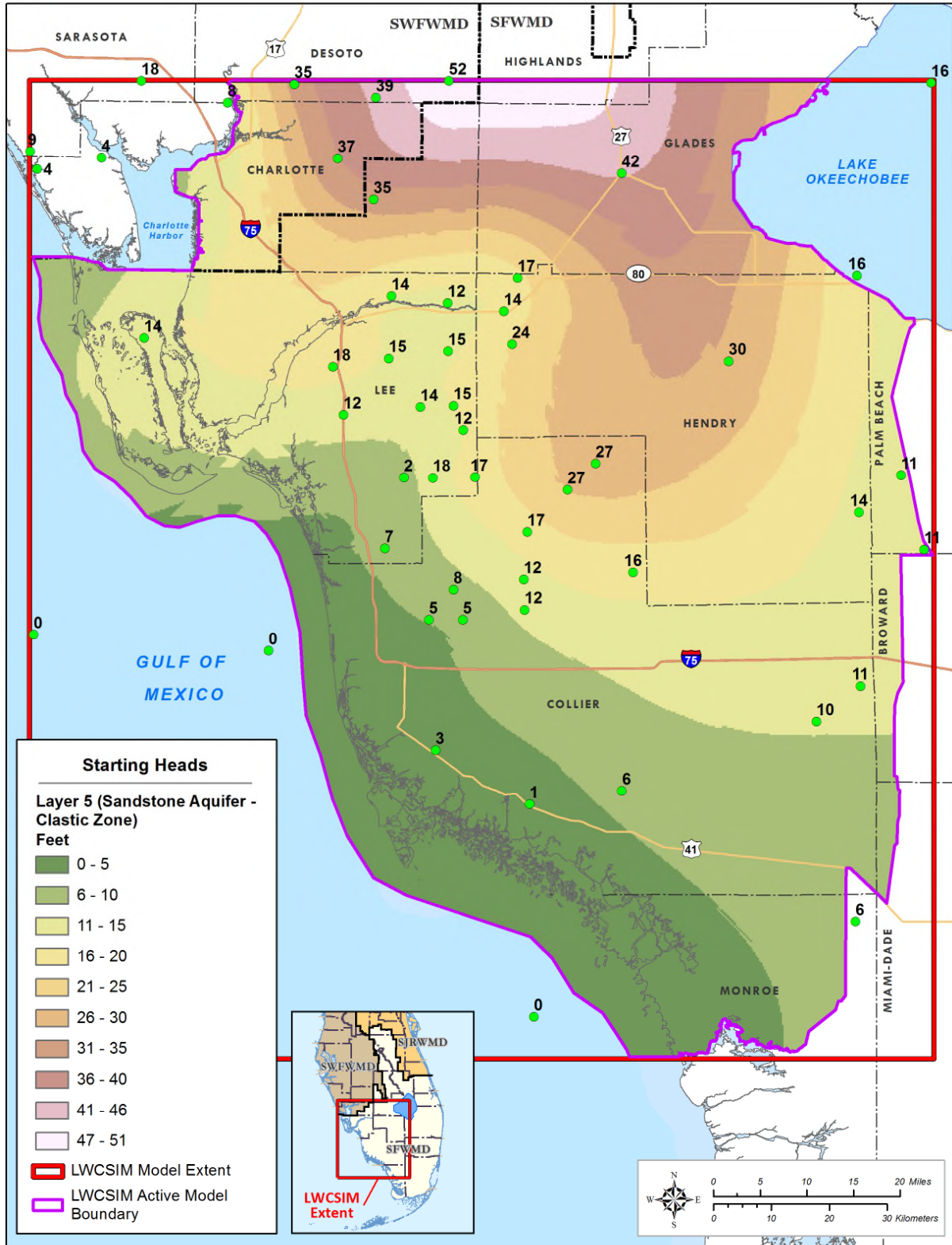


Figure 5-7. Starting heads of the Lower Tamiami aquifer.



\\ad.sfwmd.gov\dfsroot\GIS\GSB\iz\WS\LWCSIM\Report_Figures\mxd\StartingHeads_UHC_Lyr4.mxd

Figure 5-8. Starting heads of the Upper Hawthorn confining unit.



\\ad.sfwmd.gov\dfsroot\GIS\GSBizi\SWLWCSIM\Report_Figures\mxd\StartingHeads_SAC_Lyr5.mxd

Figure 5-9. Starting heads of the Sandstone aquifer, clastic zone.

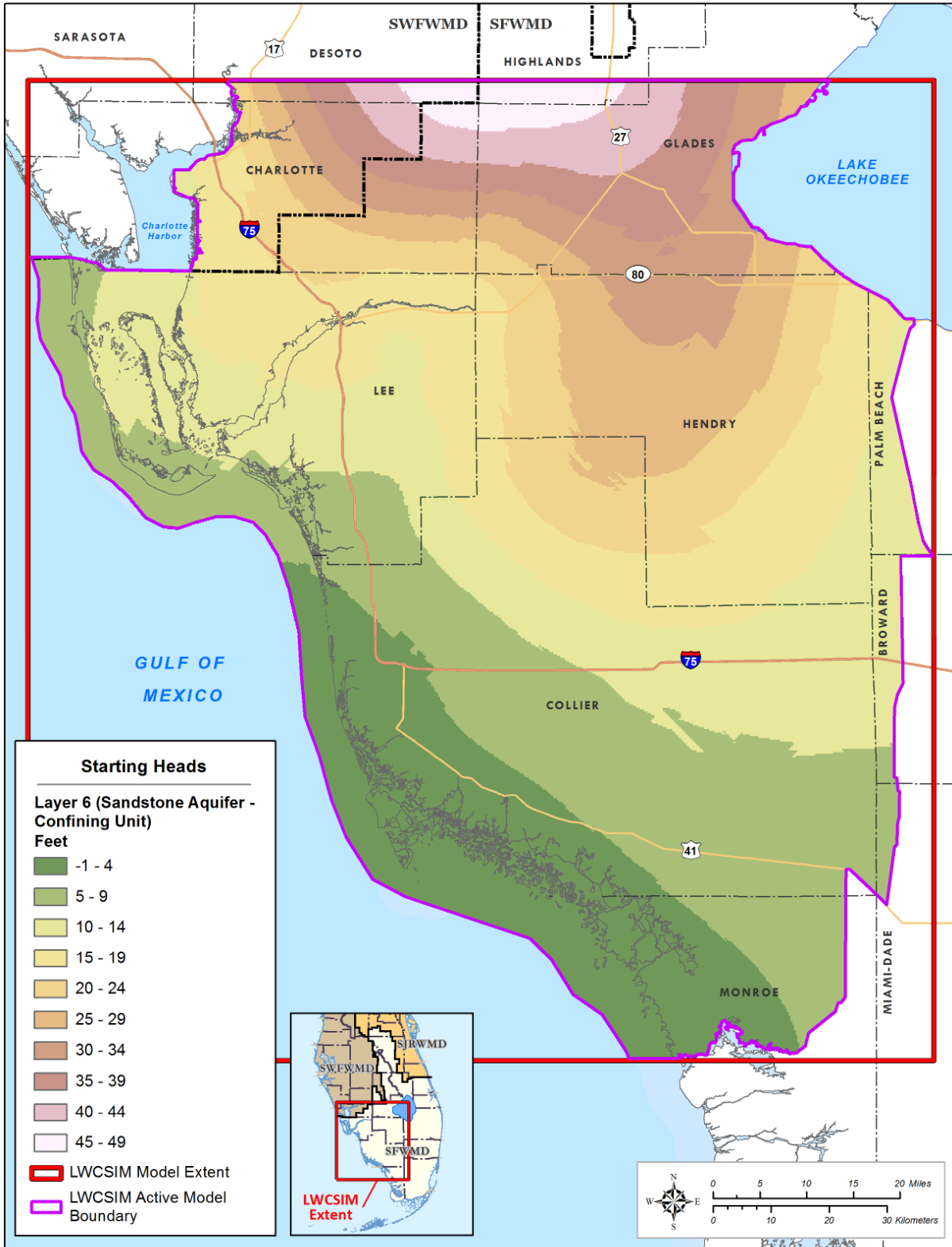
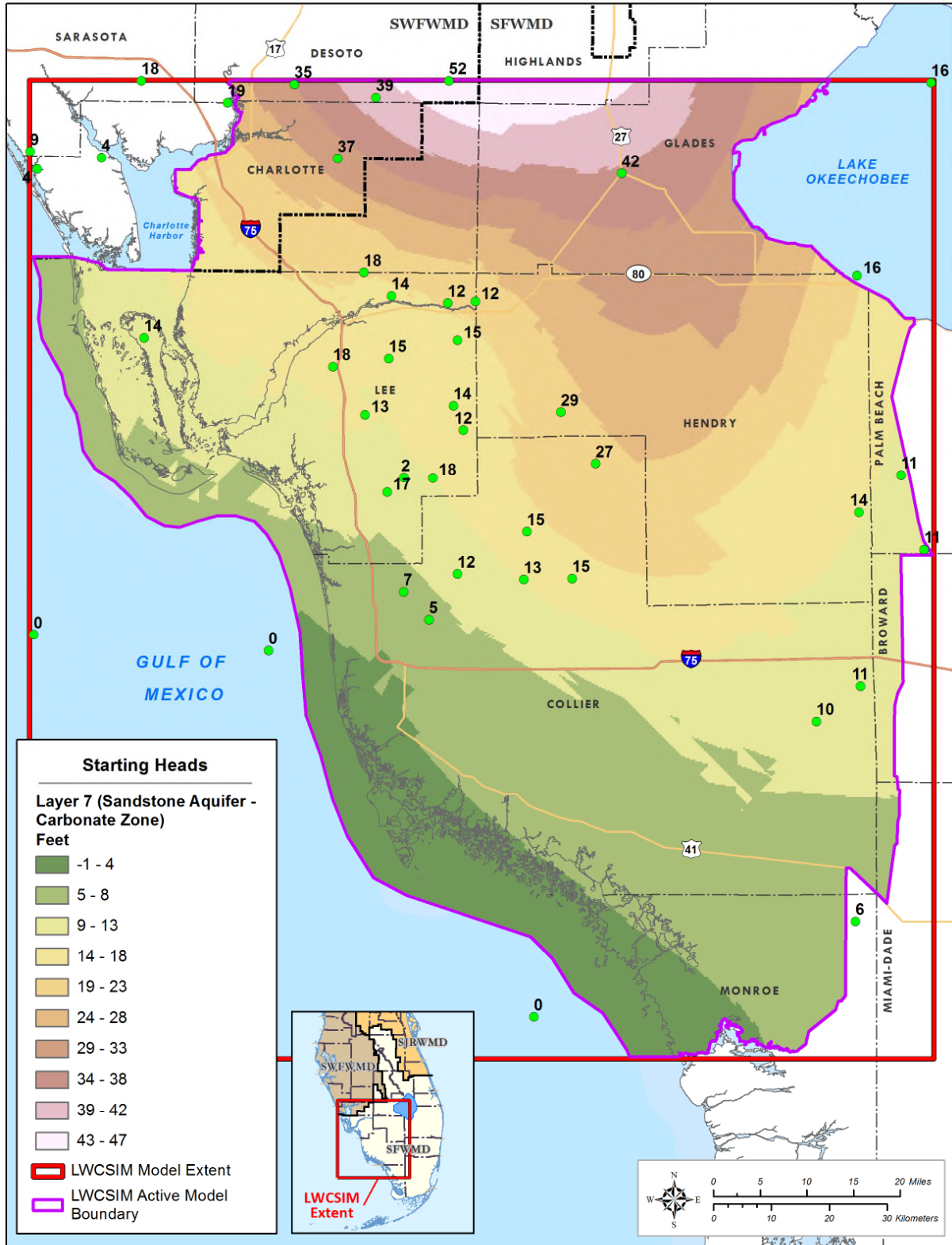
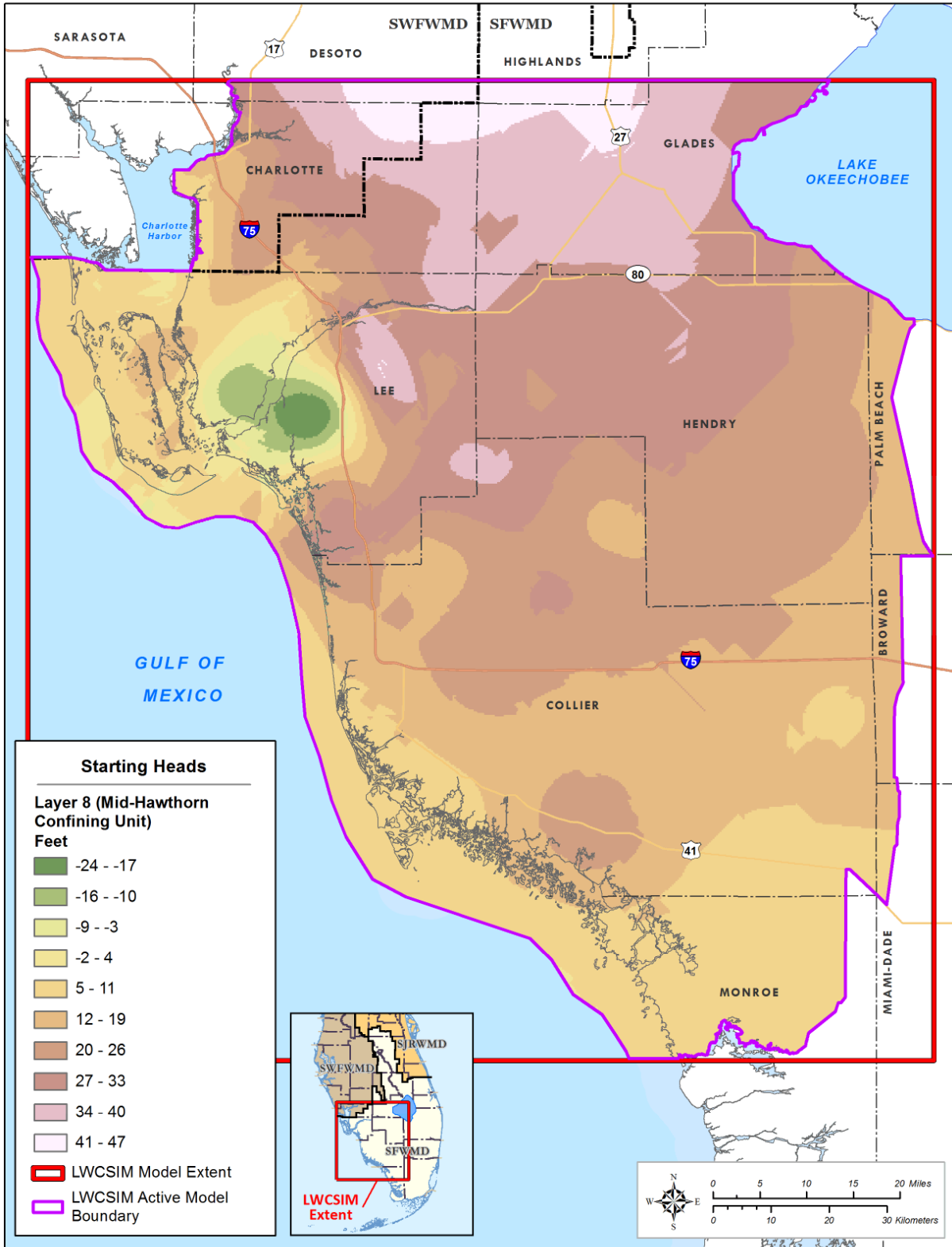


Figure 5-10. Starting heads of the Sandstone aquifer confining unit.



\\ad.sfwmd.gov\dfsroot\GIS\GISBizi\WS\LWCSIM\Report_Figures\mxr\d\StartingHeads_SAC_Lyr7.mxd

Figure 5-11. Starting heads of the Sandstone aquifer, carbonate zone.



\\ad.sfwmd.gov\dfsroot\GIS\GISBiz\IWS\LWCSIM\Report_Figures\mxd\StartingHeads_MHC_Lyr8.mxd

Figure 5-12. Starting heads of the Mid-Hawthorn confining unit.

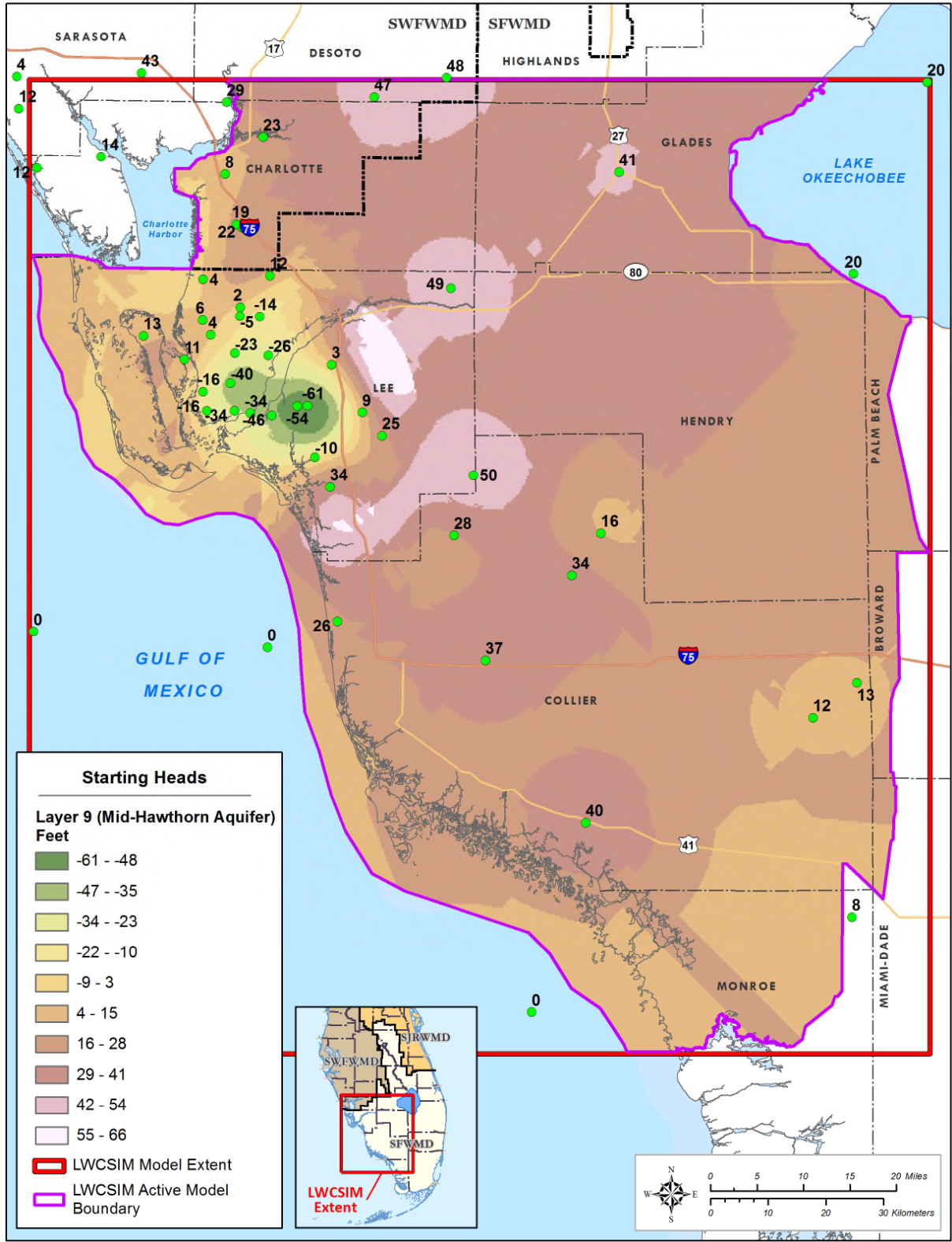


Figure 5-13. Starting heads of the Mid-Hawthorn aquifer.

5.3 Rivers

The primary and secondary rivers/canals data set of the SFWMD's Arc Hydro Enhanced Database and the USGS's National Hydrography Dataset were overlaid to evaluate the consistency of the data. The rivers/canals attributes were triangulated and accessed from:

1. Caloosahatchee River Basin Integrated Surface Water – Groundwater Model (SFWMD 2004). The model uses SFWMD surveys and past study documentations of canal design and surveys.
2. SFWMD river/canal surveys.
3. BCB Integrated Hydrological Model (DHI Water and Environment 2002, Atkins 2011). The DHI Water and Environment (2002) study covers the Tidal Caloosahatchee River Basin, Estero Bay, the BCB, the freshwater Caloosahatchee (C-43) River, and the Picayune Strand Restoration Project.
4. The DHI Water and Environment (2002) report claims data were acquired from United States Army Corps of Engineers (USACE) and SFWMD surveys as well as past studies.
5. South Florida Regional Simulation Model canal input data documentation, with data from SFWMD and USACE surveys and studies regarding:
 - a. Central and Southern Florida Flood Control Project (C&SF Project) primary canals for the Lower East Coast Planning Area and water conservation areas, including selected secondary canals for the Lower East Coast Planning Area
 - b. C-44 Canal attributes from the WaSh (URS 2008) modeling study
 - c. Everglades Agricultural Area MIKE-SHE modeling study canals
 - d. South West Florida Feasibility Regional Simulation Model study canals
6. The LWC SAS model (Marco Water Engineering, Inc. 2006), which considered the canal detail designs from the USACE, multi-version canal GIS coverages used in the Regional Simulation Model, and canal cross-section data used in the MIKE11 model for a previous SFWMD project in the Naples area.

Rivers in the LWCSIM principally include the SFWMD's primary and secondary canals and other perennial rivers and streams (**Figure 5-14**). In addition to rivers and streams, surface water bodies that were not included in the Wetlands package were included in the River package. Thus, Lake Trafford was modeled as a river. The LWCSIM uses the MODFLOW River package to simulate river flows. The MODFLOW River package was used instead of the more advanced MODFLOW Stream Flow Routing package to keep model execution and preprocessing times manageable.

In MODFLOW, a river is a head-dependent boundary condition. The MODFLOW River package requires riverbed conductance and river stage as inputs to estimate the river-aquifer leakage. Riverbed conductance (C) is calculated by equation (13):

$$C = (K \times L \times W) \div M \quad (13)$$

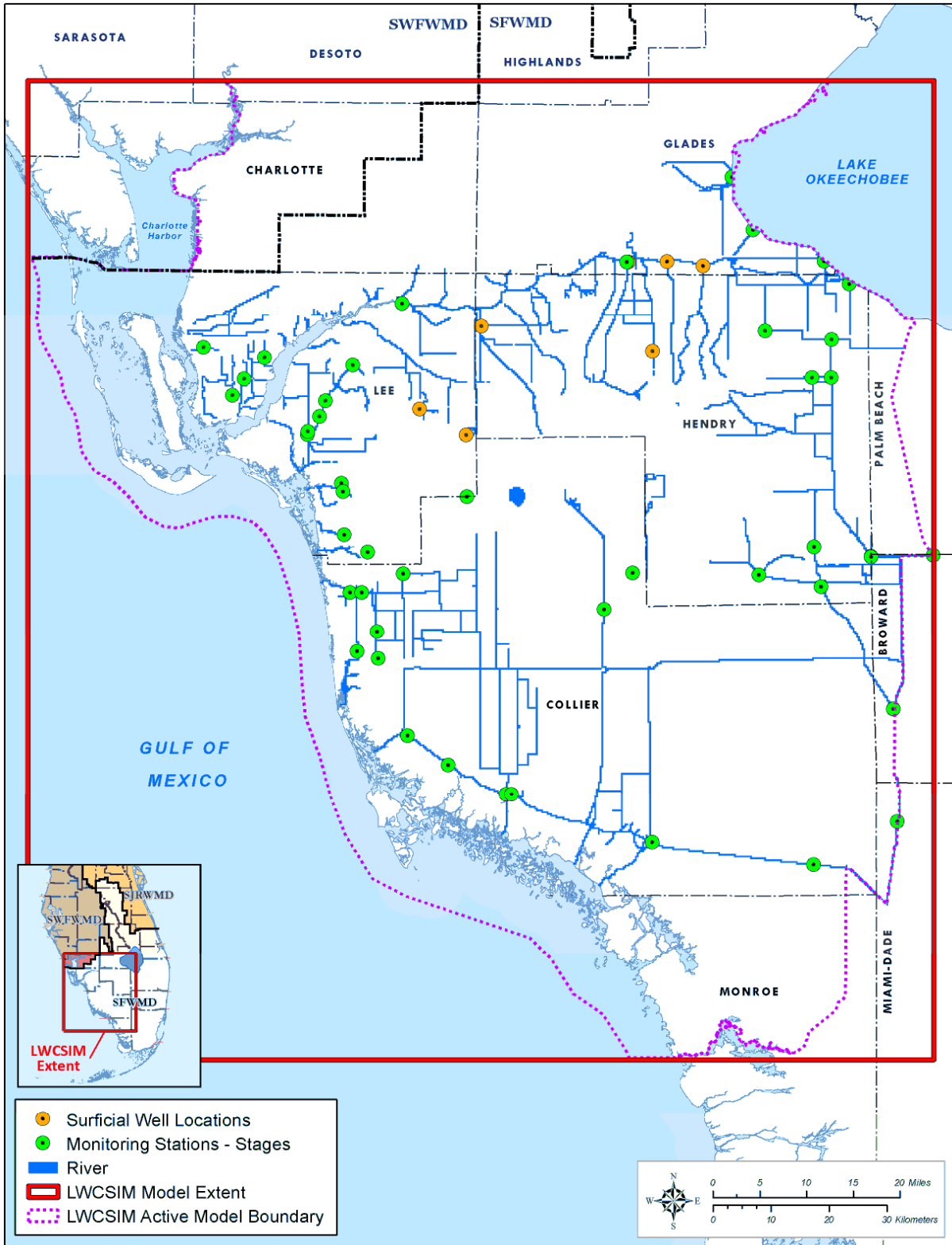
Where:

K is the vertical hydraulic conductivity of the riverbed sediment

W is the width of the riverbed

L is the length of the river segment within a model cell

M is the thickness of the riverbed sediment



\\ad.sfwmd.gov\dfsroot\GIS\GISBz\WS\LWCSIM\Report_Figures\mxd\LWCSIM_Rivers.mxd

Figure 5-14. Location of rivers simulated in the model.

Cross-sectional and hydraulic characteristics were assigned to each model cell where rivers were identified. This included assigning reaches to model grid cells and determining river bottom elevations and area within each cell. As stated earlier, the cross-sectional data were triangulated from multiple sources, whereas K and riverbed sediment thickness data, except for Lake Trafford, were obtained from the calibrated values of the Marco Water Engineering, Inc. (2006) model. The calibrated K and sediment thickness were used as initial values for the LWCSIM. Aerial photographs were used for triangulation and estimation of the interpolated canal top widths. The missing bottom elevations of primary or secondary canals were estimated from USACE (1957, 1961, 1962, 1969) design books or GIS coverages from other SFWMD projects. River lengths were obtained from the National Hydrography Dataset or the Arc Hydro Enhanced Database. For Lake Trafford, bathymetric data were obtained from the SFWMD, sediment thickness was derived from ART Engineering, LLC's (2004) geophysical survey, and K was estimated based on the nearest riverbed values.

River stage data were needed to estimate leakance in and out of the rivers to the aquifers. When gauge stations were available, observed stages were used. However, in many cases river tributaries are not monitored; thus, various methods were used for river stage estimation depending on the circumstance.

- **Method 1:** River stage level was interpolated for model cells between two gauge stations. Linear interpolation was based on river flow direction(s) and calculating a slope between two gauge stations' water levels and the distance of each grid node from the origin of one of the stations.
- **Method 2:** For some river grid cells, especially tributaries of main rivers where the upstream monitoring station is absent, water levels from shallow groundwater wells near tributaries on the upstream side were used as surface water level approximations. Where tributary rivers are connected to gauged rivers, the interpolated data of the model cell at the junction of the center of the tributary and the main river were used as the downstream data source.
- **Method 3:** Some tributaries in the Caloosahatchee River do not have surface water gauge stations or shallow groundwater wells. In these cases, riverbank elevations, riverbed elevations, and aerial imagery of the rivers were analyzed. The stage in these cells was estimated to be 4 ft below the riverbank elevation.
- **Method 4:** For the Cape Coral area, where a complex network of canals exists and water level slopes seem unrealistic, the stage was estimated as the average from multiple stations.

In addition to areas where gauge stations were not present, there also were instances when river stage data were missing. For this modeling effort, incomplete stage data at multiple monitoring stations were filled using the method described in **Appendix D** (Chebud and Melesse 2011).

5.4 Drains

Drains in the LWCSIM represent most of the SFWMD's tertiary canals in the region (**Figure 5-15**). These are surface water routing features and are restricted to the top layer of the model. The SFWMD's Wetlands package was used in the steady-state and transient models to represent wetlands in the top layer.

In MODFLOW, a drain is a head-dependent boundary condition. In a drain cell, the flow of water out of the aquifer depends on the assigned head and the conductance term. The head is compared to the computed head in the aquifer for the cell containing the drain. If the aquifer head is higher than the drain head, then the drain removes water from the aquifer. If the drain head is higher than the aquifer head, then the drain is considered to be dry and no water is removed or added to the aquifer. The amount of water removed is based on the conductance calculated by equation (13).

To develop the LWCSIM Drain coverage, two GIS coverages were used: 1) the National Hydrography Dataset, medium resolution, and 2) the digital elevation model for South Florida, light detection and ranging (LiDAR) 10 ft, found in the SFWMD's Geospatial Data Library. The procedure used to extract the drain coverage for use in MODFLOW is described in detail in **Appendix E**.

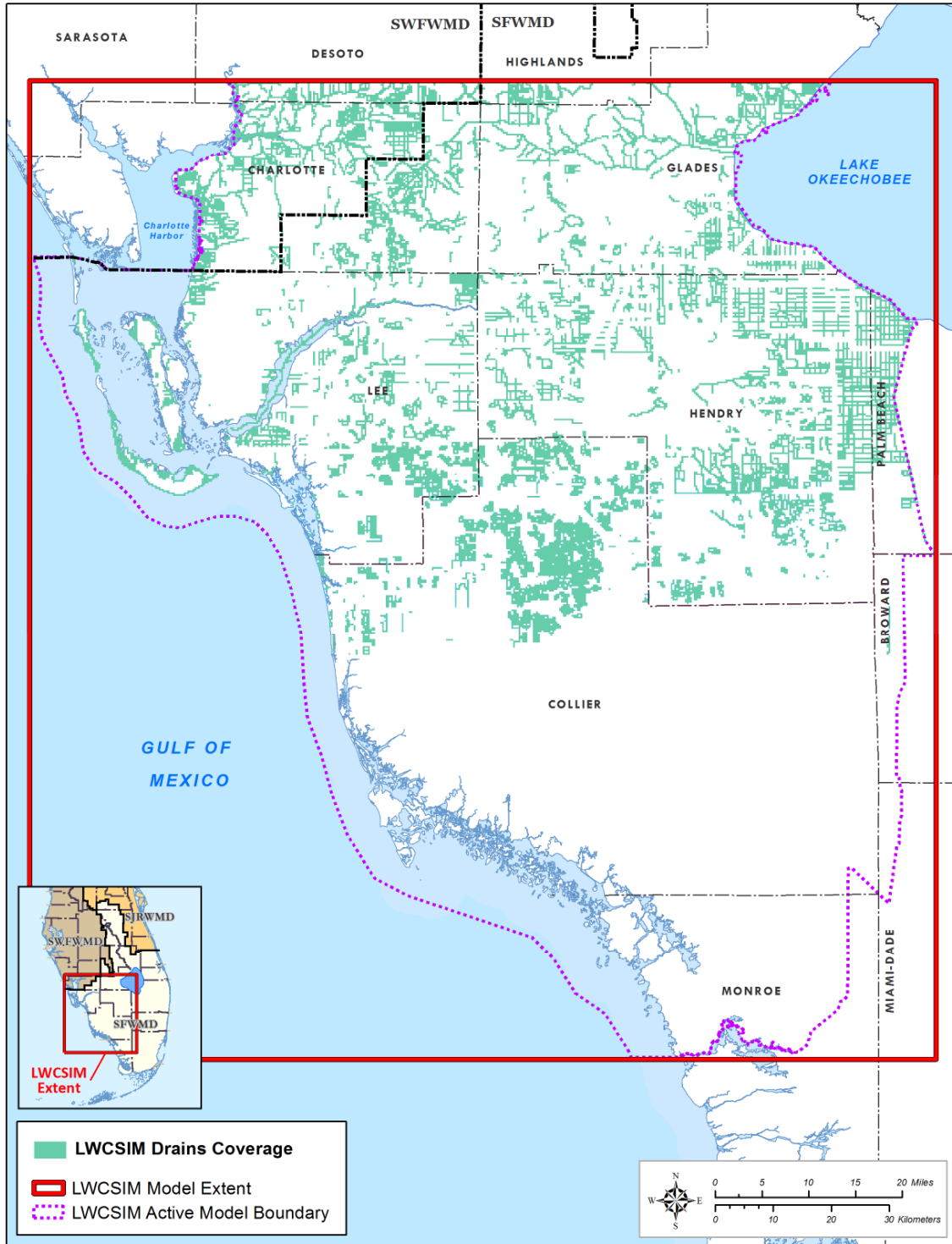


Figure 5-15. Location of drains used in the model.

5.5 Wetlands

The 2000 land use/land cover map (**Figure 2-12**) of the LWC Planning Area shows a substantial portion of the top layer of the model area is covered in wetlands, especially in the southern half of the model area (**Figure 5-16**). The Wetlands package was developed in 1998 by the SFWMD and the Hydrological Research Center at Florida Atlantic University to fulfill the need for a sound, physically based representation of wetlands and surface water/groundwater interaction. The Wetlands package accounts for sheet flow, wetting and drying, ET, and the vertical and horizontal flux components of the wetland/aquifer interaction (Restrepo et al. 1998).

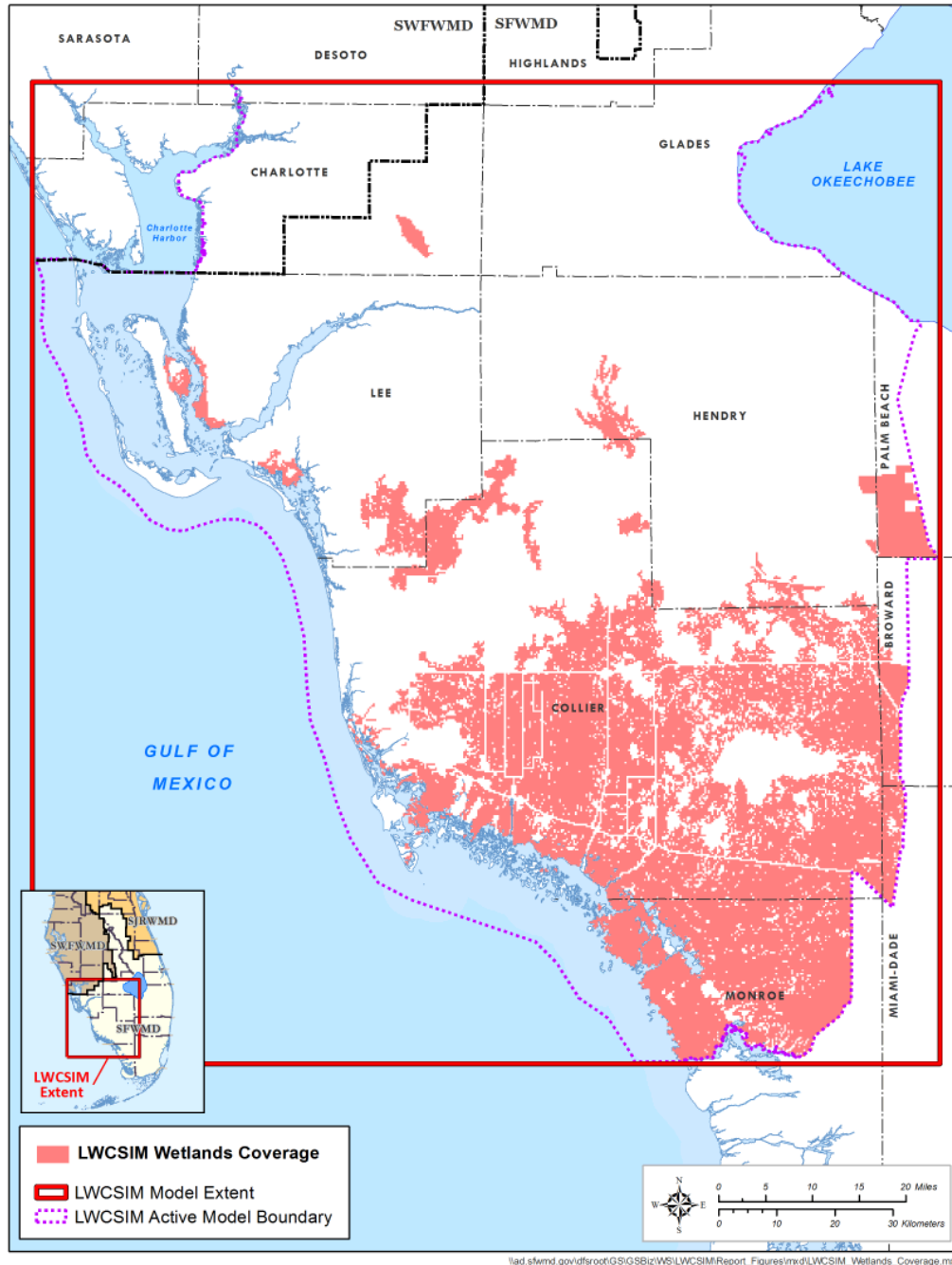


Figure 5-16. Wetlands coverage in the model.

Surface water flow is treated in two broad categories: sheet flow through dense vegetation, and channel flow through a slough network. The Wetlands package uses a semi-empirical Manning-type equation rather than Darcy’s Law to represent surface water movement through dense vegetation. An explanation of the mathematical formulations for the Wetlands package may be found in Restrepo et al. (1998). Wetland cells are always simulated in layer 1. This package gives the user the option of simulating the wetland as an individual layer or embedding it within the aquifer.

Channel flow in wetlands can occur through sloughs, canals, airboat trails, and lakes, which act as preferential flow paths for surface water in wetlands. Levees also can influence flow patterns in wetlands by acting as barriers to surface water flow. Preferential flow paths created by channels or local flow barriers can be simulated by specifying different anisotropic ratios for each wetland cell. This feature of the Wetlands package required modification to the original MODFLOW Block Centered Flow package, which holds the anisotropy factor constant throughout the layer. The establishment of preferential flow paths requires the user to specify which cell faces in the modeled feature are perpendicular to flow (in the case of barriers) or toward the direction of flow (for channels). Cell faces are numbered by convention as shown in **Figure 5-17**.

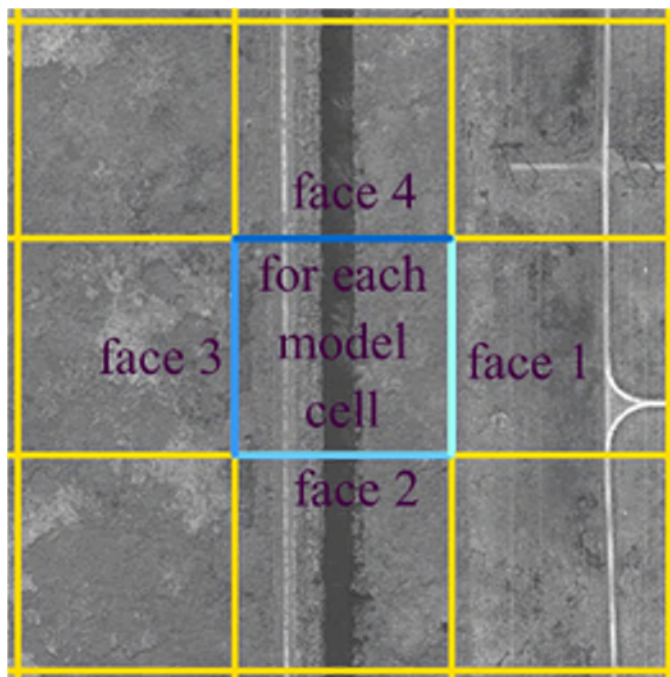


Figure 5-17. Convention for numbering cell faces in the MODFLOW Wetlands package.

Multipliers were applied to the selected cell faces to increase (in the case of channels) or decrease (in the case of levees) the interblock conductivity. **Figure 5-18** represents a levee (in orange) acting as a barrier to flow occurring from left to right across the graphic, by specifying cell faces 2 and 3. In this case, face 3 is designated as primary and face 2 is secondary.

Use of the Wetlands package in MODFLOW 2005 required several input data files defining the wetland cell, Kh of the soil type in that cell, vertical anisotropy, capillary fringe, and Kadlec number. These are prepared separately from the MODFLOW model, and the inclusion of a call file and the above data files in the MODFLOW name file incorporate the Wetlands package into the model run. **Appendix F** presents a detailed description of the GIS procedure used to build the wetlands coverage.

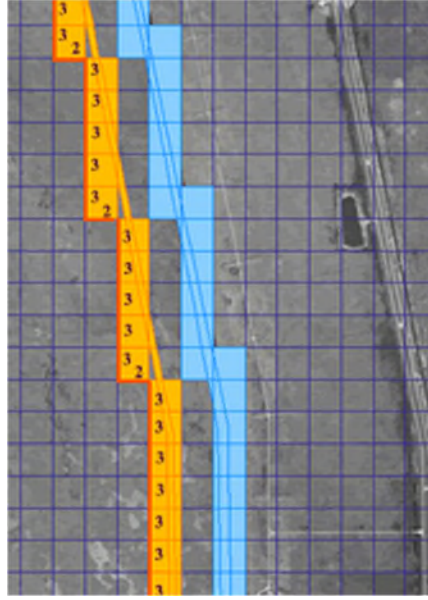


Figure 5-18. Example of a levee acting as a barrier to flow in the MODFLOW Wetlands package.

5.6 Landscape Irrigation Return Flow

Landscape irrigation (LSI) occurs generally in the residential/commercial mixed land use areas served by PS utility systems. LSI is an important component of the water balance that accommodates a portion of the reclaimed water flow and is combined with rainfall, potable water, and other irrigation water to satisfy landscape irrigation needs. The combined irrigation water applied to the land satisfies plant water needs, evaporates or is transpired, runs off, or infiltrates into the ground and percolates to the water table to complete the water cycle.

PS utility service areas are the areas defined to receive LSI. The service areas are aggregated at the county level because of the complexity of characterizing the distribution of reclaimed water in the utility service areas for all the utilities in the LWC Planning Area. There often are instances where utilities' potable water, wastewater, and reclaimed water service areas overlap, and other instances where utilities serve potable, wastewater, and reclaimed water outside their service areas via agreements between utilities. Adequately capturing these complexities in the time frame available for this modeling effort was deemed infeasible. Therefore, distributing LSI water at the county level is considered a reasonable simplifying assumption to address this issue.

Potable and reclaimed water are the two sources of LSI water associated with PS systems. The portion of potable water applied as LSI (i.e., outdoor water use) was estimated by subtracting indoor water use from total PS pumping. For return flow, the total PS pumping includes not only pumping from the SAS/IAS but also from the Floridan aquifer system. Indoor water use is assumed to be equal to wastewater flow. The annual potable water use for LSI during the calibration period in the LWCSIM is shown in **Figure 5-19**. Only a portion of reclaimed water generated is used for LSI purposes, which was considered in this analysis. Historical wastewater treatment flows and reclaimed water use data were obtained from the Florida Department of Environmental Protection for municipal wastewater systems. Historical reclaimed water LSI quantities were extracted based on the assumptions noted above. Reclaimed water used for LSI during the calibration period for Lee and Collier counties is shown in **Figure 5-20**. These calculations were compiled at the county level for input to the LWCSIM. There are no major potable or reclaimed water uses outside Lee and Collier counties; thus, LSI return flows were not calculated for Charlotte, Hendry, Glades, or Monroe counties.

Once the LSI rates were developed, they were added to the rainfall array and processed through the CN method to estimate recharge and runoff. Spatial distribution of LSI application rates from 1999 are shown in **Figure 5-21**. Development of the LSI data set for the LWCSIM is described in **Appendix G**.

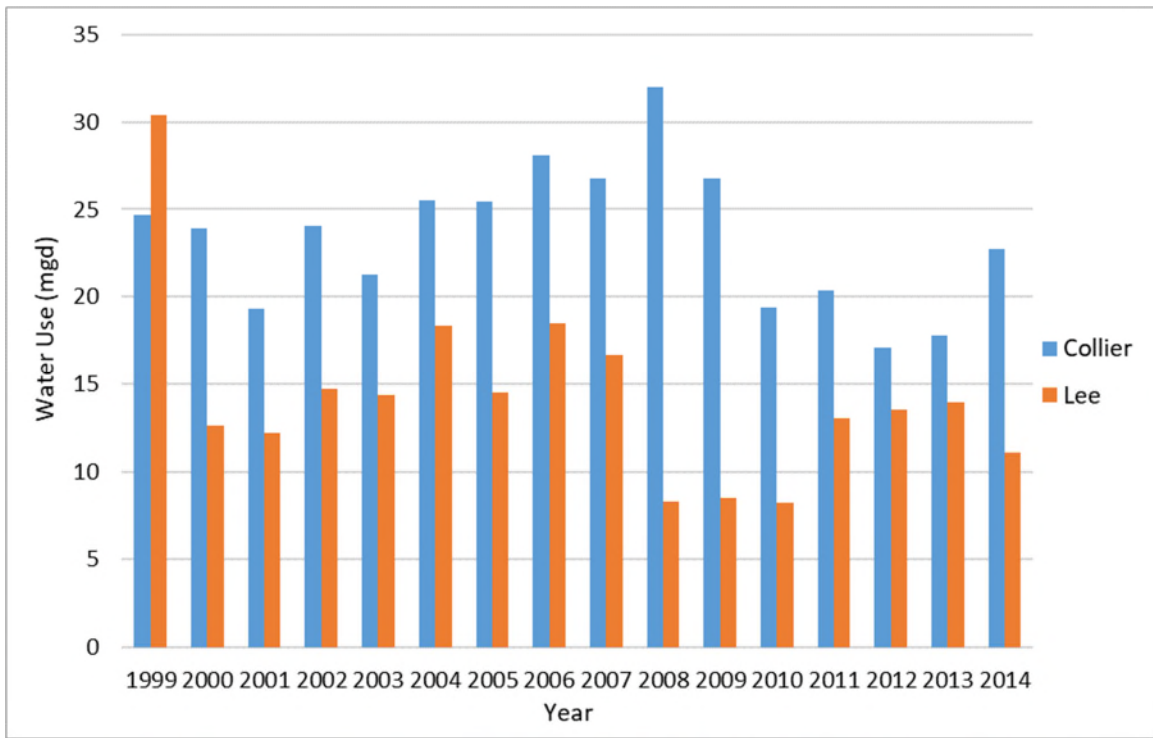


Figure 5-19. Potable water used for landscape irrigation in the model.

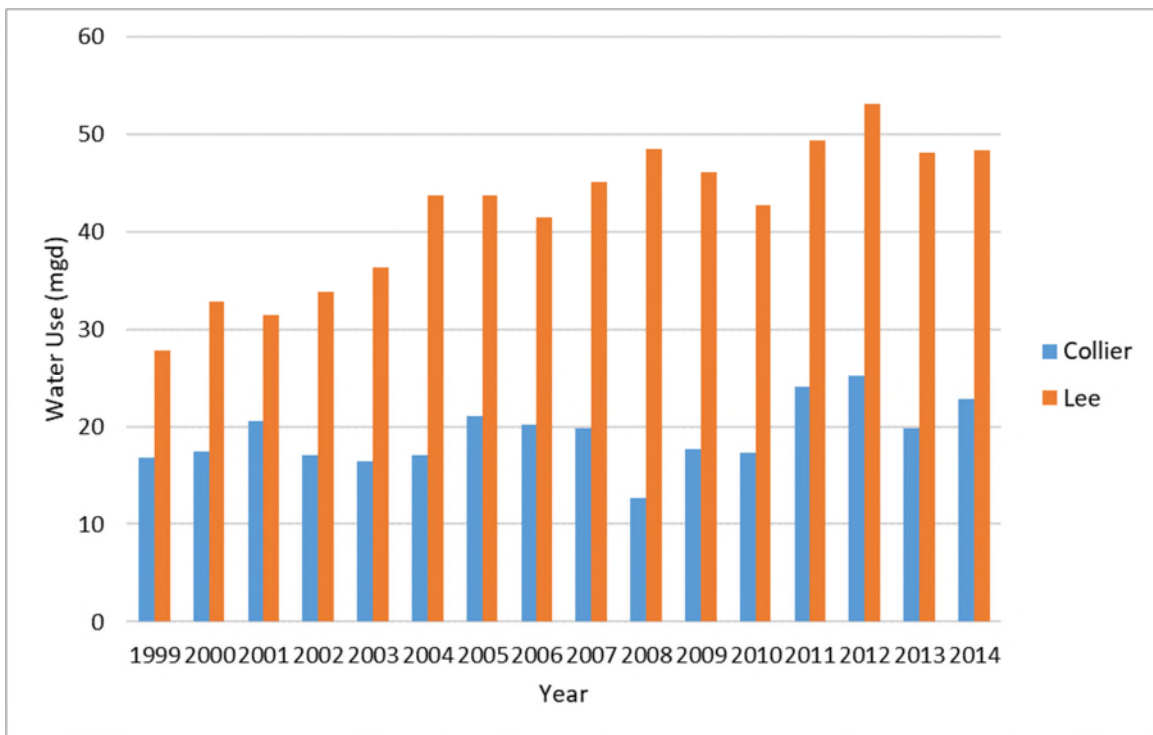


Figure 5-20. Reclaimed water used for landscape irrigation in the model.

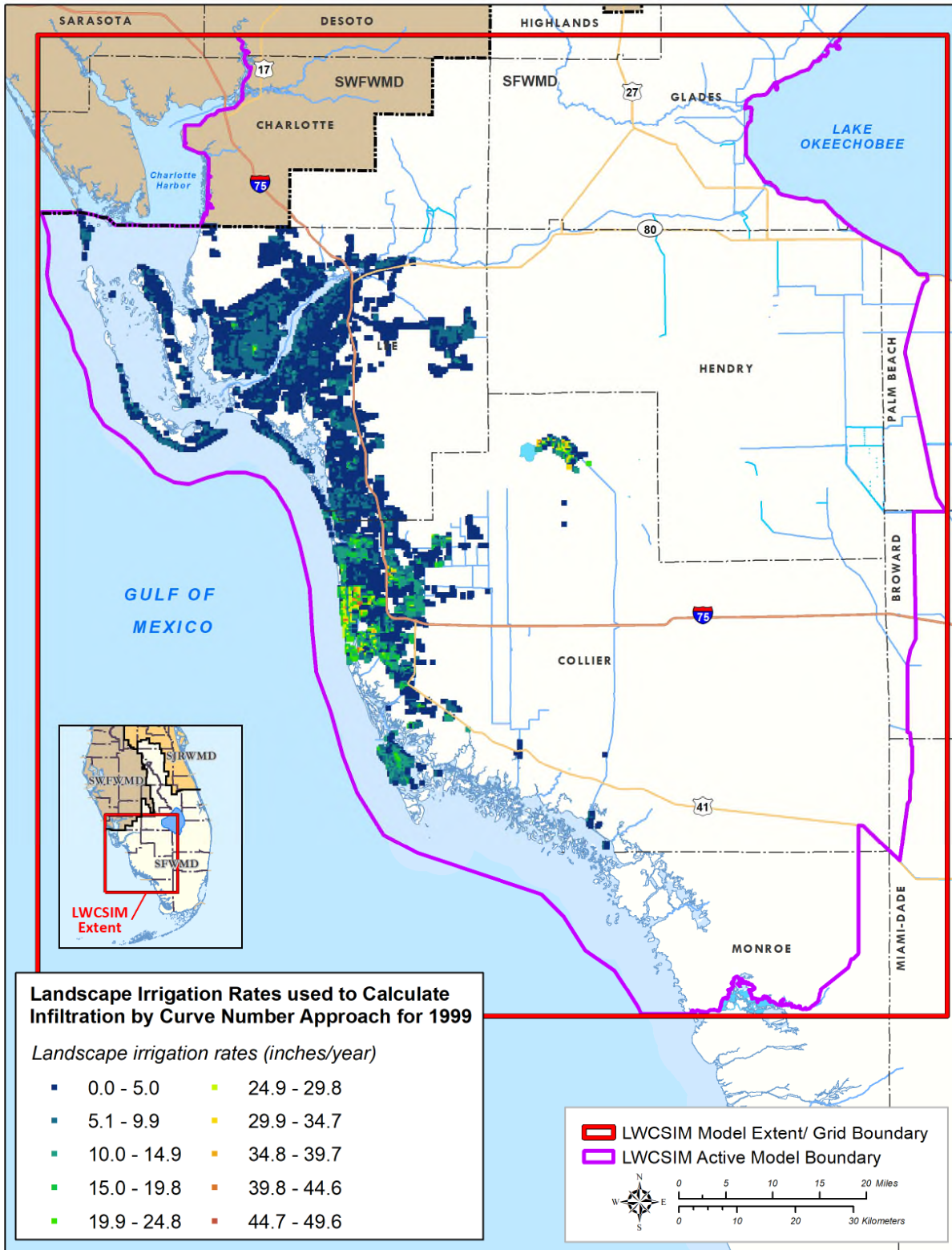


Figure 5-21. Landscape irrigation application rates used to calculate infiltration by curve number method for 1999.

5.7 ET-Recharge-Runoff Methodology

The methodology used to develop ET and recharge to the SAS uses AFSIRS (Smajstrla 1990) with the NRCS CN method for partitioning rainfall and runoff (Restrepo and Giddings 1994). A FORTRAN program was written to call AFSIRS for different land use polygons to calculate daily ET and recharge requirements, which are translated into model cell values (ET-Recharge-Runoff program, Bandara 2018). The ET-Recharge-Runoff program uses time-dependent data such as rainfall, irrigation return flows, potential ET, land use, and crop type, as well as time-independent data such as drainage basins, soil types, irrigated fractions, and irrigation efficiencies. Input requirements and how each of the processes are connected in the ET-Recharge-Runoff program are shown in **Figure 5-22**.

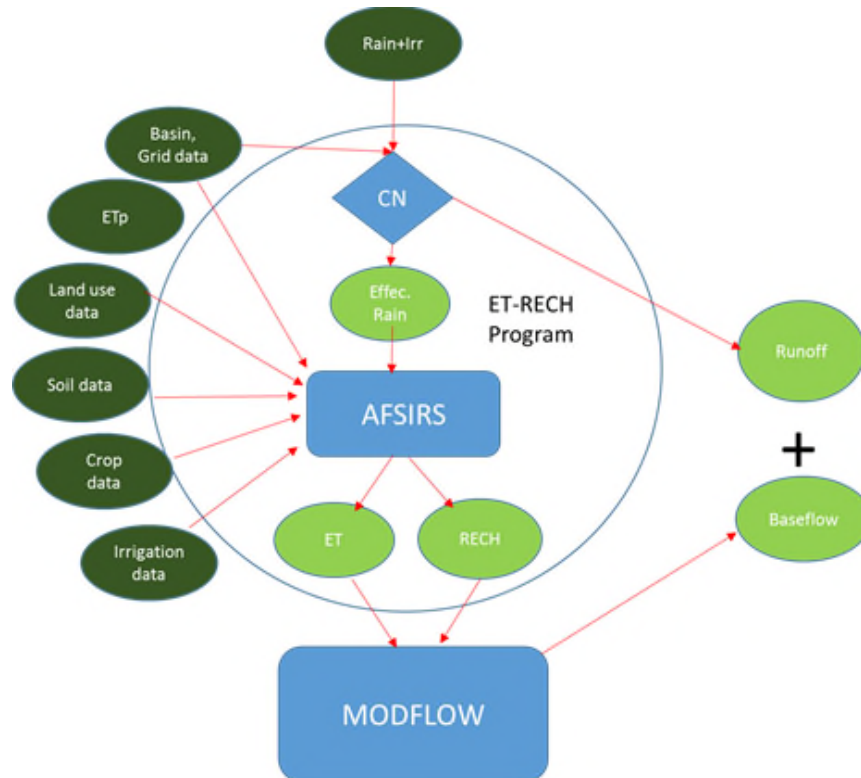


Figure 5-22. Inputs and outputs for the ET-Recharge-Runoff program.

5.7.1 Input Requirements

GIS Coverage Input: The ET-Recharge-Runoff program reads spatially referenced data that overlay the model grid. GIS coverages were created for land use, soil type, topography, and climate. These are the main inputs to the program and were produced using an area-weighted value for each model cell.

Model Grid Arrays: The main inputs to the program related to model-grid-referenced data include basin identification (ID) for water budget calibration purposes, basin ID for runoff CN, and cell ID for active/inactive designation. (Note: CNs are empirical parameters used to estimate runoff from rainfall based on land uses.)

Reference Land Use Table: Look-up tables relate land use to the following: crop type, CN, growing season, percent vegetation, impervious area, switching (indicating if a polygon is irrigated or not), and water use type classification. Irrigated land use categories include citrus, sugar cane, vegetables, pasture, and sod. Non-irrigated land use categories include rangeland and upland forests.

Evapotranspiration Input: The District’s ET data set (Brown 2013) was used to assign reference ET values for each cell in the model domain. The potential ET was computed from the reference ET and K_c .

Rainfall Input: The District’s NEXRAD rainfall data set (Brown 2014) was used to assign a rainfall value to each cell in the model domain.

Return Flow Input: LSI flows and other applications that introduce water into the unsaturated zone were added directly into the rainfall arrays. Septic tank return flows were added directly to recharge arrays.

5.7.2 Evapotranspiration

ET is the sum of vaporization by the combined process of evaporation and transpiration (Jensen et al. 1990, Doherty et al. 2010). ET is the largest loss in the water budget in Florida. The ET rate from a crop depends on the type of crop, stage of growth, soil moisture content, and amount of energy available. The reference crop ET was used to represent a baseline rate of ET for actively growing grass, which has an unlimited supply of soil water. Potential ET for other crops was calculated as the product of the reference ET and K_c .

The reference ET data came from the SFWMD’s updated ET data set (Brown 2013). The K_c value depends on several factors, including growth stage, development of the crop canopy, and amount of rainfall. K_c ranges between 0.4 and 1.2 for most agricultural crops and varies from month to month. Low K_c values occur early in the growing seasons when vegetation canopies are incomplete, whereas high K_c values occur during peak growth stages. The K_c value increases following rain or irrigation due to increased evaporation from wet soil. AFSIRS provides tables of monthly crop coefficients for perennial and annual crops. Daily K_c values were calculated within the AFSIRS program using linear interpolation and adjusted based on the daily rainfall. Because the AFSIRS program is designed to estimate AG demands, it does not provide K_c values for non-irrigated crop types such as upland forests. In such cases, the K_c values were determined by comparing the crop type in the land use GIS coverages with the AFSIRS crop description. During the calibration process, the assumed K_c values were adjusted, if necessary, to better match observed data. Total crop ET was calculated as the sum of unsaturated zone ET and groundwater ET (equation 14).

$$ET_c = ET_{UZ} + ET_{GW} \quad (14)$$

Unsaturated zone ET was calculated within the AFSIRS program. The AFSIRS program does not directly output unsaturated zone ET, so the source code was modified to properly account for and output unsaturated zone ET. Once unsaturated zone ET is calculated, maximum groundwater ET was calculated. The maximum groundwater ET was provided as an input to MODFLOW, which used the simulated depth to the water table and the crop root zone depth to calculate the actual groundwater ET. Actual groundwater ET varies linearly with water table depth, with maximum ET rate at ground level and zero at the root zone depth. Groundwater ET for a model cell, $V_{cell,ET}$ is calculated as:

$$V_{cell,ET} = \sum_{i=1}^{nLU} (ET_{C,P,i} - ET_{UZ,i}) * A_{perv,i} \quad (15)$$

Where: $A_{perv,i}$ is the pervious area of the land use class i . Pervious areas were calculated using data from the National Land Cover Database. In well-irrigated areas, the crop ET requirement was assumed to be met by irrigation. Therefore, in well-irrigated areas, groundwater ET approaches zero. In open-water conditions where surface water and groundwater are connected, the ET requirement was assumed to be completely met by groundwater and, therefore, groundwater ET approaches potential ET.

5.7.3 Runoff Calculations

The CN method developed by the NRCS, formerly known as the Soil Conservation Service (1989), was used to compute runoff. Net rainfall (infiltration and retention) was computed as rainfall, plus return flows, minus runoff; however, additional criteria were used to consider antecedent conditions and high rainfall conditions.

CNs were selected according to the antecedent moisture contents as per the Soil Conservation Service (1972, Table 42) classification. According to this classification, a dry condition was when the total 5-day antecedent rainfall was less than 0.5 inches during the dormant season or less than 1.4 inches during the growing season. A wet condition was when the total 5-day antecedent rainfall was more than 1.1 inches during the dormant season or more than 2.1 inches during the growing season. The condition in between these two are defined as normal conditions. CNs were selected from antecedent moisture content I, II, or III categories for the dry, normal, and wet conditions, respectively.

If dry conditions existed, an additional retention factor was added to the NRCS initial abstraction. The retention factor is a user input and was adjusted during calibration. This procedure considers antecedent conditions to limit runoff when there is potential for additional soil storage.

The majority of southwestern Florida soils are sandy with very high infiltration capacity; therefore, runoff generation occurs mainly due to a saturation excess mechanism. Runoff was calculated for each model cell and accumulated by watershed. Runoff volume for each model cell ($V_{cell,roff}$) was calculated as:

$$V_{cell,roff} = \sum_{i=1}^{nLU} D_{roff,i} * A_{roff,i} \quad (16)$$

Where:

i is the land use class within the model cell

$D_{roff,i}$ is the runoff depth

$A_{roff,i}$ is the area of runoff

nLU is the number of land uses within the cell

For this modeling effort, nLU was limited to three predominant land use categories. The area of runoff was the area directly connected to drainage features that contributed to the basin outflows. The directly connected areas were calculated using Sutherland's (2000) equations. Directly connected areas convey runoff from an originating point to a destination such as a drain or a river. Runoff volumes are obtained by multiplying runoff depths by directly connected areas.

In open-water conditions, runoff was assumed to be negligible during the dry season and high during the wet season. Thus, the model calculated runoff only during the wet season, using a higher CN. In closed basins, where runoff does not leave the basin and ridge physiographic province areas and where runoff potential is very small, runoff was assumed to be zero.

Effective Rainfall

Effective rainfall is the portion of rainfall available for plant ET. It is calculated as rainfall minus runoff and initial abstraction. For closed basins and in ridge areas, runoff was assumed to stay within the watershed. Thus, the total rainfall was effective after accounting for initial losses in closed basins and ridge areas.

Routed Runoff (Muskingum)

The ET-Recharge-Runoff program was used to transform the direct runoff (from NRCS) to a routed flood hydrograph using the Muskingum hydrologic routing procedure (Cunge 1969). The direct runoff computed with the NRCS equation for all areas was accumulated by basin in preparation for the Muskingum hydrologic routing procedure.

The Muskingum method is a hydrologic river routing technique based on the continuity equation and the linear reservoir relationship. The Muskingum method is adaptable to a simple mathematical solution with variables such as weighting factors for inflow and outflow rates, a storage time constant, and travel time constant. The inflow hydrograph was made up of the direct runoff from each basin. The result of the Muskingum transformation was a routed hydrograph curve with an equivalent volume to the inflow hydrograph curve. The Muskingum parameters were calibrated by correlating routed runoff with actual observed flow values.

5.7.4 Recharge to the Saturated Zone

AFSIRS simulates a daily water balance in the unsaturated zone. Originally developed to determine irrigation demands, AFSIRS was adapted to simulate the unsaturated zone water balance in non-irrigated areas as well. Data for AFSIRS come from crop, irrigation, and soil databases. The crop database includes crop type, monthly crop coefficients, total and irrigated crop root depths, and allowable soil water depletion by month. The irrigation database contains irrigation system type, application efficiency of the irrigation system, percent irrigated soil surface area, and the ET fraction assumed to be extracted from the irrigated portion of the crop root zone. The soils database includes available soil type, vertical hydraulic conductivity (Kv), and porosity.

The AFSIRS model is based on a water budget of the crop root zone, and the concept of crop ET can be estimated from potential ET. The water budget includes inputs to the crop root zone from rain and irrigation and losses from initial abstraction, runoff, deep percolation, and root zone/unsaturated zone ET. The water balance equation within the crop root zone of a polygon can be written as:

$$\Delta STO = Rain + IRR - RCH - Runoff - IA - UZET \quad (17)$$

Where (in inches):

ΔSTO is the change in soil storage

IRR is irrigation (In non-irrigated areas, IRR becomes zero.)

RCH is the deep percolation or gross groundwater recharge

IA is the initial abstraction

$UZET$ is the unsaturated zone ET

In AFSIRS, the control volume is the available water content of the plant's root zone. If incoming rainfall (or irrigation) exceeds this control volume, the excess volume ("drainage") is discarded as the combined process of runoff and recharge to the saturated zone. For this modeling effort, runoff (from the CN calculations) was removed from the daily rainfall (i.e., effective rainfall) and used as an input to AFSIRS. This made the AFSIRS drainage output equal to the recharge in the saturated zone, which was passed to the MODFLOW model.

Recharge volume for a model cell ($V_{cell,RCH}$) is calculated as:

$$V_{cell,RCH} = \sum_{i=1}^{nLU} DRN_i * A_{perv,i} + Rain_{eff} * (A_{imperv,i} - DCIA_i) \quad (18)$$

Where: $A_{imperv,i}$ is the impervious area of the land use polygon i . The second term in the equation represents the groundwater recharge that can occur within impervious areas (e.g., urban developments) where runoff is routed to on-site lakes or ponds.

For non-irrigated areas, vegetation used available water in the unsaturated zone and, if the plant's water extraction depth was deep enough, supplemented the additional demands from the water table. AFSIRS was used to calculate the overall potential crop ET (reference ET \times K_c) and the amount of water extracted from the unsaturated zone. Unsaturated zone ET is based on the daily water balance of rainfall, potential crop ET, and available soil water storage. The potential saturated zone ET is equal to the potential crop ET minus the unsaturated zone ET. The potential saturated zone ET was passed to MODFLOW, which calculated actual saturated zone ET based on the distance from the ET surface to the water table and on the extinction depth for a specific crop type.

In sufficiently irrigated areas, the calculations were the same except irrigation was applied when the soil moisture storage was depleted to a specified level (the maximum allowable depletion). Thus, the potential saturated zone ET approached zero for irrigated areas. Nonetheless, the potential saturated zone ET for irrigated areas was passed to MODFLOW. Both ET and recharge were assumed to be negligible in impervious areas due to runoff.

Figure 5-23 describes the steps of the ET-Recharge-Runoff program. The program was successfully verified against field measured data within the LWCSIM domain.

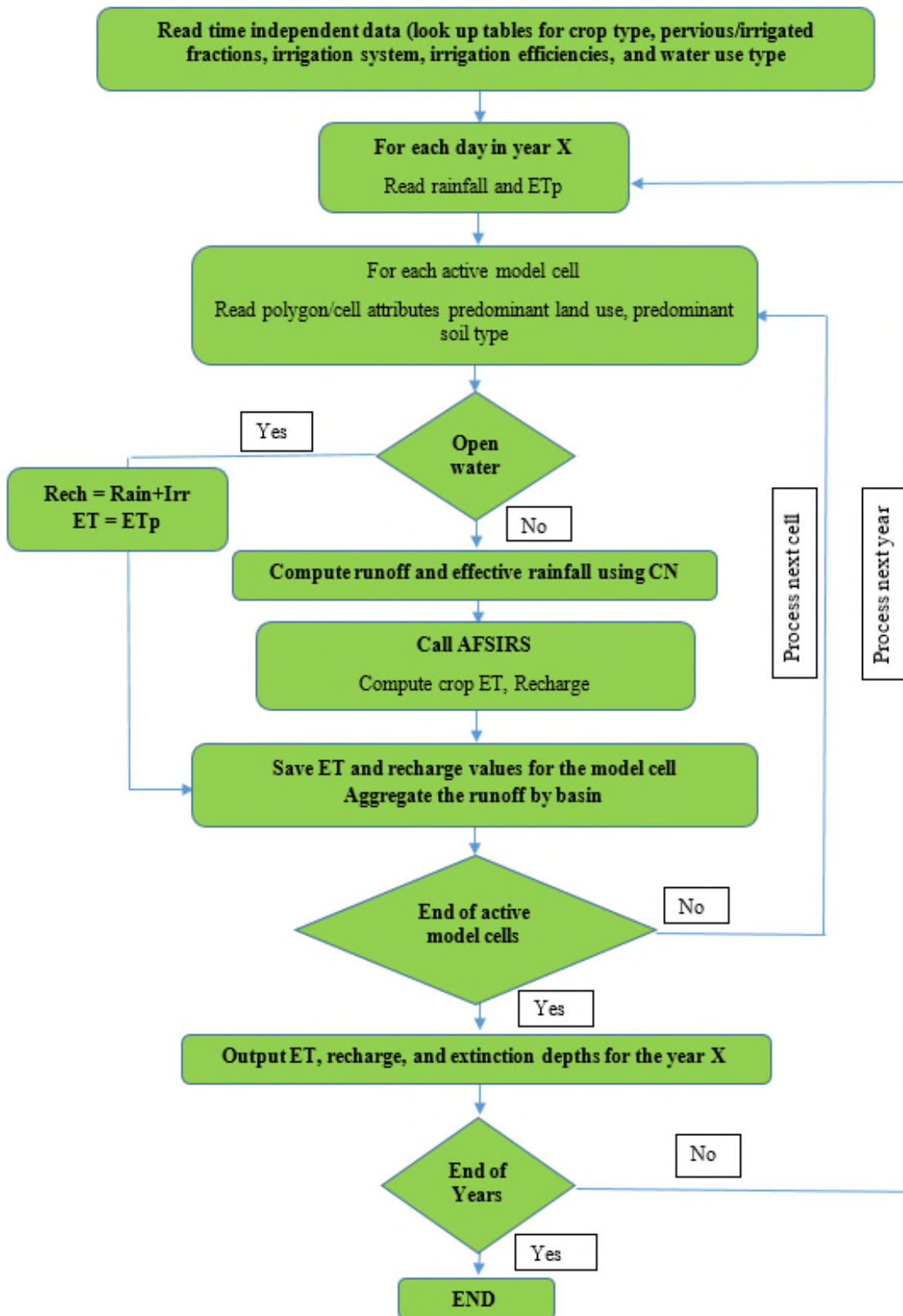


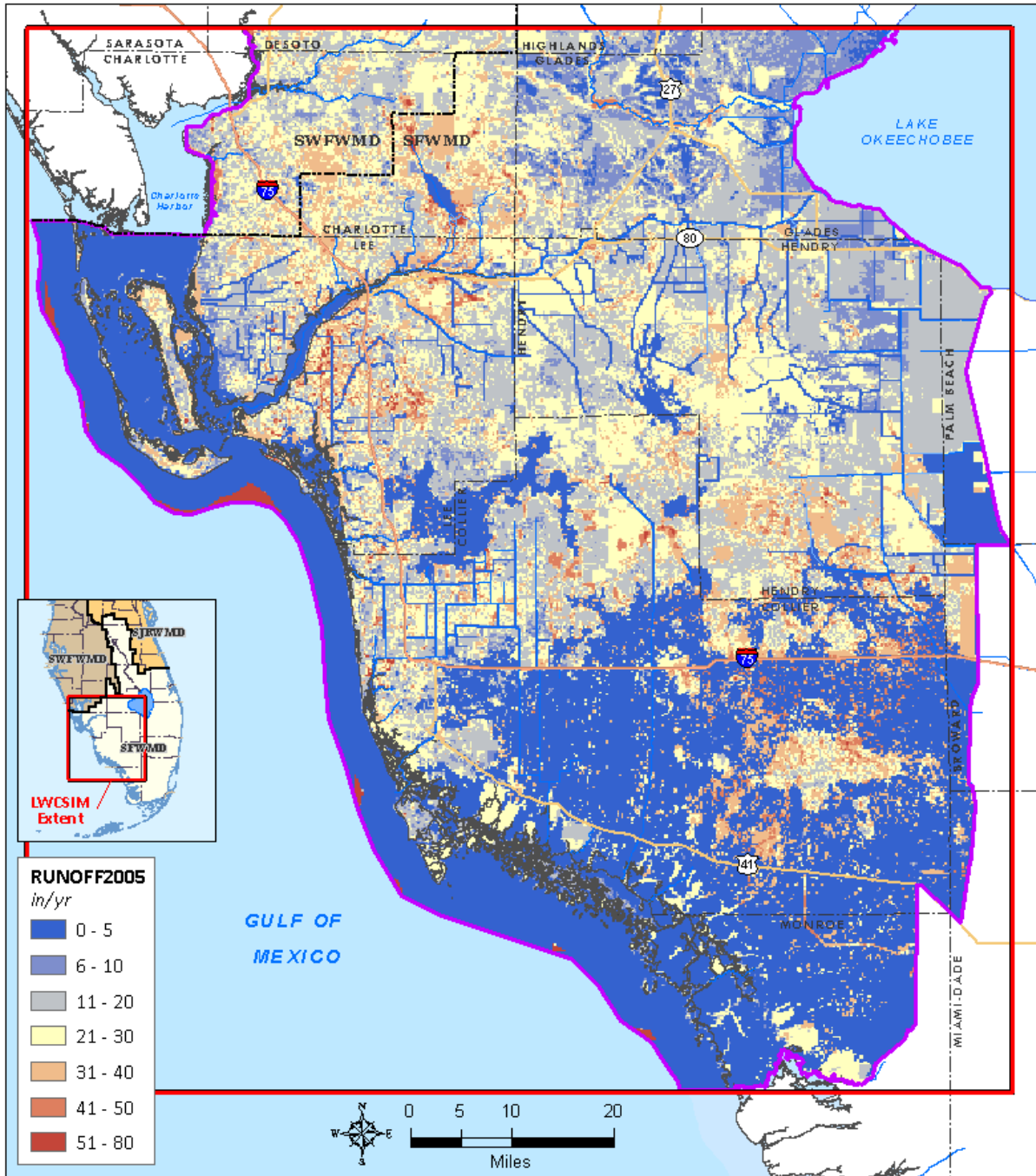
Figure 5-23. Flow chart describing the ET-Recharge-Runoff program.

Figures 5-24 and 5-25 show the spatial distribution of simulated runoff for 2005 (wet year) and 2007 (dry year), respectively. Using the ET-Recharge-Runoff pre-processor, simulated runoff generally was lowest in the southern portion of the LWCSIM domain, which is primarily wetland areas such as Everglades National Park and Big Cypress National Preserve. This is because the overland flow over wetland areas were routed using the Wetlands package and runoff was not removed from the ET-Recharge-Runoff pre-processor. Simulated runoff generally was highest in areas with the most impervious land coverage (e.g., urban areas in Lee and Collier counties) and in areas where the soil is poorly drained and the water table is shallow (e.g., along the Caloosahatchee River floodplain).

Figures 5-26 and 5-27 show the spatial distribution of unsaturated zone ET developed using the ET-Recharge-Runoff program for 2005 (wet year) and 2007 (dry year), respectively. Unsaturated zone ET is higher when the thickness of the unsaturated zone is greater. Unsaturated zone ET is lowest when the thickness of the unsaturated zone is small to non-existent or in shallow water table conditions (e.g., river floodplains). Generally, the unsaturated zone ET is higher in irrigated areas because the crop ET requirement is mainly met by the water content in the root zone and by the irrigation water, which is applied to the unsaturated zone.

Figures 5-28 and 5-29 show the spatial distribution of maximum ET developed using the ET-Recharge-Runoff program for 2005 (wet year) and 2007 (dry year), respectively. Maximum ET is an input to MODFLOW and is highest in open water bodies and shallow water table conditions, while it is lowest in deep water table conditions. **Figures 5-30 and 5-31** show the spatial distribution of gross recharge developed using the ET-Recharge-Runoff program for 2005 (wet year) and 2007 (dry year), respectively. Gross recharge is an input to MODFLOW and is highest in highly drained soil conditions, deep water table conditions, closed basins, or open water bodies. It is lowest in poorly drained soil conditions or shallow water table conditions.

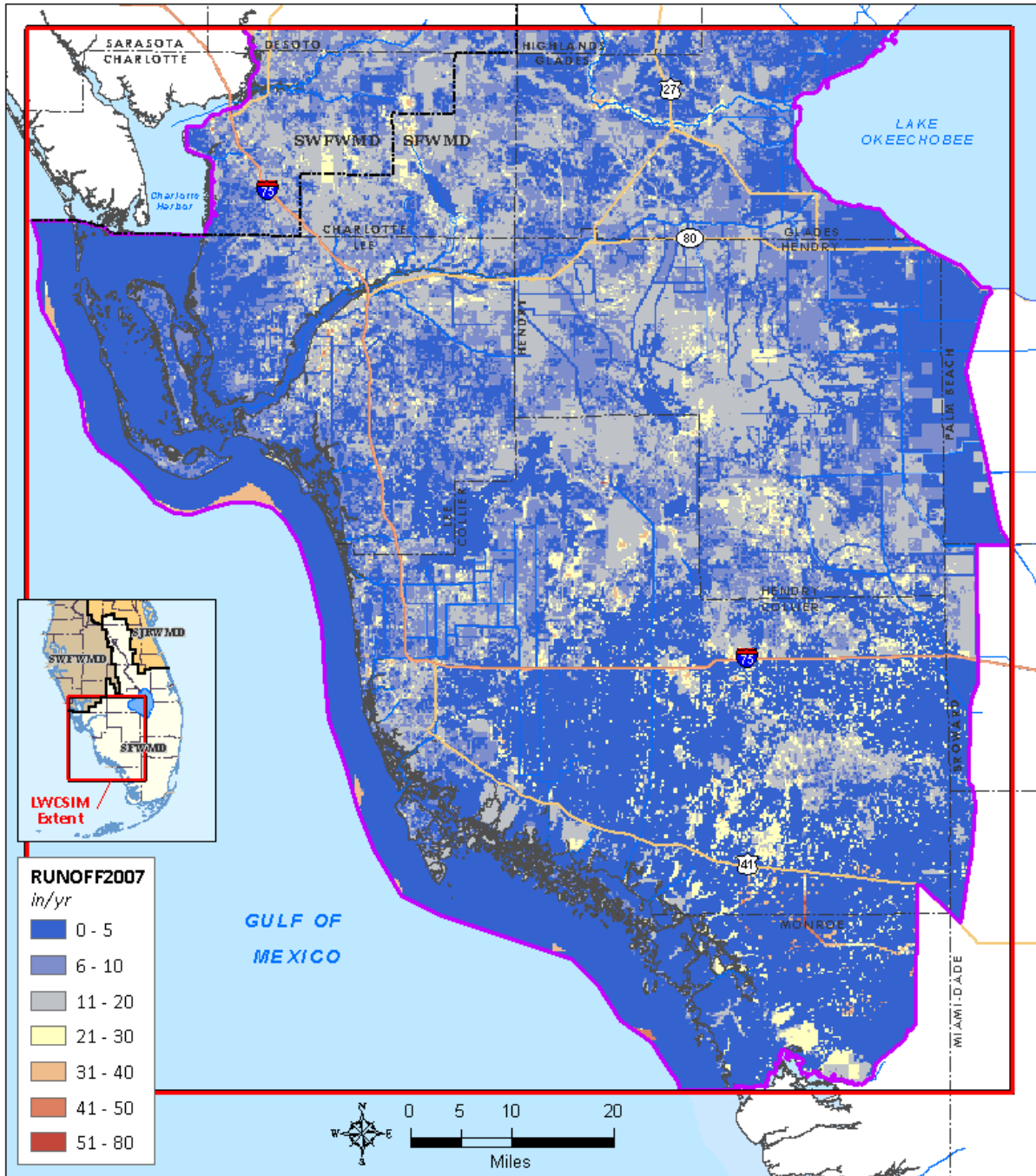
Figures 5-32 and 5-33 show the spatial distribution of MODFLOW-simulated groundwater ET for 2005 (wet year) and 2007 (dry year), respectively. MODFLOW-simulated ET depends on the maximum ET provided (**Figures 5-28 and 5-29**), simulated depth to the water table, and extinction depth of the plants. **Figure 5-34** shows the spatial distribution of extinction depths used for 2005 (Shah et al. 2007). Generally, the simulated groundwater ET is highest under open water or shallow water table conditions such as rivers, lakes, wetlands, and river floodplains. The simulated groundwater ET is lowest in deep water table conditions or in urban areas due to lack of tree cover. **Figures 5-35 and 5-36** show the spatial distribution of simulated net recharge for 2005 (wet year) and 2007 (dry year), respectively. Net recharge is the difference between gross recharge and the MODFLOW-simulated groundwater ET. Generally, net recharge is highest in highly drained soil conditions and deep water table conditions. Net recharge is lowest or negative (aquifer is discharging) in poorly drained soil conditions and shallow water table conditions such as in the Caloosahatchee River floodplain.



| | | |
|---|--|--|
| <p>Lower West Coast Planning Region</p> <p>Lower West Coast Surficial Aquifer System & Intermediate Aquifer System (LWCSIM) Modeling Results</p> | <p>LWCSIM Model Run 10/08/2018</p> <p>Runoff Inches Per Year</p> | <p> LWCSIM Model Extent</p> <p> LWCSIM Active Model Boundary</p> <p>Map Date: January 2019</p> |
|---|--|--|

User Name: a.kortart Map Produced on Date: 1/24/2019 4:56:47 PM \\ad.sfwmd.gov\dfs\root\GIS\Bz\Bz\GIS\LWCSIM\RET_RCH_Fig\res\20190123\mxd\RUNOFF_1.mxd

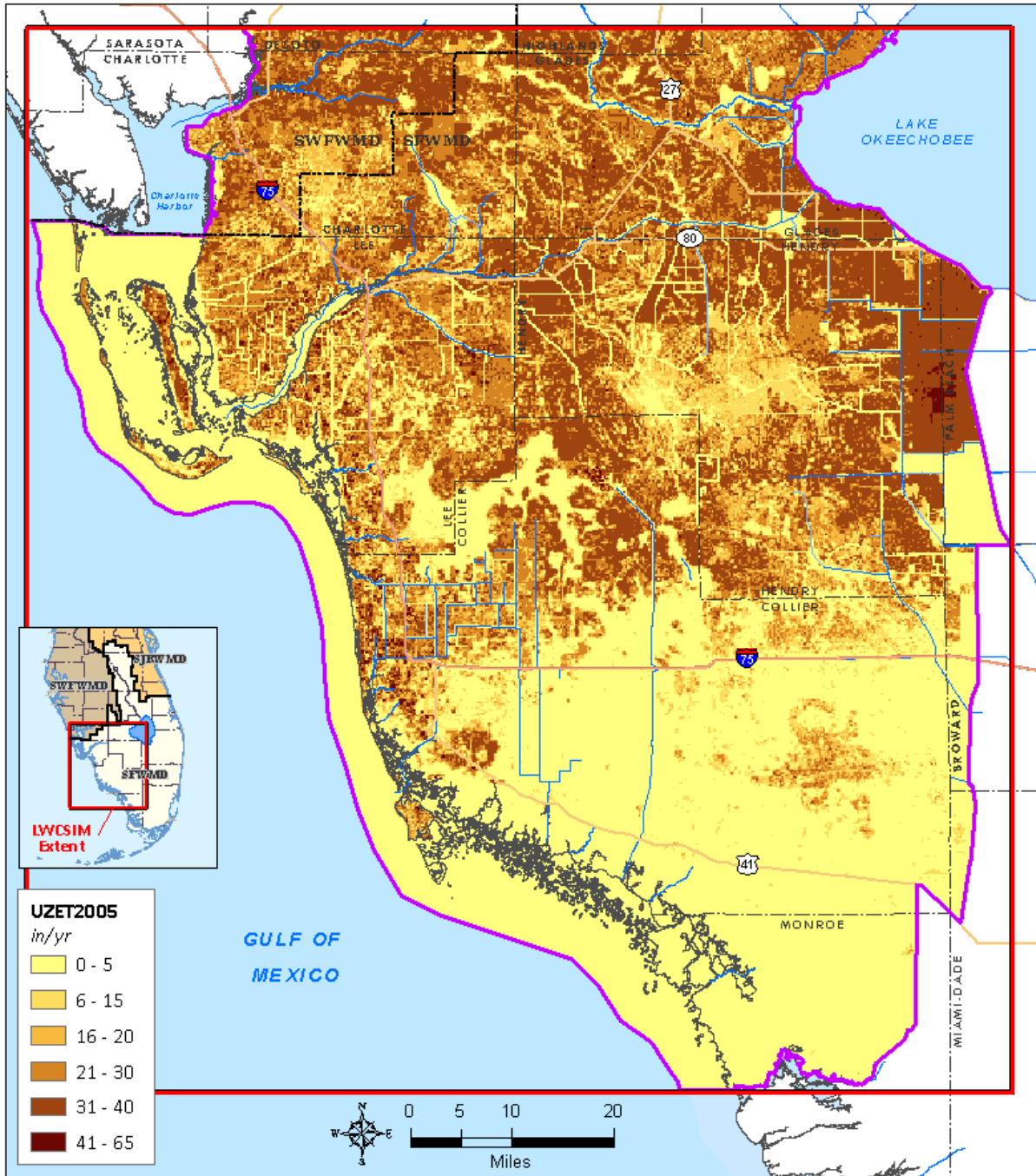
Figure 5-24. Spatial distribution of simulated runoff in 2005 (wet year).



| | | |
|--|--|--|
| <p>Lower West Coast Planning Region</p> <p>Lower West Coast Surficial Aquifer System & Intermediate Aquifer System (LWCSIM) Modeling Results</p> | <p>LWCSIM Model Run 10/08/2018</p> <p>Runoff</p> <p><i>Inches Per Year</i></p> | <p> LWCSIM Model Extent</p> <p> LWCSIM Active Model Boundary</p> <p>Map Date: January 2019</p> |
|--|--|--|

User Name: a.kortart Map Produced on Date: 1/24/2019 4:56:47 PM \\ad.sfwmd.gov\dfs\root\GIS\BIZ\GIS\LWCSIM\RET_RCH_Fig\res\20190123\mxd\RUNOFF_1.mxd

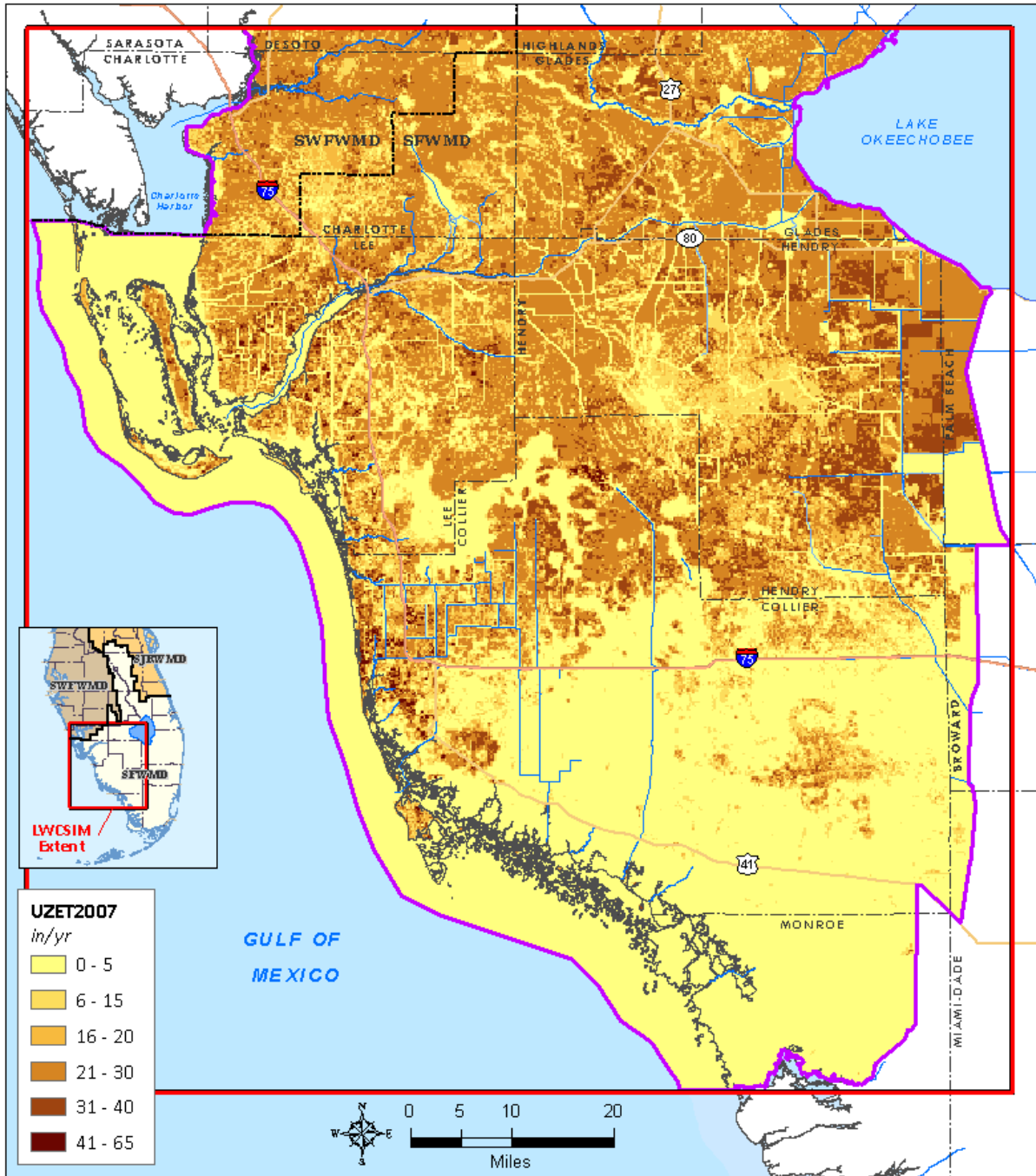
Figure 5-25. Spatial distribution of simulated runoff in 2007 (dry year).



| | | |
|---|--|--|
| <p>Lower West Coast Planning Region</p> <p>Lower West Coast Surficial Aquifer System & Intermediate Aquifer System (LWCSIM) Modeling Results</p> | <p>LWCSIM Model Run 10/08/2018</p> <p>Unsaturated Zone Evapotranspiration <i>Inches Per Year</i></p> | <p> LWCSIM Model Extent</p> <p> LWCSIM Active Model Boundary</p> <p>Map Date: January 2019</p> |
|---|--|--|

User Name: akortart Map Produced on: Date: 1/24/2019 11:50:48 AM Y:\d:\m\m\g\m\m\root\GIS\GIS\B2\WCSIM\NET_RCH_Fig\1e2\20190123\mxd\UZET_2.mxd

Figure 5-26. Spatial distribution of unsaturated zone evapotranspiration in 2005 (wet year).



| | | |
|---|--|--|
| <p>Lower West Coast Planning Region</p> <p>Lower West Coast Surficial Aquifer System & Intermediate Aquifer System (LWCSIM) Modeling Results</p> | <p>LWCSIM Model Run 10/08/2018</p> <p>Unsaturated Zone Evapotranspiration <i>Inches Per Year</i></p> | <p> LWCSIM Model Extent</p> <p> LWCSIM Active Model Boundary</p> <p>Map Date: January 2019</p> |
|---|--|--|

User Name: akortart Map Produced on: Date: 1/24/2019 11:50:48 AM Y:\s\m\g\o\ds\root\GIS\GIS\B2\WCSIM\NET_RCH_Fig\1e2\20190123\mxd\UZET_2.mxd

Figure 5-27. Spatial distribution of unsaturated zone evapotranspiration in 2007 (dry year).

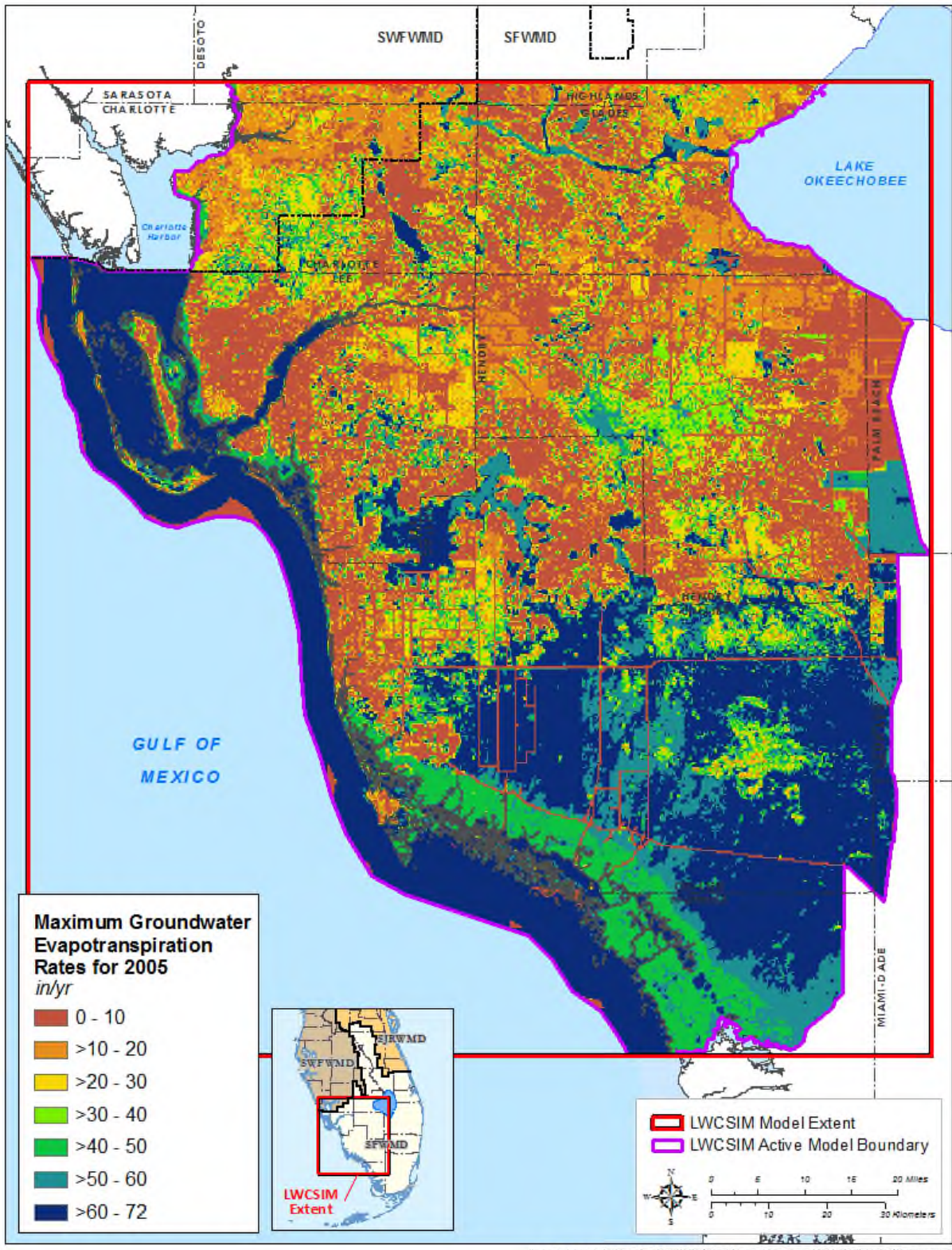


Figure 5-28. Maximum evapotranspiration in 2005 (wet year).

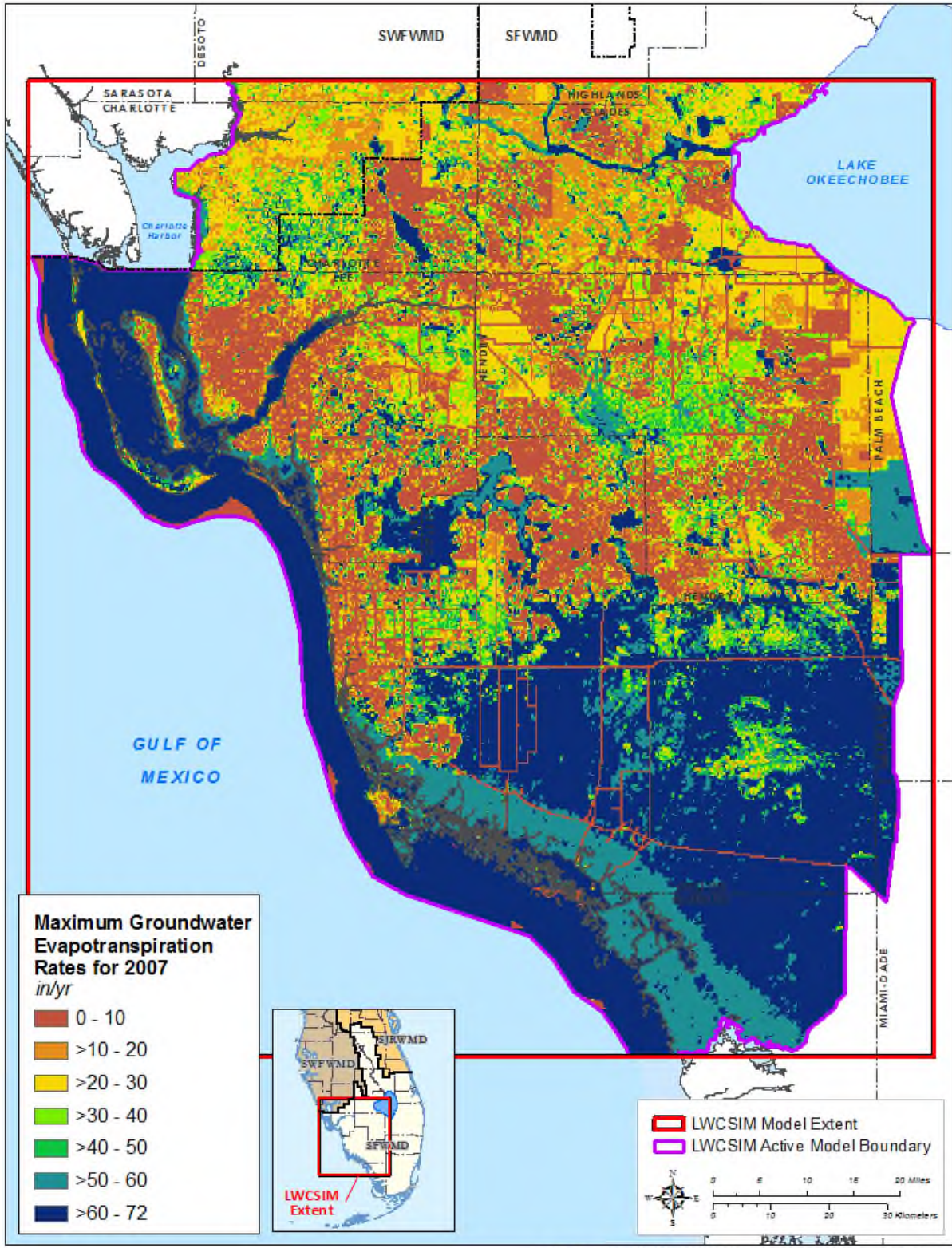


Figure 5-29. Maximum evapotranspiration in 2007 (dry year).

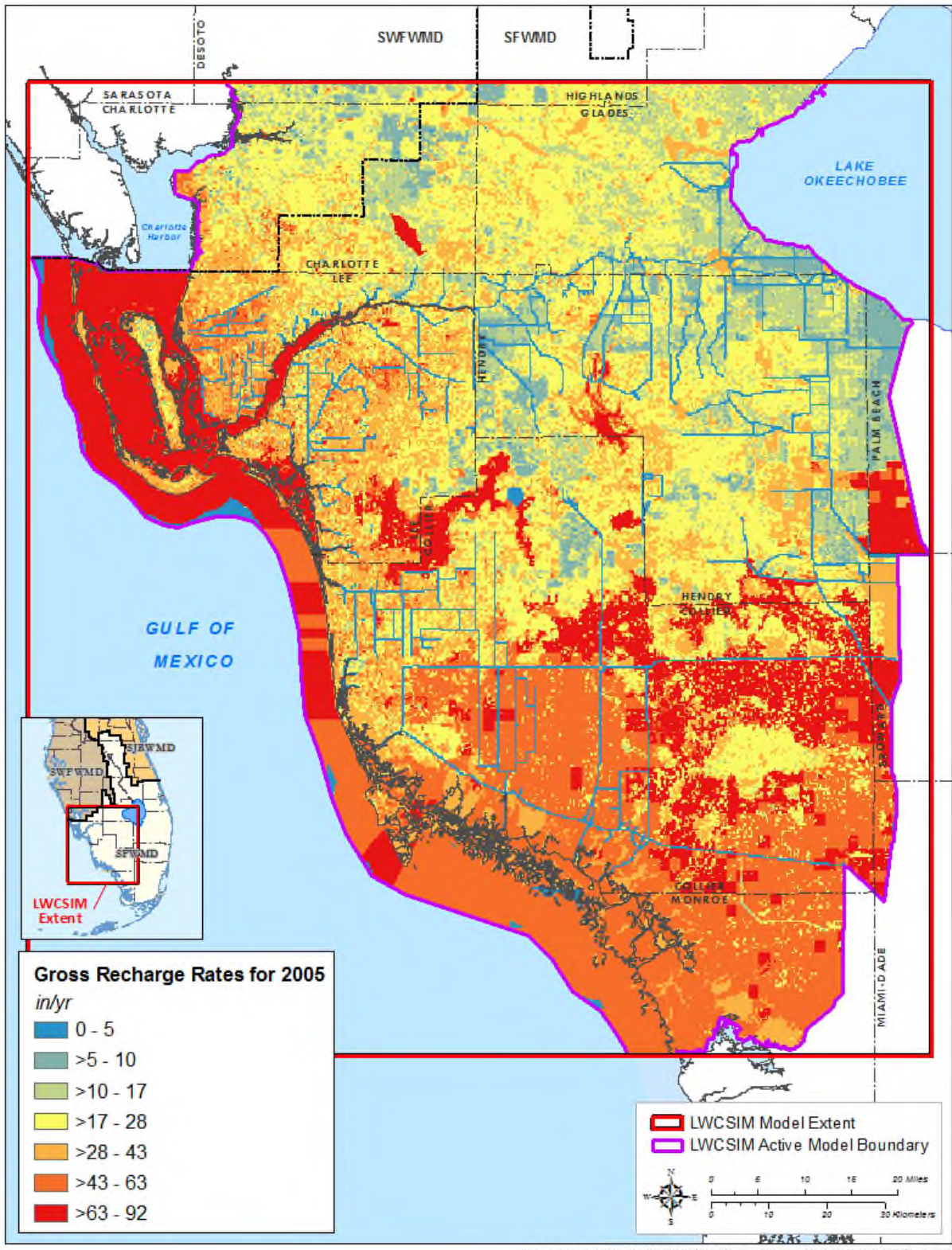


Figure 5-30. Gross recharge in 2005 (wet year).

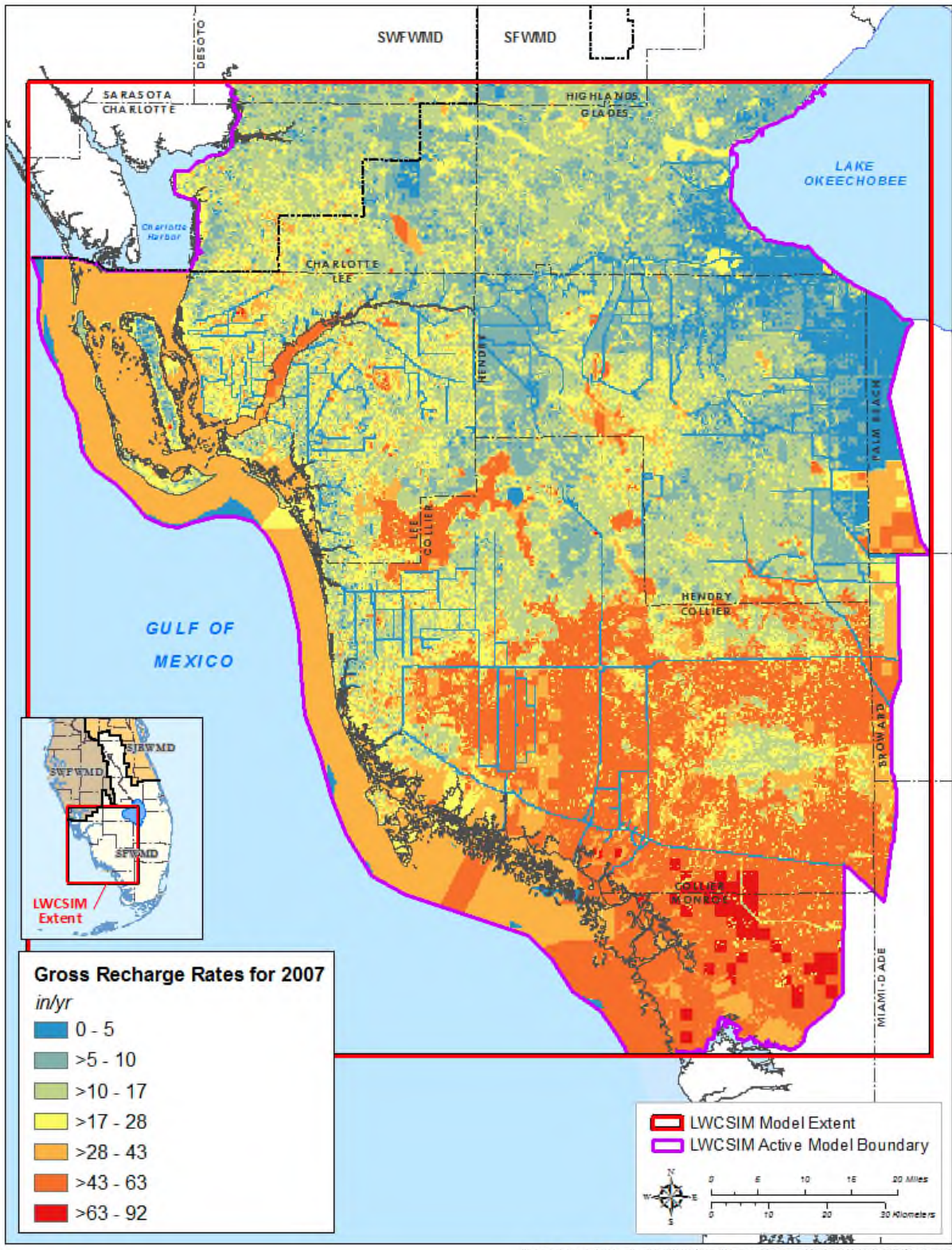


Figure 5-31. Gross recharge in 2007 (dry year).

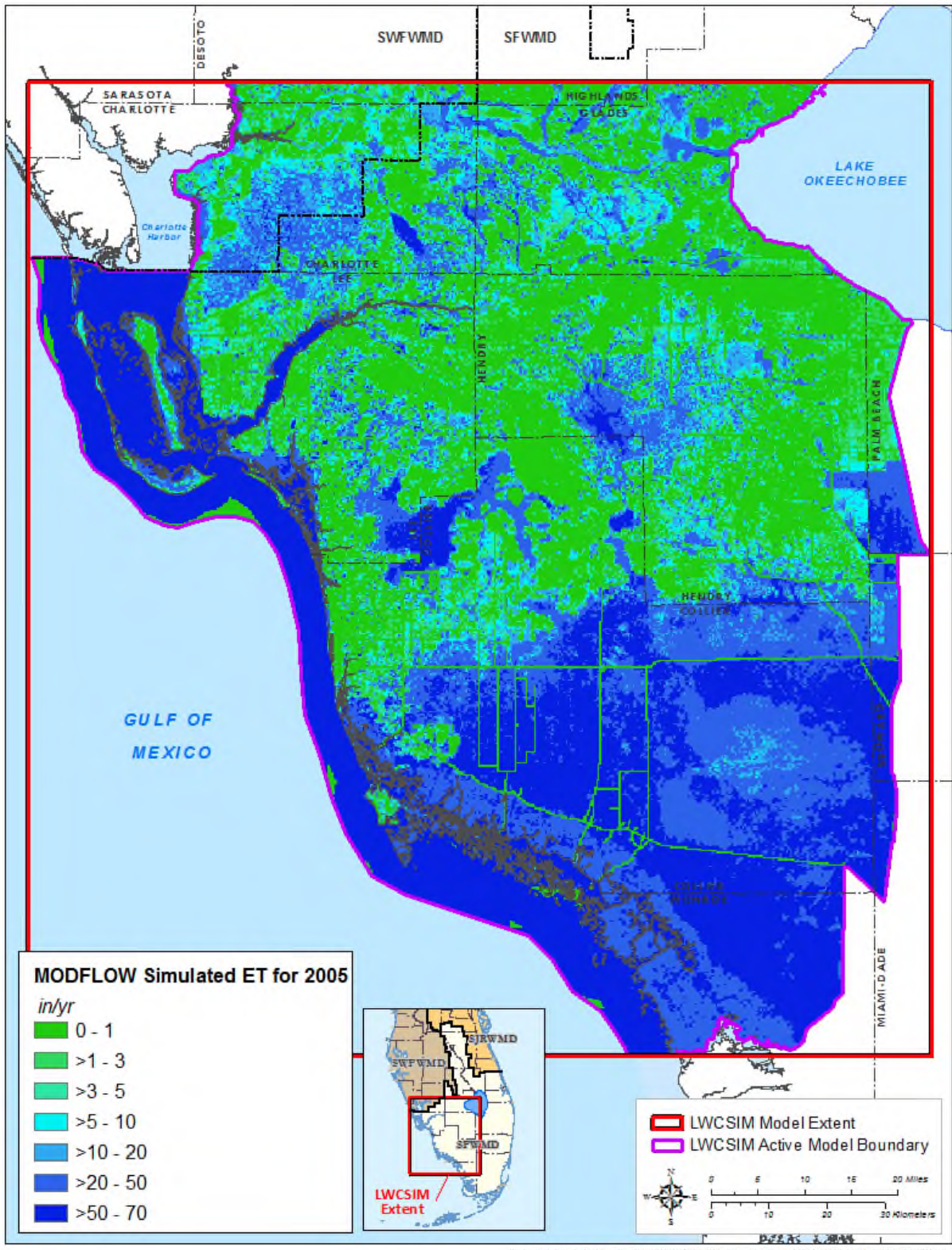


Figure 5-32. MODFLOW-simulated evapotranspiration in 2005 (wet year).

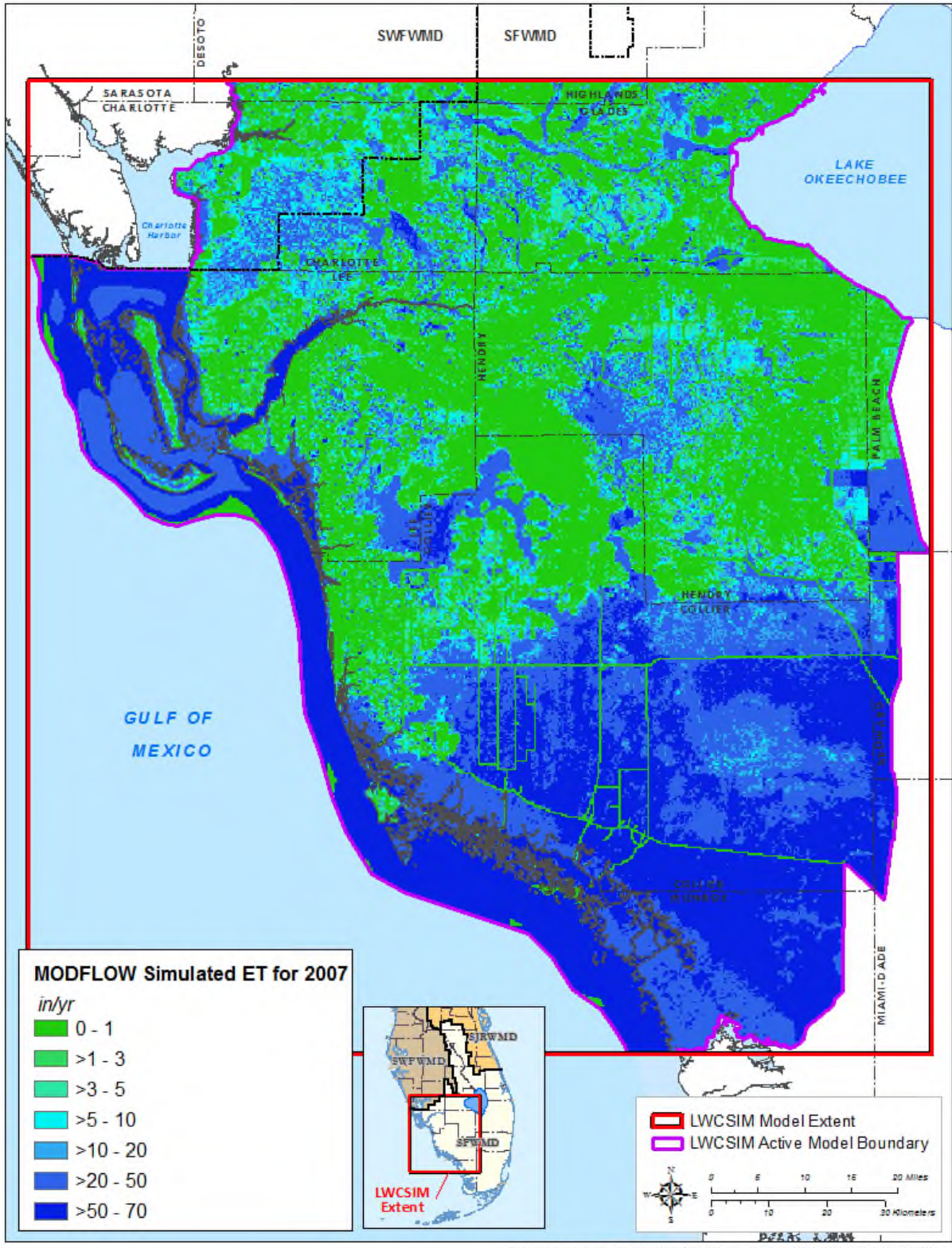
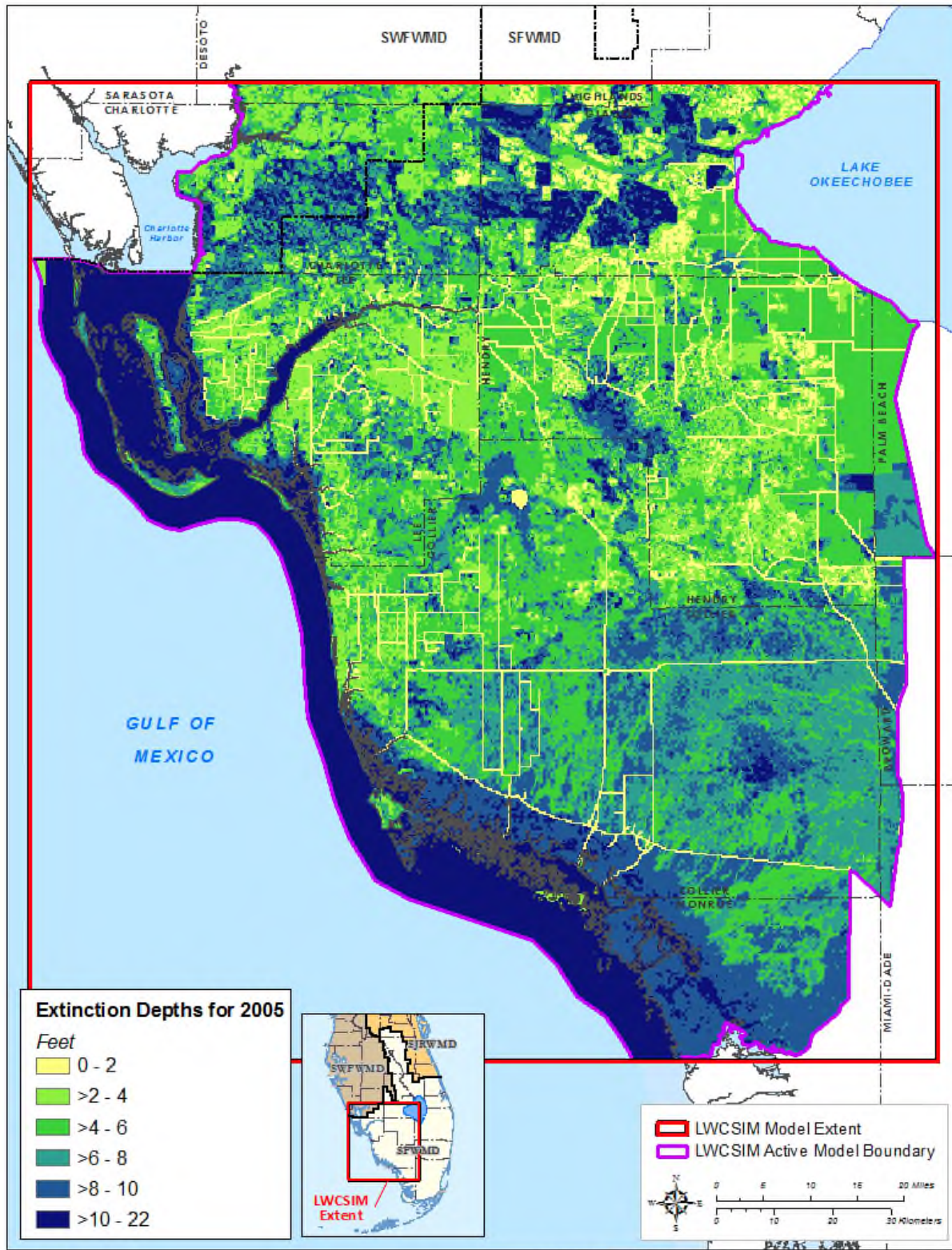


Figure 5-33. MODFLOW-simulated evapotranspiration in 2007 (dry year).



\\ad.stfwmd.gov\cfe\root\GIS\GIS\BIZ\W\WCS\IMET_RCH_Figures\20200127\mid1103\EXTD.mxd

Figure 5-34. Extinction depths in 2005.

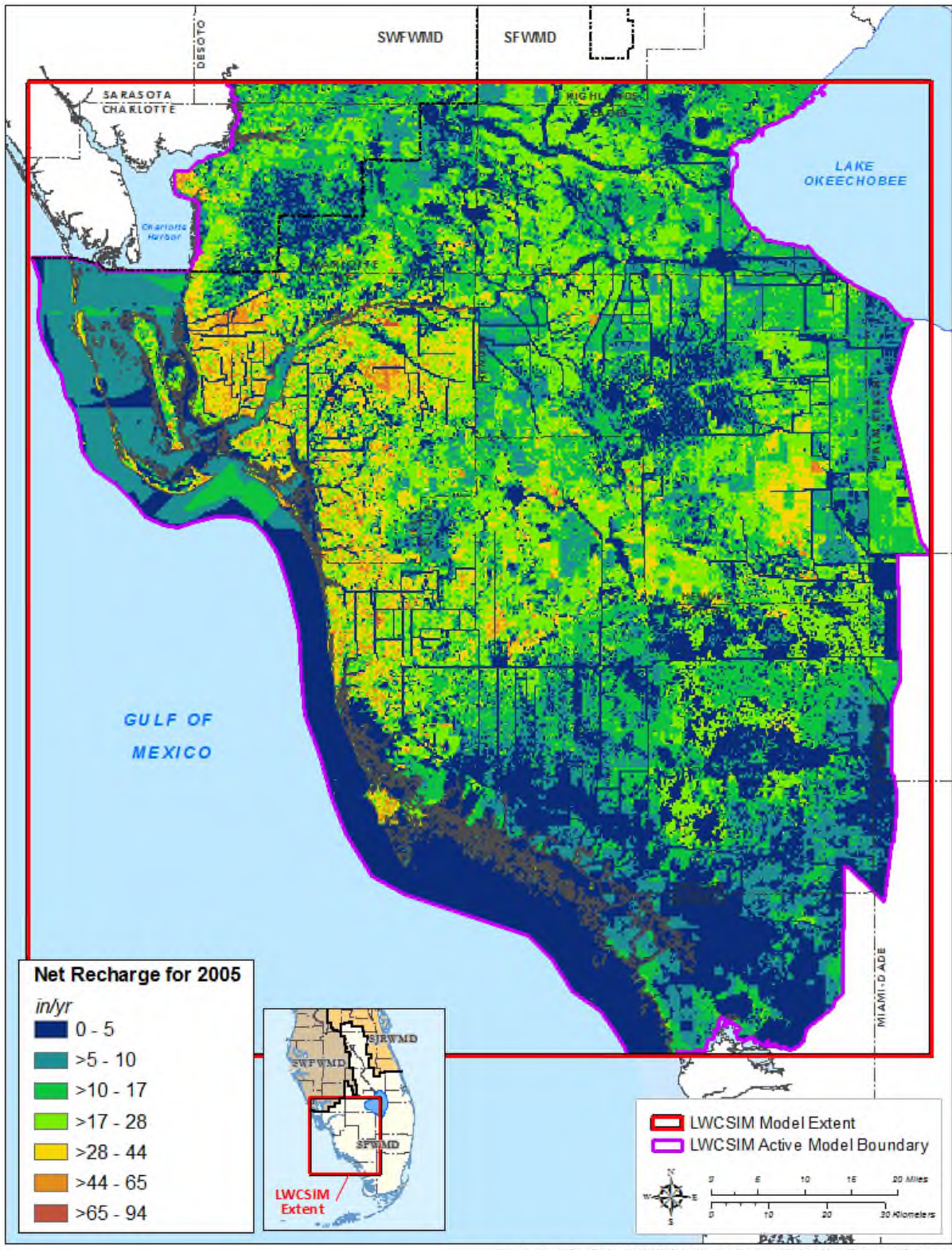


Figure 5-35. Simulated net recharge in 2005 (wet year).

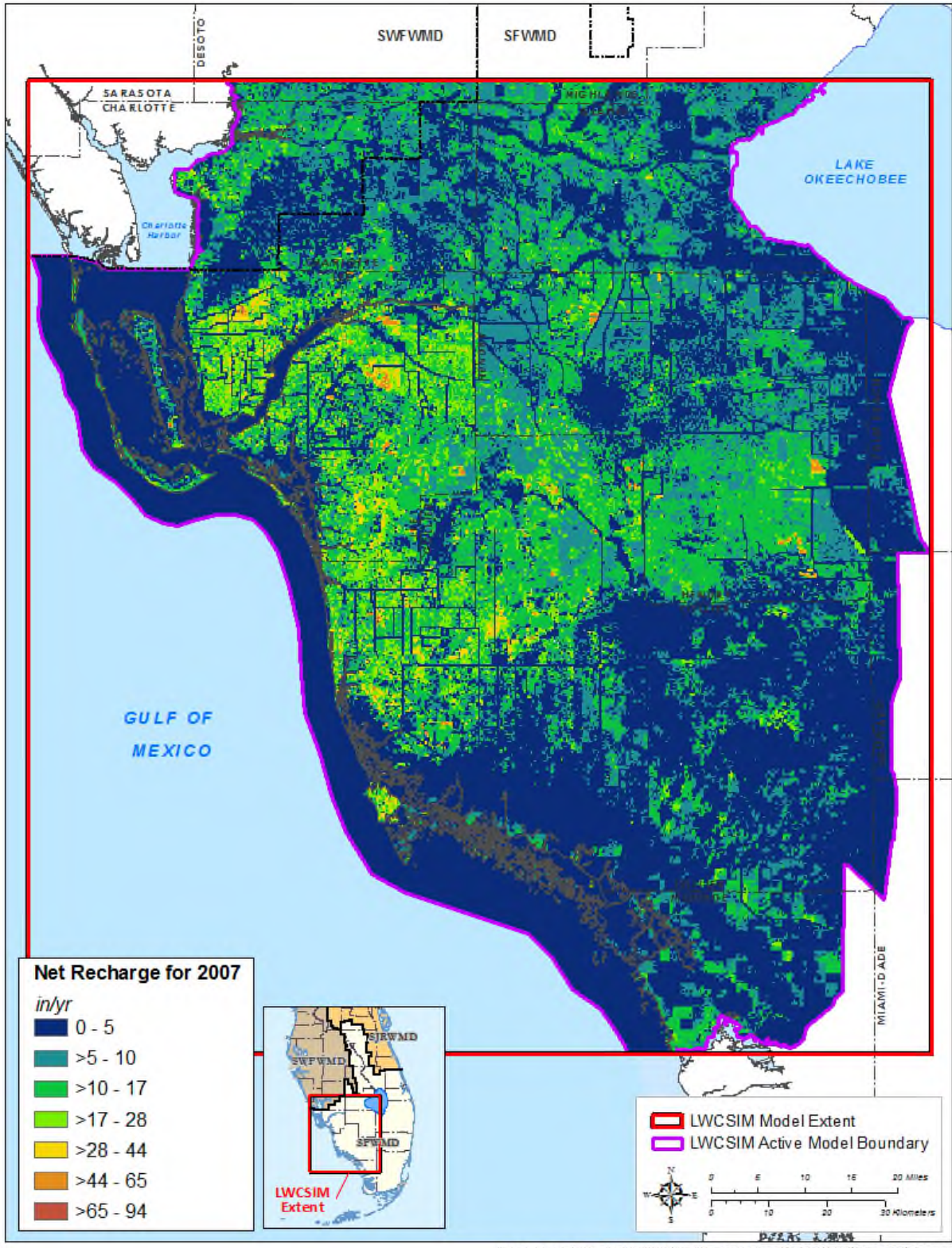


Figure 5-36. Simulated net recharge in 2007 (dry year).

5.7.5 Land Use Impact on Evapotranspiration and Recharge

Spatial distribution of ET and recharge is largely attributed to the land use categories across the LWCSIM domain. Generally, more ET occurs in wetland and open water areas, while less ET occurs in urban and built-up areas. Highest net recharge occurs in managed recharge areas, usually within urban and built-up land use types, and lowest net recharge occurs in wetland areas. In southwestern Florida wetlands, groundwater generally discharges to the surface. Variation in simulated ET, recharge, and associated parameters with land use types was studied as part of this modeling effort to ensure the simulated values demonstrated generally accepted trends. **Figure 5-37** shows the variation of gross recharge, runoff, unsaturated zone ET, actual ET, total ET, and net recharge calculated from the ET-Recharge-Runoff program with different land use types. FLUCCS codes are used to describe the land use types (SFWMD 2009). **Table 5-2** lists the major FLUCCS codes used for this modeling effort.

Table 5-2. Florida Land Use Cover Classification System (FLUCCS) descriptions.

| Land Use FLUCCS Code | Description |
|----------------------|--|
| 1000 | Urban and Built-Up |
| 2000 | Agriculture |
| 3000 | Rangeland-Upland Nonforested |
| 4000 | Upland Forest |
| 5000 | Water |
| 6000 | Wetlands |
| 7000 | Barren Land |
| 8000 | Transportation, Communications and Utilities |

Figure 5-37a shows the variation of gross recharge among various land use types. Gross recharge represents the applied recharge to MODFLOW before ET losses were accounted for. As expected, the highest average gross recharge rates were simulated in open water conditions (FLUCCS code 5000; 50 inches/year) and wetland areas (FLUCCS code 6000; 43 inches/year). Due to the absence of an unsaturated zone, gross recharge is mostly equal to rainfall in open water and wetland conditions. The third highest average gross recharge rates (24 inches/year) were simulated in urban and built-up (FLUCCS code 1000). Most built-up areas (e.g., residential communities) have on-site lakes or ponds that capture and store local runoff, which eventually recharges the water table. Irrigated agricultural areas (FLUCCS code 2000) have the lowest average gross recharge rates (14 inches/year). The greater ET requirement in agricultural areas makes less water available to infiltrate to the water table, reducing net recharge.

Figure 5-37b shows average ET-Recharge-Runoff model-generated runoff for each land use type. The highest runoff (18 inches/year) was generated in the transportation land use type (FLUCCS code 8000). The transportation land use type generally includes highly impervious areas such as highways, roads, and airports; thus, greater runoff is expected. The second highest average runoff (17 inches/year) occurred in the upland-non-forested category (FLUCCS code 3000). This FLUCCS code is used in conjunction with various land uses, including rural residential, reclaimed mining lands, abandoned mining lands, inactive land with street pattern, utility corridors, and parks and zoos, which contain a lot of impervious areas. The third highest average runoff (15 inches/year) occurred in the urban and built-up land use category (FLUCCS code 1000). This category also includes highly impervious areas such as cities, towns, villages, shopping centers, and industrial and commercial centers, which generate higher runoff.

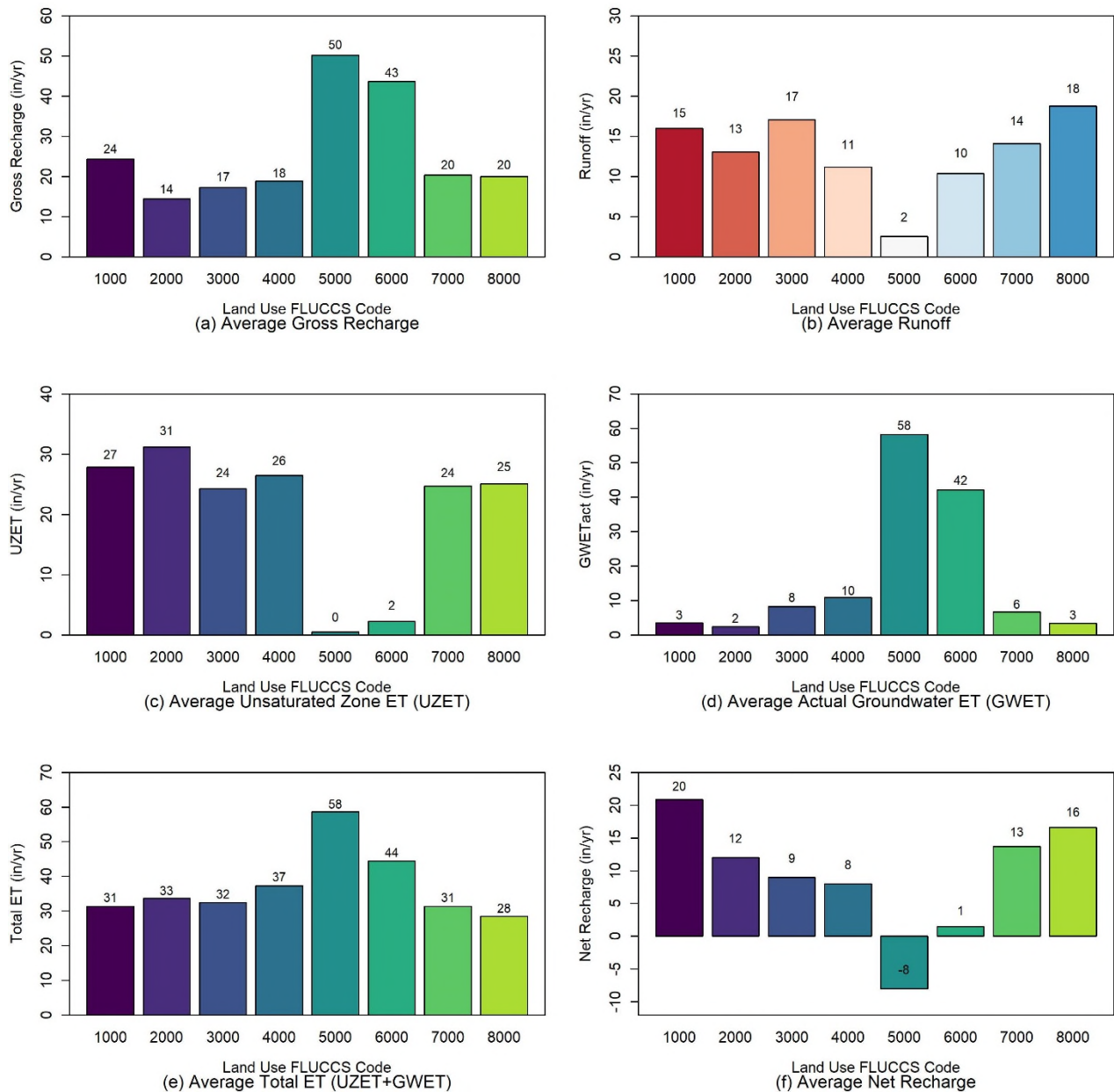


Figure 5-37. Gross recharge, runoff, unsaturated zone evapotranspiration, groundwater evapotranspiration, total evapotranspiration, and net recharge variation with land use. (Refer to **Table 5-2** for the FLUCCS codes.)

Figure 5-37c shows average unsaturated zone ET calculated by the ET-Recharge-Runoff program for various land use types. For open water conditions (FLUCCS code 5000), unsaturated zone ET was zero because of the absence of an unsaturated zone. Unsaturated zone ET was smaller (2 inches/year) in the wetland land use type (FLUCCS code 6000), possible because the unsaturated zone is completely absent or present only during the dry season. Unsaturated zone ET was highest (31 inches/year) in irrigated agricultural areas (FLUCCS code 2000) because of the supplemental crop ET demand applied as irrigation to the unsaturated zone. Average actual groundwater ET simulated by MODFLOW for different land use types is shown in **Figure 5-37d**. As expected, the highest groundwater ET was simulated in open water

conditions (FLUCCS code 5000), followed by wetlands (FLUCCS code 6000). Irrigated agricultural areas have the smallest groundwater ET (2 inches/year) because crop demand was met by applied irrigation, rainfall, and unsaturated zone water content. Urban built-up (FLUCCS code 1000) and transportation (FLUCCS code 8000) land use types also had low groundwater ET (3 inches/year). This is mainly because both land use types have higher impervious percentages, which minimizes the area available for groundwater ET to occur. Additionally, most of the pervious portions are landscaped and receive irrigation return flows to meet the crop ET demands. Total simulated ET, which is the sum of unsaturated zone ET and groundwater ET, is shown in **Figure 5-37e**. The highest total ET (58 inches/year) occurred in open water conditions (FLUCCS code 5000), followed by the wetland land use type (FLUCCS code 6000; 44 inches/year), primarily due to the higher groundwater ET contribution in these two categories. Generally, the average total ET simulated in all other land use types varied between 28 and 37 inches/year. Average simulated net recharge for various land use types is shown in **Figure 5-37f**. The highest average net recharge (20 inches/year) was simulated in the urban built-up (FLUCCS code 1000) areas. Net recharge was highest due to the combined effect of relatively higher recharge (managed recharge) and minimal groundwater ET in urban and built-up areas. Simulated net groundwater discharge was approximately 8 inches/year in open water conditions, where ET is highest and recharge is minimal because of the saturated conditions. The second lowest net recharge occurred in wetland areas (1 inch/year), also due to higher groundwater ET rates and lower recharge rates.

5.7.6 Extinction Depths Variation with Land Use Types

Extinction depth, or root zone depth, is a key parameter that controls ET. Extinction depths generally vary with crop type and thus land use type. Variation of average extinction depths with different land types are shown in **Figure 5-38**. The extinction depths in the model were highest (11 ft) for open water condition (FLUCCS code 5000). The highest extinction depths are assigned to open water to allow for maximum groundwater ET extraction in MODFLOW. The second highest average extinction depth (8 ft) was assigned to upland forest (FLUCCS code 4000) because roots generally grow deeper to extract groundwater. The lowest extinction depth (3 ft) was assigned to irrigated areas (FLUCCS code 2000), where crop water demand is mainly met with applied irrigation, in addition to the unsaturated zone water content and rainfall. Therefore, roots generally do not extend deeper to extract water from water table. The groundwater table is kept lower in most irrigated areas to avoid root damages due to saturation. The transportation land use type (FLUCCS code 8000) was assigned a smaller value (3 ft) because those areas are landscaped and well irrigated. Crop ET demands are met by the application of LSI water and roots generally do not extend deeper to extract water from the water table.

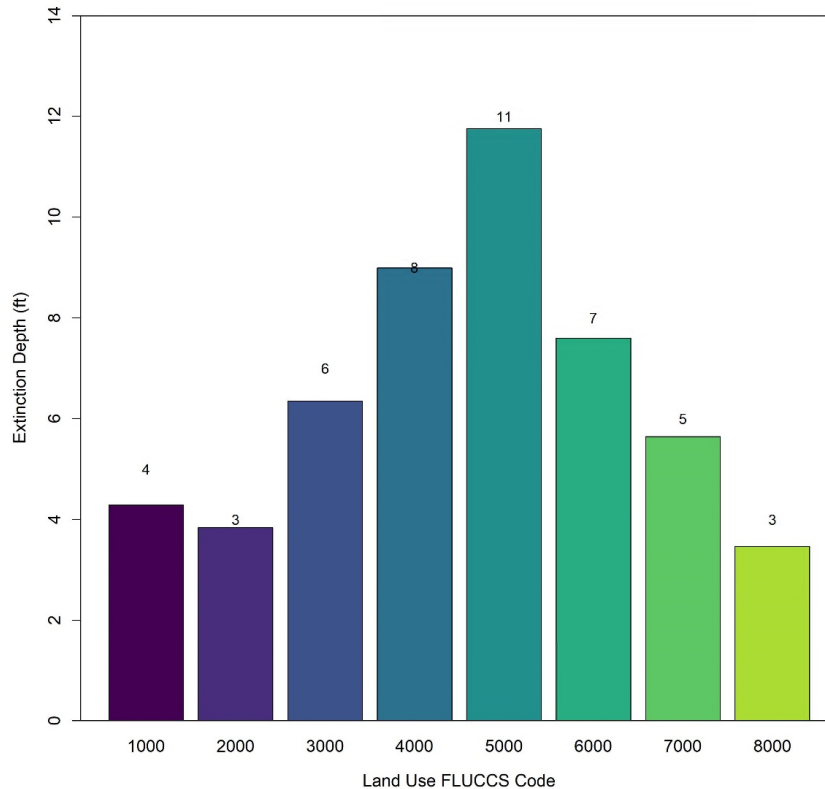


Figure 5-38. Average simulated extinction depths for different land use types. (Refer to **Table 5-2** for the FLUCCS codes.)

5.8 Pumping Wells

Pumping wells were entered into the model using the MODFLOW WEL package. The WEL package was generated using well input tables for each water use type: PS, CII, DSS, and AG with L/R. PS, CII, and DSS well input tables were constructed from measured or estimated pumping data, as described in **Section 3.3**.

Monthly reported PS and CII data were obtained from the SFWMD’s regulatory database. However, reported data for AG and L/R were incomplete. The AFSIRS program was used to generate the monthly AG and L/R data by permit. AFSIRS-generated demands were capped at 0.8 times the permitted allocation because the AFSIRS-generated demands generally are 1.2 to 1.5 ($1 \div 0.8 = 1.25$) times higher than the permitted allocations. AFSIRS demands were generated for average climatic conditions for the simulation period, while the permitted allocations represent 1-in-10 drought condition demands. Therefore, AFSIRS demands should always be less than permitted allocations. During the calibration process, AFSIRS demands were further adjusted to better match observed water levels. Monthly permit-level demands were assigned to well demands based on historical ratios, if available. If historical records were not available, the permit-level pumpage rates were equally distributed among the number of active wells.

A FORTRAN program was developed to read the individual well files and generate the MODFLOW WEL package. This program reads monthly pumpage data from each pumping well, total and casing depths of the wells, K data, and aquifer top and bottom elevations and assigns the withdrawals to the correct model layer. If a pumping well is open to multiple aquifers, the program assigns pumping rates proportional to the transmissivity of the aquifer. The use of well input tables facilitated easy editing of pumping rates, as needed, especially during manual calibration.

6 CALIBRATION

Model calibration involved adjusting model input parameters within reasonable ranges until model results (simulated water levels and/or structure flows) closely matched observed field data, while staying within the error bands of hydraulic properties observed from APTs or other information. For the LWCSIM, calibration was achieved by adjusting the parameters both manually and automatically. Manual model calibration was the process of changing one or more parameters in the model for each calibration model run. In the automatic calibration process, the model parameters were adjusted and optimized using the computer software PEST (Doherty 2010, Doherty and Hunt 2010).

Both the steady-state (1999 conditions) and the transient models were calibrated. Calibration and verification of the LWCSIM was intended to represent the hydrologic conditions from 1999 through 2012. This transient calibration period showed significant changes in population, land use, and water use as well as multiple drought and wet cycles. Prior to the calibration process, calibration goals were identified that describe reasonable tolerance limits for the goodness-of-fit of the simulation results to the measured field conditions. For this modeling effort, the comparisons were spatial and temporal. Multiple adjustments to aquifer hydraulic property types and values and to water recharge and discharge related inputs were made in a focused, trial-and-error process until the simulation results reasonably achieved calibration goals. The resulting calibrated model simulated historical and future aquifer conditions within the limits of calibration and model construction. Monthly groundwater level calibration targets were developed for the LWCSIM domain for the calibration and verification period from January 1999 through December 2014 using the District's DBHYDRO database and external county sources.

Calibration of the LWCSIM proceeded in an iterative fashion, using both automated (PEST) and manual adjustment of model parameters. The overall calibration process, from start to finish, consisted of the following steps:

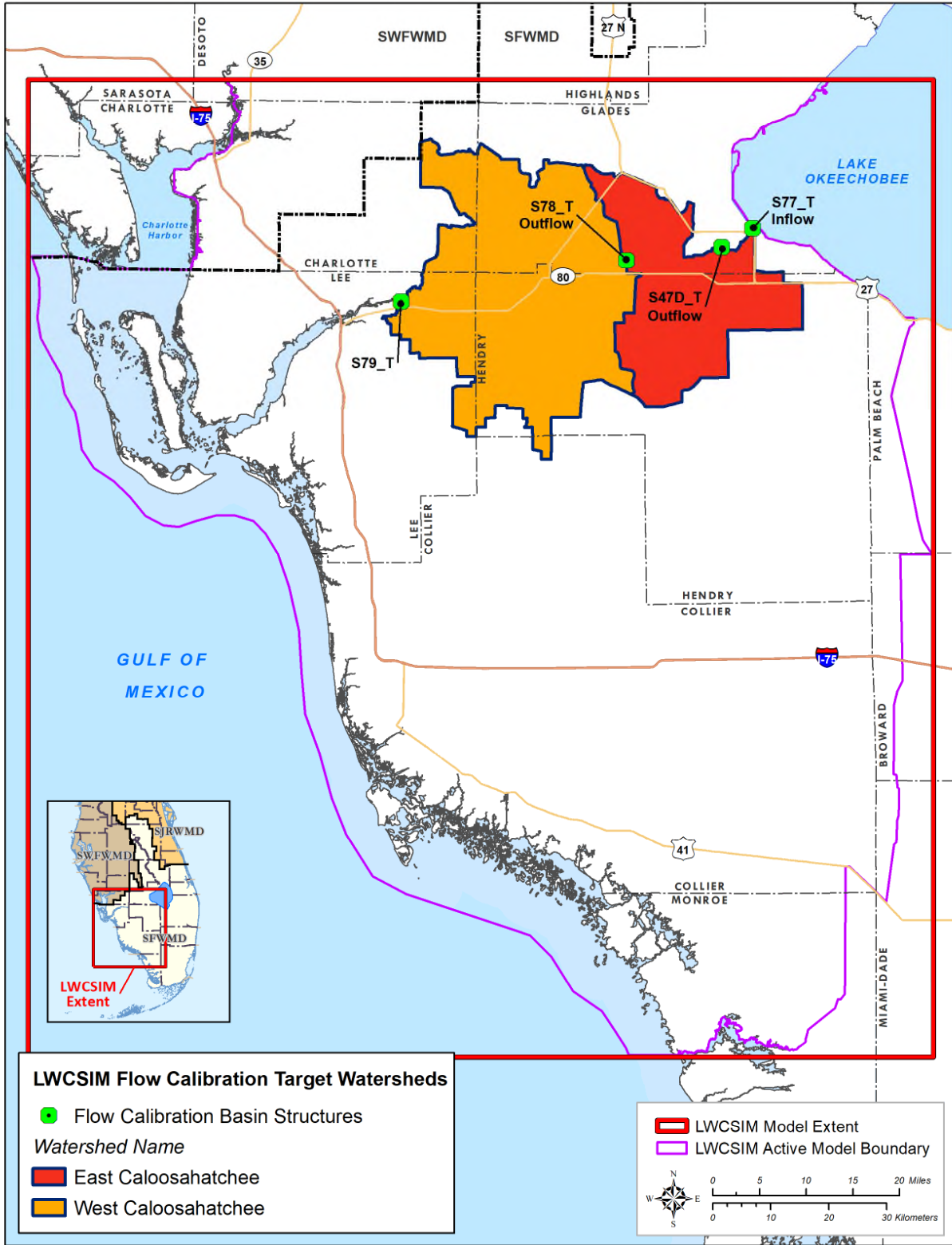
1. A steady-state model representing 1999 conditions was constructed, tested, and calibrated using PEST, varying only K_h in all nine model layers. Layer pinch-outs were not incorporated into the model for this first PEST calibration.
2. The results of step 1 were used as initial conditions for a full transient PEST calibration of the model, varying K ; river, drain, and GHB conductance; ET and recharge; and aquifer storativity. Layer pinch-outs were incorporated for the PEST transient calibration. PEST transient calibration was successful in calibrating the SAS layers (layers 1 through 3).
3. Manual calibration picked up where PEST calibration left off and was used to complete calibration of the LWCSIM, including the IAS layers (layers 4 through 9).

These were the major steps of the calibration process. of the following sections describe each calibration step, from the initial steady-state PEST calibration to the final manual transient calibration.

6.1 Methodology

6.1.1 Calibration Targets

The calibration targets were primarily groundwater monitor wells that had observed data. Calibrating a groundwater model only to groundwater levels does not guarantee a unique solution, especially when groundwater systems are highly connected to the surface water system, as they are in southwestern Florida where surface water bodies are strongly connected to the SAS through wetlands and rivers. This necessitated ensuring the surface water fluxes and water levels also were reasonable. An iterative groundwater recharge estimation process using the ET-Recharge-Runoff pre-processor and MODFLOW ensured the modeled surface water fluxes were reasonable compared to the observed structure flow data in terms of overall mass balance and the transient response. Measured structure flow from two major watersheds were selected as flow calibration targets (**Figure 6-1**). Measured water levels at 60 gauge stations in wetland areas were used as surface water level calibration targets (**Figure 6-2**). Additionally, four measured ET sites were selected as ET calibration targets (**Figure 6-3**). There were 441 groundwater monitor wells used as calibration targets, including 297 in the WTA, 72 in the LTA, 29 in the SSA-clastic, and 18 in the SSA-carbonate, and 25 in the MHA (**Figure 6-4**). The goal of model calibration was to match the model-calculated head levels, flows, and ET to the measured data at these target locations. Time-series data for groundwater heads and surface water stages were collected primarily from USGS, SFWMD, SWFWMD, Lee County, and Collier County monitor wells. Measured ET data were obtained mainly from the USGS. The monitor well data were thoroughly reviewed, and questionable well targets were removed. Observed data were summarized as averaged monthly heads. Estimated baseflows at the measured structure flow locations also were used as calibration targets. Boundary fluxes from the eastern and northern boundaries of the LWCSIM were compared with the District's LECsR Model (Giddings et al. 2006) and the SWFWMD's DWRM (Environmental Simulations, Inc. 2014), respectively.



\\ad.sfwmd.gov\dfsroot\GIS\GISBiz\W\SLWCSIM\Report_Figures\mxd\20200616_FlowCalibrationTargetWatersheds.mxd

Figure 6-1. Flow calibration targets.

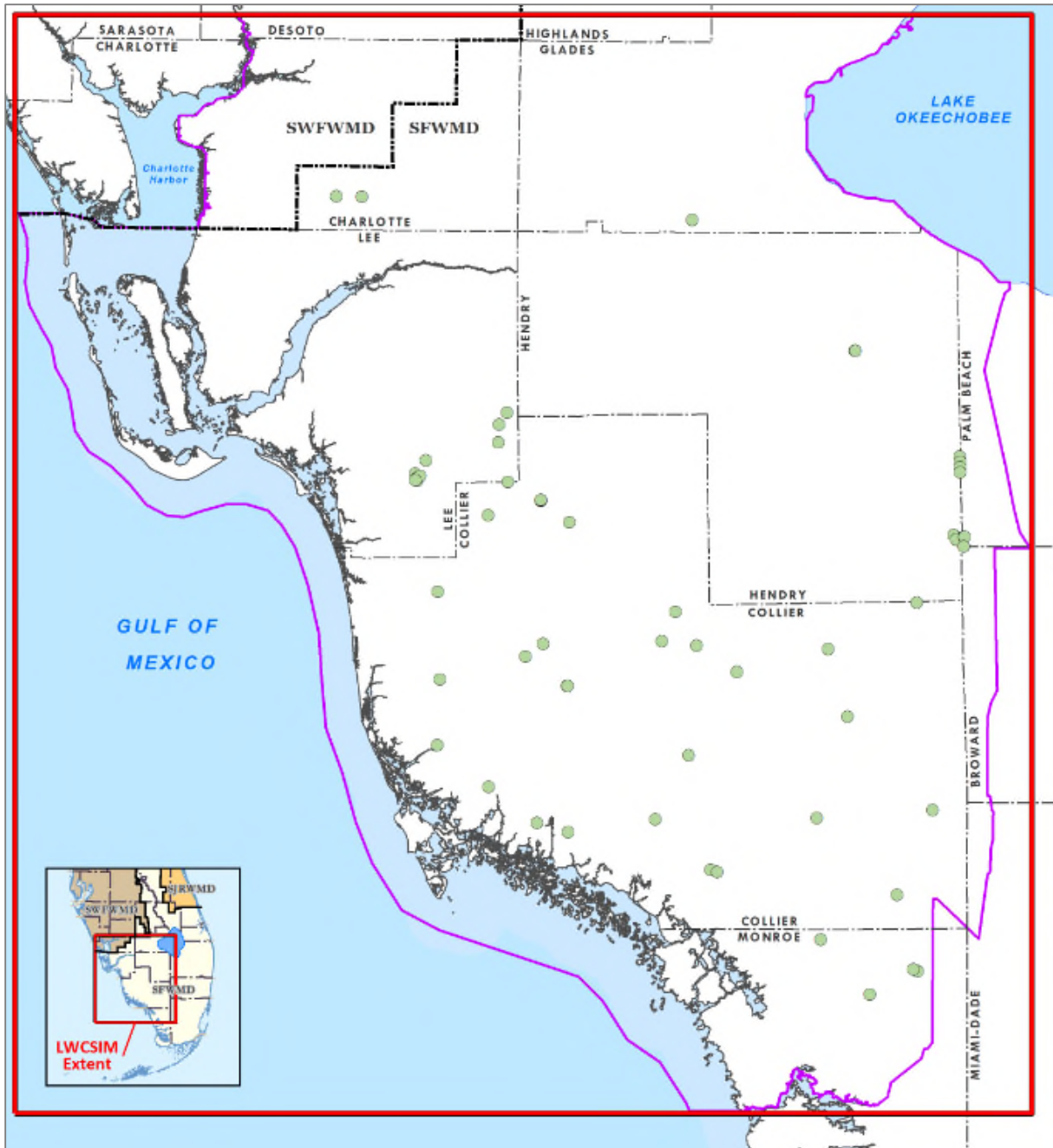


Figure 6-2. Surface water calibration targets.

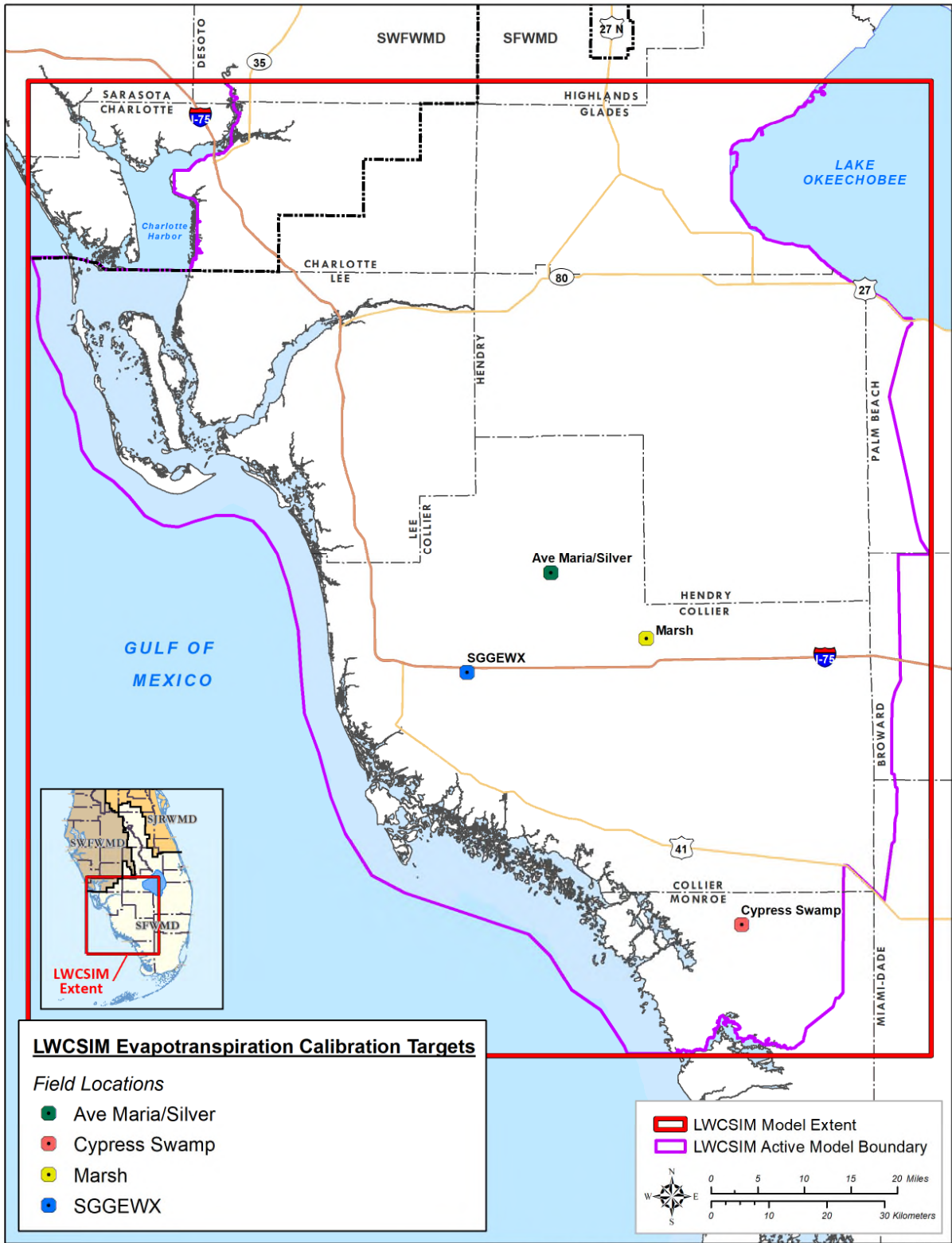
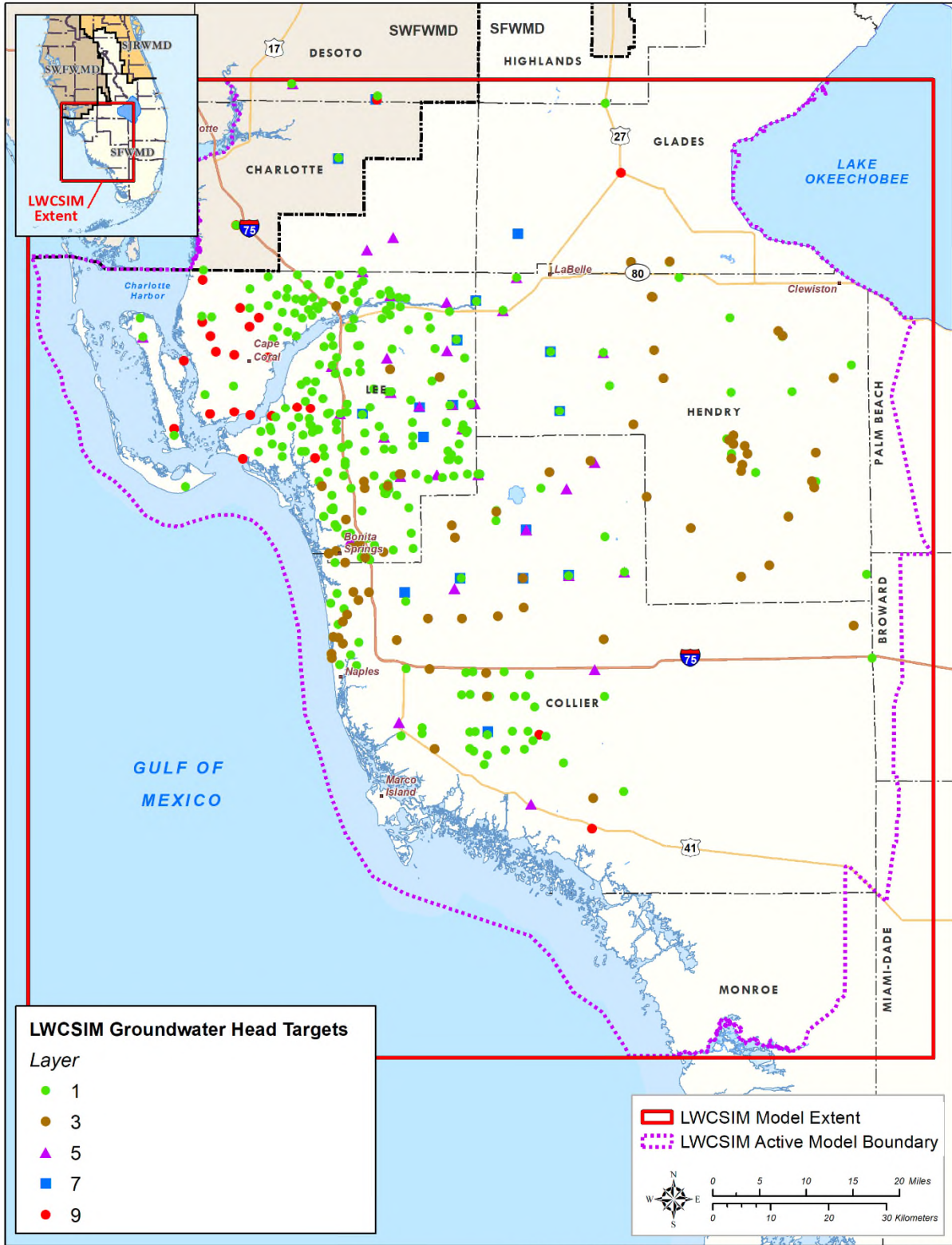


Figure 6-3. Evapotranspiration calibration targets.



\\ad.sfwmd.gov\dfsroot\GIS\GISBiz\WS\LWCSIM\Report_Figures\mxd\20200617_GWHeadTargets.mxd

Figure 6-4. Groundwater level calibration targets.

6.1.2 Automated Calibration

The LWCSIM used a combination of automated and manual calibration methods. PEST (Doherty and Hunt 2010), a model-independent parameter optimization code, was used first for automated calibration. To minimize computational time during PEST simulations, BeoPEST (Hunt et al. 2010) was used. BeoPEST manages parallel runs more efficiently than the standard PEST calibration method.

Uniqueness in model calibration is achieved through a simplification of parameters called regularization. For this model, regularization was achieved through application of Tikhonov constraints, which solves ill-posed inverse problems. Tikhonov regularization is the imposition of a “smoothing constraint” on parameters (Doherty 2010). This approach applies each parameter difference to PEST as extra “observations.” Regularization also applies expert knowledge to the parameter estimation processes. For the LWCSIM, this was accomplished by constraining the aquifer parameter values while considering APT values and prior information gained from previously developed models.

Pilot points as well as watershed-based approaches were used in the PEST calibration. Pilot points were used for parameter point values such as K and storage coefficients. The point values of these parameters at calibration are used to interpolate throughout the model domain using kriging. The pilot point technique helped to characterize heterogeneities in the hydraulic properties. Pilot points were generated following the guidelines in Doherty (2010):

- 1) Place pilot points at the center of head calibration targets
- 2) Place pilot points at locations of APTs and core samples (for Kv analysis) in the confining units
- 3) Fill gaps in the model domain with initial educated guess values
- 4) Refine the overall pilot point distribution, especially in dense areas prescribed by steps 1 and 2, resulting in an excessive number of pilot points over a small region

A logarithmic transformation was applied to parametric values such as K, as the values range over several orders of magnitude. Watershed-based parametric calibration was done for parameters such as river and drain conductance.

For the LWCSIM calibration effort, the PEST objective function (ϕ) to be minimized was defined as the sum of the weighted root mean square error of the heads and recharge fluxes. Weighting factors for each individual observation value were determined based on data reliability, number of observations, accuracy, and calibration performance.

6.2 Calibration Parameters

6.2.1 Hydraulic Conductivity

The LWCSIM was calibrated by adjusting Kh values within the major aquifers and Kv values within the confining units. Flow is dominated by Kh in a productive aquifer and Kv in the confining units between the major aquifers. Parameters selected for calibration in PEST included Kh in the permeable aquifer units (i.e., WTA, LTA, SSA-clastic, SSA-carbonate, and MHA), Kv in the confining units, and storativity in the confined aquifers. In the LWCSIM, most head targets and APTs are located in the WTA, LTA, SSA-clastic, and SSA-carbonate. Therefore, most pilot points were generated and distributed in these units. In the MHA, aquifer parameter and head observations become much sparser spatially across the domain and are primarily concentrated along the coast. Pilot points in the confining units were spatially distributed in a grid-based

fashion. During the PEST calibration process, model input parameters were adjusted within user-specified ranges. The ranges for pilot points in the permeable units were set at reasonable multiples of observed values based on data confidence. During iterative calibration, some pilot point intervals were slightly modified. The parameter ranges were set to represent a bracketed range from observed field test values.

A preliminary test run of PEST was performed in Groundwater Vistas to evaluate calibration of the 1999 steady-state flow model to observed water levels using only K_h as the variable parameter. The test run yielded results that suggested maintaining continuous K_h distributions across each model layer, as opposed to representing hydrostratigraphic layer absences by assigning properties from the layer below in areas where the layer is apparently missing. Attempts to capture local heterogeneities adversely affected steady-state model stability. Thus, the layer pinch-outs were not incorporated in the steady-state calibration. Transient model calibration began with a K distribution that did include layer pinch-outs. This is discussed in more detail in **Section 6.4.1**.

6.2.2 Leakance Values

Leakance values (K_v) of the four confining layers—layer 2: the TCU, layer 4: the Upper Hawthorn confining unit (H1), layer 6: the Sandstone aquifer confining unit (SC), and layer 8: the Mid-Hawthorn confining unit (H2)—were adjusted by including them as a variable in the automated calibration process. The calibration method developed for the LWCSIM modeling effort relied on a regional approach, where important model parameters such as K_h and K_v were adjusted in a systematic way to best match observed water levels.

6.2.3 Storage Parameters

Storage parameters for the aquifer systems were estimated as a continuous spatial field variable instead of a single parameter across a model layer. Storage parameters help describe the rate at which water is taken from the aquifer matrix and help develop the time-varying responses of the transient model. Changes in these parameters were accomplished by enabling estimation of the spatial variation, such as the approach used with the K_h values of the aquifer layers estimated in the automated calibration process.

6.2.4 Crop Coefficients

The ET-Recharge-Runoff program calculates maximum groundwater ET, recharge, and runoff as described in **Section 5.7**. The maximum groundwater ET was calculated as the supplemental crop water demand, after using the water from rain, irrigation, and soil moisture. The program used the potential ET of each crop type associated with the land use and K_c to calculate the crop ET requirement. By varying the crop ET requirement, maximum groundwater ET demands varied.

6.2.5 Extinction Depths

Extinction depth is the cutoff depth below which actual groundwater ET cannot occur. The actual groundwater ET rate is highest at the ET surface (generally ground level), gradually decreases as it goes deeper, and ceases at the extinction depth. Generally, this depth is specific to crop type. Initial extinction depth estimates were obtained from previous modeling studies in the area (Shah et al. 2007). Extinction depths were varied during the calibration process to adjust ET rates.

6.2.6 Curve Numbers

The NRCS CN method was used to separate runoff from rainfall, as described in **Section 5.7**. CNs are associated with land use, and higher CN values indicate higher runoff potential, while lower CNs indicate lower runoff potential. CNs were adjusted during the structure flow calibration process.

6.2.7 River and Drain Conductance

River and drain conductance values were adjusted to achieve better simulated baseflows, as described in **Section 5.7**. River and drain conductance values were joined with specific watersheds and assigned a watershed ID value for the grids situated within the watershed. For calibration, a similar multiplying factor was applied to each river/drain conductance within a given watershed ID. This avoided point-scale calibration of the thousands of grid cells, and instead downscaled it to a scale of four watersheds. Initial values of river/drain conductance were based on the values estimated using equation (13) in **Section 5.3**.

6.2.8 Pumping Rates

Pumping rates for AG, L/R, and DSS wells were estimated due to incomplete or poor quality data. Pumping rates were adjusted during the calibration process after the main calibration parameter changes were exhausted, particularly in situations where monitor wells showed trends in water levels (e.g., a sharp or gradual increase or decrease in water levels). DSS pumping rates were adjusted in the MHA (layer 9) pumping wells around Cape Coral to simulate the observed sharp declines in water levels over time. AG pumping rates in the SSA (layers 5 and 7) were adjusted during calibration to obtain a better match of simulated and observed water levels.

6.3 Steady-State Calibration

Calibration of the LWCSIM 1999 steady-state model was a multi-step process involving Groundwater Vistas, GIS, PEST++, and some manual adjusting of parameters. Water levels in 1999 from 177 groundwater observation wells were averaged across all nine model layers. The model was run using the K value based on an interpolation of APT values, prior to PEST calibration, to ensure convergence. The results of this initial steady-state model run indicated an absolute residual mean of 2.95 ft, with an observed head range of 60 ft. PEST was then used, varying only Kh in the nine model layers. The initial Kh, based on APTs, was assigned to pilot points arrayed in an approximate rectangular grid across the active model domain. During the initial PEST calibration run, the Kh in each model layer was changed to achieve a better fit between observed and modeled heads. The total number of water level observation points was increased to 266 (with some original points omitted), with a head range of 46.14 ft. The absolute residual mean was reduced to 1.73 ft, and the residual statistics and modeled versus observed heads are shown in **Table 6-1**. The observed versus modeled head is presented in **Figure 6-5**. The resulting head solution was used as the initial head array for the start of the transient model run. In addition, hydrostratigraphic layer absences (i.e., pinch-outs) were incorporated into the model.

Table 6-1. Residual statistics after parameter estimation (PEST) calibration of steady-state model.

| By Layer | | | Overall Statistics | |
|----------------|------------------------|---------------------|------------------------------------|-----------|
| Layer | Absolute Residual Mean | No. of Observations | | |
| 1 | 1.50 | 186 | Residual mean | -0.46 |
| 2 | 0.98 | 11 | Residual standard deviation | 2.14 |
| 3 | 2.32 | 27 | Absolute residual mean | 1.73 |
| 4 | 1.93 | 12 | Residual sum of squares | 1.27e+003 |
| 5 | 3.11 | 14 | Root-mean-square error | 2.19 |
| 6 | 4.17 | 4 | Minimum residual | -6.84 |
| 7 | 1.61 | 8 | Maximum residual | 4.86 |
| 8 | 2.69 | 2 | Range of observations | 46.14 |
| 9 | 4.93 | 2 | Scaled residual standard deviation | 0.046 |
| | | | Scaled absolute mean | 0.038 |
| Overall | 1.73 | 266 | Scaled root-mean-square | 0.047 |
| | | | Number of observations | 266 |

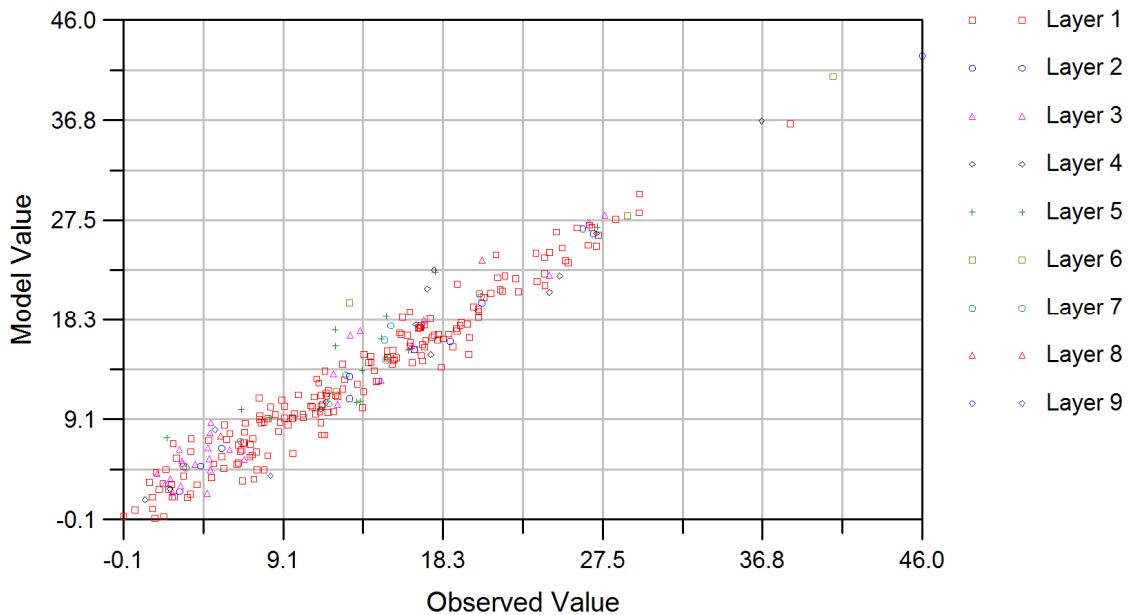


Figure 6-5. Observed versus simulated steady-state heads in all model layers.

6.4 Transient Calibration

For the transient model calibration, a combination of automated (PEST) and manual procedures was used. The main calibration targets were the monthly averaged observed water levels in 502 monitor wells and 60 wetland gauges and the monthly averaged measured structure flows from 2 watersheds. Additionally, ET rates measured from four stations were used as calibration targets. Several model parameters were varied throughout the transient calibration process, such as K; river, drain, and GHB conductance; pumping rate; CN; crop coefficient; ET and recharge rate; and aquifer storativity.

The calibration period ran from 1999 through 2012, while 2013 through 2014 were used as the verification period. The extent of flooded and dry cells, depth-to-water-table information, and regional potentiometric surfaces were used qualitatively to guide the manual transient calibration process. Additionally, GHB fluxes from saltwater boundaries were adjusted to minimize saltwater influx as artificial freshwater influx to the model.

6.4.1 Transient Calibration Setup

Prior to performing the transient model calibration, a K distribution based on the steady-state PEST calibrations, which included stratigraphic pinch-out areas in layers 1 through 7, was tested in the 1999 steady-state model. For the first pre-PEST full transient model (168 stress periods), this K configuration provided the fastest and most stable convergence (approximately 45 seconds per stress period).

In order to incorporate the layer pinch-outs in layers 1 through 7 K value surfaces, Groundwater Vistas and ArcMap (GIS) were used. The procedure was as follows:

1. Beginning with the PEST-derived K distribution in each layer, the K value was accessed and post-processed using Groundwater Vistas. From there, the K value of layer 8 was exported as a point shapefile.
2. The shapefile was brought into ArcMap and selected by location against a prepared shapefile representing layer 7 pinch-outs.
3. The selected cells were extracted and saved as a shapefile containing layer 8 K values in the shape of the layer 7 pinch-outs.
4. In Groundwater Vistas, the new shapefile was imported to the K value of layer 7. K values in the layer 7 pinch-out cells were replaced with the K values of the corresponding layer 8 cells.
5. In Groundwater Vistas, the updated K value of layer 7 was exported as a point shapefile to use against layer 6, repeating the procedure above beginning with step 2.
6. This process was repeated for the remaining model layers.

The “bullseye” patterns or anomalies in **Appendix H**, Figures H-1 to H-5, is the result of using the process above to insert adjacent layer properties in areas of layer pinch-outs.

6.4.2 Transient Calibration Procedure

Groundwater Level Calibration

Calibration consisted of manually adjusting K, leakance and specific storage, pumping rates, ET, and recharge to improve matches between simulated and observed heads, flows, and ET rates. Starting conditions and initial parameters were obtained from the steady-state calibrated model for 1999. A continuing emphasis during the calibration process was honoring the conceptualization of the system described earlier. Parameters were constrained within reasonable ranges based on prior knowledge of the hydrogeologic system.

PEST calibration focused on reducing the residuals of groundwater levels and baseflows by adjusting K, leakance, and river and drain bed conductance. PEST successfully met the calibration goals in the SAS layers of the model (layers 1 and 3, the WTA and LTA, respectively). However, no significant improvements were made by PEST to layers 5, 7, and 9 (SSA and MHA, respectively). Layers 5, 7, and 9 were manually calibrated by adjusting K, leakance, storativity, and pumping rate. The leakance between the productive aquifers (i.e., between the MHA and SSA, between the SSA and LTA) was the most sensitive parameter during manual calibration. As expected, pumping rate in the MHA was a very sensitive parameter because the MHA is not a very productive aquifer. More detailed descriptions about parameter sensitivities can be found in **Section 7**. A sharp decline (on the order of 20 to 30 ft) in MHA water level was observed

from 2000 to 2003 due to the introduction of a large number of small DSS wells, primarily in the Cape Coral area. No reported data for the DSS pumping wells were available; therefore, pumping rates were adjusted until an adequate match between the observed and simulated water levels was obtained.

Simulated ET rates were adjusted in wetland areas in the southern portion of the model to match measured ET rates. The ET rates were increased by increasing the wetland crop coefficients from 1.1 to 1.2. The simulated water levels in the southwest portion of layer 1 consistently were overestimated prior to the ET adjustments. After the ET adjustments, the simulated water levels were in good agreement with metered data.

Structure Flow Calibration

Surface water is highly connected to the SAS through rivers, drains, and wetlands in southwestern Florida. Therefore, it is important to ensure the interaction between groundwater and surface water systems are simulated reasonably well and the overall mass balance is preserved between surface water and groundwater systems. Simulated transient surface water flows were compared with measured surface water flows at gauged structures. The simulated total structure flow out of a watershed is the sum of runoff and baseflow within the watershed. Runoff was simulated using the ET-Recharge-Runoff program, and the simulated baseflow was extracted from MODFLOW river and drain leakages, as described in **Section 5.7**. The ET-Recharge-Runoff program is not coupled to MODFLOW; therefore, a process was developed to iteratively calibrate canal net flows between the two programs. Interaction between the surface water and groundwater systems was facilitated by a simple canal water budget program and the ET-Recharge-Runoff program. The simple canal water budget program neglects storage in the canals and is represented by equation 19:

$$[\text{Runoff} + \text{Baseflow}]_{\sim \text{NET FLOW}} = \text{Structure canal outflows} + \text{Pumpage} - \text{Structure canal inflows} - \text{Return flows from lakes} \quad (19)$$

Where runoff is the routed runoff computed with the NRCS/Muskingum method, structure canal inflows and outflows are obtained from measured flow at gauges, and baseflow (Q) is calculated using equation 20 from MODFLOW:

$$Q_{\text{baseflow}} = ((K \times L \times W) \div M) \times (h_{\text{river}} - h) \quad (20)$$

Where:

h_{river} is the river stage

h is the aquifer hydraulic head

K is the hydraulic conductivity of riverbed material

L is the length of the reach

W is the width of the river

M is the thickness of riverbed sediments

The first step was to develop initial ET and recharge values for MODFLOW using the ET-Recharge-Runoff program. MODFLOW was executed using the initial ET and recharge values, and the baseflow components were extracted from the River and Drain package outputs. For the selected basins, an instantaneous hydrograph of runoff was derived by subtracting estimated baseflow from observed stream flow hydrograph data and compared with runoff calculated from the ET-Recharge-Runoff program. Baseflows were estimated from net flows using the Web-based Hydrologic Analytical Tool (WHAT) program (<https://engineering.purdue.edu/mapserve/WHAT/>). The WHAT program uses frequency analysis of flows to conduct baseflow separation from managed watersheds. The WHAT results were compared against other

methods used by the USGS such as the Baseflow Index, stream flow hydrograph separation (HYSEP), and Partitioning to estimate daily discharge. The result shows the WHAT program has a better performance over the Baseflow Index for watersheds (larger than 500 square miles).

Runoff and baseflow components were adjusted to achieve a reasonable match with the observed stream flow hydrograph. Runoff calibration was achieved by adjusting the CN of the model cells within the basin. Where the drainage basin area was significantly larger, the outflow hydrograph peak can be less pronounced and takes more time to occur than the instantaneous hydrograph. In such situations, runoff was routed using the Muskingum method to correct the time lag and attenuate the peak of the output flood hydrograph. Baseflows were adjusted based on the estimated values by adjusting the river and drain bed conductance. The ET-Recharge-Runoff program was re-run using the adjusted CNs, and then ET and recharge values were passed to MODFLOW. MODFLOW was re-run with adjusted river/drain bed conductance values. This procedure was repeated until a reasonable match between the observed and simulated runoff and baseflow hydrographs was achieved.

Due to the size of the model cells (1,000 ft × 1,000 ft), there can be several different land use types within a cell. The initial CN for a given cell was calculated based on the three predominant land uses in the cell. Because CNs depend on the antecedent moisture content of the soil, they were adjusted based on the daily rainfall events during the calibration period, as described in **Section 5.7**. The model domain underwent substantial land use changes during the calibration period. To capture the effects of land use change on ET and recharge, four land use maps were used: 2000, 2004, 2010, and 2014. CNs were adjusted to reflect land use changes over the calibration period.

Within the LWCSIM domain, two major watersheds were selected for calibration based on the availability of continuously measured structure flow data. Gauged basins were delineated by combining multiple HUC12 watersheds to ensure the availability of inlet and outlet stream gauging stations.

Surface Water Level Calibration

The LWCSIM routes overland flow over wetland areas, where the Wetlands package is used. Thus, wetland area water levels simulated with the Wetlands package can be directly compared to observed water level data. Initial Kh values were assigned based on kriged data, using the APT and other field data, and adjusted during calibration. Initial Kadlec coefficients were used from the LECsR Model and adjusted during calibration. In southwestern Florida, most wetlands are hydraulically connected to the water table; therefore, wetlands respond highly to groundwater changes.

6.4.3 Transient Calibration Criteria

Statistical calibration goals for the LWCSIM were established based on comparing modeled and measured water levels in 502 groundwater observation wells, providing monthly groundwater levels for the period of record. Not all 502 observation wells have data for every month of the period of record; therefore, not all wells were used in every model stress period. Model performance statistics were calculated by finding the differences between the measured and modeled values (referred to as the residuals) for each stress period and then assessing the result against the metric via direct comparison or calculating statistics on the residuals.

The calibration goals for groundwater observation wells in LWCSIM were:

1. A mean residual error for the five aquifer layers of less than 1 ft.
2. An absolute residual mean and root mean square error of less than 5 ft.

3. 50% of the mean absolute simulated head residuals for all wells in the five aquifer layers had to be within 2.5 ft of observed.
4. 80% of the mean absolute simulated head residuals for all wells in the five aquifer layers had to be within 5 ft of observed.
5. 60% of the observed versus simulated hydrographs in the five aquifer layers had to have a Pearson coefficient of correlation (R^2) value greater than 0.4.
6. 60% of the observed versus simulated hydrographs in the five aquifer layers had to have a transformed Nash-Sutcliffe efficiency (TNSE) coefficient value of greater than 0.4.

R^2 is defined as:

$$R^2 = \frac{(\sum_i^N (S_i - \bar{S}_i)(O_i - \bar{O}_i))^2}{\sum_i^N (S_i - \bar{S}_i)^2 \sum_i^N (O_i - \bar{O}_i)^2} \quad (21)$$

Where:

S_i = the i^{th} simulated head at the monitor well

O_i = the i^{th} observed head at the monitor well

\bar{S}_i = the average simulated head at the monitor well

\bar{O}_i = the average observed head at the monitor well

The TNSE was determined for all aquifer layer transient groundwater calibration targets as an additional indicator of transient model fit. Through statistical comparison with the R^2 value, it was determined that a TNSE value of 0 or higher roughly corresponds to an R^2 value of 0.4 or higher, allowing for determination of a TNSE calibration criterion for the LWCSIM that is similar to the R^2 . The TNSE was determined using the following equation:

$$TNSE = 1 - \frac{\sum_{i=1}^n (X_i - Z_i)^2}{\sum_{i=1}^n (X_i - \bar{X})^2} \quad (22)$$

Where:

X_i = the i^{th} transformed observed head value at a particular observation well

$X_i = O_i - \bar{O}$

\bar{X} = the mean of the transformed simulated head values at the observation well (this should be zero)

Z_i = the i^{th} transformed simulated head value at the same well location

$Z_i = S_i - \bar{S}$

\bar{S} = the mean of the simulated head values at the observation well

\bar{S}_i = the average simulated head at the monitor well

O_i , \bar{O} , and S_i as previously defined

To be more precise, the R^2 quantile for an R^2 of 0.4 is about 0.262 (i.e., approximately 26% of R^2 values are less than 0.4). The TNSE quantile for a TNSE of about 0.063 is 0.262 (i.e., approximately 26% of TNSE values are less than 0.063). The TNSE quantile for a TNSE of zero is about 0.252. Based on the above, three categories of model fit were created based on the TNSE:

- $TNSE < 0$: Model quality is less than null model of observed mean
- $0 \leq TNSE < 0.5$: Low-quality fit
- $0.5 \leq TNSE$: Moderate- to high-quality fit

Based on the above, a TNSE cutoff of 0 was chosen.

The calibration criteria were derived from the recently calibrated, peer-reviewed East Central Florida Transient Expanded (ECFTX) Model (Central Florida Water Initiative Hydrologic Assessment Team 2020). A summary of the transient calibration criteria is provided at the end of this section.

An alternative method for using calibration statistics to assess the fit of the model to observed water levels was to use the range in head values as the basis for establishing calibration goals. For example, requiring the absolute mean head error and the root mean square error to be less than 5% to 10% of the range in head. In other words, if the range in head in any given month is 100 ft, then the goal would be 5 to 10 ft.

The same calibration criteria were used for surface water level calibration. The calibration criteria for structure flows were selected based on the criteria used in previous regional models (Central Florida Water Initiative Hydrologic Assessment Team 2020) and are as follows.

1. Deviation of volume less than 15%
2. Nash-Sutcliffe efficiency coefficient greater than 0.5
3. R^2 greater than 0.5

Deviation of volume (DV) is defined as:

$$DV = \frac{\sum_{i=1}^N (S_i - O_i)}{\sum_{i=1}^N O_i} * 100 \quad (23)$$

Nash-Sutcliffe efficiency (NSE) is defined as:

$$NSE = 1 - \frac{\sum_i^N (O_i - S_i)^2}{\sum_i^N (O_i - \bar{O}_i)^2} \quad (24)$$

R^2 is defined as:

$$R^2 = \frac{(\sum_i^N (S_i - \bar{S}_i)(O_i - \bar{O}_i))^2}{\sum_i^N (S_i - \bar{S}_i)^2 \sum_i^N (O_i - \bar{O}_i)^2} \quad (25)$$

Where:

S_i = the i^{th} simulated flow value at the structure

O_i = the i^{th} observed flow value at the structure

\bar{S}_i = the average simulated flow value at the structure

\bar{O}_i = the average observed flow value at the structure

Final Calibrated Model Properties

Appendix H contains figures showing the end result of the manual transient calibration: property distributions in the LWCSIM layers. Field test measurements of Kh are overlaid to show the calibrated Kh distributions stayed within an order of magnitude of field measured values during the calibration process throughout the LWCSIM domain. Transmissivity, leakance, and storage coefficient distribution figures also are presented in **Appendix H**.

6.4.4 Model Fit/Statistics

Groundwater Level Calibration

The result of transient calibration is presented in the summary of calibration statistics (**Table 6-2**). The majority of the monitor wells are open to the WTA (297 wells) and LTA (72 wells). All water level calibration criteria were achieved for all aquifers of the model except mean absolute error (MAE) in the MHA. The calibration criteria for average mean error is ± 1 ft for all aquifers. In the WTA, the mean error was -0.27 ft, indicating a slight underprediction of water levels. In the LTA, the SSA-clastic and SSA-carbonate had mean errors of 0.58 ft, 0.52 ft, and 0.7 ft, respectively, indicating a slight overprediction of water levels. The average mean error in the MHA was -1.08 ft, indicating an underprediction of water levels. The calibration criteria for standard deviation, MAE, and root mean square error were 5 ft for all aquifers. These three criteria were met for all aquifers except the MAE criteria in the MHA. Minimum and maximum residuals generally are 10 ft or lower in all aquifers. More than 90% of monitor wells in all aquifers showed less than 5 ft of error. At least 59% of monitor wells showed an error less than 2.5 ft in all the aquifers. The calculated R^2 and TNSE values indicate a very good transient response of the simulated water levels. The calculated R^2 values show that at least 65% of monitor wells had R^2 values greater than 0.4. At least 72% of the monitor wells had TNSE values greater than zero in all aquifers.

Table 6-2. Transient model calibration statistics of the target monitoring wells in the model.

| Statistics | Criteria | Aquifer | | | | |
|------------------------------|------------|---------|-------|-------------|---------------|-------|
| | | WTA | LTA | SSA-clastic | SSA-carbonate | MHA |
| Mean error | ± 1 ft | -0.29 | 0.58 | 0.46 | 0.61 | -1.08 |
| Error standard deviation | <5 ft | 2.31 | 3.11 | 3.77 | 2.11 | 2.45 |
| Mean absolute error (MAE) | <5 ft | 1.99 | 2.82 | 3.74 | 3.26 | 5.95 |
| Root mean square error | <5 ft | 2.32 | 3.14 | 3.73 | 2.15 | 2.63 |
| Minimum residual | | -9.12 | -4.12 | -9.91 | -3.28 | -7.38 |
| Maximum residual | | 6.45 | 9.35 | 5.27 | 3.78 | 4.39 |
| Number of observation points | | 297 | 72 | 29 | 18 | 23 |
| Percentage with MAE < 2.5 ft | >50% | 71 | 60 | 59 | 78 | 78 |
| Percentage with MAE < 5.0 ft | >80% | 97 | 92 | 90 | 100 | 91 |
| Percentage with $R^2 > 0.4$ | >60% | 76 | 81 | 69 | 83 | 65 |
| Percentage with TNSE > 0 | >60% | 78 | 89 | 83 | 89 | 72 |

LTA = Lower Tamiami aquifer; MHA = Mid-Hawthorn aquifer; R^2 = Pearson coefficient of correlation; SSA = Sandstone aquifer; TNSE = transformed Nash-Sutcliffe efficiency; WTA = Water Table aquifer.

Green font indicates compliance with calibration criteria.

Calibration period: 1999 to 2012.

Appendix I contains all calibration target hydrographs and a summary table for all model layers. Spatial distribution of groundwater monitor wells and their average simulated errors (residuals) for the WTA, LTA, SSA-clastic, SSA-carbonate, and MHA are shown in **Figures 6-6 to 6-10**. Monitor wells shown in red represent where average simulated water levels are lower than average measured water levels, indicating an underprediction. Monitor wells shown in blue represent locations where average simulated water levels are higher than average measured water levels, indicating an overprediction. The size of the symbols is proportional to the average residual at that location. **Figure 6-6** shows monitor wells in the WTA (layer 1) are located mainly along the Gulf coast where the WTA is heavily used (e.g., Naples, Bonita Springs, Fort Myers, Cape Coral). Overall, the model shows a very good distribution of residuals with no significant spatial bias in the WTA. However, there is a consistent, slight overestimation of simulated water levels in the Picayune Strand area of southern Collier County.

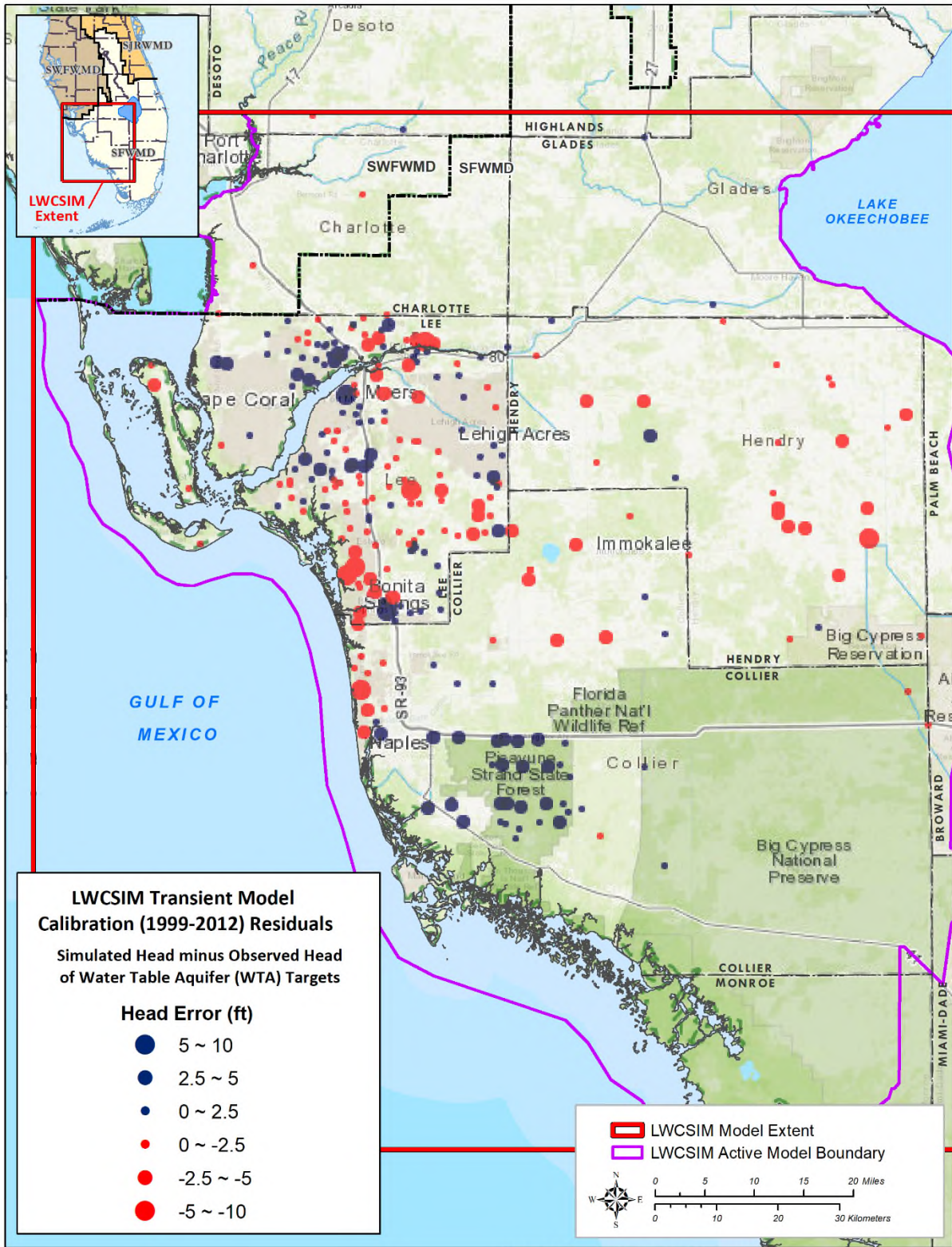
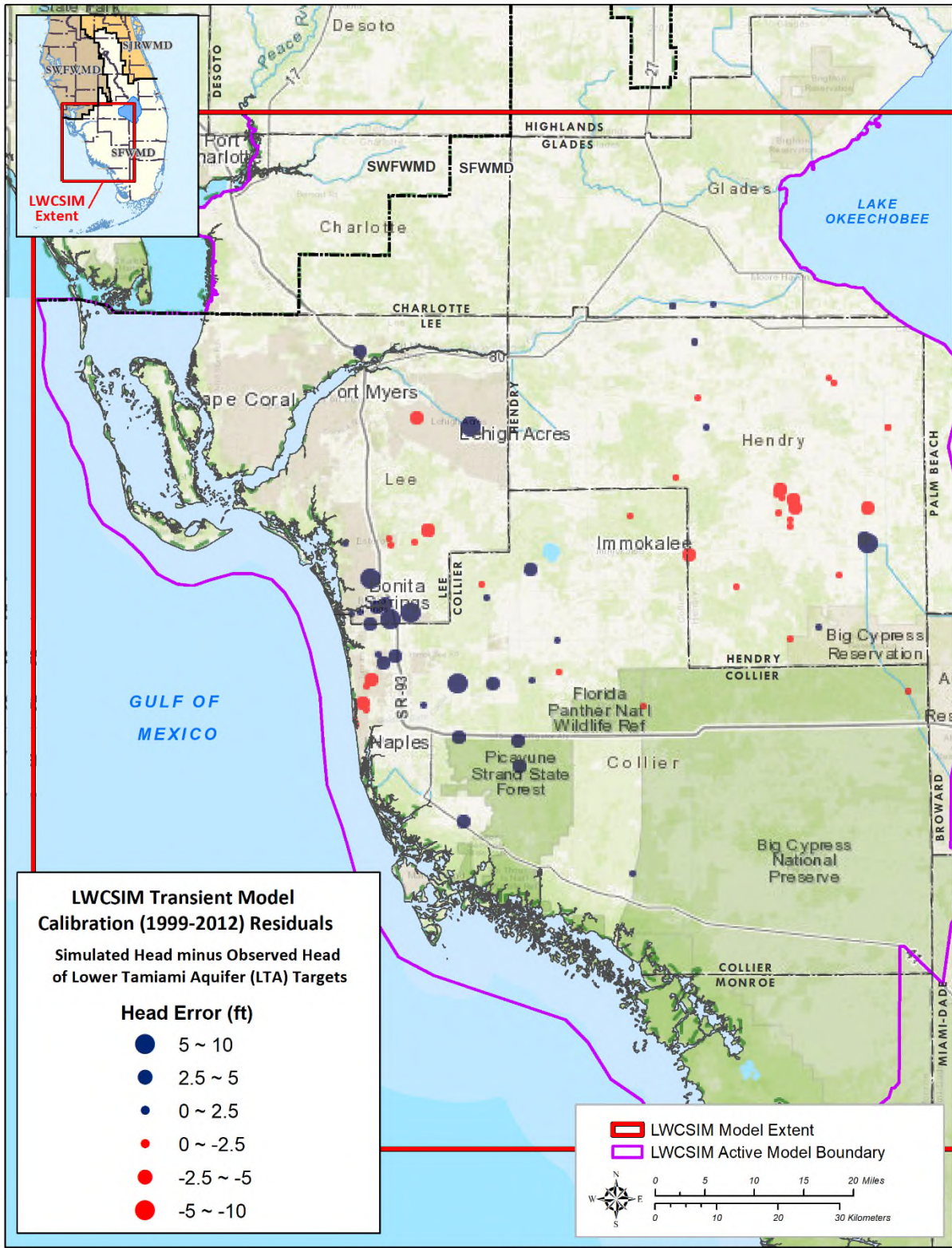
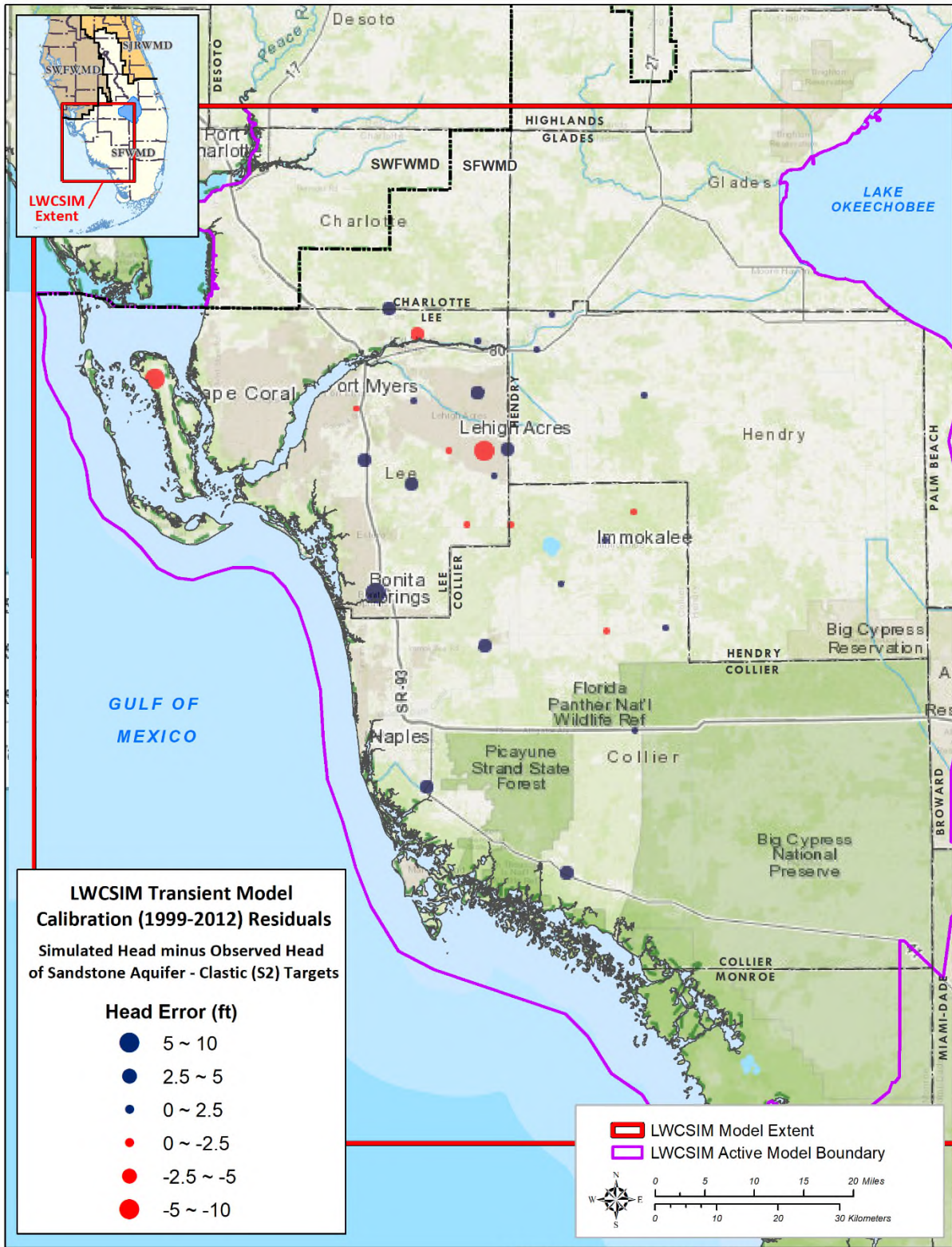


Figure 6-6. Spatial distribution of groundwater target wells and the average errors of simulated heads in the Water Table aquifer (layer 1).



\\lad.sfwmd.gov\dfsroot\GIS\GSBiz\WS\LWCSIM\mxd\FLOW\20200812ResidualHeadError_Lyr\LTA.mxd

Figure 6-7. Spatial distribution of groundwater target wells and the average errors of simulated heads in the Lower Tamiami aquifer (layer 3).



\\vad.sfwmd.gov\dfsroot\GIS\GSBiz\WLS\LWCSIM\mxd\VFLOW\20200812ResidualHeadError_LyrSA2.mxd

Figure 6-8. Spatial distribution of groundwater target wells and the average errors of simulated heads in the Sandstone aquifer – clastic zone (layer 5).

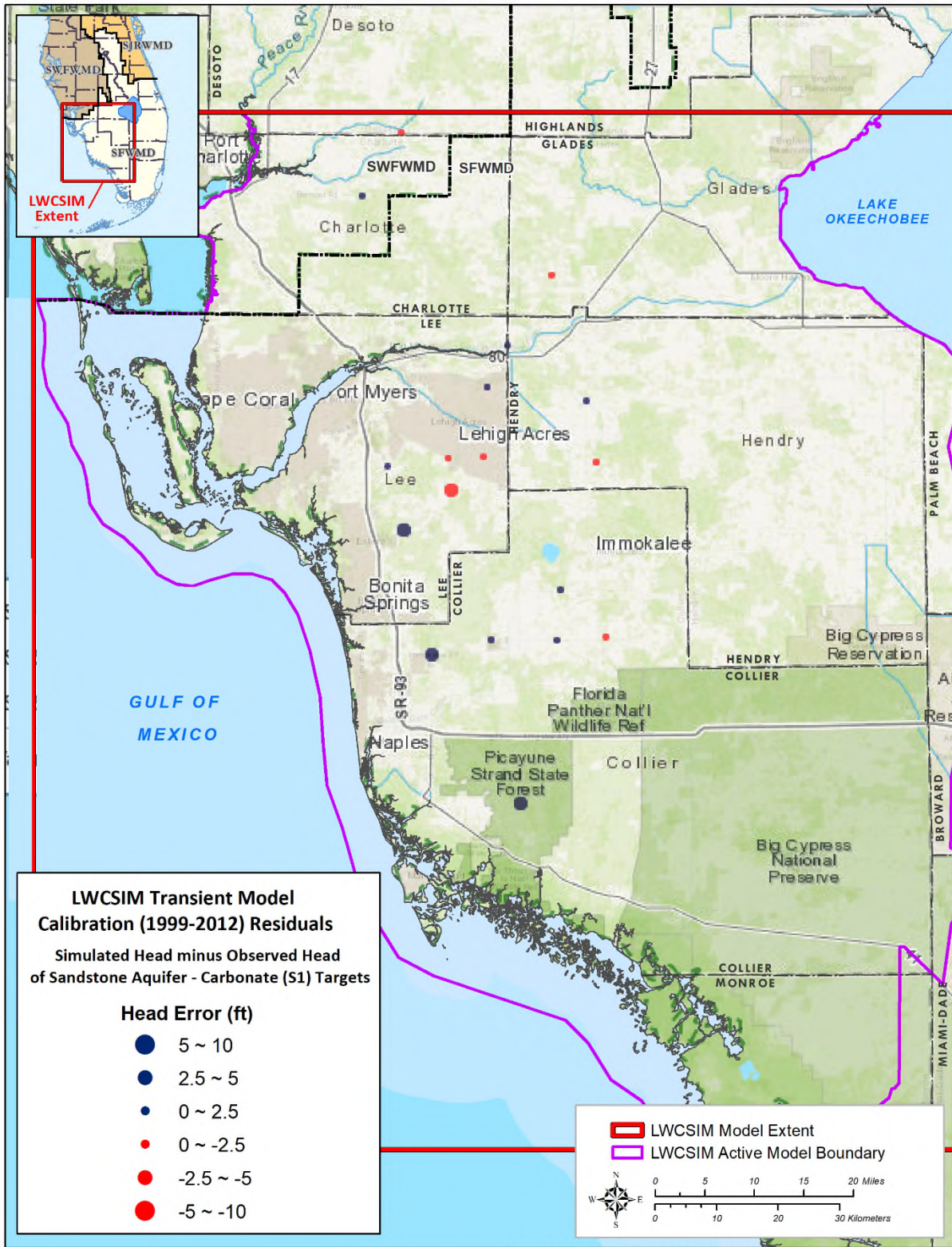


Figure 6-9. Spatial distribution of groundwater target wells and the average errors of simulated heads in the Sandstone aquifer – carbonate zone (layer 7).

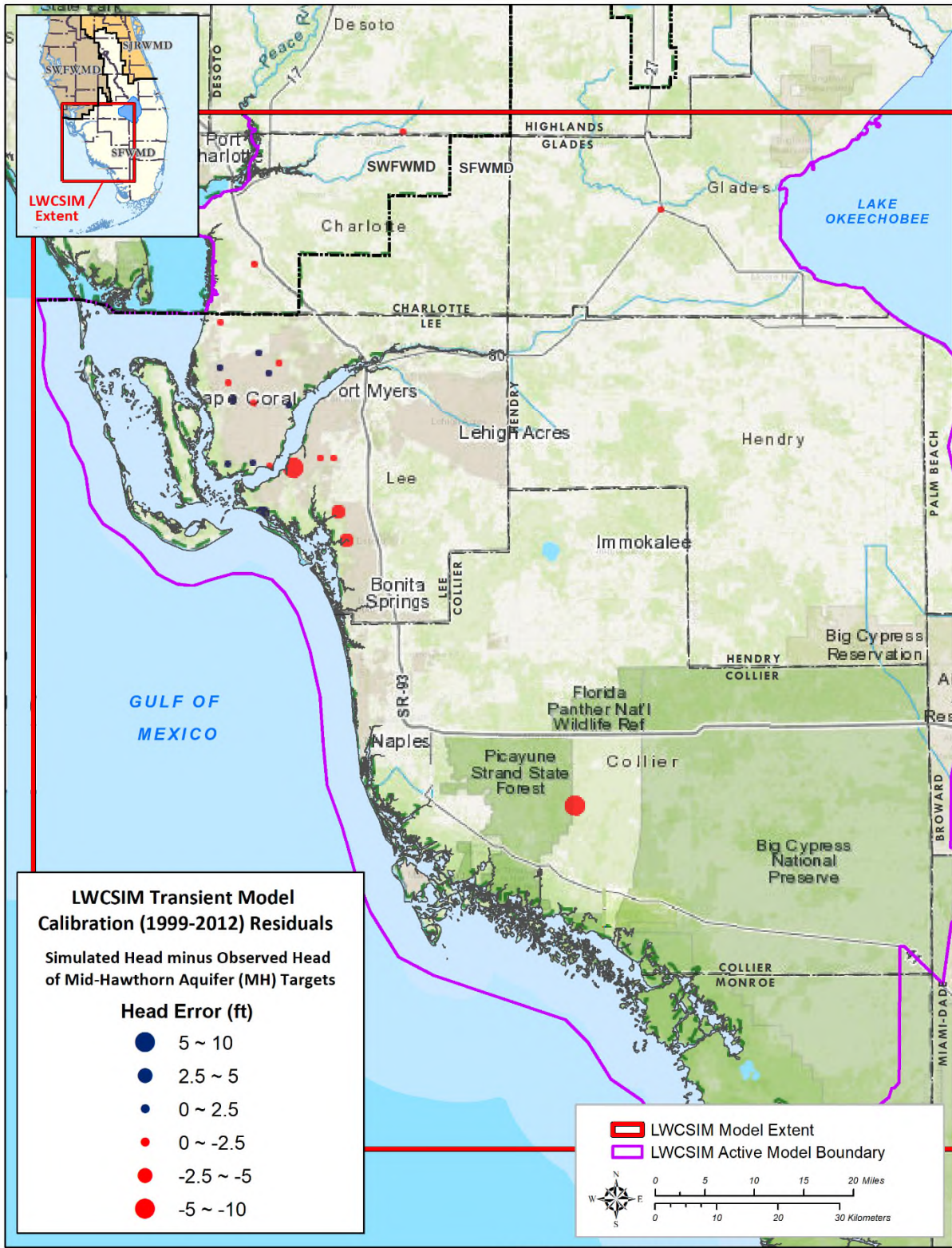


Figure 6-10. Spatial distribution of groundwater target wells and the average errors of simulated heads in the Mid-Hawthorn aquifer (layer 9).

As shown in **Figures 6-7 to 6-9**, the LTA and SSA-carbonate/clastic aquifers show very good spatial distribution of errors with no significant bias. Most MHA monitor wells are in the Cape Coral area, and no significant bias is observed (**Figure 6-10**). The two MHA monitor wells (DBKeys 1660 and 37311) in southern Collier County indicate water levels are greater than 40 ft above the mean sea level, which is an artesian condition. The model, however, underestimates these water levels by more than 5 ft, and it was not possible to move the simulated water levels higher with reasonable parameter adjustments to match the observed levels. Observed water levels in the UFA (adjusted for equivalent freshwater heads) are slightly higher (approximately 42.5 ft) than MHA levels in this area. According to Geddes et al. (2015), confinement between the MHA and the Lower Hawthorn aquifer in western Collier County is not very thick. Bennett (2004) noted the separation between the MHA and UFA is weak, and there is an apparent hydraulic connection between the two aquifers in Collier County. Analysis of the nearest cluster wells open to the MHA (BICY-MZ1) and UFA (BICY-MZ2) indicates a very good correlation between the water levels in the two aquifers (**Figure 6-11**). This further confirms that separation between the MHA and UFA is semi-confined, suggesting there can be upward flow from the UFA to the MHA in western Collier County. However, the LWCSIM assumes no hydraulic connection between the two aquifers and uses a no-flow boundary at the bottom of the model, which may not be a true representation of the area. Therefore, the LWCSIM may be unable to accurately simulate the groundwater system in southwestern Collier County, and users are cautioned against relying on the model predictions of the MHA in this area. Because of this conceptual limitation, BICY-MZ1 and BICY-MZ2 were removed when calculating the layer-specific calibration statistics for the MHA.

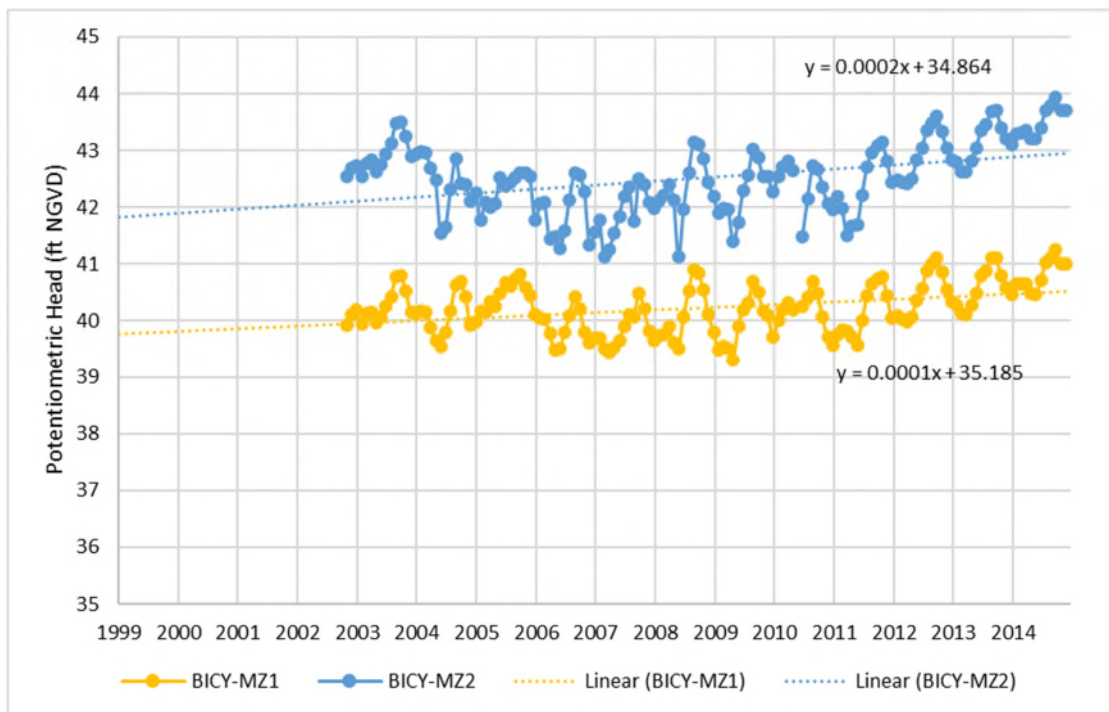


Figure 6-11. Comparison of observed water levels in cluster wells open to Mid-Hawthorn aquifer (BICY-MZ1) and Upper Floridan aquifer (BICY-MZ2).

Regression plots of simulated versus observed water levels for the WTA, LTA, SSA-clastic, SSA-carbonate, and MHA are shown in **Figures 6-12 to 6-16**. Most simulated data show good agreement with the observed data. Histogram plots of simulated versus observed water levels for the WTA, LTA, SSA-clastic, SSA-carbonate, and MHA, including a quantitative distribution of errors in each aquifer, are shown in **Figures 6-17 to 6-21**. **Appendix J** contains figures of the spatial distribution of TNSE and R^2 values for each aquifer.

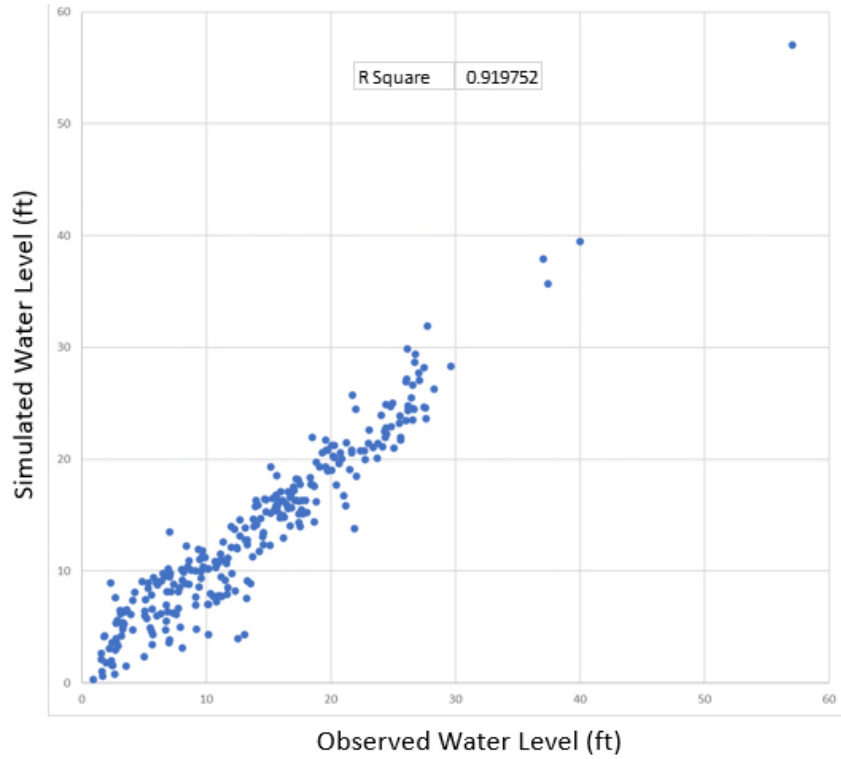


Figure 6-12. Mean simulated versus observed water levels in the Water Table aquifer.

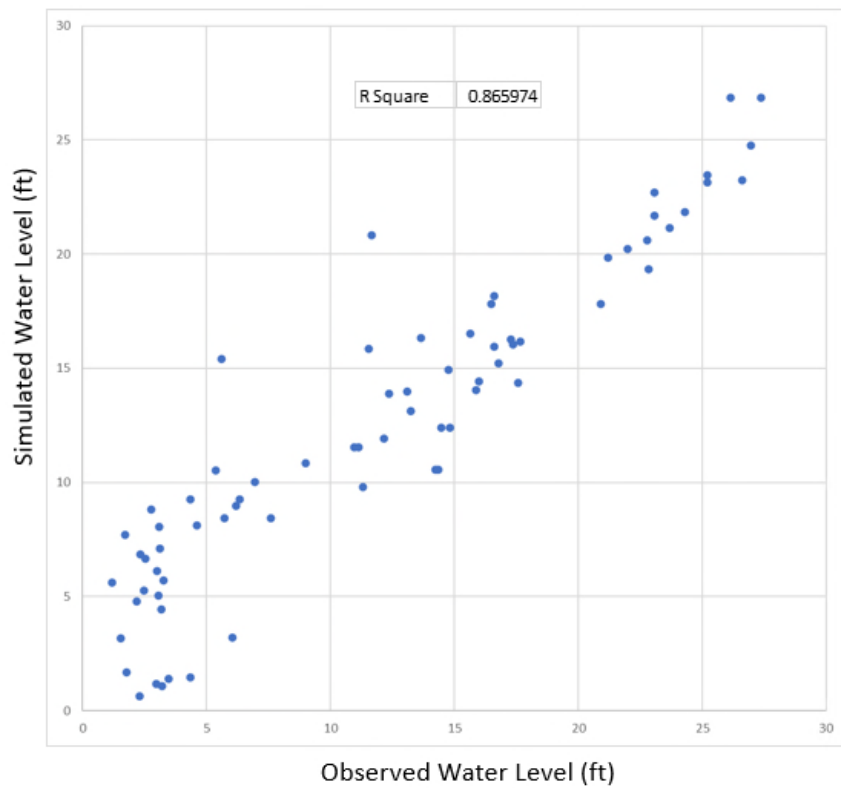


Figure 6-13. Mean simulated versus observed water levels in the Lower Tamiami aquifer.

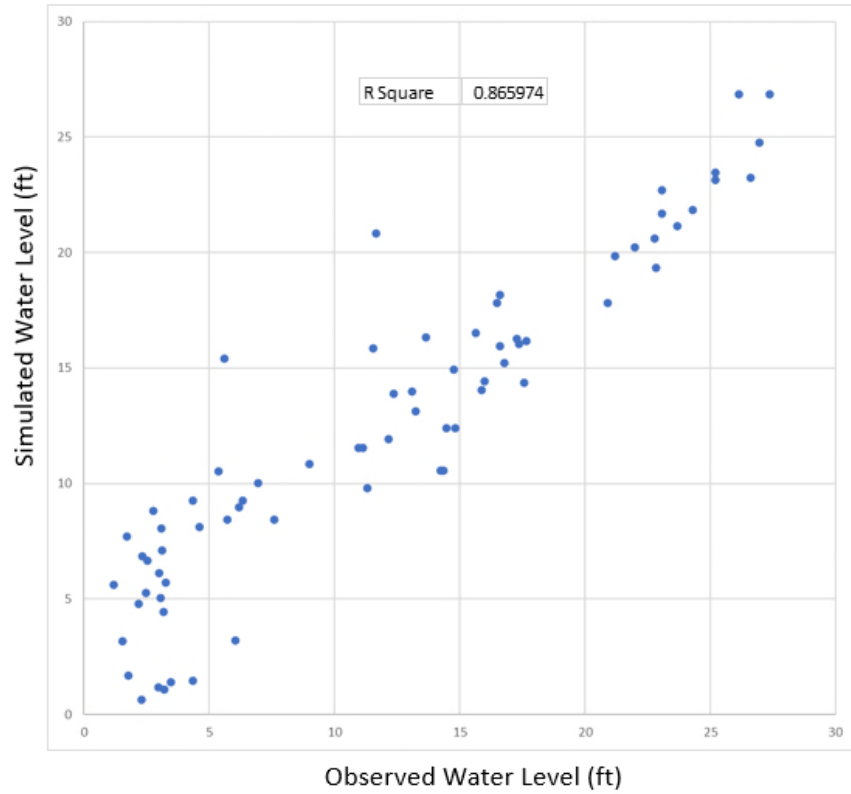


Figure 6-14. Mean simulated versus observed water levels in the Sandstone aquifer – clastic zone.

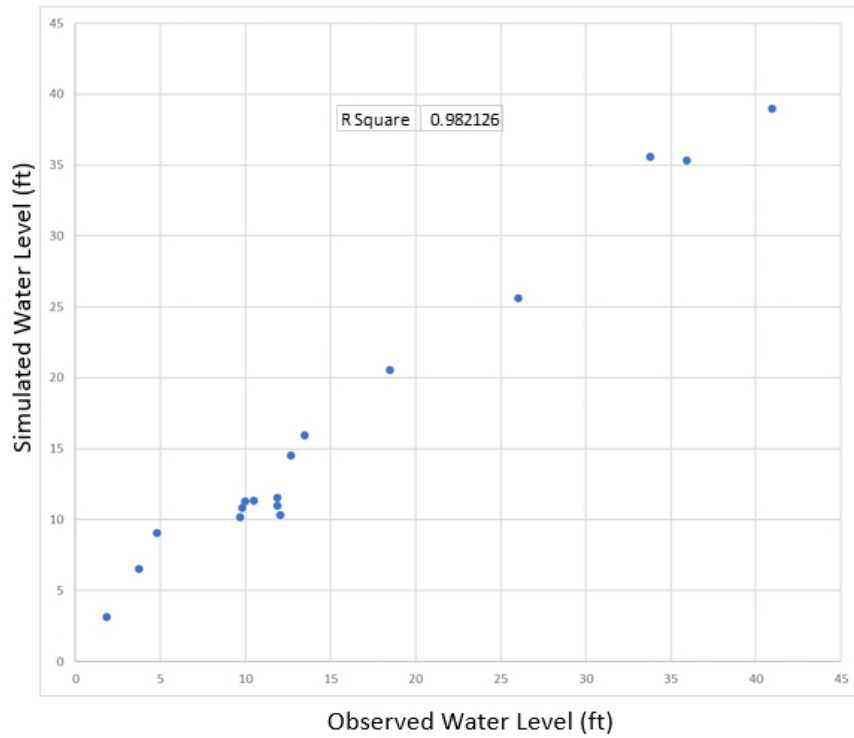


Figure 6-15. Mean simulated versus observed water levels in the Sandstone aquifer – carbonate zone.

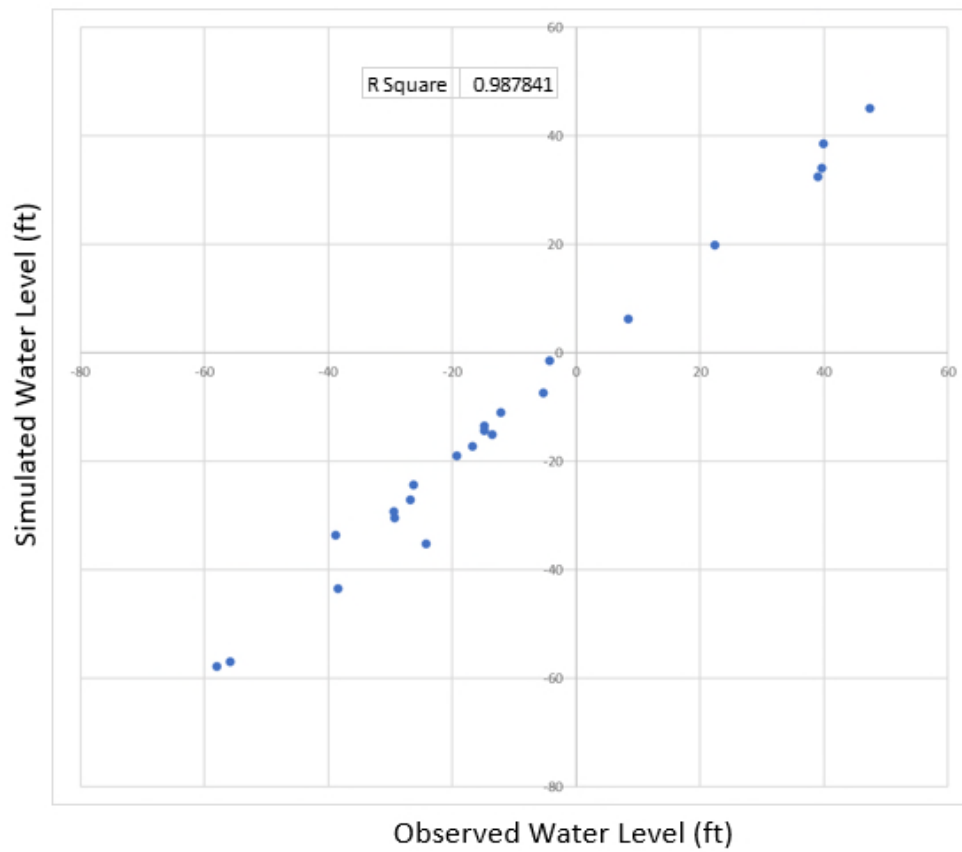


Figure 6-16. Mean simulated versus observed water levels in the Mid-Hawthorn aquifer.

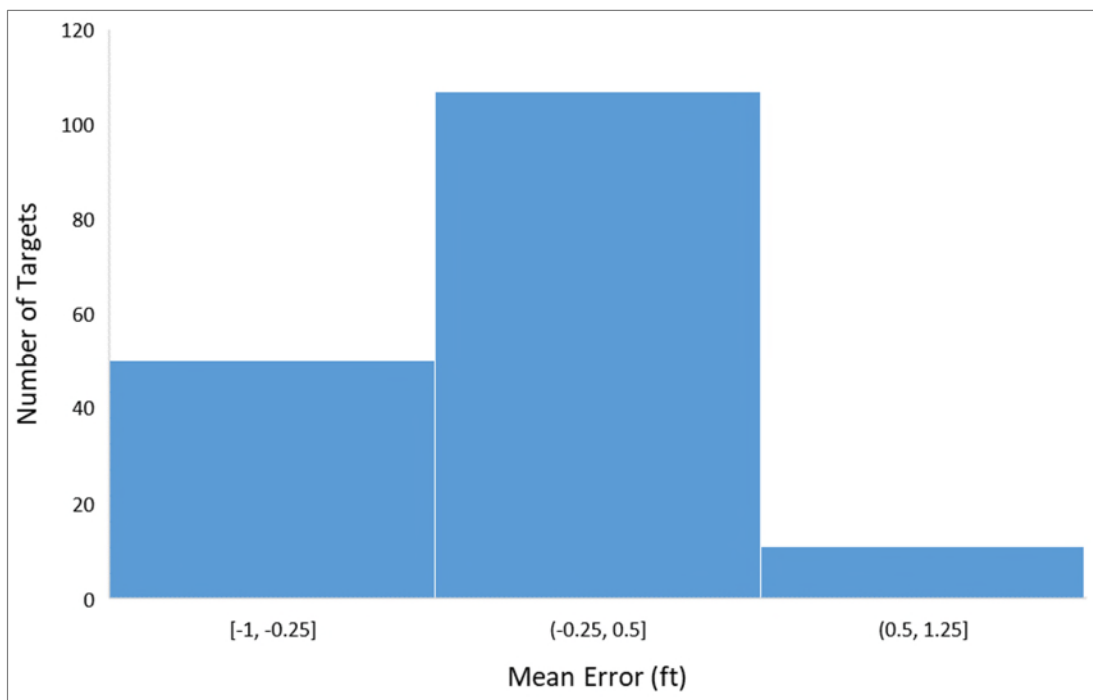


Figure 6-17. Histogram of simulated versus observed water level differences in the Water Table aquifer.

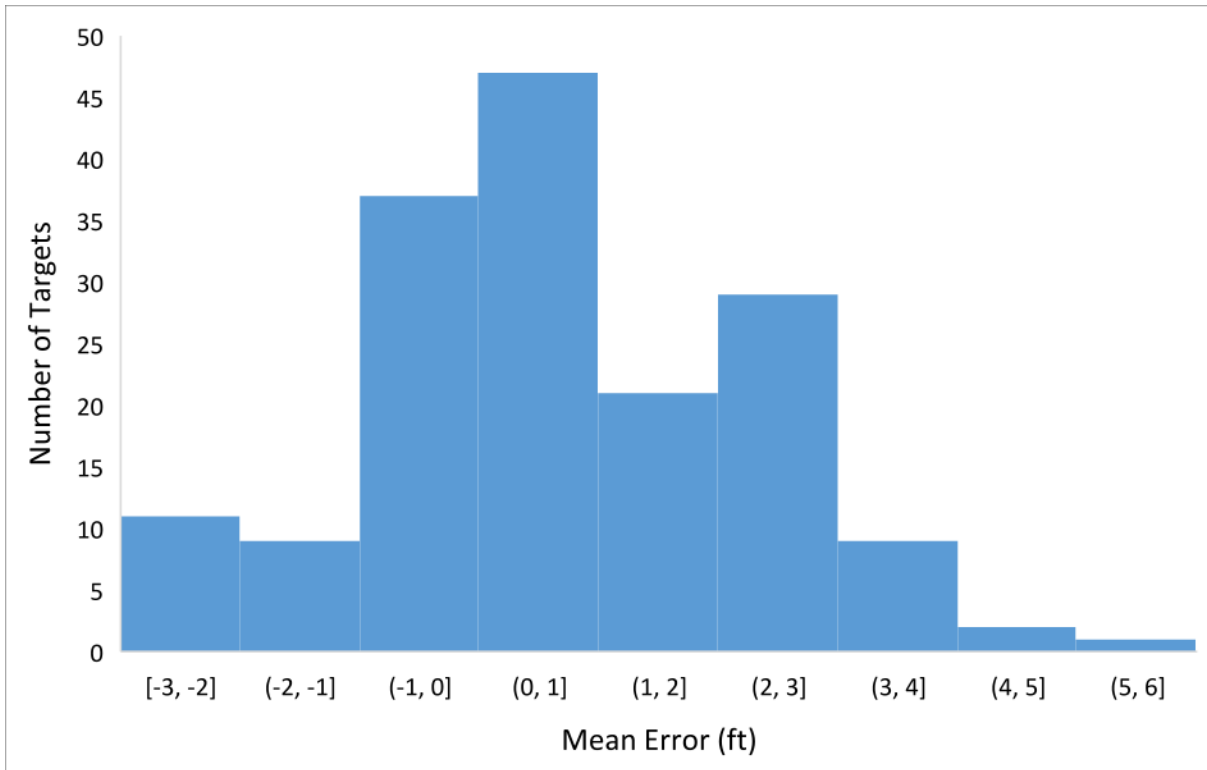


Figure 6-18. Histogram of simulated versus observed water level differences in the Lower Tamiami aquifer.

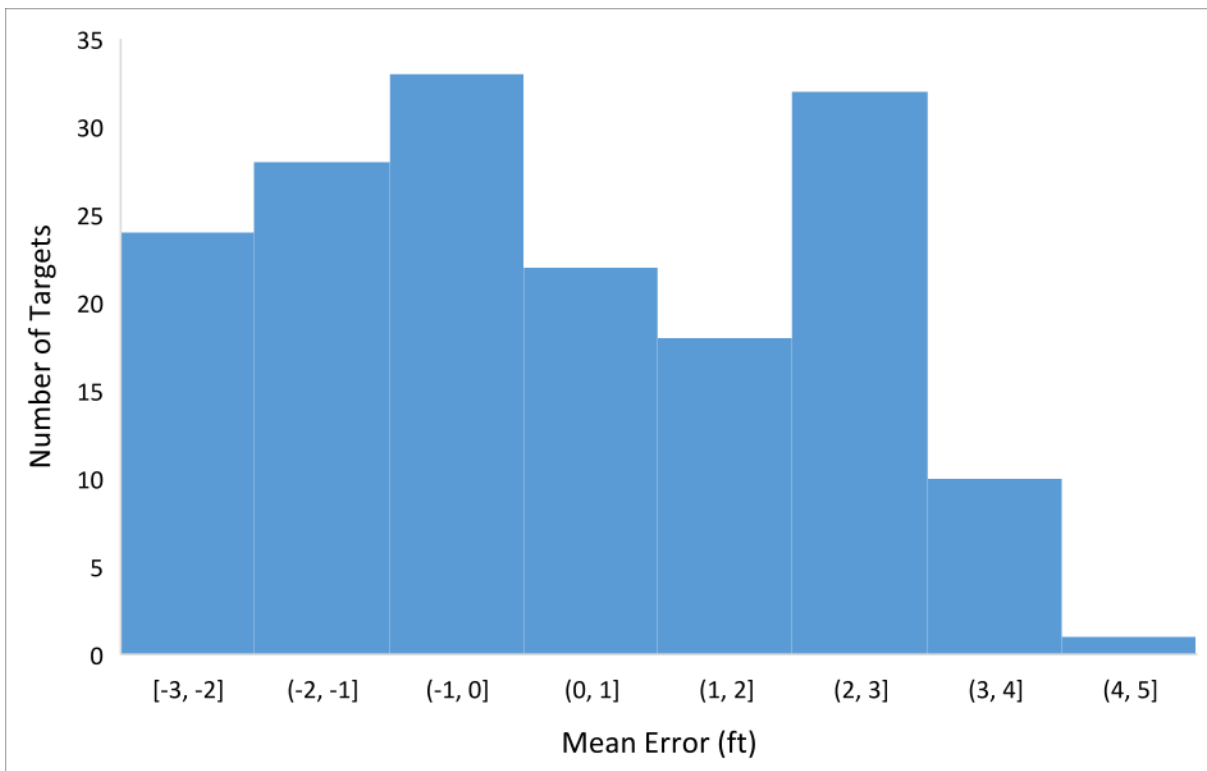


Figure 6-19. Histogram of simulated versus observed water level differences in the Sandstone aquifer – clastic zone.

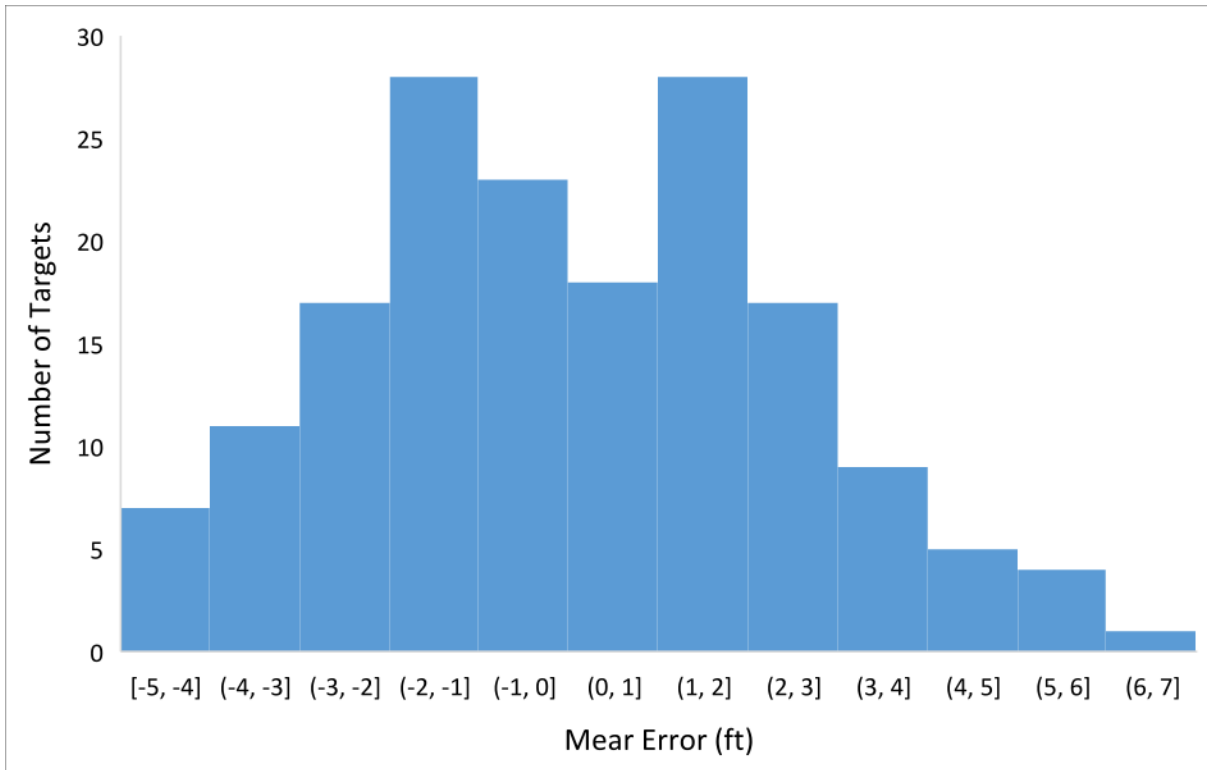


Figure 6-20. Histogram of simulated versus observed water level differences in the Sandstone aquifer – carbonate zone.

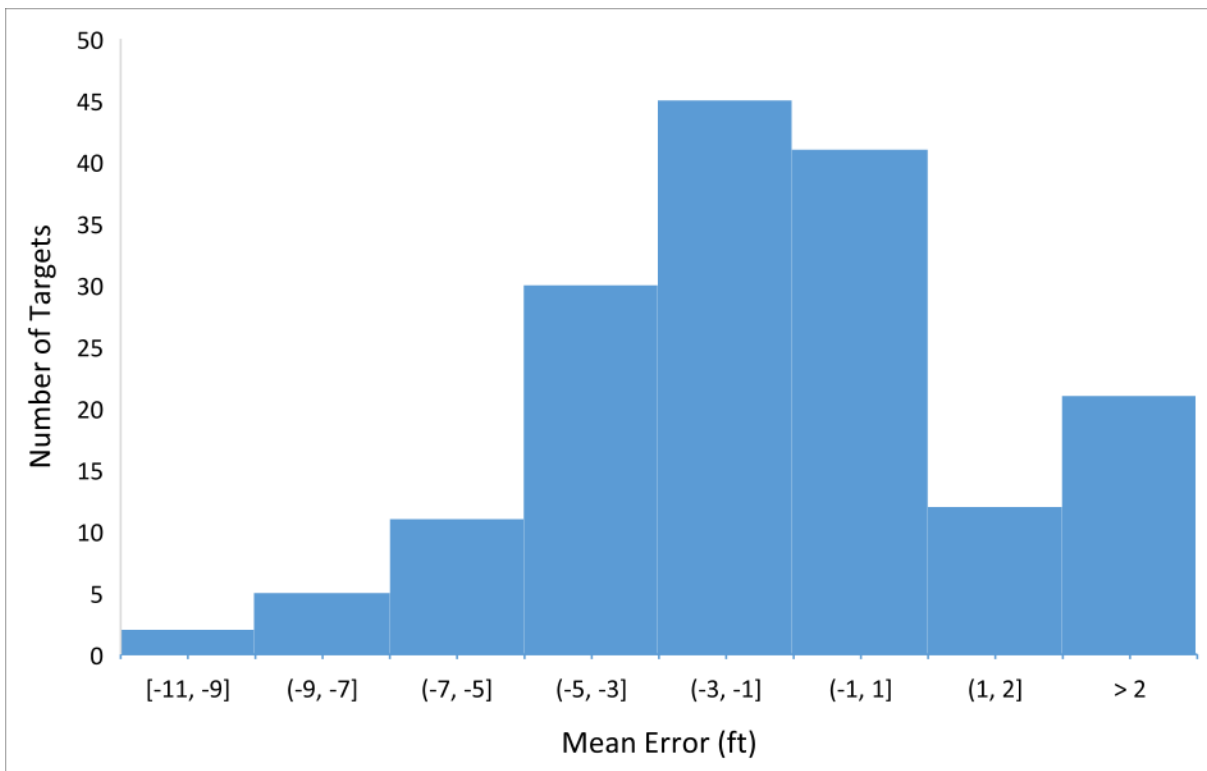


Figure 6-21. Histogram of simulated versus observed water level differences in the Mid-Hawthorn aquifer.

Surface Water Flow Calibration

Figures 6-22 and **6-23** compare observed and simulated structure flow data for two major watersheds in the LWCSIM domain: West Caloosahatchee and East Caloosahatchee, respectively. Each figure shows the estimated versus simulated runoff, estimated versus simulated baseflow, total structure flow, and cumulative flow. Simulated runoff was obtained by subtracting the estimated baseflow from the total observed stream flow. Total observed flow at a watershed outlet was calculated as:

$$\text{Total watershed outflow} = \text{Observed flow at the basin outlet} - \text{Observed flow at the basin inlet}$$

Total simulated flow was calculated as:

$$\text{Total simulated outflow} = \text{Runoff} + \text{Baseflow from rivers and drains}$$

As described in the *Structure Flow Calibration* section, deviation of volume, the Nash-Sutcliffe efficiency value, and R^2 were used to evaluate the goodness of fit.

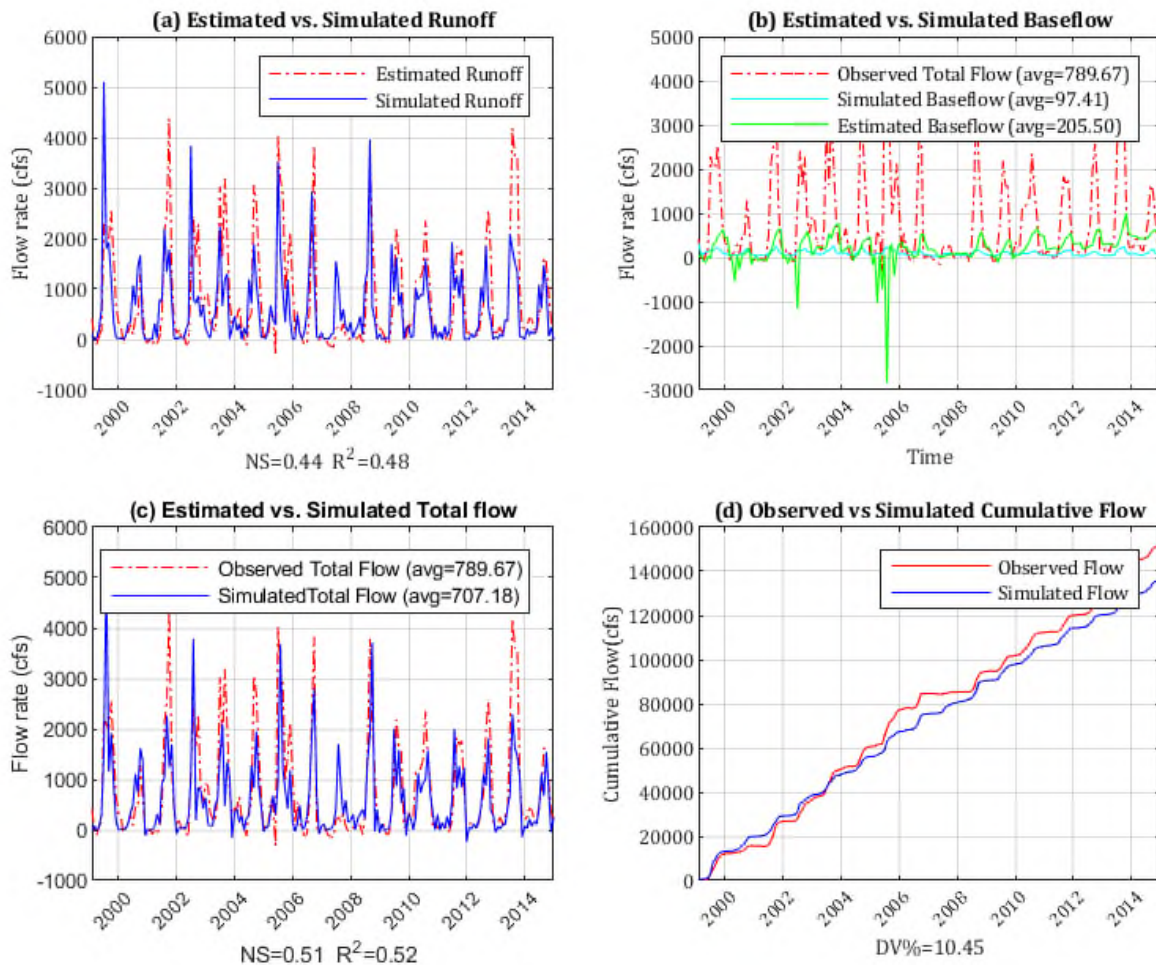


Figure 6-22. Observed versus simulated structure flow in the West Caloosahatchee watershed.

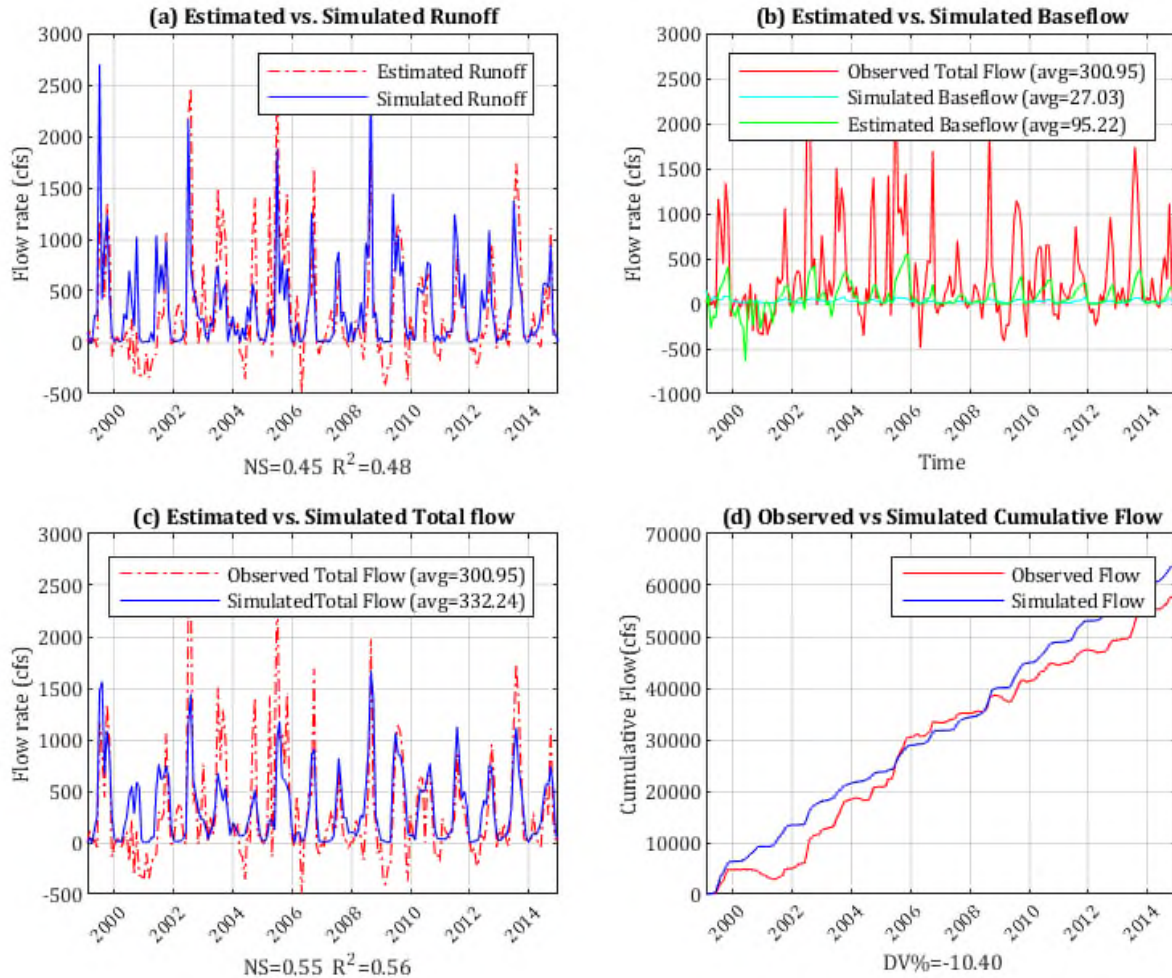


Figure 6-23. Observed versus simulated structure flow in the East Caloosahatchee watershed.

The total simulated structure flow for the West Caloosahatchee watershed (**Figure 6-22c**) indicates the model captures most of the peaks during the simulation period. However, there are a couple years when the model was not able to capture peak flows (2001 and 2013), especially when the peak flows were significantly higher than average. These peaks are associated with how the inflow (S-78) and outflow (S-79) structures were operated during high rainfall/hurricane events, which were not simulated by the LWCSIM. The mass balance error (10.45% of deviation of volume in **Figure 6-22d**) occurred primarily due to not capturing these peak flows. The model indicated a significant groundwater contribution to the West Caloosahatchee watershed river flow during the calibration period. On average, the groundwater baseflow contribution is approximately 97 cubic feet per second (cfs), which is about 12% of the total stream flow (789 cfs) within the West Caloosahatchee watershed (**Figure 6-22b**).

The total simulated structure flow for the East Caloosahatchee watershed (**Figure 6-23c**) indicates the model captures peak flows about half of the time during the simulation period. This is because the complex operational schedule of the inflow and outflow structures (S-77 and S-78) was not incorporated into the LWCSIM. In some situations, total outflow becomes negative when the outflow structure, S-78, releases less flow than the inflow structure, S-77, within the model time step (1 month). The model simulated mass balance error was approximately 3.72%. The model indicates that, on average, groundwater baseflow contribution is approximately 27 cfs, which is about 7% of the total stream flow (374 cfs) within the East Caloosahatchee watershed (**Figure 6-23b**).

Figures 6-22 and **6-23** indicate the simulated total structure flows are in good agreement with observed data, especially given the complexity of structure operations was not incorporated into the LWCSIM. **Table 6-3** shows calibration statistics of the West Caloosahatchee and East Caloosahatchee watersheds. Indicated by the green font in the table, both watersheds met all three established calibration criteria (deviation of volume, Nash-Sutcliffe efficiency, and R^2).

Table 6-3. Transient structure flow calibration statistics for major watersheds in LWCSIM

| Statistic | Criterion | East Caloosahatchee | West Caloosahatchee |
|--|-----------|---------------------|---------------------|
| Deviation of volume | <15% | 3.72% | 10.45% |
| Nash-Sutcliffe efficiency | >0.5 | 0.55 | 0.51 |
| Pearson coefficient of correlation (R^2) | >0.5 | 0.58 | 0.52 |

Green font indicates compliance with calibration criteria.
Calibration period: 1999 to 2012.

Surface Water Level Calibration

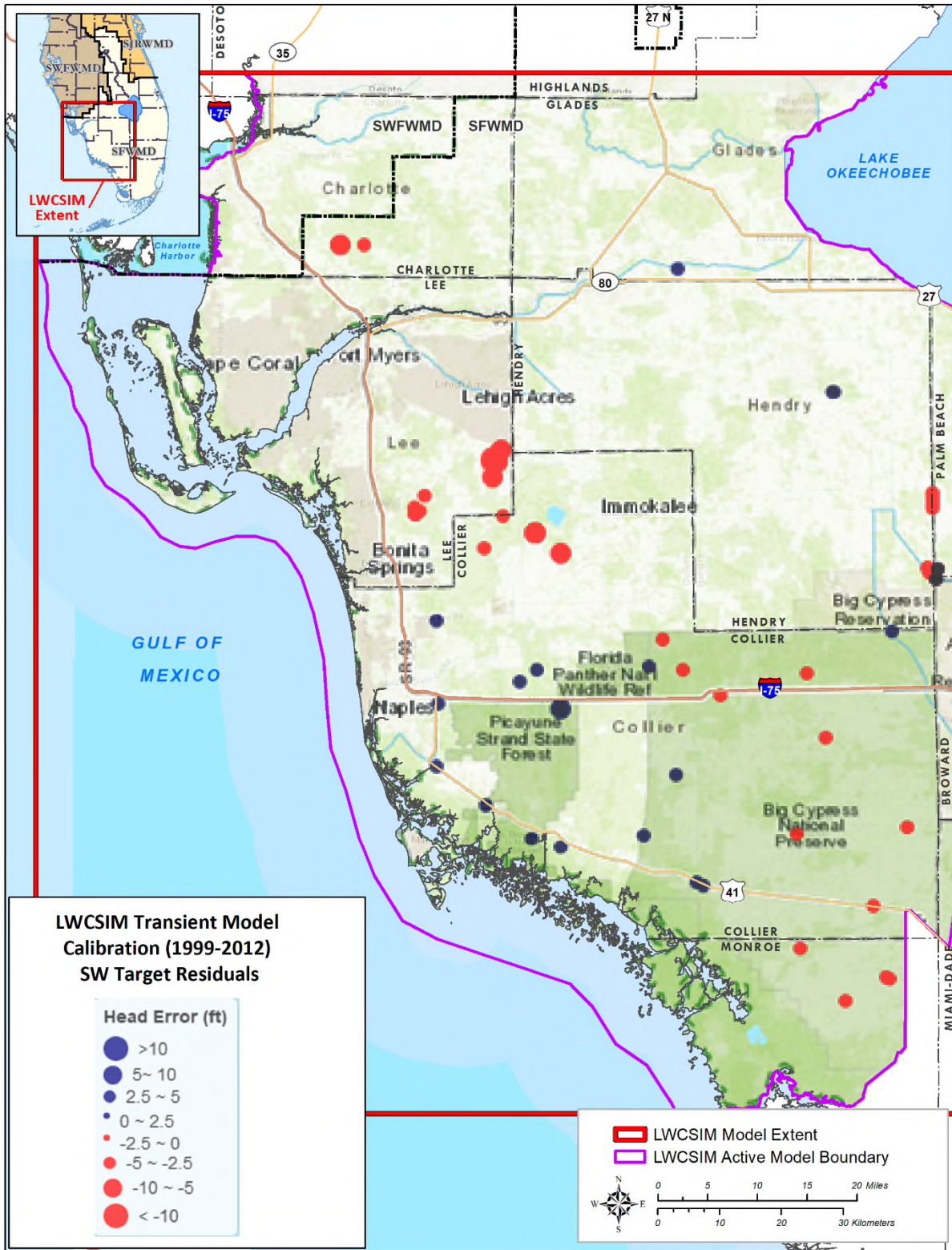
A summary of surface water calibration at 60 wetland gauge stations is provided in **Table 6-4**. As indicated by the green font in the table, the LWCSIM met the established calibration criteria. Average mean error of all gauge stations was -0.76 ft, indicating a slight underestimation. Of the gauge stations, 85% had less than 2.5 ft mean absolute error, 97% had less than 5 ft mean absolute error, and 63% had 60% of R^2 and modified Nash-Sutcliffe efficiency, indicating a very good overall transient response of the model.

Table 6-4. Transient wetland water level calibration statistics in the model.

| Statistic | Criterion | Feet or % |
|------------------------------|--------------|-----------|
| Mean error | < \pm 1 ft | -0.76 |
| Error standard deviation | <5 ft | 1.98 |
| Mean absolute error (MAE) | <5 ft | 1.62 |
| Root mean square error | <5 ft | 2.11 |
| Minimum residual | | -8.52 |
| Maximum residual | | 4.26 |
| Number of observation points | 60 | |
| Percentage with MAE < 2.5 ft | >50% | 85 |
| Percentage with MAE < 5.0 ft | >80% | 97 |
| Percentage with R^2 > 0.4 | >60% | 63 |
| Percentage with TNSE > 0 | >60% | 63 |

R^2 = Pearson coefficient of correlation; TNSE = transformed Nash-Sutcliffe efficiency.
Green font indicates compliance with calibration criteria.
Calibration period: 1999 to 2012.

Spatial distribution of wetland gauge stations and their average simulated errors are shown in **Figure 6-24**. Hydrographs for the simulated and measured water levels are shown in the **Appendix I**. Gauge stations shown in red represent where average simulated water levels are lower than average measured water levels, indicating an underprediction. Gauge stations shown in blue represent where average simulated water levels are higher than average measured water levels, indicating an overprediction. The size of the symbols is proportional to the average residual at that location.



\\ad.sfwmd.gov\dfsroot\GIS\GSBiz\WS\LWCSIM\Report_Figures\mxd\20200804ResidualSWTargets.mxd

Figure 6-24. Spatial distribution of wetland surface water gauges and the average errors of simulated water levels.

Figures 6-25 to 6-28 compare simulated and measured ET data at four stations. The four stations represent different land use types, including agricultural land use (Figures 6-25 and 6-28), marsh land (Figure 6-26), and Cypress swamp (Figure 6-27). Simulated ET was adjusted using crop coefficients to better match the measured data. Figures 6-25 to 6-28 show a good agreement between the final simulated and measured ET data.

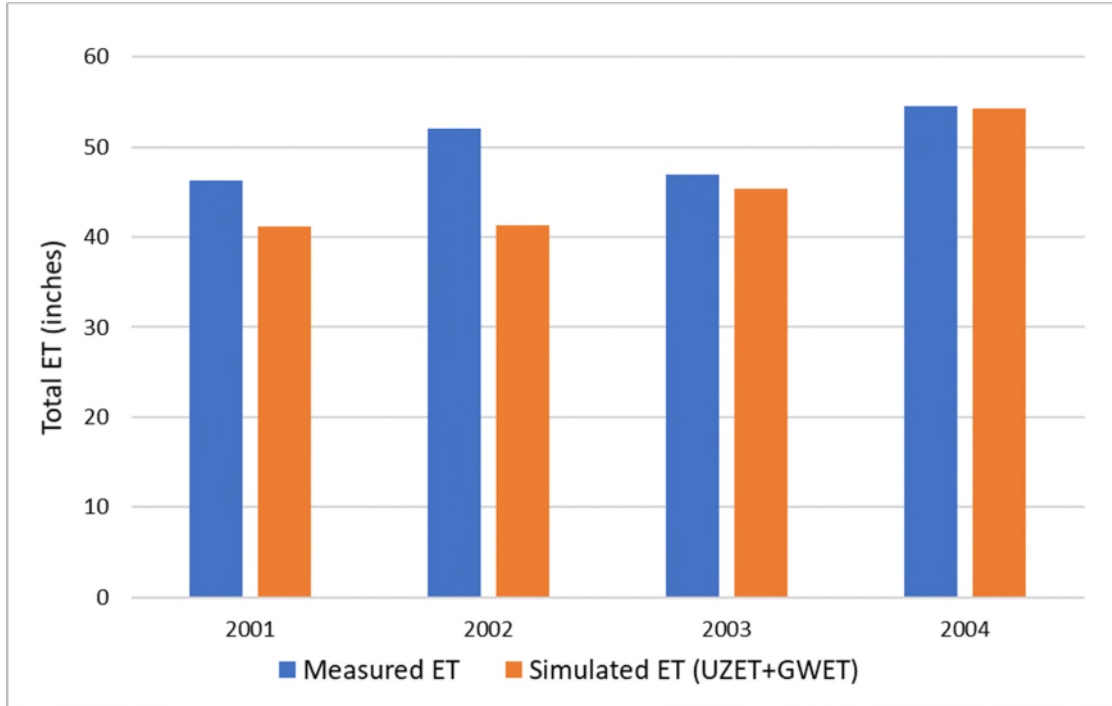


Figure 6-25. Measured versus simulated total evapotranspiration at the Ave Maria agricultural site.

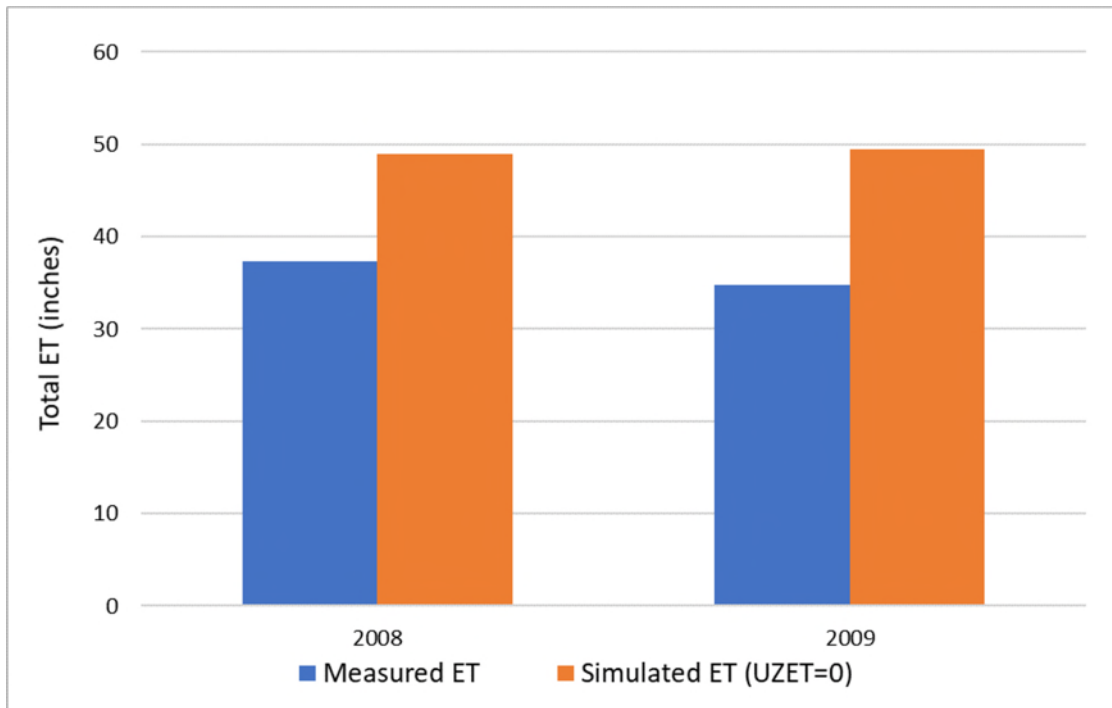


Figure 6-26. Measured versus simulated total evapotranspiration at the marsh site.

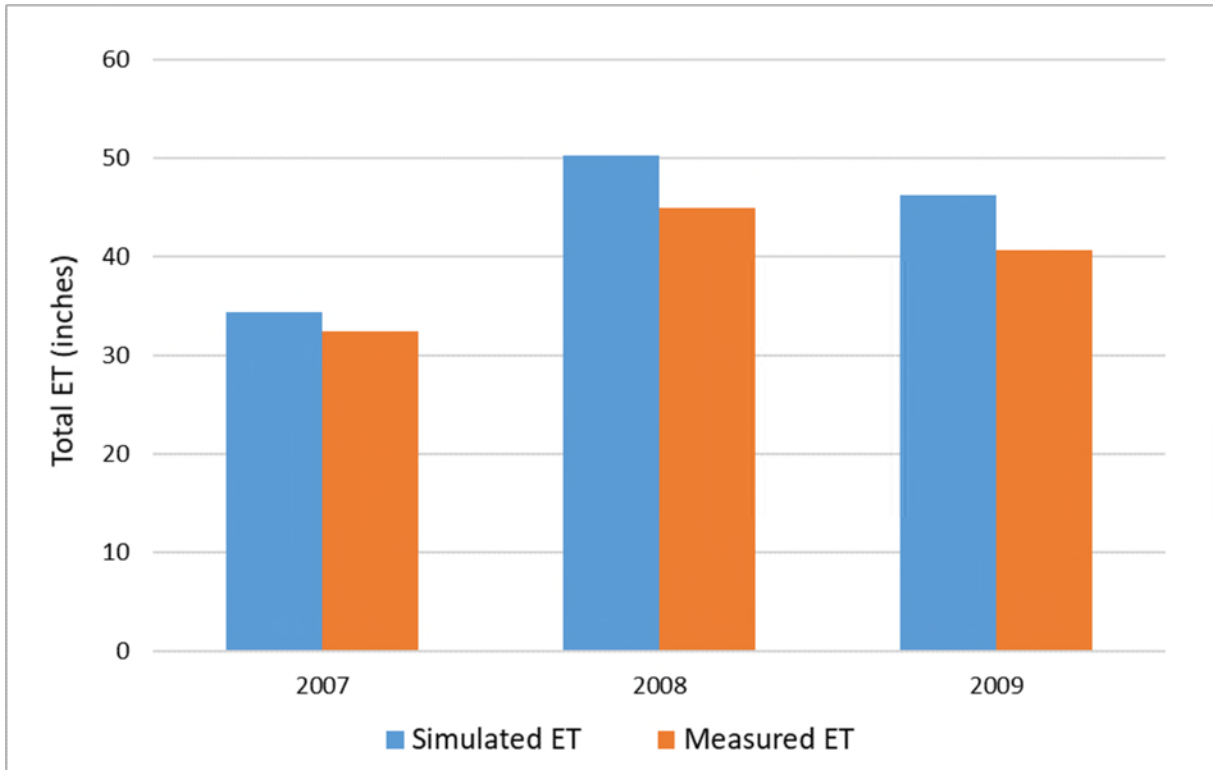


Figure 6-27. Measured versus simulated total evapotranspiration at the Cypress swamp site.

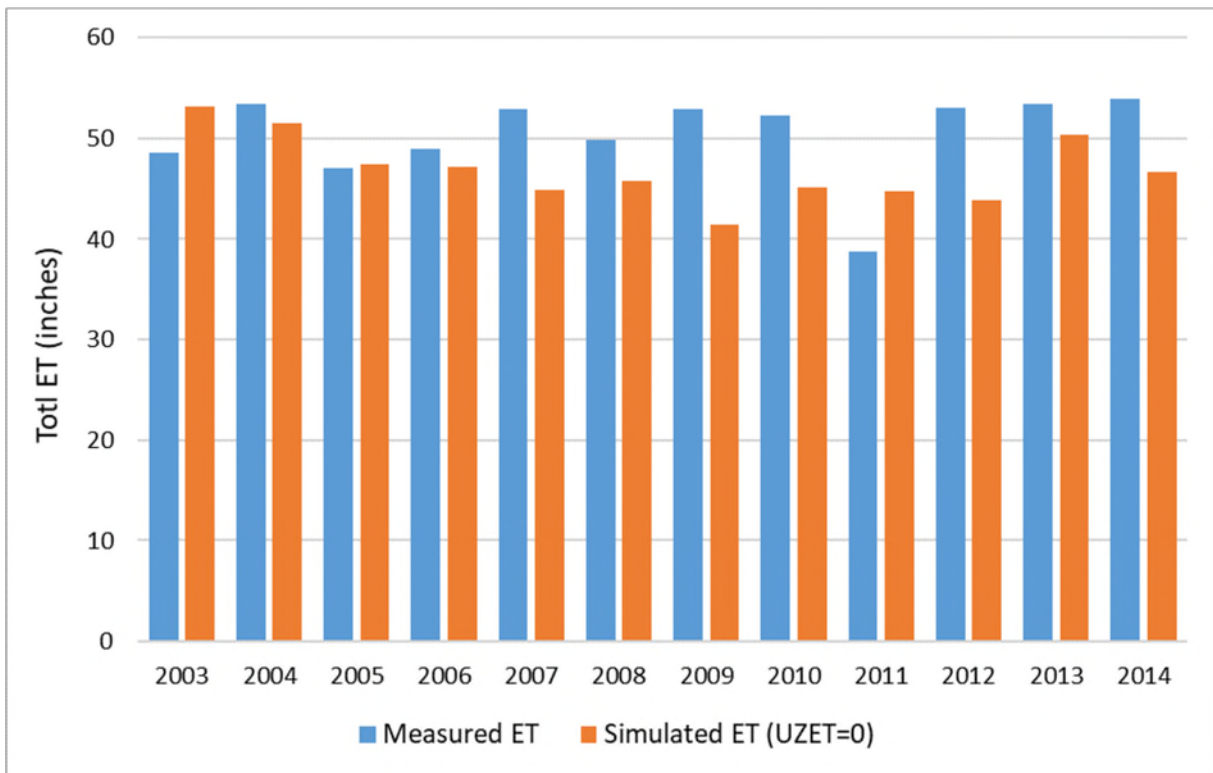


Figure 6-28. Measured versus simulated evapotranspiration at the SGGWEX agricultural site.

6.5 Model Verification

Once a model is deemed calibrated, a verification period outside of the calibration period is selected to evaluate the model's performance and determine if the simulation continues to meet the calibration metrics previously assigned. In this case, the 2-year monthly transient period from 2013 through 2014 was selected as the LWCSIM verification period.

Table 6-5 provides a summary of the LWCSIM verification statistics. Within the model domain, there were 242, 48, 23, 14, and 15 monitor wells within model layers 1, 3, 5, 7, and 9, respectively, to compare simulated and observed water levels during the verification period. Calibration criteria were achieved for layers 1, 3, 5, and 7, and were comparable to the calibrated model; however, some of the calibration criteria were not met in layer 9. Layer 9 had fewer targets (15 targets during the verification period as opposed to 25 targets during the calibration period) for the verification period, and many of those targets had significant data gaps. In addition, increased reclaimed water use in the Cape Coral area may have offset some of the DSS withdrawals in the MHA, making some DSS pumping rate assumptions invalid for the verification period. Layer 9 did meet the R^2 criterion and showed a residual mean error of 0.45 ft. In general, it can be expected that some targets would not meet the criteria during the verification period because calibration parameters can no longer be adjusted as they were during calibration. That very few wells did not meet the calibration criteria during the verification period indicates the model is reasonably calibrated and can be used for its intended purposes.

Table 6-5. Transient model verification statistics of the target monitor wells.

| Statistics | Criteria | Aquifer | | | | |
|------------------------------|----------|---------|-------|-------|-------|-------|
| | | WTA | LTA | SSA-2 | SSA-1 | MHA |
| Mean error | ±1 ft | -0.05 | 0.68 | -1.14 | -0.17 | 0.62 |
| Error standard deviation | <5 ft | 2.33 | 3.1 | 3.8 | 1.88 | 6.57 |
| Mean absolute error (MAE) | <5 ft | 1.95 | 2.79 | 3.13 | 2.36 | 5.77 |
| Root mean square error | <5 ft | 2.33 | 3.14 | 3.89 | 1.82 | 6.36 |
| Minimum residual | | -9.12 | -4.12 | -9.91 | -3.28 | -7.38 |
| Maximum residual | | 6.45 | 9.35 | 5.27 | 3.78 | 4.39 |
| Number of observation points | | 297 | 72 | 29 | 18 | 23 |
| Percentage with MAE < 2.5 ft | >50% | 71 | 56 | 70 | 86 | 29 |
| Percentage with MAE < 5.0 ft | >80% | 97 | 90 | 91 | 100 | 57 |
| Percentage with $R^2 > 0.4$ | >60% | 83 | 85 | 74 | 86 | 71 |
| Percentage with TNSE > 0 | >60% | 72 | 86 | 87 | 93 | 64 |

R^2 = Pearson coefficient of correlation; TNSE = transformed Nash-Sutcliffe efficiency.

Green font indicates compliance with calibration criteria.

Verification period: 2013 through 2014.

6.6 Simulated Heads

Figures 6-29 to 6-33 present the simulated potentiometric surfaces of the five LWCSIM aquifers. These are average head surfaces produced for each aquifer from the calibrated transient model after a full 192-stress-period model run. **Figure 6-29** shows water levels in the WTA, which represents regional groundwater flow patterns reasonably well. The regional groundwater high is near Polk City in Polk County (outside the LWCSIM domain), and groundwater flows radially outward in every direction. Southeasterly flow from the Polk City high enters the LWCSIM through the northern model boundary. The regional groundwater flow that enters the model domain continues to flow southwest and eventually discharge to the Gulf of Mexico. The highest water levels along the northern boundary are 60 to 70 ft National Geodetic Vertical Datum of 1929 (NGVD29) near the Highlands-Glades county line. Another regional high water level area in the WTA is the Immokalee area, south of the Caloosahatchee River. The highest water levels in this area are 30 to 40 ft NGVD29, and groundwater flows radially outwards in every direction from this high. Northerly flow ends up in the Caloosahatchee River, while flows to the west and southwest discharge to the Gulf of Mexico. Low water levels along the Caloosahatchee River indicate groundwater flow towards the river from the north and south. The simulated potentiometric surfaces in the LTA, SSA-clastic, and SSA-carbonate shown in are similar to regional patterns in the WTA (**Figures 6-30** to **6-32**). The lowest potentiometric heads are in the MHA in the Cape Coral area, where water levels are -70 to -80 ft NGVD29.

Figures 6-34 to **6-37** present the potentiometric surface (head) differences between the LWCSIM aquifer layers. The potentiometric head difference maps can help understand the regional flow vertical gradients within the model domain. These were produced by subtracting the average potentiometric surfaces between aquifer layers. For example, **Figure 6-34** presents the average head difference between the WTA and LTA. This was produced by subtracting the average LTA head from the WTA head. Most of the time, WTA heads are 5 to 15 ft higher than LTA heads where the LTA is productive (i.e., within Lee, Collier, and Hendry counties). **Figure 6-35** shows the simulated potentiometric head difference between the LTA and SSA-clastic. The potentiometric heads in the LTA are 10 to 15 ft higher in Lee County, indicating a flow gradient from the LTA to the SSA-clastic. **Figure 6-36** shows the simulated potentiometric head difference between the SSA-clastic and SSA-carbonate. There is a potentiometric head difference from -10 to +10 ft within Lee County, indicating both upward and downward flow gradients. In the Cape Coral area, the potentiometric head in the SSA-clastic is approximately 10 ft higher than the head in the SSA-carbonate. **Figure 6-37** shows the simulated potentiometric head difference between the SSA-carbonate and the MHA. In Cape Coral and Fort Myers within Lee County, SSA-carbonate heads are 15 ft higher than in the MHA, indicating a flow gradient from the SSA-carbonate to the MHA. In southern Collier County and eastern Glades County, MHA heads are greater than SSA-carbonate heads by approximately 10 ft, indicating an upward flow gradient from the MHA to the SSA-carbonate.

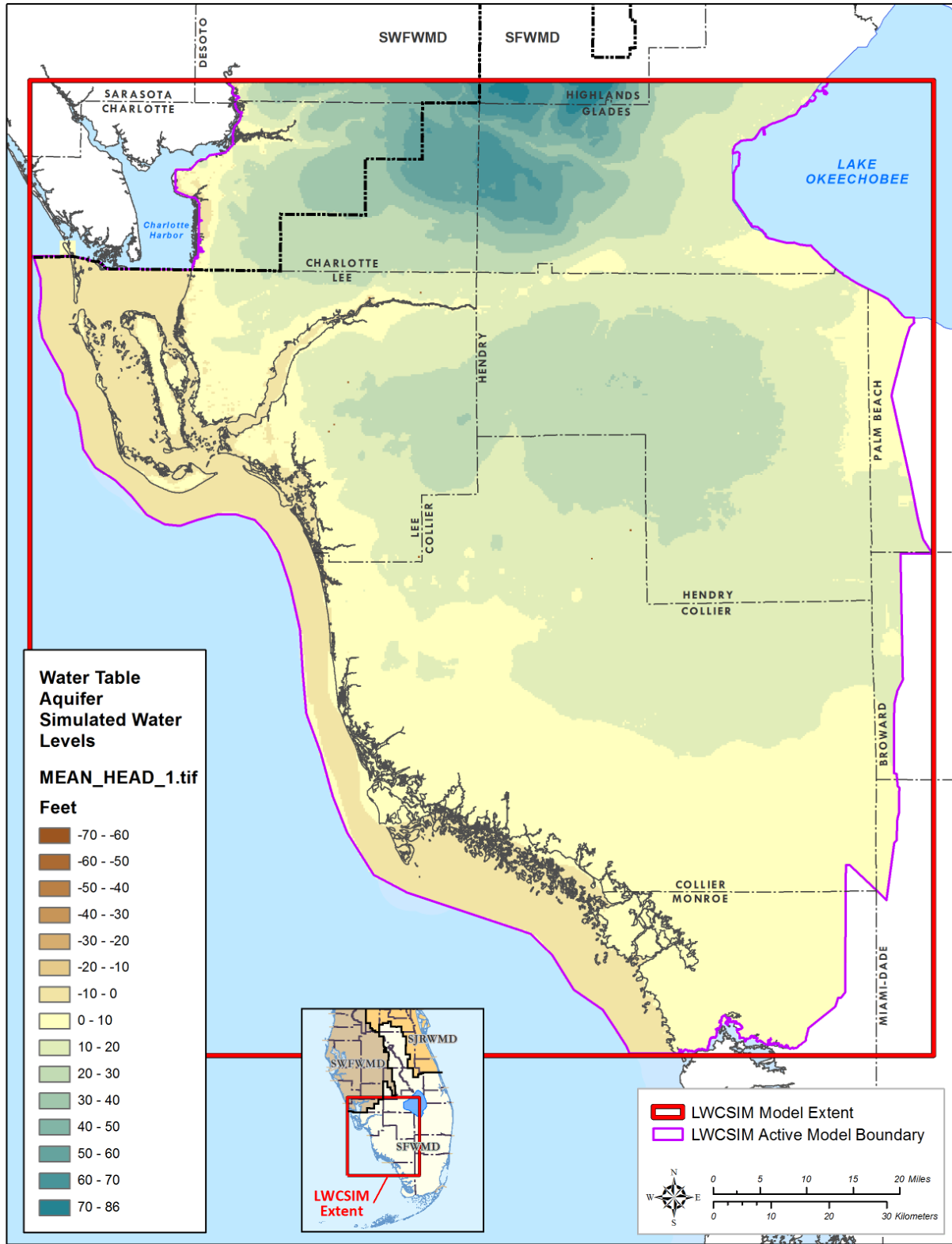


Figure 6-29. Simulated water levels for the Water Table aquifer.

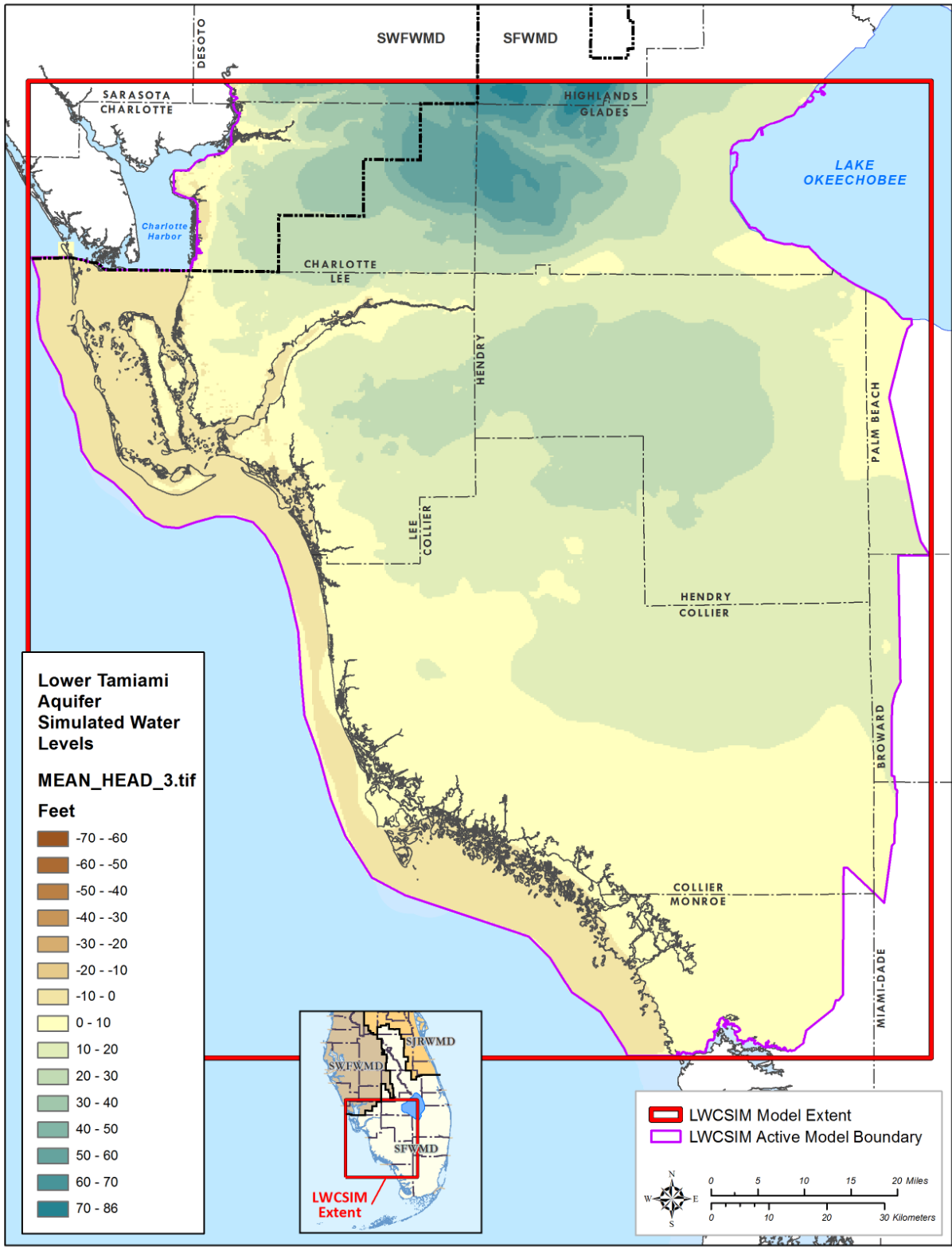


Figure 6-30. Simulated water levels for the Lower Tamiami aquifer.

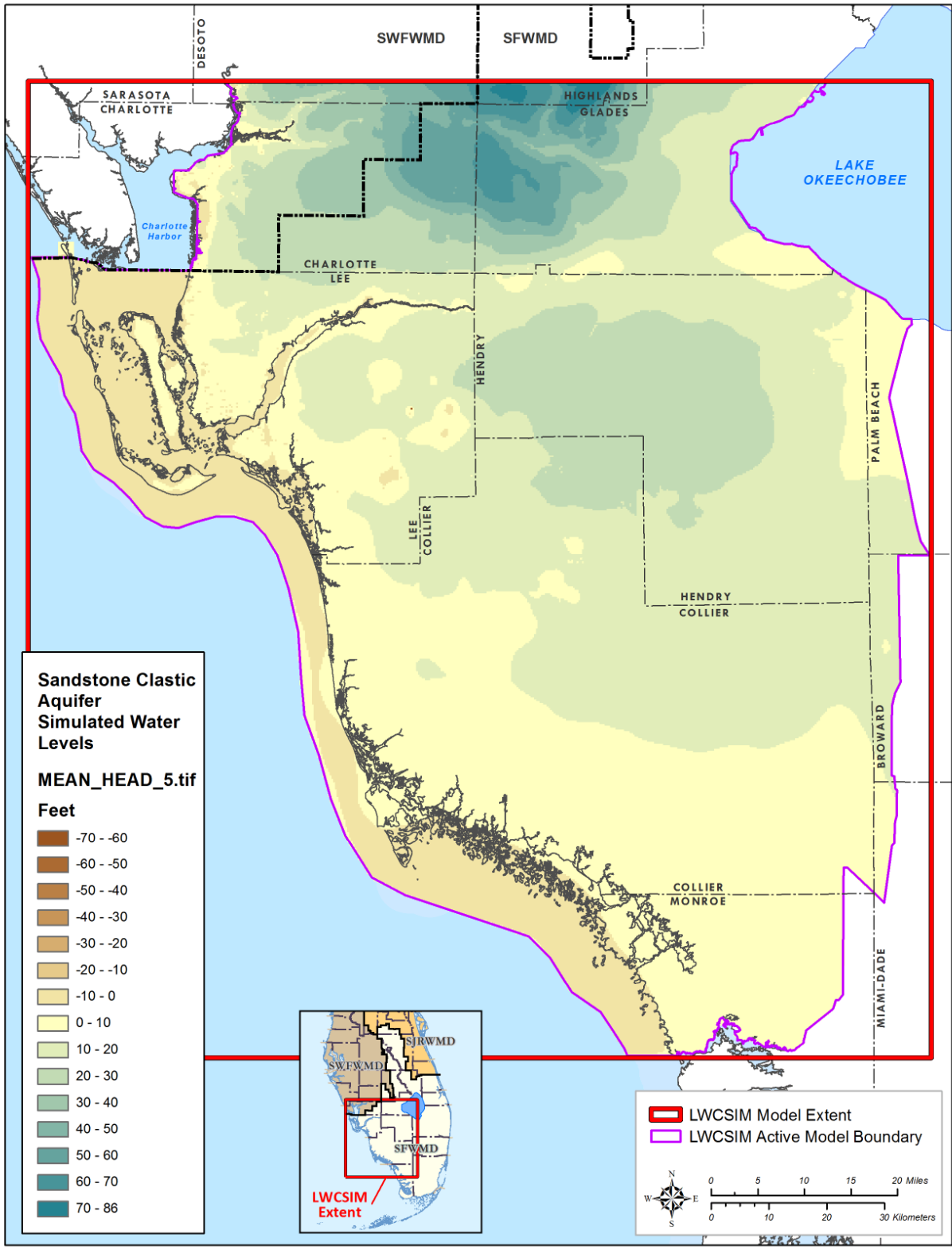


Figure 6-31. Simulated water levels for the Sandstone aquifer – clastic zone.

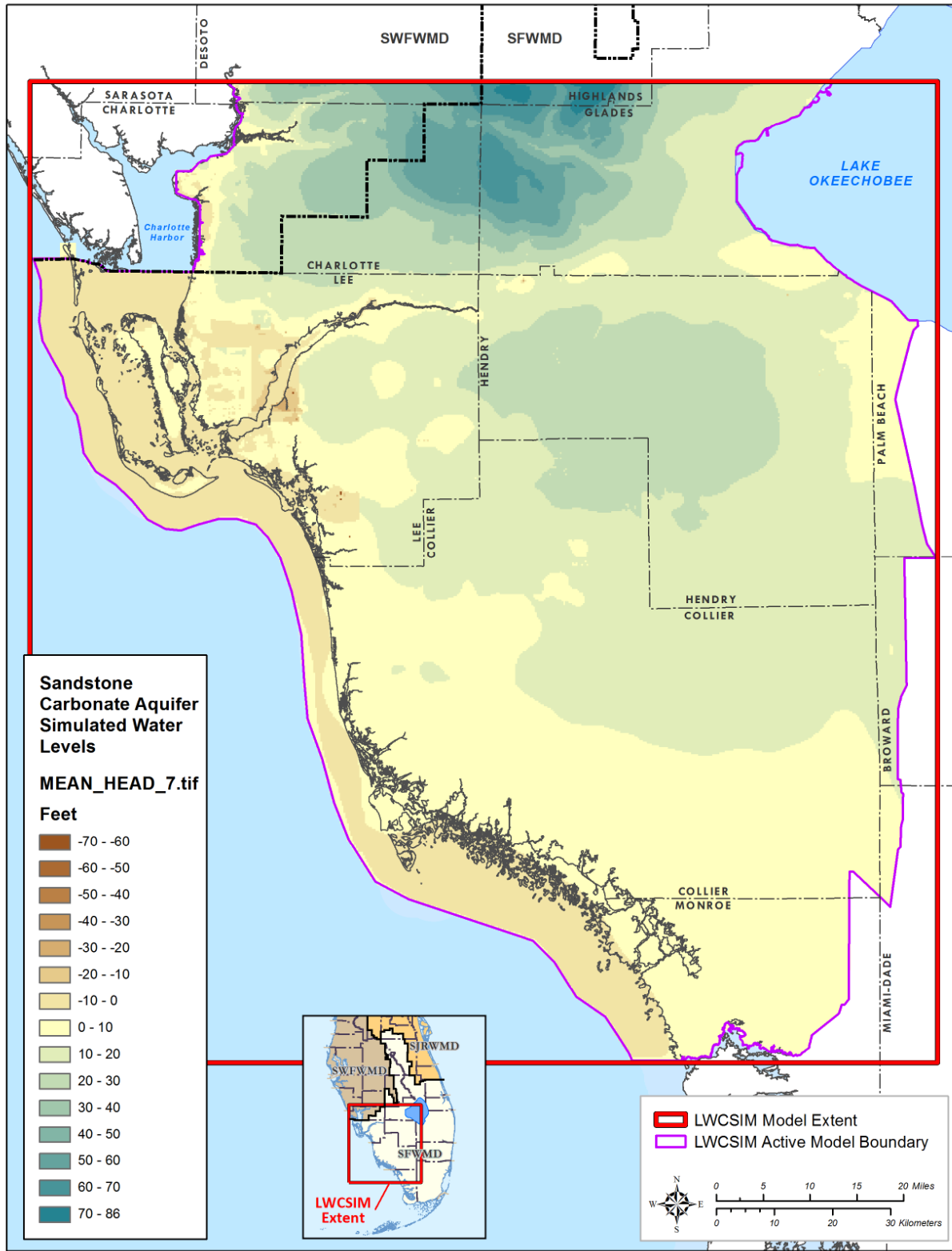


Figure 6-32. Simulated water levels for the Sandstone aquifer – carbonate zone.

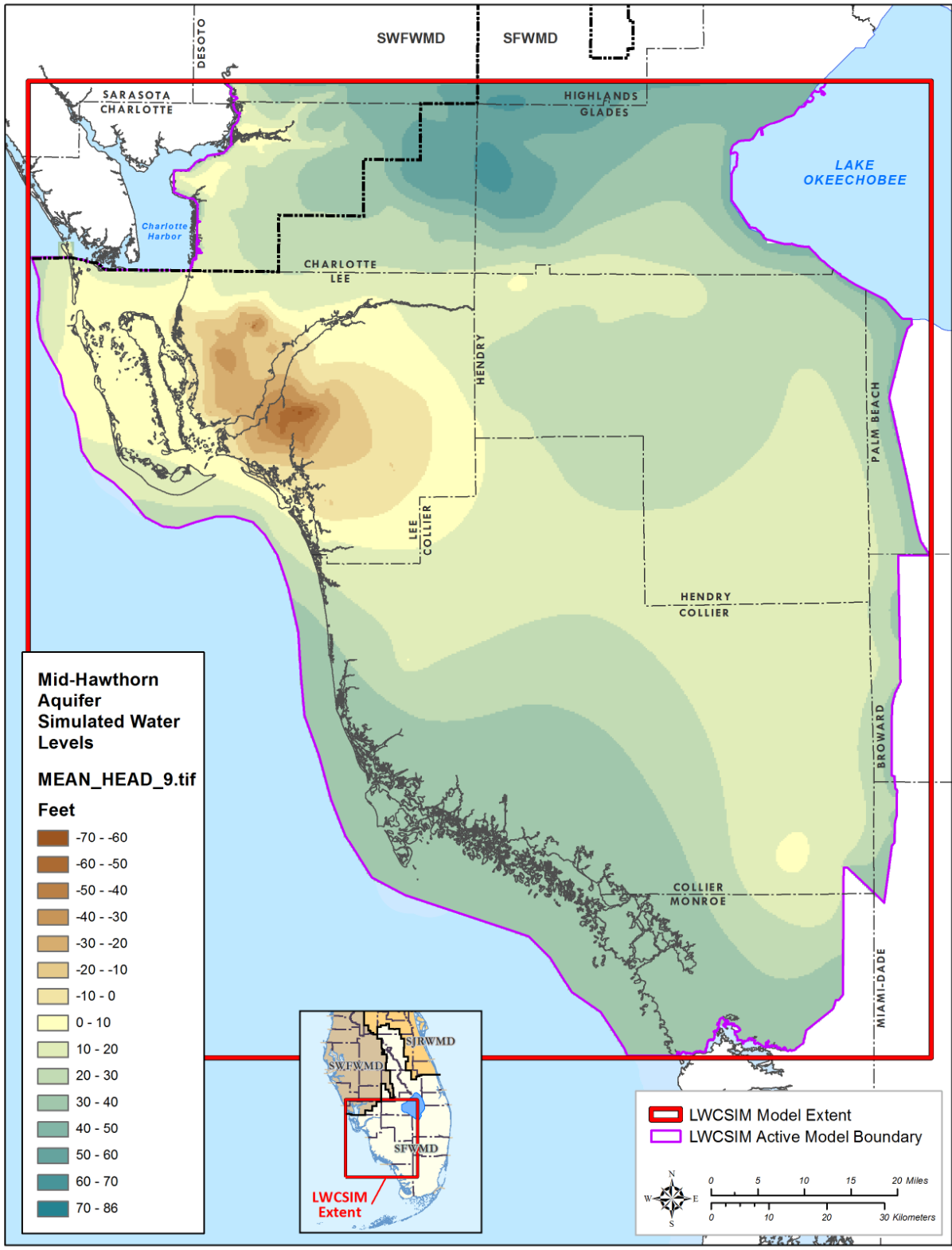


Figure 6-33. Simulated water levels for the Mid-Hawthorn aquifer.

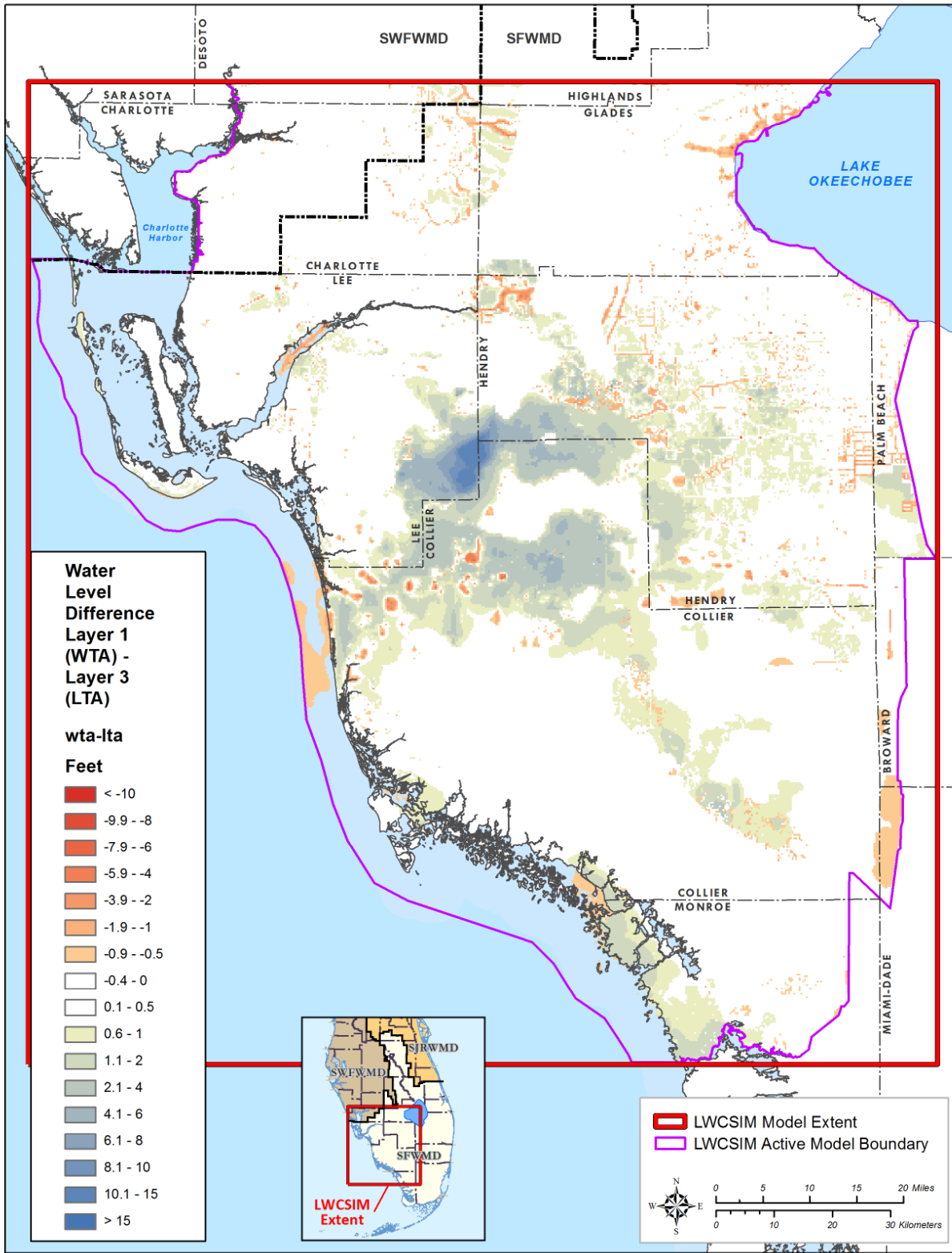


Figure 6-34. Simulated potentiometric surface differences between the Water Table aquifer and the Lower Tamiami aquifer.

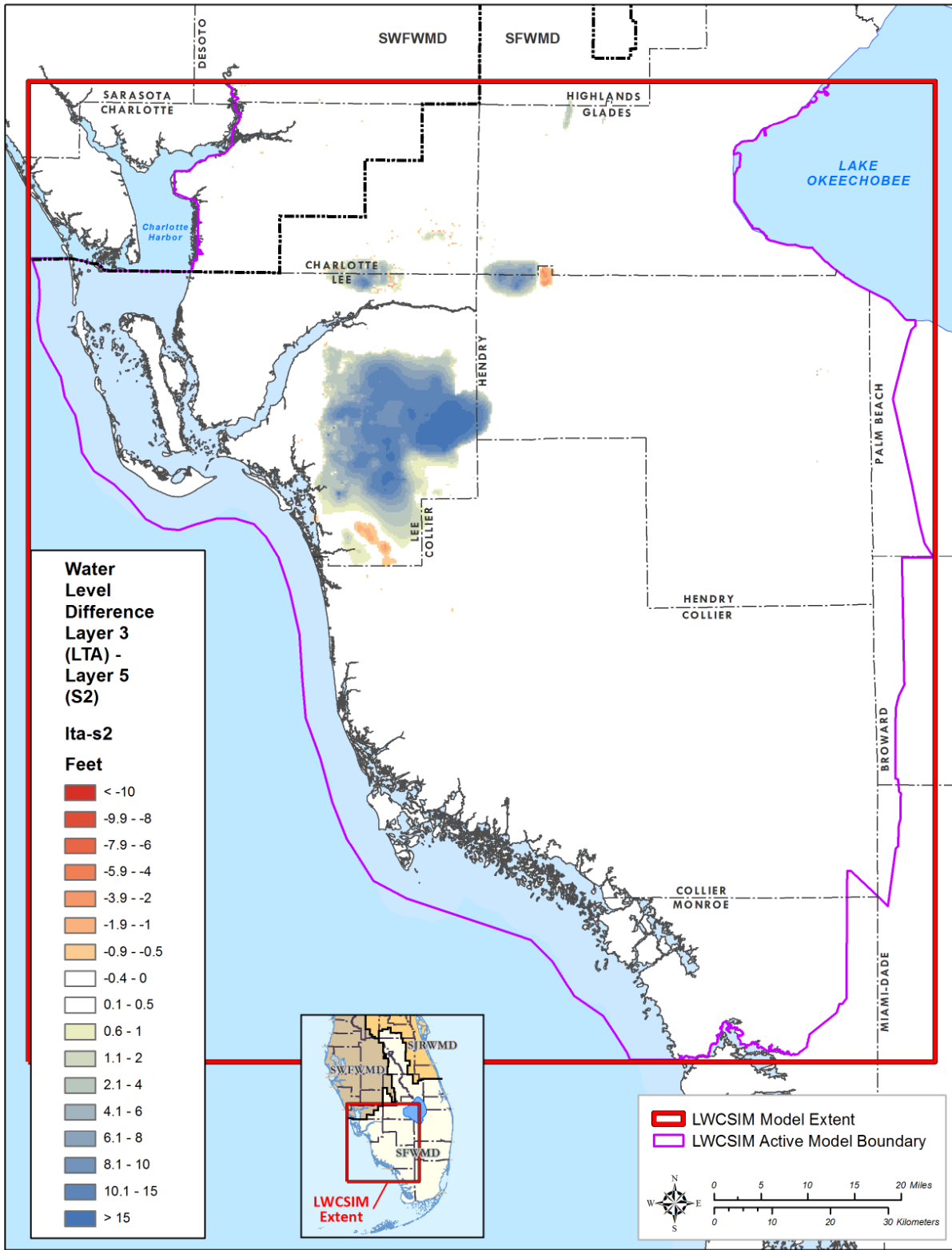


Figure 6-35. Simulated potentiometric surface differences between the Lower Tamiamiqi aquifer and the Sandstone aquifer – clastic zone.

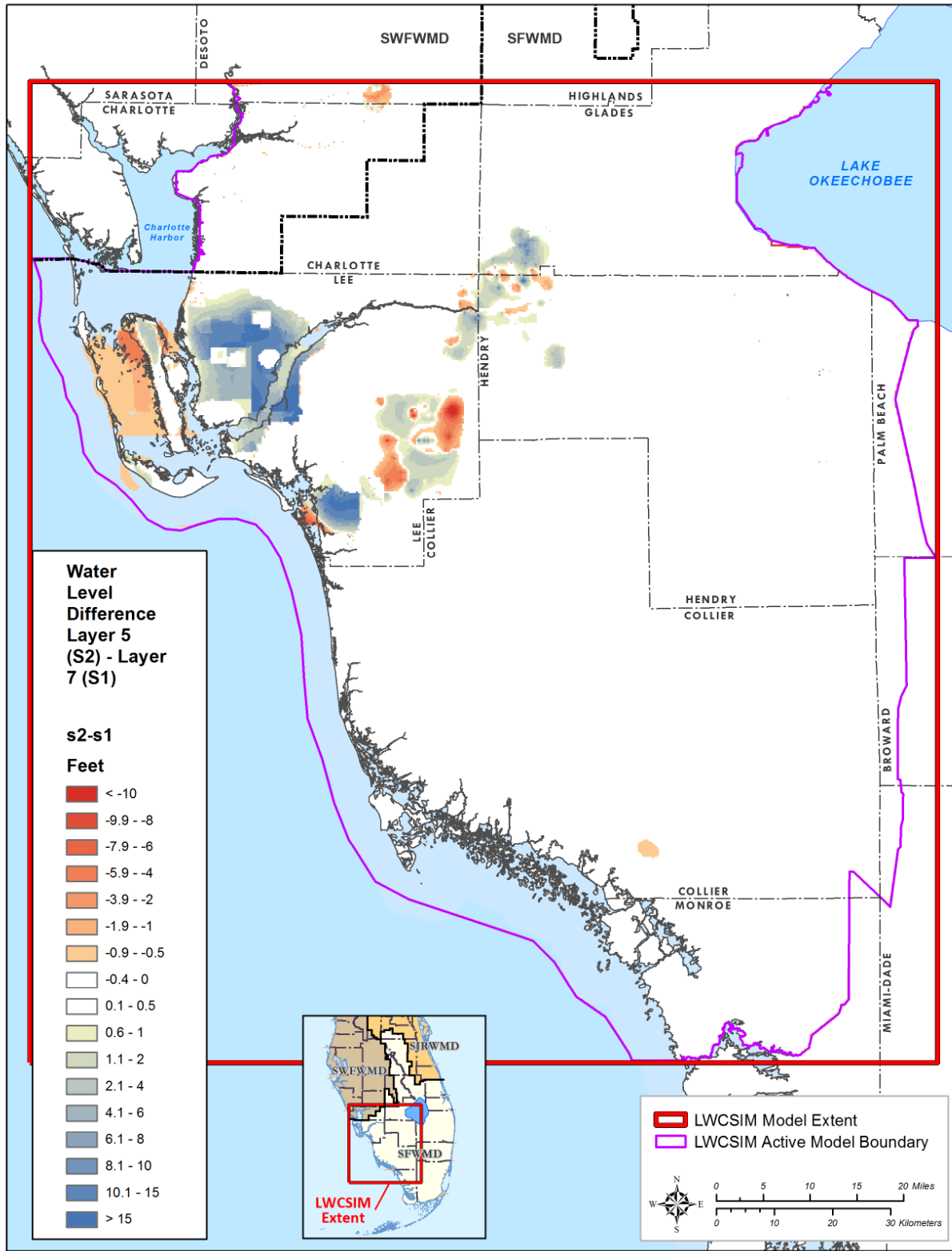


Figure 6-36. Simulated potentiometric surface differences between the Sandstone aquifer – clastic zone and carbonate zone.

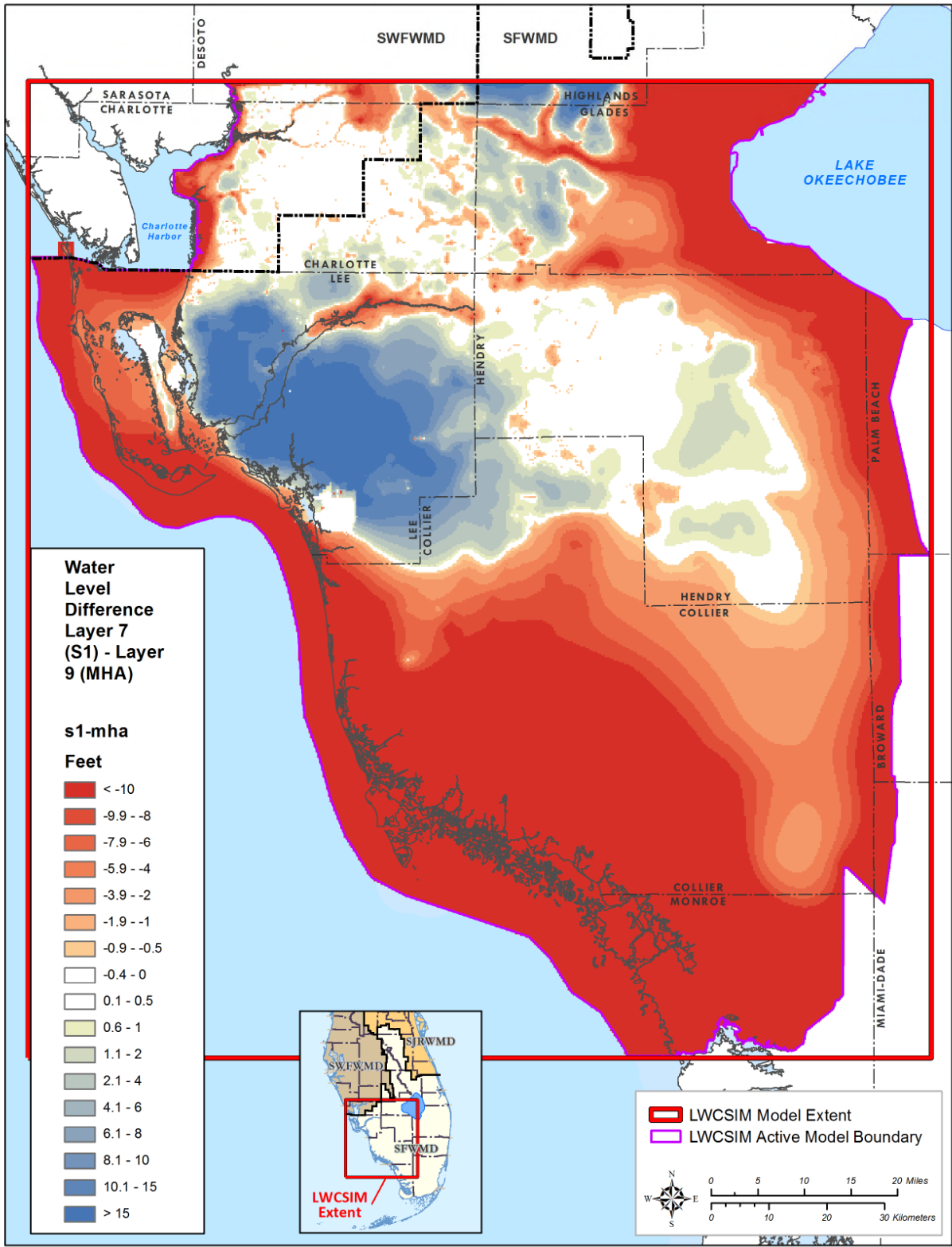


Figure 6-37. Simulated potentiometric surface differences between the Sandstone aquifer – carbonate zone and the Mid-Hawthorn aquifer.

6.7 Water Budget

Water budget analysis was done for surface water and groundwater budget components. The surface water budget was analyzed using the budget terms produced in the ET-Recharge-Runoff program, including rainfall, runoff, gross recharge, unsaturated zone ET, maximum groundwater ET provided to MODFLOW, actual groundwater ET simulated by MODFLOW, net recharge, and change in soil water content. Water use withdrawal from all aquifers was included for comparison purposes. The groundwater budget was analyzed using the budget terms produced during the MODFLOW model run, including GHBs, wells, drains, rivers, recharge/ET, change in storage, and top/bottom flux.

6.7.1 Surface Water Budget

Using the ET-Recharge-Runoff program, average simulated water budgets for each county are shown **Figure 6-38**. Charlotte, Glades, and Hendry counties predominantly consist of agricultural areas; Collier County primarily consists of wetlands and agricultural areas; and Lee County mainly consists of urban areas. Agricultural and landscape irrigation combined (IRR in **Figure 6-38**) was highest in Hendry County (5.5 inches/year) followed by Lee County (3.5 inches/year). Hendry County's total irrigation was mostly due to agricultural irrigation, whereas it was mainly due to landscape and golf course irrigation in Lee County. The rest of the budget terms are compared with respect to rainfall values because of different rainfall values in each county.

Runoff rate was highest in Charlotte County, approximately 26% of rainfall ($14.5 \div 55 \times 100 = 26\%$), while the lowest percentage of runoff occurred in Collier County, 15.7% of rainfall ($8.9 \div 56.4 \times 100 = 15.7\%$). Although, the predominant land use is agriculture in Charlotte County, the portion within the LWCSIM is mostly urban. Therefore, runoff generated within Charlotte County is higher than the other counties within the model domain. Most of Collier County is covered with wetland areas. Runoff in wetland areas is not accounted for here because runoff is not separate from rainfall in the ET-Recharge-Runoff program; instead, runoff is routed through the Wetlands package.

Unsaturated zone ET typically is highest in irrigated areas because it is assumed that the supplemental crop ET requirement is met by applied irrigation. Percentage of unsaturated zone ET with respect to rainfall was highest in Glades ($25 \div 48.8 \times 100 = 51.2\%$), Hendry ($23.3 \div 52.7 \times 100 = 44.2\%$), and Charlotte ($21.1 \div 55 \times 100 = 38.2\%$) counties. Groundwater ET rates were lowest in irrigated areas such as Glades ($8.2 \div 48.8 \times 100 = 16.8\%$), Hendry ($13 \div 52.7 \times 100 = 24.7\%$), and Charlotte ($14.7 \div 55 \times 100 = 26.7\%$) counties. Groundwater ET was highest in wetland-dominated areas such as Collier County, 72% of rainfall ($40.6 \div 56.4 \times 100 = 72\%$). Thus, total ET (unsaturated zone ET + groundwater ET) was highest in wetland-dominated areas such as Collier County, 83% of rainfall ($46.8 \div 56.4 \times 100 = 83\%$), because of the higher contribution from groundwater ET.

Net recharge rate was highest in Lee County, approximately 18.2% of rainfall ($11.3 \div 56.7 \times 100 = 19.9\%$). Lee County also has the highest estimated water use withdrawal rates from the SAS and IAS, approximately 3.4 inches/year. However, because of the greater net recharge rate (11.3 inches/year), water use withdrawals are unlikely to cause a significant threat to the SAS or IAS. Net recharge was lowest in Collier County, approximately 3.7% of rainfall ($2.1 \div 56.4 \times 100 = 3.7\%$) because throughout much of the county, the water table exists either very close to or above ground surface, especially in wetland areas, causing groundwater to discharge to the surface. The estimated water use withdrawal rate from the SAS and IAS in Collier County was 1.8 inches/year, which was greater than the county's net recharge. However, it could be misleading to use net recharge to represent the entire county because about half of Collier County is wetland areas. Therefore, comparison of water use withdrawals and net recharge may not be accurate.

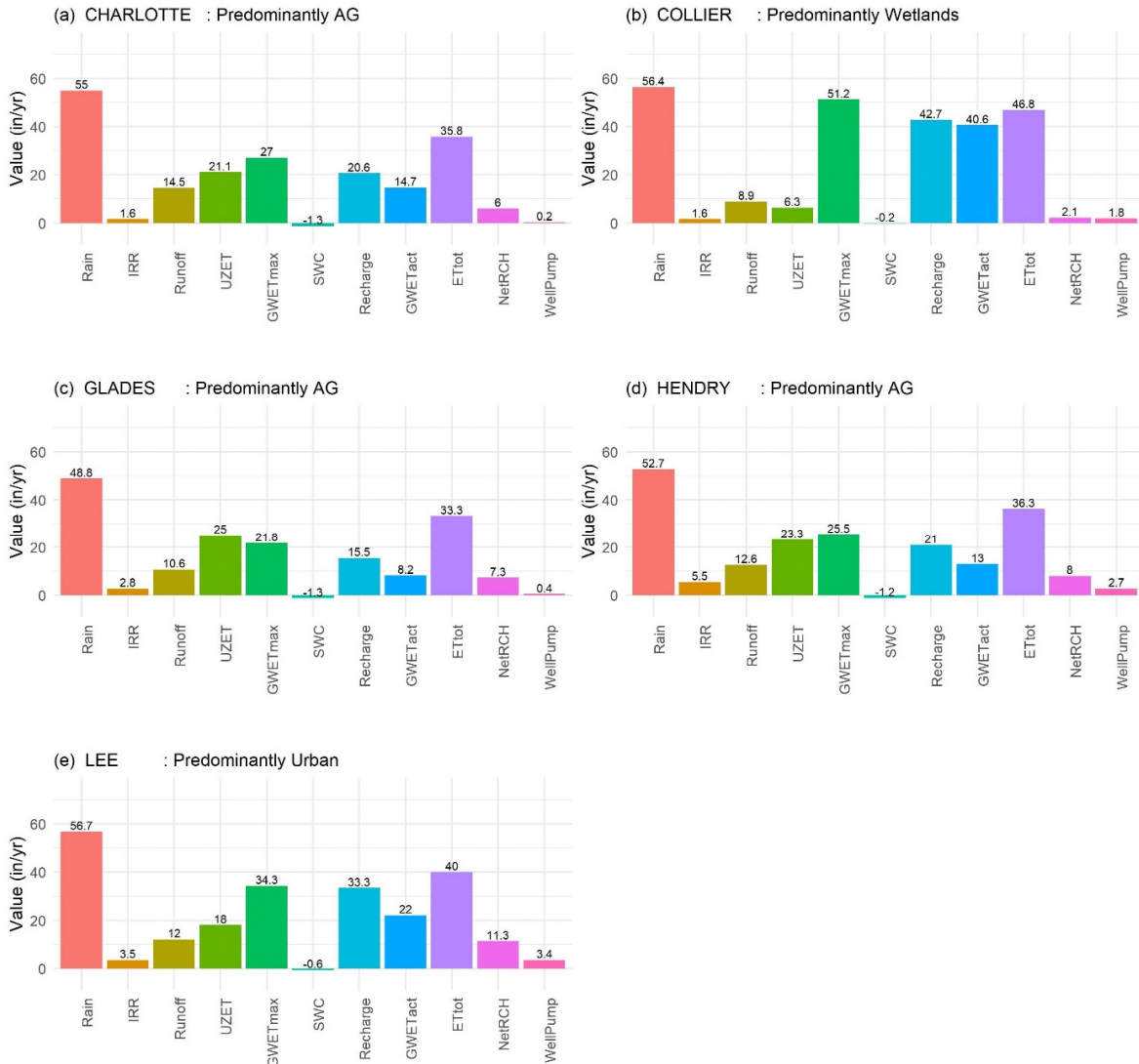


Figure 6-38. Average water budgets, by county, as simulated in the ET-Recharge-Runoff program.

6.7.2 Groundwater Water Budget

A simulated average water budget, by model layer, from 1999 to 2014 is provided in **Table 6-6**. Average net recharge to the WTA was approximately 5.81 inches/year across the model domain (gross recharge – ET = 30.294 – 24.48 = 5.81). Average GHB lateral fluxes were 1.47 inches/year into the model domain. GHB lateral fluxes represent regional groundwater inflows to the model domain from the north/northeast minus groundwater discharge to the Gulf of Mexico. Average well withdrawal rate from the model domain was 1.842 inches/year. Most withdrawals came from the WTA and LTA. Total drain and river leakages from the model domain were 4.97 and 0.75 inches/year, respectively, mostly from the WTA. Drain and river leakages represent groundwater discharge as baseflows. Total average baseflow was approximately 5.7 inches/year (4.97 + 0.720 + 0.025 = 5.715), which is comparable to the net recharge (5.81 inches/year). Generally, the SAS is highly connected to surface water bodies in southwestern Florida, so higher baseflows are expected. Total storage change was approximately 0.28 inches/year, indicating an increase in groundwater storage. This indicates groundwater withdrawals have not caused adverse impact to the SAS-IAS groundwater system overall.

Table 6-6. Simulated water budget summary.

| Layer | GHB Fluxes | Wells | Drains | River Leakage | Gross Recharge | ET | Change in Storage | Vertical Flow | | Error |
|--------------|--------------|---------------|---------------|---------------|----------------|----------------|-------------------|---------------|---------------|--------------|
| | | | | | | | | Top | Bottom | |
| 1 | 0.573 | -0.378 | -4.974 | -0.720 | 30.294 | -24.480 | 0.274 | 0.000 | -0.590 | 0.000 |
| 2 | 0.000 | 0.000 | 0.000 | -0.025 | 0.001 | | 0.000 | 0.590 | -0.566 | 0.000 |
| 3 | 0.472 | -0.793 | 0.000 | 0.000 | | | 0.001 | 0.566 | -0.245 | 0.000 |
| 4 | 0.016 | 0.000 | 0.000 | 0.000 | | | 0.000 | 0.245 | -0.261 | 0.000 |
| 5 | 0.029 | -0.343 | 0.000 | 0.000 | | | 0.000 | 0.261 | 0.053 | 0.000 |
| 6 | 0.019 | 0.000 | 0.000 | 0.000 | | | 0.000 | -0.053 | 0.034 | 0.000 |
| 7 | 0.017 | -0.237 | 0.000 | 0.000 | | | 0.001 | -0.034 | 0.253 | 0.000 |
| 8 | 0.048 | 0.000 | 0.000 | 0.000 | | | 0.000 | -0.253 | 0.205 | 0.000 |
| 9 | 0.297 | -0.093 | 0.000 | 0.000 | | | 0.000 | -0.205 | 0.000 | 0.000 |
| Total | 1.470 | -1.842 | -4.974 | -0.745 | 30.295 | -24.480 | 0.276 | 1.117 | -1.117 | 0.000 |

ET = evapotranspiration; GHB = general head boundary.

Note: All values are presented in inches per year.

During the simulation period, the WTA provided an average recharge of approximately 0.59 inches/year to the underlying TCU, which eventually recharges the LTA. The WTA received 0.57 inches/year of net average groundwater recharge from the regional system from north/northeast of the model domain through GHB fluxes. Higher water levels along the northern/northeastern boundary and lower levels in the southwestern portion of the model indicate a northeast to southwest regional flow gradient (**Figure 6-29**). The WTA lost approximately 0.38 inches/year due to water use withdrawals, 4.98 inches/year through drains as baseflows, and 0.72 inches/year through rivers as baseflows. During the simulation period, there was a net increase in groundwater storage in the WTA of approximately 0.27 inches/year, indicating no negative impacts to the WTA from water use withdrawals.

The LTA received 0.57 inches/year of recharge from the overlying WTA. Generally, the average potentiometric levels of the WTA are 5 to 15 ft higher than the LTA potentiometric levels where the LTA is productive (**Figure 6-34**). Therefore, a downward flow gradient is expected from the WTA to the LTA. The LTA received approximately 0.47 inches/year of net groundwater recharge from the regional system through the northern/northeastern model boundary. Higher potentiometric heads along the northern/northeastern boundary and lower potentiometric heads in the southwestern portion of the model indicate a northeast to southwest regional flow gradient (**Figure 6-30**). The water use withdrawal rate from the LTA was approximately 0.378 inches/year, making the LTA the most used aquifer in southwestern Florida. Despite higher withdrawals, there was a slight increase in groundwater storage (0.001 inches/year) within the LTA, indicating no significant harm to the LTA from water use withdrawals.

The LTA provided approximately 0.26 inches/year average recharge to the underlying SSA-clastic zone through the confining zone. **Figure 6-35** shows the LTA potentiometric heads are 10 to 15 ft higher than the SSA-clastic zone potentiometric heads; therefore, a downward flow gradient from the LTA to the SSA-clastic zone is expected. The SSA-clastic zone received 0.03 inches/year of groundwater flow from the regional system, and 0.343 inches/year were withdrawn for water use purposes. No change in groundwater storage within the SSA-clastic zone occurred. The SSA-carbonate zone received approximately 0.032 inches/year of average recharge from the overlying SSA-clastic zone and 0.2 inches/year from the underlying MHA. The simulated potentiometric surfaces indicate there are areas in MHA with higher potentiometric levels than the overlying SSA-carbonate zone, especially in the southwestern portion of the model domain (**Figure 6-37**). Thus, an upward gradient from the MHA to the SSA-carbonate zone is expected. Approximately 0.24 inches/year of average water use withdrawals occurred from the SSA-carbonate zone; however, groundwater storage slightly increased (0.001 inches/year).

The MHA provided approximately 0.2 inches/year of average recharge to the overlying SSA. The MHA received 0.297 inches/year of net average groundwater recharge from the regional system through GHB fluxes from north and northeast of the model domain. Regional flow from northeast to southwest is clearly shown in the simulated potentiometric heads (**Figure 6-33**). Approximately 0.9 inches/year of average water use withdrawals occurred from the MHA; however, there were no changes in groundwater storage.

Figures 6-39 to 6-43 present the average GHB fluxes into and out of the LWCSIM for the five aquifer layers. These represent one of the extracted MODFLOW budget terms and indicate the magnitude of groundwater flux entering and leaving the model under a regional groundwater gradient. Shades of green represent water flowing into the model domain and shades of yellow to red represent water flowing out of the model domain. In layers 1, 3, 5 and 7, the general flow across the model domain is from the northeast to the southwest, or from the Lake Okeechobee down and out to the Gulf of Mexico. This represents the known pattern of regional groundwater flow across the model domain. The GHB flux in layer 9 is mostly inflow from the Gulf of Mexico. There is a known area of artesian conditions in the southwestern portion of the MHA, as indicated by measured water levels in the two monitor wells in southwestern Collier County. Artesian conditions were simulated by defining higher stages in the GHBs along the Gulf coast, particularly in this area of the model. GHB boundary fluxes were checked to ensure there were no major fluxes on the western boundary indicating saltwater coming into the model domain, with the exception of layer 9. Western boundary fluxes show very little flow to the east because the corrected GHB heads for fresh water are higher than adjacent freshwater heads.

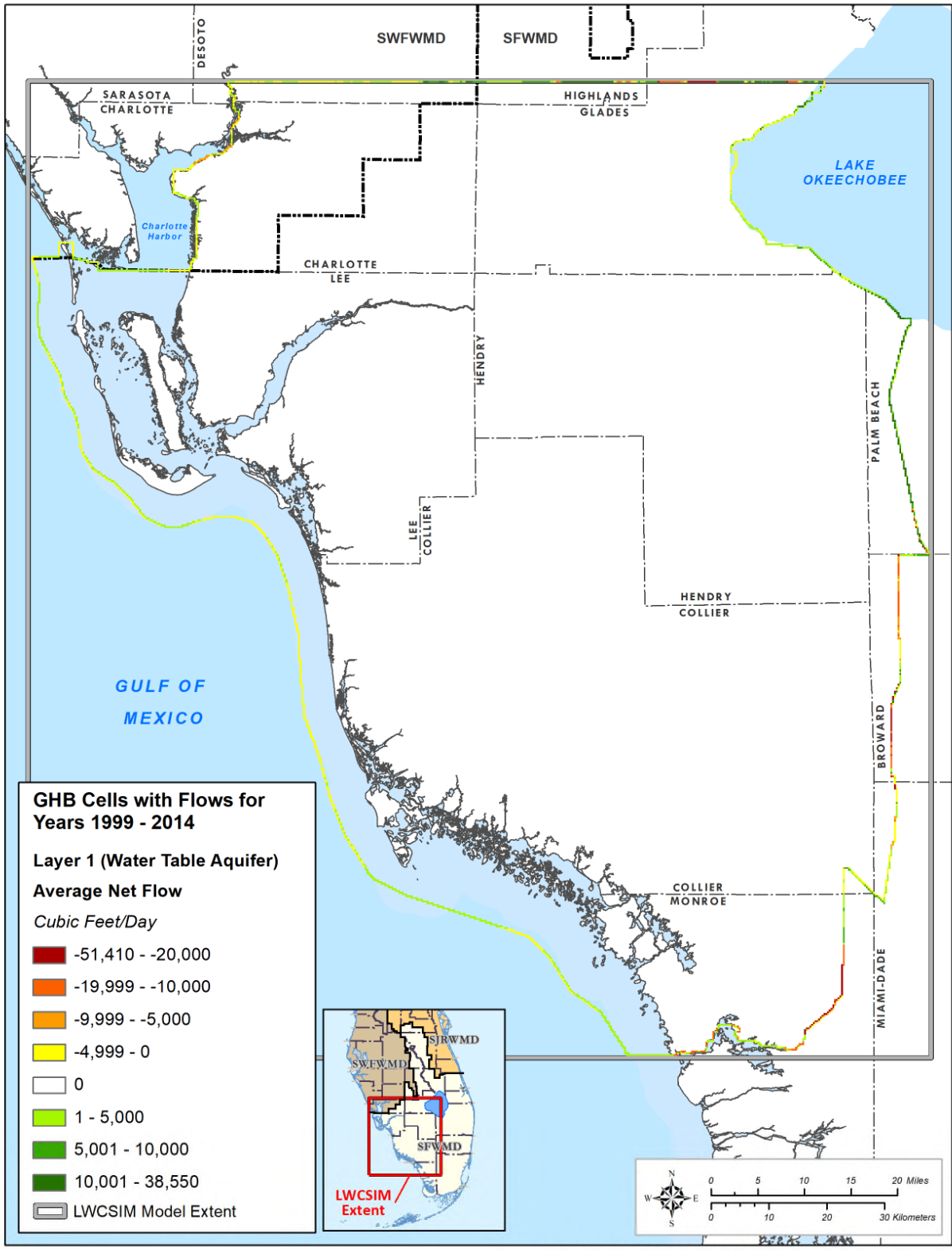


Figure 6-39. Average net general head boundary flow in the Water Table aquifer.

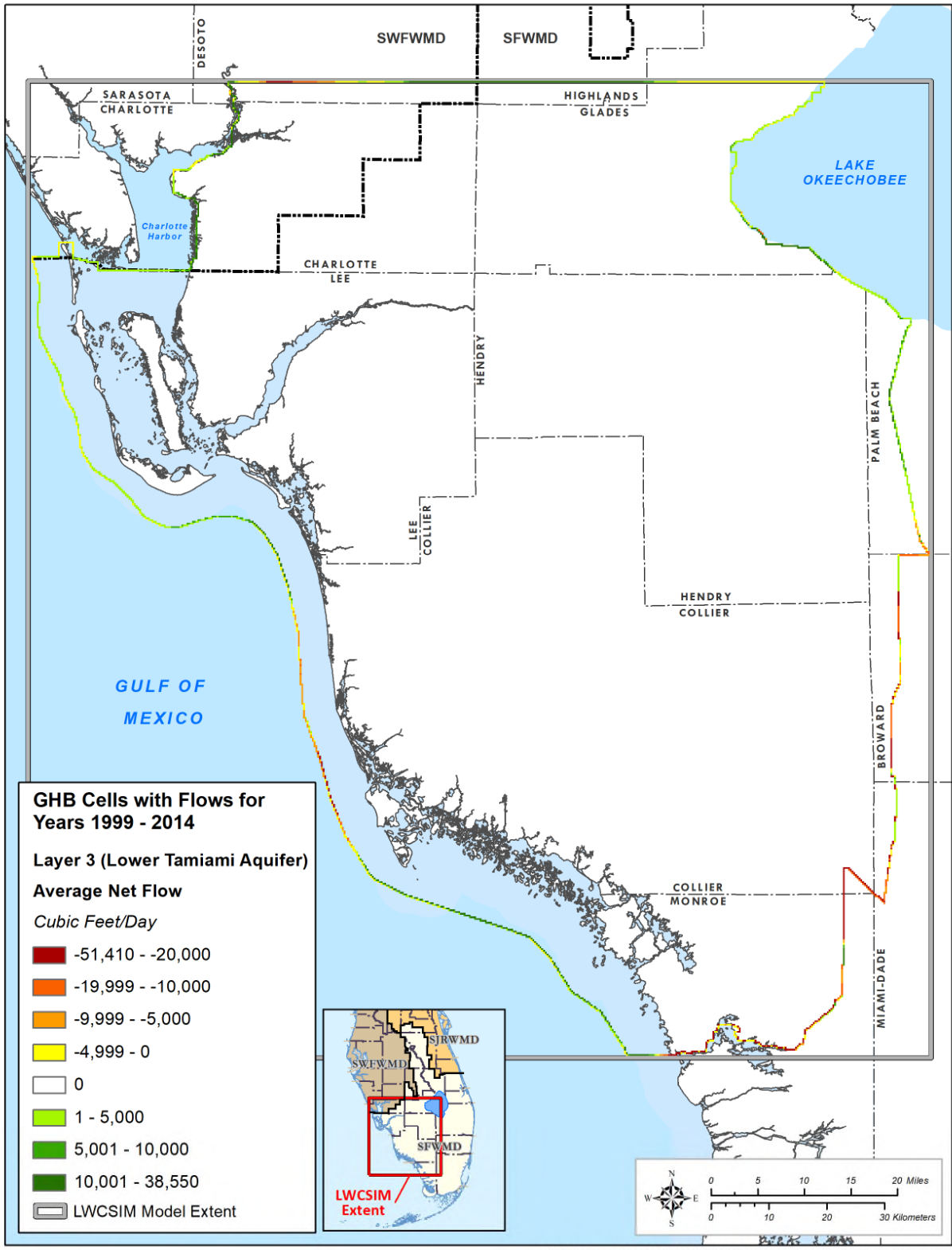


Figure 6-40. Average net general head boundary flow in the Lower Tamiami aquifer.

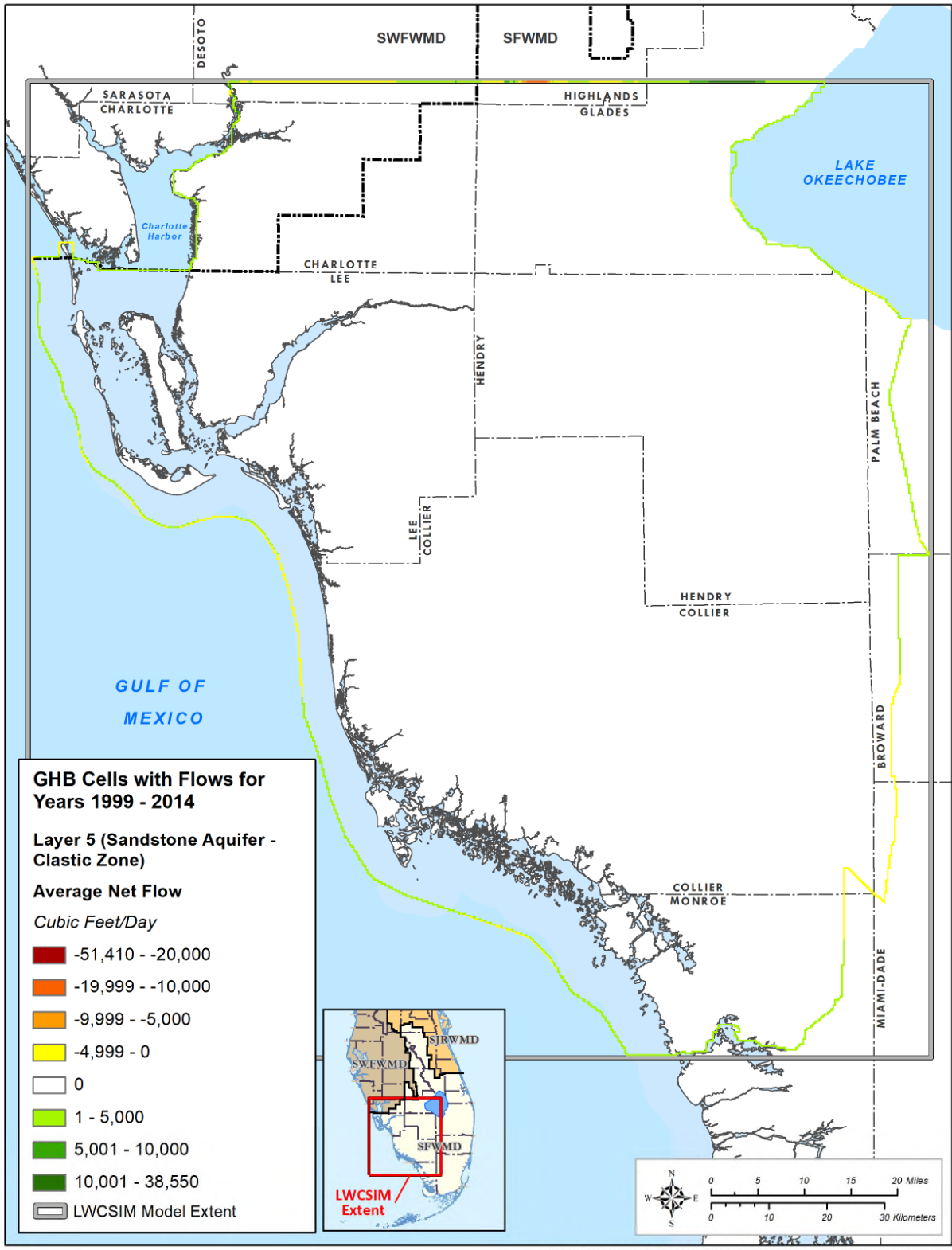


Figure 6-41. Average net general head boundary flow in the Sandstone aquifer – clastic zone.

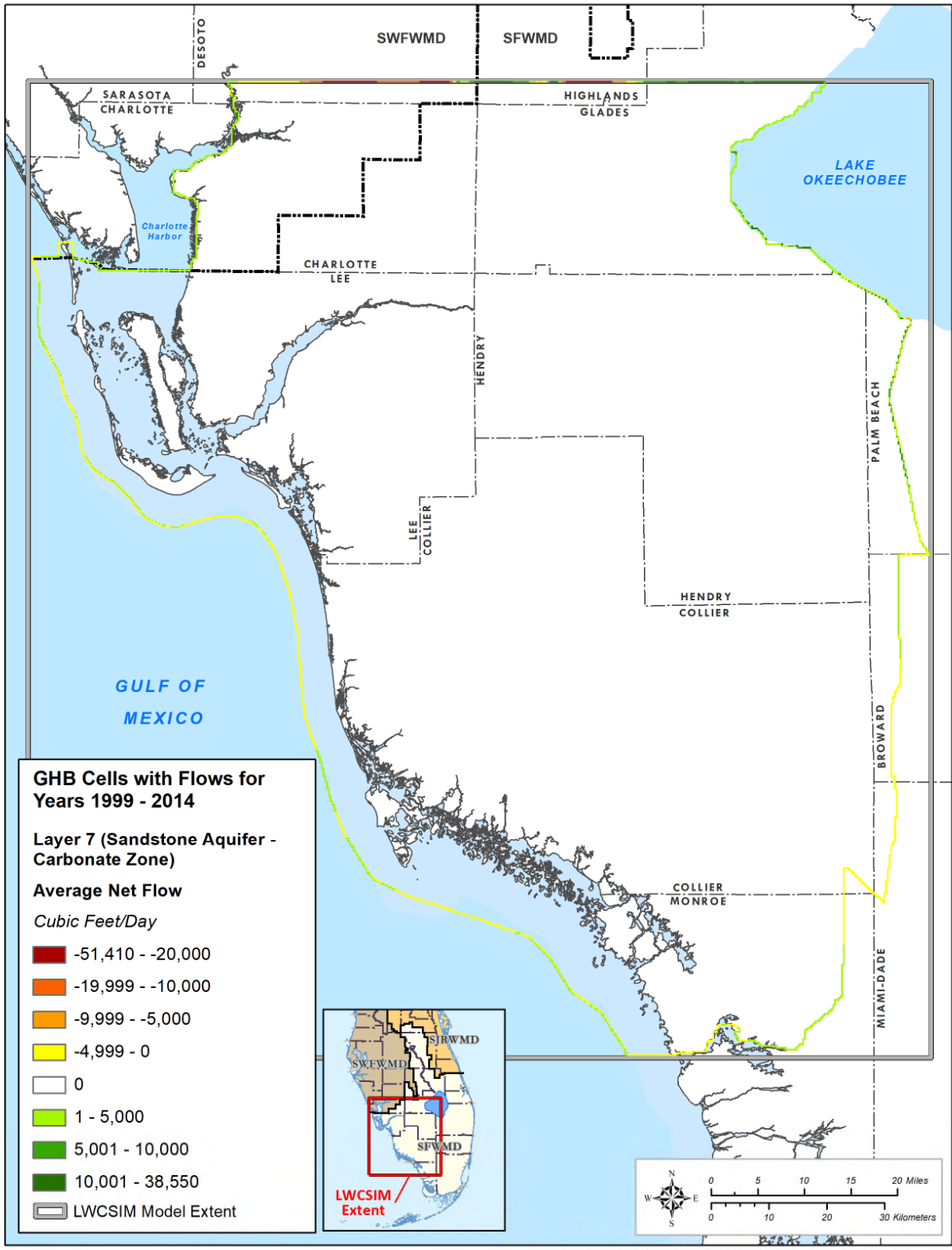


Figure 6-42. Average net general head boundary flow in the Sandstone aquifer – carbonate zone.

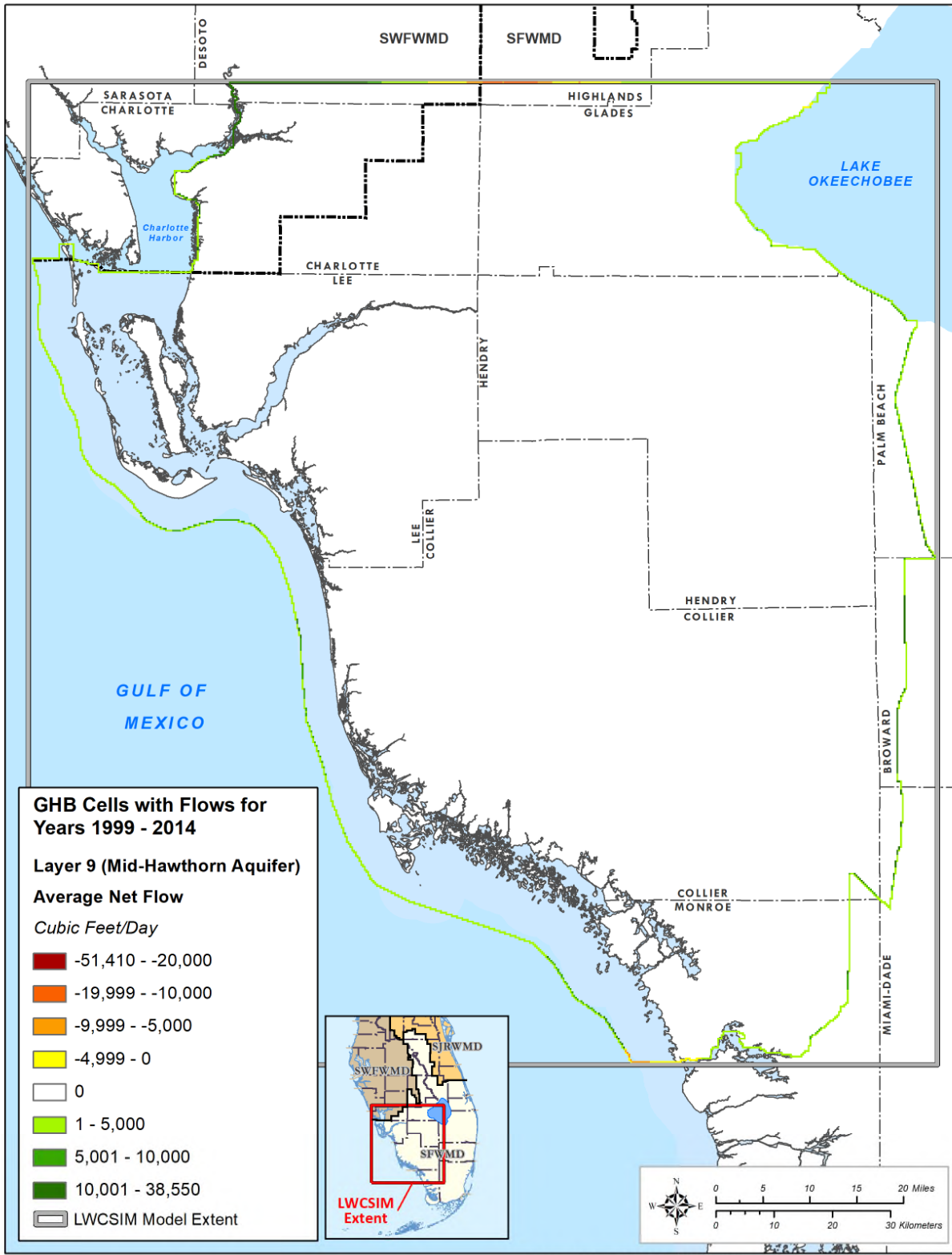


Figure 6-43. Average net general head boundary flow in the Mid-Hawthorn aquifer.

7 SENSITIVITY ANALYSIS

A sensitivity analysis is a process of quantifying the degree to which model outputs are influenced by model inputs. Model inputs include parameters that are conceptually constant or fixed, but whose values are not known with great precision. A sensitivity analysis may reveal the degree of calibration of a calibrated model. Under this concept, a sensitivity analysis is interpreted as a kind of inverse model; rather than estimating model performance for given inputs, error bars about the inputs are estimated. All models have some error. Useful models have errors that are not significant relative to the answers to the questions that are asked of the model.

Whereas calibration is a minimization problem in which parameters are adjusted until model error is minimized, sensitivity analysis is descriptive; it explores the parameter space in the neighborhood of the calibration. Whereas the result of calibration is a single point, a list of specific parameters and their values, the result of sensitivity analysis is a collection of such lists.

A model highly sensitive to a given parameter exhibits significantly increased error with deviation from the calibrated parameter value. Conversely, a model that is insensitive to a given parameter will not exhibit significant increases in error with such deviation.

7.1 Parameters and Methodology

Model sensitivity to several parameters was assessed by constructing several alternative parameter sets and computing relative model response. The result was several dozen pairs of deviations of parameter and response. Scenarios differ from the calibrated model by a single parameter, so the effect of that parameter's variations on the model could be individually assessed. Parameter ranges were varied, within acceptable ranges, based on a predetermined data range for each parameter calculated from known values. **Table 7-1** shows the model input parameters used in the sensitivity analysis and the different multipliers applied to the calibration parameters.

Table 7-1. Parameters varied by model layer.

| | |
|------------------------------|--|
| Each Layer* | Horizontal hydraulic conductivity |
| | Specific yield |
| Each Pair of Adjacent Layers | Vertical hydraulic conductivity |
| Layer 1 | Horizontal hydraulic conductivity of muck/peat |
| | Specific yield of muck/peat |
| | Specific yield of surface water body |
| | Kadlec conductance coefficient |
| | Drain conductance |
| | River conductance |
| | Recharge |
| | Evapotranspiration |
| Each of Layers 2 to 9 | Evapotranspiration extinction depth |
| | Specific storage |

* The distinction between "Each Layer" and "All Layers" is that for the former, each layer is considered to have its own parameter, whereas for the latter, a single parameter is shared by all the layers.

Additional model runs replacing time-varying heads in selected GHB cells with a constant-head boundary in addition to a no-flow boundary (GHB conductance equal to 0) in model layers 1 through 9 also were simulated. For each parameter, several model runs were completed using the various multipliers identified in **Table 7-2**. The simulation period for the sensitivity analysis was from January 1, 1999 to December 31, 2012 (168 months). To complete the sensitivity analysis, 178 model runs were conducted; of these, 170 converged (ran to completion).

Table 7-2. Parameters and multipliers of sensitivity analysis for the model.

| Description | Multipliers | | | |
|--|-------------|-------|-------|--------------|
| | 0.1 | 0.2 | 5 | 10 |
| Horizontal hydraulic conductivity | 0.1 | 0.2 | 5 | 10 |
| (Layer 1) specific yield | 0.25 | 0.5 | 0.75 | 1.25 |
| (Layers 2, 3, 4, 6, 8, and 9) specific storage | 0.01 | 0.1 | 10 | 100 |
| (Layers 5 and 7) specific storage | 0.0015 | 0.015 | 0.15 | 0.2 |
| (Layers 2, 3, 4, 6, 8, and 9) specific yield | 0.05 | 0.1 | 0.2 | 0.25 |
| (Layers 5 and 7) specific yield | 0.0015 | 0.015 | 0.15 | 0.2 |
| (Layers 1 to 8) vertical hydraulic conductivity ^a | 0.1 | 0.2 | 5 | 10 |
| Drain conductance | 0.01 | 0.1 | 10 | 100 |
| Evapotranspiration | 0.8 | 0.9 | 1.1 | 1.2 |
| Evapotranspiration extinction depth | 0.8 | 0.9 | 1.1 | 1.2 |
| General head boundary conductance | 0.01 | 0.1 | 10 | 100 |
| General head boundary conductance ^b | N = 0 | W = 0 | E = 0 | ^c |
| Recharge | 0.8 | 0.9 | 1.1 | 1.2 |
| River conductance | 0.01 | 0.1 | 10 | 100 |
| Kadlec conductance coefficient ^d | 0.1 | 0.2 | 5 | 10 |
| Horizontal hydraulic conductivity of muck/peat ^d | 0.1 | 0.2 | 5 | 10 |
| Specific yield of muck/peat ^d | 0.75 | 0.875 | 1.125 | 1.25 |
| Specific yield of surface water body ^d | 0.894 | 0.947 | 1.042 | ^c |

^a The model parameter varied for vertical hydraulic conductivity was actually leakance, but because the variation is by a factor, this is equivalent to varying vertical hydraulic conductivity.

^b Three scenarios where the north, east, or west general head boundary conductance was set to zero.

^c Only three variations.

^d Wetlands only.

7.2 Sensitivity Results

Sensitivity results are grouped by aquifer and subdivided into four sensitivity categories. Categories are defined by the magnitude of the difference between mean absolute error for the scenario and for the calibrated model (expression EXP1).

$$| \text{Sensitivity MAE} - \text{Calibrated Model MAE} | \quad (\text{EXP1})$$

Specifically, the difference categories are:

- Less than 0.1 ft: not sensitive
- From 0.1 to less than 0.5 ft: slightly sensitive
- From 0.5 to less than 1.0 ft: moderately sensitive
- 1.0 ft or greater: sensitive

A complete set of sensitivity plots, grouped by parameter type, is presented in **Appendix K**. There is one plot per parameter. The parameter value is plotted on the horizontal axis, and the responses (deviations from the base MAE for each aquifer) are plotted on the vertical axis.

There is only one scenario for which there is an overall improvement in model performance: where Kh for layer 6 is reduced by a factor of five. However, this comes at the expense of an increase of relative MAE in layer 1 that approaches 2 ft. **Table 7-3** provides additional details. In **Table 7-3**, the values are rounded to the nearest 0.1 ft. Layer 1 exhibits significant diminishment in performance for some stations.

Table 7-3. Range of relative mean absolute error, by aquifer, for the scenario Kh (layer 6) = 0.2×.

| Layer | Range of Relative Mean Absolute Error | |
|-------|---------------------------------------|---------|
| | Minimum | Maximum |
| 1 | -1.4 | 1.8 |
| 3 | -0.3 | 0.5 |
| 5 | -0.7 | 0.3 |
| 7 | -0.8 | 0.2 |
| 9 | -0.0 | 0.1 |

Kh = horizontal hydraulic conductivity.

7.3 Monitor Well Water Level Sensitivity

Monitor well water levels were most sensitive to the parameters presented in **Table 7-4**. The LWCSIM was not sensitive in any aquifer to the scenarios not listed in the table. The model appeared most sensitive to Kh, Kv, and riverbed conductance.

Table 7-4. Parameters with significant sensitivity.

| Parameter | Layer | Multiplier | Aquifer Rank | | | | | Rank Sum |
|--------------------|-------|------------|--------------|-----|-------------|---------------|-----|----------|
| | | | WTA | LTA | SSA-clastic | SSA-carbonate | MHA | |
| Kv | 2 | 0.1 | 1 | 3 | 4 | 4 | 1 | 13 |
| River conductance | N/A | 0.01 | 2 | 2 | 2 | 2 | 4 | 12 |
| Kv | 1 | 0.1 | 2 | 2 | 3 | 3 | 1 | 11 |
| Kh | 3 | 10 | 2 | 3 | 2 | 2 | 2 | 11 |
| Kv | 4 | 0.2 | 1 | 1 | 4 | 4 | 1 | 11 |
| Kv | 4 | 0.1 | 1 | 1 | 4 | 4 | 1 | 11 |
| River conductance | N/A | 0.1 | 2 | 1 | 2 | 2 | 4 | 11 |
| Kh | 1 | 0.2 | 2 | 2 | 2 | 2 | 2 | 10 |
| Kh | 1 | 0.1 | 2 | 2 | 2 | 2 | 2 | 10 |
| Kv | 2 | 0.2 | 1 | 2 | 4 | 2 | 1 | 10 |
| Kv | 4 | 10 | 1 | 1 | 3 | 4 | 1 | 10 |
| Kv | 4 | 5 | 1 | 1 | 3 | 4 | 1 | 10 |
| Kv | 6 | 0.1 | 1 | 1 | 2 | 2 | 4 | 10 |
| Evapotranspiration | N/A | 0.8 | 2 | 2 | 2 | 2 | 2 | 10 |
| Kh | 1 | 5 | 2 | 2 | 1 | 2 | 2 | 9 |
| Specific yield | 1 | 0.25 | 2 | 2 | 2 | 1 | 2 | 9 |
| Kh | 5 | 10 | 2 | 1 | 3 | 2 | 1 | 9 |
| Kh | 5 | 0.1 | 1 | 1 | 4 | 2 | 1 | 9 |
| Kv | 6 | 0.2 | 1 | 1 | 2 | 1 | 4 | 9 |
| Kh | 9 | 10 | 1 | 1 | 1 | 2 | 4 | 9 |
| Kh | 9 | 5 | 1 | 1 | 1 | 2 | 4 | 9 |
| Kh | 9 | 0.1 | 1 | 1 | 1 | 2 | 4 | 9 |

| Parameter | Layer | Multiplier | Aquifer Rank | | | | | Rank Sum |
|-----------------------|-------|------------|--------------|-----|-------------|---------------|-----|----------|
| | | | WTA | LTA | SSA-clastic | SSA-carbonate | MHA | |
| Drain conductance | N/A | 0.01 | 1 | 2 | 2 | 3 | 1 | 9 |
| River conductance | N/A | 10 | 1 | 2 | 2 | 2 | 2 | 9 |
| Recharge | N/A | 1.2 | 2 | 2 | 2 | 2 | 1 | 9 |
| Kv | 1 | 0.2 | 1 | 2 | 2 | 2 | 1 | 8 |
| Kh | 3 | 0.1 | 1 | 2 | 2 | 2 | 1 | 8 |
| Kv | 5 | 0.2 | 1 | 1 | 1 | 1 | 4 | 8 |
| Kv | 5 | 0.1 | 1 | 1 | 1 | 1 | 4 | 8 |
| Kh | 6 | 10 | 2 | 1 | 2 | 2 | 1 | 8 |
| Kh | 6 | 5 | 2 | 1 | 2 | 2 | 1 | 8 |
| Kv | 6 | 10 | 1 | 1 | 1 | 2 | 3 | 8 |
| Kh | 7 | 10 | 1 | 1 | 2 | 3 | 1 | 8 |
| Kv | 7 | 10 | 1 | 1 | 1 | 1 | 4 | 8 |
| Kv | 7 | 5 | 1 | 1 | 1 | 1 | 4 | 8 |
| Kv | 7 | 0.2 | 1 | 1 | 1 | 1 | 4 | 8 |
| Kv | 7 | 0.1 | 1 | 1 | 1 | 1 | 4 | 8 |
| Kv | 8 | 10 | 1 | 1 | 1 | 1 | 4 | 8 |
| Kv | 8 | 5 | 1 | 1 | 1 | 1 | 4 | 8 |
| Kv | 8 | 0.2 | 1 | 1 | 1 | 1 | 4 | 8 |
| Kv | 8 | 0.1 | 1 | 1 | 1 | 1 | 4 | 8 |
| Kh | 9 | 0.2 | 1 | 1 | 1 | 1 | 4 | 8 |
| Specific storage | 9 | 100 | 1 | 1 | 1 | 1 | 4 | 8 |
| GHB conductance | N/A | 0.1 | 1 | 1 | 1 | 1 | 4 | 8 |
| GHB conductance | N/A | 0.01 | 1 | 1 | 1 | 1 | 4 | 8 |
| West GHB conductance | N/A | N/A | 1 | 1 | 1 | 1 | 4 | 8 |
| River conductance | N/A | 100 | 1 | 2 | 1 | 2 | 2 | 8 |
| Specific yield | 1 | 0.5 | 2 | 1 | 2 | 1 | 1 | 7 |
| Kh | 2 | 10 | 1 | 1 | 1 | 2 | 2 | 7 |
| Kh | 3 | 5 | 2 | 2 | 1 | 1 | 1 | 7 |
| Kh | 3 | 0.2 | 1 | 2 | 1 | 2 | 1 | 7 |
| Kh | 5 | 5 | 1 | 1 | 2 | 2 | 1 | 7 |
| Kh | 5 | 0.2 | 1 | 1 | 3 | 1 | 1 | 7 |
| Kv | 5 | 10 | 1 | 1 | 1 | 1 | 3 | 7 |
| Kv | 5 | 5 | 1 | 1 | 1 | 1 | 3 | 7 |
| Kv | 6 | 5 | 1 | 1 | 1 | 2 | 2 | 7 |
| Kh | 7 | 5 | 1 | 1 | 2 | 2 | 1 | 7 |
| Kh | 7 | 0.2 | 1 | 1 | 3 | 1 | 1 | 7 |
| Kh | 7 | 0.1 | 1 | 1 | 3 | 1 | 1 | 7 |
| Drain conductance | N/A | 0.1 | 2 | 1 | 1 | 2 | 1 | 7 |
| GHB conductance | N/A | 100 | 1 | 1 | 1 | 1 | 3 | 7 |
| Recharge | N/A | 0.8 | 2 | 1 | 1 | 1 | 2 | 7 |
| Kv | 2 | 10 | 1 | 2 | 1 | 1 | 1 | 6 |
| Kv | 2 | 5 | 1 | 2 | 1 | 1 | 1 | 6 |
| Kh | 4 | 10 | 1 | 1 | 1 | 1 | 2 | 6 |
| Specific storage | 8 | 100 | 1 | 1 | 1 | 2 | 1 | 6 |
| Specific storage | 9 | 0.1 | 1 | 1 | 1 | 1 | 2 | 6 |
| GHB conductance | N/A | 10 | 1 | 1 | 1 | 1 | 2 | 6 |
| North GHB conductance | N/A | N/A | 1 | 1 | 1 | 1 | 2 | 6 |
| Evapotranspiration | N/A | 1.2 | 1 | 1 | 1 | 1 | 2 | 6 |
| Recharge | N/A | 0.9 | 1 | 1 | 1 | 1 | 2 | 6 |

GHB = general head boundary; Kh = horizontal hydraulic conductivity; Kv = vertical hydraulic conductivity; LTA = Lower Tamiami aquifer; MHA = Mid-Hawthorn aquifer; N/A = not applicable; SSA = Sandstone aquifer; WTA = Water Table aquifer.

Rank was assigned by sorting the four sensitivity categories, with “not sensitive” ranked as 1. Based on rank sum, among the parameters included in the sensitivity analysis, the LWCSIM was most sensitive to Kv for layer 2. A multiplier of 0.1 versus the base scenario effects an average of more than 1 ft in deviation from the base scenario (rank 4), in terms of MAE, for the SSA-clastic and SSA-carbonate. The LTA was moderately sensitive (rank 3). At least one model layer was sensitive (rank 4) or moderately sensitive (rank 3) to Kv for layers 1, 4, 5, 6, 7, and 8.

7.4 Results by Layer Parameter

This section describes model sensitivity by aquifer, which is summarized in **Table 7-5**. **Tables 7-6** to **7-10** provide further details for each aquifer.

Table 7-5. Summary of sensitive parameters by aquifer.

| Aquifer | Sensitive Parameters |
|--|---|
| Water Table aquifer (layer 1) | Slightly sensitive to hydraulic conductivity, drain-river leakance, and recharge |
| Lower Tamiami aquifer (layer 3) | Moderately sensitive to vertical hydraulic conductivity between layers 3 and 4 and to its own horizontal hydraulic conductivity |
| Sandstone aquifer – clastic zone (layer 5) | <ul style="list-style-type: none"> • Sensitive to vertical hydraulic conductivity between layers 2 and 3, between layers 4 and 5, and between layers 5 and 6. • Moderately sensitive (rank 3) to vertical hydraulic conductivity between layers 1 and 2 and between layers 4 and 5 • Moderately sensitive to horizontal hydraulic conductivity of layers 5 and 7 |
| Sandstone aquifer – carbonate zone (layer 7) | <ul style="list-style-type: none"> • Sensitive (rank 4) to vertical hydraulic conductivity between layers 2 and 3 and between layers 4 and 5 • Moderately sensitive (rank 3) to vertical hydraulic conductivity between layers 1 and 2 and between layers 4 and 5 |
| Mid-Hawthorn aquifer (layer 9) | <p>The aquifer is sensitive (rank 4) to:</p> <ul style="list-style-type: none"> • Vertical hydraulic conductivity between layers 5 and 6, layers 6 and 7, layers 7 and 8, and layers 8 and 9 • Its own horizontal hydraulic conductivity • Its own specific storage • The boundary condition conductance • River conductance |

Table 7-6. Significant sensitivity of the Water Table aquifer.

| Parameter | Layer | Multiplier | Rank |
|----------------|-------|------------|------|
| Kh | 1 | 5 | 2 |
| Kh | 1 | 0.2 | 2 |
| Kh | 1 | 0.1 | 2 |
| Kv | 1 | 0.1 | 2 |
| Specific yield | 1 | 0.5 | 2 |
| Specific yield | 1 | 0.25 | 2 |
| Kh | 3 | 10 | 2 |
| Kh | 3 | 5 | 2 |
| Kh | 5 | 10 | 2 |
| Kh | 6 | 10 | 2 |
| Kh | 6 | 5 | 2 |

| | | | |
|--------------------|-----|------|---|
| Drain conductance | N/A | 0.1 | 2 |
| River conductance | N/A | 0.1 | 2 |
| River conductance | N/A | 0.01 | 2 |
| Evapotranspiration | N/A | 0.8 | 2 |
| Recharge | N/A | 1.2 | 2 |
| Recharge | N/A | 0.8 | 2 |

Kh = horizontal hydraulic conductivity; Kv = vertical hydraulic conductivity; N/A = not applicable.

Table 7-7. Significant sensitivity of the Lower Tamiami aquifer.

| Parameter | Layer | Multiplier | Rank |
|--------------------|-------|------------|------|
| Kv | 2 | 0.1 | 3 |
| Kh | 3 | 10 | 3 |
| Kh | 1 | 5 | 2 |
| Kh | 1 | 0.2 | 2 |
| Kh | 1 | 0.1 | 2 |
| Kv | 1 | 0.2 | 2 |
| Kv | 1 | 0.1 | 2 |
| Specific yield | 1 | 0.25 | 2 |
| Kv | 2 | 10 | 2 |
| Kv | 2 | 5 | 2 |
| Kv | 2 | 0.2 | 2 |
| Kh | 3 | 5 | 2 |
| Kh | 3 | 0.2 | 2 |
| Kh | 3 | 0.1 | 2 |
| Drain conductance | N/A | 0.01 | 2 |
| River conductance | N/A | 100 | 2 |
| River conductance | N/A | 10 | 2 |
| River conductance | N/A | 0.01 | 2 |
| Evapotranspiration | N/A | 0.8 | 2 |
| Recharge | N/A | 1.2 | 2 |

Kh = horizontal hydraulic conductivity; Kv = vertical hydraulic conductivity; N/A = not applicable.

Table 7-8. Significant sensitivity of the Sandstone aquifer – clastic zone.

| Parameter | Layer | Multiplier | Rank |
|--------------------|-------|------------|------|
| Kv | 2 | 0.2 | 4 |
| Kv | 2 | 0.1 | 4 |
| Kv | 4 | 0.2 | 4 |
| Kv | 4 | 0.1 | 4 |
| Kh | 5 | 0.1 | 4 |
| Kv | 1 | 0.1 | 3 |
| Kv | 4 | 10 | 3 |
| Kv | 4 | 5 | 3 |
| Kh | 5 | 10 | 3 |
| Kh | 5 | 0.2 | 3 |
| Kh | 7 | 0.2 | 3 |
| Kh | 7 | 0.1 | 3 |
| Kh | 1 | 0.2 | 2 |
| Kh | 1 | 0.1 | 2 |
| Kv | 1 | 0.2 | 2 |
| Specific yield | 1 | 0.5 | 2 |
| Specific yield | 1 | 0.25 | 2 |
| Kh | 3 | 10 | 2 |
| Kh | 3 | 0.1 | 2 |
| Kh | 5 | 5 | 2 |
| Kh | 6 | 10 | 2 |
| Kh | 6 | 5 | 2 |
| Kv | 6 | 0.2 | 2 |
| Kv | 6 | 0.1 | 2 |
| Kh | 7 | 10 | 2 |
| Kh | 7 | 5 | 2 |
| Drain conductance | N/A | 0.01 | 2 |
| River conductance | N/A | 10 | 2 |
| River conductance | N/A | 0.1 | 2 |
| River conductance | N/A | 0.01 | 2 |
| Evapotranspiration | N/A | 0.8 | 2 |
| Recharge | N/A | 1.2 | 2 |

Kh = horizontal hydraulic conductivity; Kv = vertical hydraulic conductivity; N/A = not applicable.

Table 7-9. Significant sensitivity of the Sandstone aquifer – carbonate zone.

| Parameter | Layer | Multiplier | Rank |
|--------------------|-------|------------|------|
| Kv | 2 | 0.1 | 4 |
| Kv | 4 | 10 | 4 |
| Kv | 4 | 5 | 4 |
| Kv | 4 | 0.2 | 4 |
| Kv | 4 | 0.1 | 4 |
| Kv | 1 | 0.1 | 3 |
| Kh | 7 | 10 | 3 |
| Drain conductance | N/A | 0.01 | 3 |
| Kh | 1 | 5 | 2 |
| Kh | 1 | 0.2 | 2 |
| Kh | 1 | 0.1 | 2 |
| Kv | 1 | 0.2 | 2 |
| Kh | 2 | 10 | 2 |
| Kv | 2 | 0.2 | 2 |
| Kh | 3 | 10 | 2 |
| Kh | 3 | 0.2 | 2 |
| Kh | 3 | 0.1 | 2 |
| Kh | 5 | 10 | 2 |
| Kh | 5 | 5 | 2 |
| Kh | 5 | 0.1 | 2 |
| Kh | 6 | 10 | 2 |
| Kh | 6 | 5 | 2 |
| Kv | 6 | 10 | 2 |
| Kv | 6 | 5 | 2 |
| Kv | 6 | 0.1 | 2 |
| Kh | 7 | 5 | 2 |
| Specific storage | 8 | 100 | 2 |
| Kh | 9 | 10 | 2 |
| Kh | 9 | 5 | 2 |
| Kh | 9 | 0.1 | 2 |
| Drain conductance | N/A | 0.1 | 2 |
| River conductance | N/A | 100 | 2 |
| River conductance | N/A | 10 | 2 |
| River conductance | N/A | 0.1 | 2 |
| River conductance | N/A | 0.01 | 2 |
| Evapotranspiration | N/A | 0.8 | 2 |
| Recharge | N/A | 1.2 | 2 |

Kh = horizontal hydraulic conductivity; Kv = vertical hydraulic conductivity; N/A = not applicable.

Table 7-10. Significant sensitivity of the Mid-Hawthorn aquifer.

| Parameter | Layer | Multiplier | Rank |
|-----------------------|-------|------------|------|
| Kv | 5 | 0.2 | 4 |
| Kv | 5 | 0.1 | 4 |
| Kv | 6 | 0.2 | 4 |
| Kv | 6 | 0.1 | 4 |
| Kv | 7 | 10 | 4 |
| Kv | 7 | 5 | 4 |
| Kv | 7 | 0.2 | 4 |
| Kv | 7 | 0.1 | 4 |
| Kv | 8 | 10 | 4 |
| Kv | 8 | 5 | 4 |
| Kv | 8 | 0.2 | 4 |
| Kv | 8 | 0.1 | 4 |
| Kh | 9 | 10 | 4 |
| Kh | 9 | 5 | 4 |
| Kh | 9 | 0.2 | 4 |
| Kh | 9 | 0.1 | 4 |
| Specific storage | 9 | 100 | 4 |
| GHB conductance | N/A | 0.1 | 4 |
| GHB conductance | N/A | 0.01 | 4 |
| West GHB conductance | N/A | N/A | 4 |
| River conductance | N/A | 0.1 | 4 |
| River conductance | N/A | 0.01 | 4 |
| Kv | 5 | 10 | 3 |
| Kv | 5 | 5 | 3 |
| Kv | 6 | 10 | 3 |
| GHB conductance | N/A | 100 | 3 |
| Kh | 1 | 5 | 2 |
| Kh | 1 | 0.2 | 2 |
| Kh | 1 | 0.1 | 2 |
| Specific yield | 1 | 0.25 | 2 |
| Kh | 2 | 10 | 2 |
| Kh | 3 | 10 | 2 |
| Kh | 4 | 10 | 2 |
| Kv | 6 | 5 | 2 |
| Specific storage | 9 | 0.1 | 2 |
| GHB conductance | N/A | 10 | 2 |
| North GHB conductance | N/A | N/A | 2 |
| River conductance | N/A | 100 | 2 |
| River conductance | N/A | 10 | 2 |
| Evapotranspiration | N/A | 1.2 | 2 |
| Evapotranspiration | N/A | 0.8 | 2 |
| Recharge | N/A | 0.9 | 2 |
| Recharge | N/A | 0.8 | 2 |

GHB = general head boundary; Kh = horizontal hydraulic conductivity; Kv = vertical hydraulic conductivity; N/A = not applicable.

7.4.1 Stresses and Related Variables

The sensitivity scenarios included scaling back ET and recharge by factors of 0.8, 0.9, 1.1, and 1.2 versus the calibrated model. Four runs scaled ET and four runs scaled recharge. **Table 7-11** presents the sensitivity results for the ET and recharge scenarios that exhibited at least slight sensitivity (rank 2). Of the ET scenarios, only 0.8- and 1.2-scaled runs exhibited slight model sensitivity, and only the 0.8-scaled run exhibited sensitivity in all aquifers. Extinction depth also was varied in four scenarios by the same scale factors; however, none of the scenarios exhibited even slight sensitivity (rank 2). Model sensitivity to gross recharge was slight (rank 2) for all aquifers. Gross recharge is the recharge input provided to MODFLOW and should not be confused with net recharge, which is the combined effect of gross recharge and ET.

Table 7-11. Significant sensitivity to stresses.

| Parameter | Multiplier | Aquifer Rank | | | | | Rank Sum |
|--------------------|------------|--------------|-----|-------------|---------------|-----|----------|
| | | WTA | LTA | SSA-clastic | SSA-carbonate | MHA | |
| Evapotranspiration | 0.8 | 2 | 2 | 2 | 2 | 2 | 10 |
| Evapotranspiration | 1.2 | 1 | 1 | 1 | 1 | 2 | 6 |
| Recharge | 1.2 | 2 | 2 | 2 | 2 | 1 | 9 |
| Recharge | 0.9 | 1 | 1 | 1 | 1 | 2 | 6 |
| Recharge | 0.8 | 2 | 1 | 1 | 1 | 2 | 7 |

LTA = Lower Tamiami aquifer; MHA = Mid-Hawthorn aquifer; SSA = Sandstone aquifer; WTA = Water Table aquifer.

7.4.2 Conclusion of the Sensitivity Analysis

The model appeared reasonably calibrated; any change decreased model performance. The results from the global model sensitivity analysis showed that model-wide changes to any considered parameter did not improve the overall model calibration. Modifying the most sensitive parameters generally resulted in a net degradation of model performance. The sole exception (aside from perhaps miniscule improvements), discussed above (layer 6 Kh of 0.2× that of the calibrated model) results in the range of relative MAE extending upwards nearly 2 ft in the WTA.

The calibration run was superior when considering the MAE across the model domain. While there may be instances where a sensitivity run might appear superior to the calibration run for one or more parameters at the local scale, or even for one or a few aquifers, this comes at the expense of poorer performance elsewhere.

8 MODEL LIMITATIONS

Overall, the transient groundwater flow model reasonably simulates regional hydrologic conditions across the model domain. Simulated potentiometric surfaces are in good visual agreement with regional potentiometric surface maps. Residual statistics also demonstrate good agreement between observed and simulated water levels.

Although the LWCSIM adequately represents the groundwater flow patterns and fluxes within the model domain, there are a few areas where model residual head errors are significant, particularly in the Cape Coral area of model layer 9. Localized head changes near some major wellfields were difficult to simulate given the regional nature of the application. Furthermore, although the model generally reproduces temporal water level trends at most monitor wells, there are significant differences between observed and simulated temporal water level response at specific wells. These differences are not unexpected given the use of aquifer parameter zones during calibration and the limitations of available pumpage and hydrogeologic

data. In these instances, qualitative and quantitative calibration criteria were balanced to achieve the best overall calibration. Despite these differences, the calibrated model reasonably simulates the regional and three-dimensional hydrogeologic features of the model domain.

Potential users of the LWCSIM should note because of recognized data limitations, model simulation is more appropriate at sub-regional and regional scales rather than very local or site-specific scales for simulation of hydrologic conditions. Grid cell sizes are a uniform 1,000 ft. Any simulation results at a scale of a few hundred feet would be problematic unless a finer grid discretization is used. The conceptual model used to construct the model is a simplified representation of the true groundwater flow system. The SAS and IAS in the LWC Planning Area can be characterized as a complex, heterogeneous aquifer system.

Various model parameters and boundary conditions were determined based on land use distribution, configuration of waterways and other surface water bodies, and climatic conditions during the calibration period. If any of these factors were to significantly change, parameters such as recharge, ET, and river conductance may need to be modified.

9 RECOMMENDATIONS FOR FUTURE DATA COLLECTION

9.1 Water Use Data

Currently, the SFWMD has a good data reporting system in place for PS water use. For a variety of reasons, the reported water use data for AG, L/R, and DSS are less reliable. Therefore, modelers use various tools to estimate water use from each category and eventually use those as model calibration parameters. Better data for these water use categories would result in greater confidence in model calibration to support water supply planning efforts.

9.2 Water Level (Head) Data

The assessment of model performance is based on available data. At many stations where data are available, there are months with no data points, which makes it difficult, and sometimes impossible, to assess model performance at a local scale or over short time periods (e.g., a single dry season). It probably is more valuable to have a moderately accurate measure of mean head over a time interval than to have a highly accurate measure at one instant. One recommendation is to collect groundwater data at more locations, especially in places that are well connected to withdrawal areas and are far away from areas where data already are collected. In addition, it may be more valuable to collect more groundwater data during times of extreme water levels and less during the transitions between extremes. Again, better data to support model calibration, especially during extreme events, result in greater confidence in the model's predictive capabilities.

9.3 Hydraulic Conductivity Data

In general, there is a good coverage of field data for all the aquifers to determine hydraulic properties, especially where the aquifers are heavily used. However, where the aquifers are not heavily used, there is a scarcity of field data, especially in the SSA and MHA. It is essential to characterize system hydraulic properties as accurately as possible when building a regional groundwater model. Due to the complex heterogeneity of the subsurface system, interpolating hydraulic properties from known areas to areas where the field measurements are not available can introduce significant errors in the model. Therefore, it is recommended that additional wells be installed and aquifer tests be conducted in the SSA and MHA of the LWC Planning Area.

LITERATURE CITED

- Anderson, M. and W. Woessner. 1992. *Applied Groundwater Modeling*. Academic Press, San Diego, CA.
- ART Engineering, LLC. 2004. *Lake Trafford Critical Restoration Project – AquaScan Radar Survey Report*. Tampa, FL.
- Atkins. 2011. *Collier County Watershed Management Plan. Final Report, Volume 4A: Technical Report Assessment of Existing Conditions and Performance Measures*. Prepared for Collier County.
- Bandara, U.C. 2018. Development and verification of a numerical model to simulate evapotranspiration and recharge for regional scale groundwater models. Florida Water Resource Conference, April 15-18, 2018, Daytona Beach, FL.
- Beach, M. and J. Hood. 2003. Conversion of observed water levels to equivalent freshwater heads to establish and monitor the minimum aquifer level of the ETB MIA. Southwest Florida Water Management District internal memo.
- Bennett, M.W. 2004. Hydrogeologic investigation of the Floridan aquifer system, Big Cypress Preserve Collier County, Florida. Technical Publication WS-18. South Florida Water Management District, West Palm Beach, FL.
- Brown, C. 2013. Reference evapotranspiration (1948 – 2013) using 51-year hydrological reanalysis and North American regional reanalysis. South Florida Water Management District, West Palm Beach, FL.
- Brown, C. 2014. QA/QC of NEXRAD rainfall (2001 – 2012). South Florida Water Management District, West Palm Beach, FL.
- Bryan, J., R. Green, and G. Means. 2013. *An illustrated guide to the identification of hydrogeologically important formations in the South Florida Water Management District*. South Florida Water Management District, West Palm Beach, FL.
- Central Florida Water Initiative Hydrologic Analysis Team. 2020. *Model Documentation Report for the East-Central Florida Transient Expanded (ECFTX) Model*. 275 pp. + app.
- Chebud, Y. and A. Melesse. 2011. Operational prediction of groundwater fluctuation in South Florida using sequence based Markovian stochastic model. *Water Resources Management* 25:2,279-2,294.
- Copp, R.A. 2015. *Lehigh Acres groundwater model notes*. A.D.A. Engineering, Inc.
- Cunge, J.A. 1969. On the Subject of a Flood Propagation Computation Method (Muskingum Method). *Journal of Hydraulic Research* 7(2):205-230.
- DHI Water and Environment. 2002. *Big Cypress Basin Integrated Hydrologic-Hydraulic Model. Final report*. Prepared for the South Florida Water Management District, West Palm Beach, FL.
- Doherty, J. 2010. *PEST: Model-independent Parameter Estimation User's Manual*. 5th edition. Watermark Numerical Computing.

- Doherty, J. and R. Hunt. 2010. Approaches to highly parameterized inversion: A guide to using PEST for groundwater-model calibration. United States Geological Survey Scientific Investigations Report 2010-5169.
- Doherty, J., M. Fienen, and R. Hunt. 2010. Approaches to highly parameterized inversion: Pilot-point theory, guidelines, and research directions. United States Geological Survey Scientific Investigations Report 2010-5168.
- Environmental Simulations, Inc. 2014. Development and calibration of the District Wide Regulation Model (DWRM), Version 3, for the Southwest Florida Water Management District.
- Franke, O.L., T.E. Reilly, and G.D. Bennett. 1987. Chapter B5: Definition of boundary and initial conditions in the analysis of saturated ground-water flow systems – An introduction. In: U.S. Survey Techniques of Water-Resources Investigations of the United States Geological Survey.
- Geddes, E., E. Richardson, and A. Dodd. 2015. Hydrogeologic mapping update for the Lower West Coast water supply planning area. Technical Publication WS-35. South Florida Water Management District, West Palm Beach, FL.
- Giddings, J., L. Kuebler, J. Restrepo, K. Rodberg, A. Montoya, and H. Radin. 2006. Lower West Coast Subregional (LECsR) MODFLOW Model Documentation. South Florida Water Management District, West Palm Beach, FL.
- Goudenhoofd, E. and L. Delobbe. 2009. Evaluation of radar-gauge merging methods for quantitative precipitation estimates. *Hydrology and Earth System Sciences* 13(2):195-203.
- Harbaugh, A.W. 2005. MODFLOW-2005, the U.S. Geological Survey modular ground-water model – the ground-water flow process. United States Geological Survey Techniques and Methods 6-A16.
- Harvey, J.W., S.L. Krupa, and J.M. Krest. 2006. Ground water recharge and discharge in the Central Everglades. *Groundwater* 42(7):1,090-1,102.
- Helsel, D.R. and R.M. Hirsch. 1992. *Statistical Methods in Water Resources*. Studies in Environmental Science 49. 522 pp.
- Heimstra, P.H., E.J. Pebesma, C.J.W. Twenhöfel, and G.B.M. Heuvelink. 2009. Real-time automatic interpolation of ambient gamma dose rates from the Dutch radioactivity monitoring network. *Computers & Geosciences* 35(8):1,711-1,721.
- Hunt, R.J., J. Luchette, W.A. Schreuder, J.O. Rumbaugh, J. Doherty, M.J. Tonkin, and D.B. Rumbaugh. 2010. Using a cloud to replenish parched groundwater modeling efforts. *Groundwater* 48(3):360-365.
- Jensen, M.E., R.D. Burman, and R.G. Allen (eds). 1990. *Evapotranspiration and Irrigation Water Requirements*. Manuals and Reports on Engineering Practice No. 70. American Society of Civil Engineers, New York, NY. ISBN 0-87262-763-2. 360 pp.
- Luszczynski, N. 1961. Head and flow of ground water of variable density. *Journal of Geophysical Research* 66:4,247-4,256.

- Maechler, M., P. Rousseeuw, A. Struyf, M. Hubert, and K. Hornik. 2018. Cluster: Cluster Analysis Basics and Extensions. R package version 2.0.7-1.
- Marco Water Engineering, Inc. 2006. Lower West Coast Surficial Aquifer System Model Report.
- McDonald, M. and A. Harbaugh. 1988. A modular, three-dimensional finite-difference groundwater flow model. Techniques of Water Resources Investigations of the United States Geological Survey.
- Müllner, D. 2013. Fastcluster: Fast hierarchical, agglomerative clustering routines for R and Python. *Journal of Statistical Software* 53(9):1-18.
- National Oceanic and Atmospheric Administration. 2015. NOAA Tidal Stations. <http://tidesandcurrents.noaa.gov>.
- R Development Core Team. 2018. R: A language and environment for statistical computing. R Foundation for Statistical Computing, Vienna, Austria. ISBN 3-900051-07-0.
- Reilly, T.E. 2001. Chapter B8: System and boundary conceptualization in ground-water flow simulation. In: U.S. Survey Techniques of Water-Resources Investigations of the United States Geological Survey.
- Reilly, T.E. and A.W. Harbaugh. 2004. Guidelines for evaluating ground-water flow models. United States Geological Survey. 30 pp.
- Restrepo, J.I. and J.B. Giddings. 1994. Physical based methods to estimate ET and recharge rates using GIS. In: Effects of Human-Induced Changes on Hydrologic Systems, American Water Resources Association, Bethesda, MD.
- Restrepo, J., A. Montoya, and J. Obeysekera. 1998. A wetland simulation module for the MODFLOW ground water model. *Groundwater* 36(5):764-770.
- Scott, T. 1988. The lithostratigraphy of the Hawthorn Group (Miocene) of Florida. Bulletin 59. Florida Geological Survey, Tallahassee, FL.
- Scott, T. 2001. Text to accompany the geologic map of Florida. Florida Geological Survey, Tallahassee, FL.
- Shah, N., M. Nachabe, and M. Ross. 2007. Extinction depth and evapotranspiration from groundwater under land covers. *Groundwater* 45(3):329-338.
- Shoemaker, W.B., C.D. Lopez, and M.J. Duever. 2011. Evapotranspiration over spatially extensive plant communities in the Big Cypress National Preserve, southern Florida, 2007–2010. United States Geological Survey Scientific Investigations Report 2011-5212. 46 pp.
- Smajstrla, A. 1990. User's Guide: Agricultural Field Scale Irrigation Requirements Simulation (AFSIRS) Model. University of Florida.
- Smith, B. and S. Rodriguez. 2017. Spatial analysis of high-resolution radar rainfall and citizen-reported flash flood data in ultra-urban New York City. *Water* 9(736). 17 pp.
- Soil Conservation Service. 1989. Runoff curve number computations. Engineering Hydrology Training Series Module 104. United States Department of Agriculture.

- South Florida Water Management District. 2004. Caloosahatchee River Basin Integrated Surface Water - Groundwater Model. Version 11. West Palm Beach, FL.
- South Florida Water Management District. 2009. 2009 SFWMD Photointerpretation Key. West Palm Beach, FL. Available at: https://www.sfwmd.gov/sites/default/files/documents/2009_pi-key.pdf.
- South Florida Water Management District. 2012. 2012 Lower West Coast Water Supply Plan Update. West Palm Beach, FL.
- South Florida Water Management District. 2014. Merged isochlor. Version 1.2. West Palm Beach, FL.
- South Florida Water Management District. 2017. 2017 Lower West Coast Water Supply Plan Update. West Palm Beach, FL.
- Steiner, M., J.A. Smith, S.J. Burges, C.V. Alonso, and R.W. Darden. 1999. Effect of bias adjustments and rain gauge data quality control on radar rainfall estimation. *Water Resources Research* 35(8):2,487-2,503.
- Sutherland. 2000. Methods for estimating effective impervious cover. *The Practice of Watershed Protection Article 32*. Center for Watershed Protection, Ellicott City, MD.
- United States Army Corps of Engineers. 1957. Central and Southern Florida Project, Part IV, Lake Okeechobee and Outlets Supplement 6 – General Design Memorandum, Caloosahatchee River and Control Structures (Canal 43, and Lock and Spillway Structures 77, 78, and 79). April 24, 1975. Jacksonville, FL.
- United States Army Corps of Engineers. 1961. Central and Southern Florida Project, Part IV, Lake Okeechobee and Outlets Supplement 15 – Detail Design Memorandum, Canal 43, Section 2 (Caloosahatchee River). August 4, 1961. Jacksonville, FL.
- United States Army Corps of Engineers. 1962. Central and Southern Florida Project, Part IV, Lake Okeechobee and Outlets Supplement 17 – Detail Design Memorandum Canal 43, Section 4 and 5 (Caloosahatchee River). August 22, 1962. Jacksonville, FL.
- United States Army Corps of Engineers. 1969. Central and Southern Florida Project, Part IV, Lake Okeechobee and Outlets Supplement 23 – Detail Design Memorandum Canal 43, Section 4 and 5 (Caloosahatchee River). September 9, 1969. Jacksonville, FL.
- URS. 2008. WaSh (Watershed Quality Model) User's Manual. Prepared for the South Florida Water Management District, West Palm Beach, FL. URS, Tallahassee, FL.
- United States Department of Agriculture. 1986. Urban Hydrology for Small Watersheds. Technical Release 55. Natural Resources Conservation Service, Conservation Engineering Division. Washington, D.C.
- White, W.A. 1970. The Geomorphology of the Florida Peninsula. Florida Bureau of Geology Bulletin No. 51. 164 pp.

APPENDICES

**APPENDIX A:
NEXRAD CORRECTION**

INTRODUCTION

Rainfall plays a prominent role in the development and application of hydrologic models and water budgets. Traditionally, rain gauges have been used to measure and estimate the rainfall input needed for hydrologic models and water budgets. However, errors associated with rain gauge measurements limit their use and increase the uncertainties in the results (Habib et al. 2009, Skinner et al. 2009, Craciun and Catrina 2016). In addition, estimating rainfall over large areas requires maintaining a large network of rain gauge stations, which can be costly and limited by accessibility to remote station locations. Advances in radar technology and continuous improvement in rainfall volume detection and estimation have made radar-derived rainfall data useful for hydrologic applications (Habib et al. 2007, 2009; Skinner et al. 2009; Craciun and Catrina 2016).

In the early 1990s, the National Weather Service established the Next-Generation Weather Radar (NEXRAD) system (approximately 160 ground-based radar stations) across the United States, including five stations in Florida (Habib et al. 2009, Skinner et al. 2009). Unlike rain gauge networks, NEXRAD can estimate rainfall over a large area by providing a better representation of rainfall distribution (Skinner et al. 2009). However, there are multiple forms of error associated with radar-derived data, including systematic bias, random error, and temporal and spatial radar error (Habib et al. 2007). These, errors greatly affect the accuracy of rainfall estimates; therefore, in most cases, evaluation and correction of radar data are needed to reduce uncertainties. Comparisons of rain gauge and radar estimates indicate radar tends to overestimate small rain volumes and underestimate large rain volumes (Over et al. 2007, Hardegree et al. 2008, Skinner et al. 2009).

Improvement of radar-derived data can be achieved by correcting for inherent bias using adjustment factors; however, systematic deviations in radar data from reference surface rainfall (rain gauges) can remain after correction (Habib et al. 2007). Several approaches for correcting NEXRAD data have been investigated and implemented successfully depending on period, resolution, and area of interest (Chumchean et al. 2006, Hanchoo Wong et al. 2012, Vernimmen et al. 2012, Smith and Rodriguez 2017).

The South Florida Water Management District (SFWMD) uses NEXRAD products in the development of water budgets and application of hydrologic models. However, there are concerns about the accuracy of the NEXRAD rainfall data, which is a key component in these model applications (Beeson et al. 2011). Multiple evaluations have been completed to address these concerns (Skinner et al. 2009, Brown 2014, Trimble 2018).

The objectives of this study were to 1) evaluate the relationship between rain gauge and NEXRAD rainfall estimates during a 16-year period (1999 to 2014) in the Lower West Coast (LWC) Planning Area of South Florida; 2) determine the amount of error in the NEXRAD data set; and 3) develop a simple systematic approach for correcting daily NEXRAD rainfall using adjustment factors derived from the bias between rain gauge and NEXRAD rainfall. In this study, rain gauges were assumed to offer a better representation of rainfall accumulation than NEXRAD at specific locations because they are direct measurements. Therefore, rain gauges were used as a ground truth for rainfall despite the presumed inaccuracies and limitations of the rain gauge data set.

METHODS

Study Area

The LWC Planning Area encompasses approximately 5,130 square miles in the southwestern region of Florida between the Gulf of Mexico and the western edge of the Everglades, extending north to the Southwest Florida Water Management District jurisdictional boundary and south to include portions of Everglades National Park (**Figure A-1**). The LWC Planning Area average elevation is approximately 16 feet National Geodetic Vertical Datum of 1929 (NGVD29), with elevations ranging from slightly above sea level to as high as 65 feet NGVD29 (SFWMD 2017). Most rainfall in the LWC Planning Area occurs during the wet season, which normally is from June through September; the remaining months typically are considered dry months. The amount of rain varies on a monthly and yearly basis and is greatly affected by climatic disturbances such as regional droughts, seasonal storm events, and hurricanes. In addition, rainfall can vary spatially depending on the geographic features of the area. Rainfall estimates in the LWC Planning Area were derived using the extensive rain gauge network maintained by the SFWMD (**Figure A-1**) and/or using NEXRAD.

Rain Gauge and NEXRAD Data

Rainfall data in the LWC Planning Area are collected by a network of rain gauges maintained by the SFWMD. The number of active rain gauges varied from 65 to 82 gauges during the study period (1999 to 2014). During the study period, the SFWMD operated four rain gauge recording types: tipping buckets, weighing buckets, float-type, and simple standard. Long-term variability in the number of available rain gauges was due to optimization of the monitoring network, while short-term changes likely were associated with equipment maintenance and/or malfunction. Therefore, missing data values are common over time. A comprehensive quality assurance and quality control (QA/QC) process was conducted by the SFWMD to address possible data problems before data were loaded into the agency's DBHYDRO database. In addition, rain gauge data quality and accuracy can be affected by wind speed, canopy coverage, and physical obstructions that may be difficult to discern during the QA/QC process. However, a 2014 QA/QC evaluation indicated rain gauge measurement data better represents rainfall amounts at co-located rain gauge and NEXRAD pixels (Brown 2014). Daily rain gauge values generally are the result of daily sum values; therefore, finer time resolution may be available at some rain gauge stations

The SFWMD acquires NEXRAD data as part of an agreement with a private vendor, who provides data to all five water management districts within the State of Florida. NEXRAD data are obtained in near real time at 15-minute intervals, which is aggregated into hourly and daily values. Prior to delivery, the near-real-time data are adjusted by the vendor using selected rain gauge data, which are incorporated into the algorithm computation (Brown 2014) and used to validate and calibrate real-time radar rainfall data (Craciun and Catrina 2016). NEXRAD data are delivered to the SFWMD in a 2×2 -kilometer grid format that includes a 35-mile buffer around the SFWMD's boundary; however, database queries only provide access to pixel data within the SFWMD's jurisdictional boundary. Each 2×2 -kilometer grid is equivalent to 1 pixel, which is identified by a unique pixel identification number in DBHYDRO (**Figure A-2**). For this study, a grid of 4,763 pixels covering the entire LWC Planning Area was used. All rain gauge and NEXRAD data used in this evaluation were obtained from DBHYDRO.



Figure A-1. Rain gauge stations within the Lower West Coast Planning Area.

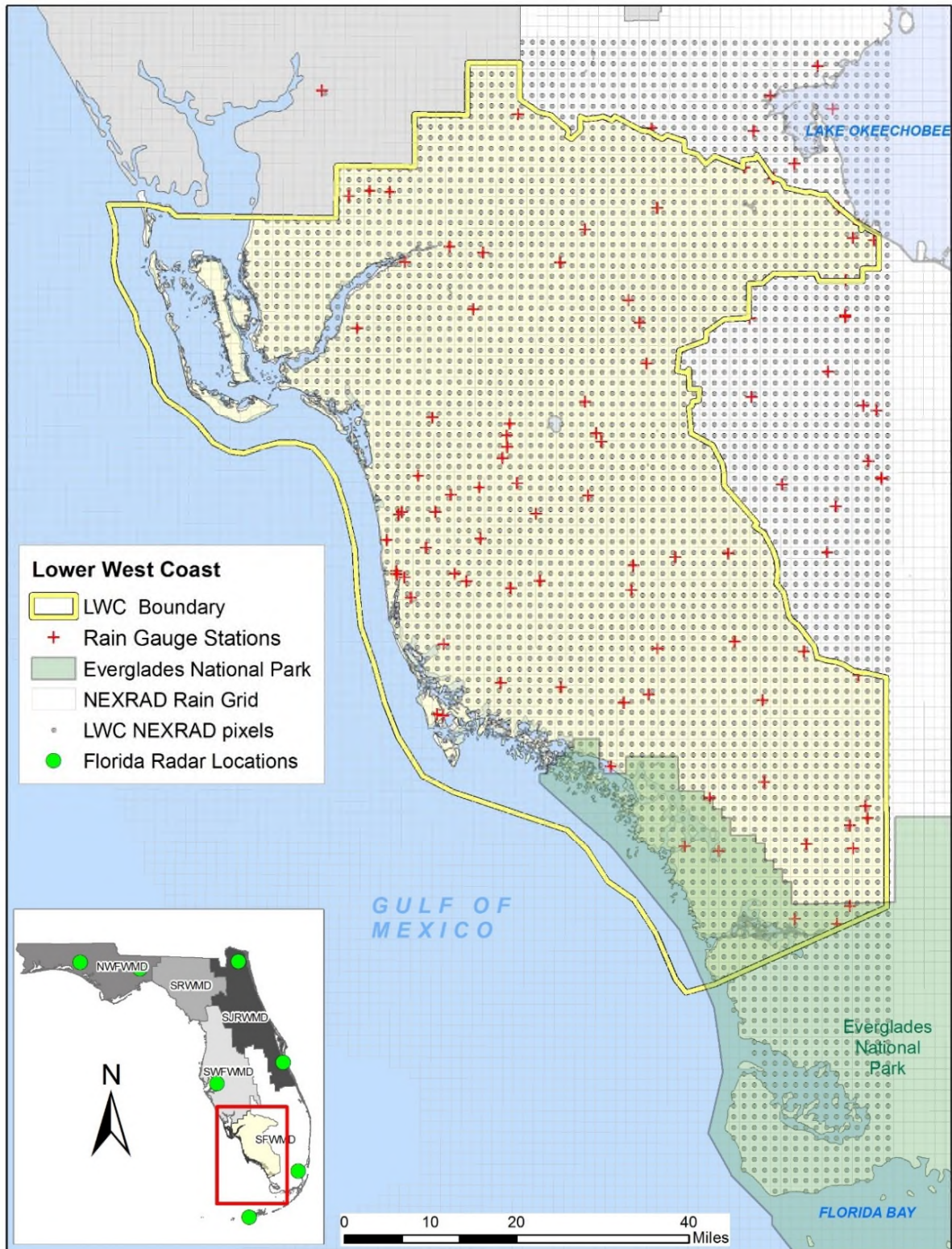


Figure A-2. Florida radar locations and the Next-Generation Weather Radar (NEXRAD) rain grid along with corresponding pixels in reference to rain gauge stations in the Lower West Coast Planning Area.

Statistical and Spatial Methods

Each rain gauge and associated 2 × 2-kilometer pixel were compared on a daily, monthly, and yearly basis from 1999 to 2014. Mean rainfall volume difference for monthly and yearly totals was calculated as follows:

$$RD = \overline{NRD}_i - \overline{RG}_i \quad (1)$$

Where RD is the mean rainfall difference, and NRD_i and RG_i represent the mean rainfall estimated by NEXRAD and recorded by the rain gauge, respectively. The relative bias between the monthly and yearly recorded rain gauge and estimated NEXRAD rainfall totals was calculated as follows:

$$Relative\ bias = \frac{\sum NRD_i - \sum RG_i}{\sum RG_i} \times 100 \quad (2)$$

Linear regression of yearly, monthly, and daily rain gauge and NEXRAD rainfall totals was performed to evaluate the overall relationship between the variables. Furthermore, the Kolmogorov-Smirnov statistical test for normality showed a marked positive skew of the daily values, indicating a considerable number of small values near or equal to zero; this observation was not surprising because it does not rain every day. Therefore, the relationship between NEXRAD data and individual rain gauges was evaluated using Kendall's tau (τ) rank-based correlation method (Helsel and Hirsch 1992). Monthly correlation for each rain gauge and NEXRAD pixel pair was calculated using daily values ($n \geq 14$), and correlation coefficients were used to discern which rain gauges displayed a good relationship ($\tau \geq 0.75$) with the NEXRAD pixels. Rain gauges showing a poor relationship with the NEXRAD pixels were excluded from further analysis. Yearly and monthly rain gauge and NEXRAD totals were calculated. The bias between the rain gauge and NEXRAD was determined by the ratio between the two (Steiner et al. 1999, Goudenhoofdt and Delobbe 2009, Smith and Rodriguez 2017). The resulting value was used as the NEXRAD adjustment factor, calculated as follows:

$$AdjF(bias) = \sum \frac{RG_i}{n_1} / \sum \frac{NRD_i}{n_1} \quad (3)$$

Where $AdjF$ is the multiplicative factor used to adjust the daily NEXRAD value, and RG_i and NRD_i are the monthly rainfall recorded by the rain gauge and estimated by NEXRAD, respectively, during an equally match-paired number of days ($n \geq 14$). To prevent overcorrection of NEXRAD daily values and to include most adjustment factors, the adjustment factor was arbitrarily capped at not greater than three. Therefore, daily NEXRAD values with adjustments factors greater than three received a maximum adjustment factor of three. Visual examination of the resulting bias showed several rain gauges located less than 2 kilometers from each other, which can produce inconsistencies in the bias arising from high and low values in spatially close stations. Therefore, the resulting monthly bias value at each rain gauge station was normalized using a complete hierarchical cluster analysis (Müllner 2013, Mächler et al. 2018), in which bias points were the result of the averaged bias of each rain gauge located within 2 kilometers of each other. The resulting monthly bias was used as the multiplicative adjustment factor to correct the daily NEXRAD pixel value using geostatistical processes.

Adjustment factors were interpolated across the NEXRAD grid using the automated autoKriging method described by Hiemstra et al. (2009). The autoKriging function tests different interpolation models (linear, spherical, exponential, Gaussian, and Matern) by estimating semi-variograms and selecting the best fit kriging model (Hiemstra et al. 2009). This process produced a monthly bias grid with adjustment factors at each NEXRAD pixel; these adjustment factors were applied to the uncorrected NEXRAD values to produce corrected NEXRAD values. Point values for the bias and the uncorrected and corrected NEXRAD were converted into a raster for visual evaluation. During this process, a few inconsistencies associated with the

NEXRAD and rain gauge pairing were observed in the corrected NEXRAD raster. These inconsistencies resulted from mismatched NEXRAD and rain gauge daily values. The data were examined and removed from daily values. Subsequently, the entire process described above was repeated and a new set of raster plots was created. The difference or change in rain was calculated by subtracting the corrected from the uncorrected NEXRAD, and the results were displayed in a separate raster. All statistical and spatial data analyses were performed using R programming language (version 3.5.1; R Development Core Team 2018).

Previous analysis of the NEXRAD data set reported missing rainfall for April 2001 (Brown 2014). To maintain a continuous record, the missing rainfall data were produced using the methods described in the documentation for the South Florida Water Management Model version 5.5 (SFWMD 2005).

RESULTS

Comparison of Rain Gauge and Uncorrected NEXRAD

Rain gauge and estimated NEXRAD monthly average rainfall for the LWC Planning Area from 1999 to 2014 followed similar trends, with slight differences in magnitude associated with periods of higher rainfall volumes (**Figure A-3a**). Yearly comparisons of monthly averages for rain gauge and estimated NEXRAD rainfall showed marked differences in values reported from 2002 through 2004 (**Figure A-3b**). The mean rainfall volume difference between the rain gauge and NEXRAD monthly totals showed a large underestimation of rainfall by NEXRAD from 2002 to 2004; this trend was less noticeable but consistent through 2007. While 2008 and 2009 showed a consistent overestimation of NEXRAD monthly rainfall totals (**Figure A-4**), subsequent years showed greater agreement between the rain gauge and NEXRAD monthly totals.

Scatter plots comparing daily, monthly, and yearly rainfall totals between the rain gauges and associated uncorrected NEXRAD pixels indicated a better fit or higher relationship of the data using monthly totals (**Figure A-5**). The monthly coefficient of determination (denoted by R^2) obtained from the linear regression for the entire period was greater than the yearly and daily coefficients. Further comparison of regression coefficients calculated from the daily, monthly, and yearly totals confirmed that monthly relationships were considerably better than yearly and daily relationships for all years. However, the daily relationships between rain gauge and NEXRAD data improved from 2007 through 2014 (**Table A-1**). Monthly totals were determined to be more appropriate in the calculation of bias between the rain gauge and corresponding NEXRAD pixel. In addition, monthly bias was expected to be suitable to capture seasonal changes and climate disturbances such as droughts and storm events through the years. To ensure appropriate adjustment of the daily rainfall NEXRAD values, the calculated bias was restricted using correlation coefficients ($\tau \geq 0.75$) derived from the monthly rain gauge and NEXRAD relationship. The restriction was based on the potential for using inaccurately paired rain gauge and NEXRAD values to calculate the bias due to inherent errors that exist in both methods. Therefore, after the correlation restriction, the number of rain gauge stations and associated bias used for the NEXRAD correction was reduced by 32% from 1999 to 2014. Excluding these rain gauge stations during the spatial interpolation reduced the potential transfer of errors across the entire area. In addition, higher correlations on paired rain gauge and NEXRAD values may be the result of prior adjustment to the NEXRAD data by the vendor when incorporating rain gauge data into the algorithm calculation.

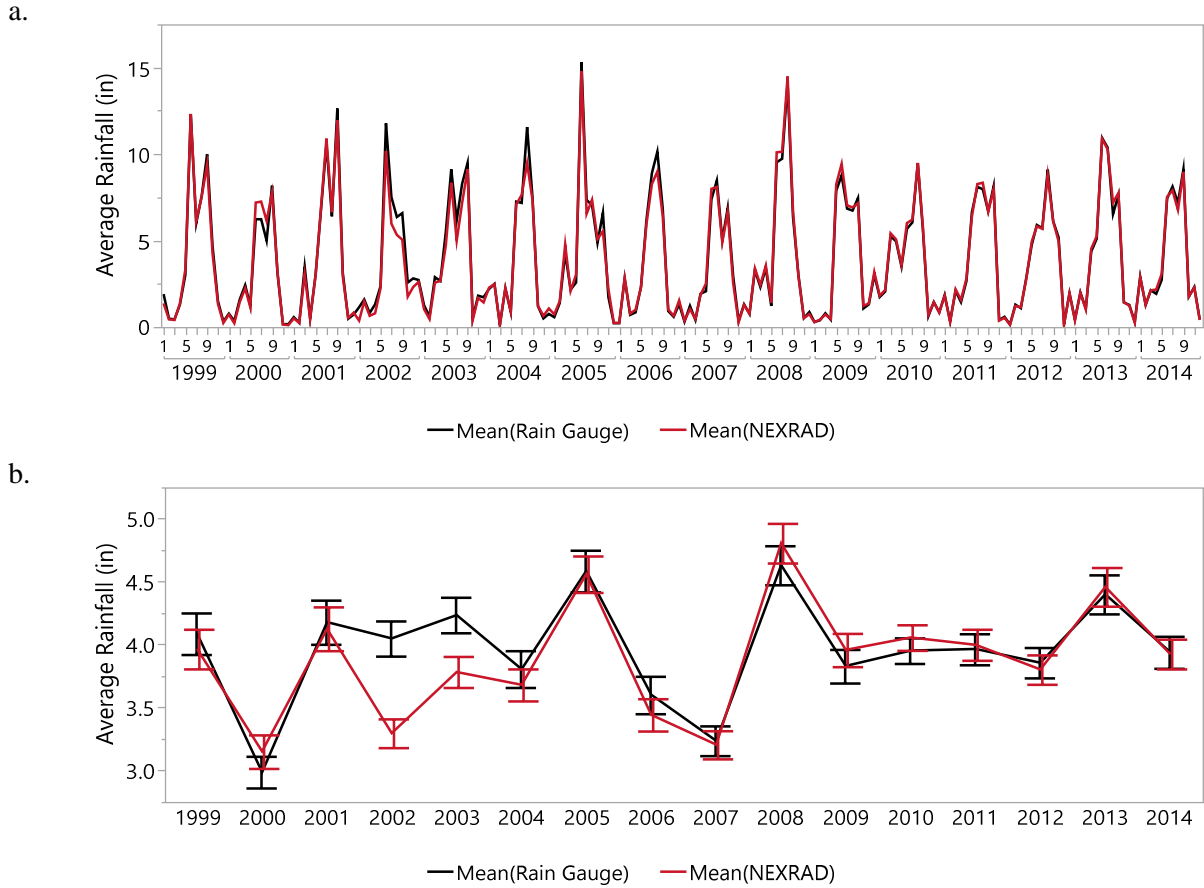


Figure A-3. Comparison of monthly average rainfall in the Lower West Coast Planning Area from rain gauges and Next-Generation Weather Radar (NEXRAD) values for (a) continuous period and (b) yearly average.

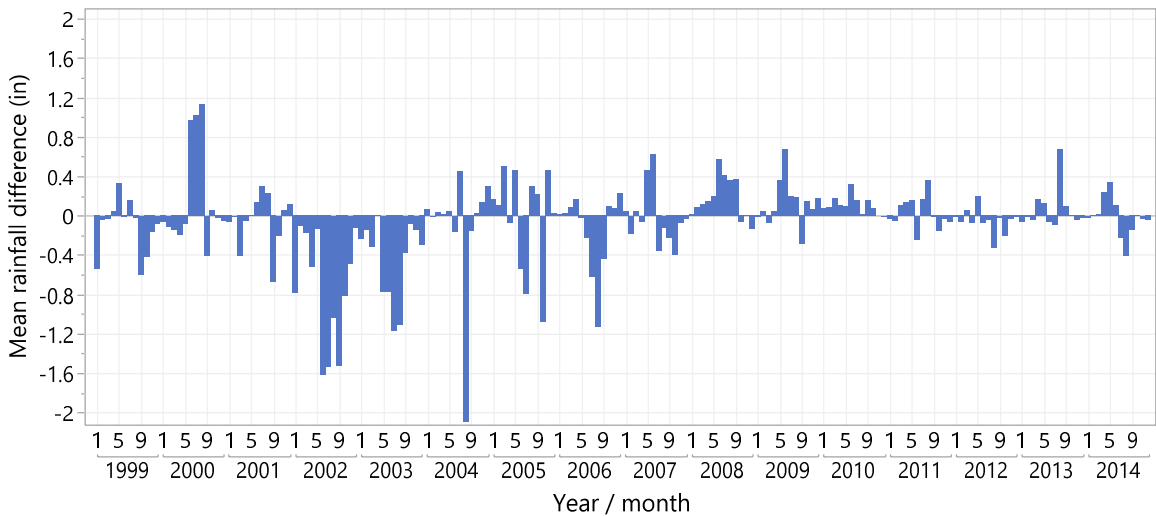


Figure A-4. Mean rainfall difference between Next-Generation Weather Radar (NEXRAD) and rain gauge data for monthly totals in the Lower West Coast Planning Area. Negative values indicate rainfall underestimation, while positive values represent periods of overestimation of rainfall.

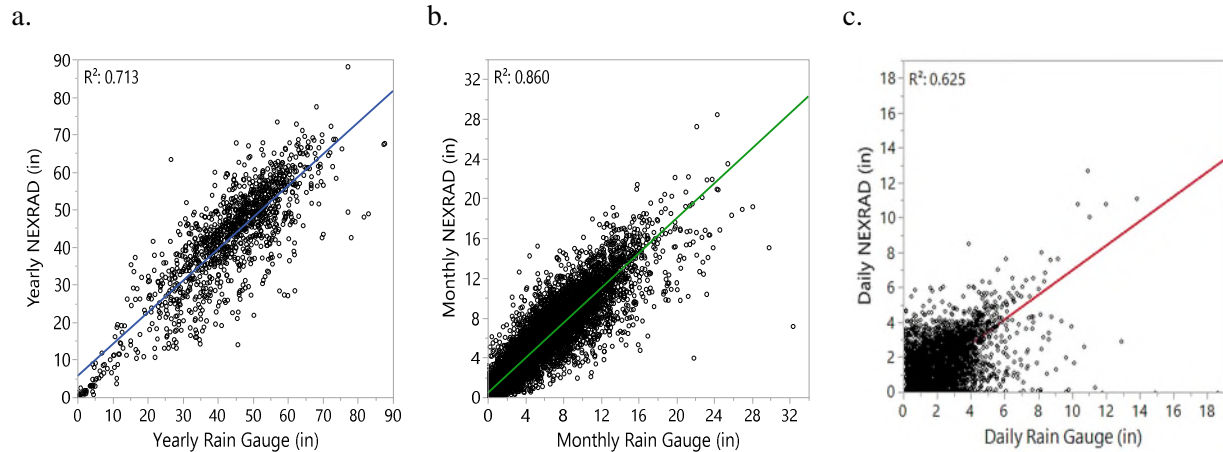


Figure A-5. Scatter plots comparing all paired rain gauge and estimated uncorrected Next-Generation Weather Radar (NEXRAD) for (a) yearly, (b) monthly, and (c) daily rainfall totals, in inches, from 1999 to 2014.

Table A-1. Yearly coefficients of determination (R^2) calculated from the relationship between all paired rain gauges and uncorrected Next-Generation Weather Radar (NEXRAD) data using yearly, monthly, and daily totals. The number of observations (n) indicates the number of rain gauge and uncorrected NEXRAD pairs available for each year.

| Year | Yearly Totals | | Monthly Totals | | Daily Totals | |
|------|---------------|-------|----------------|-------|--------------|-------|
| | n | R^2 | n | R^2 | n | R^2 |
| 1999 | 75 | 0.63 | 740 | 0.82 | 19,461 | 0.49 |
| 2000 | 74 | 0.79 | 690 | 0.85 | 19,496 | 0.6 |
| 2001 | 76 | 0.79 | 700 | 0.88 | 19,753 | 0.5 |
| 2002 | 73 | 0.42 | 748 | 0.8 | 19,935 | 0.53 |
| 2003 | 79 | 0.81 | 797 | 0.85 | 21,576 | 0.57 |
| 2004 | 79 | 0.7 | 813 | 0.84 | 23,206 | 0.57 |
| 2005 | 77 | 0.61 | 856 | 0.81 | 22,685 | 0.56 |
| 2006 | 76 | 0.73 | 783 | 0.86 | 22,801 | 0.59 |
| 2007 | 82 | 0.78 | 841 | 0.84 | 23,222 | 0.6 |
| 2008 | 81 | 0.67 | 889 | 0.91 | 25,579 | 0.76 |
| 2009 | 79 | 0.67 | 882 | 0.91 | 25,544 | 0.71 |
| 2010 | 81 | 0.65 | 928 | 0.89 | 26,133 | 0.7 |
| 2011 | 81 | 0.73 | 859 | 0.9 | 24,894 | 0.69 |
| 2012 | 65 | 0.7 | 726 | 0.9 | 21,513 | 0.74 |
| 2013 | 65 | 0.6 | 742 | 0.92 | 21,432 | 0.74 |
| 2014 | 66 | 0.57 | 756 | 0.88 | 21,106 | 0.73 |

Uncorrected versus Corrected NEXRAD

Comparison of monthly totals for selected paired rain gauge and uncorrected and bias-corrected NEXRAD data between 1999 and 2014 showed an improvement in the coefficient of determination (R^2) and relationship (**Figure A-6**). Yearly regression coefficients calculated from monthly totals showed similar improvement after bias correction was applied to the daily NEXRAD values (**Table A-2**). In addition, yearly rain gauge and corrected NEXRAD rainfall totals were more equivalent than uncorrected NEXRAD totals (**Figure A-7**). The mean yearly relative bias of monthly totals between the rain gauge and uncorrected NEXRAD data indicated that, on average, NEXRAD underestimated rainfall from 1999 to 2003 by as much as 23%. Subsequent years showed slight (1% to 7%) overestimation and underestimation of NEXRAD yearly totals (**Figure A-8**). The percent error between the rain gauge and NEXRAD data was greatly reduced (less than 5%) for all years after the correction was applied to the daily NEXRAD values. When NEXRAD underestimated rainfall, the corrected NEXRAD data resulted in a slight overestimation compared to rain gauge yearly values, which suggests a possible overcorrection of the NEXRAD daily values (**Figure A-8**).

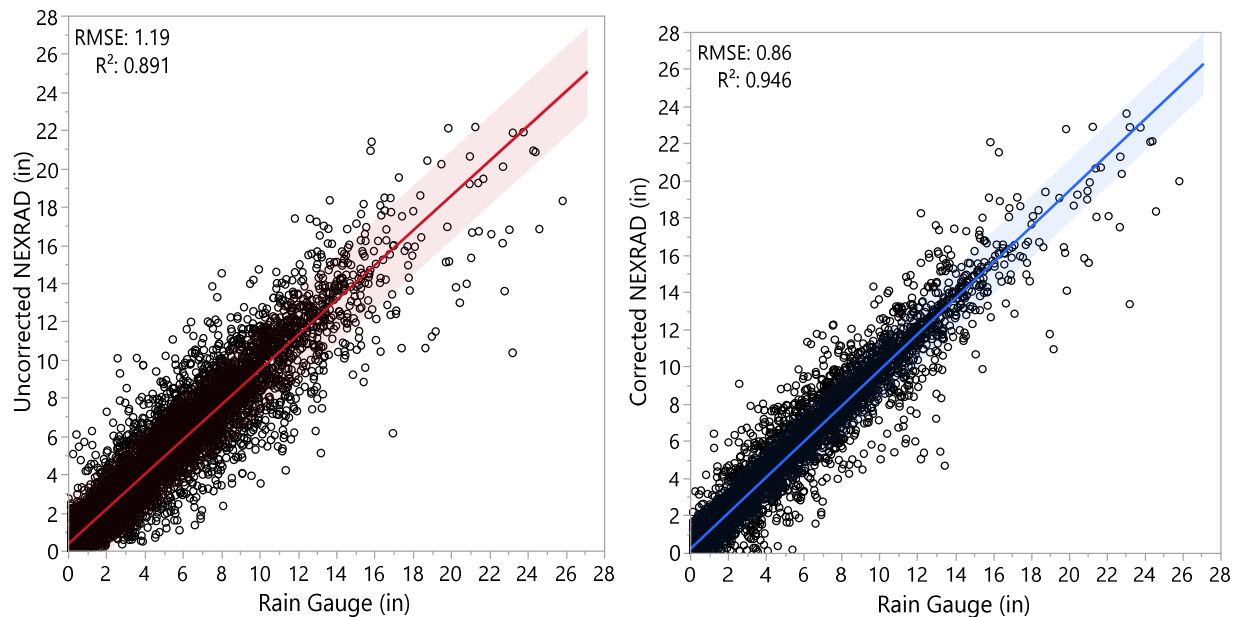


Figure A-6. Scatter plots comparing selected paired rain gauge and estimated Next-Generation Weather Radar (NEXRAD) monthly rainfall totals, in inches, for daily uncorrected and corrected NEXRAD values from 1999 to 2014. Circles represent a monthly value for each rain gauge and NEXRAD pixel located within the Lower West Coast Planning Area.

Table A-2. Yearly coefficients of determination (R^2) calculated from the relationship between selected paired rain gauges and Next-Generation Weather Radar (NEXRAD) monthly rainfall totals before and after correction. The number of observations (n) indicates the number of rain gauge and NEXRAD monthly pairs available for each year with a good correlation ($\tau \geq 0.75$).

| Year | Uncorrected NEXRAD | | Bias-Corrected NEXRAD | |
|------|--------------------|-------|-----------------------|-------|
| | n | R^2 | n | R^2 |
| 1999 | 740 | 0.82 | 752 | 0.85 |
| 2000 | 690 | 0.85 | 696 | 0.88 |
| 2001 | 700 | 0.88 | 701 | 0.88 |
| 2002 | 748 | 0.8 | 755 | 0.86 |
| 2003 | 797 | 0.85 | 807 | 0.87 |
| 2004 | 813 | 0.84 | 816 | 0.88 |
| 2005 | 856 | 0.81 | 859 | 0.86 |
| 2006 | 783 | 0.86 | 787 | 0.9 |
| 2007 | 841 | 0.84 | 845 | 0.89 |
| 2008 | 889 | 0.91 | 893 | 0.93 |
| 2009 | 882 | 0.91 | 880 | 0.94 |
| 2010 | 928 | 0.89 | 927 | 0.96 |
| 2011 | 859 | 0.9 | 867 | 0.91 |
| 2012 | 726 | 0.9 | 725 | 0.93 |
| 2013 | 742 | 0.92 | 745 | 0.94 |
| 2014 | 756 | 0.88 | 756 | 0.9 |

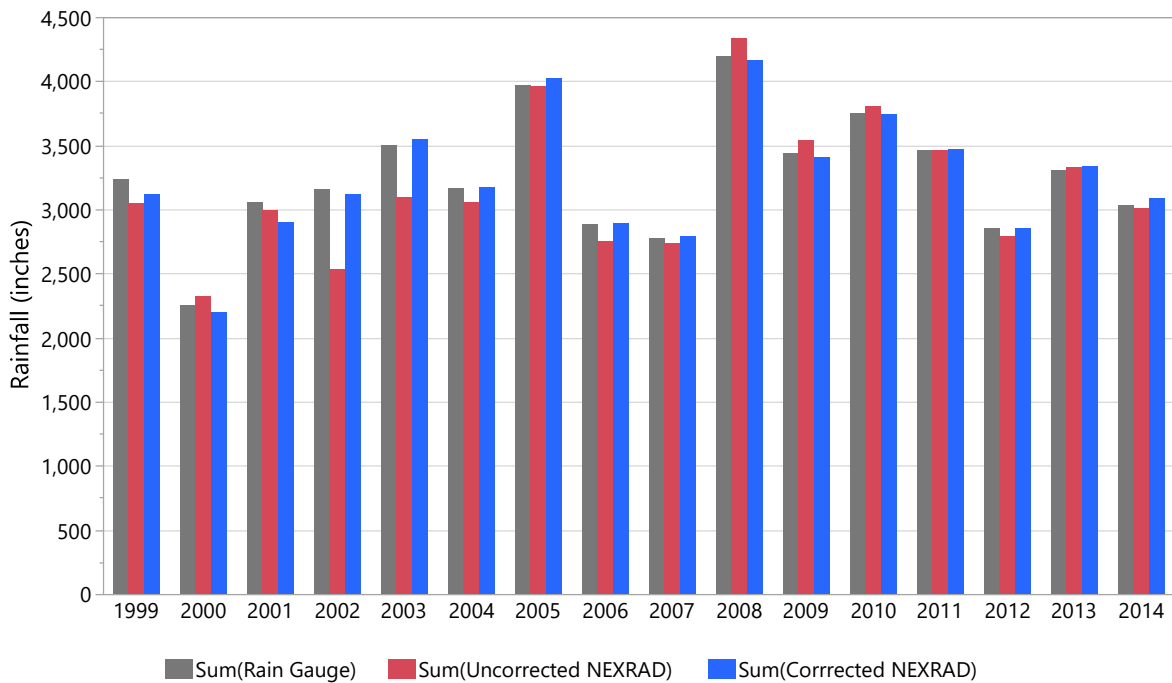


Figure A-7. Comparison of paired rain gauge and estimated Next-Generation Weather Radar (NEXRAD) yearly rainfall totals, in inches, for uncorrected and corrected NEXRAD values from 1999 to 2014.

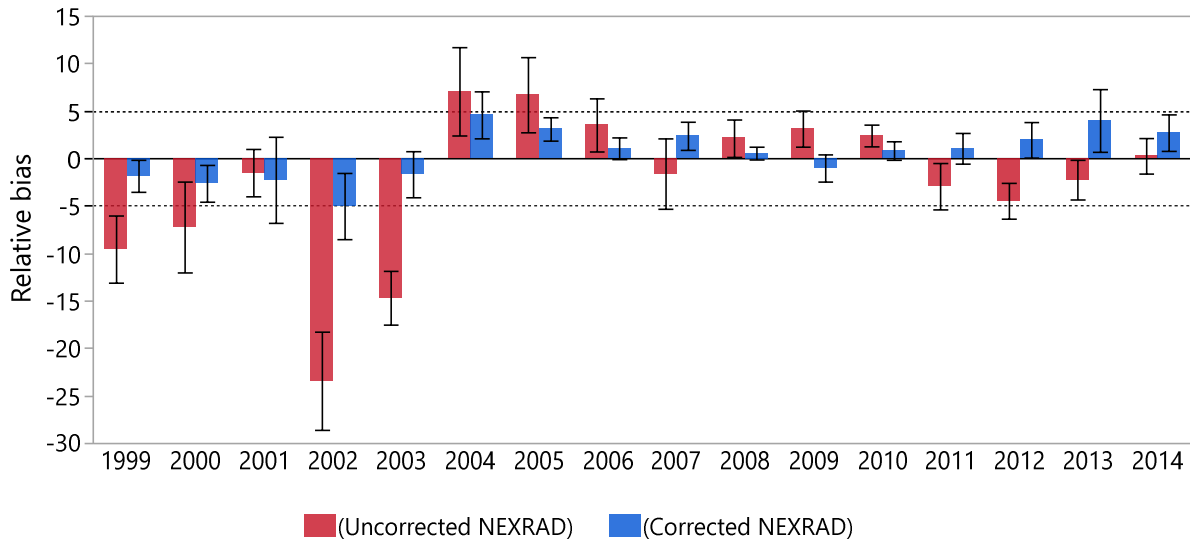


Figure A-8. Mean yearly relative bias of monthly totals between available rain gauges and the uncorrected and corrected Next-Generation Weather Radar (NEXRAD). Error bars represent ± 1 standard error of the mean.

Bias

The monthly bias, or adjustment factor, is defined by the sum of daily rainfall values recorded by the rain gauge divided by the sum of the associated estimated daily rainfall NEXRAD value. Monthly bias values greater than 1 indicated underestimation, while bias values lower than 1 suggested overestimation of rainfall by NEXRAD. Monthly bias derived from the difference between the rain gauge and NEXRAD rainfall resulted in approximately 2.7% of the bias greater than 3, suggesting a gross underestimation of NEXRAD rainfall. When the bias value was greater than 3, a maximum bias or adjustment factor of 3 was applied to the daily NEXRAD value to prevent overcorrection. Bias values for the uncorrected NEXRAD appeared normally distributed, suggesting a tendency to equally overestimate and underestimate monthly rainfall totals (**Figure A-9a**). As bias is calculated monthly and applied to the daily NEXRAD value, some bias is anticipated to remain in the corrected NEXRAD monthly totals. Evaluation of the remaining monthly bias after NEXRAD rainfall correction showed a substantial reduction in the differences between the rain gauge and NEXRAD data (**Figure A-9b**). Overall, the 1999 to 2014 monthly bias after correction of the NEXRAD rainfall showed a statistically tighter proximity to 1 compared to the uncorrected NEXRAD bias (**Table A-3**). Further evaluation of the bias showed an improvement of the uncorrected NEXRAD data after 2007. This trend also was highlighted in the previous comparison of uncorrected and corrected NEXRAD rainfall yearly totals. Finally, continuous improvement of the NEXRAD correction methodology by the vendor has resulted in better estimation of NEXRAD rainfall data compared to previous years.

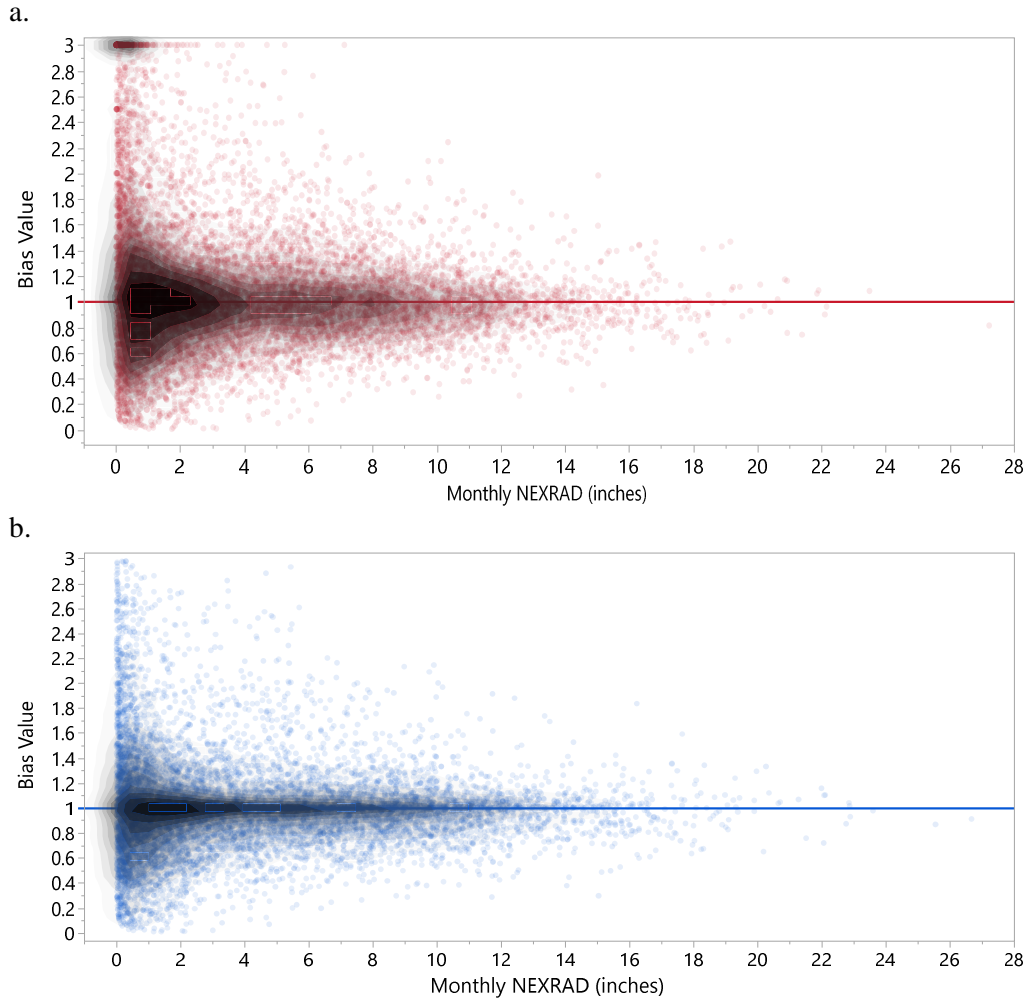


Figure A-9. Density plot comparison of monthly bias from 1999 to 2014 at each rain gauge station (a) before and (b) after Next-Generation Weather Radar (NEXRAD) rainfall correction. Values greater or lower than 1 represent overestimation or underestimation, respectively, of NEXRAD rainfall monthly values, in inches.

Table A-3. Summary statistic comparison of monthly bias from 1999 to 2014 for uncorrected and corrected Next-Generation Weather Radar (NEXRAD) rainfall.

| Statistic | Bias | |
|-----------------------------|-----------------------------|---------------------------|
| | Uncorrected NEXRAD Rainfall | Corrected NEXRAD Rainfall |
| Maximum | 3.000 | 2.978 |
| 90 th percentile | 1.667 | 1.351 |
| 75 th percentile | 1.224 | 1.079 |
| Mean | 1.095 | 1.007 |
| Standard Deviation | 0.529 | 0.354 |
| Standard Error Mean | 0.005 | 0.003 |
| Median | 1.000 | 0.994 |
| 25 th percentile | 0.811 | 0.853 |
| 10 th percentile | 0.596 | 0.644 |
| Minimum | 0.006 | 0.007 |

Spatial Analysis

The monthly bias, or adjustment factors, derived from the relationship between the rain gauge and NEXRAD rainfall were interpolated across the LWC Planning Area to produce 192 raster plots, one for each month between 1999 and 2014. The interpolated NEXRAD bias did not show any spatial or temporal trends in the distribution and variability of the bias. Instead, the variability of the bias appeared to be influenced primarily by the relationship between the rain gauge and NEXRAD pixel. Results showed large variability in the number of rain gauges available for each month, which was heavily influenced by the rain gauge data quality, the amount of rainfall recorded, and the number of paired rain gauge and NEXRAD observations available for each month. In addition, the southernmost portion of the LWC Planning Area has a lack of rain gauge monitoring stations, whereas the middle to northern region has a larger concentration and clustering of rain gauge monitoring stations. Overall, the NEXRAD bias appeared localized in relation to rain gauge locations.

As described earlier, the clustering of rain gauge stations was minimized by normalizing adjustment factors that appeared within 2 kilometers of each other. The remaining adjustment factors were used to correct the daily NEXRAD pixel values (**Figure A-10**). Two additional raster plots were produced to visually compare the uncorrected and corrected NEXRAD monthly totals. In some cases, differences between the uncorrected and corrected NEXRAD values were visually discernable, particularly during months with higher rainfall (**Figure A-10a**). However, months with low rainfall did not appear to visually differ (**Figure A-10b**). Large variability in monthly rainfall volumes occurred across the LWC Planning Area, suggesting heavy downpours in localized areas. The change in monthly rainfall total was spatially depicted by the difference between the uncorrected and corrected NEXRAD values. The resulting raster plot (denoted by Change in NEXRAD) showed where the monthly NEXRAD total rainfall in inches was increased or reduced above the zero mark (**Figure A-10**).

As shown in the monthly total raster plots, one advantage of applying monthly bias adjustments to the daily NEXRAD values is the process can capture seasonal changes and climate disturbances such as droughts and storm events through the years. This is particularly important for periods associated with tropical storms and hurricanes when rain gauge data may be limited or nonexistent in areas severely affected by the storm.

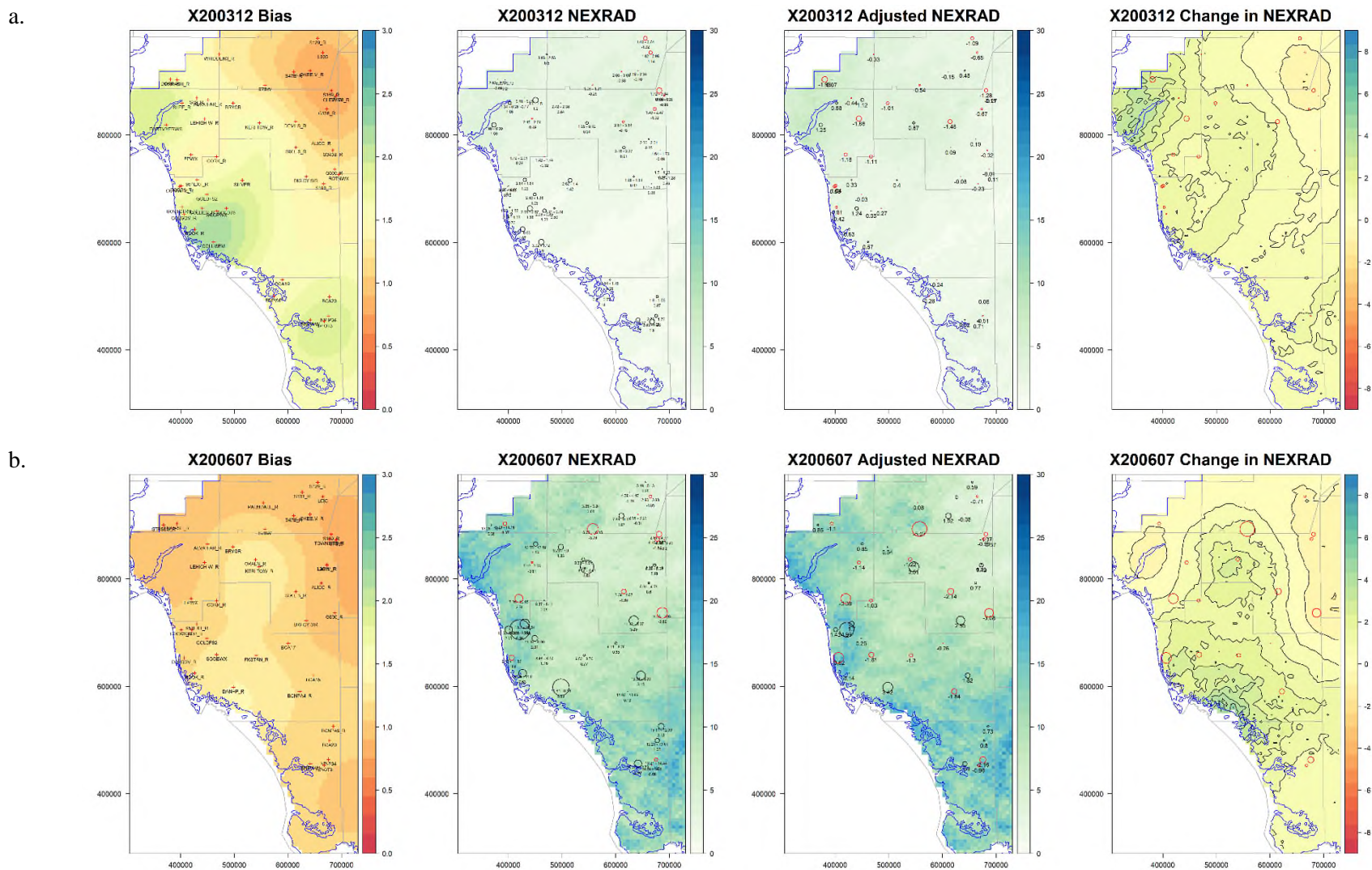


Figure A-10. Lower West Coast Planning Area raster maps showing the calculated monthly bias, monthly rainfall totals (in inches) for uncorrected and corrected Next-Generation Weather Radar (NEXRAD), and net change in NEXRAD after the adjustment is applied for (a) a dry season month in December 2003 (X200312), and (b) a rainy season month in July 2006 (X200606).

SUMMARY AND CONCLUSION

The main objectives of this study were to 1) evaluate the relationship between rain gauge measurements and estimated NEXRAD values using yearly, monthly, and daily rainfall totals in the LWC Planning Area of Florida during a 16-year period (1999 to 2014); and 2) develop a method to correct NEXRAD rainfall bias using adjustment factors derived from the relationship of co-located rain gauge and NEXRAD pixel pairs. An important assumption in this study was that rain gauge measurements offer a better representation of rainfall accumulation than estimated NEXRAD values at the same location. Although, the quality and continuity of the rain gauge measurement data can be affected by multiple factors, previous QA/QC evaluations indicated rain gauge measurements are a better representation of rainfall than NEXRAD values at co-located rain gauge and NEXRAD pixels (Brown 2014).

Overall, NEXRAD underestimated rainfall in the LWC Planning Area from 1999 to 2003 by as much as 23%, while only slight (1% to 7%) overestimations and underestimations were observed in subsequent years. Results showed improvement in the quality of NEXRAD data provided by the vendor from 2007 through 2014, as indicated by higher coefficients of determination derived from the rain gauge and NEXRAD daily and monthly rainfall totals.

Comparison of rain gauge measurements and estimated NEXRAD values showed a stronger correlation using monthly totals than yearly and daily totals. As a result, monthly correction factors were determined to be better suited for the correction of daily NEXRAD values. Furthermore, adjustment of daily NEXRAD values using monthly bias factors provided a way to capture seasonal changes and climate disturbances such as droughts and storm events. This was particularly important for periods associated with tropical storms and hurricanes when rain gauge data appeared affected, limited, or nonexistent in areas severely affected by the storm.

Correction of the NEXRAD daily rainfall data was achieved using a systematic approach in which calculated monthly adjustment factors were interpolated across the LWC Planning Area and applied to the daily values. Although corrections of daily NEXRAD data were applied systematically to all 4,763 pixel values in the LWC Planning Area, there were minor inconsistencies in daily rainfall values at co-located rain gauge and NEXRAD pixel pairs that could have resulted in localized overestimation or underestimation of rainfall. Therefore, further examination of the raster plots was necessary to find and manually remove inconsistencies before producing the final adjusted NEXRAD data set. Rather than completely eliminating the bias between the rain gauge and NEXRAD values, the process developed in this study attempted to reduce the bias while errors associated with rain gauges were preserved.

After applying the monthly correction to the daily NEXRAD value, differences in rain gauge and NEXRAD daily, monthly, and yearly rainfall totals were reduced. The monthly relationship of co-located rain gauge and NEXRAD pixel pairs increased after the correction, while monthly bias between the rain gauge and NEXRAD decreased.

Finally, results showed rain gauge data can be used to improve the accuracy of estimated NEXRAD daily rainfall volumes. In addition, the process for correcting large NEXRAD data sets was optimized and partially automated using R scripts. This process reduced the time and effort needed to evaluate the relationship between the rain gauge and NEXRAD rainfall, allowed for the use of yearly and monthly adjustment factors, and expedited the production of corrected NEXRAD data and raster plots. The method described in this study can be applied to different areas of the SFWMD. The corrected NEXRAD data can be used as an alternative data set for the application and development of hydrologic models and water budgets.

LITERATURE CITED

- Beeson, P.C., P.C. Doraiswamy, A.M. Sadeghi, M. Di Luzio, M.D. Tomer, J.G. Arnold, and C.S.T. Daughtry. 2011. Treatments of precipitation inputs to hydrologic models. *Transactions of the American Society of Agricultural and Biological Engineers* 54(6):2,011-2,020.
- Brown, C. 2014. QA/QC of NEXRAD Rainfall (2001-2012). South Florida Water Management District, West Palm Beach, FL.
- Chumchean, S., A. Seed, and A. Sharma. 2006. Correcting of real-time radar rainfall bias using a Kalman filtering approach. *Journal of Hydrology* 137(1-2):123-137.
- Craciun, C. and O. Catrina. 2016. An objective approach for comparing radar estimated and rain gauge measured precipitation. *Meteorological Applications* 23:683-690.
- Goudenhoofd, E. and L. Delobbe. 2009. Evaluation of radar-gauge merging methods for quantitative precipitation estimates. *Hydrology and Earth System Sciences* 13:195-203.
- Habib, E., A.V. Aduvala, and E.A. Meselhe. 2007. Effect of radar-rainfall errors on rainfall-runoff modeling. *Proceedings of the 2007 World Environmental and Water Resources Congress*. 11 pp.
- Habib, E., B.F. Larson, and J. Grascel. 2009. Validation of NEXRAD multisensory precipitation estimates using an experimental dense rain gauge network in south Louisiana. *Journal of Hydrology* 373(3-4):463-478.
- Hanchowong, R., U. Weesakul, and S. Chumchean. 2012. Bias correction of radar rainfall estimates based on a geostatistical technique. *ScienceAsia* 38:373-385.
- Hardegree, S.P., S.S. Van Vactor, D.H. Levinson, and A.H. Winstral. 2008. Evaluation of NEXRAD radar precipitation products for natural resource applications. *Rangeland Ecology & Management* 61(3):346-353.
- Helsel, D.R. and R.M. Hirsch. 1992. *Statistical methods in water resources*. Studies in Environmental Science Volume 49. Elsevier, Amsterdam, The Netherlands. 522 pp.
- Hiemstra, P.H., E.J. Pebesma, C.J.W. Twenhöfel, and G.B.M. Heuvelink. 2009. Real-time automatic interpolation of ambient gamma dose rates from the Dutch radioactivity monitoring network. *Computers & Geosciences* 35(8):1,711-1,721.
- Mächler, M., P. Rousseeuw, A. Struyf, M. Hubert, and K. Hornik. 2018. *Cluster: Cluster Analysis Basics and Extensions*. R package version 2.0.7-1.
- Müllner, D. 2013. Fastcluster: Fast Hierarchical, Agglomerative Clustering Routines for R and Python. *Journal of Statistical Software* 53(9):1-18.
- Over, T.M., E.A. Murphy, T.W. Ortel, and A.L. Ishii. 2007. Comparisons between NEXRAD radar and tipping-bucket gage rainfall data: A case study for DuPage County, Illinois. *Proceedings of the 2007 World Environmental and Water Resources Congress*. 14 pp.
- R Development Core Team. 2018. *R: A language and environment for statistical computing*. R Foundation for Statistical Computing, Vienna, Austria. ISBN 3-900051-07-0.

- SFWMD. 2005. South Florida Water Management Model version 5.5 documentation. South Florida Water Management District, West Palm Beach, FL.
- SFWMD. 2017. 2017 Lower West Coast Water Supply Plan Update. South Florida Water Management District, West Palm Beach, FL.
- Skinner, C., F. Bloetscher, and C.S. Pathak. 2009. Comparison of NEXRAD and rain gauge precipitation measurements in South Florida. *Journal of Hydrologic Engineering* 14(3):248-260.
- Smith, B. and S. Rodriguez. 2017. Spatial Analysis of High-Resolution Radar Rainfall and Citizen-Reported Flash Flood Data in Ultra-Urban New York City. *Water* 9(736). 17 pp.
- Steiner, M., J.A. Smith, S.J. Burges, C.V. Alonso, and R.W. Darden. 1999. Effect of bias adjustment and rain gauge data quality control on radar rainfall estimation. *Water Resources Research* 35(8):2,487-2,503.
- Trimble, P. 2018. Caloosahatchee Basin NEXRAD Rainfall Report. Draft Memorandum Report. August 2018.
- Vernimmen, R.R.E., A. Hooijer, M. Mamenun, E. Aldrian, and A.I.J.M. van Dijk. 2012. Evaluation and bias correction of satellite rainfall data for drought monitoring in Indonesia. *Hydrology and Earth System Sciences* 16:133-146.

**APPENDIX B:
LAYER TOPS/BOTTOMS AND THICKNESSES**

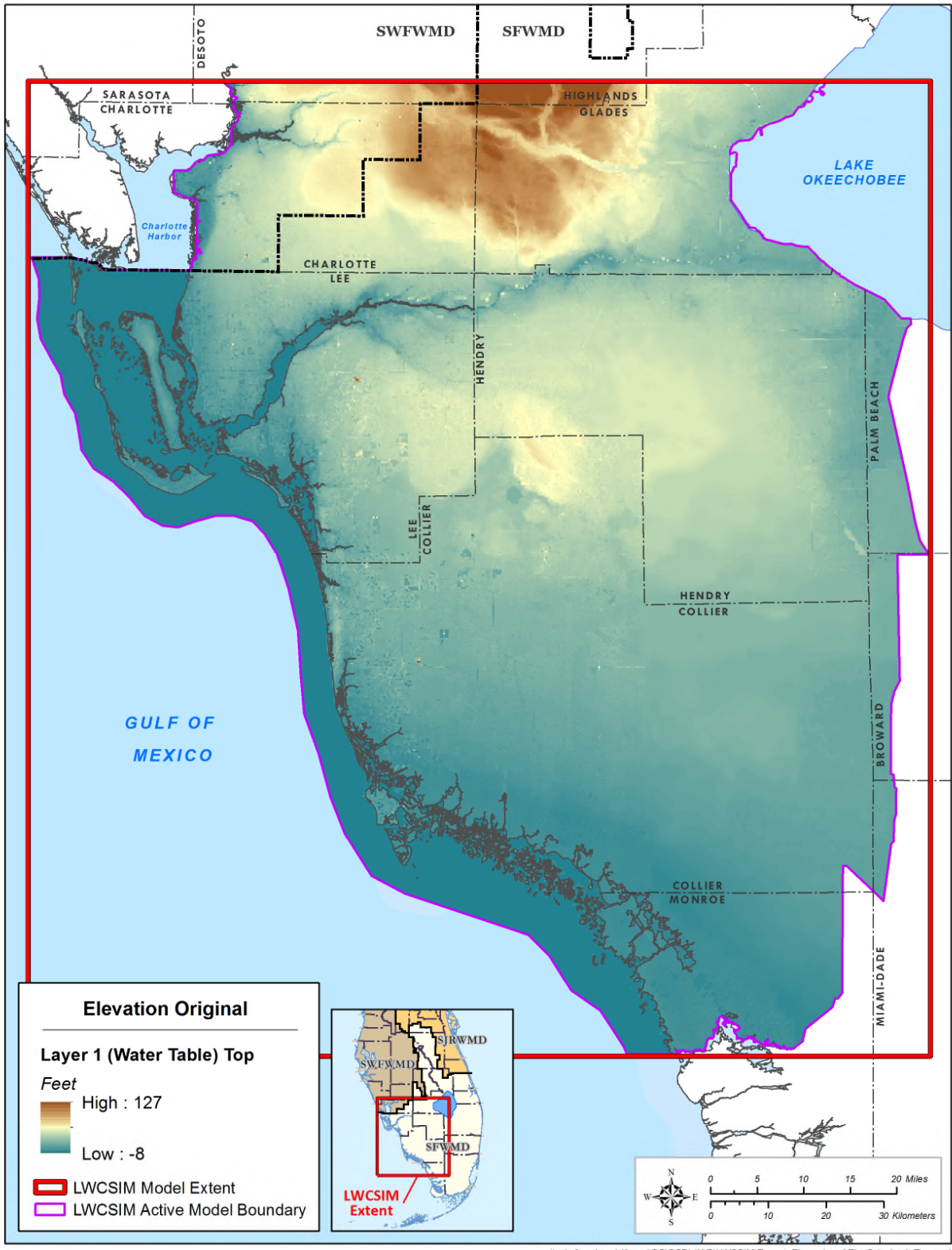


Figure B-1. Topographic surface elevation of the Water Table aquifer.

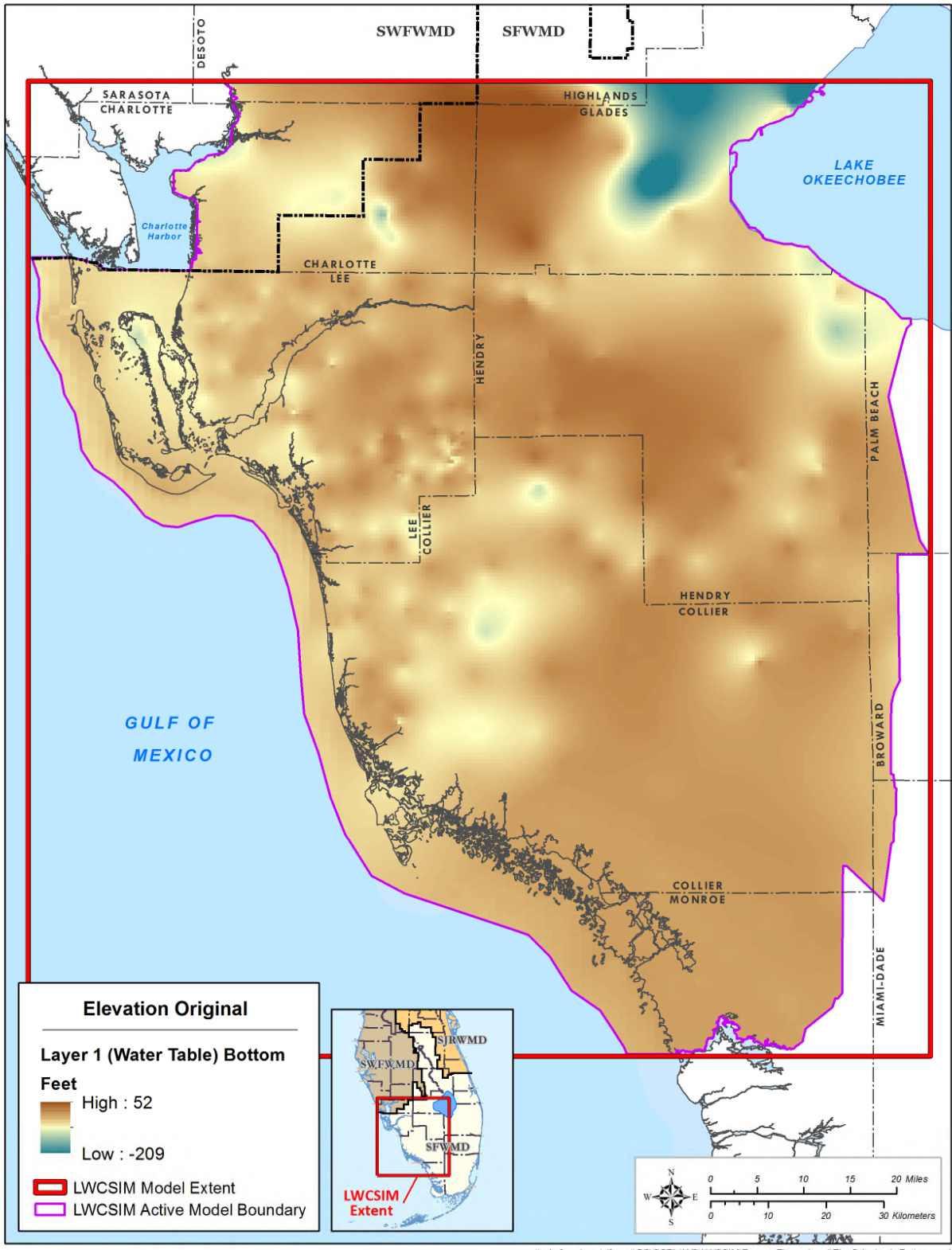
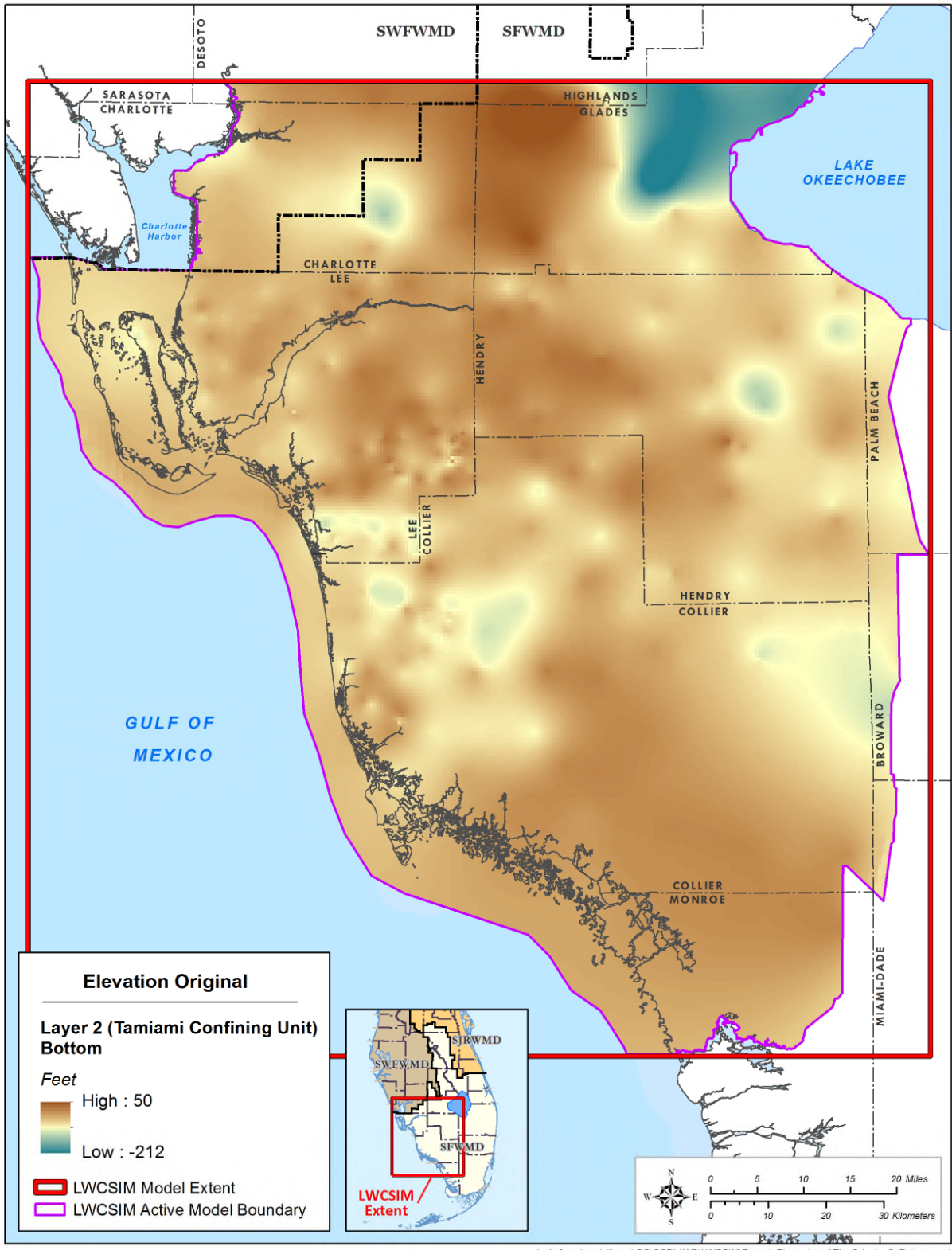


Figure B-2. Bottom elevation of the Water Table aquifer.



\\ad.sfwmd.gov\dfsroot\GIS\GSBiz\WS\LWCSIM\Report_Figures\mxd\ElevOrig_Lyr2_Bottom.mxd

Figure B-3. Bottom elevation of the Tamiami confining unit.

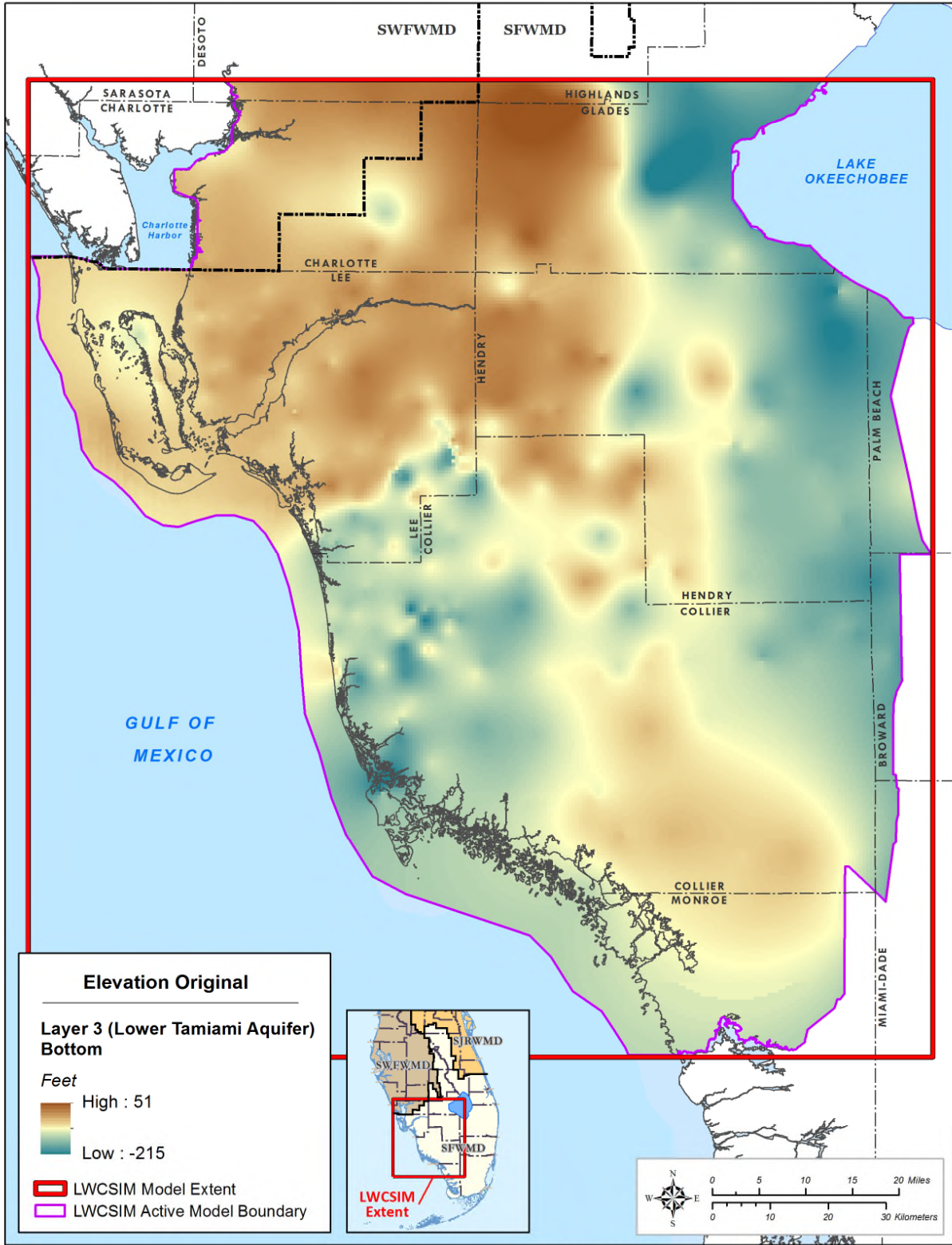


Figure B-4. Bottom elevation of the Lower Tamiami aquifer.

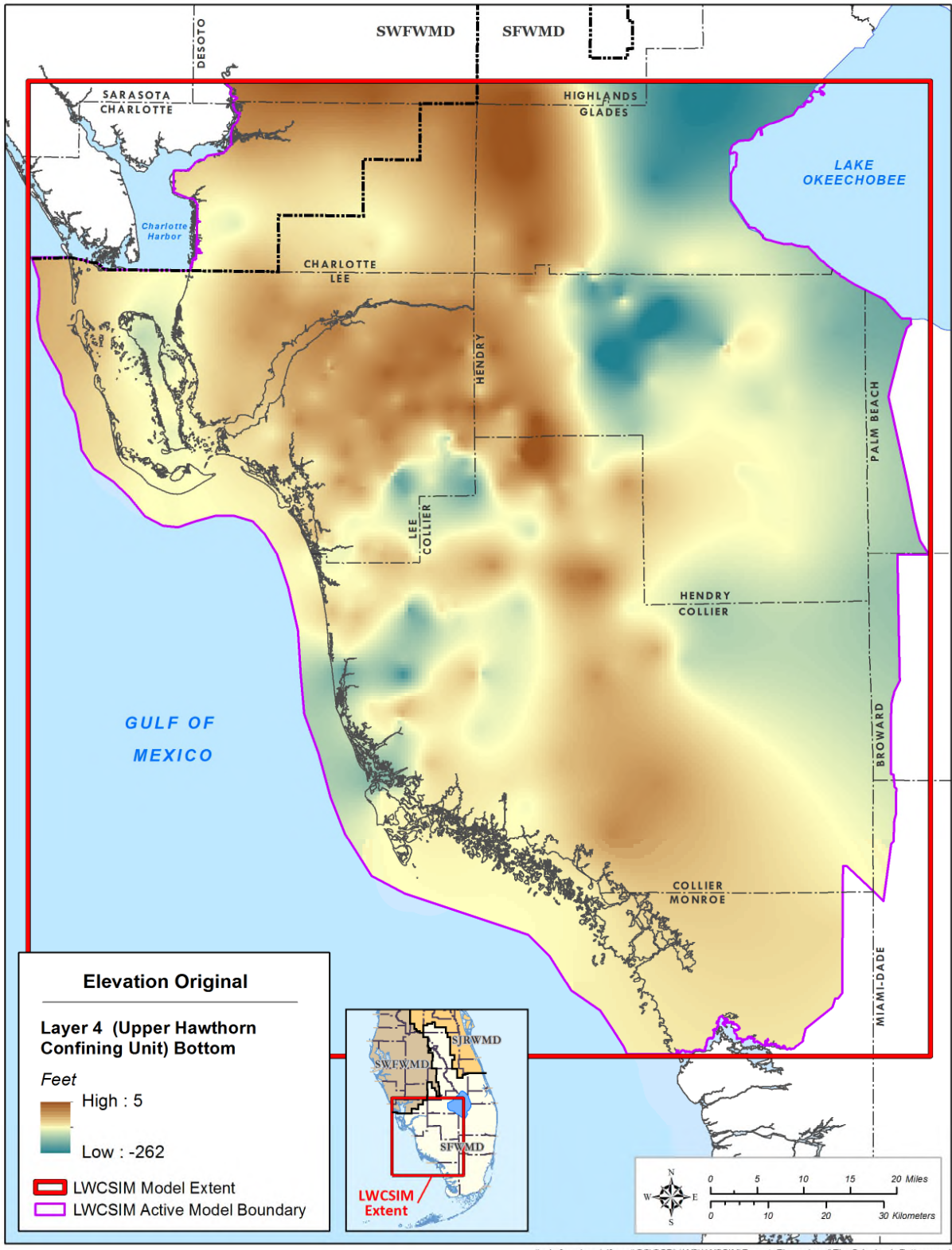


Figure B-5. Bottom elevation of the Upper Hawthorn confining unit.

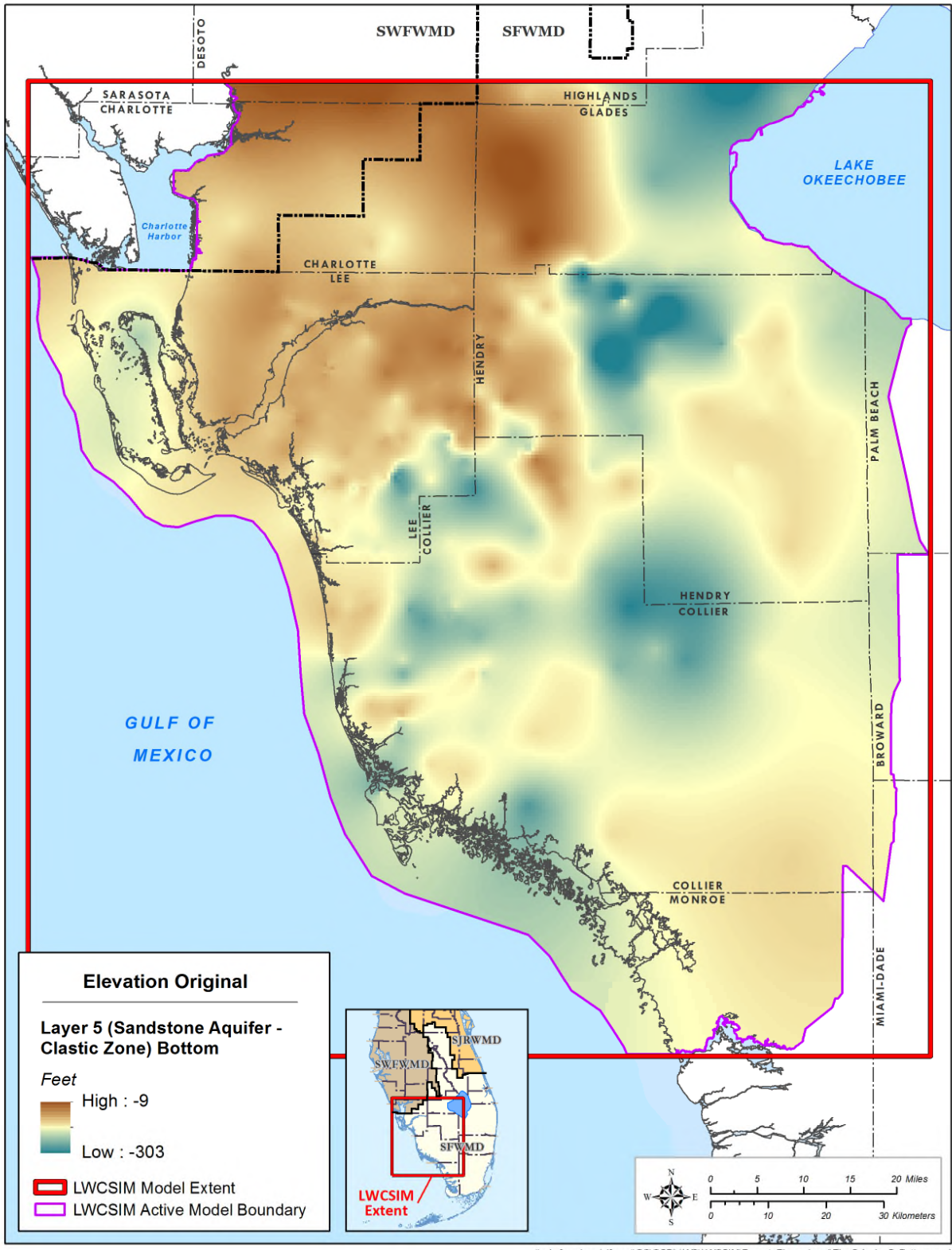


Figure B-6. Bottom elevation of the Sandstone aquifer – clastic zone.

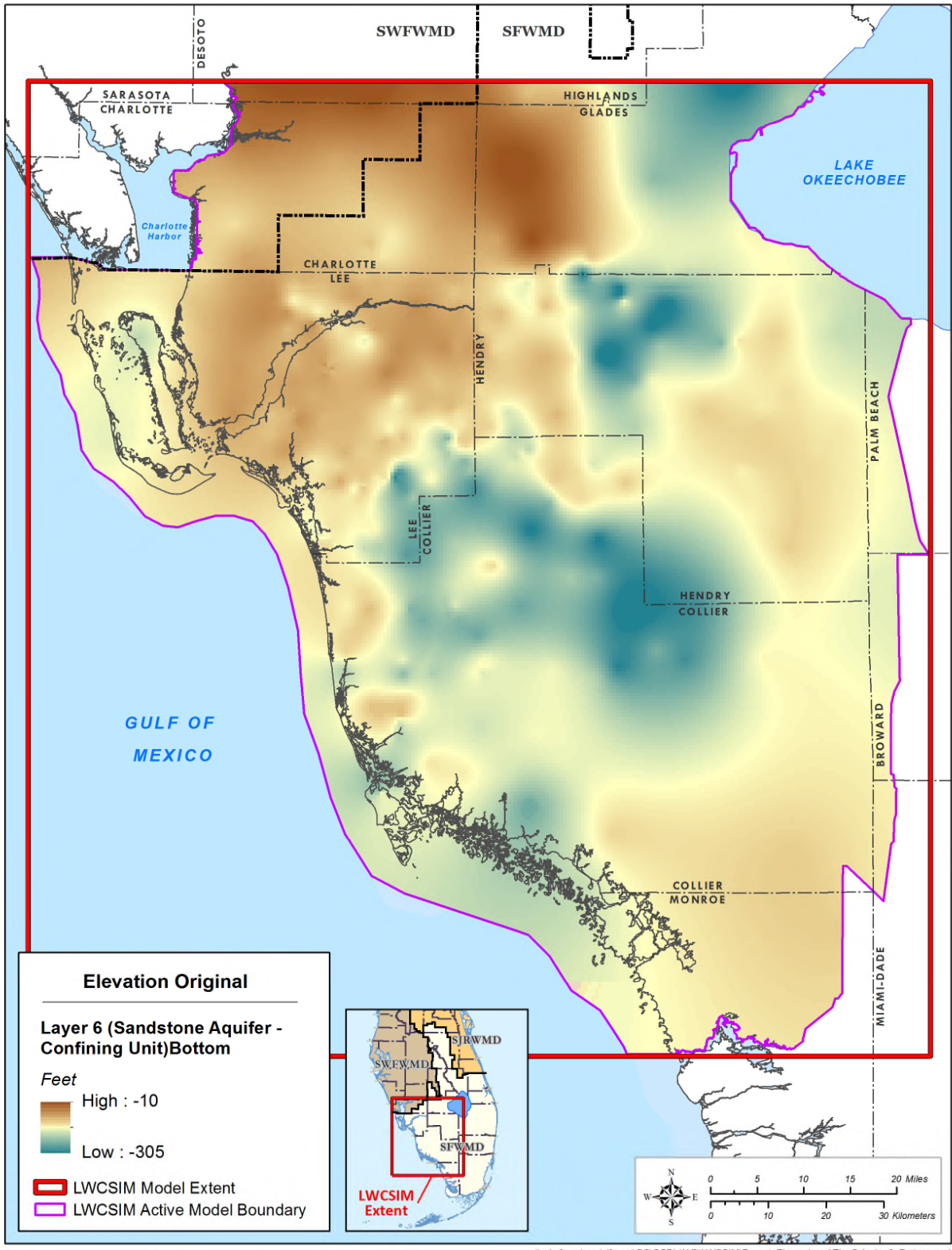


Figure B-7. Bottom elevation of the Sandstone aquifer confining unit.

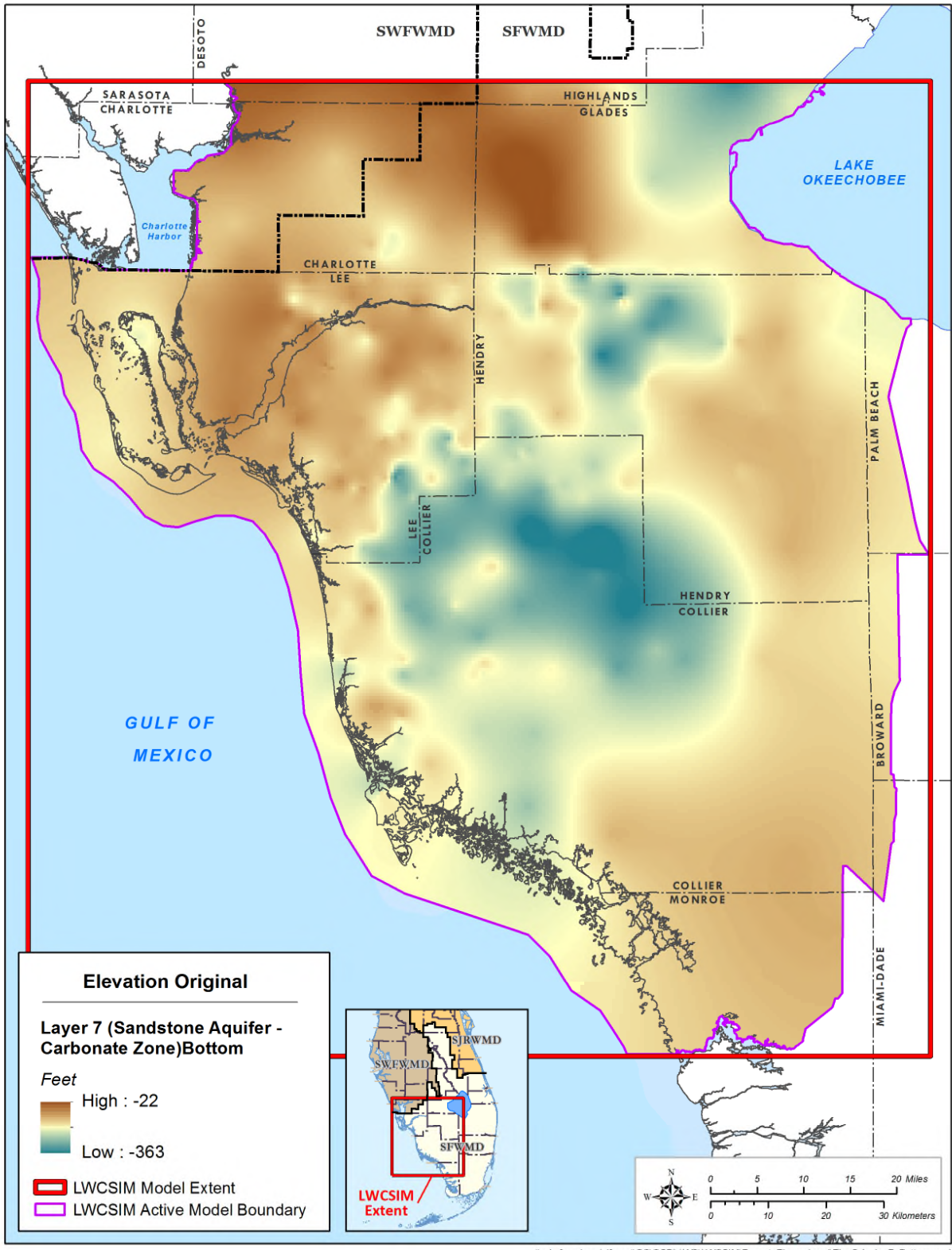


Figure B-8. Bottom elevation of the Sandstone aquifer – carbonate zone.

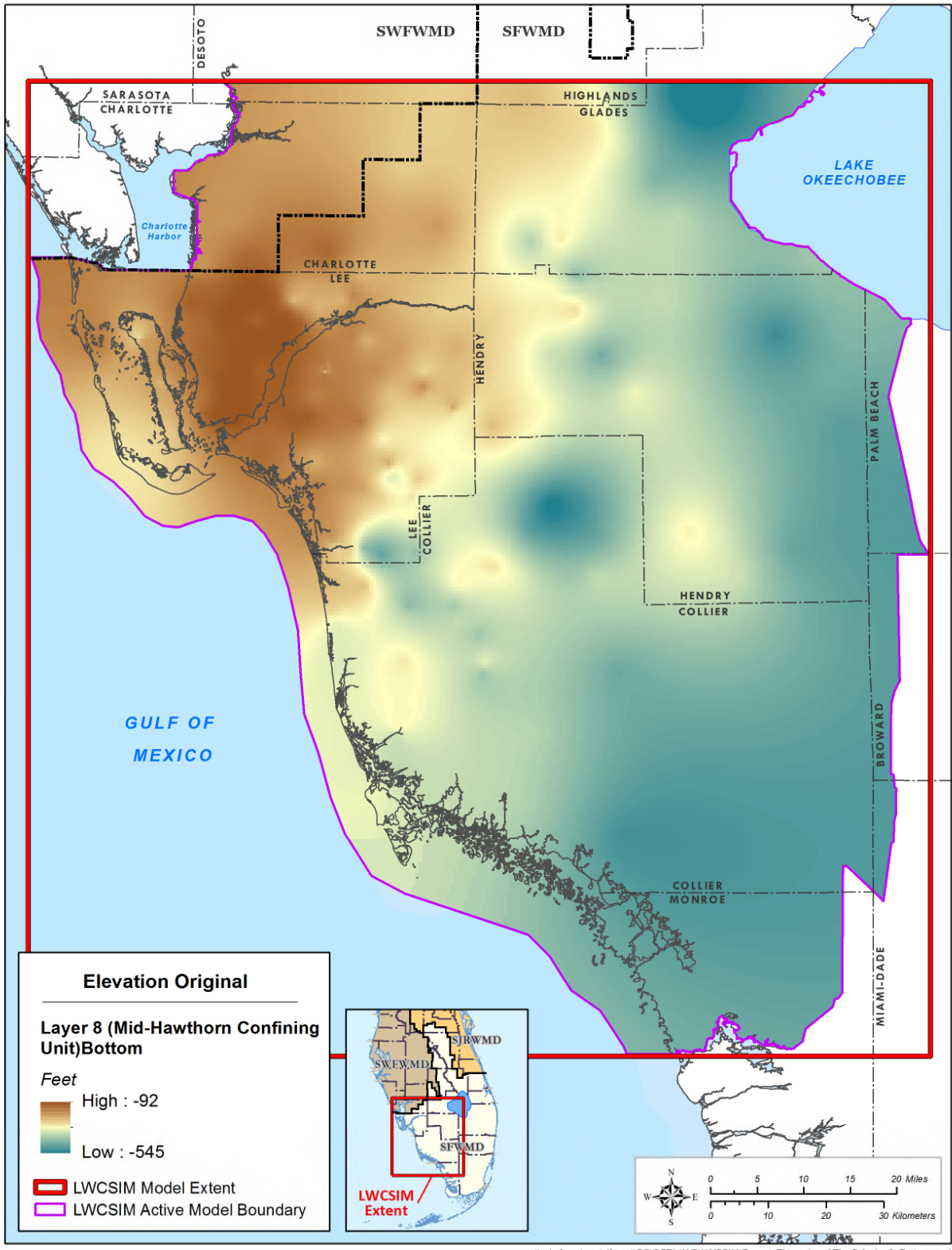


Figure B-9. Bottom elevation of the Mid-Hawthorn confining unit.

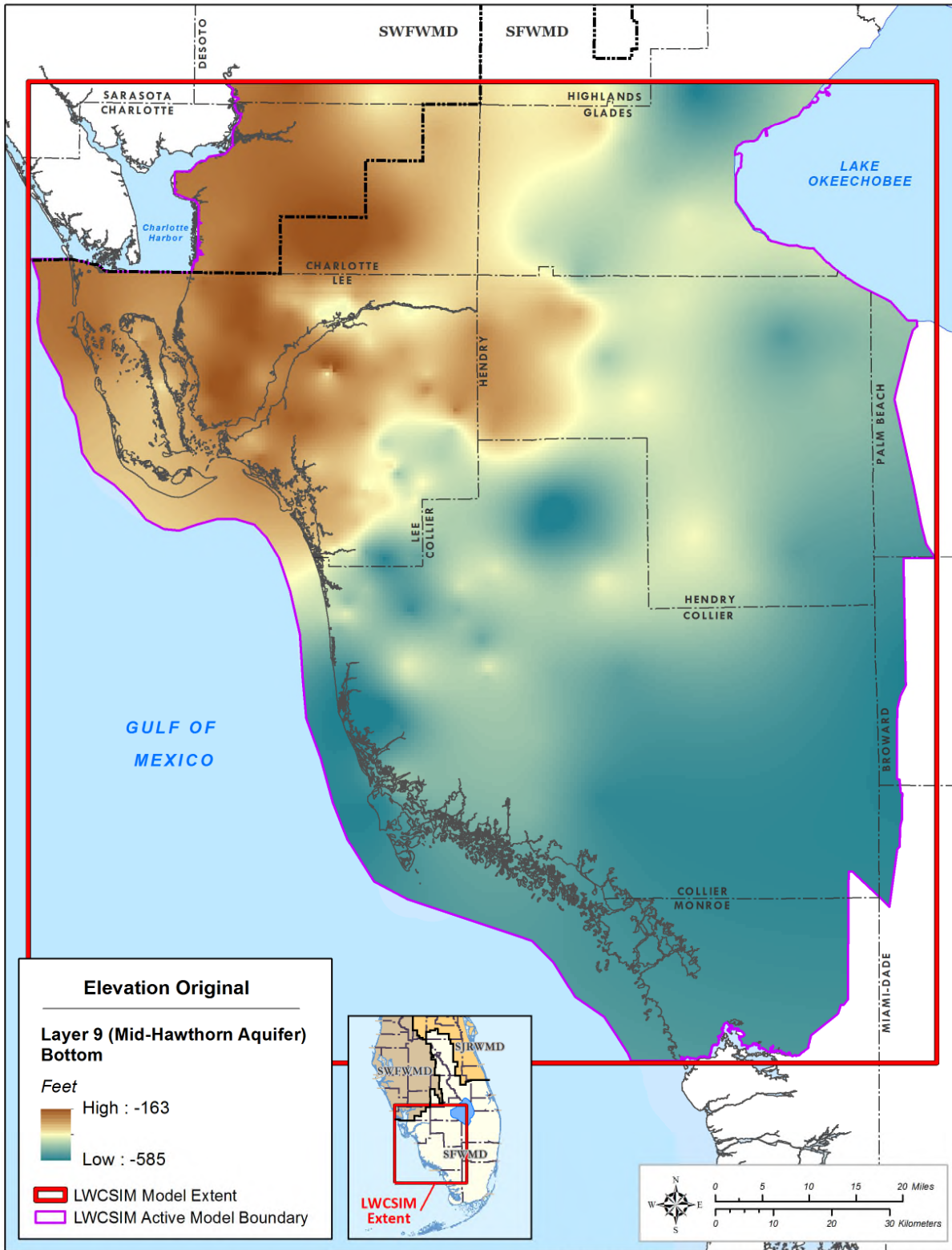


Figure B-10. Bottom elevation of the Mid-Hawthorn aquifer.

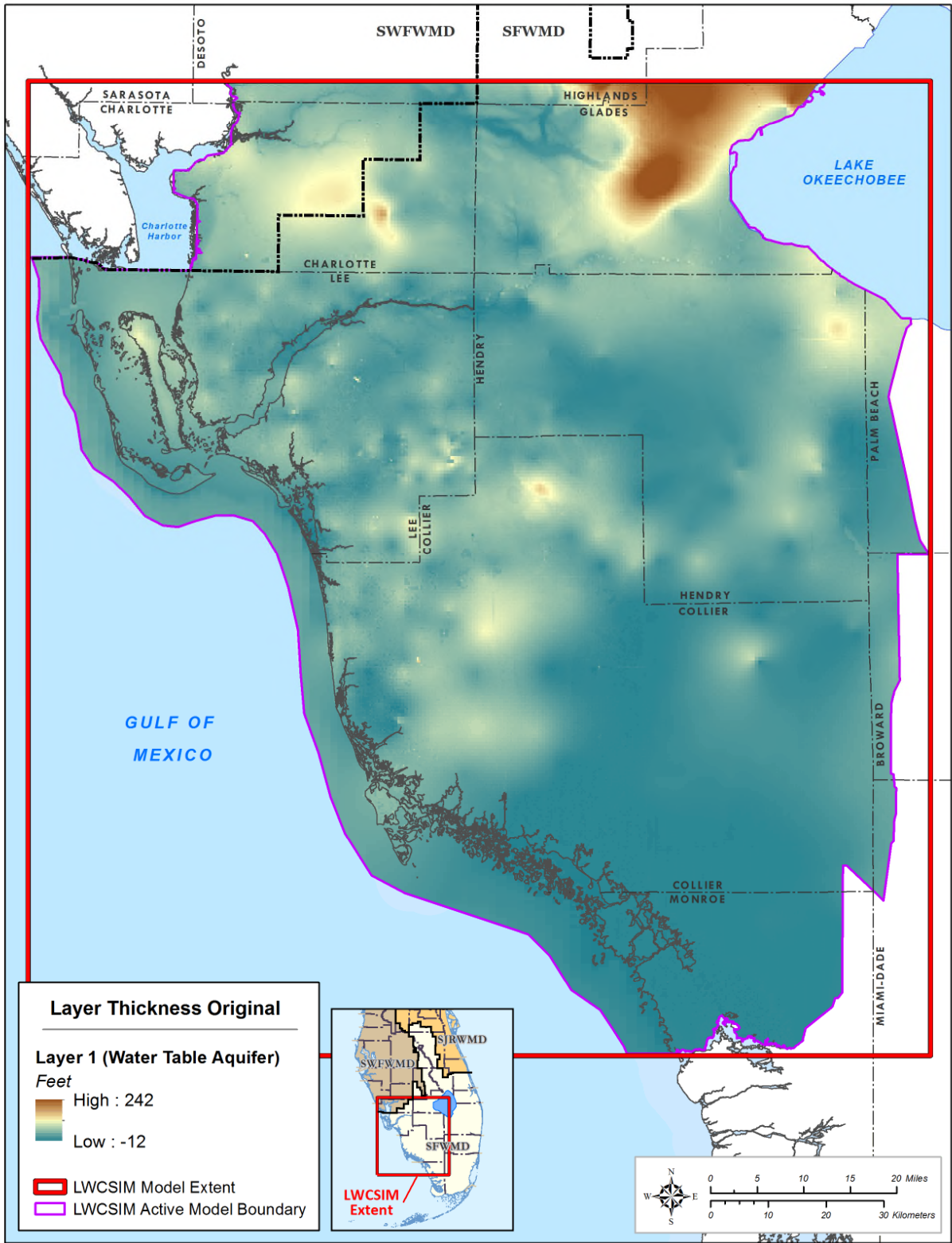


Figure B-11. Thickness of the Water Table aquifer.

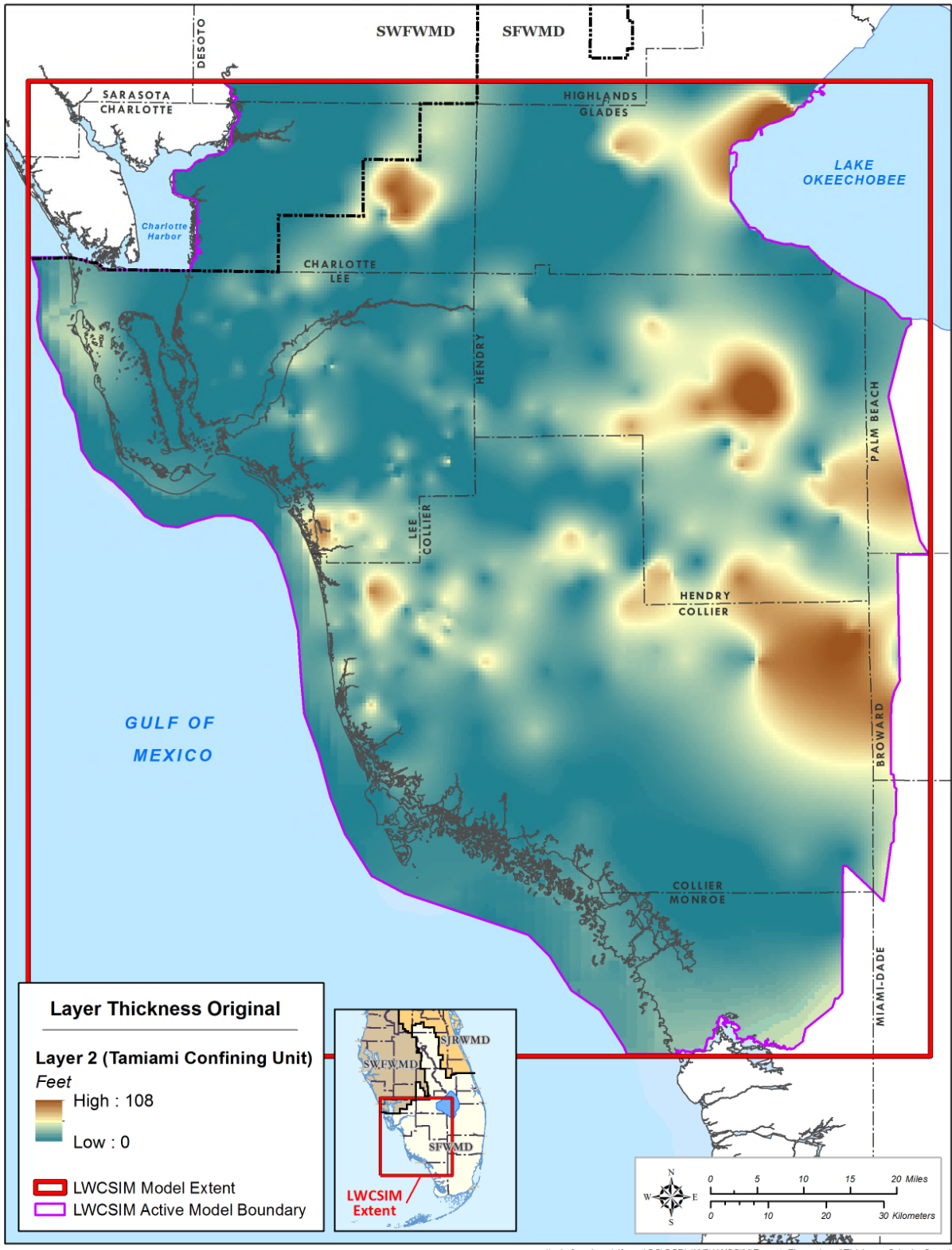


Figure B-12. Thickness of the Tamiami confining unit.

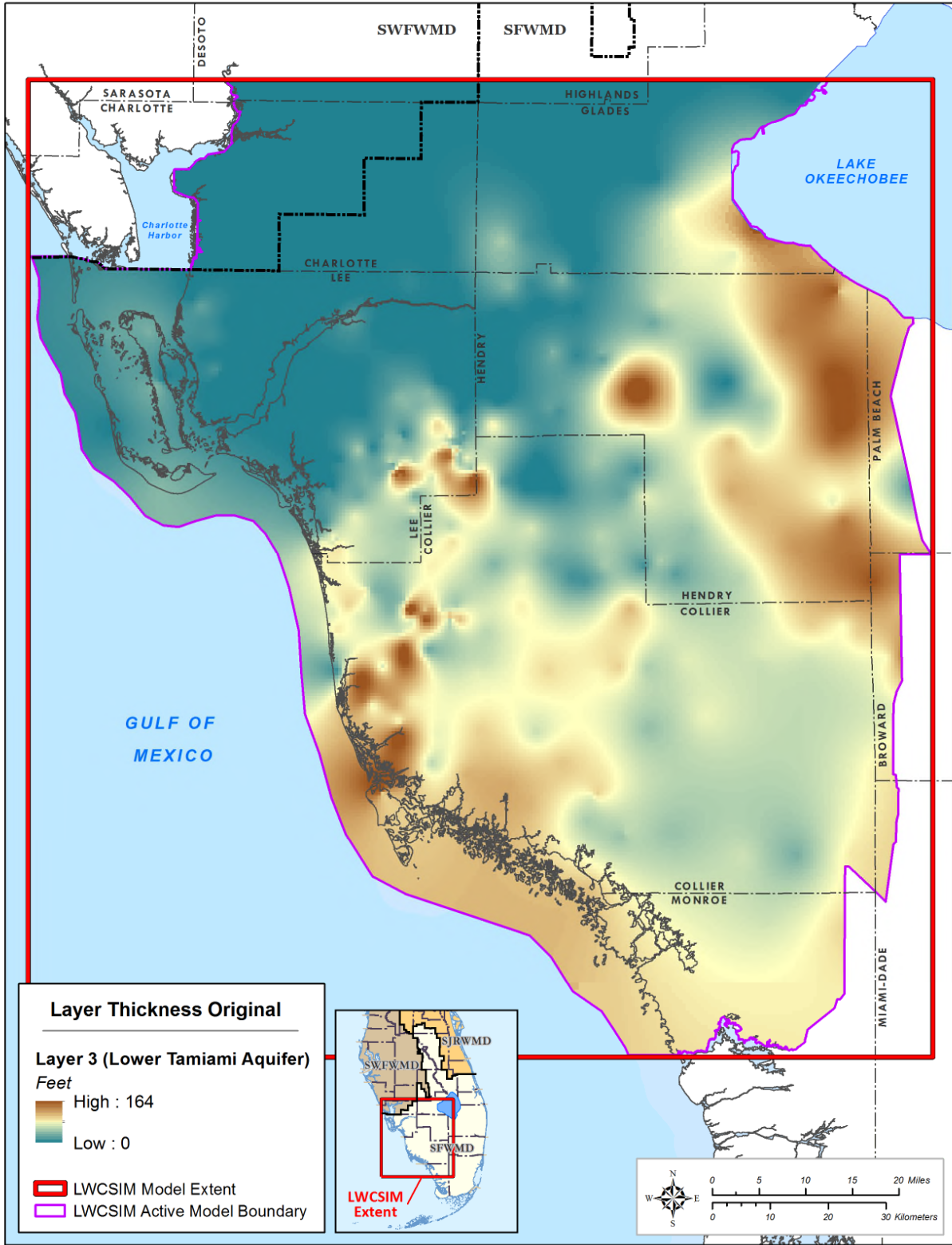


Figure B-13. Thickness of the Lower Tamiamiqi aquifer.

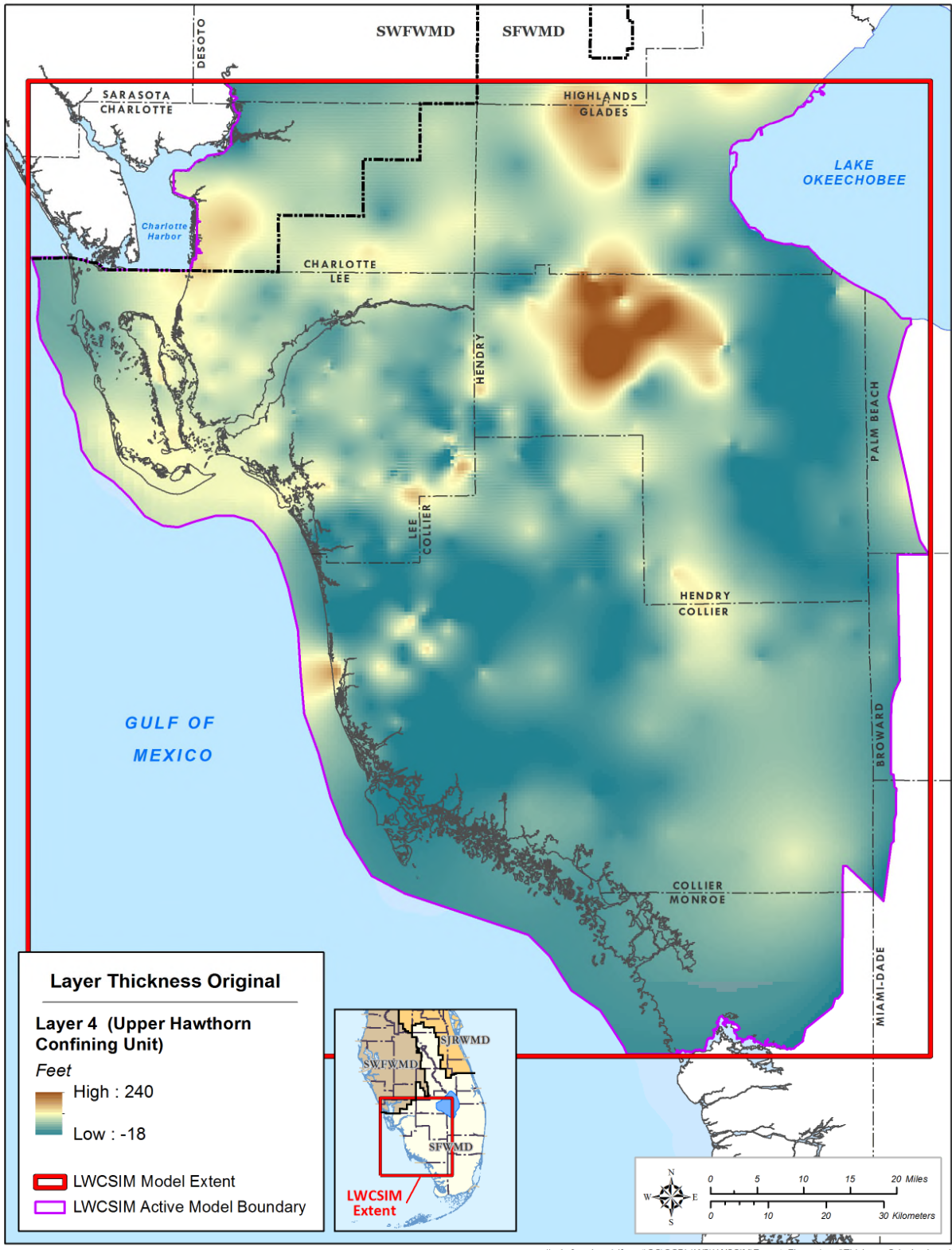


Figure B-14. Thickness of the Upper Hawthorn confining unit.

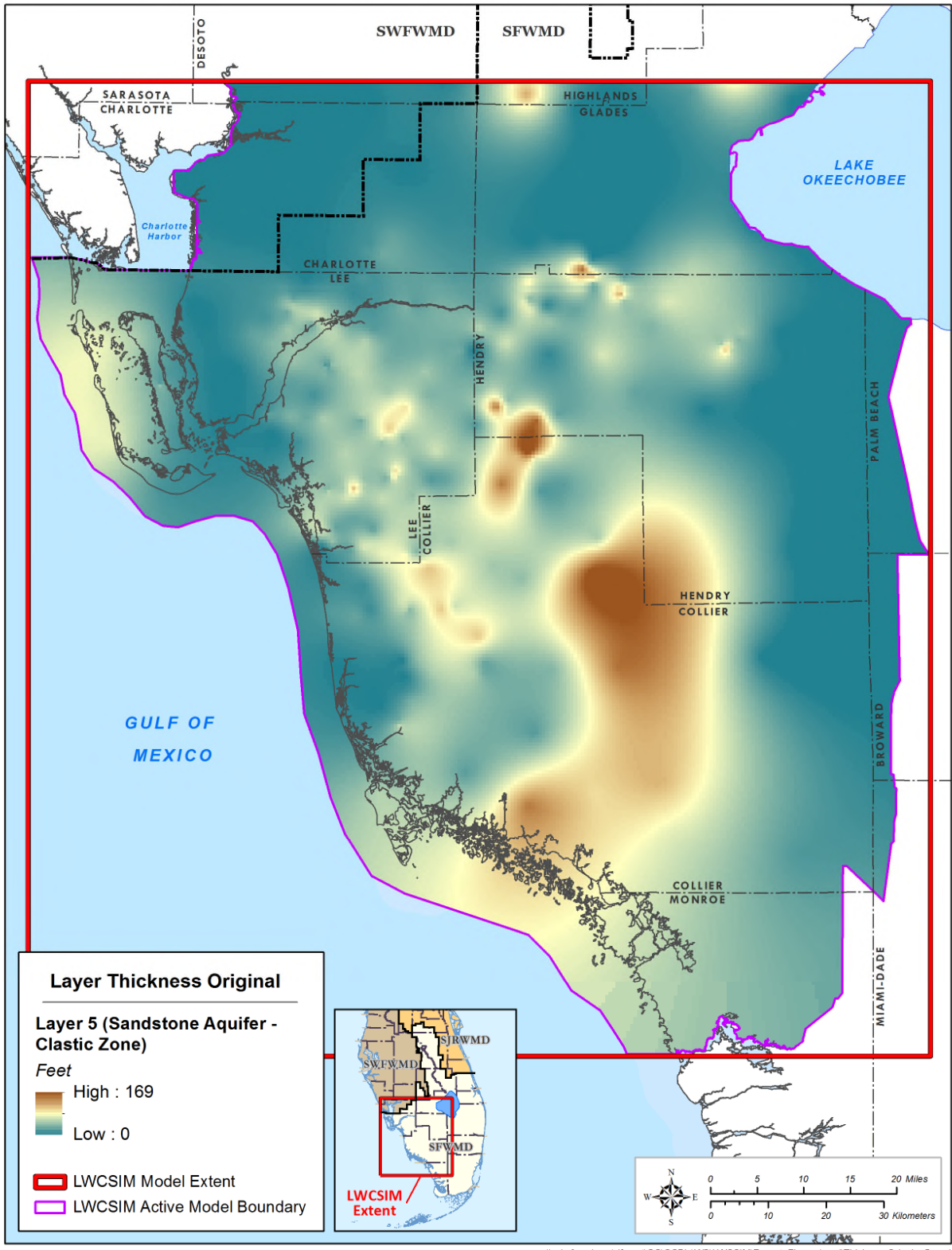


Figure B-15. Thickness of the Sandstone aquifer – clastic zone.

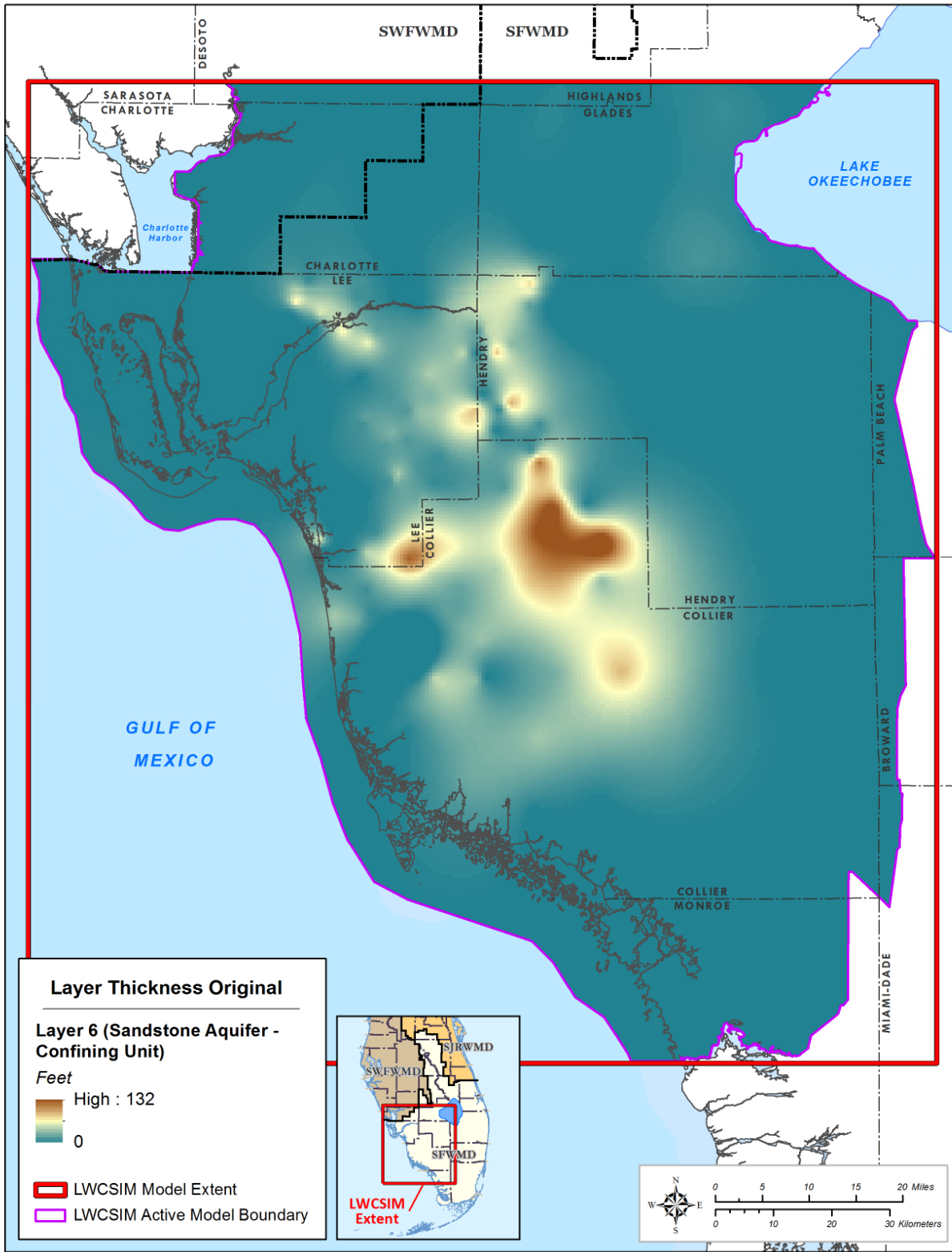
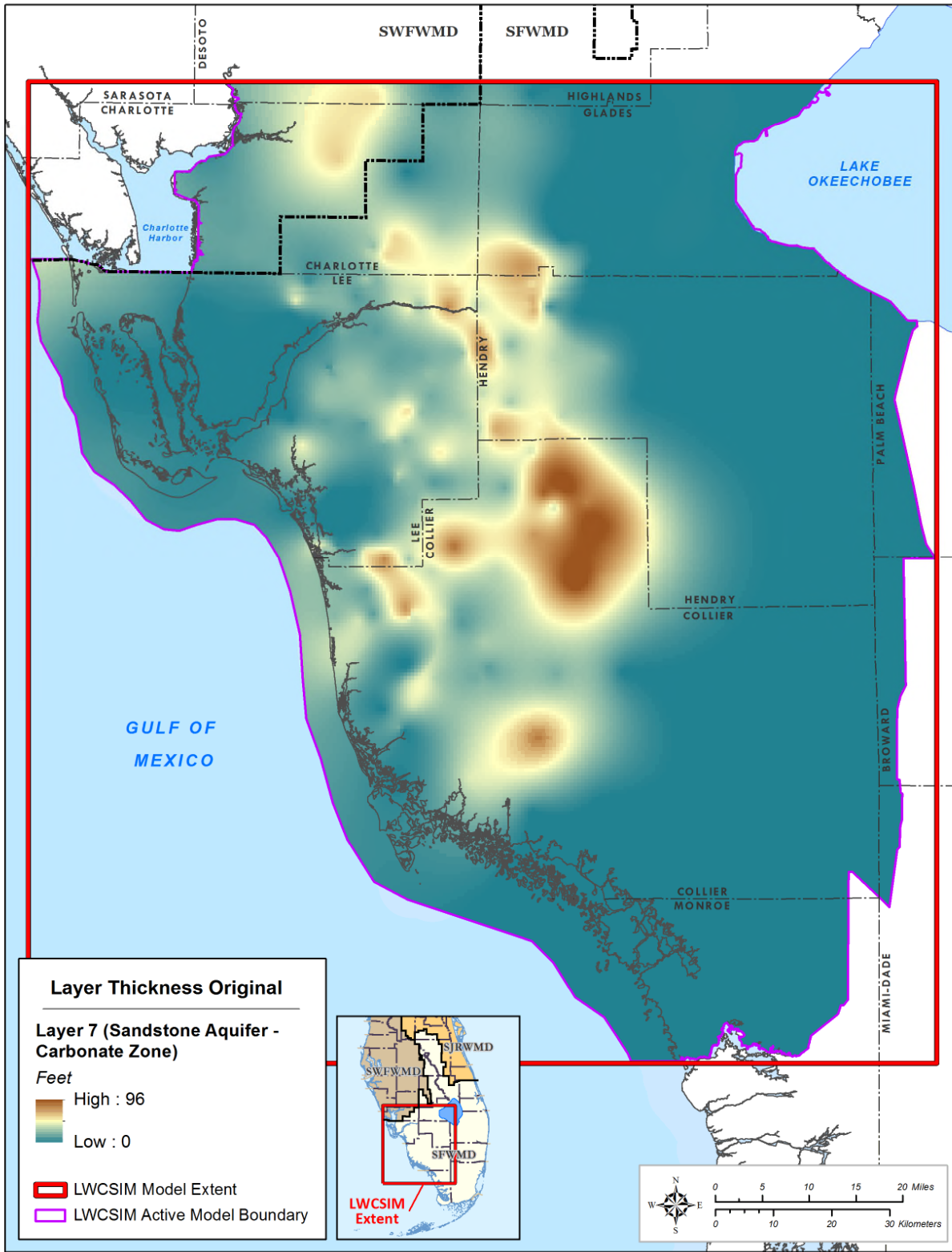


Figure B-16. Thickness of the Sandstone aquifer confining unit.



\\ad.sfwmd.gov\dfsroot\GIS\GSBiz\WS\LWCSIM\Report_Figures\mxd\ThicknessOrig_Lyr7.mxd

Figure B-17. Thickness of the Sandstone aquifer – carbonate zone.

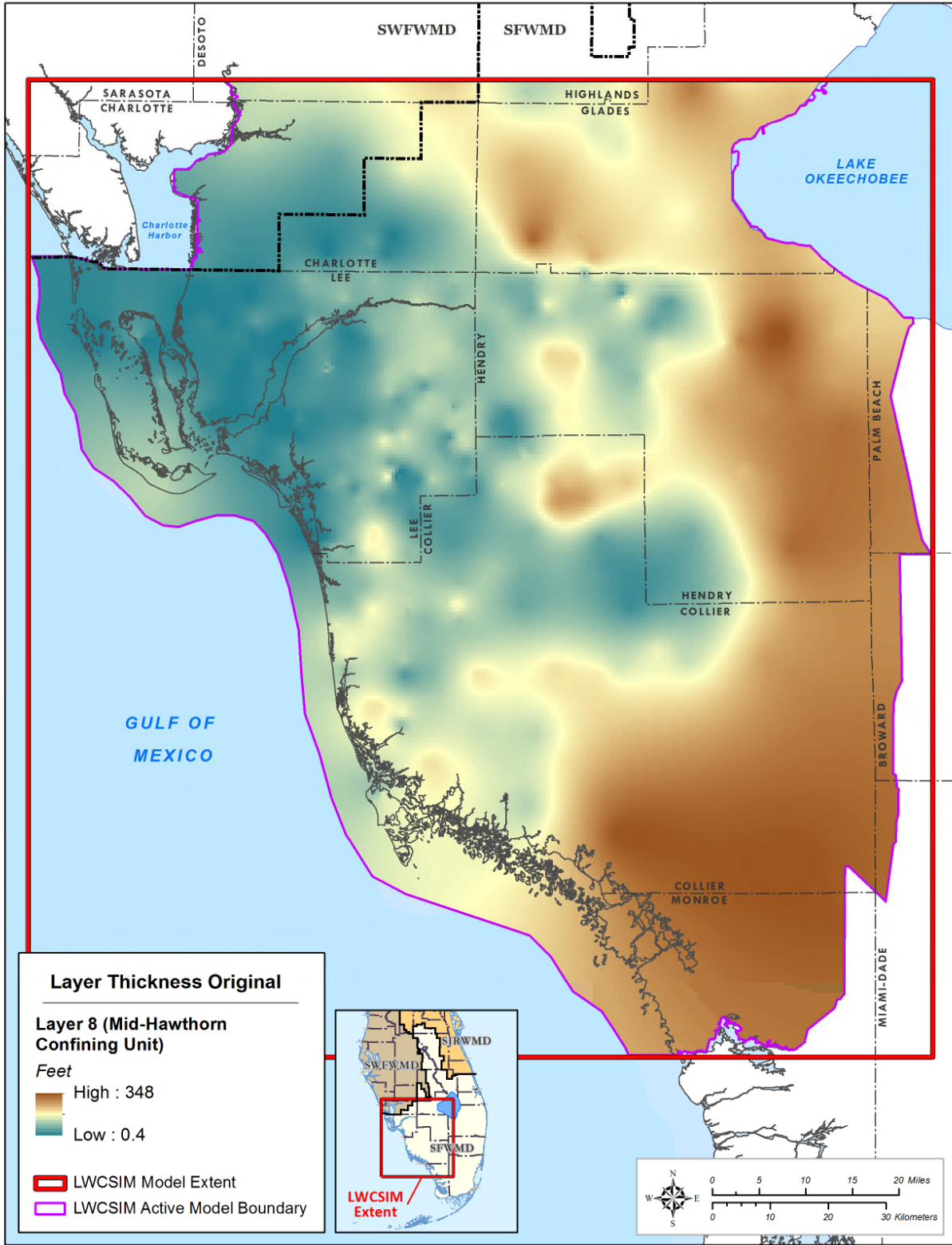


Figure B-18. Thickness of the Mid-Hawthorn confining unit.

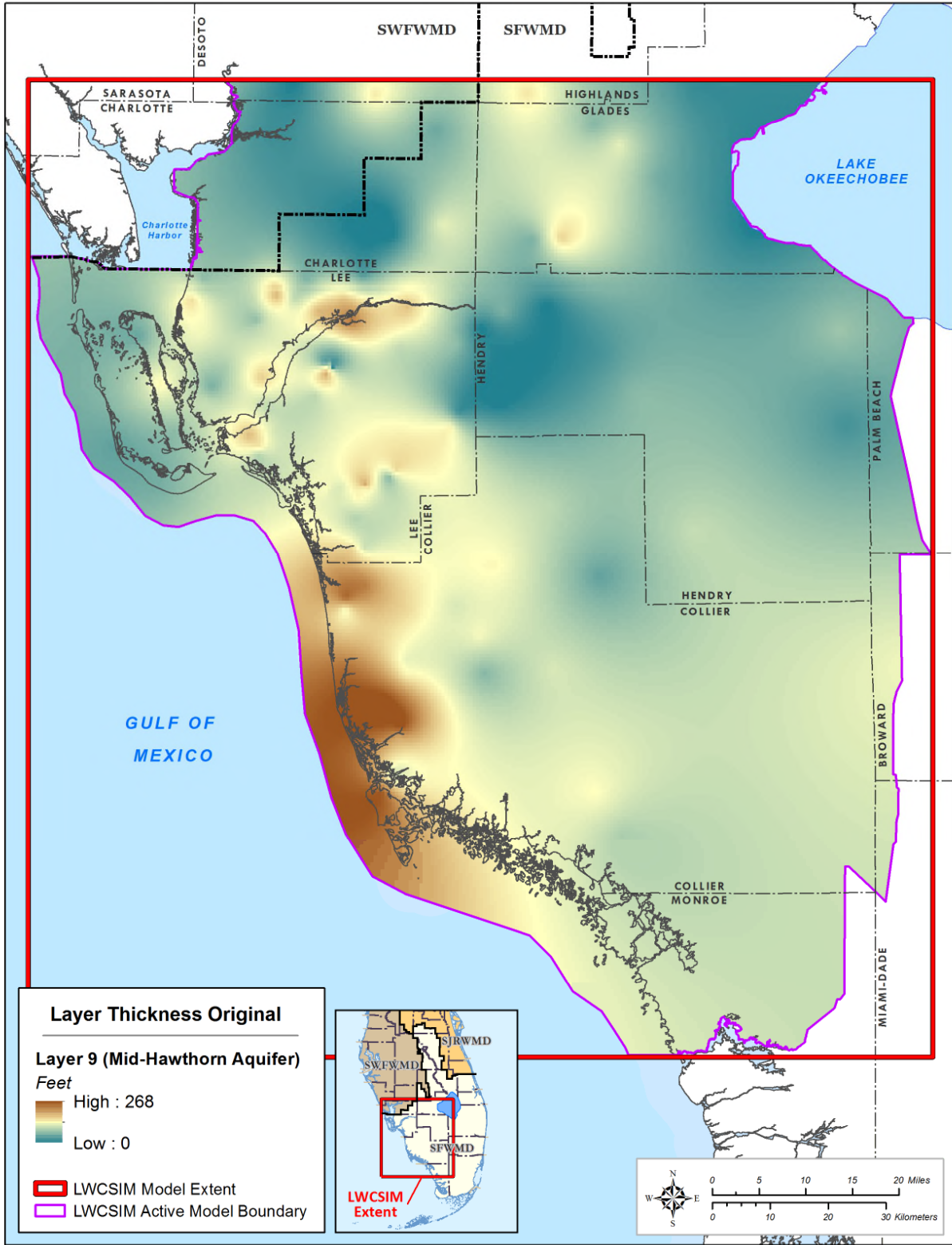


Figure B-19. Thickness of the Mid-Hawthorn aquifer.

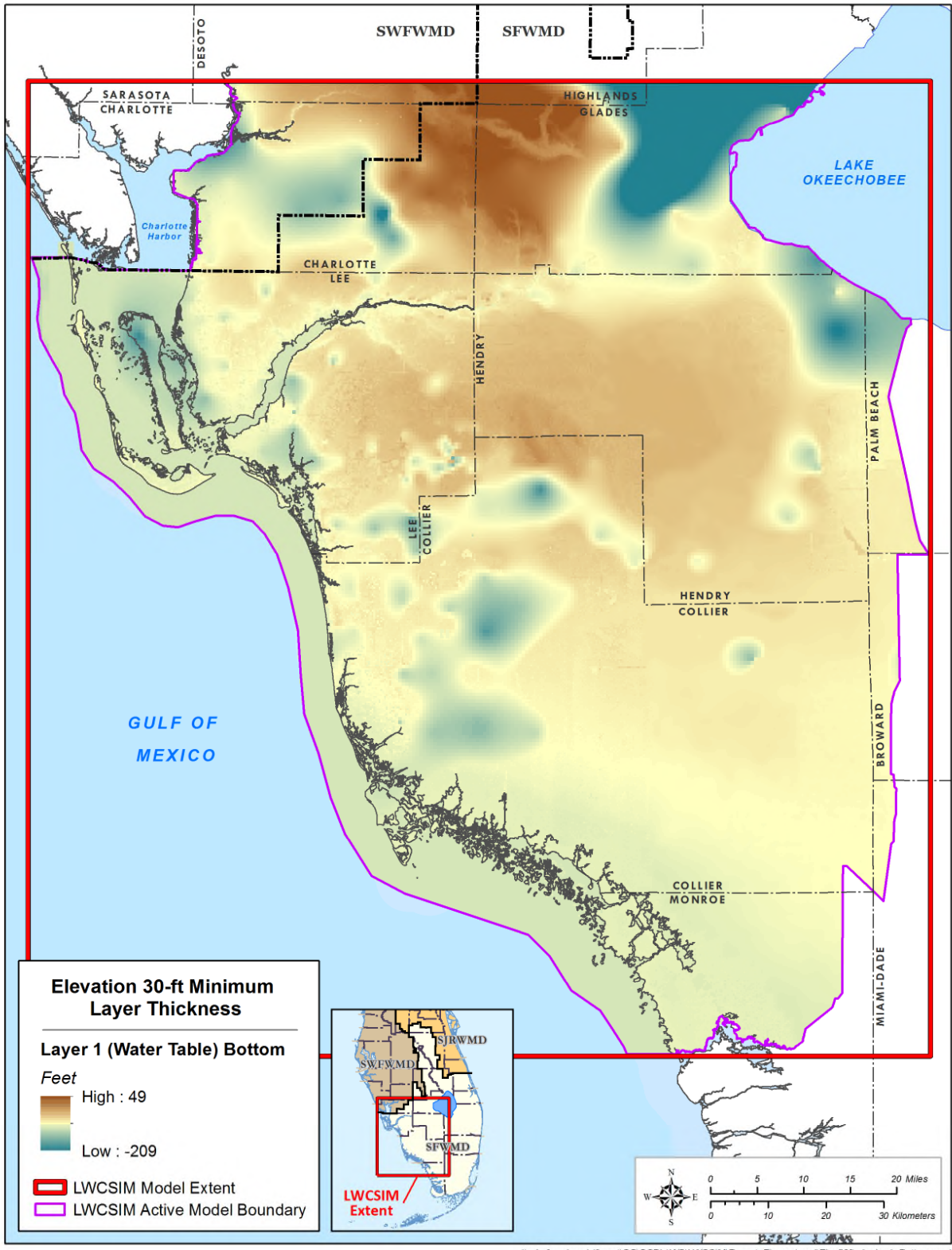


Figure B-20. Simulated bottom elevation of the Water Table aquifer.

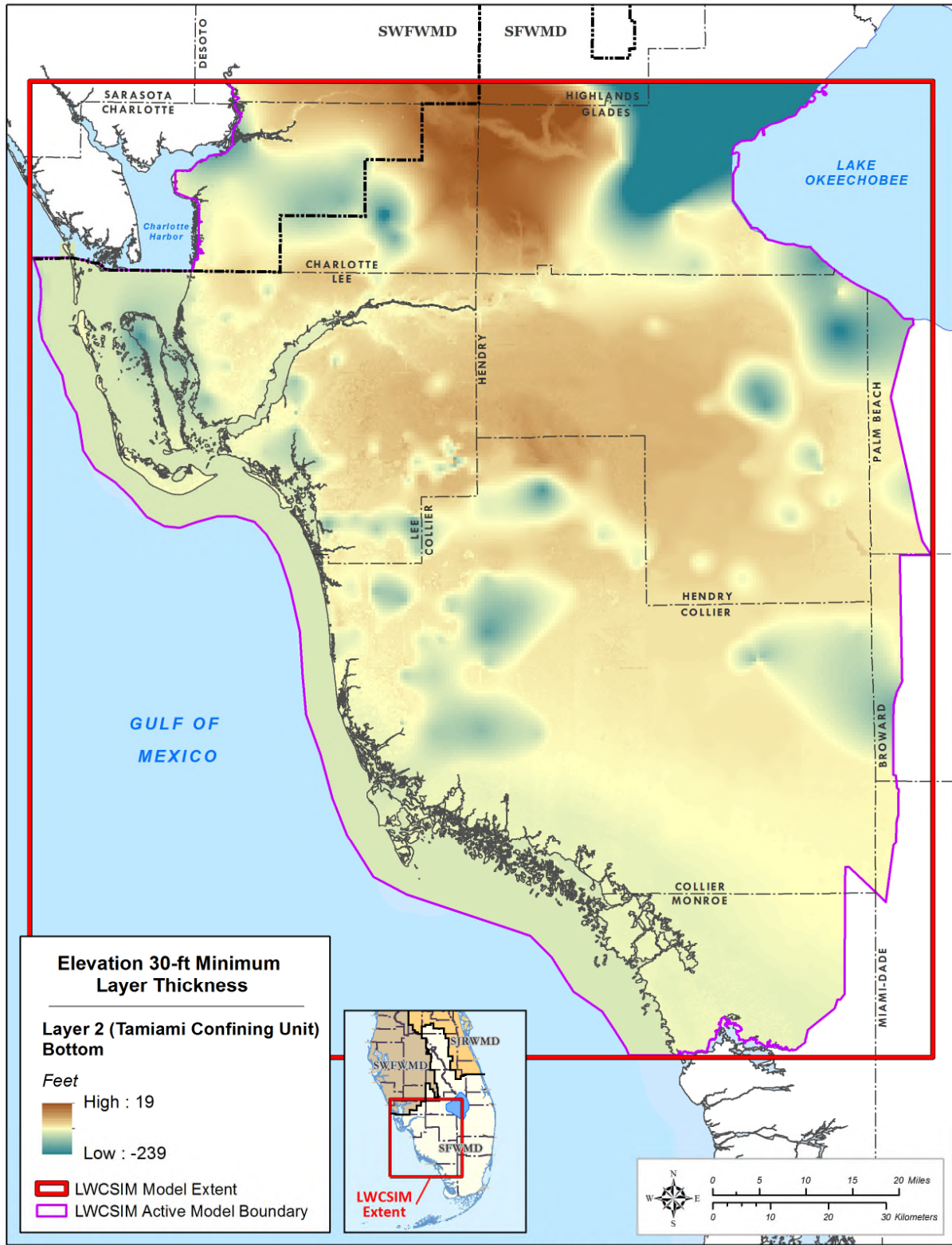


Figure B-21. Simulated bottom elevation of the Tamiami confining unit.

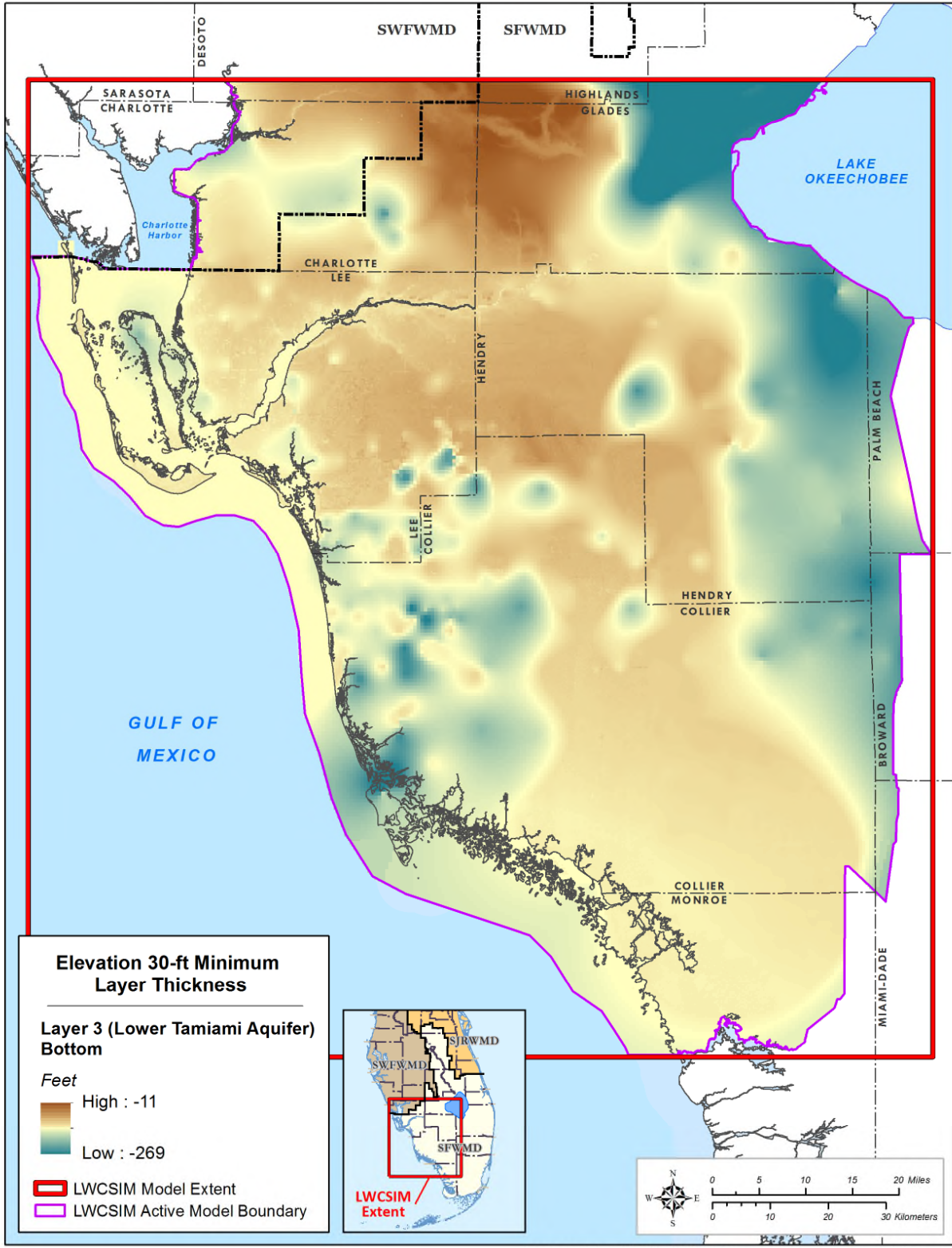


Figure B-22. Simulated bottom elevation of the Lower Tamiami aquifer.

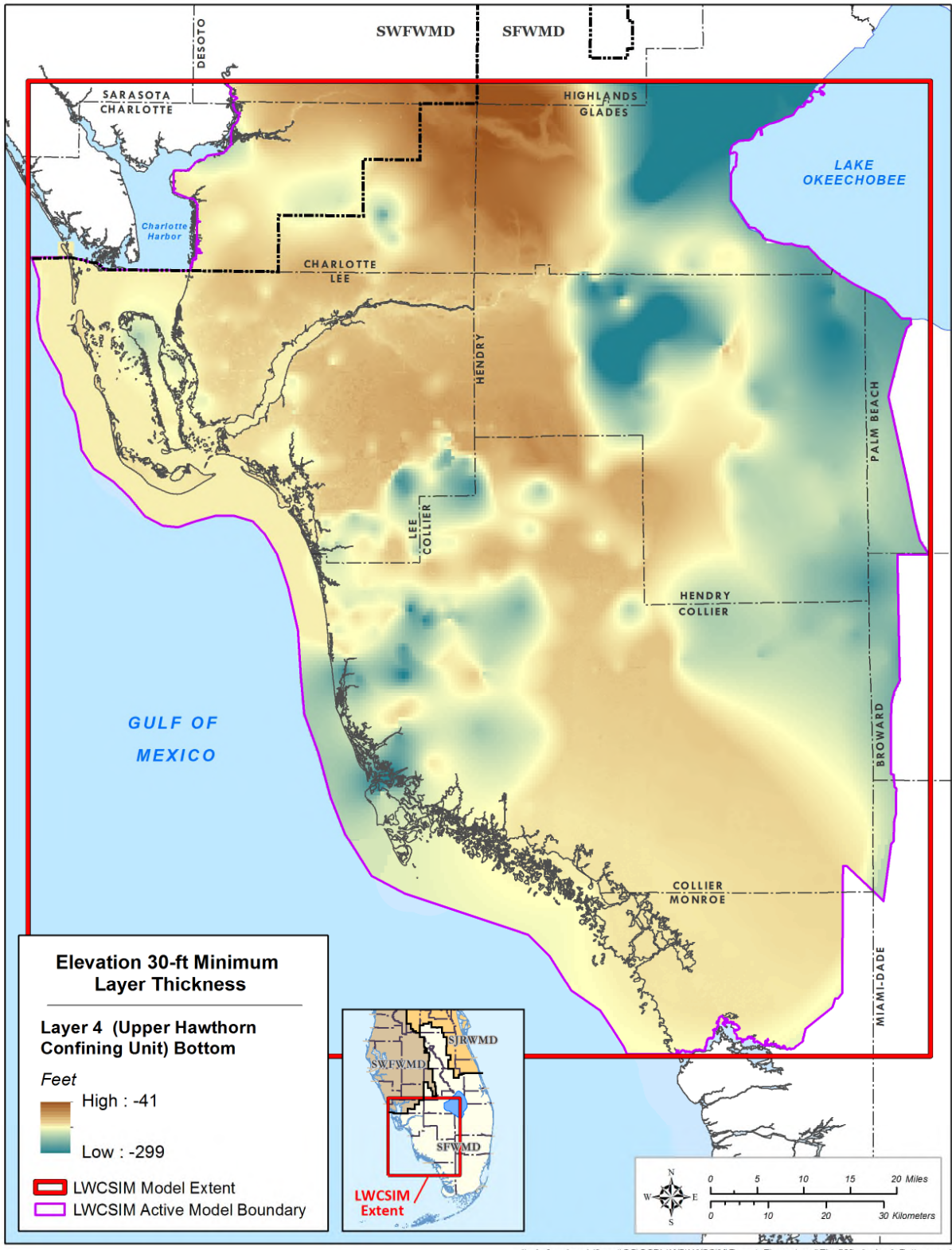


Figure B-23. Simulated bottom elevation of the Upper Hawthorn confining unit.

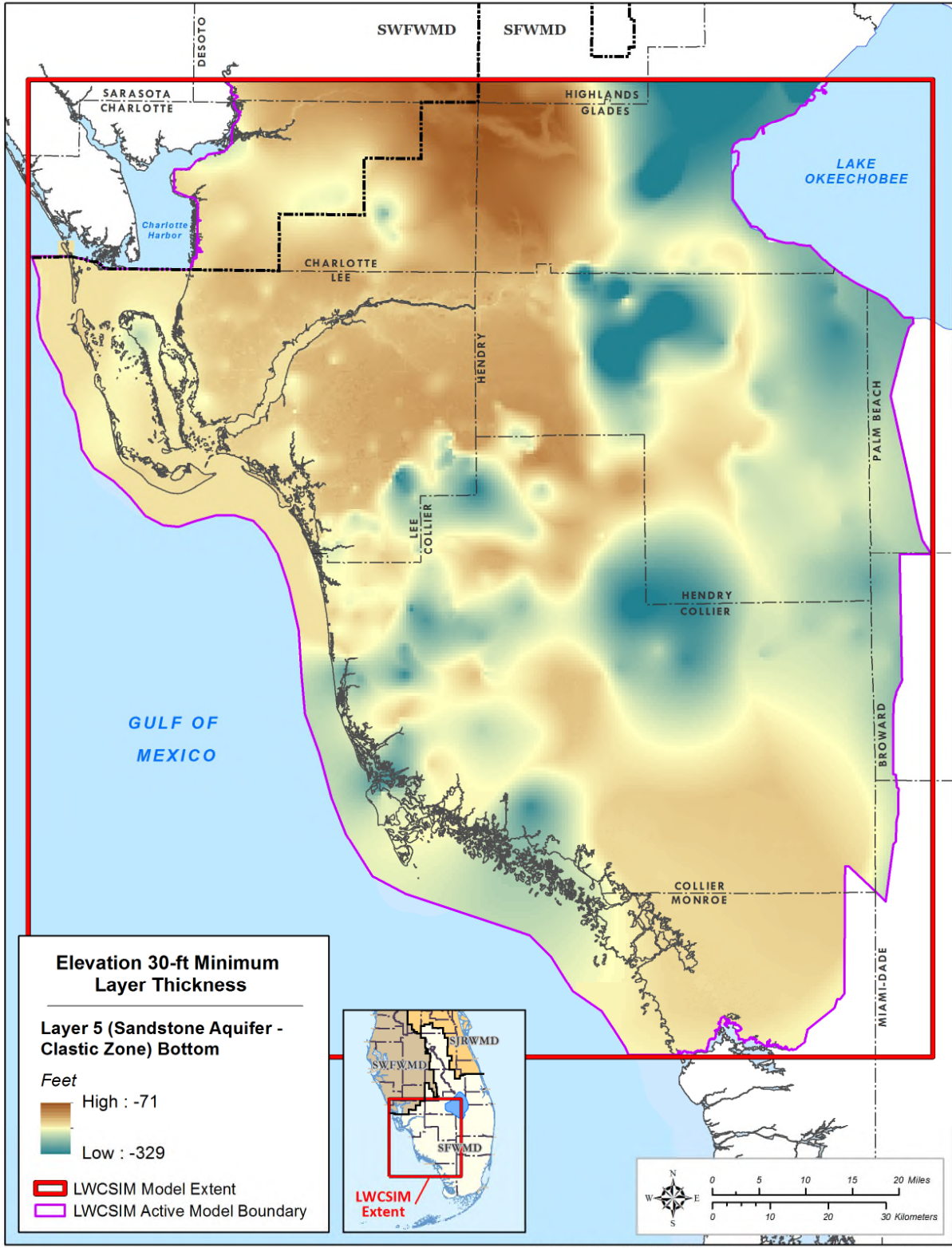


Figure B-24. Simulated bottom elevation of the Sandstone aquifer – clastic zone.

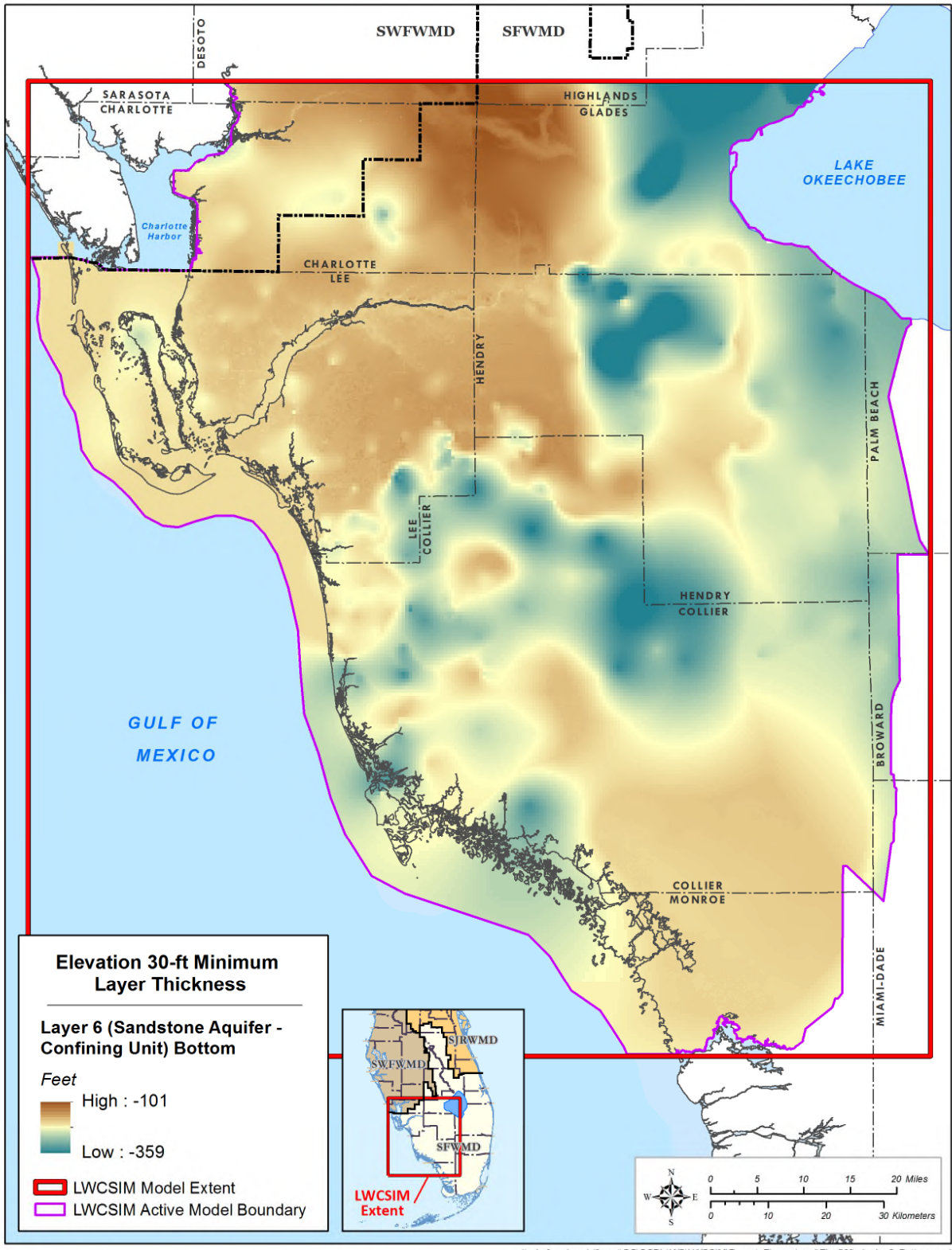


Figure B-25. Simulated bottom elevation of the Sandstone aquifer confining unit.

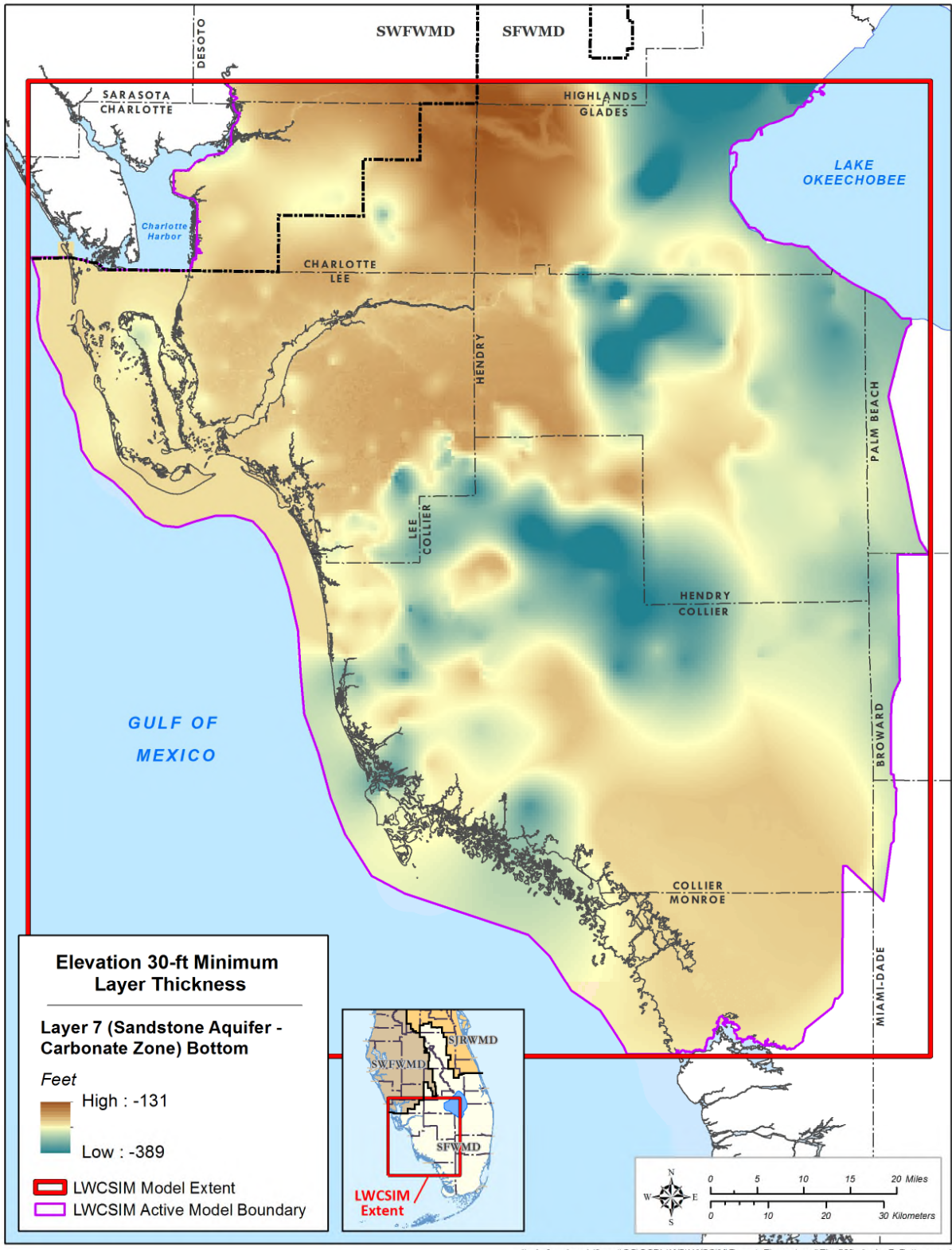


Figure B-26. Simulated bottom elevation of the Sandstone aquifer – carbonate zone.

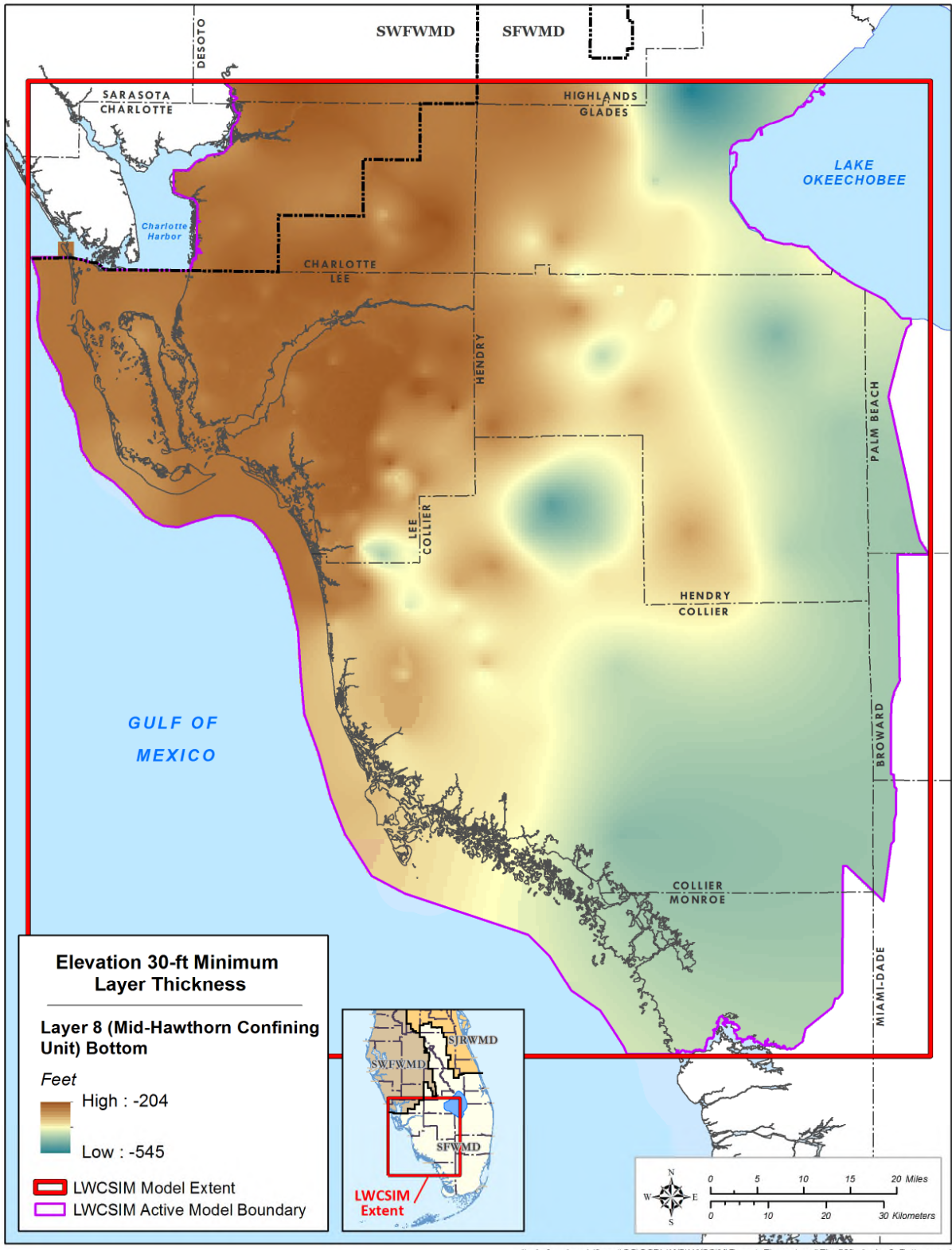


Figure B-27. Simulated bottom elevation of the Mid-Hawthorn confining unit.

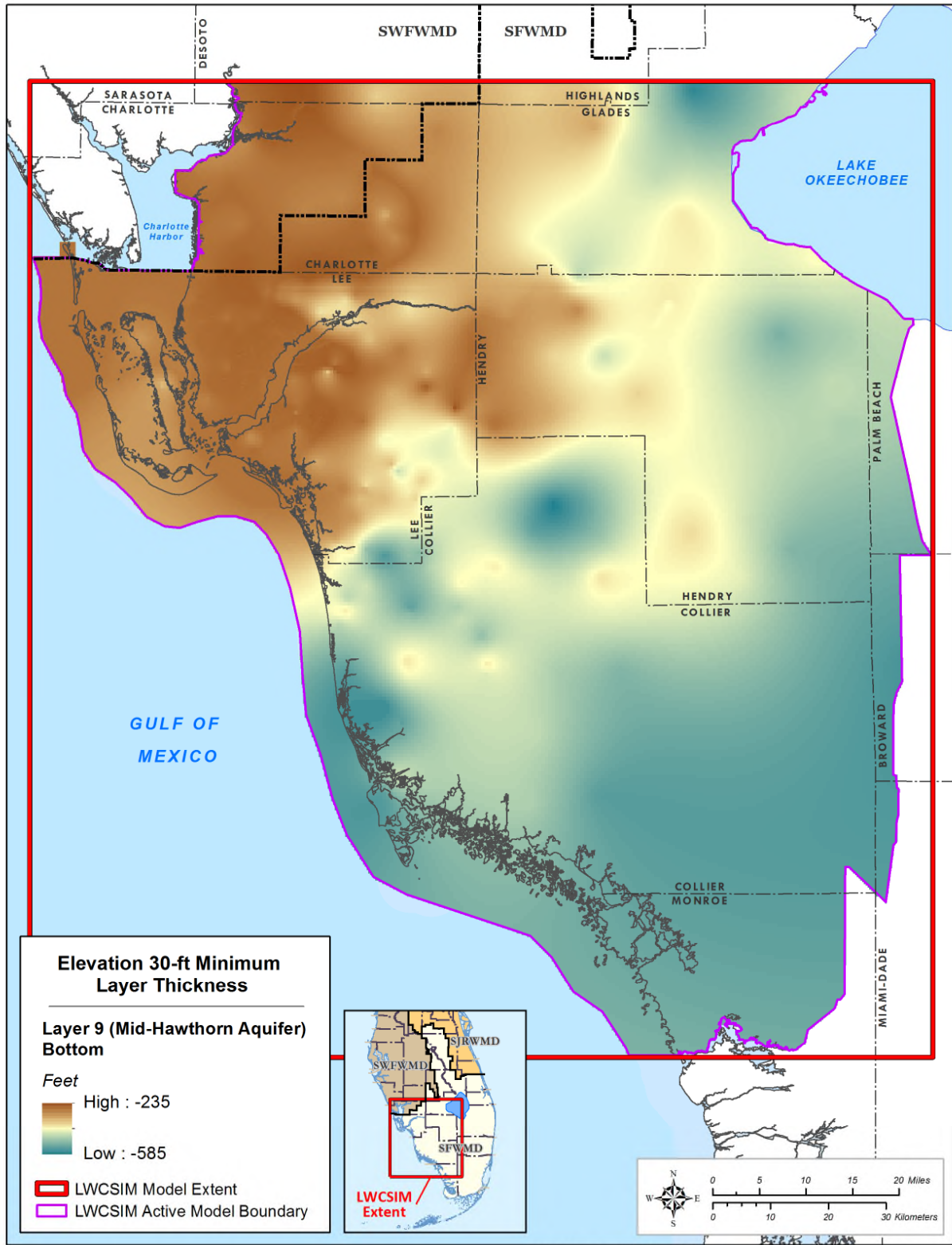


Figure B-28. Simulated bottom elevation of the Mid-Hawthorn aquifer.

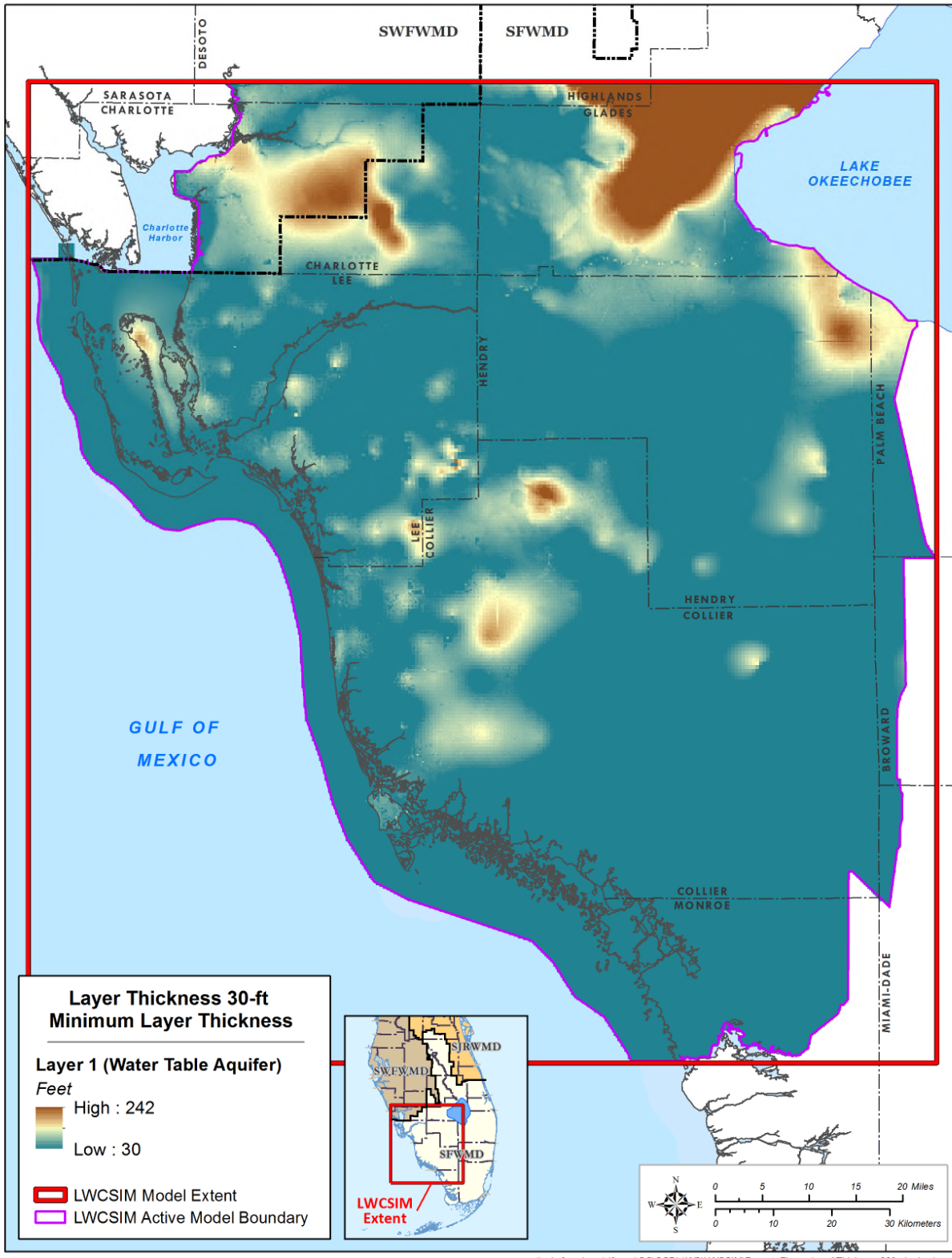


Figure B-29. Simulated thickness of the Water Table aquifer.

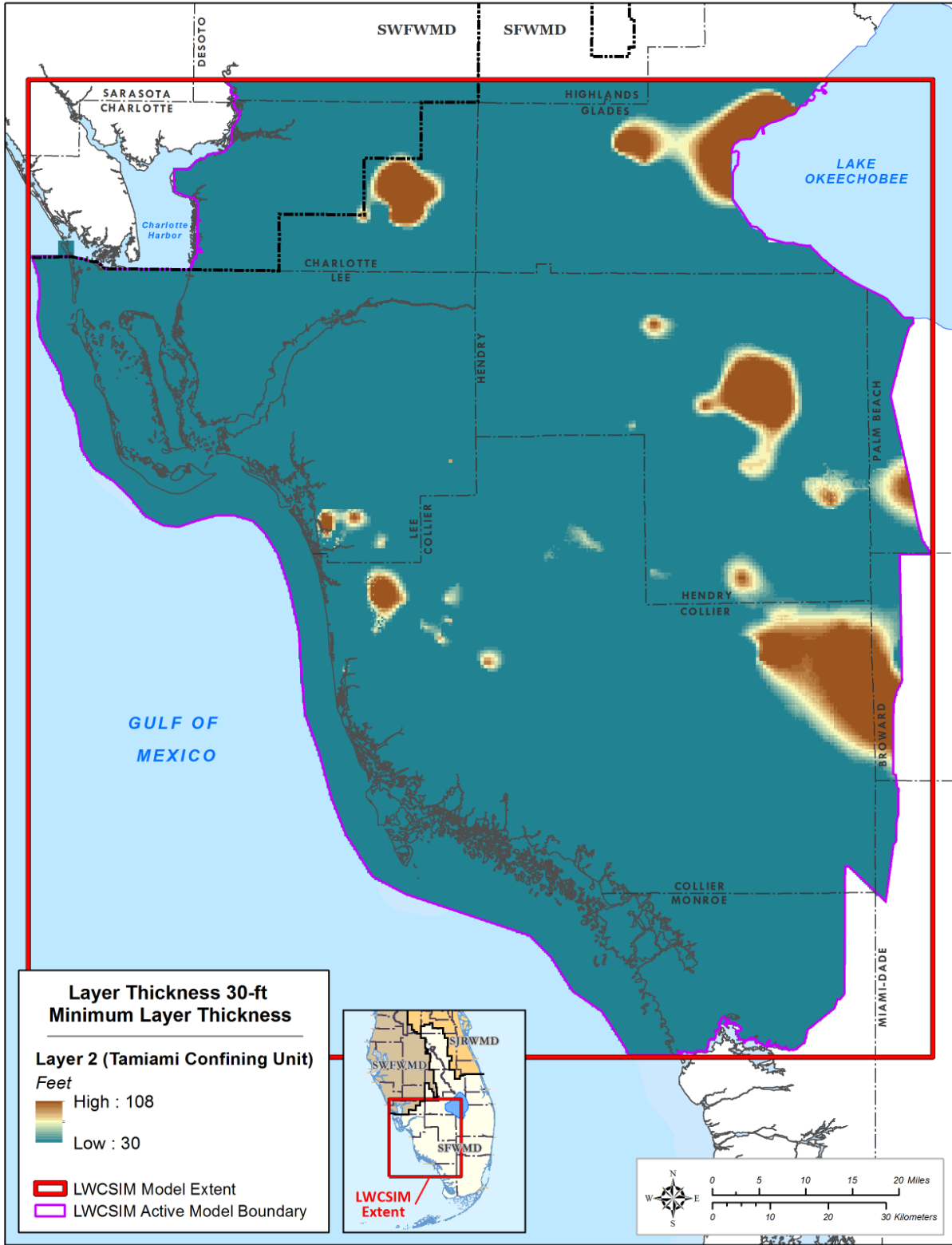


Figure B-30. Simulated thickness of the Tamiami confining unit.

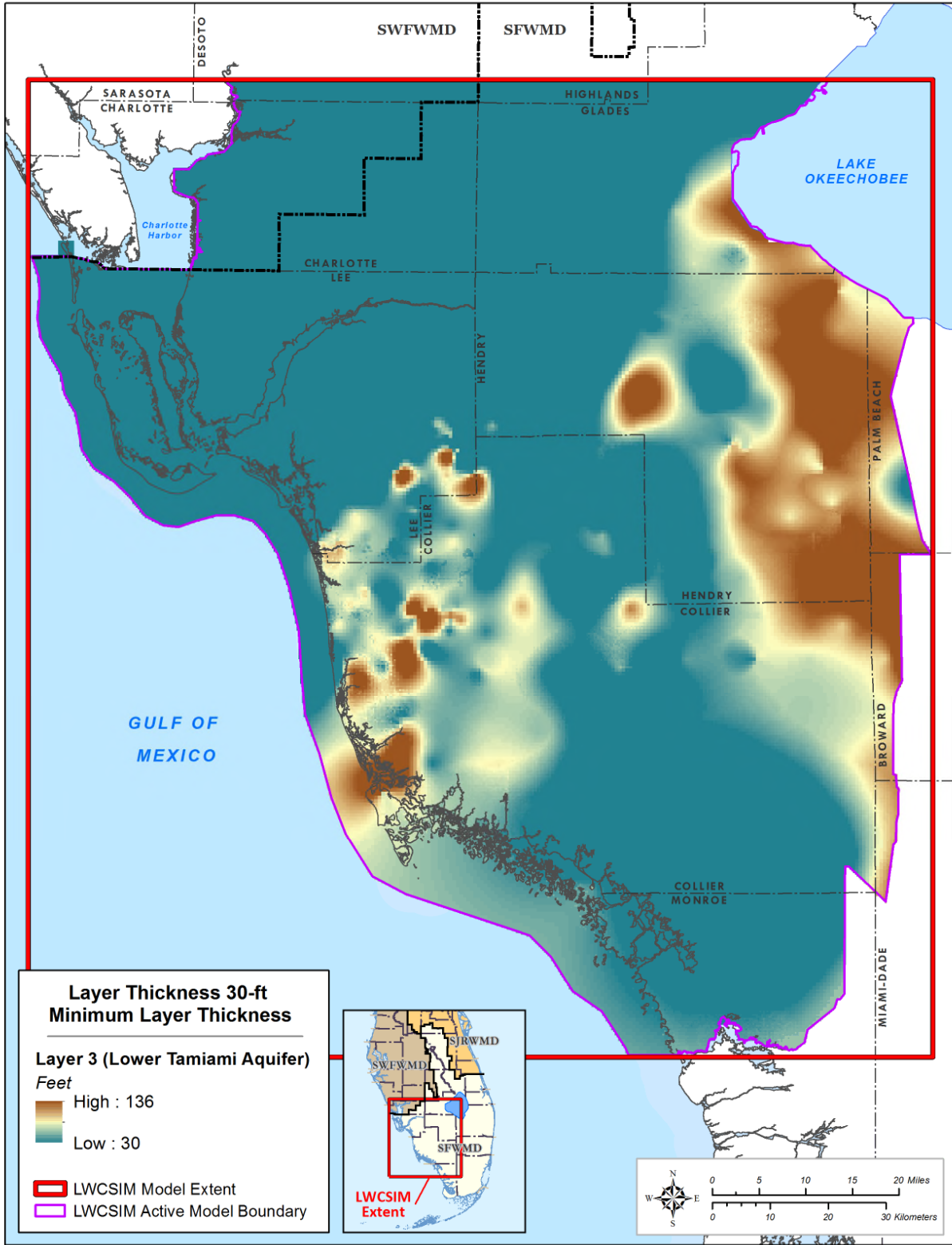


Figure B-31. Simulated thickness of the Lower Tamiami aquifer.

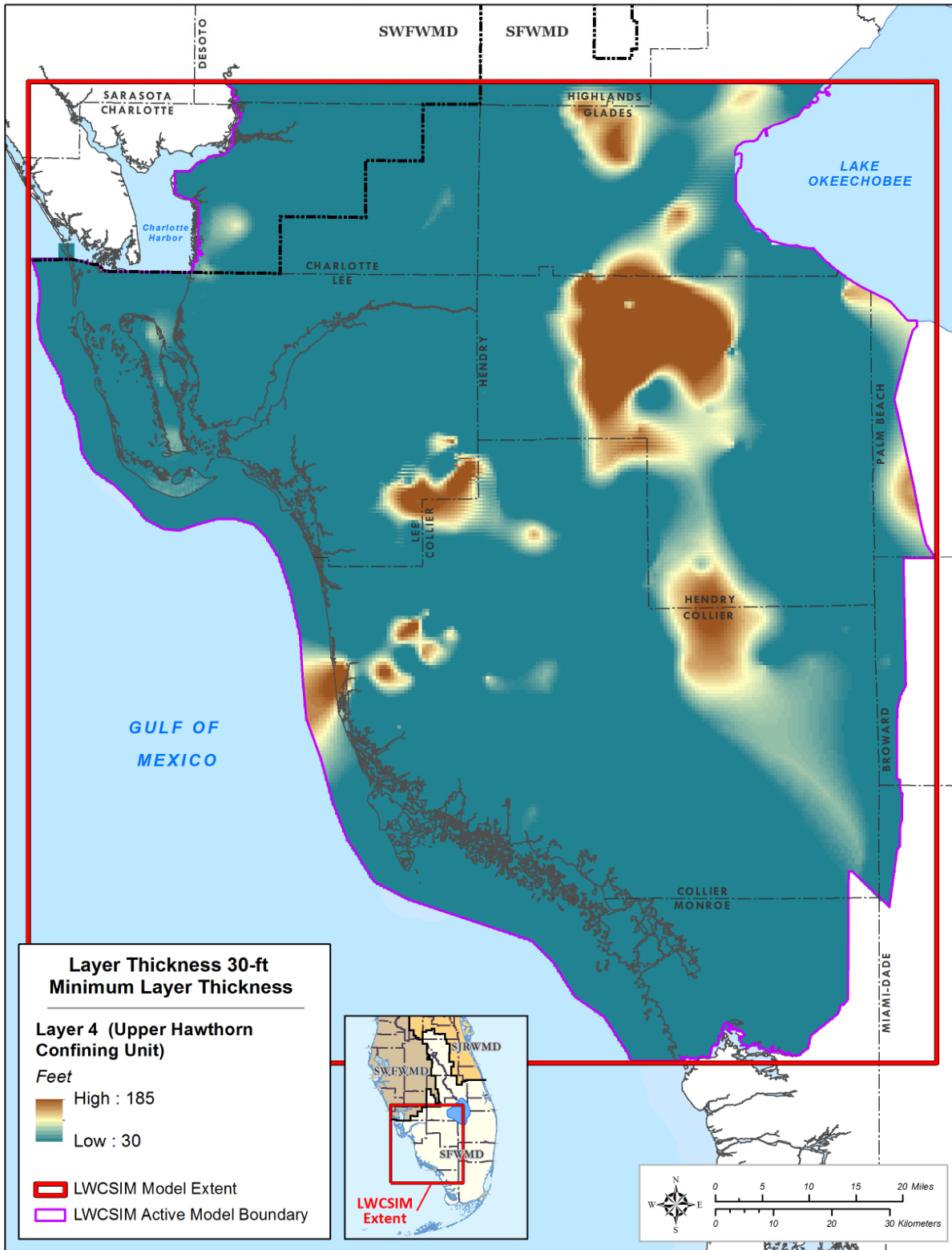


Figure B-32. Simulated thickness of the Upper Hawthorn confining unit.

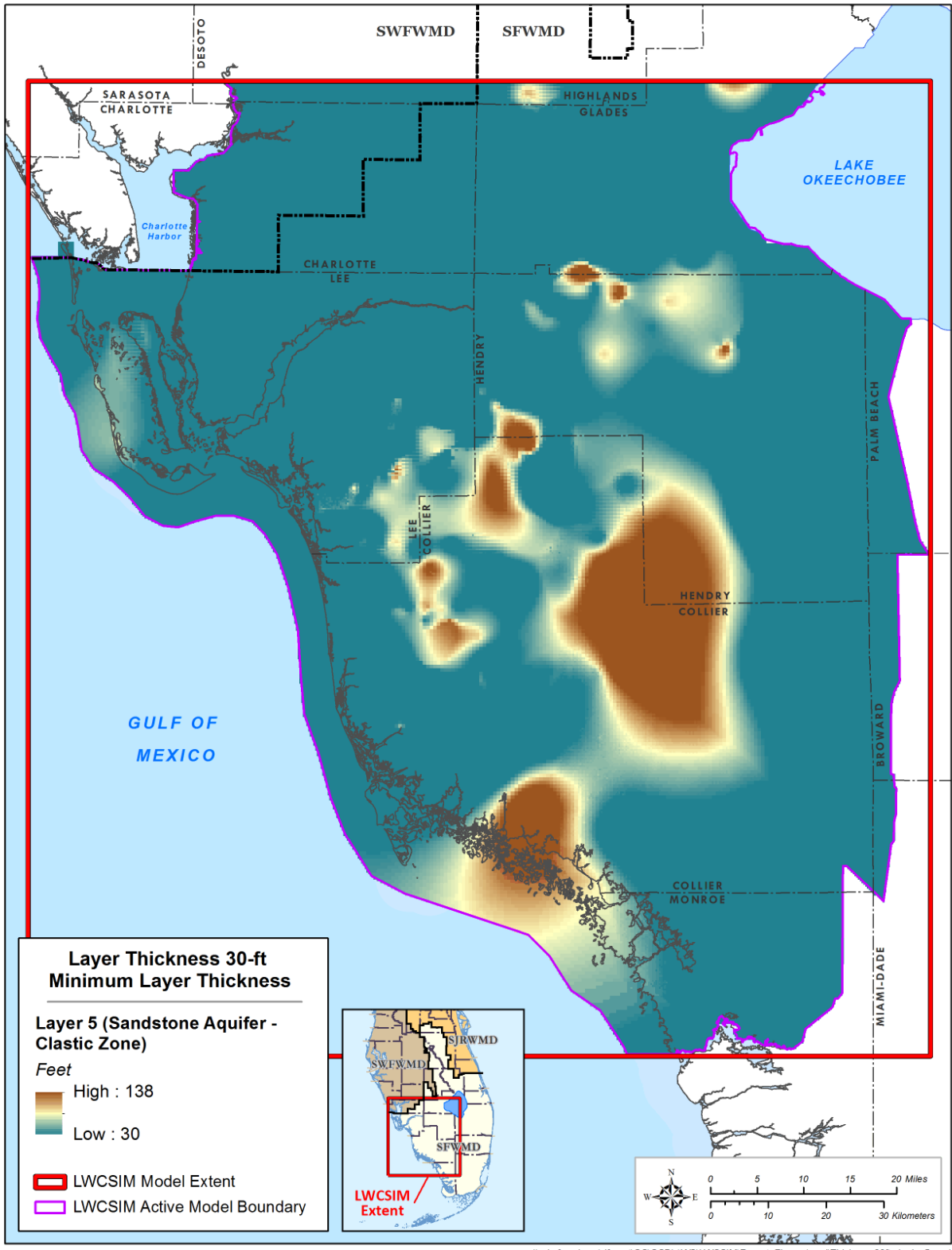


Figure B-33. Simulated thickness of the Sandstone aquifer – clastic zone.

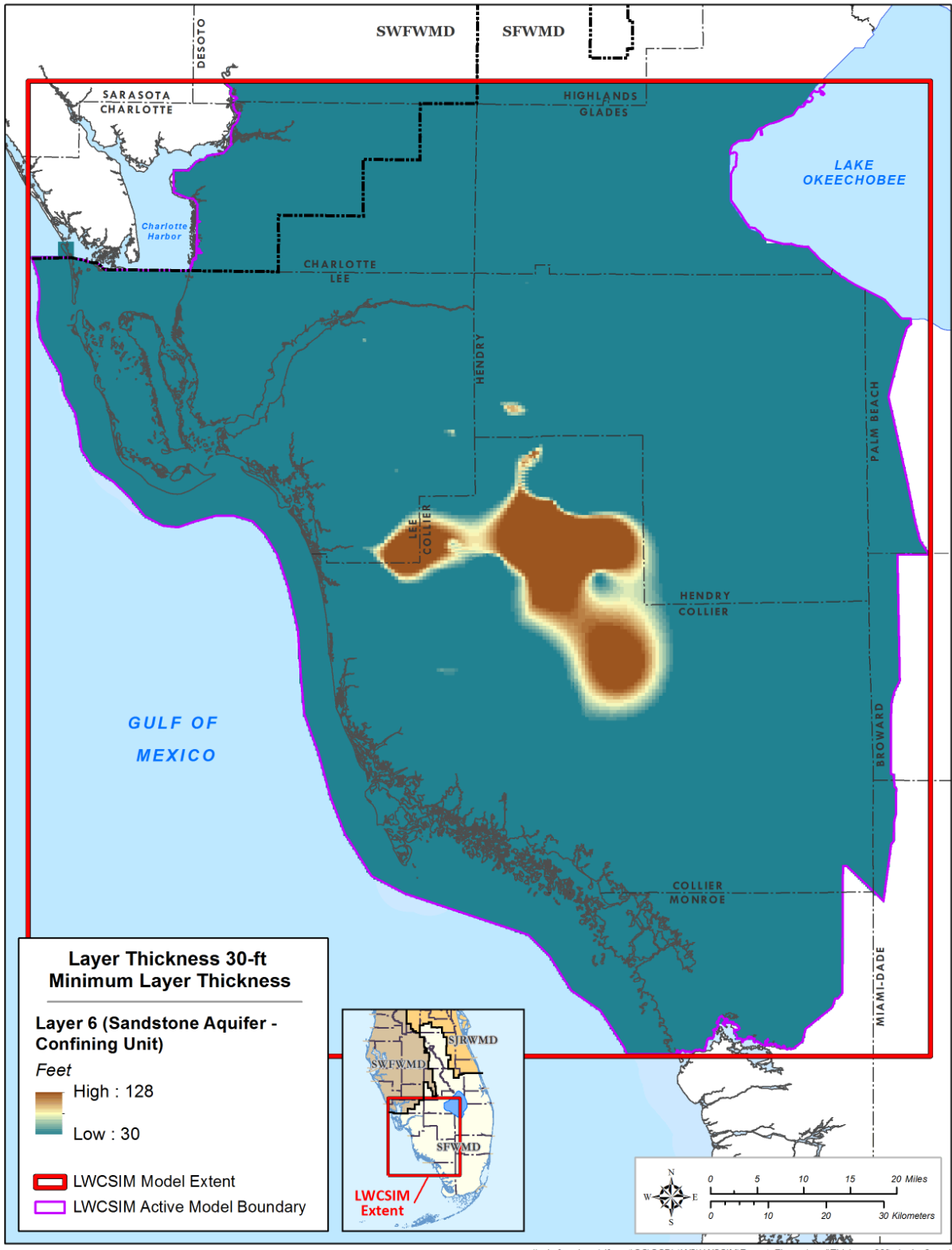


Figure B-34. Simulated thickness of the Sandstone aquifer confining unit.

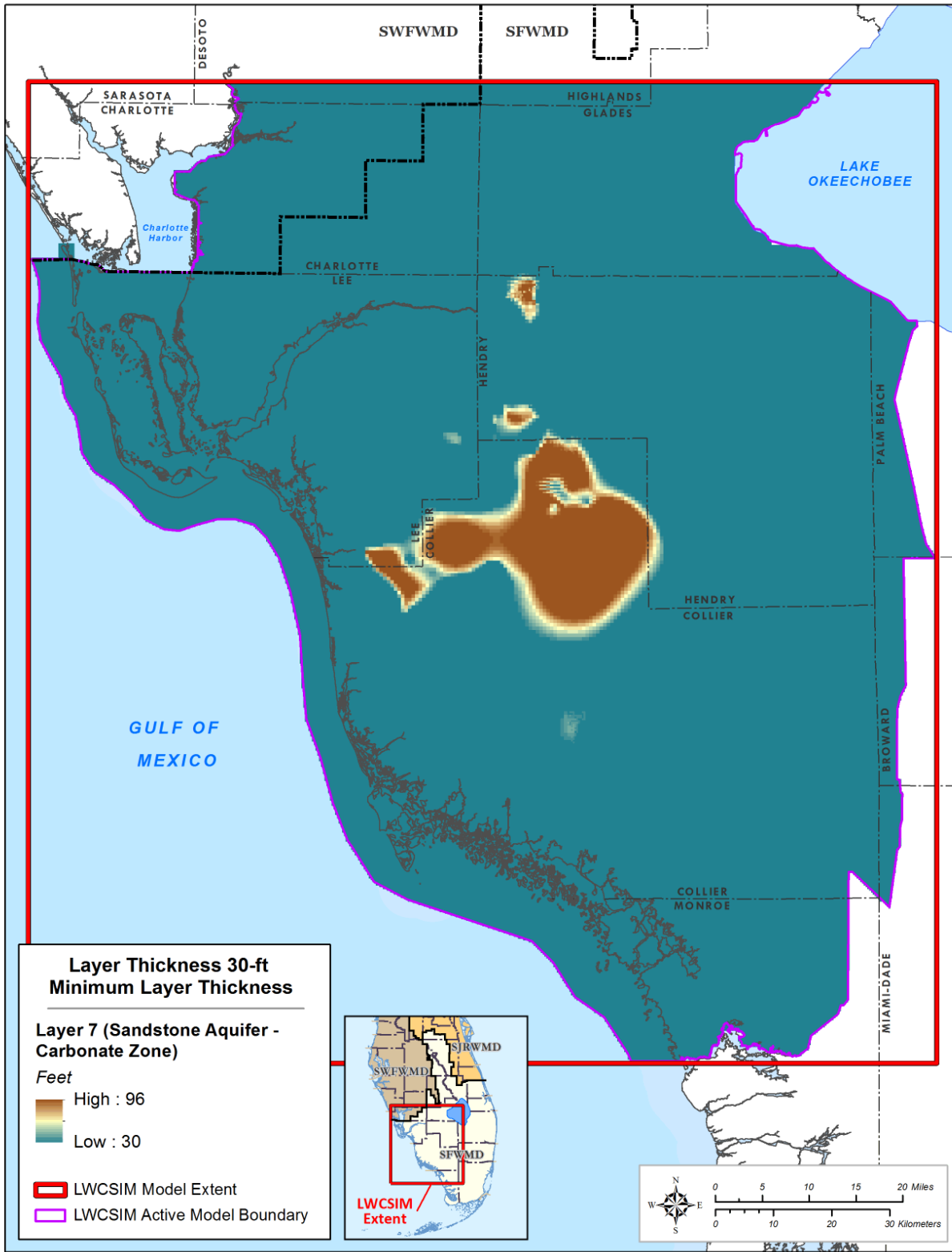


Figure B-35. Simulated thickness of the Sandstone aquifer – carbonate zone.

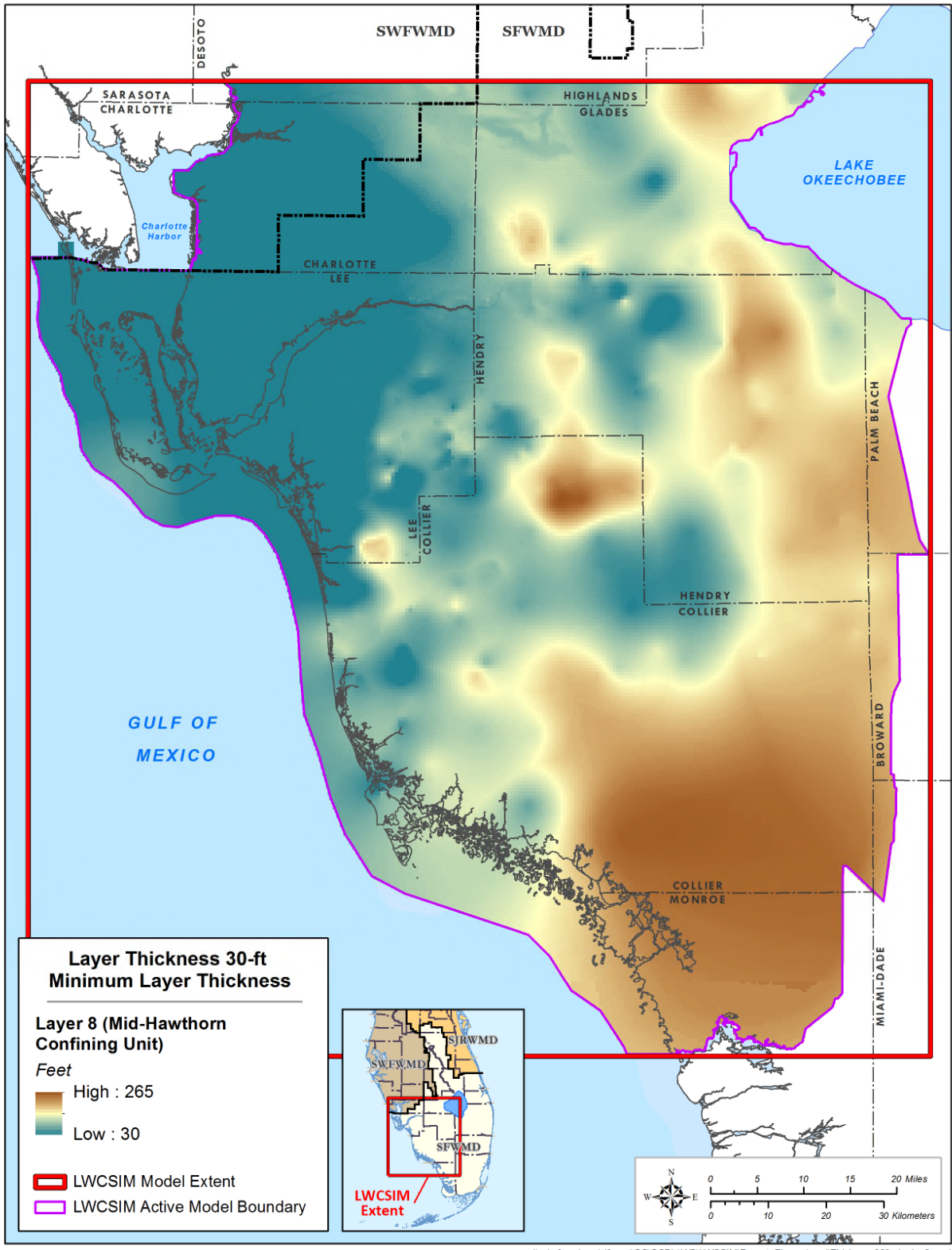


Figure B-36. Simulated thickness of the Mid-Hawthorn confining unit.

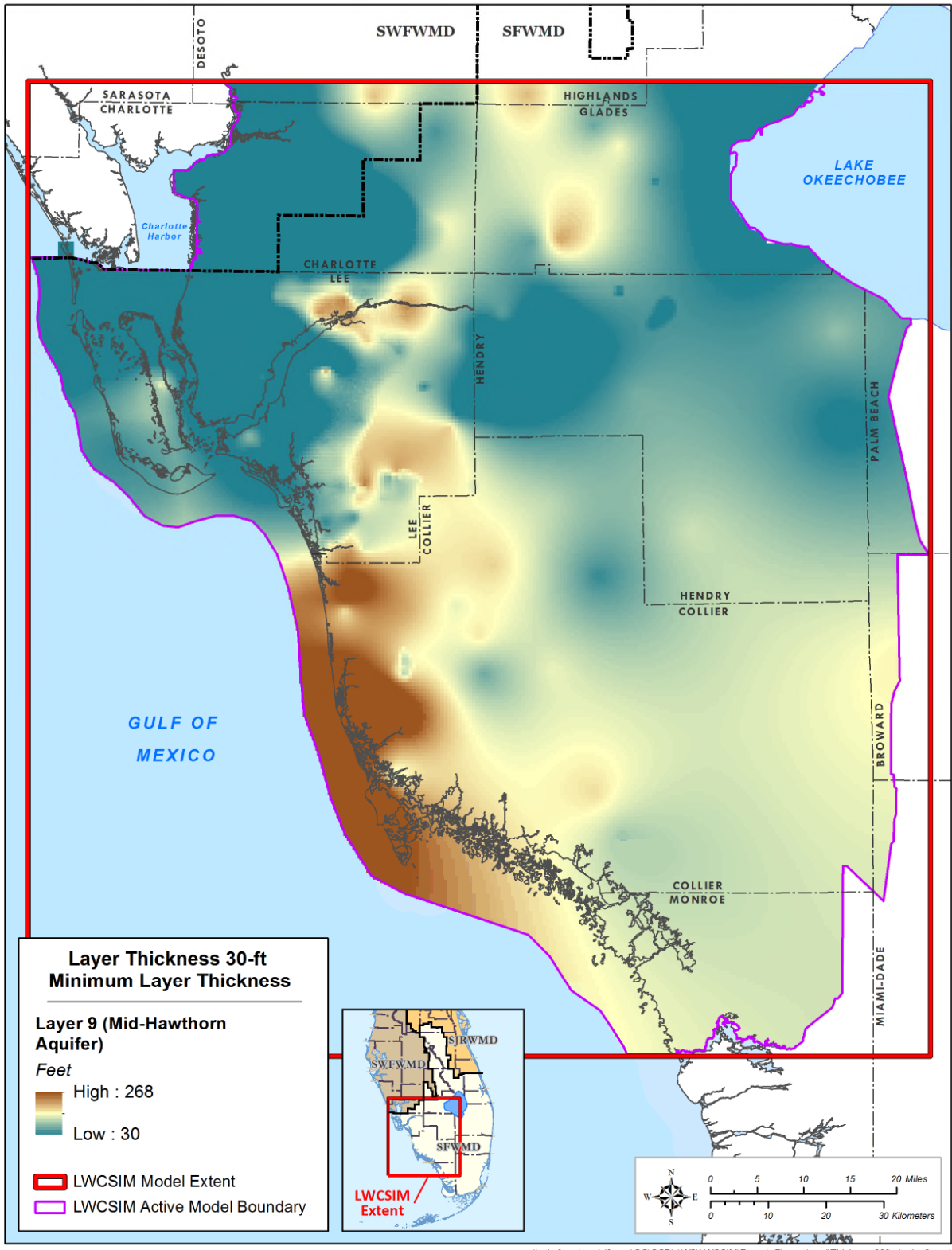


Figure B-37. Simulated thickness of the Mid-Hawthorn aquifer.

**APPENDIX C:
DOMESTIC SELF-SUPPLY COVERAGE PROCEDURE**

An important part of the Lower West Coast Surficial and Intermediate Aquifer Systems Model (LWCSIM) is the placement of pumping wells via the WEL package. The WEL package includes wells representing the full range of water being extracted from the various shallow and intermediate aquifers throughout the Lower West Coast (LWC) Planning Area. Public supply wells, agricultural and commercial irrigation wells, and domestic self-supply (DSS) wells are represented in the model. This memo describes the compilation of DSS wells for the WEL package.

DSS well data from Lee, Collier, Glades, and Hendry counties were compiled from several sources. The initial source was the Marco Water Engineering, Inc. (2006) groundwater flow model of the LWC Planning Area surficial aquifer system. Chapter 2 of the Marco Water Engineering, Inc. (2006) report explained that, while residential water use represents the smallest demand compared to other categories, the projected population increase in coastal regions (primarily in Lee and Collier counties) could significantly impact (increase) groundwater demand. Due to limited funding and well data availability, Marco Water Engineering, Inc. (2006) only considered the 18,432 DSS wells in Lee County (**Figure C-1**).

The Marco Water Engineering, Inc. (2006) model report did not detail how the DSS well coverage was derived. Therefore, the South Florida Water Management District (SFWMD) chose to compile the LWCSIM DSS well coverage using a combination of internal (SFWMD) and external (county) information sources. The SFWMD requested information on DSS wells, including location, casing depth, and total depth, from county officials in Lee, Collier, Hendry, and Glades counties. DSS well information was provided as geographic information system (GIS) shapefiles or Excel spreadsheets that were converted to GIS shapefiles so all DSS wells could be located in the model domain. Information from Lee and Collier counties was the most extensive and most complete. County DSS well data were combined into a comprehensive, consistent Excel table containing all pertinent data fields, including county, state plane coordinates, well casing depth, well total depth, and per capita use rate (PCUR). GIS was used to intersect the well locations with the LWCSIM grid to assign a row and column to each well.

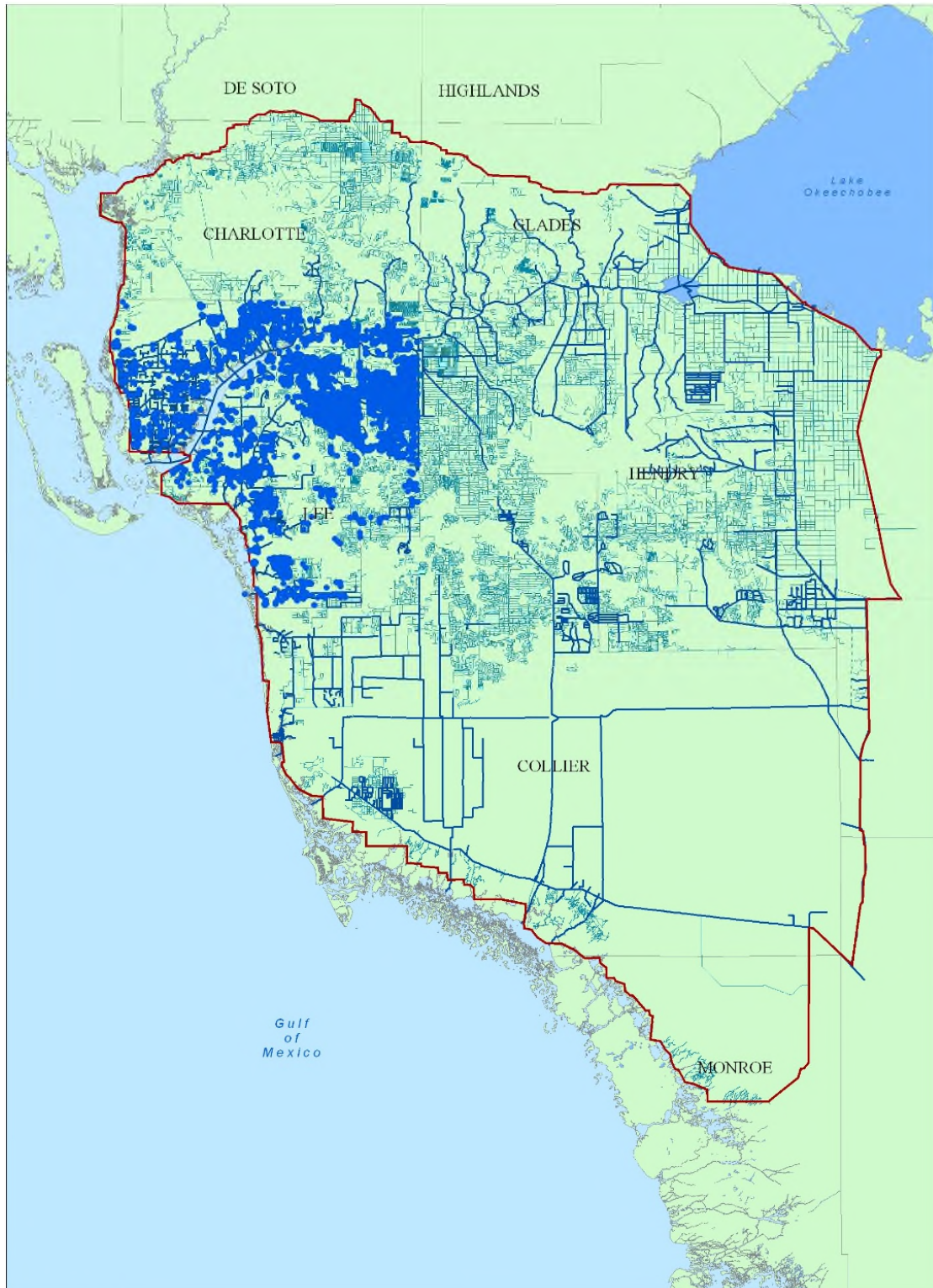
The PCUR initially was calculated from information in the 2012 LWC Water Supply Plan Update (SFWMD 2012). The plan update contains projections of DSS populations and water demand by county. Specifically, in Appendix A of the plan update, Tables A-1 to A-8 contain the data that were used to calculate a PCUR for all DSS wells in Lee, Collier, Hendry, and Glades counties. According to the plan update, the PCUR is the total annual water use divided by the permanent residents. For example, to calculate the net average PCUR for DSS wells in Lee County in 2005:

1. DSS population = 68,566 permanent residents
2. Net average DSS water demand = 8.37 million gallons per day (mgd) = 8,370,000 gallons per day (gpd)
3. $PCUR = 8,370,000 \text{ gpd} \div 68,566 \text{ permanent residents} = 122 \text{ gpd per person (gpd/p)}$

The PCUR also was calculated for net 1-in-10-year drought conditions (129 gpd/p), gross average (147 gpd/p), and gross 1-in-10-year drought conditions (156 gpd/p). The average of those four PCURs is 139 gpd/p.

Each county's overall average PCUR based on the 2012 LWC Water Supply Plan Update are as follows:

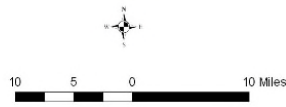
- Collier County = 219 gpd/p
- Glades County = 139 gpd/p
- Hendry County = 131 gpd/p
- Lee County = 139 gpd/p



Legend

lwc_boundary

rss wells



Residential Wells

Figure C-1. Domestic Self-Supply well coverage (From: Marco Water Engineering, Inc. 2006).

Discussions with SFWMD Water Supply Planning staff indicated a better estimate of the PCUR might be obtained using the SFWMD's Water Supply Utility Project (WaSUP) database of finished residential water demand as reported by each public supply utility. Based on these numbers, each county's average PCUR was adjusted to the following:

- Collier County = 123.67 gpd/p
- Glades County = 114.58 gpd/p
- Hendry County = 67.43 gpd/p
- Lee County = 71.05 gpd/p

The derived PCURs were used as starting points for assigning extraction rates to model cells representing DSS wells. Rates per model layer per model cell were determined and assigned using well casing depth and total depth to determine which model layer(s) were being tapped, accounting for model cells that contain more than one DSS well. It was decided that the PCUR represents water used per person and that each household well provides water for an average of three persons. Therefore, a factor of three was included to determine the final pumping rate per model cell. This means each DSS well represents three persons. Applied to all four counties:

- Collier County = $123.67 \text{ gpd/p} \times 3 = 371.01 \text{ gpd/well}$
- Glades County = $114.58 \text{ gpd/p} \times 3 = 343.74 \text{ gpd/well}$
- Hendry County = $67.43 \text{ gpd/p} \times 3 = 202.29 \text{ gpd/well}$
- Lee County = $71.05 \text{ gpd/p} \times 3 = 213.15 \text{ gpd/well}$

From information received from Lee County and discussions with SFWMD Water Supply Planning staff, two additional pieces of information were used to refine the DSS pumping rates. First, the DSS well average PCUR for each county was increased by a factor of one to account for private landscape irrigation. Applied to all four counties:

- Collier County = $371.01 \text{ gpd/well} + 123.67 = 494.68 \text{ gpd/well}$
- Glades County = $343.74 \text{ gpd/well} + 114.58 = 458.32 \text{ gpd/well}$
- Hendry County = $202.29 \text{ gpd/well} + 67.43 = 269.72 \text{ gpd/well}$
- Lee County = $213.15 \text{ gpd/well} + 71.05 = 284.20 \text{ gpd/well}$

Second, the pumping rates for all DSS wells were adjusted over time according to seasonal variations measured at DSS wells in a portion of Lee County. This information was obtained from a Lehigh Acres groundwater flow model being developed by A.D.A. Engineering, Inc. A.D.A. Engineering, Inc. provided the SFWMD with calibrated DSS well pumping rates based, in part, on private landscape irrigation use and monthly rate variations over the course of a 2-year period (January 2013 through December 2014). The monthly variation in DSS well pumping rates was used to derive a multiplier (ranging from 0.86 to 1.14) that was applied to the PCUR for each DSS well for each month of the LWCSIM calibration period (January 1999 through December 2012).

As a check on the above water extraction rate per well, the overall, four-county average PCUR of 373 gpd/well divided by 3 persons/well = 124 gpd/p. This number is almost identical to the 2015 finished residential water demand value in the WaSUP database for Collier County (123.67 gpd/p).

The final PCUR per well per county was assigned to the DSS wells in the model cells, with adjustment for seasonal variations applied monthly from January 1999 through December 2012.

Figure C-2 shows the locations of all DSS wells included in the LWCSIM. There are 59,340 DSS wells in Lee, Collier, Hendry, and Glades counties, represented by a total of 22,139 model cells.

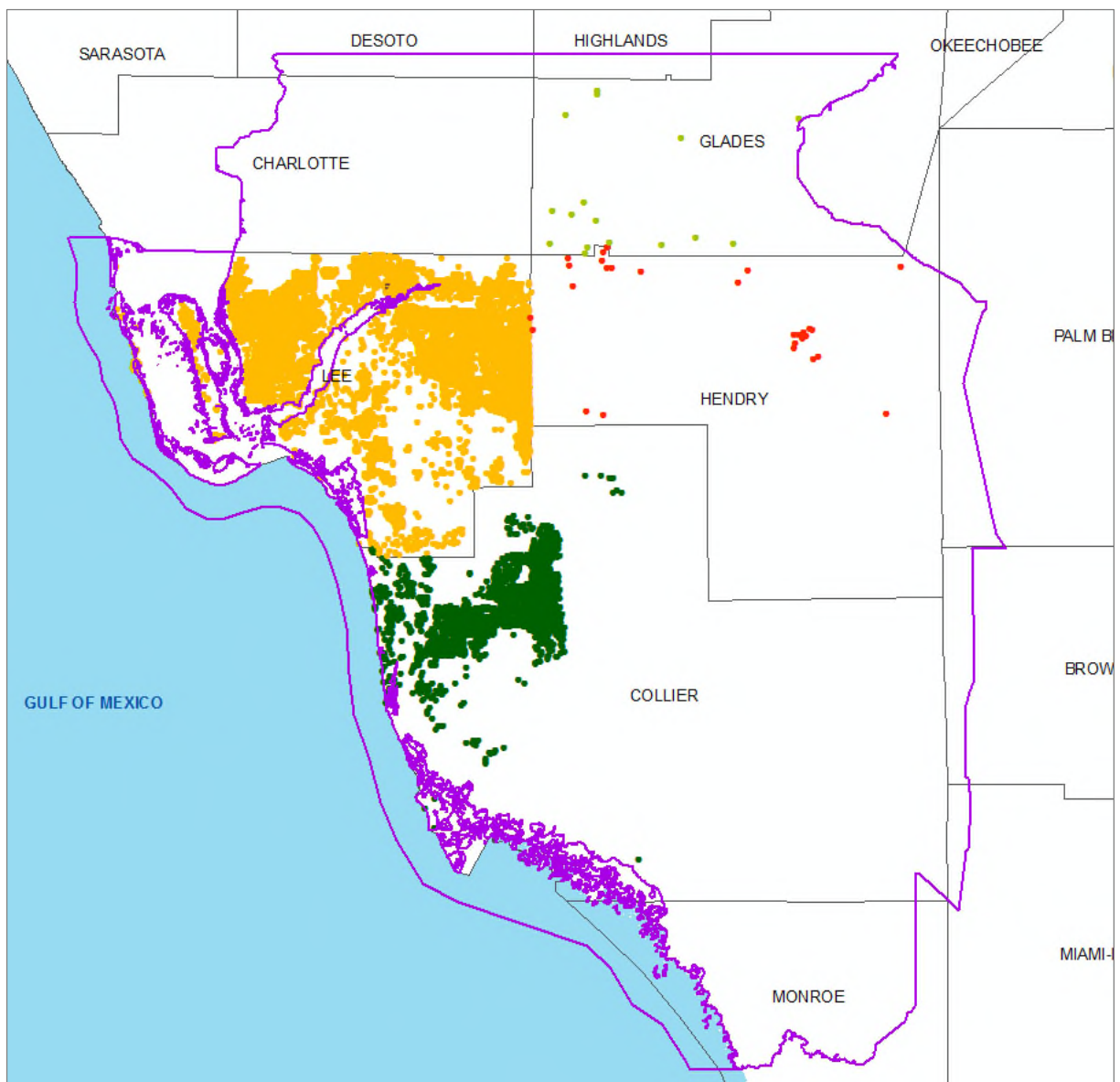


Figure C-2. Domestic Self-Supply well coverage in the model.

This DSS well coverage and an Excel pivot table were used to prepare the spreadsheet shown in **Table C-1**, which was used to build part of the WEL package for the LWCSIM. Using the procedure described earlier, DSS well data, including layer, row, column, average PCUR, and monthly per well PCUR, were entered into this spreadsheet. The data were used in the WEL package for transient MODFLOW flow modeling.

Table C-1. Domestic Self-Supply well data.

| | A | B | C | D | E | F | G | H | I | J | K | L |
|----|-------|-----|-----|-------------|-------------|-------------|-------------|-------------|-------------|-------------|-------------|-------------|
| 1 | Layer | ROW | COL | Q gpdpw | Q mgdpw | Jan-99 | Feb-99 | Mar-99 | Apr-99 | May-99 | Jun-99 | Jul-99 |
| 2 | 1 | 110 | 174 | 163.4991534 | 0.000163499 | 0.000168417 | 0.000187956 | 0.000169167 | 0.000176838 | 0.000166456 | 0.00014418 | 0.000141154 |
| 3 | 1 | 110 | 177 | 176.5850443 | 0.000176585 | 0.000181896 | 0.000203 | 0.000182707 | 0.000190992 | 0.000179779 | 0.00015572 | 0.000152451 |
| 4 | 1 | 111 | 178 | 169.56996 | 0.00016957 | 0.00017467 | 0.000194935 | 0.000175449 | 0.000183405 | 0.000172637 | 0.000149534 | 0.000146395 |
| 5 | 1 | 112 | 137 | 195.965799 | 0.000195966 | 0.00020186 | 0.000225279 | 0.00020276 | 0.000211954 | 0.00019951 | 0.000172811 | 0.000169183 |
| 6 | 1 | 112 | 171 | 159.9002048 | 0.0001599 | 0.00016471 | 0.000183819 | 0.000165444 | 0.000172946 | 0.000162792 | 0.000141007 | 0.000138047 |
| 7 | 1 | 112 | 174 | 284.2 | 0.0002842 | 0.000292748 | 0.000326712 | 0.000294053 | 0.000307387 | 0.00028934 | 0.00025062 | 0.000245359 |
| 8 | 1 | 113 | 159 | 284.2 | 0.0002842 | 0.000292748 | 0.000326712 | 0.000294053 | 0.000307387 | 0.00028934 | 0.00025062 | 0.000245359 |
| 9 | 1 | 113 | 160 | 284.2 | 0.0002842 | 0.000292748 | 0.000326712 | 0.000294053 | 0.000307387 | 0.00028934 | 0.00025062 | 0.000245359 |
| 10 | 1 | 113 | 168 | 146.944195 | 0.000146944 | 0.000151364 | 0.000168925 | 0.000152039 | 0.000158933 | 0.000149602 | 0.000129582 | 0.000126861 |
| 11 | 1 | 113 | 173 | 284.2 | 0.0002842 | 0.000292748 | 0.000326712 | 0.000294053 | 0.000307387 | 0.00028934 | 0.00025062 | 0.000245359 |
| 12 | 1 | 113 | 187 | 284.2 | 0.0002842 | 0.000292748 | 0.000326712 | 0.000294053 | 0.000307387 | 0.00028934 | 0.00025062 | 0.000245359 |
| 13 | 1 | 114 | 159 | 284.2 | 0.0002842 | 0.000292748 | 0.000326712 | 0.000294053 | 0.000307387 | 0.00028934 | 0.00025062 | 0.000245359 |
| 14 | 1 | 114 | 164 | 142.0923451 | 0.000142092 | 0.000146366 | 0.000163347 | 0.000147019 | 0.000153685 | 0.000144662 | 0.000125303 | 0.000122673 |
| 15 | 1 | 114 | 166 | 284.2 | 0.0002842 | 0.000292748 | 0.000326712 | 0.000294053 | 0.000307387 | 0.00028934 | 0.00025062 | 0.000245359 |
| 16 | 1 | 114 | 169 | 284.2 | 0.0002842 | 0.000292748 | 0.000326712 | 0.000294053 | 0.000307387 | 0.00028934 | 0.00025062 | 0.000245359 |
| 17 | 1 | 114 | 170 | 284.2 | 0.0002842 | 0.000292748 | 0.000326712 | 0.000294053 | 0.000307387 | 0.00028934 | 0.00025062 | 0.000245359 |
| 18 | 1 | 115 | 167 | 28.81442074 | 2.88144E-05 | 2.96811E-05 | 3.31246E-05 | 2.98134E-05 | 3.11653E-05 | 2.93355E-05 | 2.54098E-05 | 2.48764E-05 |
| 19 | 1 | 115 | 171 | 284.2 | 0.0002842 | 0.000292748 | 0.000326712 | 0.000294053 | 0.000307387 | 0.00028934 | 0.00025062 | 0.000245359 |
| 20 | 1 | 115 | 177 | 158.4359975 | 0.000158436 | 0.000163201 | 0.000182136 | 0.000163929 | 0.000171362 | 0.000161301 | 0.000139716 | 0.000136783 |
| 21 | 1 | 115 | 186 | 284.2 | 0.0002842 | 0.000292748 | 0.000326712 | 0.000294053 | 0.000307387 | 0.00028934 | 0.00025062 | 0.000245359 |
| 22 | 1 | 115 | 187 | 159.8681165 | 0.000159868 | 0.000164677 | 0.000183782 | 0.000165411 | 0.000172911 | 0.000162759 | 0.000140978 | 0.000138019 |
| 23 | 1 | 116 | 137 | 484.8676176 | 0.000484868 | 0.000499451 | 0.000557397 | 0.000501677 | 0.000524426 | 0.000493637 | 0.000427577 | 0.000418601 |
| 24 | 1 | 116 | 159 | 284.2 | 0.0002842 | 0.000292748 | 0.000326712 | 0.000294053 | 0.000307387 | 0.00028934 | 0.00025062 | 0.000245359 |
| 25 | 1 | 116 | 177 | 146.129343 | 0.000146129 | 0.000150525 | 0.000167988 | 0.000151195 | 0.000158051 | 0.000148772 | 0.000128863 | 0.000126158 |
| 26 | 1 | 117 | 137 | 600.6779659 | 0.000600678 | 0.000618745 | 0.00069053 | 0.000621503 | 0.000649685 | 0.000611541 | 0.000529703 | 0.000518584 |
| 27 | 1 | 117 | 138 | 206.4800919 | 0.00020648 | 0.000212691 | 0.000237366 | 0.000213638 | 0.000223326 | 0.000210214 | 0.000182083 | 0.000178261 |
| 28 | 1 | 117 | 161 | 284.2 | 0.0002842 | 0.000292748 | 0.000326712 | 0.000294053 | 0.000307387 | 0.00028934 | 0.00025062 | 0.000245359 |
| 29 | 1 | 117 | 162 | 852.5817742 | 0.000852582 | 0.000878226 | 0.000980115 | 0.00088214 | 0.000922141 | 0.000868001 | 0.000751843 | 0.00073606 |
| 30 | 1 | 117 | 163 | 284.2 | 0.0002842 | 0.000292748 | 0.000326712 | 0.000294053 | 0.000307387 | 0.00028934 | 0.00025062 | 0.000245359 |
| 31 | 1 | 117 | 167 | 284.2 | 0.0002842 | 0.000292748 | 0.000326712 | 0.000294053 | 0.000307387 | 0.00028934 | 0.00025062 | 0.000245359 |
| 32 | 1 | 117 | 178 | 147.0996218 | 0.0001471 | 0.000151524 | 0.000169104 | 0.000152199 | 0.000159101 | 0.00014976 | 0.000129719 | 0.000126996 |
| 33 | 1 | 117 | 180 | 142.090377 | 0.00014209 | 0.000146364 | 0.000163345 | 0.000147016 | 0.000153683 | 0.00014466 | 0.000125301 | 0.000122671 |

In summary, the steps used to arrive at the input table (Table C-1) for the MODFLOW WEL package are as follows:

1. Gather DSS well locations, casing depths, and total well depths from each county. County health departments are a good starting point for this information. Lee and Collier counties were able to provide GIS shapefiles and Excel spreadsheets with enough information to locate all DSS wells.
2. Create a GIS point coverage of all DSS wells. Intersect the DSS points with the LWCSIM grid to assign a row and column to each DSS well.
3. Run this coverage and the model layer coverage through a GIS analysis tool to assign layers to each DSS well point.
4. Develop a PCUR for DSS wells in each county.
5. Create a master DSS well Excel spreadsheet with the following fields: row, column, county, X, Y, case depth, total depth, PCUR per well, PCUR per layer, top of uppermost layer tapped, bottom of lowermost layer tapped.
6. Create a pivot table in this spreadsheet that sums the PCURs in cells containing multiple DSS wells and assigns a PCUR to each model cell.
7. Create a MODFLOW WEL Package spreadsheet that contains the following fields: layer, row, column, PCUR (gpd/well), PCUR (mgd/well), and a monthly time series of PCURs for transient flow model runs.

LITERATURE CITED

Marco Water Engineering, Inc. 2006. Lower West Coast Surficial Aquifer System Model Report.

South Florida Water Management District. 2012. 2012 Lower West Coast Water Supply Plan Update. West Palm Beach, FL.

**APPENDIX D:
RIVER STAGE MISSING DATA GAP FILLING**

For this modeling effort, incomplete stage data at multiple monitoring stations were filled using two methods: 1) a simple averaging, and 2) a sequence-based Markovian stochastic model (Assegid and Melesse 2011).

1. For stations with incomplete stage data of 2 years or less, the monthly average of 1999 to 2014 was used to fill the gap.
2. For stations with incomplete stage data of greater than 2 years, a sequence-based Markovian stochastic model (Assegid and Melesse 2011) was used. The method was tested for groundwater fluctuation simulation in South Florida and extended to surface water level prediction using the same analogy of groundwater fluctuation to the stage level fluctuation simulation. The result was presented to hydrologists and a consensus was reached on its use. Accordingly, the model was used to fill missing data for three river monitoring stations and three shallow groundwater stations (**Table D-1**). The shallow groundwater stations are in close proximity to ungauged rivers and thus serve as proxies for water level in the absence of monitoring.

Table D-1. Missing data by station.

| Station | Status | Missing Data Years | Duration (years) | Root Mean Square Error |
|---------|--------|--------------------|------------------|------------------------|
| VALI75 | Stage | 1999 – 2005 | 6 | 0.4 |
| HF3_G | Well | 1999, 2013 – 2014 | 1, 2 | 1.2, 1.1 |
| WF1_G | Well | 1999, 2003 – 2014 | 1, 12 | 1.0, 1.1 |

The stochastic method simulated monthly water level fluctuations based on available data. The data were used to develop and test the stochastic model. The parameters were later used to predict the period of time missing data were observed. The model used the least root mean square error and maximum likelihood ratio of 90% at the time of simulation and testing. In all cases of the forecast, the variance of the observed was preserved to uphold the stationarity assumption of the Markovian approach. The result suggests as an acceptable error for all cases: a root mean square error of 0.1 to 1.5 ft (3% to 5% of the head). A similarity of patterns between the observed and simulated outputs was observed, as indicated in **Figures D-1 to D-3**.

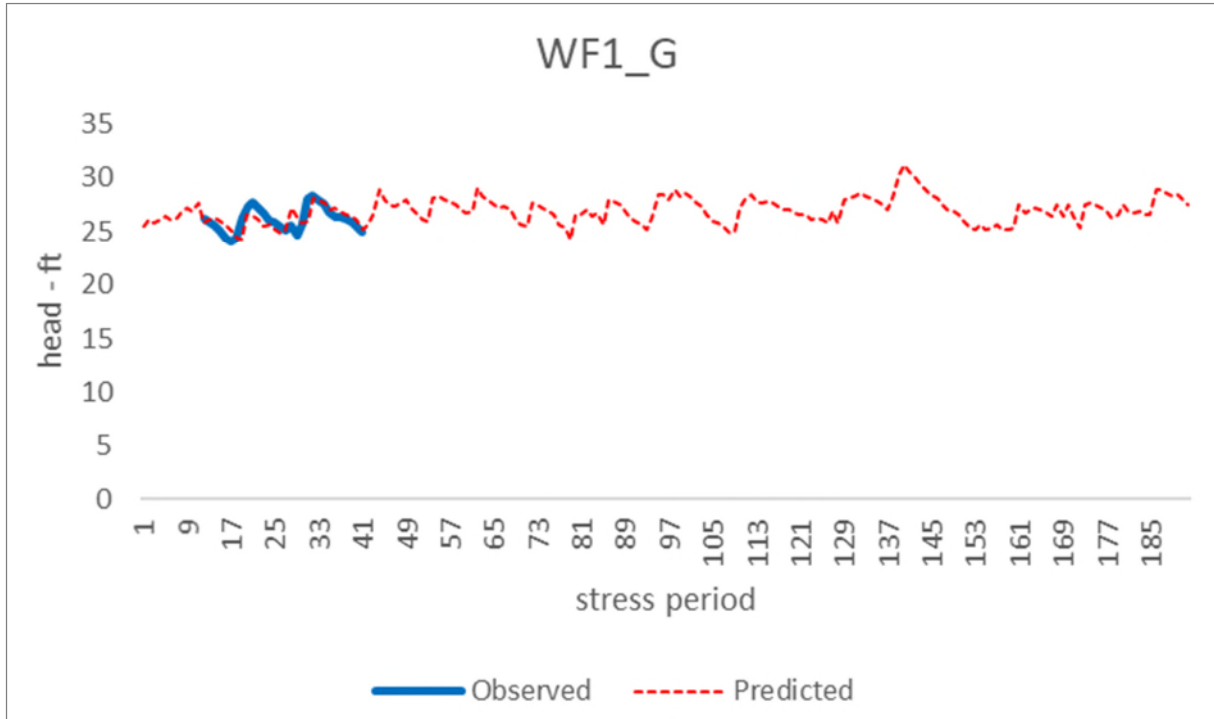


Figure D-1. Observed versus predicted values for the missing data gap at the WF1_G shallow well.

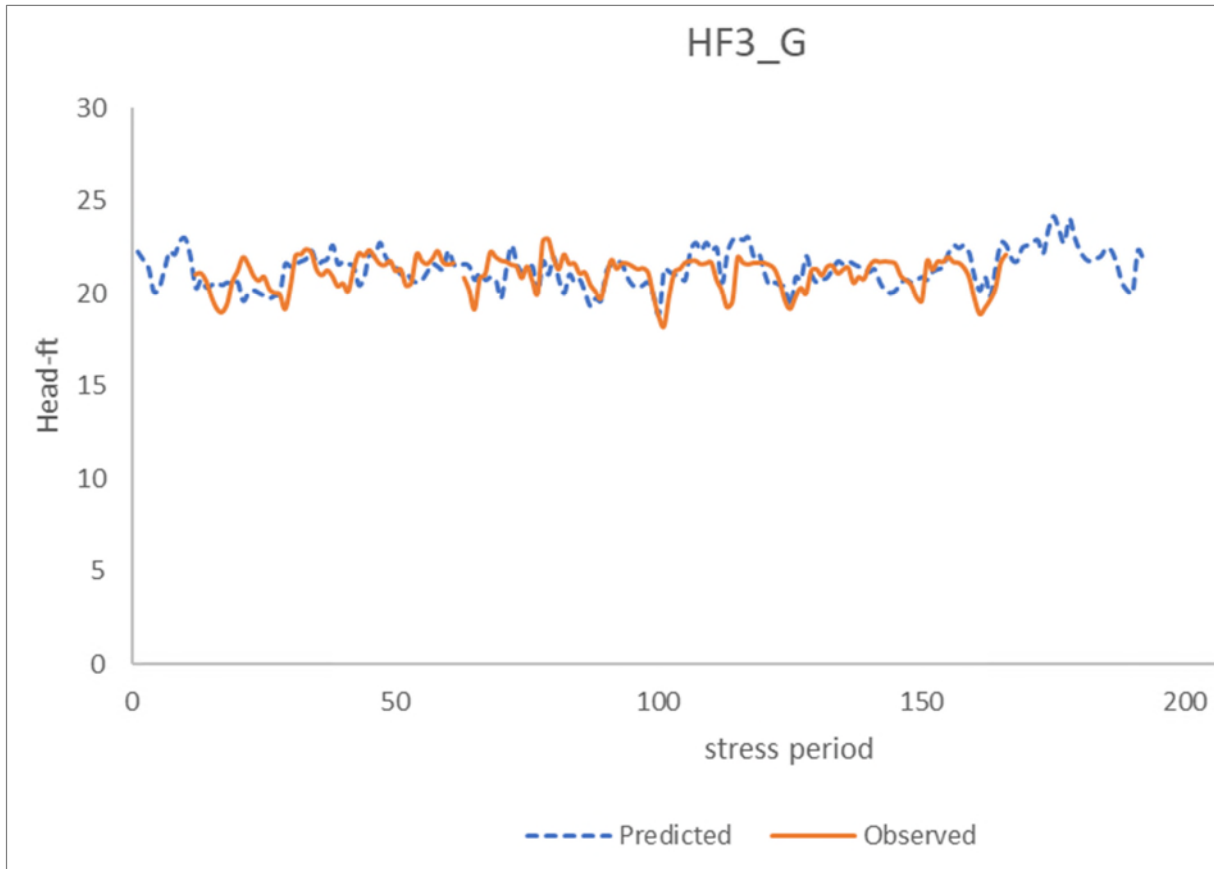


Figure D-2. Observed versus predicted values for the missing data gap at the HF3_G shallow well.

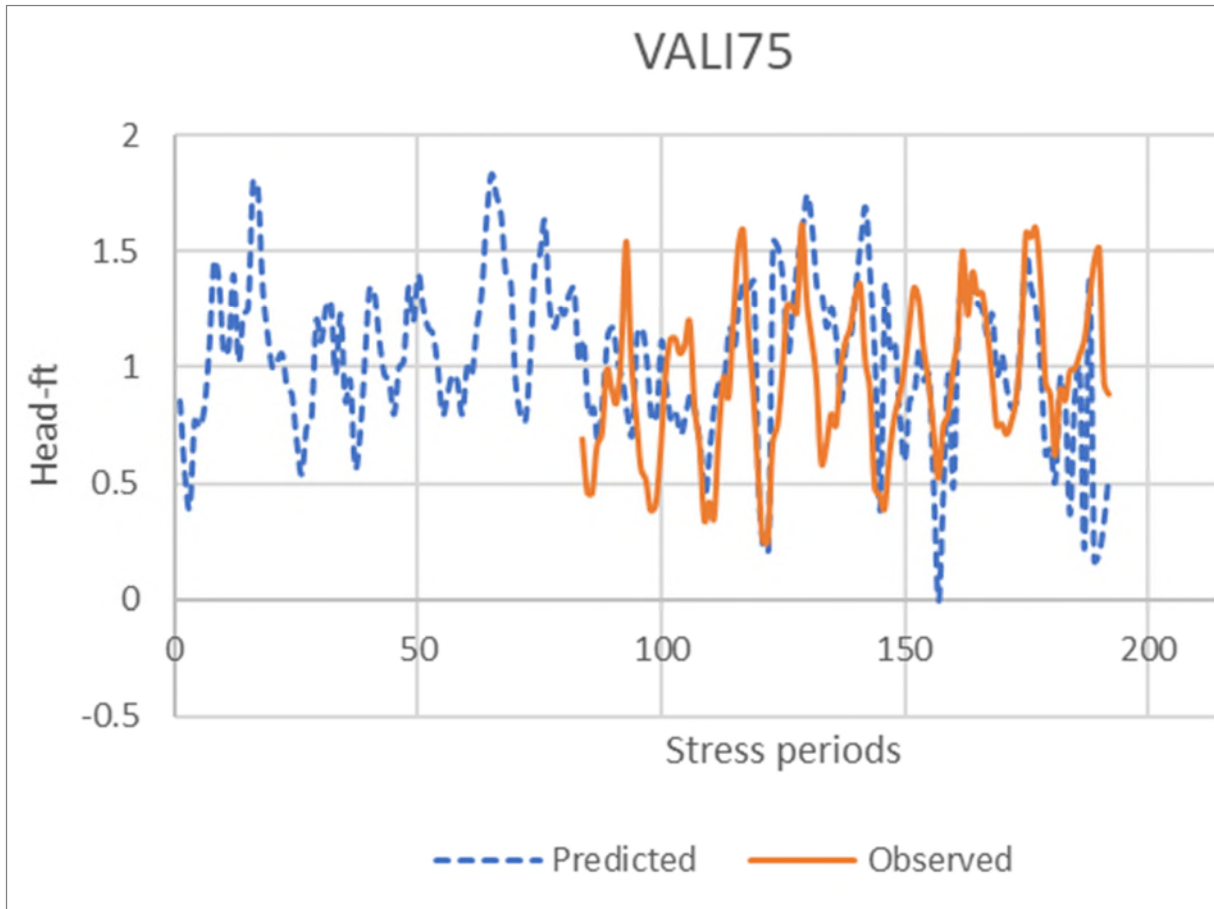


Figure D-3. Observed versus predicted values for the missing data gap at the VALI75 gauging station.

LITERATURE CITED

Assegid, Y. and A. Melesse. 2011. Operational prediction of groundwater fluctuation in South Florida using sequence-based Markovian stochastic model. *Water Resources Management* 25(9):2,279-2,294.

**APPENDIX E:
DRAIN COVERAGE PROCEDURE**

All shapefiles and feature classes illustrated in this appendix as well as the ArcMap projects used to assemble the coverages are stored on the South Florida Water Management District's (SFWMD's) server at: [\\ad.sfwmd.gov/dfsRoot\data\wsd\MOD\RCE](http://ad.sfwmd.gov/dfsRoot/data/wsd/MOD/RCE).

Two coverages were needed to prepare the drains coverage for MODFLOW: 1) National Hydrography Dataset (<http://nhd.usgs.gov/>) medium resolution (NHDM), and 2) the digital elevation model (DEM) for South Florida, light detection and ranging (LiDAR) 100 feet (ft), found in the SFWMD's Geospatial Data Library.

The NHDM was clipped to the Lower West Coast Surficial and Intermediate Aquifer Systems Model (LWCSIM) domain and saved as a feature class. After eliminating all but StreamRiver, CanalDitch, and ArtificialPath from the coverage, the remaining drain flow polylines in the LWCSIM domain are shown in **Figure E-1**.

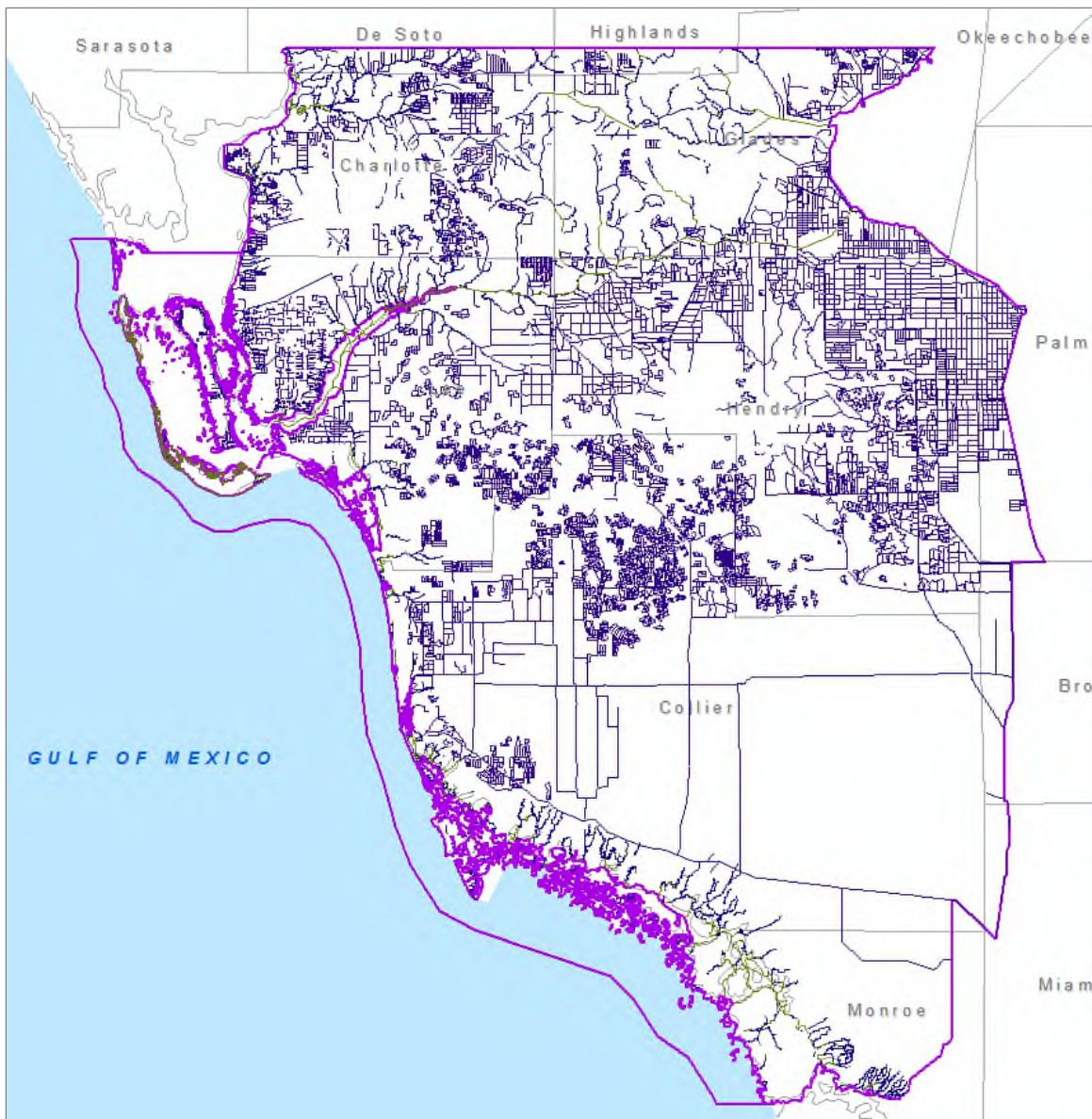


Figure E-1. Drains in the model area.

Intersect the drain flow polylines with the LWCSIM 1,000 ft × 1,000 ft grid mesh:

```
arcpy.Intersect_analysis(in_features="NHDMflow_clipped_101215 #;'LWCSIM Model Grid  
Grp/LWCSIM_mesh' #",out_feature_class="//ad.sfwmd.gov/dfsRoot/data/wsd/MOD/RCE/LWCSIM  
DRNs.gdb/NHDMflow_clipped_intMesh_101215",join_attributes="ALL",cluster_tolerance="#",output_t  
ype="INPUT")
```

Results in flow line segments inside model cells (**Figure E-2**).

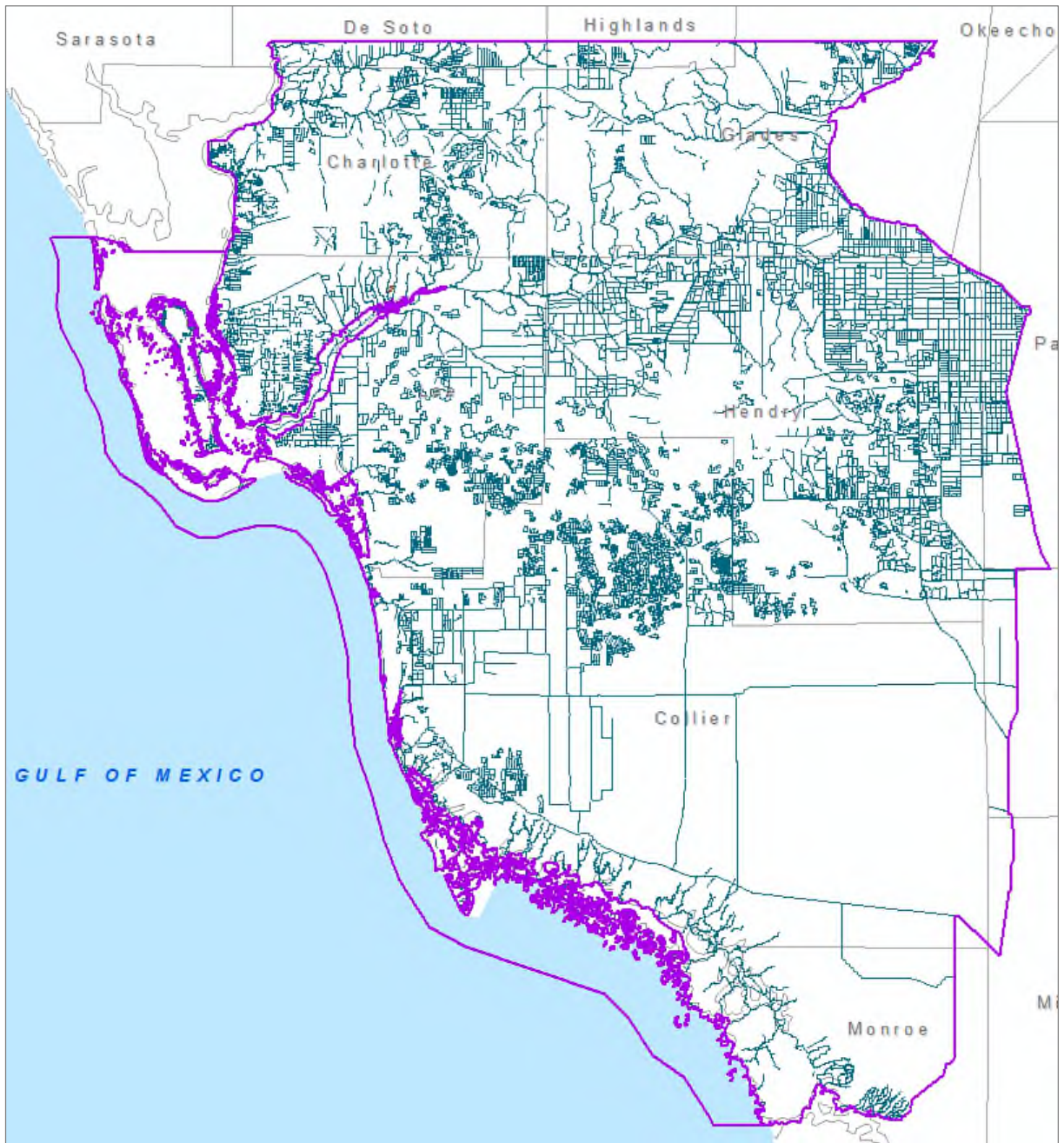


Figure E-2. Drains inside model cells.

The next coverage used was the DEM for South Florida, LiDAR 100 ft (DEM E(South Florida) Y(2013) S(FDEM, SFWMD) (LiDAR, 100 ft)), loaded from the SFWMD's Geospatial Data Library. This raster coverage was clipped to the active model domain boundary (**Figure E-3**).

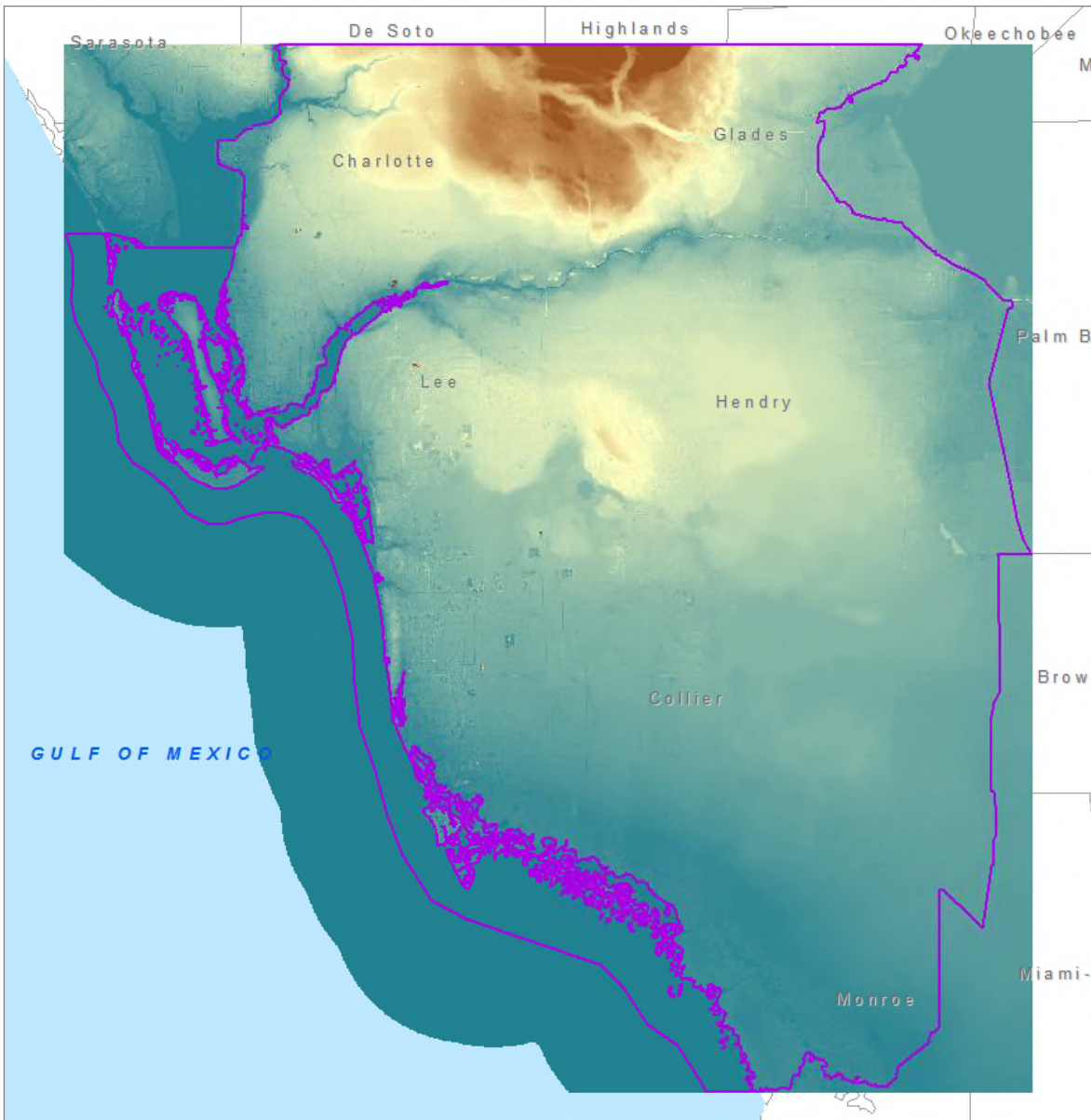


Figure E-3. Digital elevation model within the model area.

The clipped DEM was integerized using the Raster Calculator to multiply "NAVD88Raster" by 100. Then Extract by Mask was used on the previous two coverages (**Figure E-4**).

The following inputs are layers or table views: "DEM E(South Florida) Y(2013) S(FDEM, SFWMD) (LiDAR, 100 feet)", "NHDMflow_clipped_intMesh_101215"

arcpy.gp.ExtractByMask_sa("DEM E(South Florida) Y(2013) S(FDEM, SFWMD) (LiDAR, 100 feet)", "NHDMflow_clipped_intMesh_101215", "//ad.sfwmd.gov/dfsRoot/data/wsd/MOD/RCE/LWCSIM DRN 02.gdb/FlowLineDEMInt")

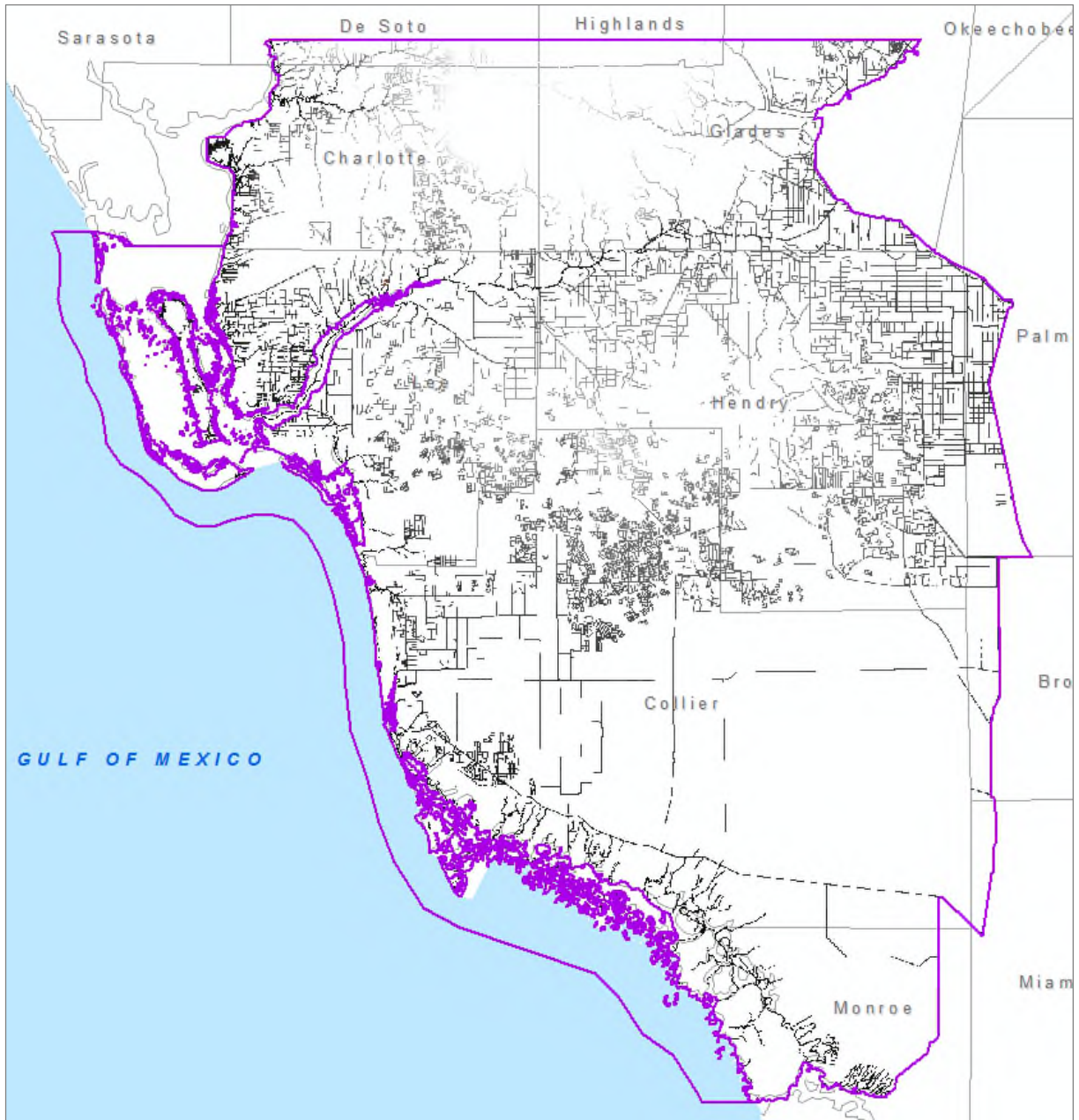


Figure E-4. Drain segments in model cells with elevation data added.

The Aggregate tool was used to calculate the mean of the integerized elevations (**Figure E-5**).

The following inputs are layers or table views: "FlowLineDEMInt"

```
arcpy.gp.Aggregate_sa("FlowLineDEMInt", "///ad.sfwmd.gov/dfsRoot/data/wsd/MOD/RCE/LWCSIM DRN 02.gdb/DrnCellDEM", "10", "MEAN", "EXPAND", "DATA")
```

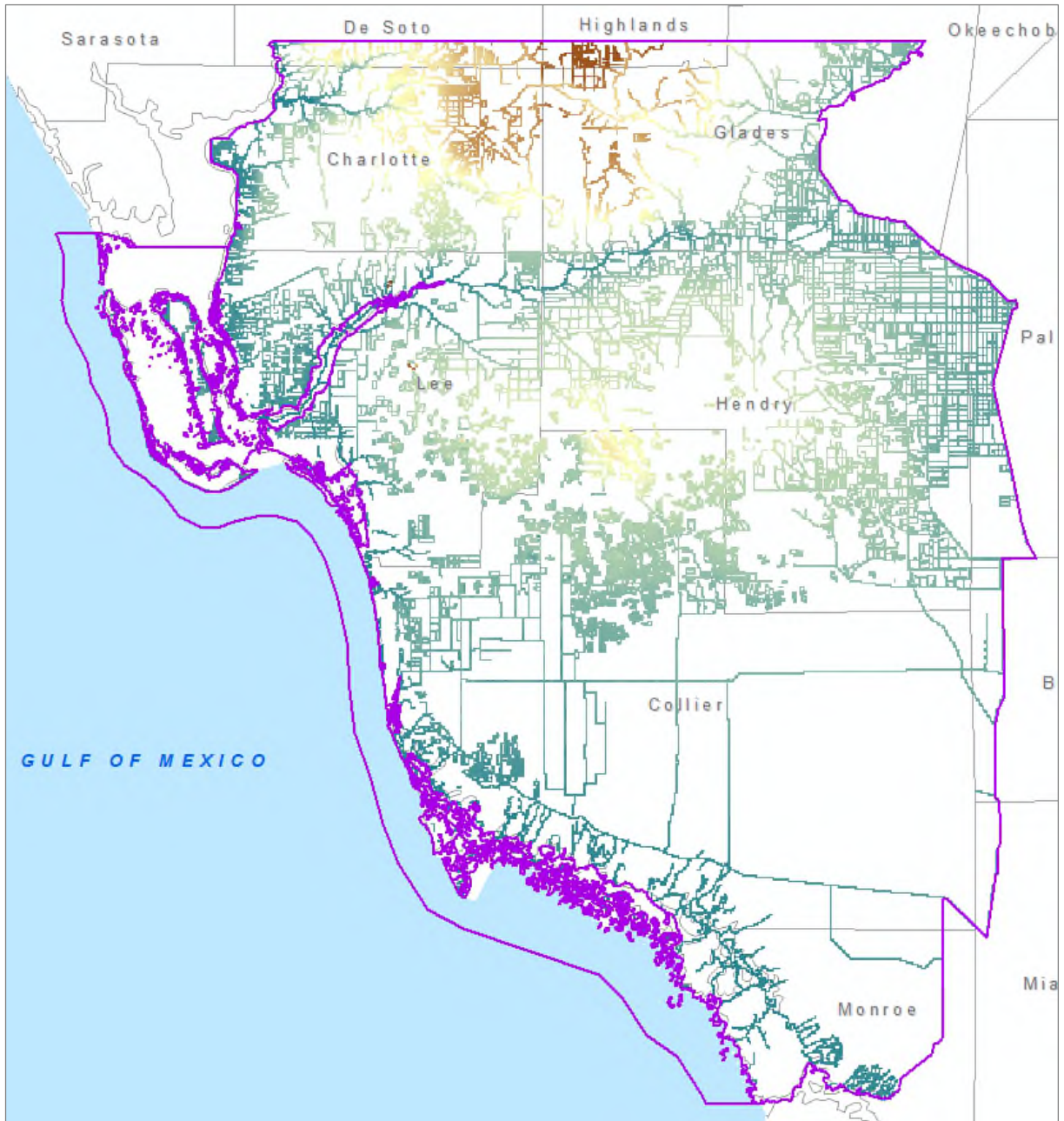


Figure E-5. Model cell drain segments with average elevation data.

The mean elevations were intergerized again using the Raster Calculator (**Figure E-6**).

```
arcpy.gp.RasterCalculator_sa("""Int("DrnCellDEM")""", "///ad.sfwmd.gov/dfsRoot/data/wsd/MOD/RCE/LWCSIM DRN 02.gdb/DrnCellDEMint")
```

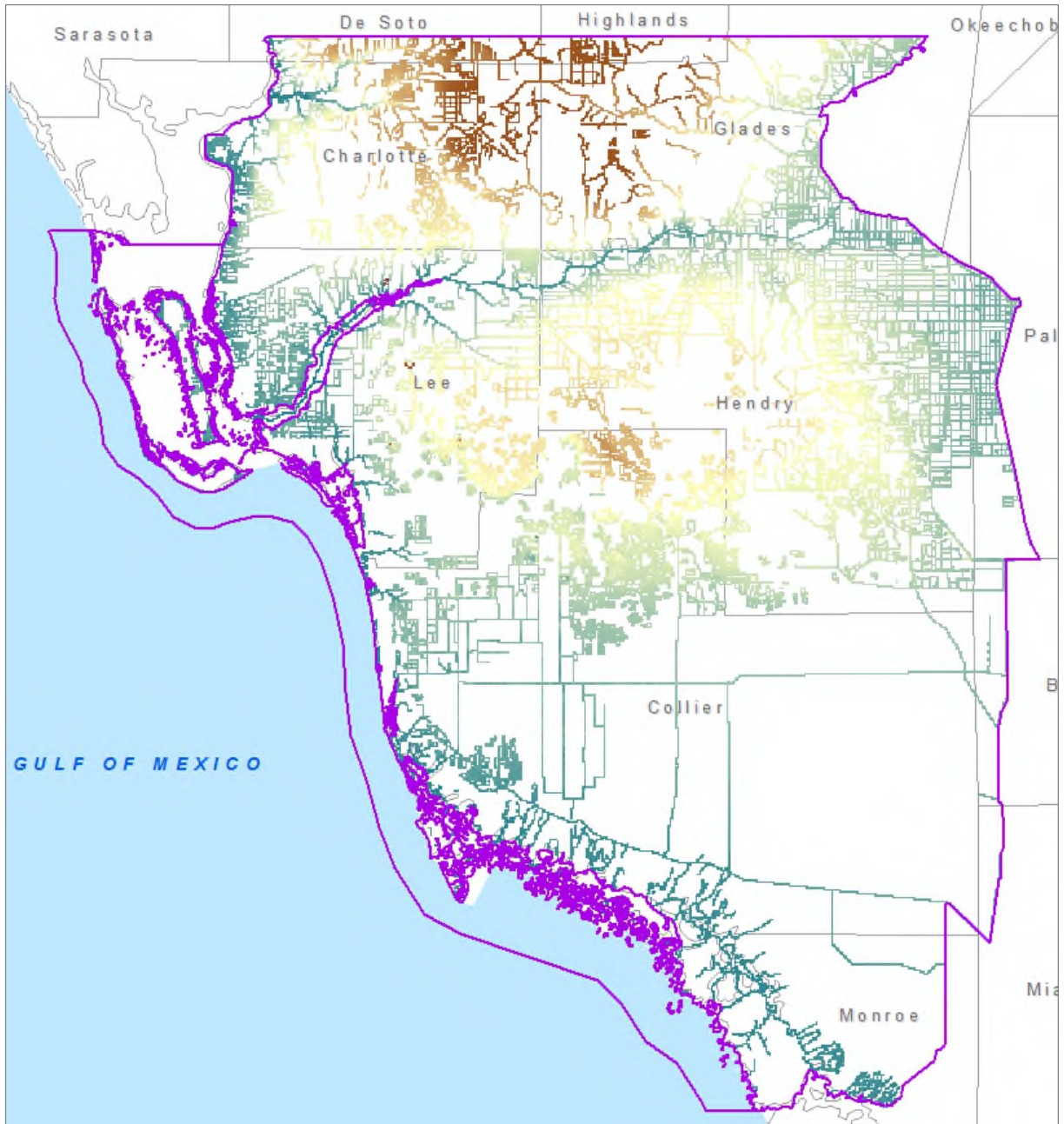


Figure E-6. Model cell drain segments with average elevation data integrated.

The Raster to Polygon tool was used to create polygons of the model drain segments (**Figure E-7**).

The following inputs are layers or table views: "DrnCellDEMint"

```
arcpy.RasterToPolygon_conversion(in_raster="DrnCellDEMint",out_polygon_features="//ad.sfwmd.gov/dfsRoot/data/wsd/MOD/RCE/LWCSIM DRN
02.gdb/DRNcellDEMPoly",simplify="NO_SIMPLIFY",raster_field="Value")
```

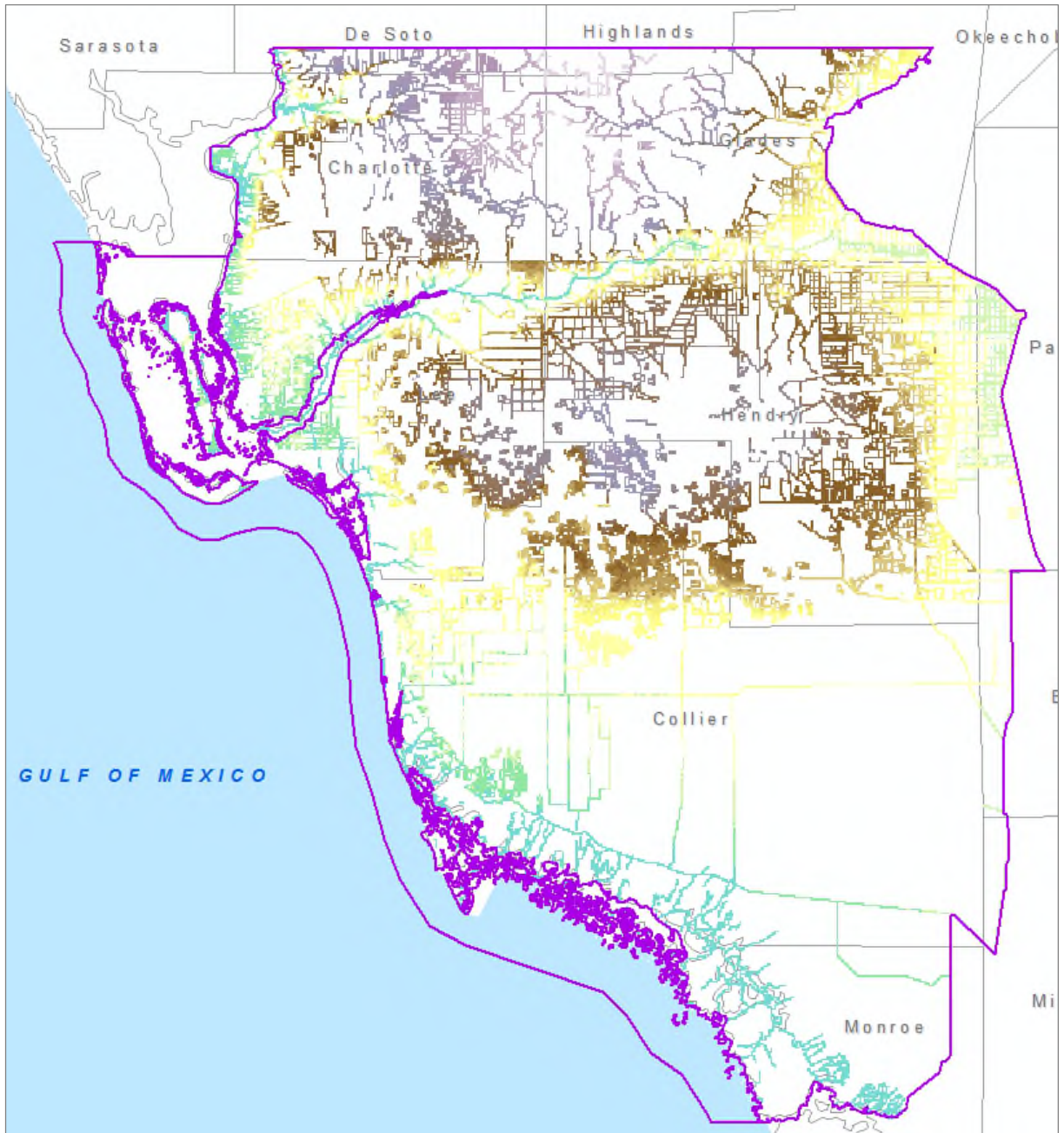


Figure E-7. Model drain cell segments converted to polygons.

The Calculate Field tool was used on this coverage to create a new field in the attribute table called DRN_Elev.

The following inputs are layers or table views: "DRNcellDEMPoly"

```
arcpy.CalculateField_management(in_table="DRNcellDEMPoly",field="DRN_Elev",expression="[grid code]/100",expression_type="VB",code_block="#")
```

The previous steps were important because the elevation data from the DEM raster were needed to assign elevations to each drain flow segment.

The coverage *NHDMflow_clipped_intMesh_101215* was intersected with *DRNcellDEMPoly* to create *FlowLineElevRoCo*, which contains the drain flow lines inside mesh cells, drain elevations, and row/column (**Figure E-8**).

```
arcpy.Intersect_analysis(in_features="NHDMflow_clipped_intMesh_101215 #;DRNcellDEMPoly #",out_feature_class="//ad.sfwmd.gov/dfsRoot/data/wsd/MOD/RCE/LWCSIM DRN 02.gdb/FlowLineElevRoCo",join_attributes="ALL",cluster_tolerance="#",output_type="INPUT")
```

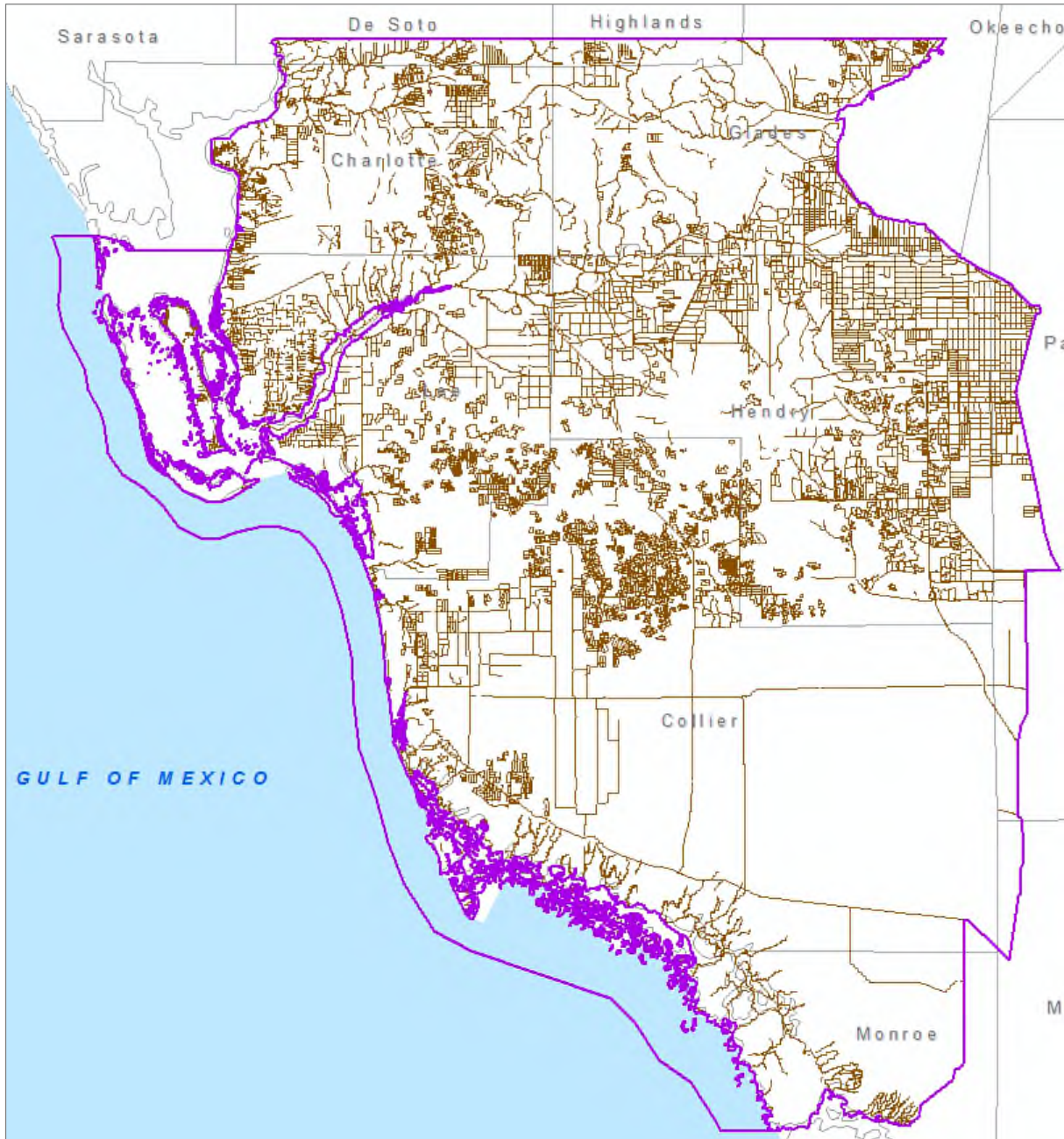


Figure E-8. Final drain segments with elevation data and row/column.

This was intersected with *LWCSIM_Soils_082515* to create the final coverage (**Figure E-9**), which contains all the pertinent data for the DRN package (row, column, segment length, drain elevation, and soil texture).

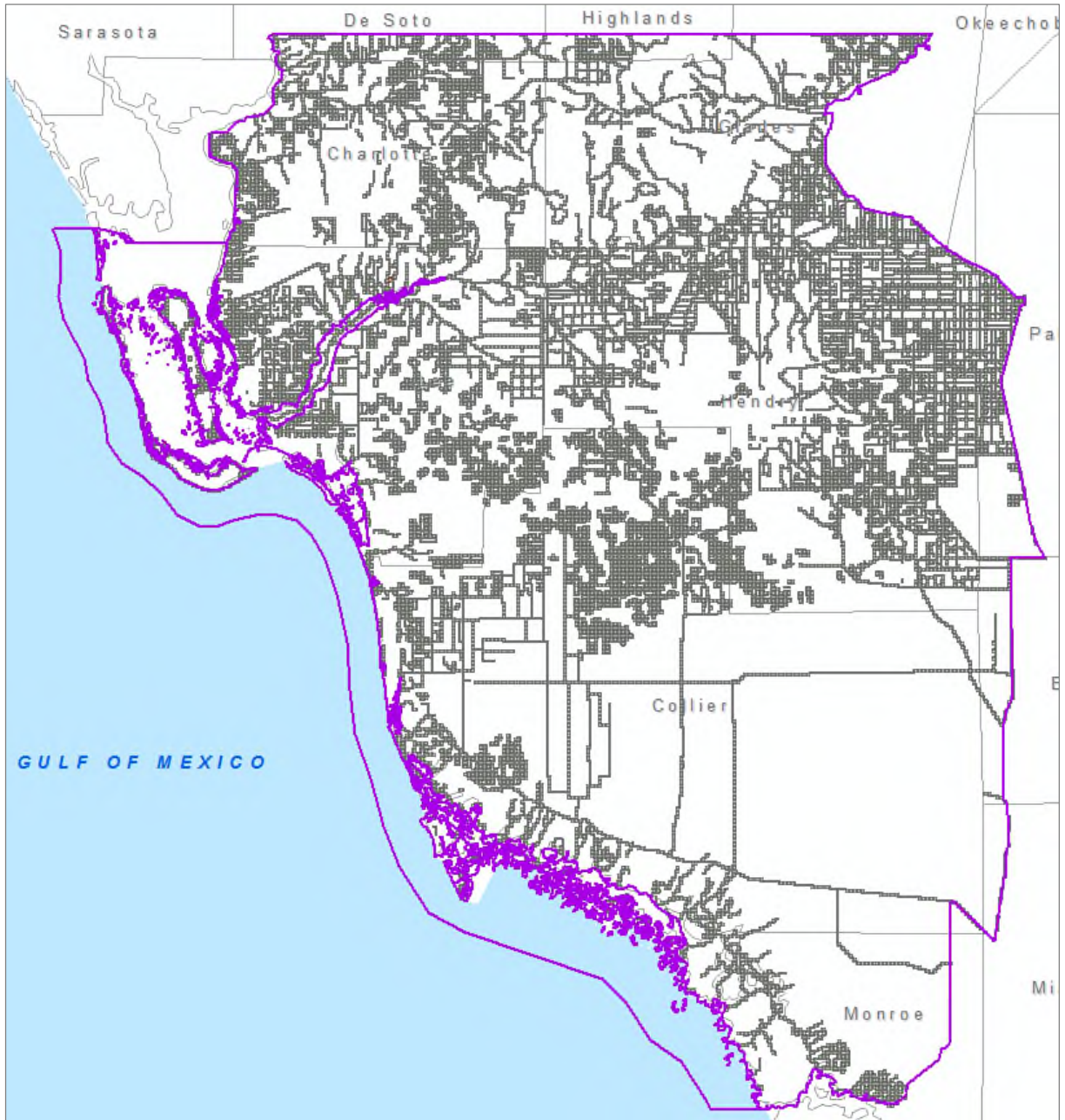


Figure E-9. Final drain segments with soil textures added.

```
arcpy.Intersect_analysis(in_features="DRN_FlowSumLenRoCo_MeanElev #;'Soils  
Grp/LWCSIM_Soils_082515'  
#",out_feature_class="//ad.sfwmd.gov/dfsRoot/data/wsd/MOD/RCE/LWCSIM DRN  
02.gdb/Final_DRN_Coverage_101415",join_attributes="ALL",cluster_tolerance="#",output_type="INP  
UT")
```

The River coverage was subtracted from the final drain coverage to eliminate overlap with stream features that are considered Rivers in the LWCSIM (Figure E-10).

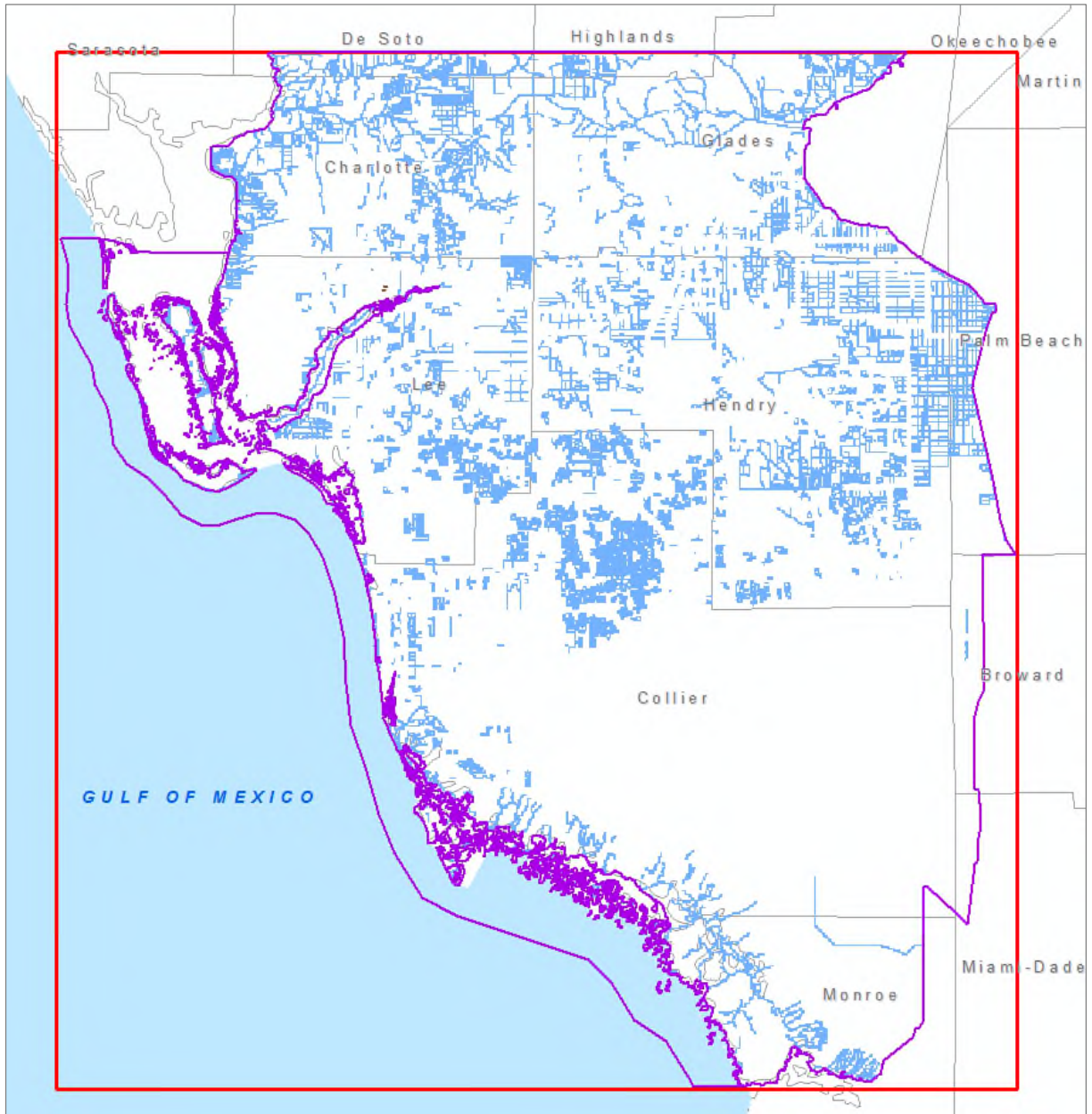


Figure E-10. Drains without rivers.

The features were exported to create the Excel spreadsheet shown in **Table E-1**, which was used to generate the DRN package for MODFLOW.

Table E-1. Drains coverage information.

| | A | B | C | D | E | F | G | H | I | J | K | L |
|----|-------|-----|-----|--------|------------|---------|---------|-------------|-------------------------------|---------|-------|---|
| | LAYER | ROW | COL | ROWCO | ELEV f msl | WIDTH f | THICK f | SEGLENGTH f | CONDUCTANCE f ² /d | Texture | K f/d | |
| 1 | 1 | 548 | 425 | 548425 | 0.1 | 30 | 1 | 255.7869372 | 107430.5136 | FS | 14 | |
| 2 | 1 | 548 | 426 | 548426 | 1.48 | 30 | 1 | 1017.369013 | 427294.9855 | FS | 14 | |
| 3 | 1 | 548 | 427 | 548427 | 1.48 | 30 | 1 | 501.5893038 | 210667.5076 | FS | 14 | |
| 4 | 1 | 548 | 430 | 548430 | 1.76 | 30 | 1 | 1029.448798 | 432368.4952 | FS | 14 | |
| 5 | 1 | 547 | 421 | 547421 | -0.76 | 30 | 1 | 416.9044981 | 175099.8892 | FS | 14 | |
| 6 | 1 | 547 | 422 | 547422 | -0.76 | 30 | 1 | 36.59626064 | 15370.42947 | FS | 14 | |
| 7 | 1 | 547 | 423 | 547423 | 0.35 | 30 | 1 | 413.9235281 | 173847.8818 | FS | 14 | |
| 8 | 1 | 547 | 424 | 547424 | 0.08 | 30 | 1 | 339.6062004 | 142634.6042 | FS | 14 | |
| 9 | 1 | 547 | 427 | 547427 | 1.48 | 30 | 1 | 647.7809808 | 272068.0119 | FS | 14 | |
| 10 | 1 | 547 | 428 | 547428 | 1.18 | 30 | 1 | 1108.805493 | 465698.3071 | FS | 14 | |
| 11 | 1 | 547 | 429 | 547429 | 1.18 | 30 | 1 | 306.609305 | 128775.9081 | FS | 14 | |
| 12 | 1 | 547 | 430 | 547430 | 1.18 | 30 | 1 | 999.4502819 | 419769.1184 | FS | 14 | |
| 13 | 1 | 546 | 421 | 546421 | 0.81 | 30 | 1 | 983.9156952 | 413244.592 | FS | 14 | |
| 14 | 1 | 546 | 422 | 546422 | 0.81 | 30 | 1 | 1434.51678 | 602497.0476 | FS | 14 | |
| 15 | 1 | 546 | 423 | 546423 | 0.51 | 30 | 1 | 1098.716915 | 461461.1043 | FS | 14 | |
| 16 | 1 | 546 | 425 | 546425 | 0.47 | 30 | 1 | 367.1718938 | 154212.1954 | FS | 14 | |
| 17 | 1 | 546 | 429 | 546429 | 1.12 | 30 | 1 | 1295.863012 | 544262.465 | FS | 14 | |
| 18 | 1 | 546 | 430 | 546430 | 1.12 | 30 | 1 | 147.2199574 | 61832.38211 | FS | 14 | |
| 19 | 1 | 545 | 421 | 545421 | 0.03 | 30 | 1 | 978.7979272 | 411095.1294 | FS | 14 | |
| 20 | 1 | 545 | 422 | 545422 | 0.3 | 30 | 1 | 100.4156987 | 42174.59345 | FS | 14 | |
| 21 | 1 | 545 | 423 | 545423 | 0.33 | 30 | 1 | 323.1706273 | 135731.6635 | FS | 14 | |
| 22 | 1 | 545 | 424 | 545424 | 0.33 | 30 | 1 | 1993.125476 | 837112.6999 | FS | 14 | |
| 23 | 1 | 545 | 425 | 545425 | 0.33 | 30 | 1 | 2159.429875 | 906960.5475 | FS | 14 | |
| 24 | 1 | 545 | 426 | 545426 | 0.79 | 30 | 1 | 1240.823006 | 521145.6625 | FS | 14 | |
| 25 | 1 | 545 | 427 | 545427 | 1.1 | 30 | 1 | 1097.421579 | 460917.0632 | FS | 14 | |
| 26 | 1 | 545 | 430 | 545430 | 1.22 | 30 | 1 | 1707.336569 | 717081.359 | FS | 14 | |

The LAYER, WIDTH f, and THICK f columns were added in Excel. All flow lines are in layer 1. Width and thickness for all flow line segments were estimated to be 30 ft wide and 1 ft thick of drain bed material. These data, along with soil textures, were used to estimate hydraulic conductivity and conductance. Hydraulic conductivity was based on soil texture and derived from literature. Conductance was calculated as:

$$C = KLW/M$$

Where:

C is the conductance (ft²/day)

K is hydraulic conductivity (ft/day)

L is length of the drain segment (ft)

W is width of the drain segment (estimated to be an average of 30 ft)

M is thickness of the drain bed sediments (estimated to be an average of 1 ft)

A final check on drain elevations was completed by comparing Marco Water Engineering, Inc. (2006) weir crest elevations with corresponding topographic elevations (**Figure E-11**).

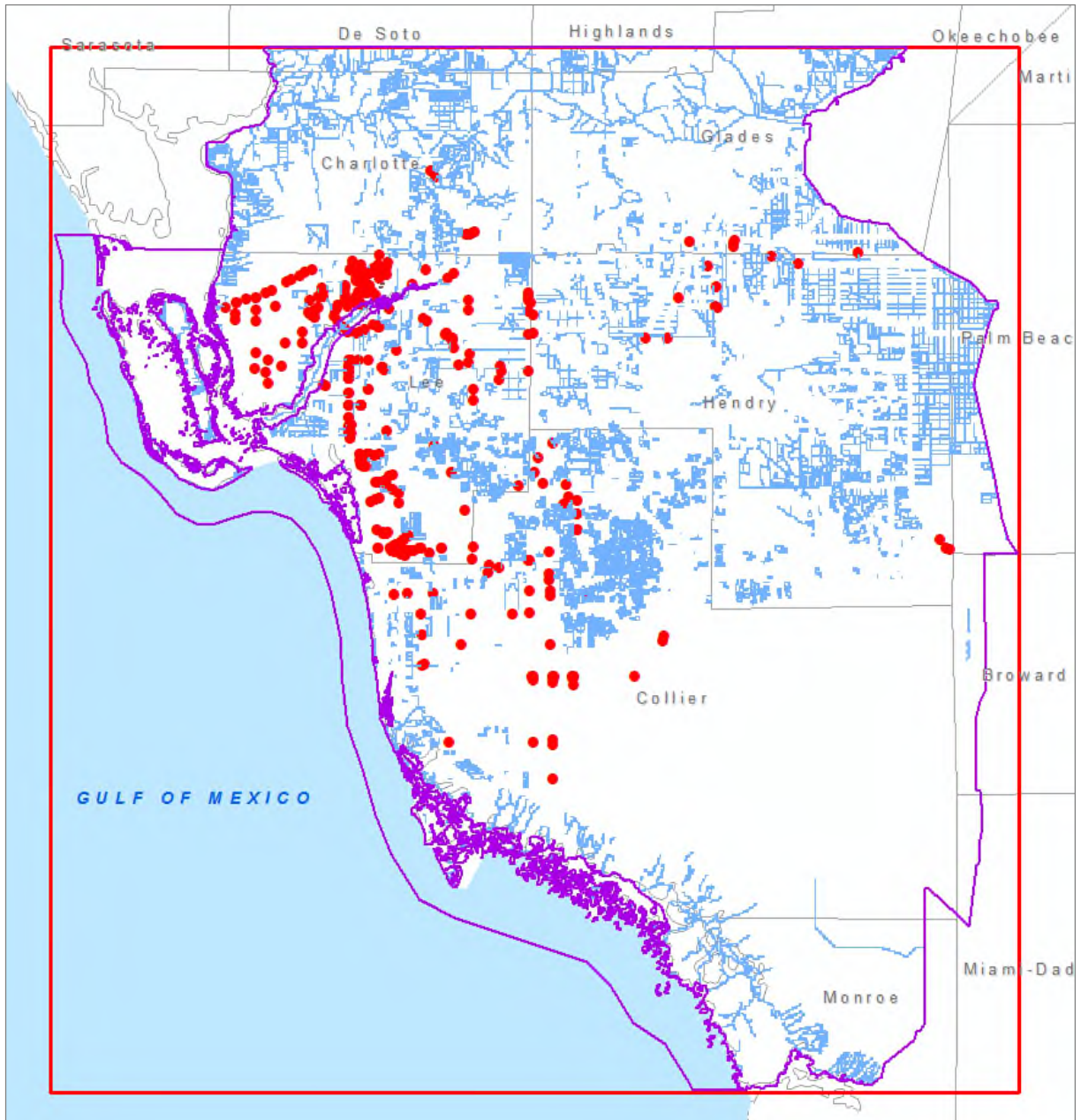


Figure E-11. Model drains and Marco Water Engineering, Inc. (2006) weir elevation data.

The average difference in elevation between land surface and the weir crest elevations was 3.4 ft lower. Therefore, an adjustment of 4 ft was applied to all drain segments in the final drain coverage.

**APPENDIX F:
WETLAND COVERAGE PROCEDURE**

This appendix describes the geographic information systems (GIS) procedure used to produce the WTL package from 2010 land use/land cover (LULC) data. LULC years 2000, 2004, and 2014 were used in similar procedures to produce WTL packages for other model years. All shapefiles and feature classes illustrated in this appendix as well as the ArcMap projects used to assemble the coverages are stored on the South Florida Water Management District's (SFWMD's) server at: <\\ad.sfwmd.gov\dfsRoot\data\wsd\MOD\RCE>.

For Wetland Year 2010:

1. In the 2010 WTL Coverage Grp, begin with LWCSIM_Wetlands_2010. This is a feature class containing LULC) data that have been reduced to only wetlands categories. These have been broken out to Levels 1, 2, and 3 and clipped to the model domain (purple boundary in **Figure F-1**). The red box is a closeup area used for the remaining figures in this appendix.

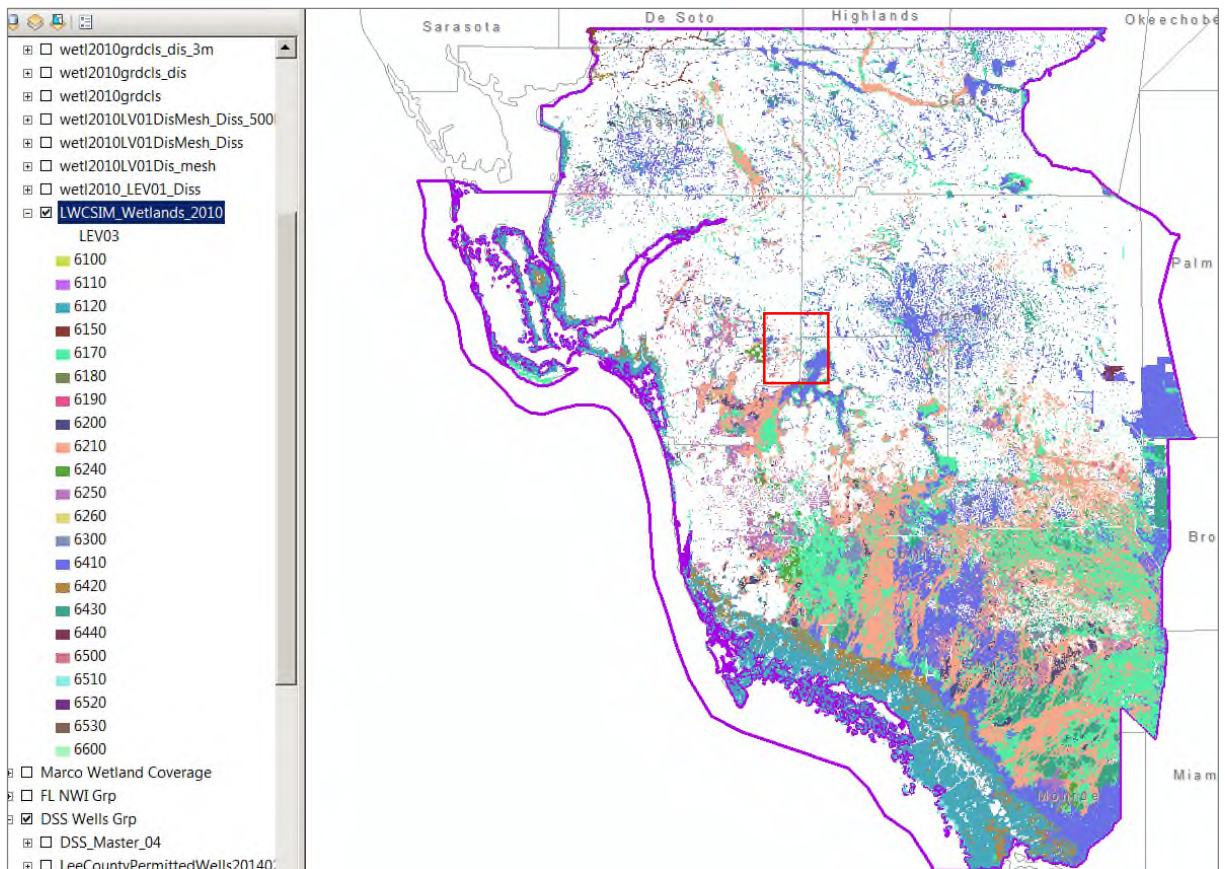


Figure F-1. Overview of wetland coverage.

2. Closeup area (Figure F-2):

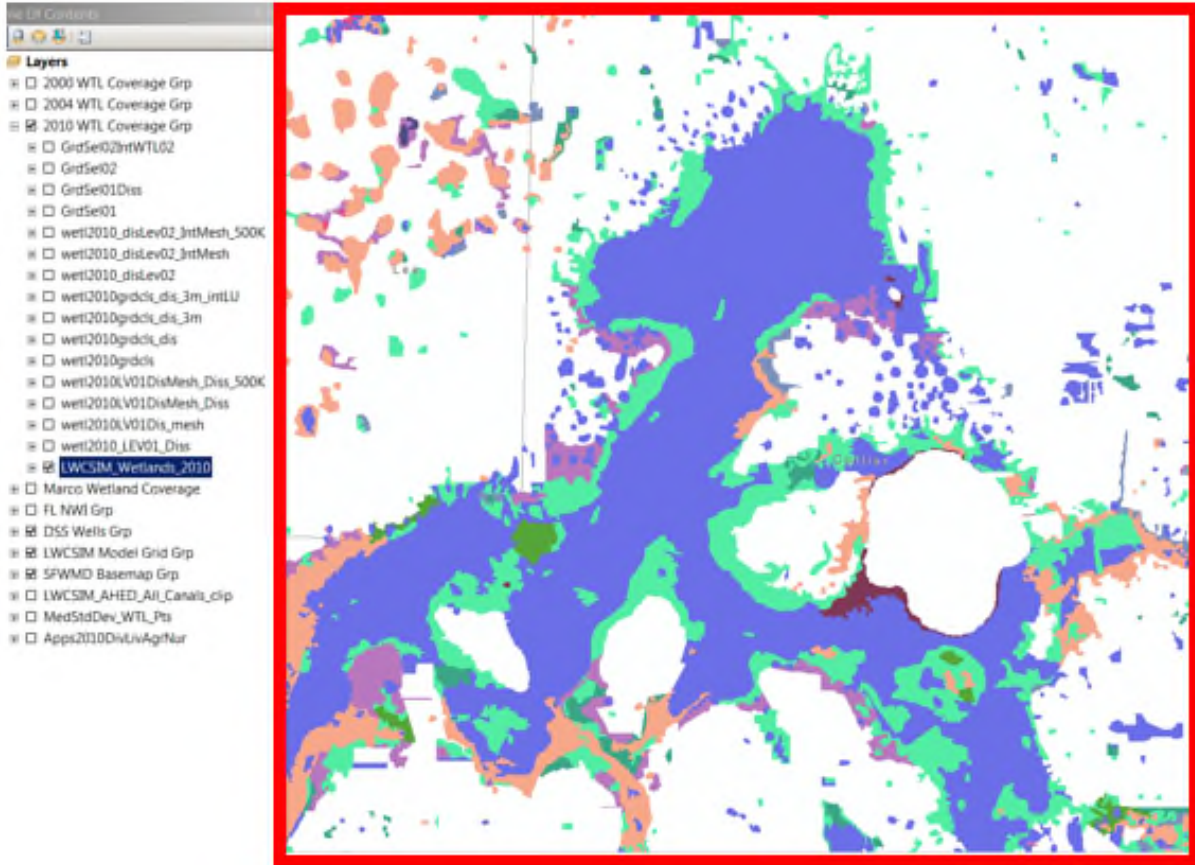


Figure F-2. Closeup.

3. Dissolve to the field LEV01, no multipart features. This step creates contiguous wetland polygons within the model area. Save the output as wetl2010_LEV01_Diss (**Figure F-3**).

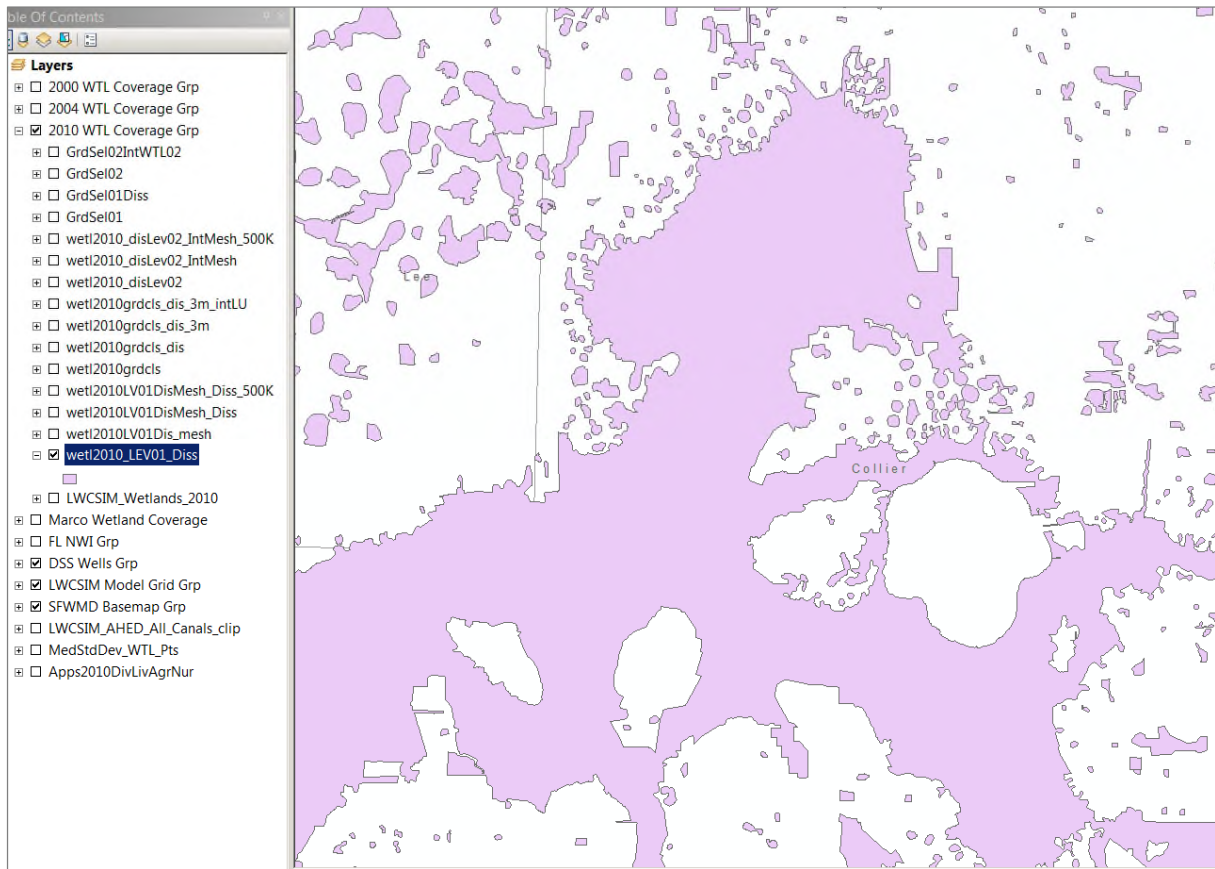


Figure F-3. Contiguous wetland polygons.

4. Take wetl2010_LEV01_Diss and intersect it with the Lower West Coast Surficial and Intermediate Aquifer Systems Model (LWCSIM) grid (LWCSIM_mesh in LWCSIM Model Grid Grp). The result is a set of polygons with model grid row and column attributes for any wetland polygons in the model area. Save the output file as wetl2010LV01Dis_mesh (**Figure F-4**).

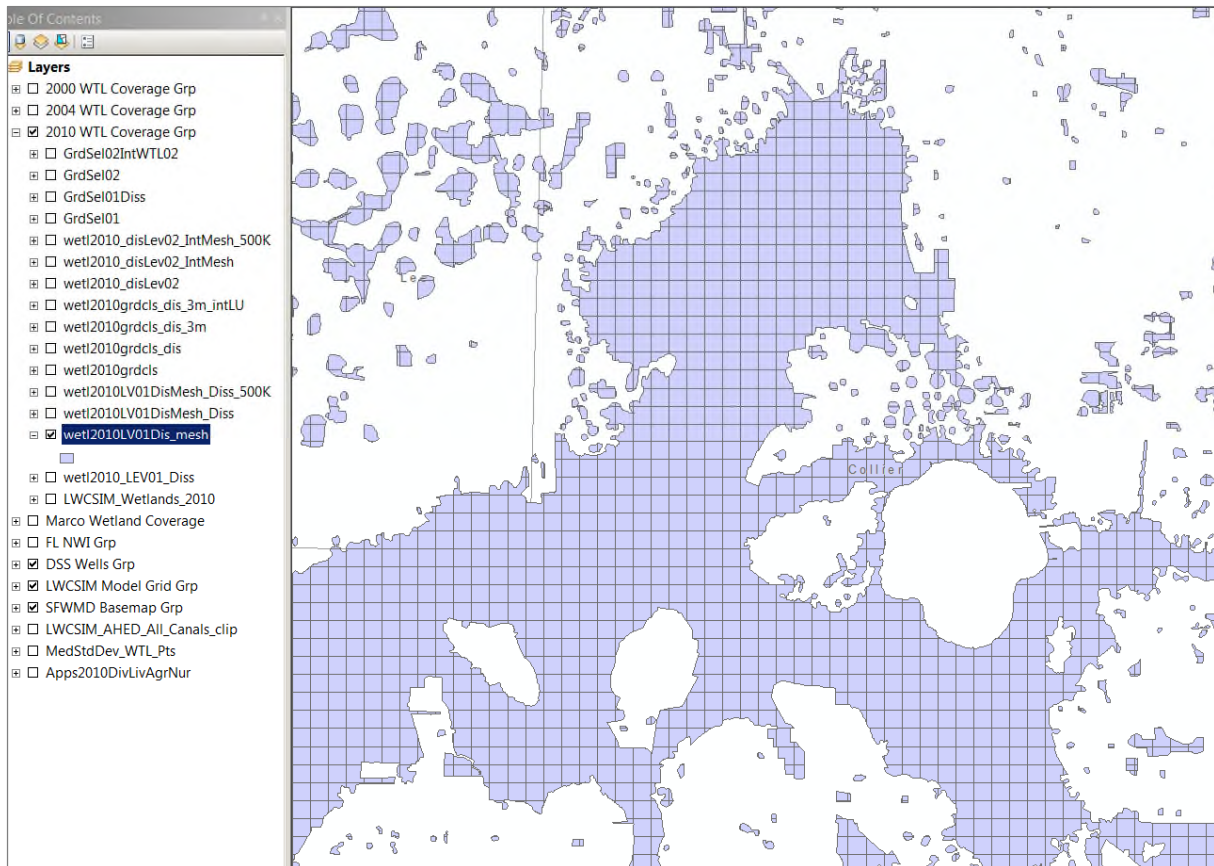


Figure F-4. Contiguous wetland polygons intersected with model grid.

5. Take wetl2010LV01Dis_mesh and dissolve to field FID_LWCSIM_mesh (this is the feature ID # assigned to the model grid cells). 'Yes' to multipart, dissolve lines. Model cells with multiple wetland polygons are merged. This file should be saved as wetl2010LV01DisMesh_Diss.

- Take wetl2010LV01DisMesh_Diss and select by attribute Shape_area $\geq 500,000$. This identifies model cells that are more than 50% wetland (500,000 is 50% of 1,000 square foot cells). Export the data to create wetl2010LV01DisMesh_Diss_500K (**Figure F-5**).

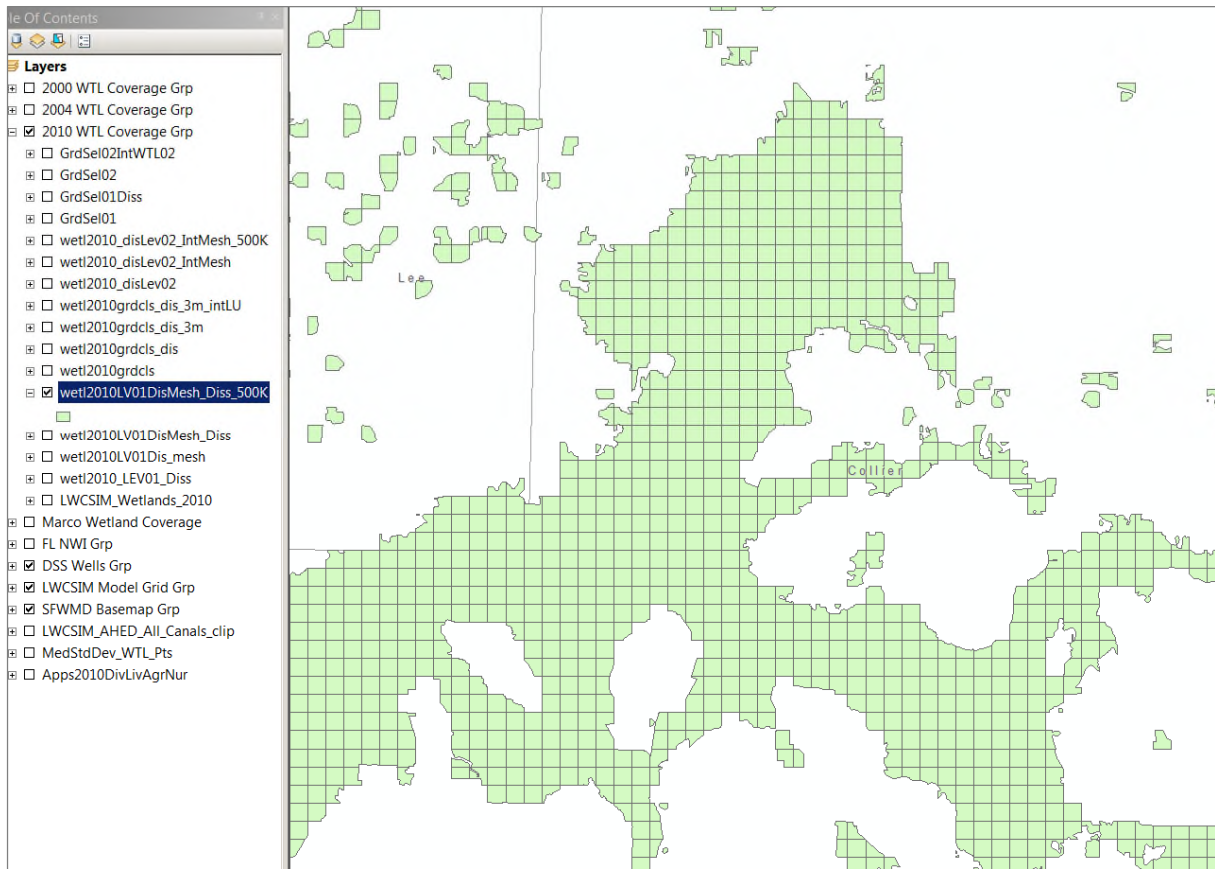


Figure F-5. Model cells containing 50% or more wetlands.

- From LWCSIM_mesh, select by location against the coverage created in step 5 (wetl2010LV01DisMesh_Diss_500K) as the source. *Spatial selection method for the target layer feature(s): contain (Clementini) the source layer features.* This will select only the cells in LWCSIM_mesh that contain (or touch) the wetlands polygons created in step 5. Export the data to the file wetl2010grdcls. This coverage contains only the cells with wetland data for the model (**Figure F-6**).

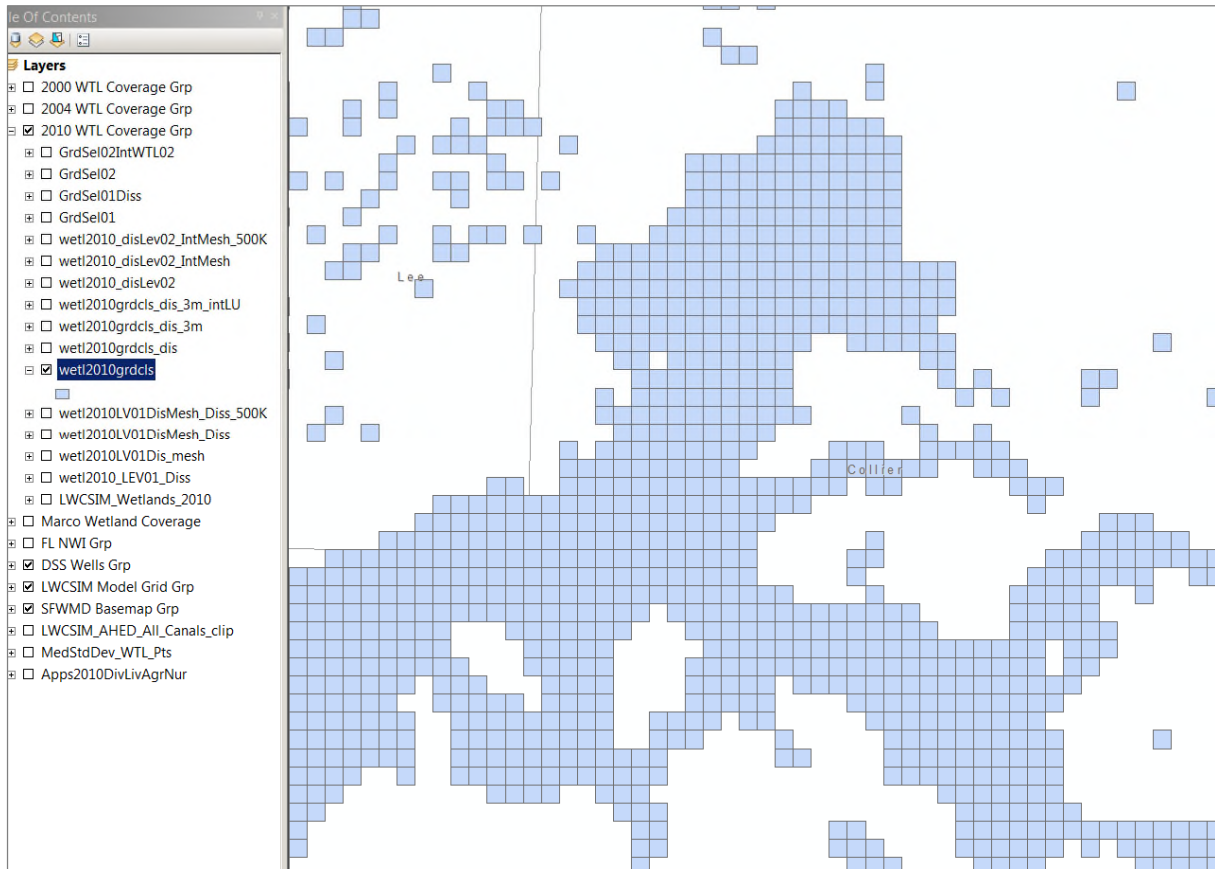


Figure F-6. Grid cells representing wetlands.

8. Dissolve wetl2010grdcls to create wetl2010grdcls_dis. This will join together adjacent grid cells to form continuous polygons (**Figure F-7**).

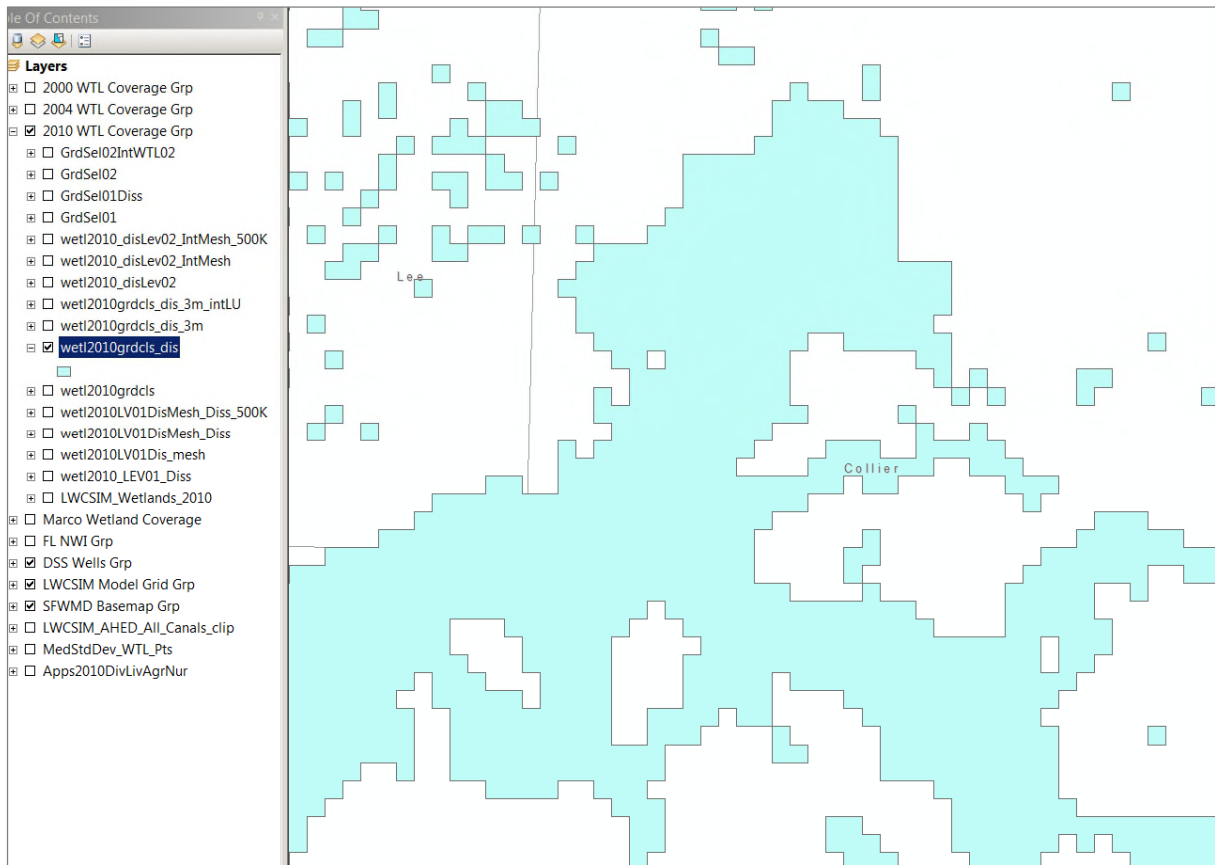


Figure F-7. Wetland grid cells dissolved into contiguous polygons.

9. From wetl2010grdcls_dis, select by attribute the polygons that are ≥ 3 million (3 grid cells in area), and export the data to wetl2010grdcls_dis_3m (Figure F-8).

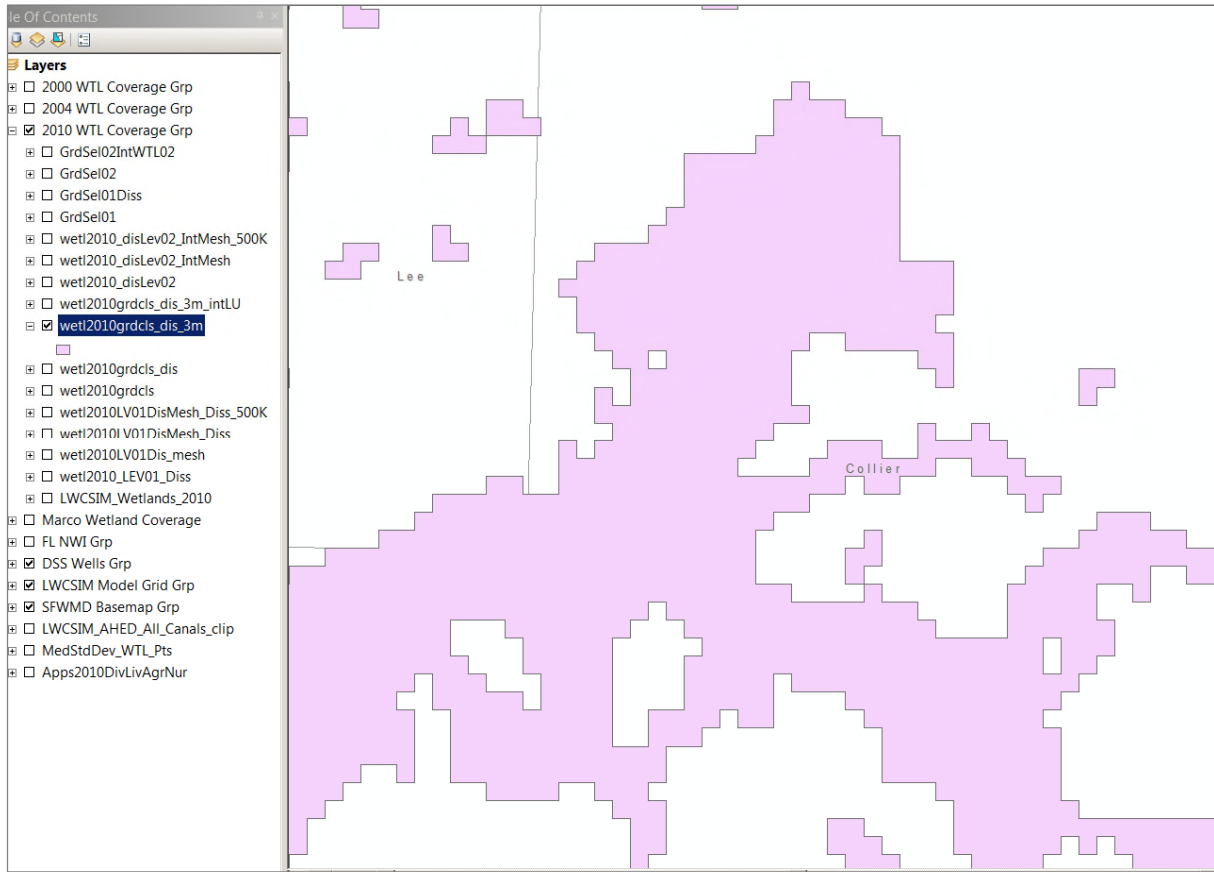


Figure F-8. Wetland grid cell polygons larger than three grid cells in size.

10. Intersect wetl2010grdcls_dis_3m with the original LWCSIM_Wetlands_2010 coverage to create wetl2010grdcls_dis_3m_intLU. This restores the original wetlands data to only the data within the model grid polygon areas arrived at in step 8 (**Figure F-9**).

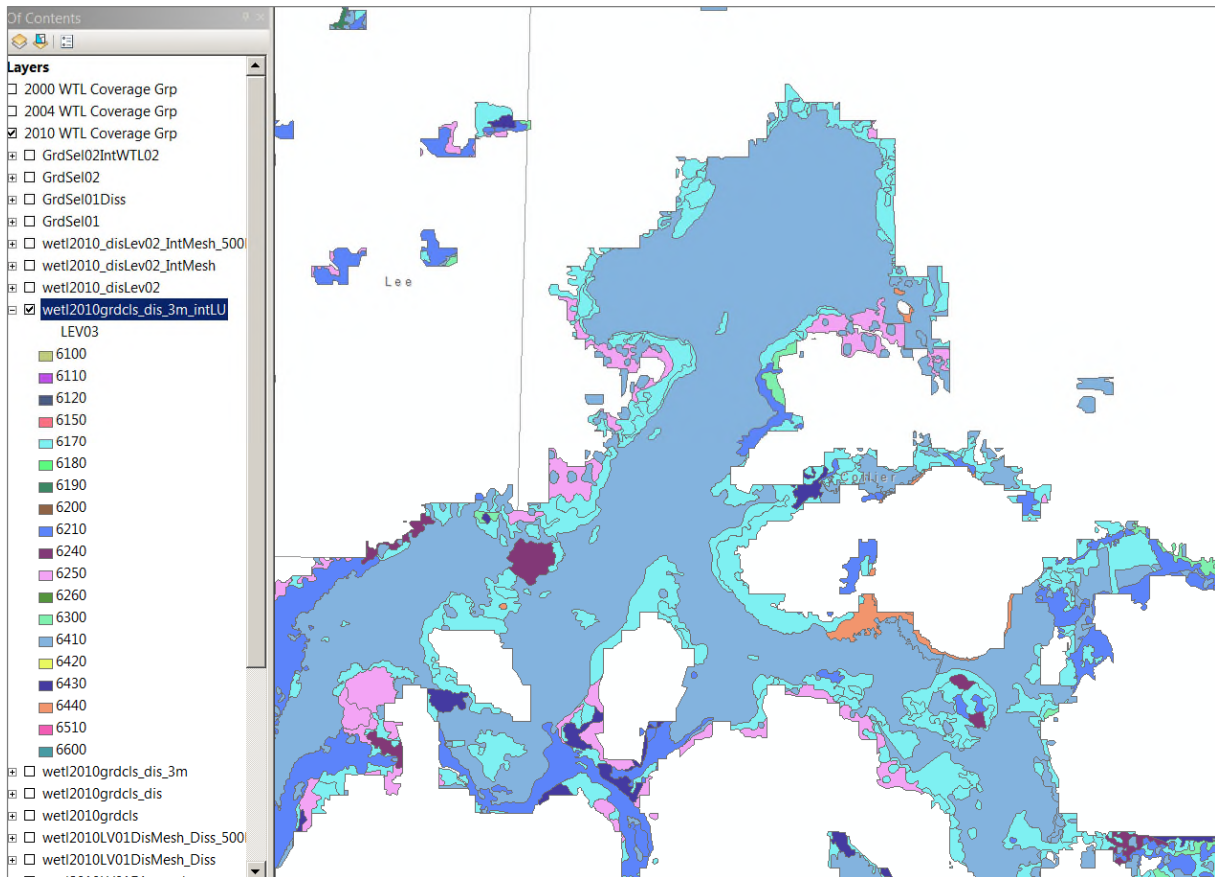


Figure F-9. Original wetland data restored to wetland grid polygons.

11. Take wetl2010grdcls_dis_3m_intLU and dissolve to the field LEV03. Output this to the file wetl2010_disLev03. This will reduce the wetlands data to Level 3 wetland categories.

12. Take wetl2010_disLev03 and intersect with the model grid (LWCSIM_mesh). Send the output to the file wetl2010_disLev03_IntMesh. This now shows only the portions of Level 3 wetlands that intersect model grid cells (**Figure F-10**).

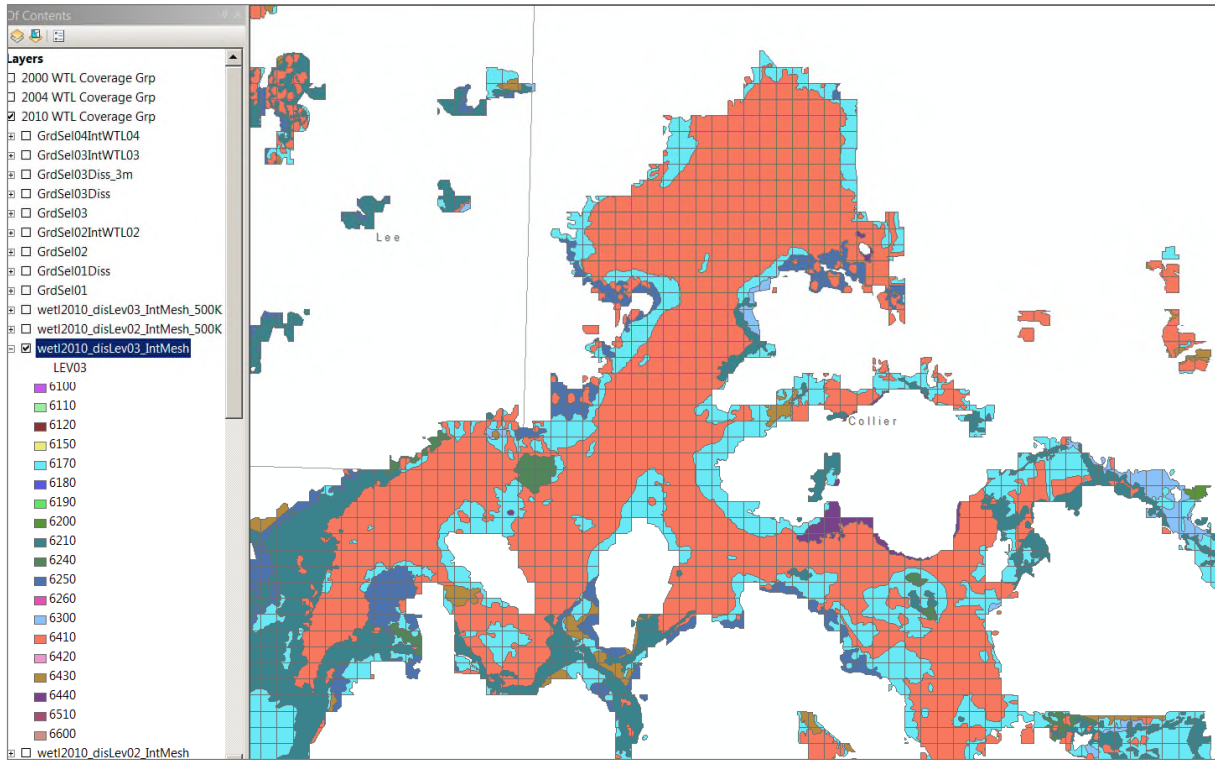


Figure F-10. Model grid cells containing only Level 3 wetlands.

13. Take wetl2010_disLev03_IntMesh, select by attribute shape_area $\geq 500,000$ and export the data to create the file wetl2010_disLev03_IntMesh_500K. This step will eliminate all wetlands polygons smaller than 50% of a model grid cell. However, individual groups of less than three cells remain. The final steps will eliminate those and leave only groups of three or more cells, each of which contains 50% or more wetland area (**Figure F-11**).

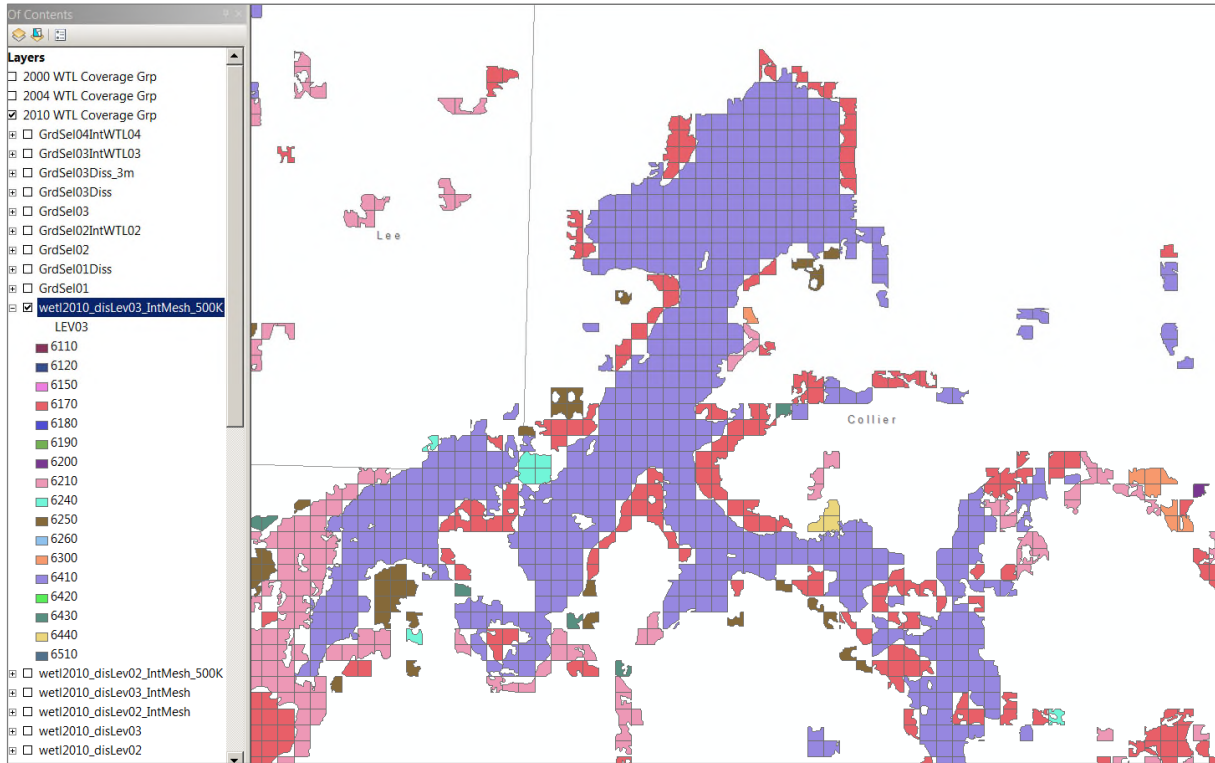


Figure F-11. Model grid cells containing 50% or more Level 3 wetlands.

14. From the mesh, select by attribute the grid cells that match with information in step 12 to create GrdSel03 (**Figure F-12**).

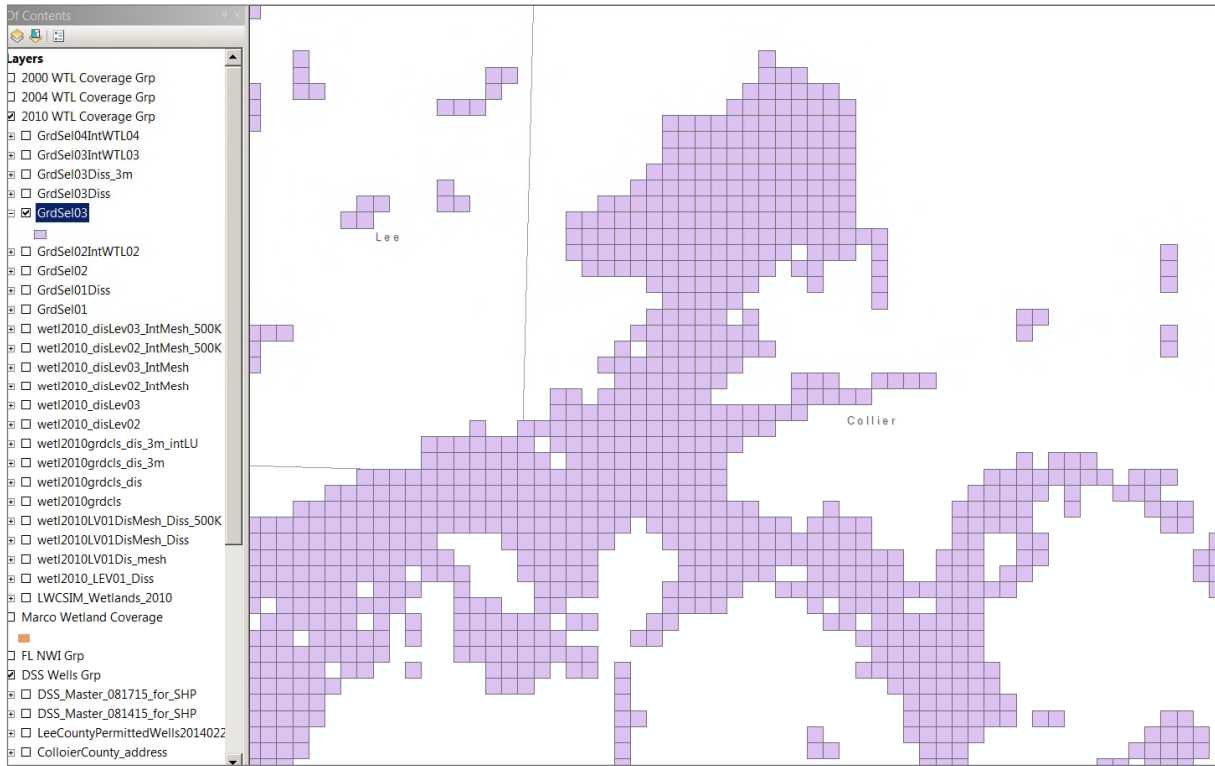


Figure F-12. Resulting selection with model grid.

15. Dissolve the cells to create contiguous polygons and save to GrdSel03Diss (Figure F-13).

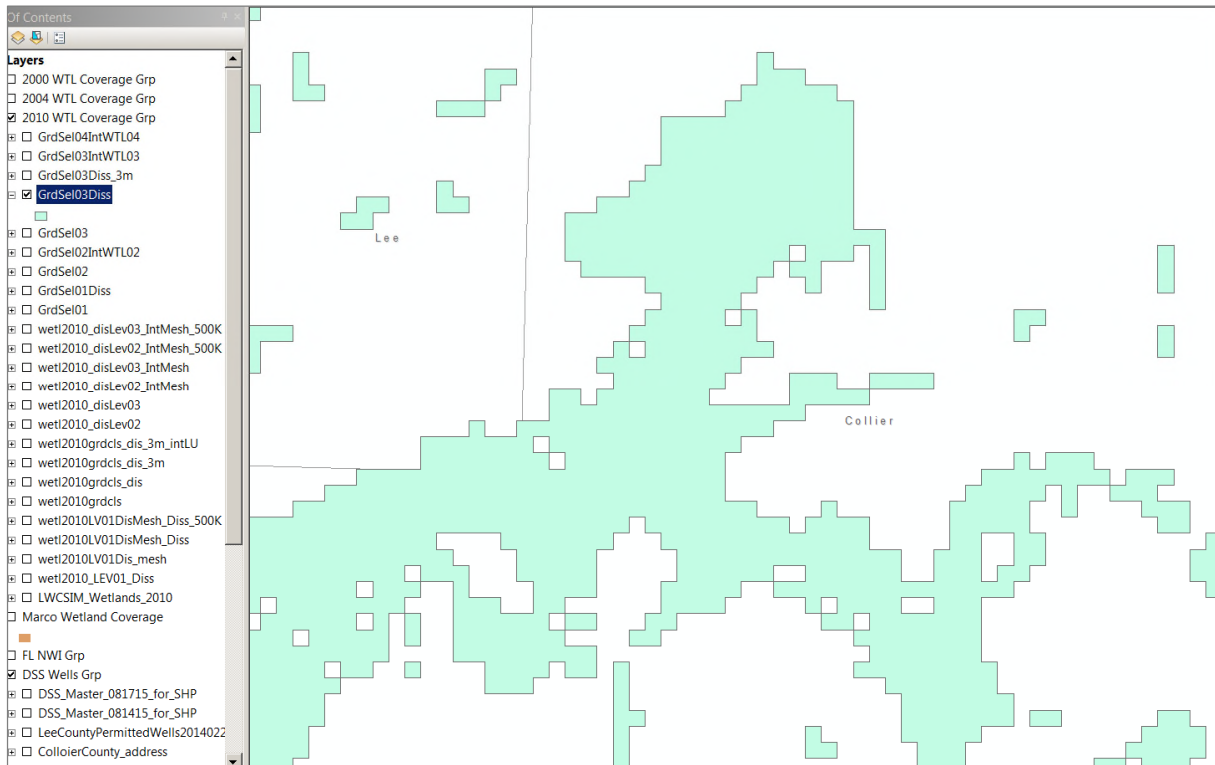


Figure F-13. Model grid selection dissolved to contiguous polygons.

16. Select only the polygons that are three cells in size (3 million square feet) or more to create GrdSel03Diss_3m (Figure F-14).

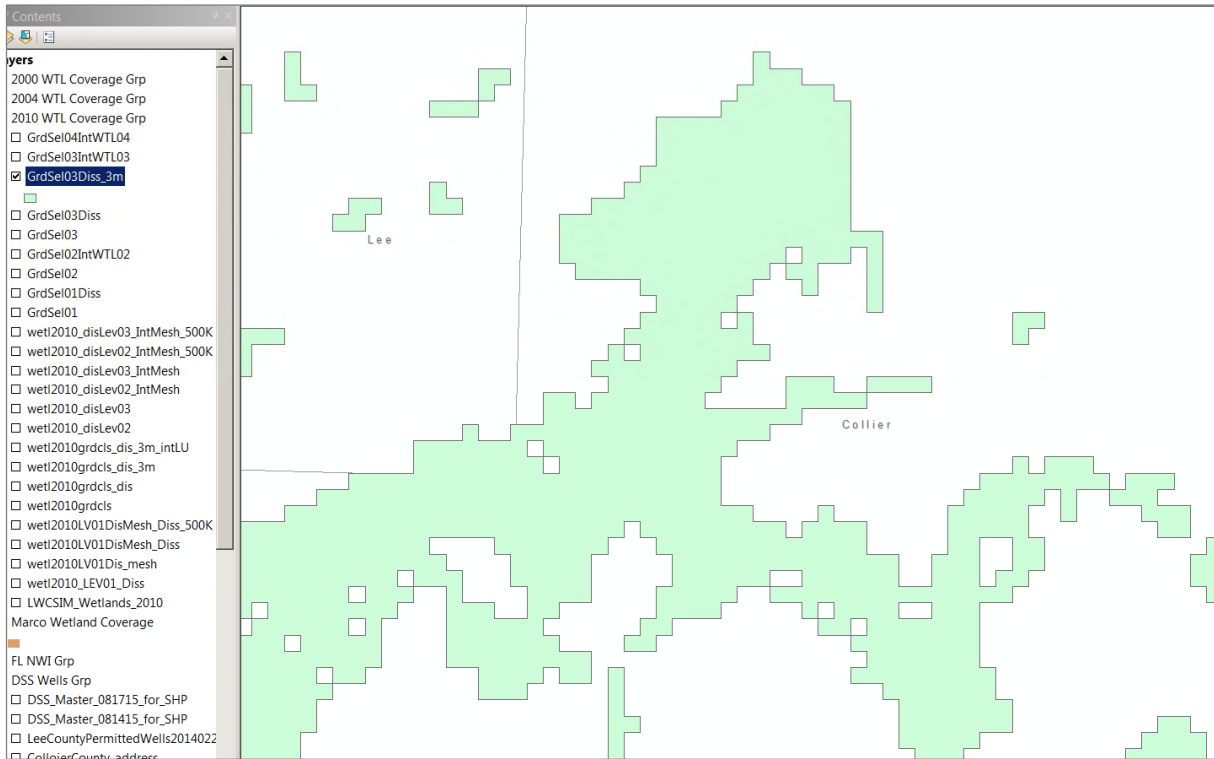


Figure F-14. Resulting grid polygons reduced to \geq grid cells in size.

17. Finally, intersect the polygons with the original wetlands LULC coverage to create GrdSel04IntWTL04. The attribute table of GrdSel04IntWTL04 will contain the critical wetland data for each active cell in the model grid (Level 3 wetland category, row, and column) (Figure F-15).

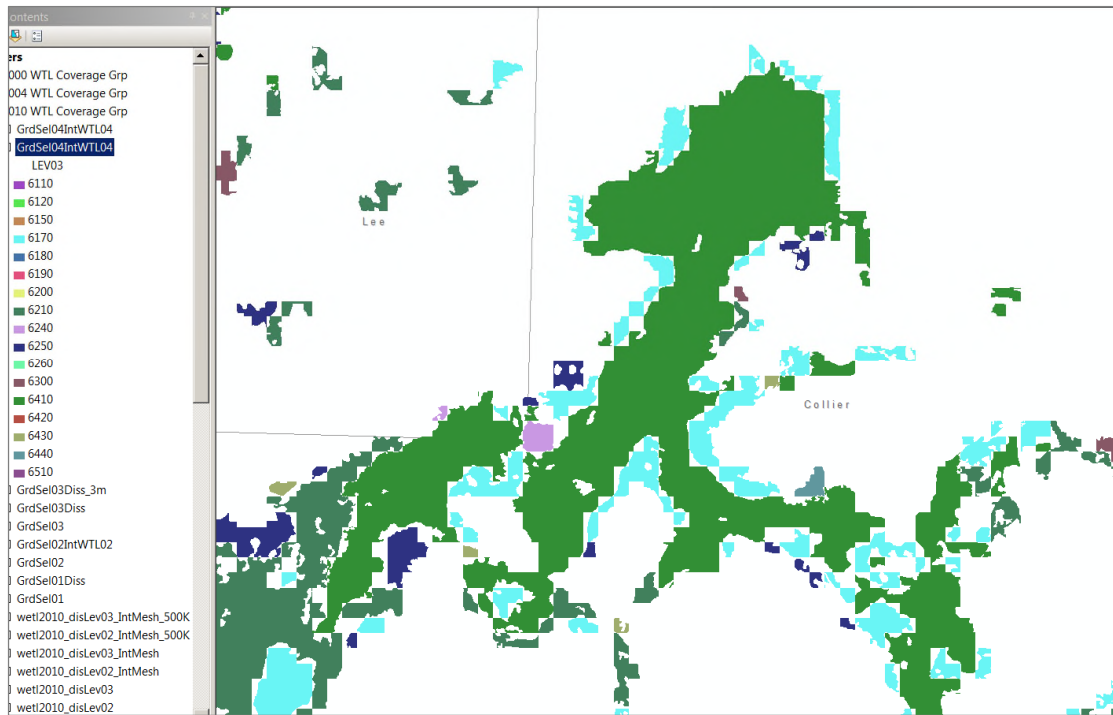


Figure F-15. Intersection with original wetland data.

This coverage was intersected with soils and model layers to produce the Excel spreadsheet shown in Table F-1.

Table F-1. Wetland coverage information.

| ROW | COL | Layer | ROWCO | Topo_NGVD2 | FLUCCS LEV03 | FLUCCS Description | REG CAT | Max Soil Area | Percent Cell Soil | MUNAME | TEXTURE | K Value f/d |
|-----|-----|---------|---------|--------------|---------------------------------|--------------------|---------|---------------|--|--------|---------|-------------|
| 362 | 490 | 1562490 | 9.74336 | 3154.536724 | 6410 Freshwater marshes | 2 | 0.32 | 0.32 | Riviera-Copeland-Boca (s1593) | SAND | 141 | |
| 442 | 279 | 1442279 | 1.0626 | 17936.72304 | 6120 Mangrove swamps | 1 | 1.79 | 1.79 | Water-Terra Cela-Perrine-Pennusco-Okeelanta (s1582) | MUCK | 0.28 | |
| 363 | 490 | 1563490 | 9.73396 | 43613.99505 | 6410 Freshwater marshes | 2 | 4.36 | 4.36 | Riviera-Copeland-Boca (s1593) | SAND | 141 | |
| 365 | 490 | 1565490 | 9.71468 | 98752.57081 | 6410 Freshwater marshes | 2 | 9.88 | 9.88 | Riviera-Copeland-Boca (s1593) | SAND | 141 | |
| 364 | 490 | 1564490 | 9.72752 | 119836.80609 | 6410 Freshwater marshes | 2 | 11.98 | 11.98 | Riviera-Copeland-Boca (s1593) | SAND | 141 | |
| 285 | 450 | 1285450 | 15.4533 | 133869.7747 | 6210 Cypress | 2 | 13.39 | 13.39 | RIVIERA SAND, LIMESTONE SUBSTRATUM, DEPRESSIONAL | SAND | 141 | |
| 257 | 394 | 1257394 | 22.9003 | 135266.6386 | 6170 Mixed wetland hardwoods | 2 | 13.53 | 13.53 | HOLOPAW SAND, DEPRESSIONAL | SAND | 141 | |
| 257 | 391 | 1257391 | 23.1885 | 147648.7544 | 6210 Cypress | 2 | 14.76 | 14.76 | CHOBEE FINE SANDY LOAM, LIMESTONE SUBSTRATUM, DEPRESSIONAL | FSL | 8 | |
| 275 | 391 | 1275391 | 20.0062 | 154449.4619 | 6240 Cypress-pine-cabbage palm | 3 | 15.44 | 15.44 | CHOBEE FINE SANDY LOAM, LIMESTONE SUBSTRATUM, DEPRESSIONAL | FSL | 8 | |
| 267 | 405 | 1267405 | 19.9912 | 161176.7175 | 6170 Mixed wetland hardwoods | 2 | 16.12 | 16.12 | JUPITER-OCHOPEE-ROCK OUTCROP COMPLEX | FS | 14 | |
| 17 | 204 | 1017204 | 43.1661 | 162978.6515 | 6300 Wetland forested mixed | - | 16.30 | 16.30 | MALABAR FINE SAND, HIGH | FS | 14 | |
| 233 | 189 | 1231189 | 16.3137 | 164669.2076 | 6210 Cypress | 2 | 16.47 | 16.47 | PIVEDA FINE SAND | FS | 14 | |
| 230 | 424 | 1230424 | 24.0095 | 166086.5379 | 6410 Freshwater marshes | 2 | 16.61 | 16.61 | BASINGER SAND | SAND | 141 | |
| 372 | 249 | 157249 | 7.42611 | 166380.2917 | 6200 Wetland coniferous forests | - | 16.64 | 16.64 | OLDSMAR FINE SAND, LIMESTONE SUBSTRATUM | FS | 14 | |
| 183 | 310 | 1583310 | 28.8782 | 167204.3198 | 6170 Mixed wetland hardwoods | 2 | 16.72 | 16.72 | CHOBEE FINE SANDY LOAM, DEPRESSIONAL | FSL | 8 | |
| 307 | 272 | 1507272 | 14.2904 | 170173.9114 | 6250 Hydric pine flatwoods | 3 | 17.02 | 17.02 | HOLOPAW FINE SAND | FS | 14 | |
| 260 | 199 | 1260199 | 15.7556 | 170289.9024 | 6250 Hydric pine flatwoods | 3 | 17.03 | 17.03 | PIVEDA FINE SAND, DEPRESSIONAL | FS | 14 | |
| 322 | 478 | 1522478 | 12.7938 | 172144.1775 | 6170 Mixed wetland hardwoods | 2 | 17.21 | 17.21 | JUPITER FINE SAND | FS | 14 | |
| 322 | 478 | 1522478 | 12.7938 | 172144.1775 | 6170 Mixed wetland hardwoods | 2 | 17.21 | 17.21 | Riviera-Copeland-Boca (s1593) | SAND | 141 | |
| 219 | 244 | 1219244 | 29.4802 | 173134.8112 | 6210 Cypress | 2 | 17.31 | 17.31 | FELDA FINE SAND, DEPRESSIONAL | FS | 14 | |
| 295 | 485 | 1295485 | 12.7506 | 174598.5322 | 6410 Freshwater marshes | 2 | 17.46 | 17.46 | CHOBEE SANDY LOAM, DEPRESSIONAL | SL | 2 | |
| 212 | 452 | 1212452 | 16.8457 | 175447.9349 | 6210 Cypress | 2 | 17.54 | 17.54 | HOLOPAW SAND | SAND | 141 | |
| 448 | 272 | 1448272 | 3.18447 | 177454.4447 | 6120 Mangrove swamps | 1 | 17.75 | 17.75 | DURBIN AND WULFERT MUCKS, FREQUENTLY FLOODED | MUCK | 0.28 | |
| 186 | 405 | 1586405 | 27.0024 | 179256.1882 | 6420 Wet prairies | 3 | 17.93 | 17.93 | WINDER FINE SAND | FS | 14 | |
| 218 | 199 | 1218199 | 20.7428 | 179426.6203 | 6300 Wetland forested mixed | - | 17.94 | 17.94 | VALKARIA FINE SAND, DEPRESSIONAL | FS | 14 | |
| 293 | 329 | 1293329 | 16.7803 | 180030.4873 | 6170 Mixed wetland hardwoods | 2 | 18.00 | 18.00 | CHOBEE, WINDER, AND GATOR SOILS, DEPRESSIONAL | FSL | 8 | |
| 296 | 309 | 1296309 | 15.594 | 180294.9219 | 6210 Cypress | 2 | 18.03 | 18.03 | BOCA FINE SAND | FS | 14 | |
| 447 | 272 | 1447272 | 2.98785 | 180923.4907 | 6120 Mangrove swamps | 1 | 18.09 | 18.09 | DURBIN AND WULFERT MUCKS, FREQUENTLY FLOODED | MUCK | 0.28 | |
| 291 | 337 | 1291337 | 16.4267 | 182322.8896 | 6300 Wetland forested mixed | - | 18.32 | 18.32 | HILOLO, JUPITER, AND MARGATE FINE SANDS | FS | 14 | |
| 205 | 264 | 1205264 | 25.4073 | 183996.648 | 6410 Freshwater marshes | 2 | 18.36 | 18.36 | TUSCOWILLA FINE SAND | FS | 14 | |
| 331 | 325 | 1531325 | 15.9546 | 184234.4491 | 6250 Hydric pine flatwoods | 3 | 18.42 | 18.42 | OCHOPEE FINE SANDY LOAM | FSL | 8 | |
| 350 | 466 | 150466 | 17.2382 | 184953.6724 | 6410 Freshwater marshes | 2 | 18.49 | 18.49 | QUANTATION MUCK | MUCK | 0.28 | |

Data from the spreadsheet were used to generate the array files needed for the WTL package for MODFLOW.

**APPENDIX G:
LANDSCAPE IRRIGATION DATA DEVELOPMENT PROCEDURE**

1. Identify landscape irrigation (LSI) locations and calculate flow rates
 - a. Delineate developed areas in geographical information systems (GIS) land use coverages.
 - b. Overlay utility service area (potable and reclaimed water) map and identify different application regions belonging to each county.
 - c. Overlay wetland/water features coverage and percent impervious coverage to delineate pervious areas within each cell and each irrigation application area.
2. Calculate monthly application rates.
 - a. Using the map produced in step 1, calculate the percent pervious areas in each cell located in developed areas in each irrigation application area in a given county.
 - b. Normalize the pervious area calculated for each cell by the total pervious area within the respective irrigation application area in a given county.
 - c. Multiply the total irrigation given by the normalized percent pervious area for each cell to calculate the flow rate for each cell. This is the average annual daily flow; therefore, the calculated LSI is the average annual daily LSI flow.

$$LSI \text{ rate in cell} = \text{Group LSI rate} * \frac{\sum_{i=1}^{num_class} A_i * f_i}{\sum_{All \text{ cells in group}} \sum_{j=1}^{num_class} A_j * f_j}$$

3. Develop the temporal variation curve for LSI.
 - a. Peaking factors were derived from the outdoor portion of the average pumping of all utilities in a given county (flow-weighted average). Utilities with larger pumping volume have more influence on the peaking factors than utilities with smaller pumping volume. The following steps describe the derivation of peaking factors and temporal variation curve for LSI.
 - i. Locate utilities that provide service within a given county.
 - ii. Calculate the total pumping volume for each of the stress periods from all wells/utilities for each county.
 - iii. Obtain the outdoor portion of the total pumping volume used for LSI for each stress period by subtracting the indoor water use from values obtained in step ii.
 - iv. The array of peaking factors for each county is obtained by dividing the outdoor potable LSI county array obtained in step iii by the total outdoor portion of the water use.
 - v. Calculate the temporal variation of LSI in each cell by multiplying the average annual daily flow by the peaking factors obtain in step iv.
 - vi. Sum all the LSI in each cell for the total number of stress periods and calculate the average to check the correct distribution of LSI within the irrigable area in each county.

4. Identify and calculate the daily irrigation rates.
 - a. During agricultural demand estimation, LSI demands were calculated using the Agricultural Field-Scale Irrigation Requirements Simulation (AFSIRS) demand model.
 - b. Using AFSIRS-generated irrigation demand curves, identify the days irrigation is required.
 - c. For a new cell that was not included in the previous approach, an average irrigation demand curve is used for the county where the cell is located.
 - d. Daily application rates are determined by multiplying the monthly average by the number of days in a given month and dividing by the number of days that actual irrigation occurs (calculated with AFSIRS). Then irrigation is applied on the AFSIRS-calculated days in a given month.
 - e. In the model, irrigation is applied to each cell as an irrigation depth, which is obtained by dividing the irrigation rates by the model cell area ($1,000 \times 1,000$ square feet).
 - f. Daily irrigation depths are added to the total rainfall array that is run through the Curve Number method to partition rainfall plus irrigation into runoff and infiltration.
 - g. The infiltrating portion is sent through the ET-Recharge-Runoff program to develop MODFLOW evapotranspiration and recharge data sets.

The LSI development flow chart is shown in **Figure G-1**.

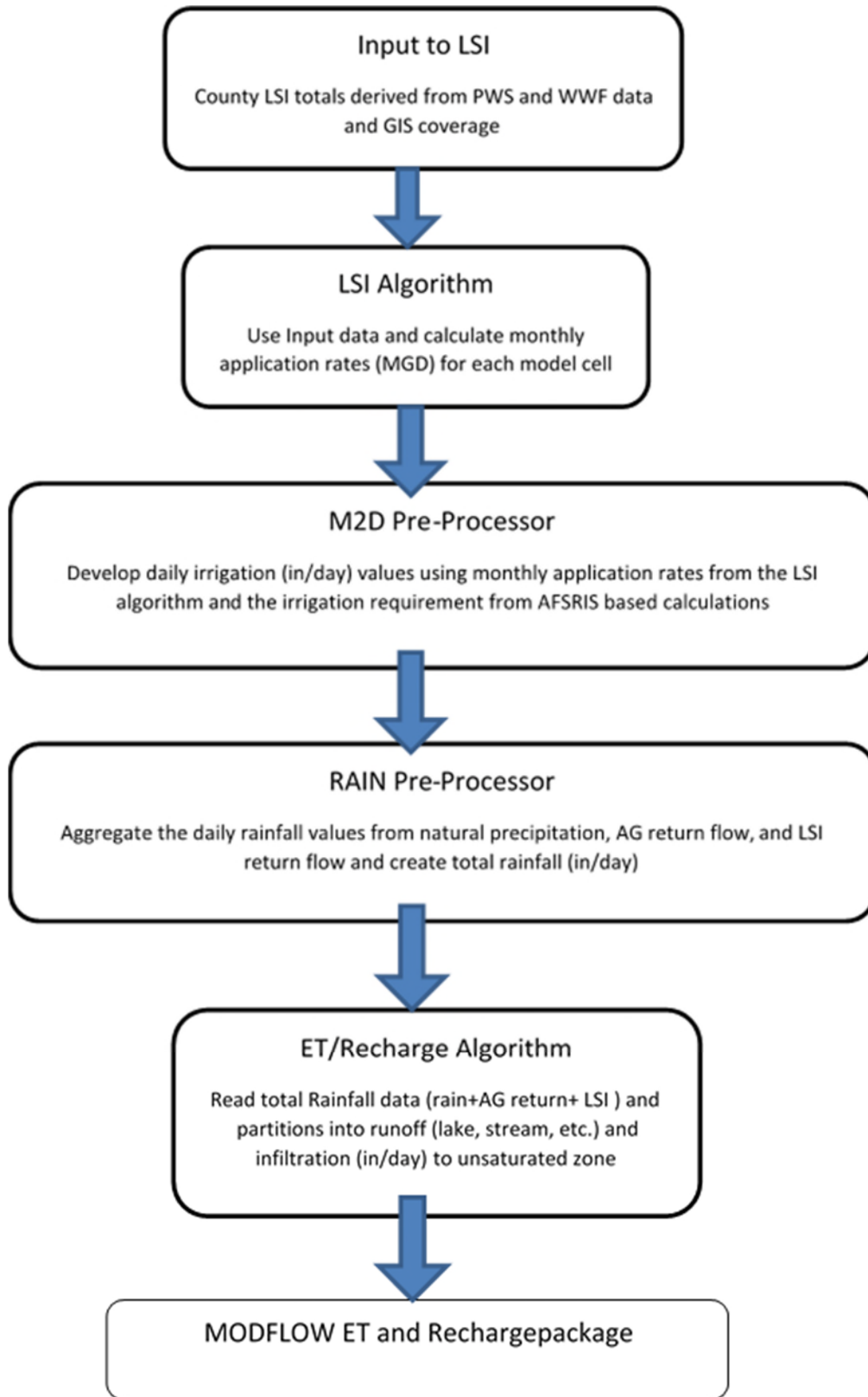


Figure G-1. Landscape irrigation data development flow chart.

**APPENDIX H:
FINAL ADJUSTED MODEL PROPERTIES**

The end result of manual transient calibration provided the following property distributions in the model layers. In **Figures H-1 to H-5**, field measurements of horizontal hydraulic conductivity were overlaid to show that the calibrated distributions were within an order of magnitude of field measured values throughout the model domain. **Figures H-6 to H-10** present the transmissivity distribution in each of the five aquifer layers. Vertical leakage was adjusted manually for layers 2, 4, 6, and 8, representing the vertical leakage between the five aquifer layers. The result of manual adjustment of vertical leakage is presented **Figures H-11 to H-14**. The storage coefficient, or storativity, in the five aquifer layers resulting from manual calibration is presented in **Figures H-15 to H-19**.

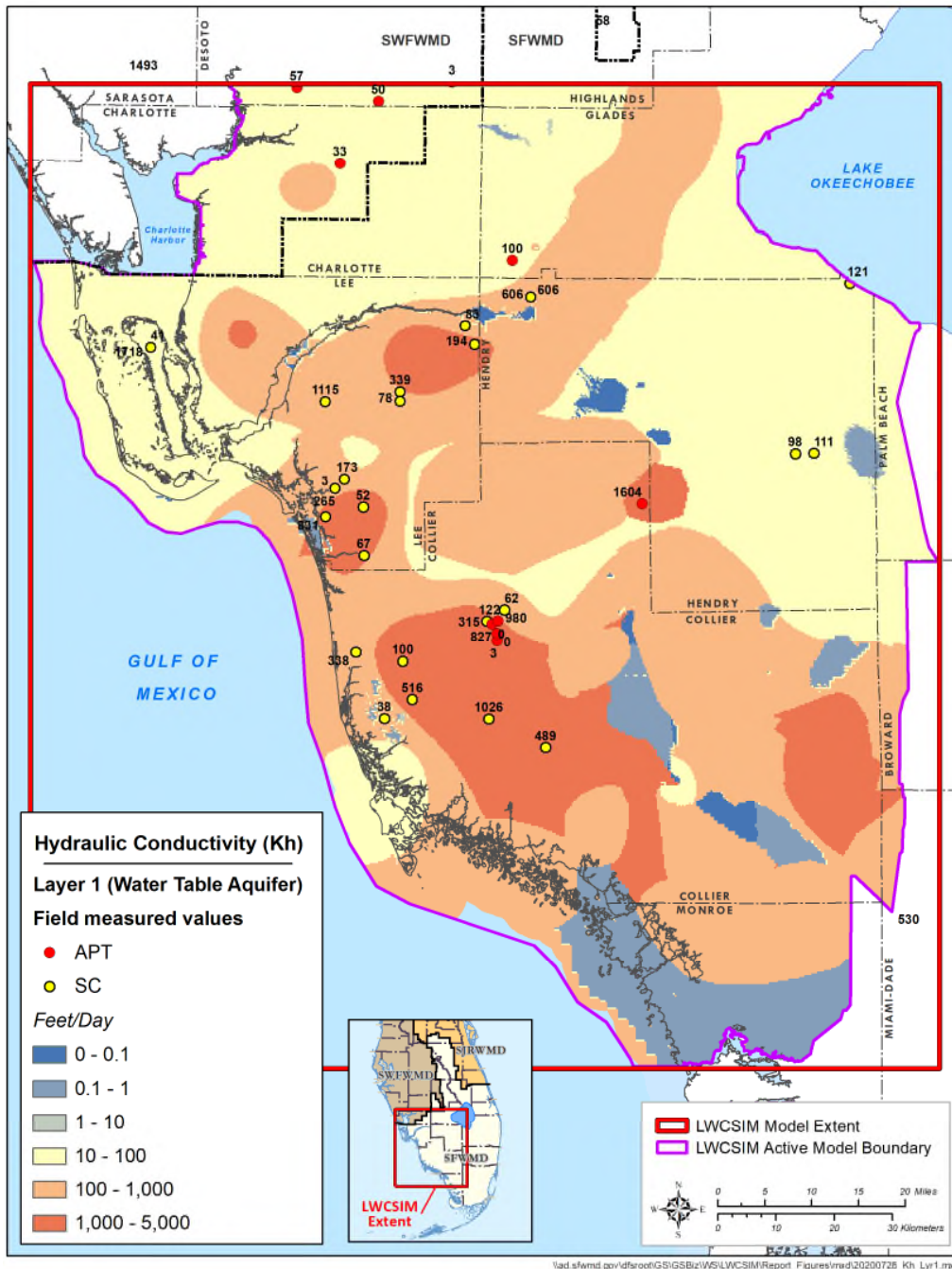


Figure H-1. Water Table aquifer (layer 1) calibrated hydraulic conductivity.

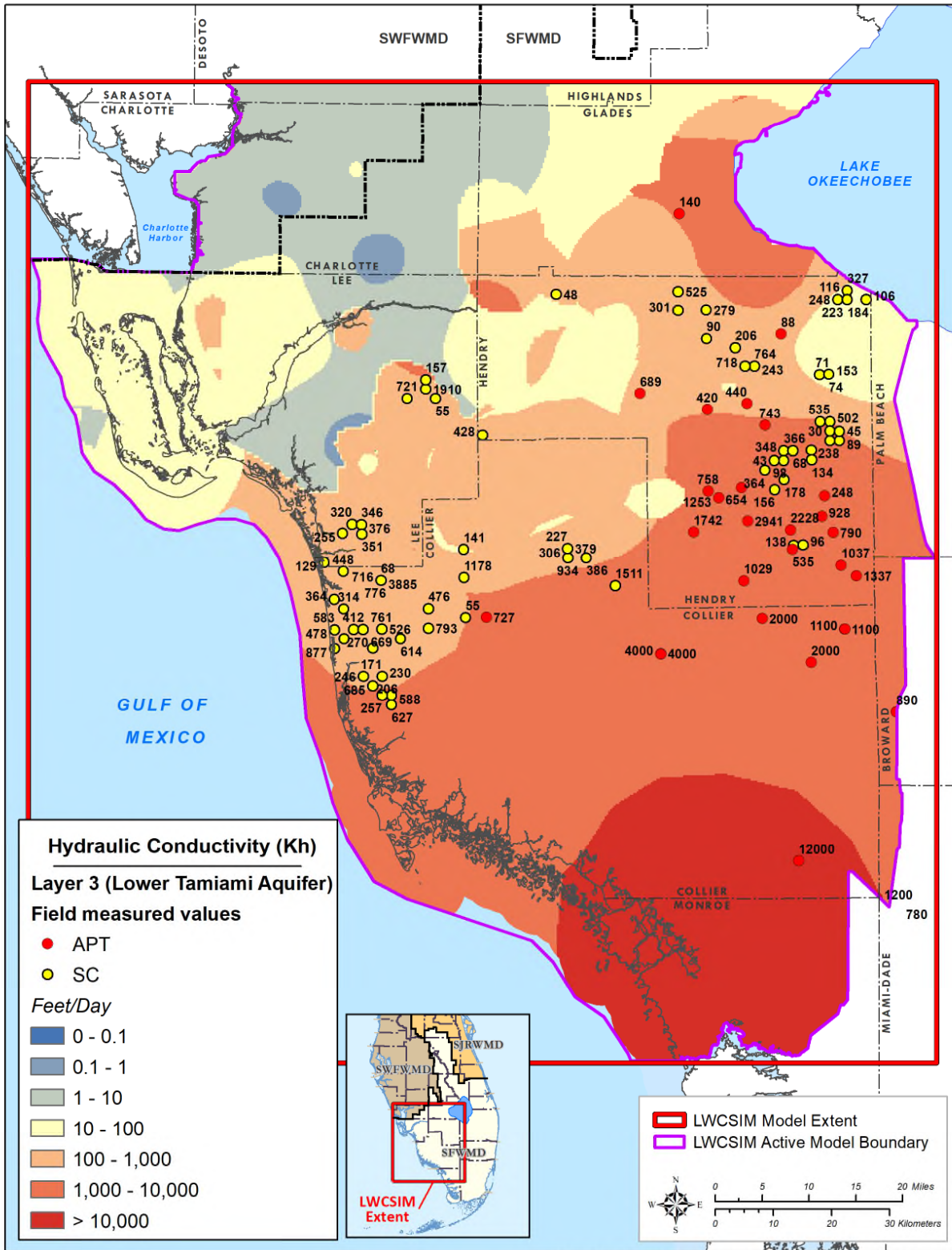
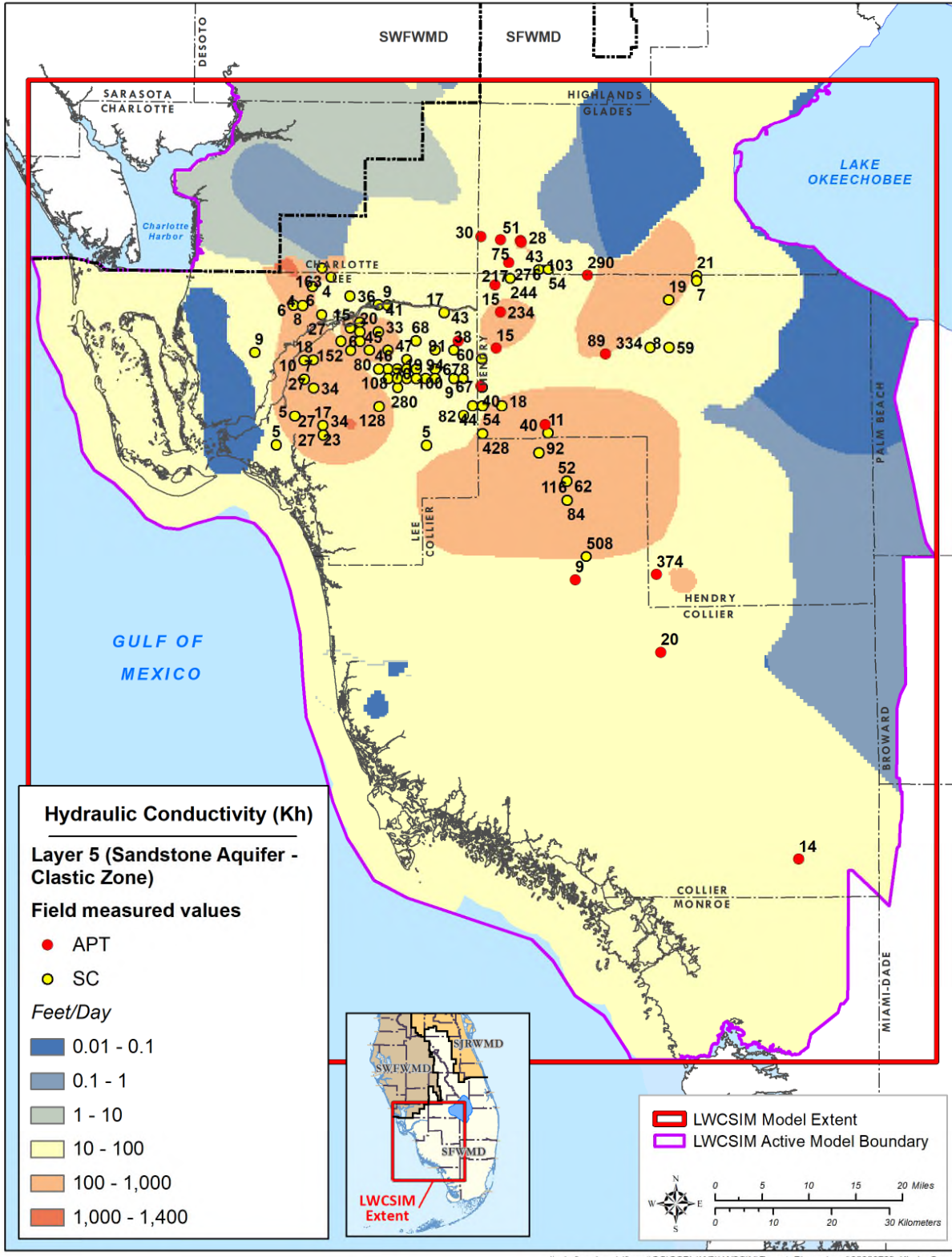


Figure H-2. Lower Tamiami aquifer (layer 3) calibrated hydraulic conductivity.



\\ad.sfwmd.gov\dfsroot\GIS\GSBiz\WS\LWCSIM\Report_Figures\mxd\20200728_Kh_Lyr5.mxd

Figure H-3. Sandstone aquifer clastic zone (layer 5) calibrated hydraulic conductivity.

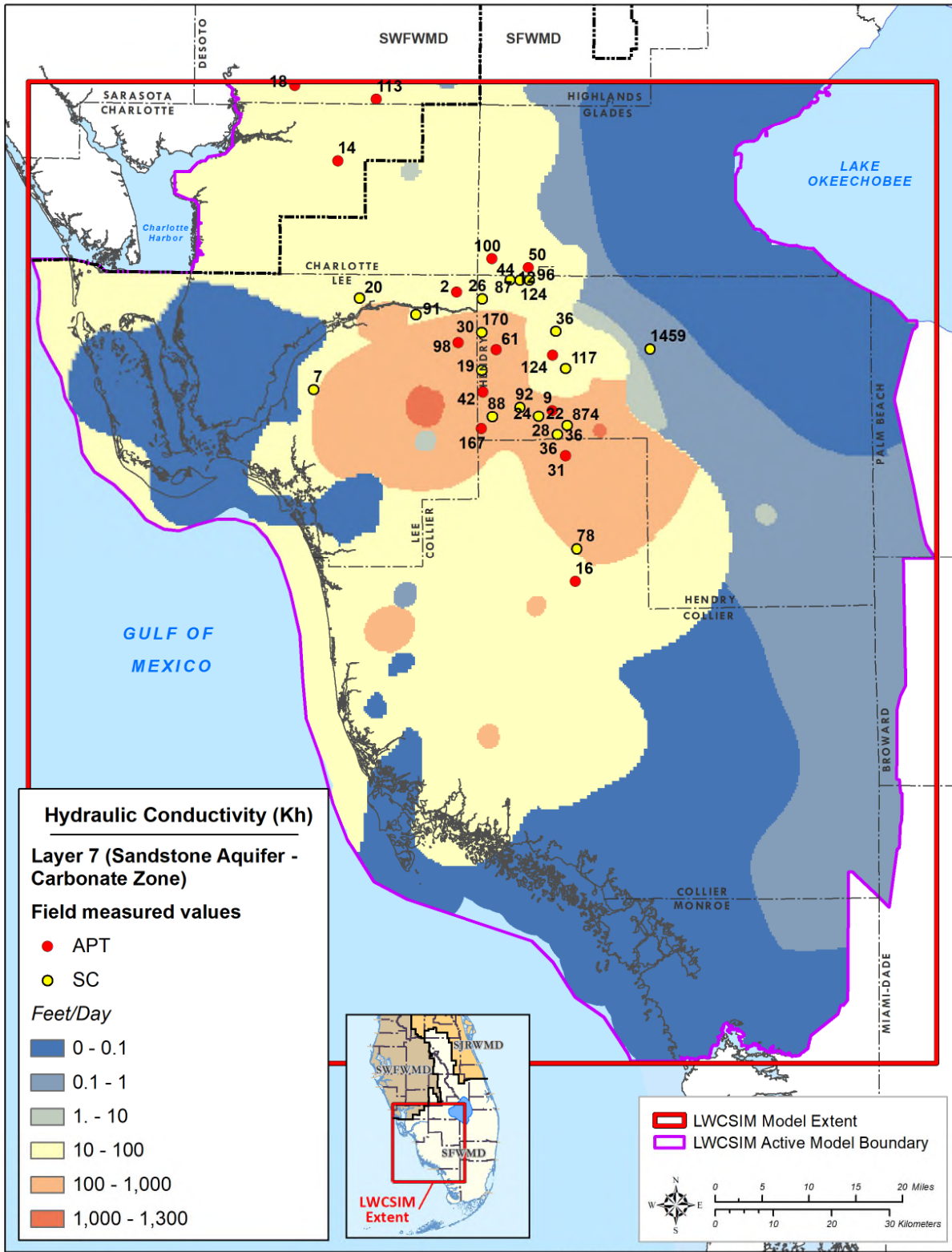
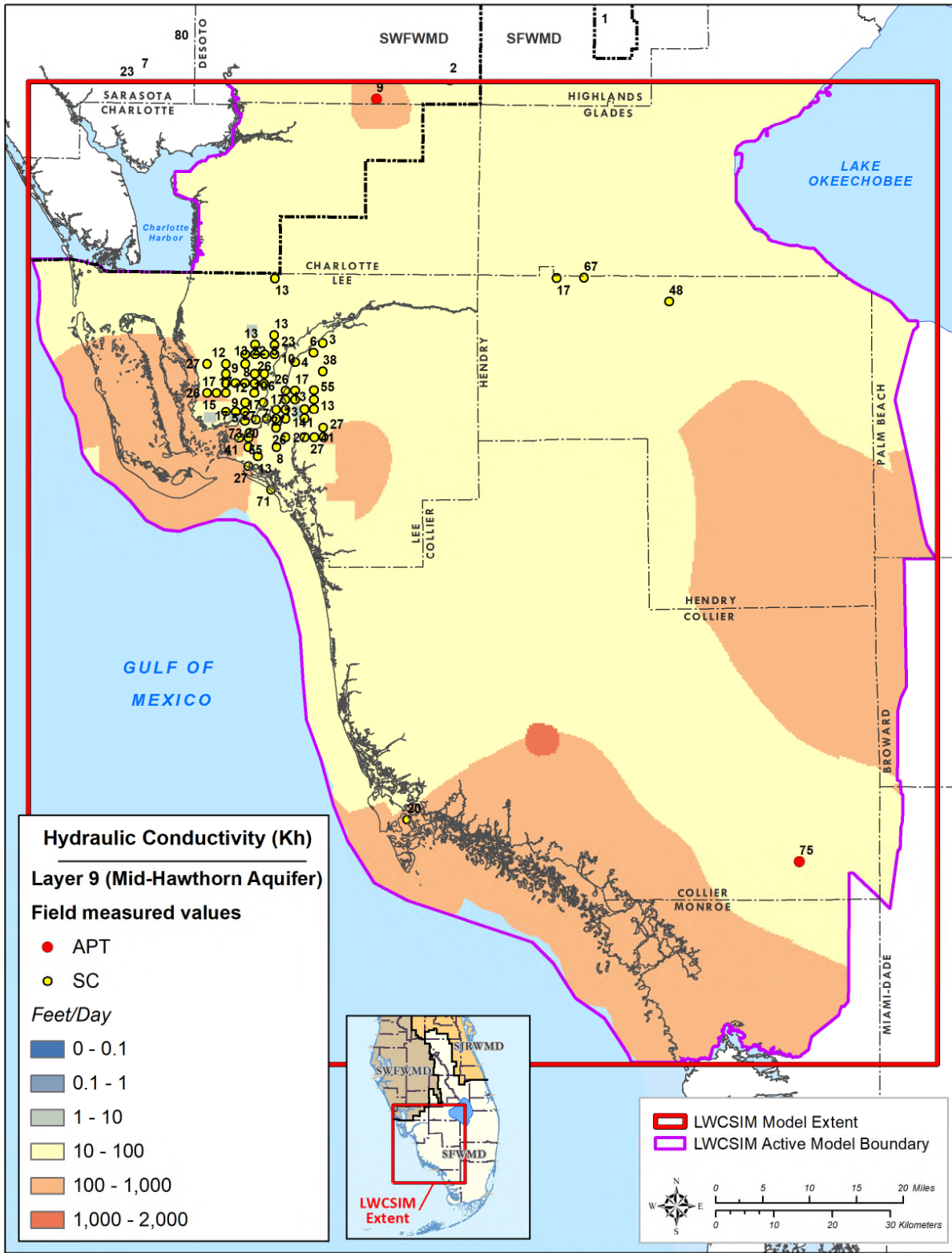


Figure H-4. Sandstone aquifer carbonate zone (layer 7) calibrated hydraulic conductivity.



\\ad.sfwmd.gov\dfsroot\GIS\GSBiz\WLS\LWCSIM\Report_Figures\mwd\20200728_Kh_Lyr9.mxd

Figure H-5. Mid-Hawthorn aquifer (layer 9) calibrated hydraulic conductivity.

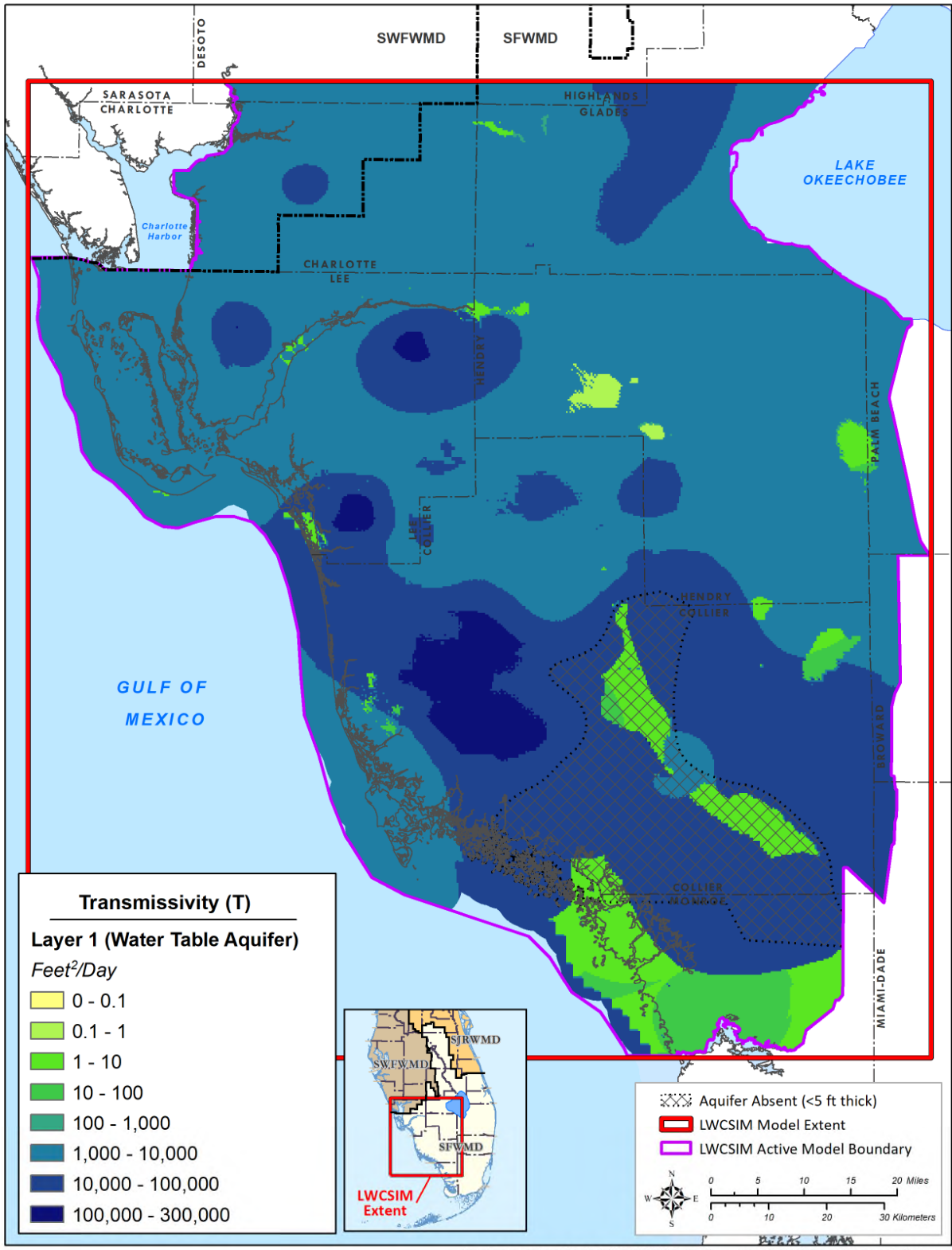


Figure H-6. Water Table aquifer (layer 1) transmissivity from the calibrated model.

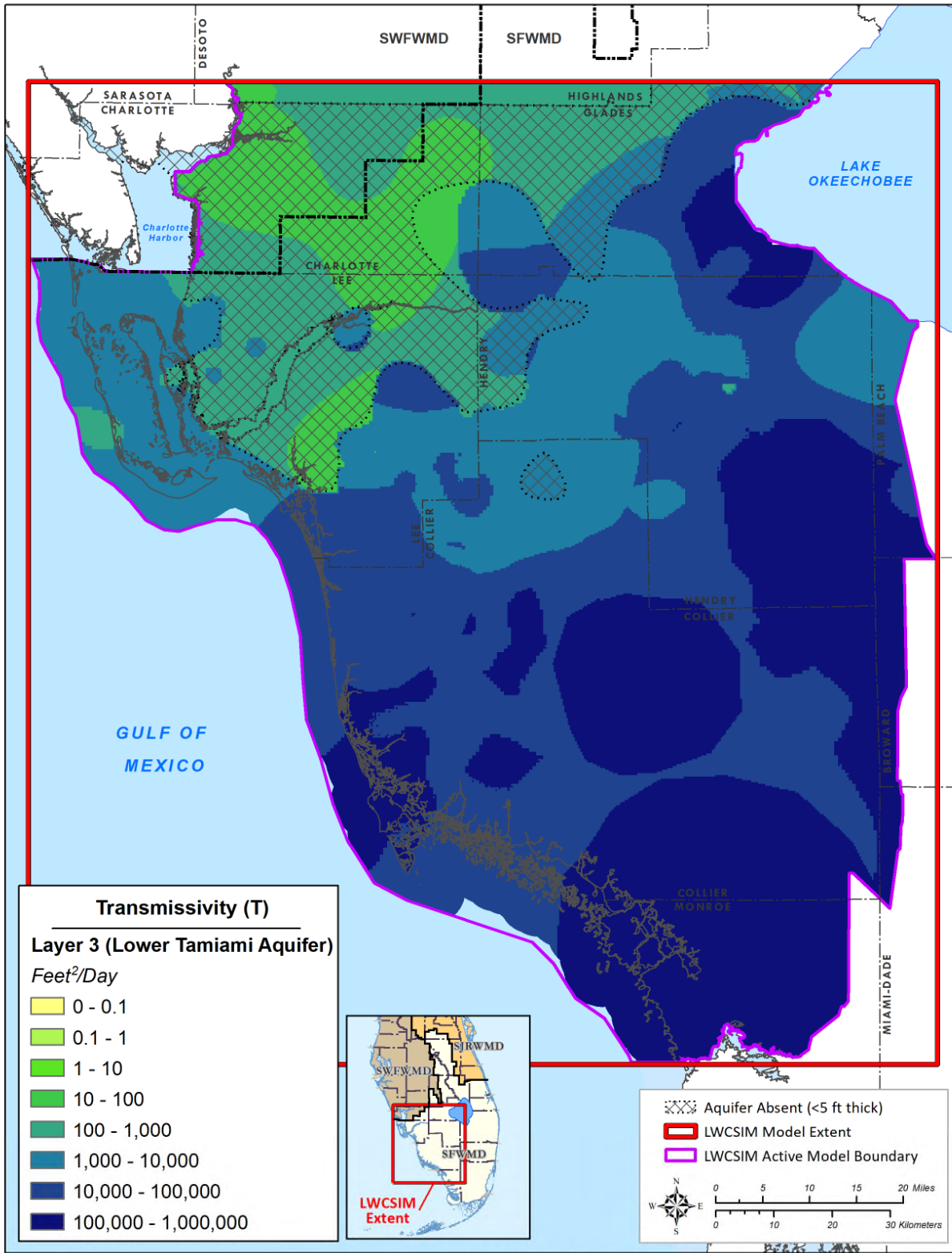


Figure H-7. Lower Tamiami aquifer (layer 3) transmissivity from the calibrated model.

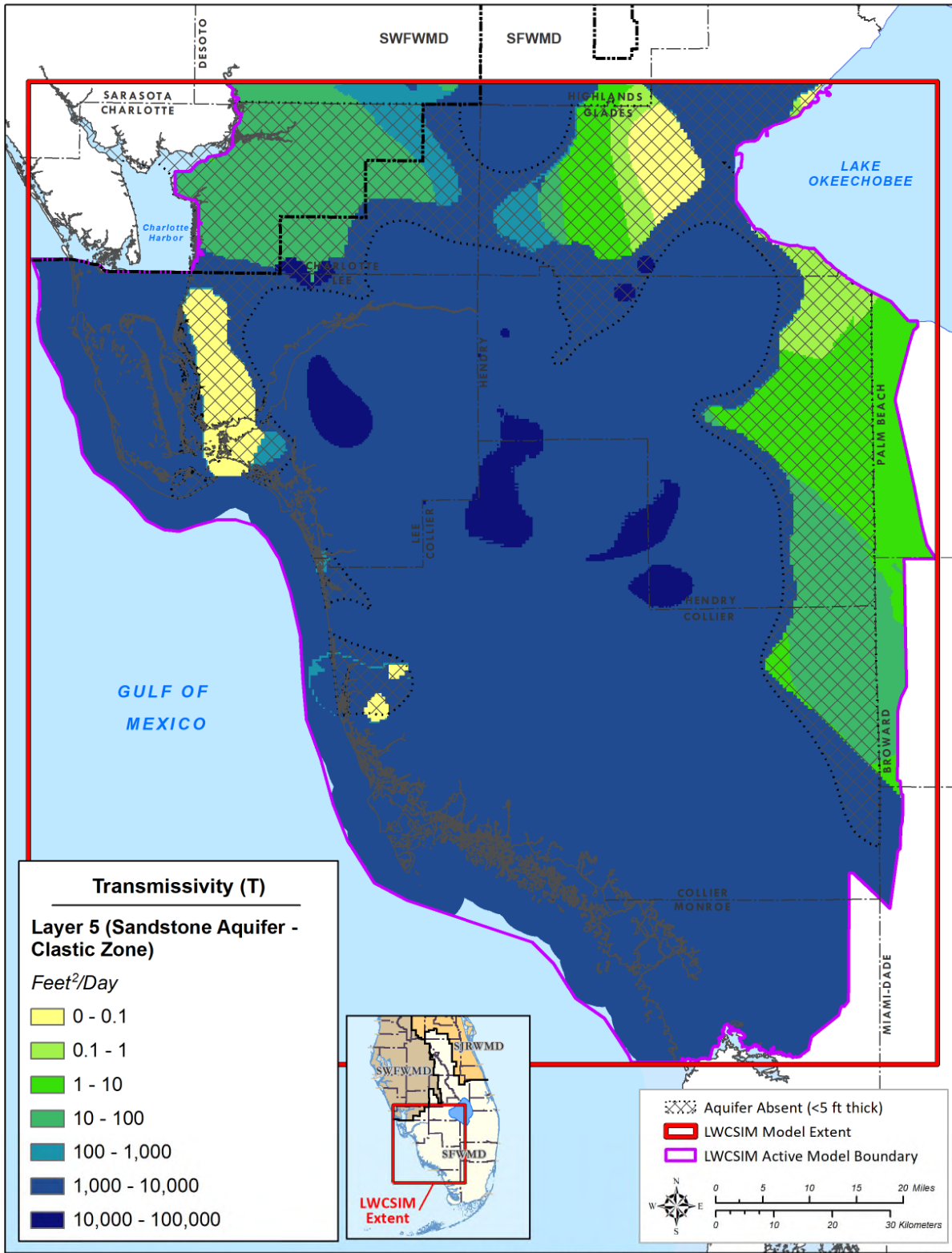


Figure H-8. Sandstone aquifer – clastic zone (layer 5) transmissivity from the calibrated model.

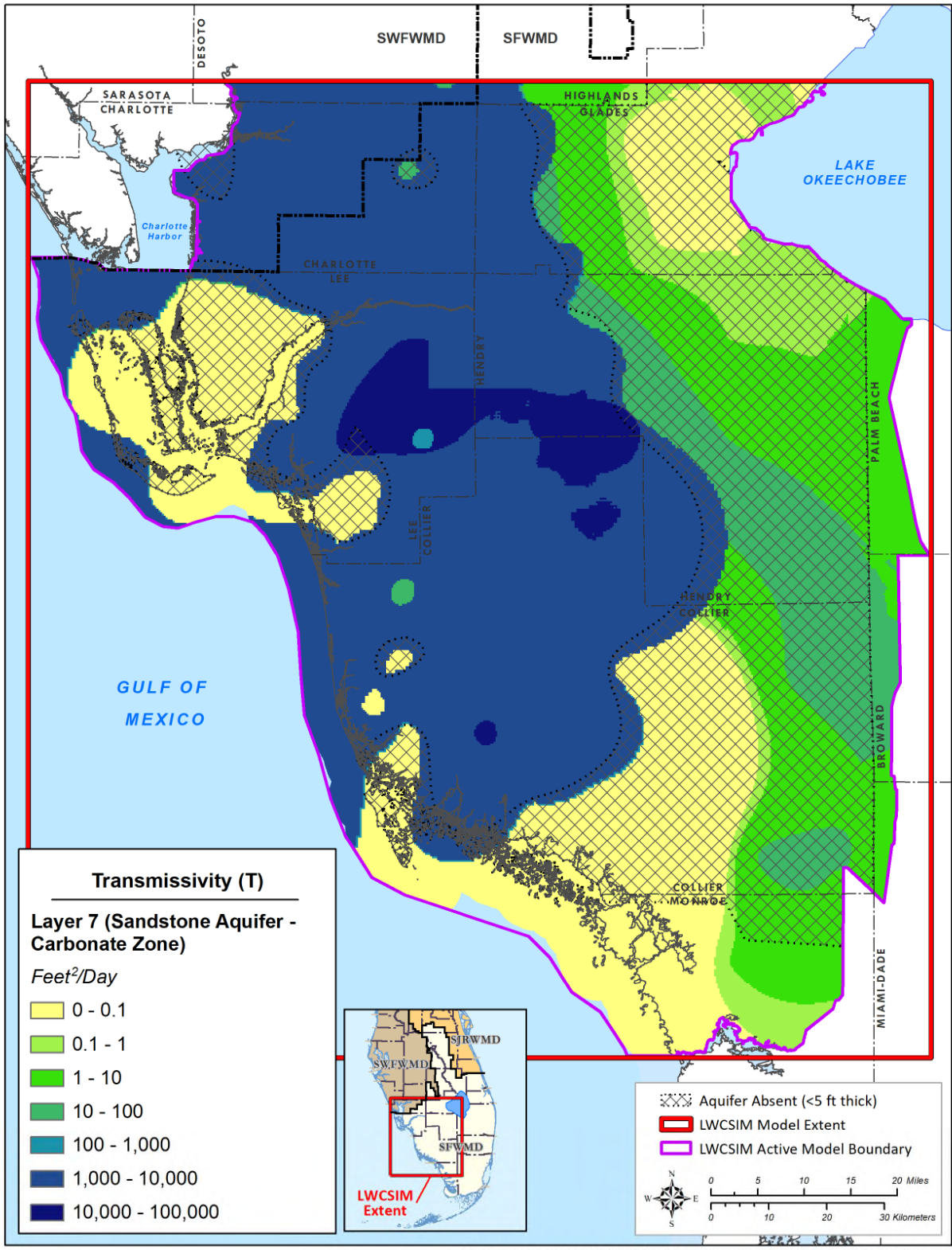


Figure H-9. Sandstone aquifer – carbonate zone (layer 7) transmissivity from the calibrated model.

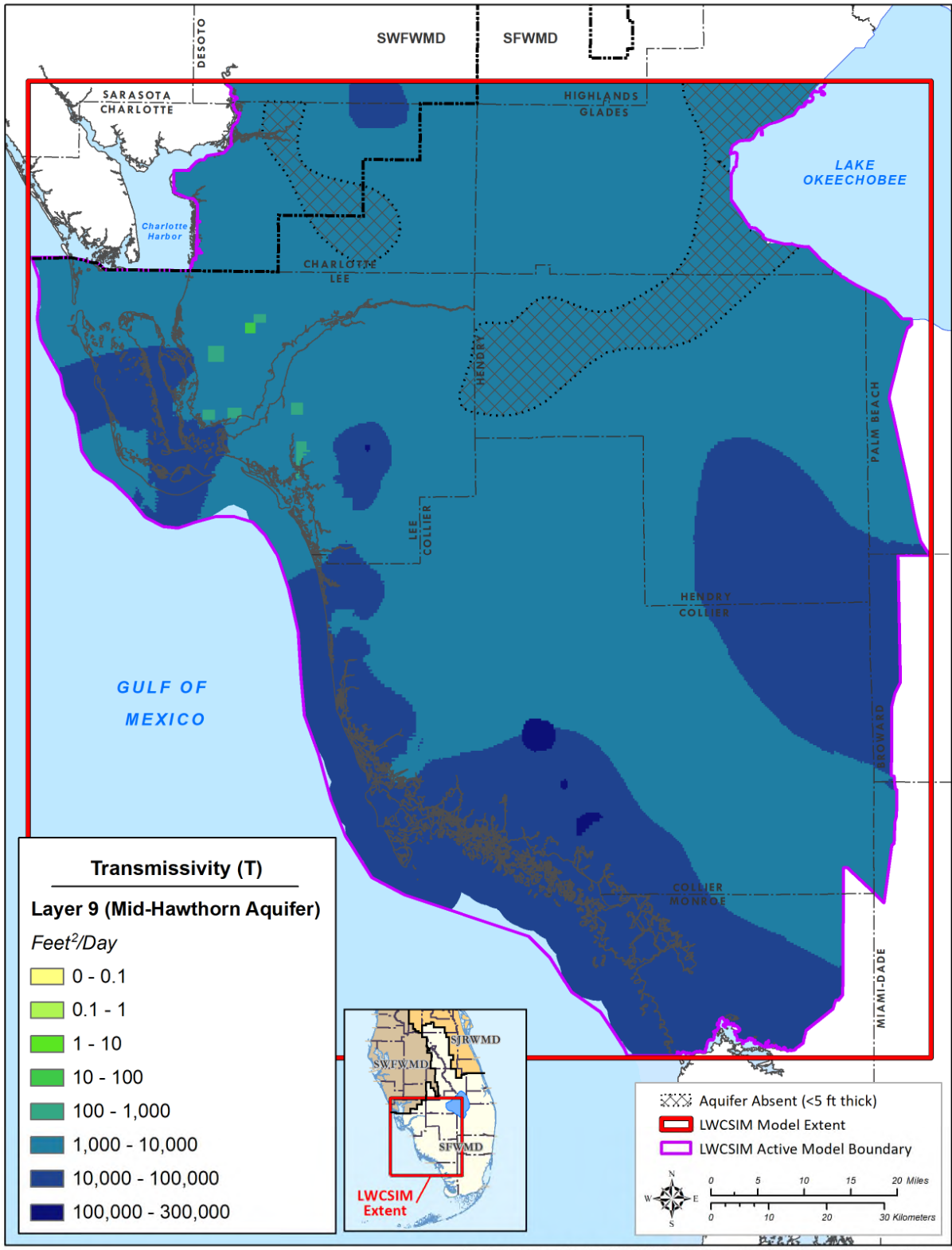
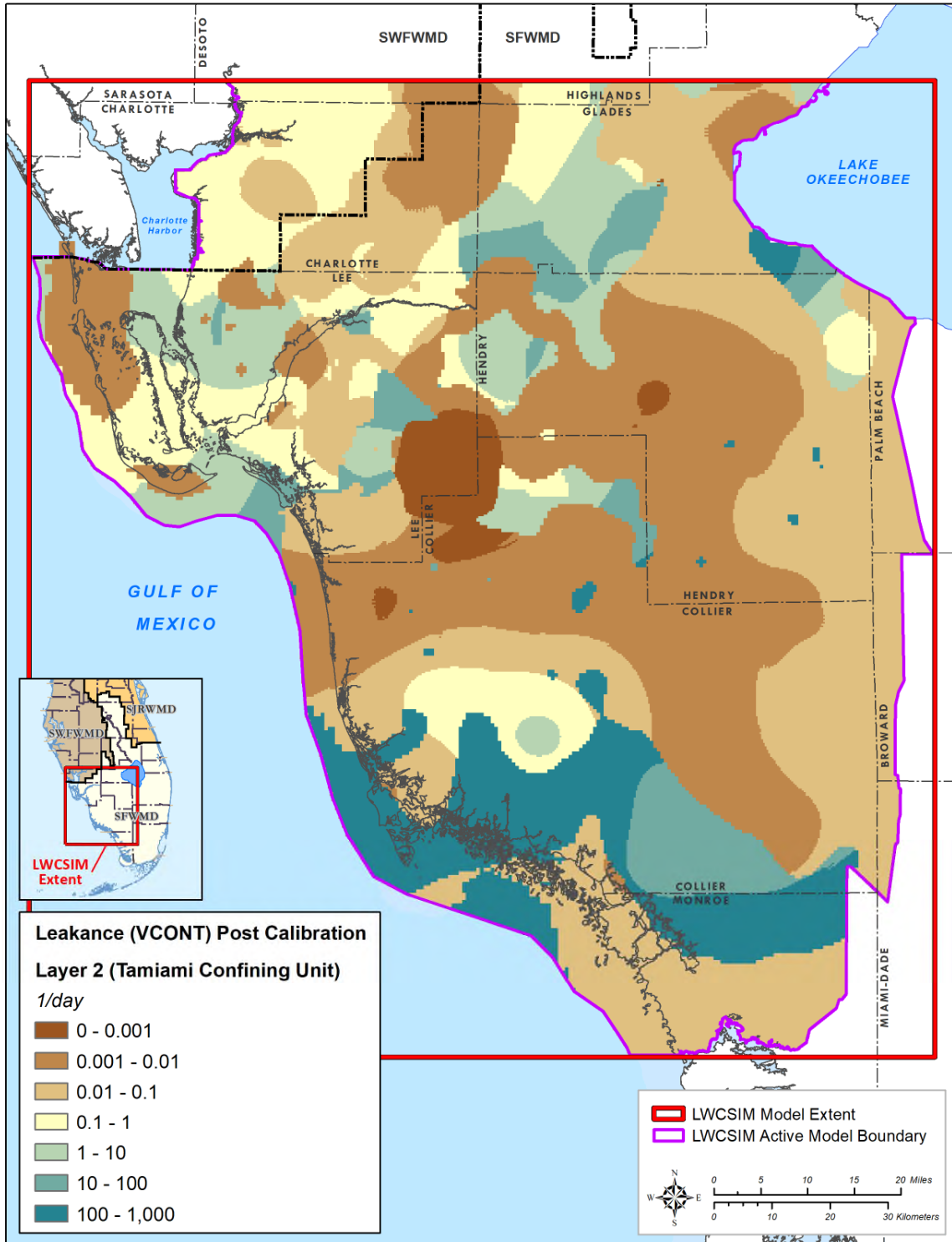
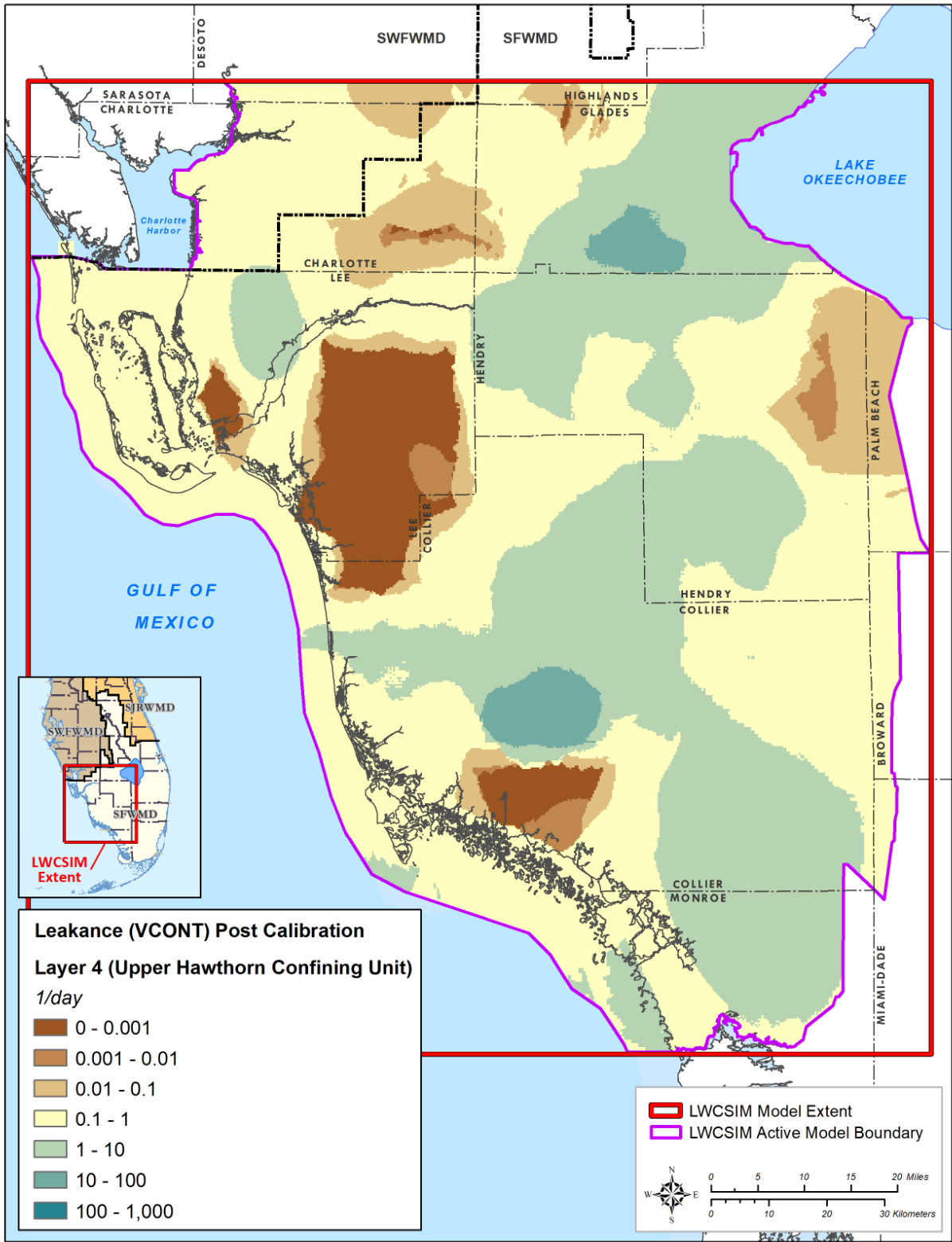


Figure H-10. Mid-Hawthorn aquifer (layer 9) transmissivity from the calibrated model.



\\ad.sfwmd.gov\dfsroot\GIS\GISBiz\WWS\LWCSIM\Report_Figures\mxd\VCONT PostCalib.mxd

Figure H-11. Calibrated leakance in the Tamiami confining unit (layer 2).



\\ad.sfwmd.gov\dfsroot\GIS\GSBz\WS\LWCSIM\Report_Figures\mxd\VCONTPostCalib.mxd

Figure H-12. Calibrated leakance in the Upper Hawthorn confining unit (layer 4).

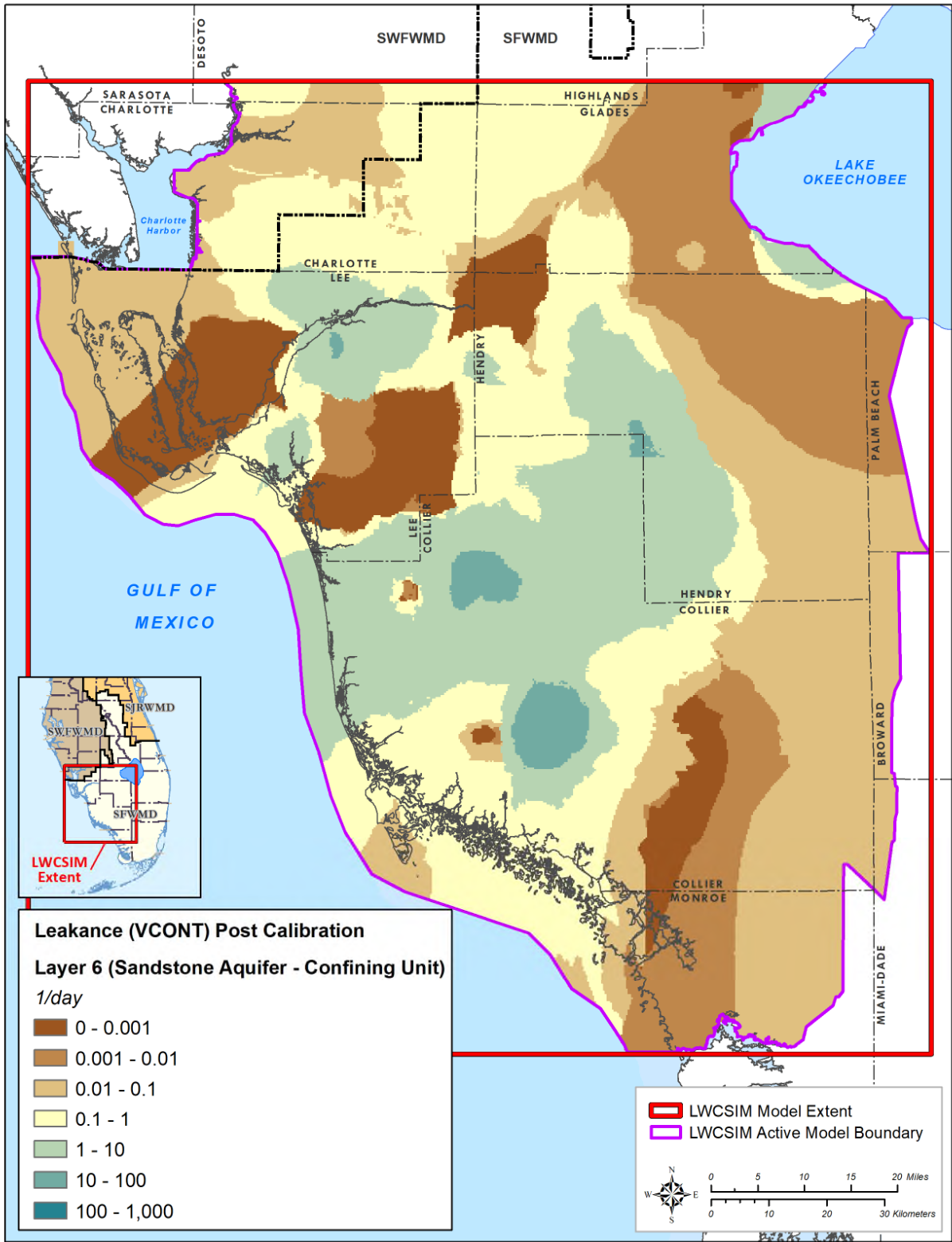


Figure H-13. Calibrated leakance in the Sandstone confining unit (layer 6).

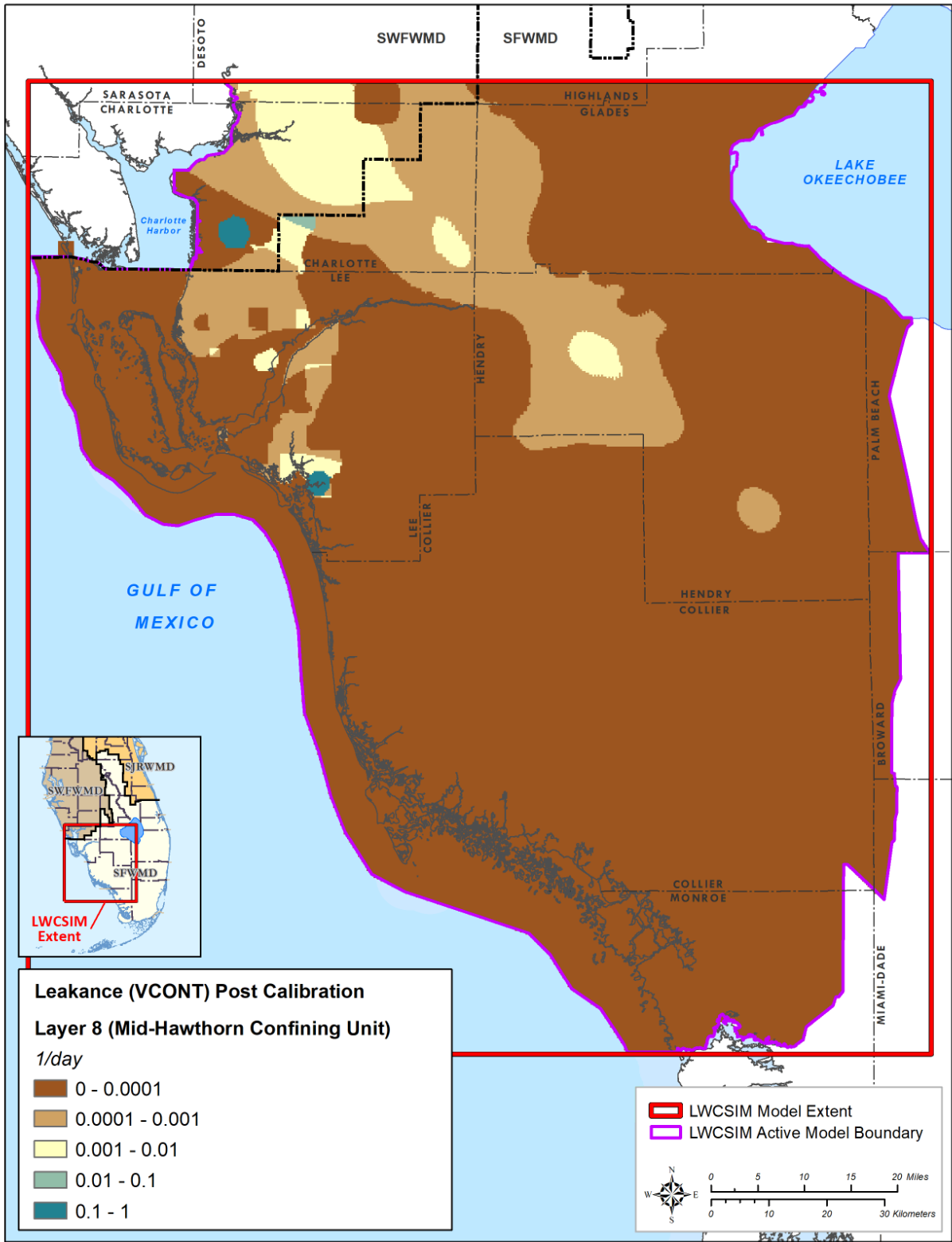


Figure H-14. Calibrated leakance in the Mid-Hawthorn confining unit (layer 8).

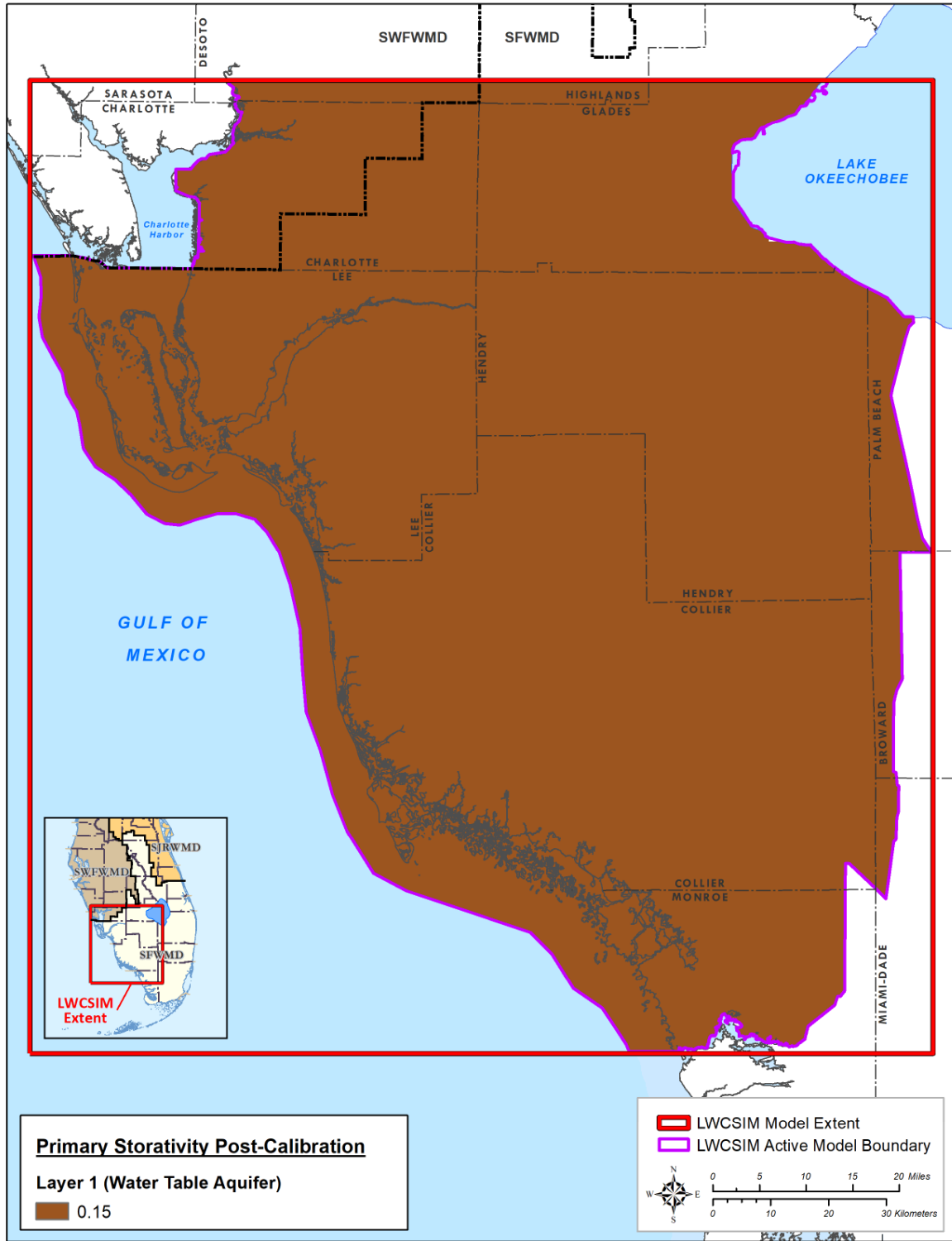


Figure H-15. Water Table aquifer (layer 1) calibrated storativity.

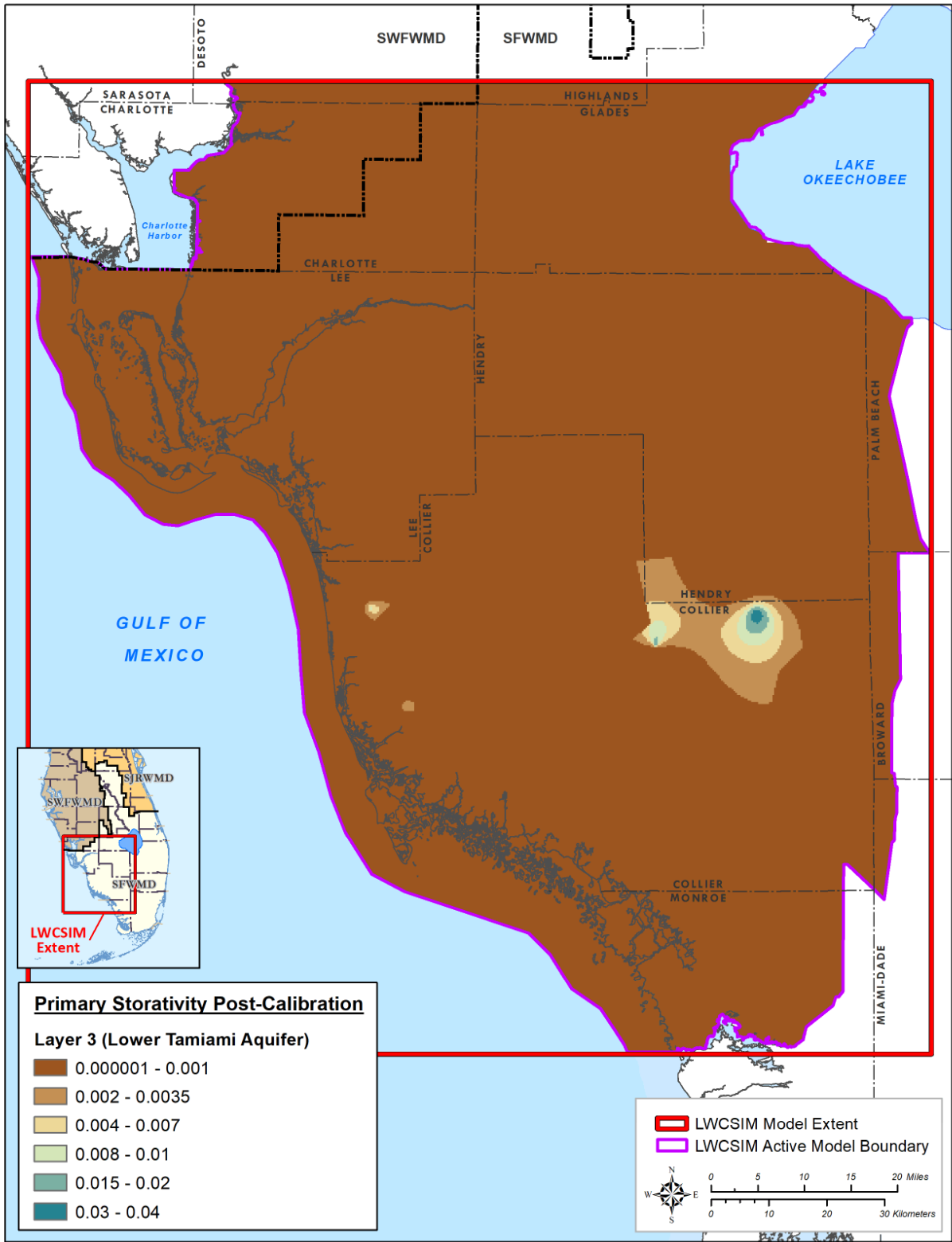


Figure H-16. Lower Tamiami aquifer (layer 3) calibrated storativity.

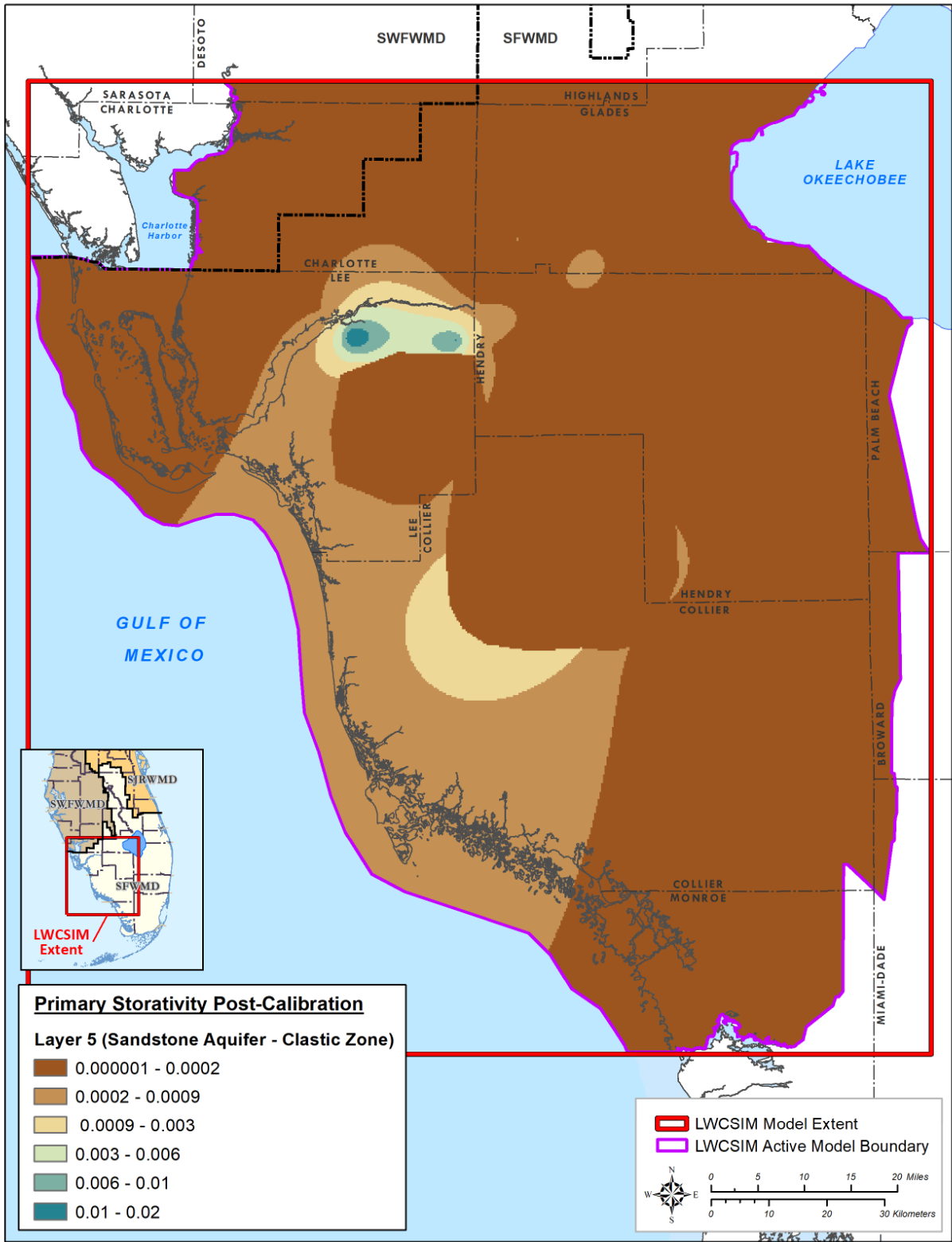


Figure H-17. Sandstone aquifer-clastic zone (layer 5) calibrated storativity.

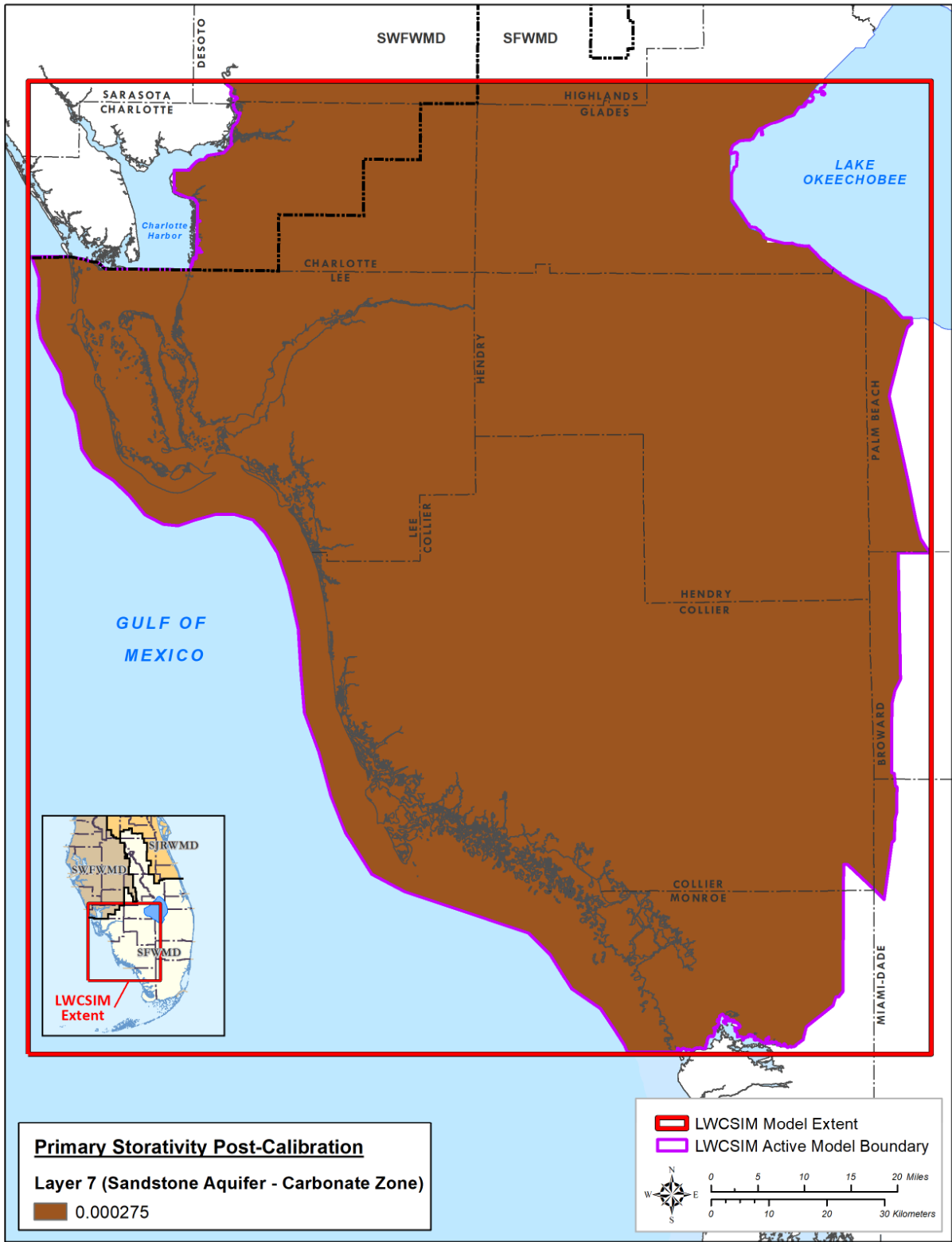


Figure H-18. Sandstone aquifer-carbonate zone (layer 7) storativity.

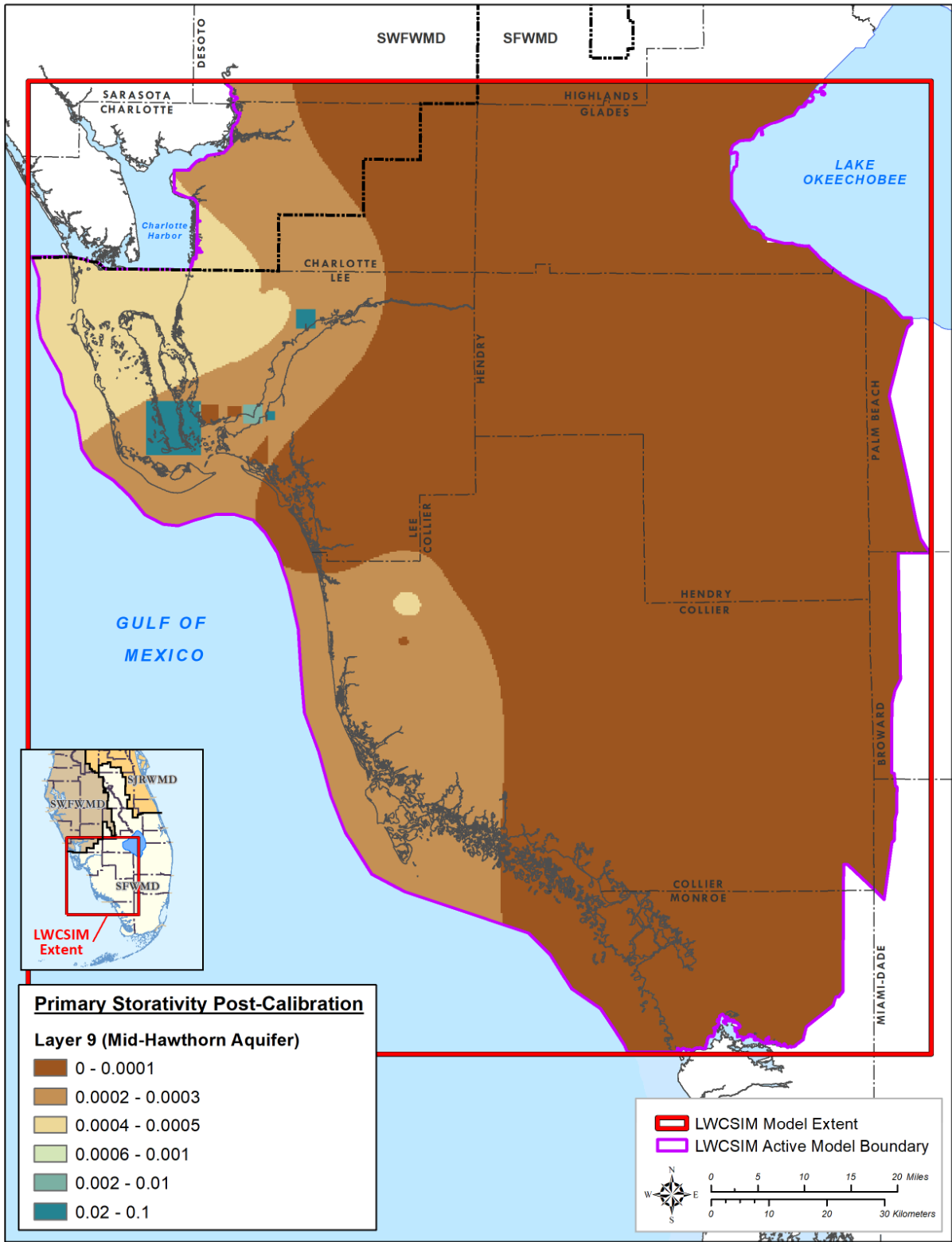


Figure H-19. Mid-Hawthorn aquifer (layer 9) calibrated storativity.

APPENDIX I: HYDROGRAPHS

**APPENDIX J:
R-SQUARED VERSUS TNSE FOR LWCSIM CALIBRATION TARGETS**

The transformed Nash-Sutcliffe efficiency (TNSE) coefficient, a derivative of the Nash-Sutcliffe efficiency (NSE) coefficient, was derived for all aquifer layer transient groundwater calibration targets as an additional indicator of transient model fit. Through statistical comparison with the R^2 value, it was determined that a TNSE value of 0 roughly corresponds to an R^2 value of 0.4, allowing for determination of a TNSE calibration criterion for the Lower West Coast Surficial and Intermediate Aquifer Systems Model (LWCSIM) that is similar to R^2 . The NSE and TNSE were determined using the following equations:

$$NSE = 1 - \frac{\sum_{i=1}^n (O_i - S_i)^2}{\sum_{i=1}^n (O_i - \bar{O})^2}$$

Where:

O_i = the i^{th} observed head value at a particular observation well

S_i = the i^{th} simulated head value at the same well location

\bar{O} = the mean of the observed head values at the observation well

$$TNSE = 1 - \frac{\sum_{i=1}^n (X_i - Z_i)^2}{\sum_{i=1}^n (X_i - \bar{X})^2}$$

Where:

X_i = the i^{th} transformed observed head value at a particular observation well

$X_i = O_i - \bar{O}$

\bar{X} = the mean of the transformed simulated head values at the observation well (this should be zero)

Z_i = the i^{th} transformed simulated head value at the same well location

$Z_i = S_i - \bar{S}$

\bar{S} = the mean of the simulated head values at the observation well

\bar{S}_i = the average simulated head at the monitor well

O_i , \bar{O} , and S_i as previously defined

Nominally, a TNSE of zero corresponds with an R^2 of 0.4 in that the quantiles for these two statistics are about equal at these two thresholds. To be more precise, the R^2 quantile for an R^2 of 0.4 is 0.262 (i.e., about 26% of R^2 values are less than 0.4). The TNSE quantile for a TNSE of 0.063 is 0.262 (i.e., about 26% of TNSE values are less than 0.063). The TNSE quantile for a TNSE of 0 is 0.252. Based on the above, there are three categories of model fit based on TNSE:

- $TNSE < 0$: Model quality is less than null-model of observed mean
- $0 \leq TNSE < 0.5$: Low-quality fit
- $0.5 \leq TNSE$: Moderate- to high-quality fit

Based on the above, the TNSE was assigned a cutoff of zero.

The summary of calibration statistics, with the TNSE values included, is presented in **Table J-1**.

Table J-1. Summary of calibration statistics.

| Statistics | Calibration | | | | |
|--|-------------|-------|-------------|---------------|-------|
| | WTA | LTA | SSA-clastic | SSA-carbonate | MHA |
| Residual mean (≤ 1) | -0.34 | 0.51 | 0.70 | 0.98 | -0.85 |
| Error standard deviation (≤ 5) | 2.27 | 2.97 | 3.22 | 1.80 | 3.21 |
| 5% of observed range* | 3.29 | 2.51 | 3.68 | 3.26 | 6.47 |
| 10% of observed range* | 6.58 | 5.02 | 7.36 | 6.52 | 12.94 |
| Mean absolute error (MAE) (≤ 5) | 1.76 | 2.44 | 2.38 | 1.68 | 2.55 |
| Root mean square error (≤ 5) | 2.29 | 2.99 | 3.24 | 2.01 | 3.25 |
| Minimum residual | -9.12 | -4.12 | -9.91 | -3.28 | -7.38 |
| Maximum residual | 6.45 | 9.35 | 5.27 | 3.78 | 4.39 |
| Number of observation points | 297 | 72 | 29 | 18 | 25 |
| Percentage with MAE < 2.5 ft (50%) | 73 | 61 | 62 | 72 | 56 |
| Percentage with MAE < 5.0 ft (80%) | 97 | 96 | 90 | 100 | 88 |
| Percentage with $R^2 > 0.4$ (60%) | 75 | 81 | 76 | 83 | 64 |
| Percentage with TNSE > 0 (60%) | 72 | 85 | 83 | 94 | 64 |

LTA = Lower Tamiami aquifer; MHA = Mid-Hawthorn aquifer; R^2 = Pearson coefficient of correlation; SSA = Sandstone aquifer; TNSE = transformed Nash-Sutcliffe efficiency; WTA = Water Table aquifer.

Green font indicates compliance with calibration criteria.

Calibration period: 1999 to 2012.

*Observed head ranges are for information only.

Figures J-1 to J-5 present the areal distribution of TNSE and R^2 values for each aquifer layer in the LWCSIM.

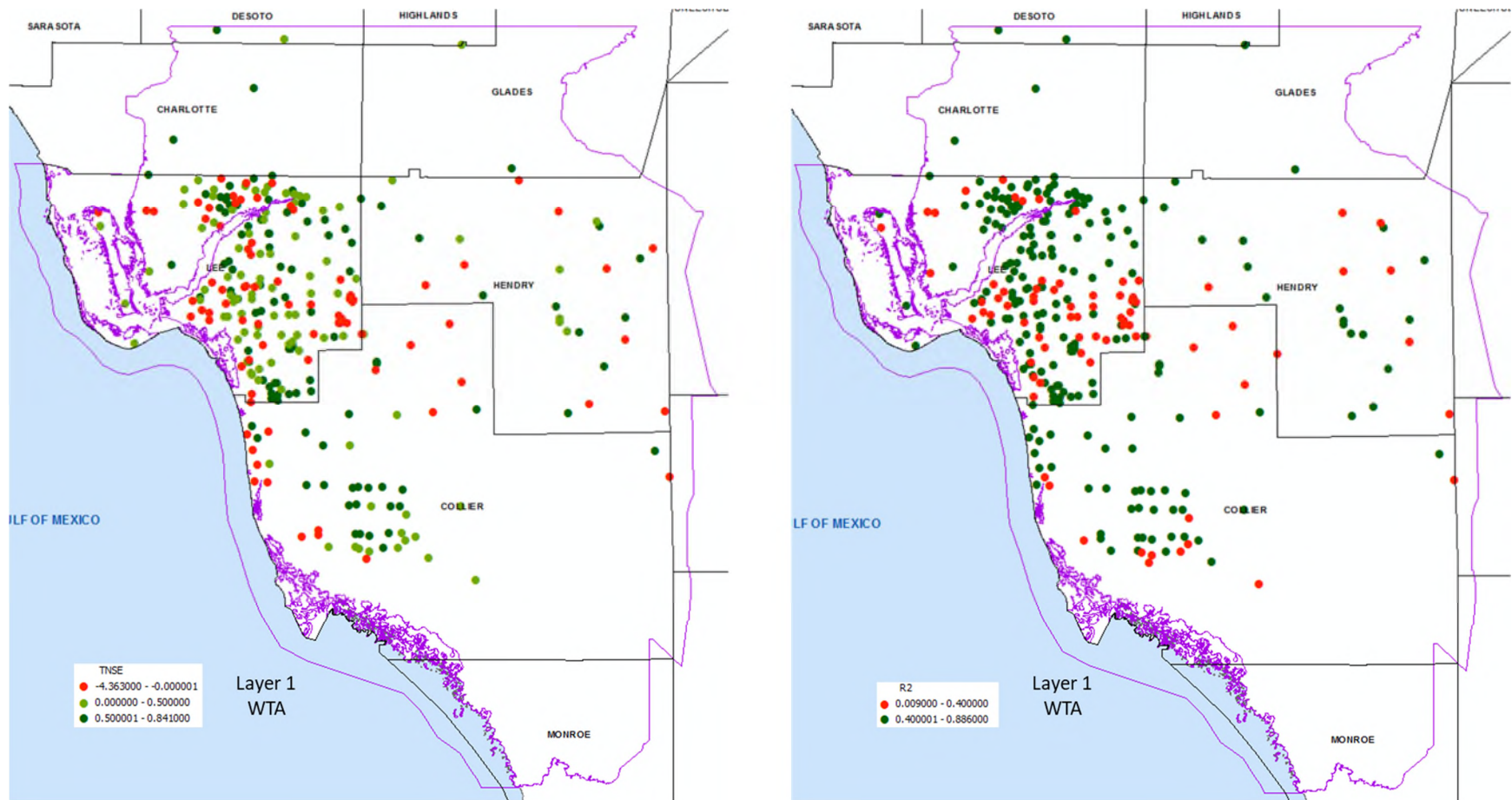


Figure J-1. Areal distribution of transformed Nash-Sutcliffe efficiency coefficient values (left) and R^2 values (right) for model layer 1.

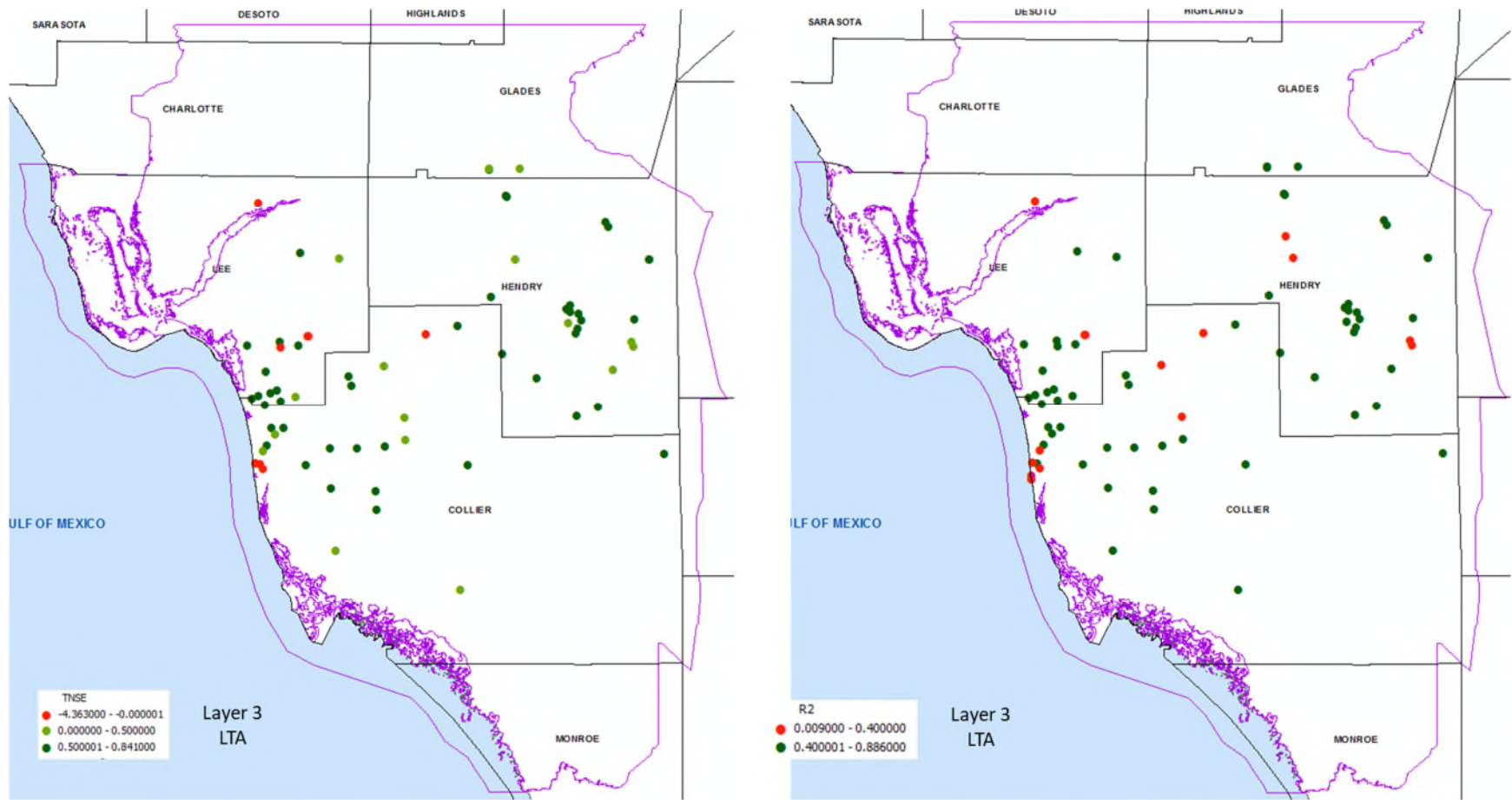


Figure J-2. Areal distribution of transformed Nash-Sutcliffe efficiency coefficient values (left) and R² values (right) for model layer 3.

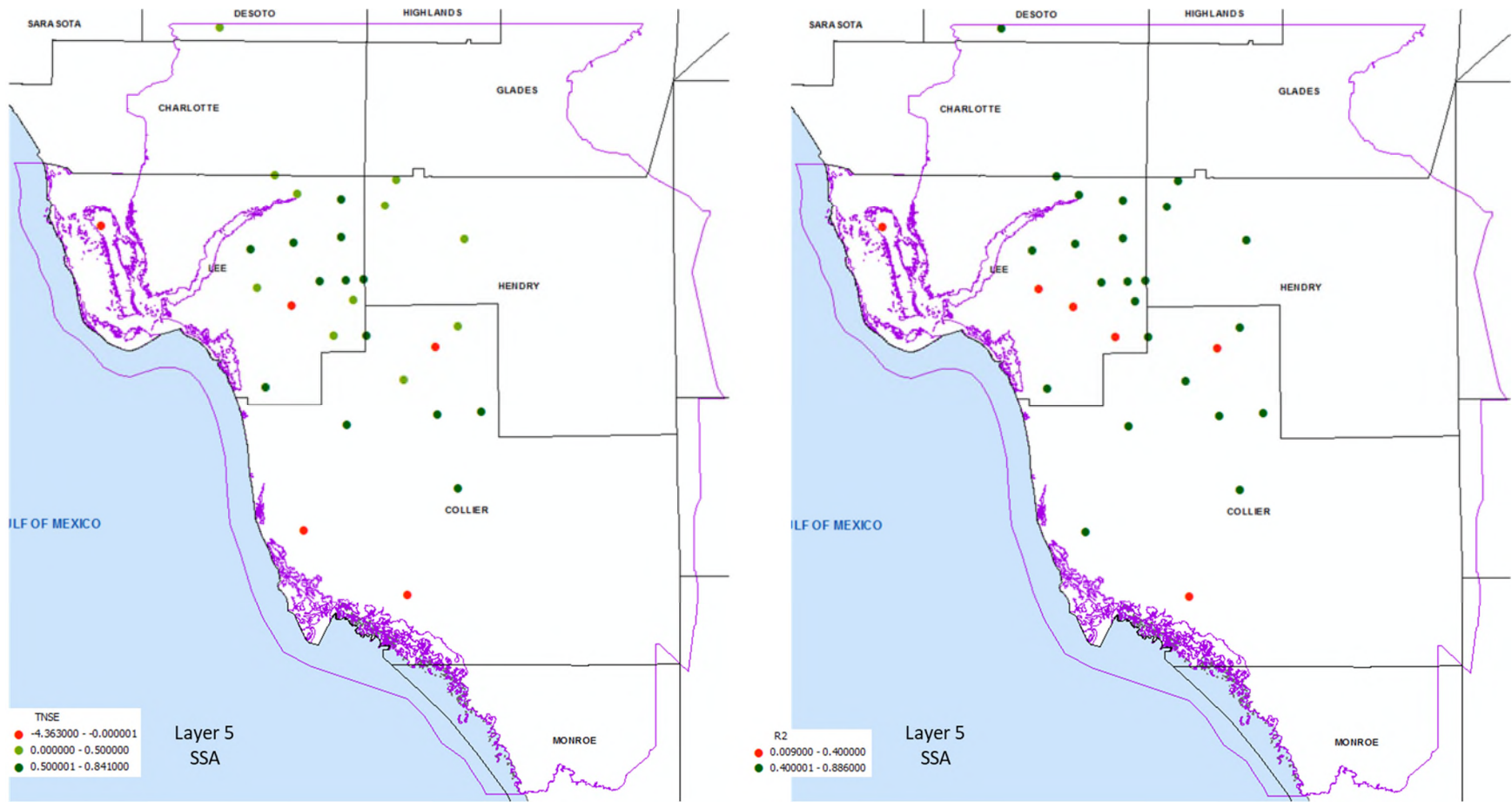


Figure J-3. Areal distribution of transformed Nash-Sutcliffe efficiency coefficient values (left) and R² values (right) for model layer 5.

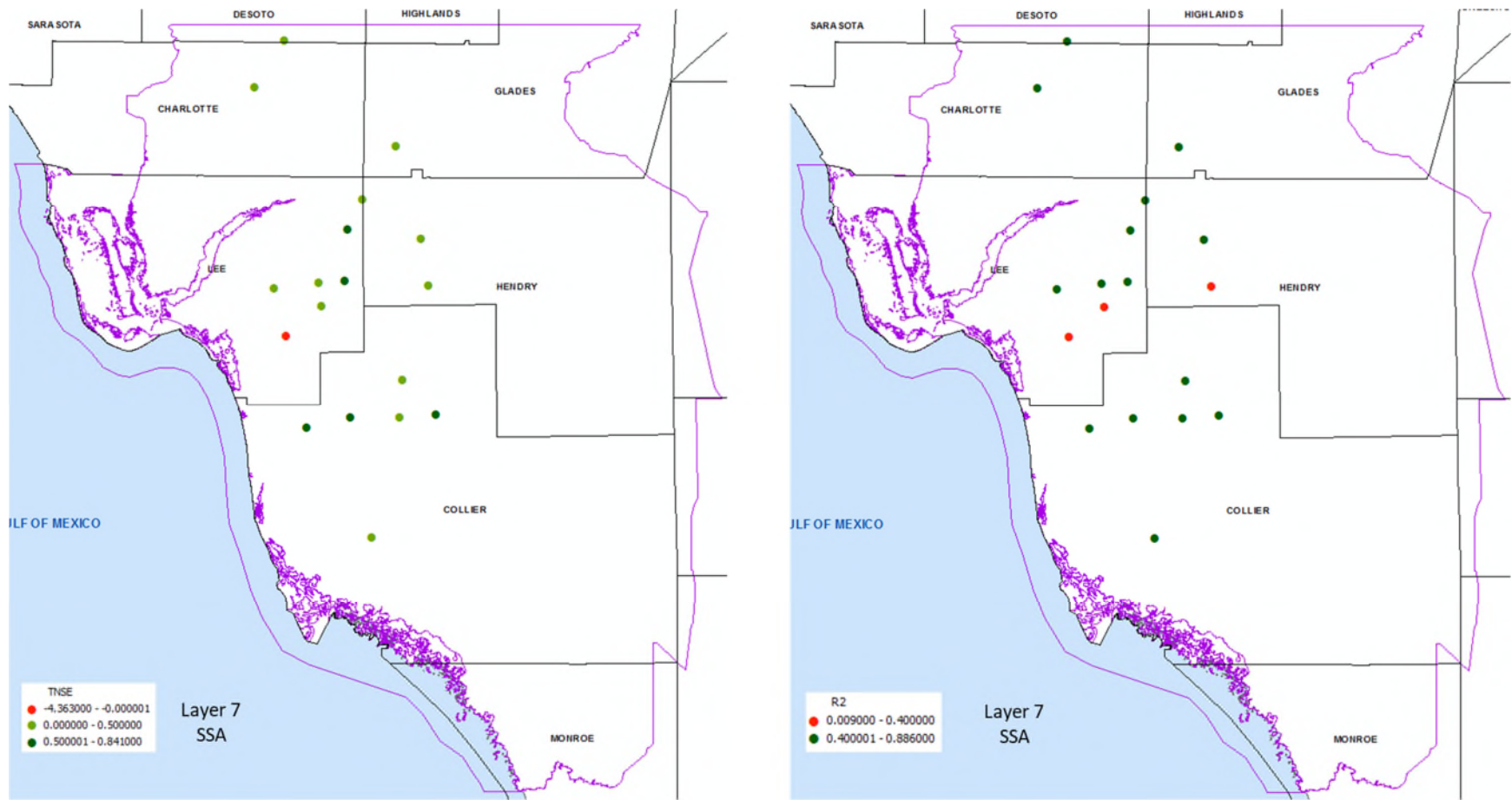


Figure J-4. Areal distribution of transformed Nash-Sutcliffe efficiency coefficient values (left) and R² values (right) for model layer 7.

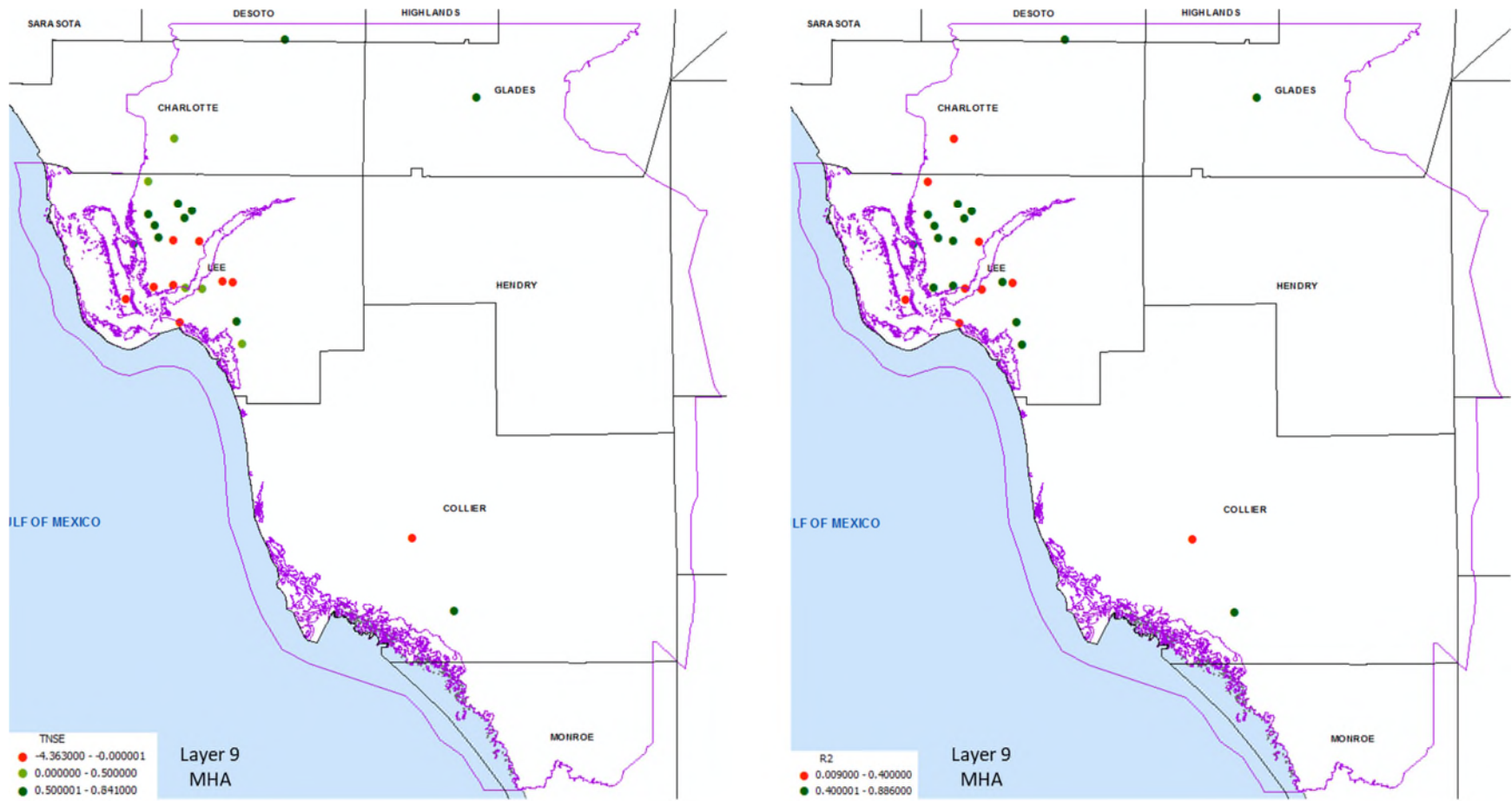


Figure J-5. Areal distribution of transformed Nash-Sutcliffe efficiency coefficient values (left) and R^2 values (right) for model layer 9.

**APPENDIX K:
SENSITIVITY RUN PLOTS**

